ΕΘΝΙΚΟ ΜΕΤΣΟΒΙΟ ΠΟΛΥΤΕΧΝΕΙΟ
ΣΧΟΛΗ ΜΗΧΑΝΟΛΟΓΩΝ ΜΗΧΑΝΙΚΩΝ
ΤΟΜΕΑΣ ΘΕΡΜΟΤΗΤΑΣ

ΥΠΟΚΑΤΑΣΤΑΣΗ ΓΑΙΑΝΘΡΑΚΑ ΑΠΟ ΕΝΑΛΛΑΚΤΙΚΑ ΚΑΙ ΥΠΟΣΤΗΡΙΚΤΙΚΑ ΚΑΥΣΙΜΑ ΣΕ ΛΕΒΗΤΕΣ ΚΟΝΙΟΠΟΙΗΜΕΝΟΥ ΚΑΥΣΙΜΟΥ ΓΙΑ ΤΗ ΜΕΙΩΣΗ ΕΚΠΟΜΠΩΝ CO_2

ΔΙΔΑΚΤΟΡΙΚΗ ΔΙΑΤΡΙΒΗ

ΜΙΧΑΗΛ Γ. ΑΓΡΑΝΙΩΤΗΣ

Επιβλέπων: Καθ. Εμμ. Κακαράς

ΑΘΗΝΑ

Δεκέμβριος 2010

Στους γονείς μου και τους δασκάλους μου

Δεῖ δή, εἶπον, ἡμᾶς τοιόνδε νομίσαι περὶ αὐτῶν, εἰ ταῦτ' ἀληθῆ· τὴν παιδείαν οὐχ οἵαν τινὲς ἐπαγγελλόμενοί φασιν εἶναι τοιαύτην καὶ εἶναι. φασὶ δέ που οὐκ ἐνούσης ἐν τῇ ψυχῇ ἐπιστήμης σφεῖς ἐντιθέναι, οἷον τυφλοῖς ὀφθαλμοῖς ὄψιν ἐντιθέντες.
Φασὶ γὰρ οὖν, ἔφη.
Ὁ δέ γε νῦν λόγος, ἦν δ' ἐγώ, σημαίνει ταύτην τὴν ἐνοῦσαν ἑκάστου δύναμιν ἐν τῇ ψυχῇ καὶ τὸ ὄργανον ᾧ καταμανθάνει ἕκαστος, […].
Τούτου τοίνυν, ἦν δ' ἐγώ, αὐτοῦ τέχνη ἂν εἴη, τῆς περιαγωγῆς, τίνα τρόπον ὡς ῥᾷστά τε καὶ ἀνυσιμώτατα μεταστραφήσεται, οὐ τοῦ ἐμποιῆσαι αὐτῷ τὸ ὁρᾶν, ἀλλ' ὡς ἔχοντι μὲν αὐτό, οὐκ ὀρθῶς δὲ τετραμμένῳ οὐδὲ βλέποντι οἷ ἔδει, τοῦτο διαμηχανήσασθαι.
Ἔοικεν γάρ, ἔφη.

Τότε [..] είπα πρέπει κι εμείς να παραδεχτούμε το εξής σχετικά με αυτά: Ότι η παιδεία δεν είναι ότι ισχυρίζονται γι' αυτήν κάποιοι, οι οποίοι έχουν για επάγγελμά τους την εκπαίδευση. Ισχυρίζονται δηλαδή ότι μέσα στην ψυχή δεν υπάρχει γνώση κι ότι κατά κάποιον τρόπο τη γνώση τη βάζουν αυτοί στην ψυχή, περίπου σαν να έβαζαν όραση σε μάτια τυφλών.
Το ισχυρίζονται πράγματι είπε
Απεναντίας, η τωρινή διερεύνησή μας, είπα εγώ δείχνει αυτή τη δύναμη της γνώσης που καθένας έχει μέσα στην ψυχή του, κι επίσης το εργαλείο με το οποίο ο καθένας φθάνει στη μάθηση [...].
Επομένως η παιδεία, είπα εγώ, θα είναι η τέχνη για αυτό το πράγμα, για τη μεταστροφή της ψυχής, με ποιον τρόπο δηλαδή η μεταστροφή θα συντελεστεί όσο το δυνατόν ευκολότερα και αποτελεσματικότερα [...].
Έτσι φαίνεται είπε.

Πλάτωνος Πολιτεία 518 b-d,
μτφ.Ν. Σκουτερόπουλου

Ευχαριστίες

Η παρούσα διατριβή εκπονήθηκε στο Εργαστήριο Ατμοκινητήρων και Λεβήτων του Τμήματος Μηχανολόγων Μηχανικών του ΕΜΠ στα πλαίσια της ερευνητικής μου ενασχόλησης από το Σεπτέμβριο του 2004 έως το Νοέμβριο του 2009.

Πρώτα από όλα θα ήθελα να ευχαριστήσω τον καθηγητή κ. Εμμ. Κακαρά για την ανάθεση της εργασίας, τη δυνατότητα που μου έδωσε να συνεργαστώ με ερευνητικές ομάδες του εξωτερικού στα πλαίσια της ερευνητικής μου δραστηριότητας και τη συνεχή υποστήριξη και εμπιστοσύνη που έδειξε στο πρόσωπό μου όλα αυτά τα χρόνια.

Θερμές ευχαριστίες θα ήθελα επίσης να απευθύνω στον ομότιμο καθηγητή κ. Ν. Παπαγεωργίου για τη διαρκή υποστήριξή του και το έμπρακτο ενδιαφέρον του για την πρόοδο της εργασίας μου.

Είμαι ακόμη υπόχρεος στο Δρ. Π. Γραμμέλη για τη συνεχή και συστηματική καθοδήγησή του, αλλά και την υποστήριξη και τη βοήθειά του σε οποιαδήποτε δυσκολία αντιμετώπισα.

Στους συναδέλφους Δρ. Σωτήρη Καρέλλα, Δρ. Βασίλη Βράγκο, Δρ. Νίκο Νικολόπουλο και Μανώλη Καραμπίνη είμαι επίσης ευγνώμων για τα ουσιαστικά σχόλια και παρατηρήσεις τους πάνω στο κείμενο.

Για την επιμέλεια του αγγλικού και ελληνικού κειμένου οφείλω επίσης θερμές ευχαριστίες στην Αλεξάνδρα Νασοπούλου και στον Παναγιώτη Βουνάτσο

Θα ήθελα επιπλέον να ευχαριστήσω όλα τα μέλη του Εργαστηρίου Ατμοπαραγωγών καθώς και του Ινστιτούτου Τεχνολογίας και Εφαρμογών Στερεών Καυσίμων (ΕΚΕΤΑ/ ΙΤΕΣΚ) για τη συνεργασία τους και την έμπρακτη συμπαράστασή τους στις δραστηριότητές μου.

Ευχαριστώ ακόμη θερμά τα υπόλοιπα μέλη της τριμελούς συμβουλευτικής επιτροπής κ. Ξ. Κακάτσιο και κ. Κ. Ρακόπουλο για τις παρατηρήσεις τους με στόχο τη βελτίωση της παρούσας εργασίας.

Στους Έλληνες και ξένους συναδέλφους, με τους οποίους συνεργάστηκα στα πλαίσια της ερευνητικής μου εργασίας οφείλω επίσης θερμές ευχαριστίες.

Τέλος στην οικογένειά μου για την αμέριστη συμπαράστασή της σε όλες τις στιγμές της πολυετούς αυτής προσπάθειας μου οφείλω μέγιστη ευγνωμοσύνη.

Μιχάλης Αγρανιώτης

Αθήνα, Οκτώβριος 2010

Σύμφωνα με απόφαση της ΓΣΕΣ της Σχολής Μηχανολόγων Μηχανικών του ΕΜΠ στις 23/11/2009 η παρούσα Διατριβή γίνεται αποδεκτή στην Αγγλική γλώσσα. Έχει επιπλέον προστεθεί ελληνική περίληψη με έκταση ίση περίπου με τον ένα τρίτο της έκτασης του αγγλικού κειμένου.

Η έγκριση της Διδακτορική Διατριβής από τη Σχολή Μηχανολόγων Μηχανικών του Εθνικού Μετσόβιου Πολυτεχνείου δεν υποδηλώνει αποδοχή των γνωμών του συγγραφέα (Ν. 5343/ 1932, Άρθρο 202)

Επιβλέπων Καθηγητής

Δρ. Εμμ. Κακαράς
Καθηγητής ΕΜΠ

Τριμελής Συμβουλευτική Επιτροπή

Δρ. Ξ. Κακάτσιος
Καθηγητής ΕΜΠ

Δρ. Κ. Ρακόπουλος
Καθηγητής ΕΜΠ

Δρ. Εμμ. Κακαράς
Καθηγητής ΕΜΠ

Table of Contents

Abbreviations

APH	Air Pre-heater
BAT	Best Available Techniques
BREF	Best Available Techniques Reference Guide
CAPEX	Capital Expenditures
CCS	Carbon Capture and Storage
CEN	European Committee for Standardisation
CFB	Circulating Fluidised Bed
CFD	Computational Fluid Dynamics
DO	Discrete Ordinates Model
EBU	Eddy Break Up Model
EN	European Norm
ESP	Electro Static Precipitator
ETS	Emissions Trading Scheme
EU	European Union
FB	Fluidised Bed
FGD	Flue Gas Desulphurisation Unit
GHG	Green House Gas
HCF	High Calorific Fraction
HM	Heavy Metals
IEA	International Energy Agency
IRR	Internal Rate of Return
LCPD	Large Combustion Plant Directive
MBM	Meat and Bone Meal
MSW	Municipal Solid Waste
MTE	Mechanical Thermal Dewatering
NAP	National Allocation Plan
NIR	Near Infrared Spectroscopy
NPV	Net Present Value
OECD	Organisation of Economic Co-operation and Development
OFA	Over Fired Air
OPEX	Operational Expenditures
PF	Pulverised Fuel
PPC	Public Power Corporation of Greece
PSD	Particle Size Distribution
RES	Renewable Energy Sources
SMP	System's Marginal Price
SRF	Solid Recovered Fuels
TCI	Total Capital Investment
TPC	Total Plant Costs
TPP	Thermal Power Plant
TS	Technical Specification
UN	United Nations
WB	Wet Bottom
WID	Waste Incineration Directive
WTA	Wirbeslchichttrocknung mit integrierter Abwaermenutzung (Fluidised Bed Drying with Integrated Waste Heat Utilisation)W
WSGGM	Weighted Sum of Grey Gases Model

Symbols

A_1	$[s^{-1}]$	pre-exponential factor in Arrhenius expression for reaction rate constant
A_p	$[m^2]$	Surface area of particle
c_p	[J/(kgK)]	specific heat
C_1	[kg / (m s Pa)]	mass diffusion limited rate constant
C_2	[kg / (m^2 s Pa)]	kinetics limited rate pre-exponential factor
d_p	[μm]	particle diameter
D_o	[kg / (m^2 s Pa)]	mass diffusion limited rate on char burnout
E	[J $kmol^{-1}$]	Activation Energy
f_{vol}	[%]	volatile fraction in the coal particle
h_{Gout}	[kJ/kg]	flue gas enthalpy at the boiler outlet after air preheater
$h_{G\_ambient}$	[kJ/kg]	flue gas enthalpy at ambient conditions
H_u	[MJ/kg]	Net Calorific Value (NCV)
m_G	[kg/s]	flue gas mass flow
k	$[s^{-1}]$	Reaction rate constant
k_∞	[W/(mK)]	Thermal conductivity in the continuous phase
m_B	[kg/s]	fuel mass flow
p	$[N/m^2]$ = [Pa]	Pressure
R	[kJ $kmol^{-1}K^{-1}$]	Universal gas constant
R_o	[kg / (m^2 s Pa)]	Kinetics limited rate on char burnout
T	[K] or [°C]	temperature
u	[m/s]	velocity
u_G	[%]	flue gas losses
u_L	[%]	Radiation losses
u_E	[%]	combustion losses

Greek Symbols

ε_p	[-]	particle emissivity
η_E	[%]	efficiency rate of the boiler heat exchanger surfaces
η_F	[%]	efficiency rate of the combustion chamber describing the percentage of the fuel, which is completely burnt. Typical value for conventional large-scale pulverised fuel boilers: 0.97 - 0.98.
θ_R	[K]	radiation temperature $\theta_R=(I/4\sigma)^{1/4}$
ρ	$[kg/m^3]$	Density
σ	$[W/(m^2K^4)]$	Stefan Boltzmann constant ($\sigma=5.67\ 10^{-8}$)

Subscripts and superscripts

∞	Ambient
dec	decomposition process
e	Electric
g	gas
melt	melting process
ox	Oxidant (O_2)
p	Particle
req	required
th	thermal power
w	wall

Summary

Scope of the present thesis is to assess the potential of two different brown coal substitution concepts as possible options to reduce CO_2 emissions in existing pulverised brown coal power plants. The substitution of brown coal by alternative fuels is the first concept examined. Alternative fuels are non fossil fuels with a high biogenic share. Agricultural or forest residues, which are fully biogenic, as well as waste derived fuels, which may have a high biogenic content, are considered as alternative fuels. In the present work a particular category of waste derived fuels, the Solid Recovered Fuels (SRF), which possess specific quality characteristics, are investigated. The second concept regarded is the substitution of raw brown coal by pre-dried brown coal, which is considered as supporting fuel and the respective integration of a fluidised bed drying system in the existing plant steam cycle. The first concept is demonstrated in a 600 MW_e pulverised brown coal boiler in Germany, while dry coal co-firing is demonstrated in a 75 MW_{th} brown coal boiler in Greece. Since the integration of a brown coal pre-drying system in an existing power plant utilising low temperature steam, has not been fully demonstrated in the large scale yet, the particular concept is investigated by thermal cycle calculations.

The evaluation and comparison of the two concepts proposed is based on specific environmental, technological and economical parameters. In order to assess the performance of the two co-firing concepts in respect with the decided criteria, different analysis approaches are used. Apart from the large scale experimental activities numerical simulations based on Computational Fluid Dynamics (CFD) analysis are also carried out for the two boilers. Through the simulations additional co-firing modes are assessed, which cannot be realised in the large scale. Different injection locations for the alternative fuel are numerically examined in the case of the 600 MW_e boiler, while the numerical investigations of the 75 MW_{th} boiler focus on the evaluation of the boiler's combustion behaviour under elevated dry coal co-firing thermal shares. Thermodynamic calculations are also carried out, so as to assess the expected plant efficiency increase by the integration of the fluidized bed drying concept in an existing Greek power plant.

The conducted small scale investigations are used as supporting work for the assessment of the co-firing concepts in the large scale. A dedicated model on SRF combustion is developed and validated against available lab scale data. The SRF combustion model is further used in the co-firing simulations of the industrial boiler. Lignite drying tests are also carried out in a lab scale fluidised bed dryer, in order to evaluate the drying behaviour of Greek lignite in comparison with the Rhenish one. An extensive experimental campaign on Greek pre-dried lignite combustion is carried out in a 1 MW_{th} experimental combustor. The experimental campaign is accompanied by numerical simulations and the simulation results are compared with the available experimental data. The simulation set up is used then in the large scale dry coal co-firing simulations. Beyond the environmental and technological aspects investigated, the economic feasibility of the regarded coal substitution concepts is also assessed by economic performance indices. The additional costs and revenues expected by applying SRF or dry lignite co-firing in the large scale are presented and compared. The respective CO_2 avoidance costs are calculated for each concept and economic indices are used for the evaluation of both co-firing scenarios in terms of return on investment.

The overall assessment implies that the realisation of both co-firing concepts in the large scale is feasible. Environmental, technical and economic aspects are thoroughly studied. Co-firing of alternative fuels in low thermal shares in existing boilers may be applied without negative impact on the boiler's operational behaviour or environmental performance. Some technological aspects have to be further examined, in order to assure the reliable boiler operation under continuous co-firing conditions. The control of chlorine induced corrosion at the boiler's heat exchanger surfaces through online monitoring tools and a continuous monitoring system of alternative fuel's quality are the recommended practices towards this direction. Considering the economic potential of SRF co-firing it is regarded as a highly profitable investment with a short payback period, due to the subsidized electricity price and the zero fuel price and has a considerable potential for reduction of CO_2 emissions.

The integration of a pre-drying concept in existing lignite power plants and the implementation of dry lignite co-firing is a more complex application, which requires increased efforts on careful planning and detailed engineering. A considerable reduction in CO_2 emissions may be achieved, if elevated co-firing thermal shares up to 25% are applied. The boiler's combustion behavior is influenced in this way in terms of furnace temperature distribution, emissions and heat balance. The performed investigations on pre-dried lignite co-firing in the case of a Greek power plant showed that large scale implementation of pre-dried lignite co-firing is feasible without specific negative impacts in terms of environmental or technological aspects. Expected changes in the boiler's heat balance may influence the overall mass balance of the power plant; a positive effect is however expected from this change, i.e. the increase of plant efficiency. The increase tendency of NO_x emissions has to be mitigated by a rearrangement of the firing system and the application of increased air staging conditions. From an economic point of view, the financial evaluation of the pre-drying concept indicates that it is not suitable as a retrofitting option for aged power plants, due the long investment payback period. It should be more regarded as an option to increase plant efficiency in new power plants or even in projects that are still in the design phase. Considerable reductions of the additional investment costs may be achieved through the effective dimensioning of the conventional milling and drying system in respect of dry lignite co-firing and the fluidised bed dryer operation.

Concluding, the evaluation and comparison of two different coal substitution practices is attempted in the present thesis. Environmental, technological and economic aspects are taken into account and several parameters are used as evaluation indices. No final result for or against a particular technology may come out from this detailed analysis. The identification and in depth investigation of positive or problematic aspects of both concepts should be considered as the main contribution of this work.

Σύνοψη

Ο σκοπός της παρούσας διατριβής είναι η αξιολόγηση δύο διαφορετικών τεχνολογιών υποκατάστασης άνθρακα ως επιλογές για την εξοικονόμηση εκπομπών CO_2 σε υπάρχοντες λιγνιτικούς σταθμούς. Η υποκατάσταση λιγνίτη από εναλλακτικά καύσιμα είναι το πρώτο τεχνολογικό σενάριο υποκατάστασης που εξετάζεται. Εναλλακτικά καύσιμα θεωρούνται τα μη ορυκτά καύσιμα με υψηλό βιογενές μέρος. Τα γεωργικά και δασικά υπολείμματα που είναι πλήρως βιογενή, όπως και τα ανακτηθέντα από απορρίμματα καύσιμα που είναι σε μεγάλο μέρος βιογενή λογίζονται ως εναλλακτικά καύσιμα. Στην παρούσα εργασία εξετάζεται μία συγκεκριμένη κατηγορία των καυσίμων από απορρίμματα, τα στερεά ανακτηθέντα καύσιμα (Solid Recovered Fuels, SRF), τα οποία έχουν συγκεκριμένα ποιοτικά χαρακτηριστικά. Η δεύτερη τεχνολογία αφορά στην υποκατάσταση του φυσικού λιγνίτη από προξηραμένο λιγνίτη, που θεωρείται ως υποστηρικτικό καύσιμο, και την ενσωμάτωση του αντίστοιχου συστήματος ρευστοποιημένης κλίνης για προξήρανση λιγνίτη στον υπάρχοντα κύκλο ατμού του υπό εξέταση λιγνιτικού σταθμού. Η επιδεικτική δράση υποκατάστασης λιγνίτη από SRF λαμβάνει χώρα σε γερμανικό λέβητα κονιοποιημένου λιγνίτη εγκατεστημένης ισχύος 600 MW_e ενώ η υποκατάσταση φυσικού λιγνίτη από προξηραμένο λαμβάνει χώρα σε ελληνικό λέβητα εγκατεστημένης ισχύος 75 MW_{th}. Εφόσον η επιδεικτική δράση του συστήματος προξήρανσης σε υπάρχοντα λιγνιτικό σταθμό, δεν έχει ολοκληρωθεί ακόμα η ενσωμάτωση της τεχνολογίας προξήρανσης σε υπάρχοντα κύκλο ατμού θα διερευνηθεί μέσω υπολογισμών θερμοδυναμικού κύκλου.

Η αξιολόγηση και η σύγκριση των δύο προτεινόμενων τεχνολογιών βασίζεται σε συγκεκριμένες περιβαλλοντικές, τεχνολογικές και οικονομικές παραμέτρους. Για να αξιολογηθούν οι επιδόσεις των δύο τεχνολογιών σε σχέση με τα δεδομένα κριτήρια, χρησιμοποιούνται διαφορετικά μεθοδολογικά εργαλεία. Εκτός από τις πειραματικές μετρήσεις στην βιομηχανική κλίμακα, πραγματοποιούνται και για τους δύο υπό εξέταση λέβητες αριθμητικές προσομοιώσεις βασισμένες σε εργαλεία Υπολογιστικής Ρευστοδυναμικής (CFD). Μέσω των υπολογιστικών προσομοιώσεων αξιολογούνται περαιτέρω σενάρια υποκατάστασης, τα οποία δεν μπορούν να υλοποιηθούν στην πράξη. Διαφορετικές θέσεις εισόδου εξετάζονται για την περίπτωση των στερεών ανακτηθέντων καυσίμων (SRF), ενώ για την περίπτωση μικτής καύσης ξηρού λιγνίτη με φυσικό εξετάζεται η επίδραση αυξημένων ποσοστών θερμικής υποκατάστασης στη συμπεριφορά καύσης στο λέβητα. Ακόμη, μέσω θερμοδυναμικών υπολογισμών εκτιμάται η δυνητική αύξηση του βαθμού απόδοσης υπάρχοντος λιγνιτικού σταθμού με την ενσωμάτωση του ξηραντήρα ρευστοποιημένης κλίνης στον υπάρχοντα κύκλο ατμού.

Οι πραγματοποιθείσες διερευνήσεις σε μικρή κλίμακα, χρησιμοποιούνται υποστηρικτικά για την αξιολόγηση των πρακτικών υποκατάστασης στη βιομηχανική κλίμακα. Ένα νέο μοντέλο καύσης για τα στερεά ανακτηθέντα καύσιμα (SRF) αναπτύσσεται. Η ακρίβειά των προλέξεων του μοντέλου πιστοποιείται με διαθέσιμα πειραματικά δεδομένα από εγκατάσταση καύσης εργαστηριακής κλίμακας. Το αναπτυχθέν μοντέλο χρησιμοποιείται στη συνέχεια στις υπολογιστικές προσομοιώσεις μικτής καύσης SRF και λιγνίτη στο βιομηχανικό λέβητα. Δοκιμές ξήρανσης λιγνίτη πραγματοποιούνται σε ξηραντήρα ρευστοποιημένης κλίνης εργαστηριακής κλίμακας, με σκοπό την εκτίμηση της συμπεριφοράς ξήρανσης ελληνικού λιγνίτη σε σύγκριση με το λιγνίτη από την περιοχή της Βόρειας Ρηνανίας Βεστφαλίας. Παρουσιάζονται στη συνέχεια τα αποτελέσματα από σειρά πειραμάτων με καύση ελληνικού προξηραμένου λιγνίτη σε πειραματική εγκατάσταση καύσης ισχύος 1 MW_{th}. Ακολουθεί η αριθμητική προσομοίωση της εγκατάστασης και τα

αποτελέσματα της προσομοίωσης συγκρίνονται με τα υπάρχοντα πειραματικά δεδομένα. Οι παράμετροι της προσομοίωσης που επιβεβαιώθηκαν από τα πειραματικά δεδομένα χρησιμοποιούνται έπειτα στις προσομοιώσεις μικτής καύσης ξηρού λιγνίτη με φυσικό στη βιομηχανική κλίμακα.
Πέρα από τις περιβαλλοντικές και τεχνολογικές παραμέτρους που εξετάζονται, αξιολογείται και η οικονομική βιωσιμότητα των προτεινόμενων τεχνολογιών μέσω δεικτών απόδοσης. Τα επιπλέον κόστη και έσοδα από την εφαρμογή μικτής καύσης SRF ή ξηρού λιγνίτη σε υπάρχοντα θερμικό σταθμό παρουσιάζονται και συγκρίνονται. Το κόστος αποφυγής CO_2 υπολογίζεται για κάθε τεχνολογία και οικονομικοί δείκτες χρησιμοποιούνται για την αξιολόγηση των δύο τεχνολογιών από την σκοπιά της οικονομικότητας και της απόδοσης της επένδυσης.
Η συνολική αξιολόγηση υποδεικνύει ότι η εφαρμογή των δύο πρακτικών υποκατάστασης στη μεγάλη κλίμακα είναι εφικτή. Περιβαλλοντικές, τεχνολογικές και οικονομικές πτυχές εξετάζονται συστηματικά. Η μικτή καύση εναλλακτικών καυσίμων σε χαμηλά ποσοστά θερμικής υποκατάστασης σε υπάρχοντες λέβητες μπορεί να εφαρμοστεί χωρίς επίπτωση στην λειτουργική συμπεριφορά του λέβητα ή την περιβαλλοντική του επίδοση Συγκεκριμένα τεχνικά ζητήματα πρέπει να εξεταστούν με σκοπό να διασφαλιστεί η ασφαλής λειτουργία ενός λέβητα σε περίπτωση συνεχούς λειτουργίας σε συνθήκες μικτής καύσης με SRF. Ο έλεγχος των φαινομένων διάβρωσης λόγω χλωρίου στις επιφάνειες των εναλλακτών θερμότητας μέσω μετρητικών ληπτών συνεχούς καταγραφής και η διασφάλιση ποιότητας του καυσίμων είναι οι προτεινόμενες πρακτικές προς αυτή την κατεύθυνση. Σχετικά με την οικονομική βιωσιμότητα ενός σεναρίου μικτής καύσης λιγνίτη και SRF, αυτό θεωρείται ως επικερδές επενδυτικό σενάριο με μικρή περίοδο αποπληρωμής, λόγω της επιδοτούμενης τιμής ηλεκτρικής ενέργειας και του μηδενικού κόστους καυσίμου, ενώ επίσης κατέχει και σημαντικό δυναμικό για την μείωση των εκπομπών CO_2.
Η ενσωμάτωση της τεχνολογίας προξήρανσης σε υπάρχοντα λιγνιτικά εργοστάσια και η μικτή καύση ξηρού λιγνίτη με φυσικό είναι μια πιο περίπλοκη εφαρμογή με αυξημένες απαιτήσεις στον αρχικό σχεδιασμό και την τελική μελέτη του συστήματος. Μια σημαντική μείωση σε εκπομπές CO_2 μπορεί να επιτευχθεί, εάν εφαρμοστούν υψηλά θερμικά ποσοστά υποκατάστασης έως 25%. Η συμπεριφορά καύσης στο λέβητα επηρεάζεται με αυτόν τον τρόπο όσον αφορά την κατανομή της θερμοκρασίας στο θάλαμο καύσης, τις εκπομπές ρύπων και το θερμικό ισοζύγιο. Η πραγματοποιθείσα διερεύνηση για τη περίπτωση των ελληνικών λιγνιτικών σταθμών καταδεικνύει ότι η εφαρμογή της συγκεκριμένης τεχνολογίας στη βιομηχανική κλίμακα είναι εφικτή χωρίς συγκεκριμένες αρνητικές επιπτώσεις σε σχέση με περιβαλλοντικές ή τεχνολογικές πτυχές. Οι αναμενόμενες αλλαγές στο θερμικό ισοζύγιο του λέβητα μπορούν να επηρεάσουν το θερμικό ισοζύγιο σε ολόκληρο το σταθμό, που εκτιμάται ότι θα οδηγήσει σε αύξηση του βαθμού απόδοσης. Η τάση αύξησης εκπομπών NO_x πρέπει να ελεγχθεί και να μειωθεί με τον ανασχεδιασμό του συστήματος καύσης και την εφαρμογή αυξημένης διαβάθμισης στον αέρα καύσης.
Από οικονομική σκοπιά, η οικονομική αξιολόγηση της τεχνολογίας προξήρανσης υποδεικνύει ότι αυτή δεν είναι κατάλληλη ως επιλογή μετασκευής σε υφιστάμενους λιγνιτικούς σταθμούς μεγάλης ηλικίας, λόγω της απαιτούμενης μεγάλης περιόδου αποπληρωμής κεφαλαίου. Θα πρέπει να θεωρείται περισσότερο ως επιλογή βελτίωσης του βαθμού απόδοσης σε νέους σταθμούς ή ακόμα σε νέα έργα υπό σχεδιασμό. Στο στάδιο σχεδιασμού είναι δυνατό να επιτευχθούν σημαντικές μειώσεις στο συνολικό κόστος επένδυσης μέσω της αποτελεσματικής διαστασιολόγησης των συμβατικών συστημάτων άλεσης και ξήρανσης λαμβάνοντας υπόψη τη λειτουργία του ξηραντήρα ρευστοποιημένης κλίνης και του συστήματος καύσης ξηρού λιγνίτη.

Εν κατακλείδι, στην παρούσα διατριβή επιχειρείται η αξιολόγηση και σύγκριση δύο διαφορετικών πρακτικών υποκατάστασης λιγνίτη. Περιβαλλοντικές, τεχνολογικές και οικονομικές πτυχές λαμβάνονται υπόψη και διαφορετικές παράμετροι χρησιμοποιούνται ως δείκτες αξιολόγησης. Από τη συγκεκριμένη ανάλυση δεν μπορεί να προκύψει κάποιο αποτέλεσμα υπέρ ή κατά μίας τεχνολογίας. Ο εντοπισμός και η σε βάθος διερεύνηση των θετικών και προβληματικών ζητημάτων που προκύπτουν από αυτές τις πρακτικές υποκατάστασης αποτελούν την κύρια προσφορά της συγκεκριμένης εργασίας.

Περίληψη στα Ελληνικά

Κεφάλαιο 1: Εισαγωγή

Η παροχή ηλεκτρισμού αλλά και γενικότερα η διαθεσιμότητα των αντίστοιχων πηγών ενέργειας θεωρούνται δύο από το τα κύρια θέματα, τα οποία καλείται να αντιμετωπίσει η διεθνής κοινότητα τις προσεχείς δεκαετίες. Σε όλη την ιστορική περίοδο μετά την βιομηχανική επανάσταση και μέχρι το τέλος του 20^{ου} αιώνα κύρια κριτήρια για την επιλογή συστημάτων παραγωγής ηλεκτρικής ενέργειας και των αντίστοιχων πρωτογενών ενεργειακών πηγών υπήρξαν, εκτός της οικονομικής βιωσιμότητας, η ασφάλεια εφοδιασμού και η αδιάλειπτη παροχή ηλεκτρικής ενέργειας. Οι πρώτες συστηματικές αντιδράσεις και κριτικές σχετικά με τις περιβαλλοντικές επιπτώσεις των τεχνολογιών παραγωγής ενέργειας, που αποτελούν και την απαρχή του περιβαλλοντικού κινήματος, εμφανίζονται στις δεκαετίες του 1970 και 1980, όταν αυξήθηκαν τα προβλήματα ατμοσφαιρικής ρύπανσης από τους σταθμούς παραγωγής ηλεκτρικής ενέργειας, κυρίως στις περιοχές έντονης βιομηχανοποίησης. Κοινωνικές ανησυχίες οδήγησαν στην ανάπτυξη αντιρρυπαντικών τεχνολογιών που είναι σήμερα σε θέση να μειώσουν δραστικά τις αντίστοιχες εκπομπές συμβατικών ρύπων SO_2, CO, NO_x και ιπτάμενης τέφρας. Με βάση αυτές τις τεχνολογικές εξελίξεις ο άνθρακας διαδραμάτισε πρωτεύοντα ρόλο στο ενεργειακό μίγμα σε όλη την ιστορική περίοδο μετά το Β' παγκόσμιο πόλεμο έως σήμερα (Σχήμα Π-1).

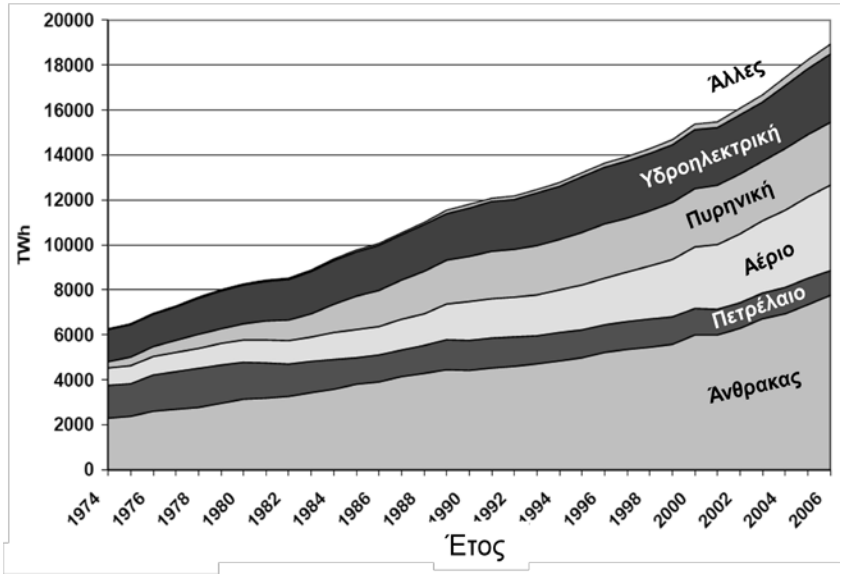

Σχήμα Π-1 : Εξέλιξη από το 1971 έως το 2006 της παγκόσμιας παραγωγής ηλεκτρικής ενέργειας (TWh) και των αντίστοιχων ενεργειακών πηγών

Στο τέλος του 20ου αιώνα, η σημασία ενός άλλου παγκόσμιου περιβαλλοντικού ζητήματος –η υπερθέρμανση του πλανήτη- γίνεται όλο και πιο κατανοητή. Με βάση πρόσφατες έρευνες, η τέταρτη έκθεση αξιολόγησης της Διακυβερνητικής Διάσκεψης για την Κλιματική Αλλαγή (IPCC), που δημοσιεύθηκε το 2007 περιγράφει τη φυσική επιστημονική βάση των παρατηρούμενων κλιματικών αλλαγών και τις συσχετίζει με τις

ανθρωπογενείς εκπομπές αερίων σε αυξημένο βαθμό σε σύγκριση με την αντίστοιχη προηγούμενη έκθεση. Τα αέρια αυτά χαρακτηρίζονται ως Αέρια του Θερμοκηπίου (Green House Gases, GHG), και τα πιο σημαντικά από αυτά, που προέρχονται από ανθρώπινες δραστηριότητες είναι το διοξείδιο του άνθρακα, CO_2, το μεθάνιο, CH_4 και υποξείδιο του αζώτου N_2O. Με την υπογραφή του Πρωτοκόλλου του Κιότο το 1997, τέθηκε ο στόχος μείωσης των εκπομπών Αερίων του Θερμοκηπίου κατά 5% έως το 2012 σε σχέση με τα επίπεδα του 1990. Μέσω του μηχανισμού του πρωτοκόλλου του Κιότο δημιουργείται επίσης μια νέα χρηματιστηριακή αγορά για την εμπορία δικαιωμάτων εκπομπών ρύπων (Emissions Trading Scheme). Σύμφωνα με στατιστικά δεδομένα της ΕΕ, ο βιομηχανικός τομέας με τις μεγαλύτερες εκπομπές αερίων του θερμοκηπίου είναι ο τομέας της παραγωγής ενέργειας. Συγκεκριμένα, περίπου το 30% της συνολικής παραγωγής αερίων του θερμοκηπίου προέρχεται από εργοστάσια παραγωγής ενέργειας.
Οι ανθρακικοί σταθμοί παραγωγής ενέργειας, λόγω της μεγάλης εγκατεστημένης ισχύος τους, έχουν τη μεγαλύτερη συμβολή στις εκπομπές αερίων του θερμοκηπίου σε σχέση με τις υπόλοιπες τεχνολογίες θερμοηλεκτρικών σταθμών. Έτσι, η μείωση των εκπομπών CO_2 σε ήδη υπάρχοντες και νέους ανθρακικούς σταθμούς αποτελεί μία από τις κορυφαίες προτεραιότητες για την επίτευξη των στόχων του Κιότο. Σε μακροπρόθεσμο ορίζοντα ωστόσο, και μετά τη λήξη του Πρωτοκόλλου του Κιότο το 2012, θα πρέπει να τεθούν στόχοι δραστικής μείωσης των εκπομπών Αερίων του Θερμοκηπίου, έτσι ώστε να ανασταλούν οι πιθανές αρνητικές επιπτώσεις από την κλιματική αλλαγή. Σύμφωνα με τη Διακυβερνητική Διάσκεψη για την Κλιματική Αλλαγή, για να είναι δυνατό κάτι τέτοιο, θα πρέπει η συγκέντρωση CO_2 στα ανώτερα στρώματα της ατμόσφαιρας να επιστρέψει στο επίπεδο των 450ppm που αντιστοιχεί στο επίπεδο συγκεντρώσεων του 1990. Ο Διεθνής Οργανισμός Ενέργειας (International Energy Agency, IEA) έχει εκπονήσει εκτεταμένη μελέτη σχετικά με τη δυνατότητα επίτευξης του συγκεκριμένου στόχου λαμβάνοντας υπόψη μία σειρά από σενάρια. Στη μελέτη αυτή η συμβολή των χωρών-μελών του ΟΟΣΑ στην αποφυγή της κλιματικής αλλαγής διαφοροποιείται από τη συμβολή των χωρών μη μελών, κυρίως της Κίνας, της Ινδίας, της Ρωσίας και των αραβικών χωρών, λόγω των διαφορετικών ρόλων και ευθυνών που έχουν αυτές στη δημιουργία του προβλήματος.
Στα πλαίσια της μελέτης Το Σενάριο αναφοράς (Business as Usual, BaU) αναλύεται αρχικά, σύμφωνα με το οποίο οι παγκόσμιες εκπομπές αερίων του θερμοκηπίου συνεχίζουν να αυξάνονται με σχεδόν σταθερό ρυθμό από τα επίπεδα των 27 Gt CO_{2eq} το έτος 2008 στους 40 Gt CO_{2eq} το 2030. Το «σενάριο σταθεροποίησης 450ppm» προβλέπει την μεγιστοποίηση των παγκόσμιων εκπομπών αερίων του θερμοκηπίου κατά την περίοδο γύρω στο 2020 και στη συνέχεια τη μείωση αυτών κατά περισσότερο από ένα τρίτο μέχρι το 2030, έτσι ώστε να επιτευχθεί ο τελικός στόχος των 26 Gt CO_{2eq} (Σχήμα Π-2). Για να επιτευχθεί αυτό είναι αναγκαία μια ριζική αναδιάρθρωση του σημερινού παγκόσμιου συστήματος παραγωγής ηλεκτρικής ενέργειας. Οι δεδομένοι στόχοι μείωσης των εκπομπών αναμένεται να επιτευχθούν σύμφωνα με τη μελέτη μέσω των ακόλουθων τριών βασικών αξόνων:

- Βελτίωση της ενεργειακής απόδοσης στα στάδια της παραγωγής ηλεκτρικής ενέργειας και της κατανάλωσης
- Αύξηση των Ανανεώσιμων Πηγών Ενέργειας (ΑΠΕ) και των βιοκαυσίμων
- Ανάπτυξη και εφαρμογή τεχνολογιών δέσμευσης και αποθήκευσης άνθρακα (CCS) στις νέες γενιές ανθρακικών σταθμών

Για την τελική επίτευξη του στόχου απαιτείται η αύξηση του μέρους των Ανανεώσιμων Πηγών Ενέργειας στο ενεργειακό μίγμα κατά 22 ποσοστιαίες μονάδες, από το 18% στο 40%, και η μείωση του μέρους των ανθρακικών σταθμών κατά 20 ποσοστιαίες μονάδες, από το 41% στο 21% (Σχήμα Π-3).

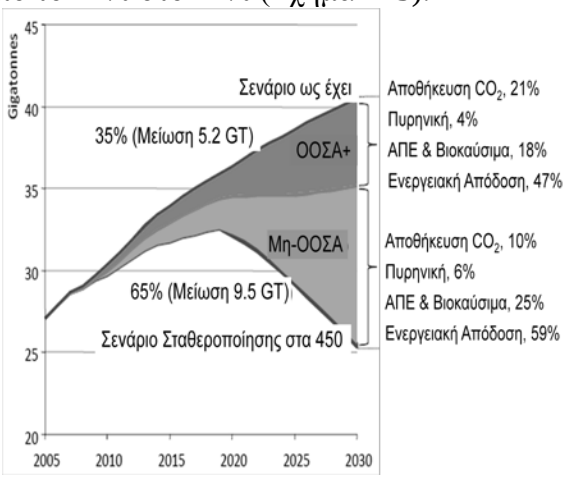

Σχήμα Π-2 : Μείωση εκπομπών CO_2 από τον ενεργειακό τομέα σύμφωνα με το σενάριο σταθεροποίησης 450ppm

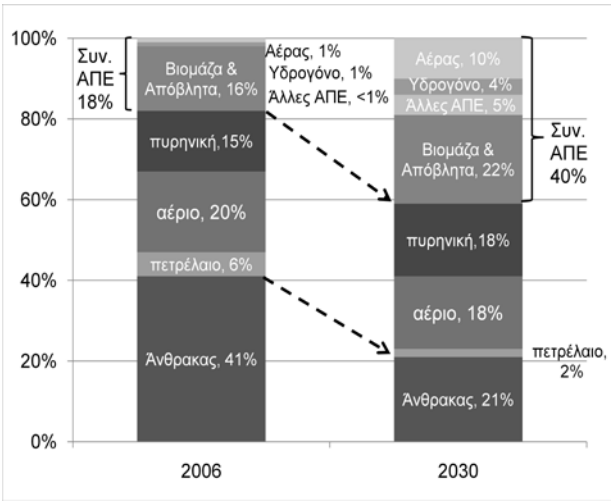

Σχήμα Π-3 : Κατανομή της παραγωγής ηλεκτρικής ενέργειας σύμφωνα με το σενάριο σταθεροποίησης 450ppm

Από την προηγούμενη ανάλυση γίνεται σαφής ο ρόλος των σταθμών παραγωγής ενέργειας με βάση τον άνθρακα στην επίτευξη των στόχων μείωσης των αερίων του θερμοκηπίου. Μια εικόνα της μέσης ηλικίας και του μεγέθους των ανθρακικών σταθμών παγκόσμια δίνεται στο παρακάτω σχήμα (Σχήμα Π-4).

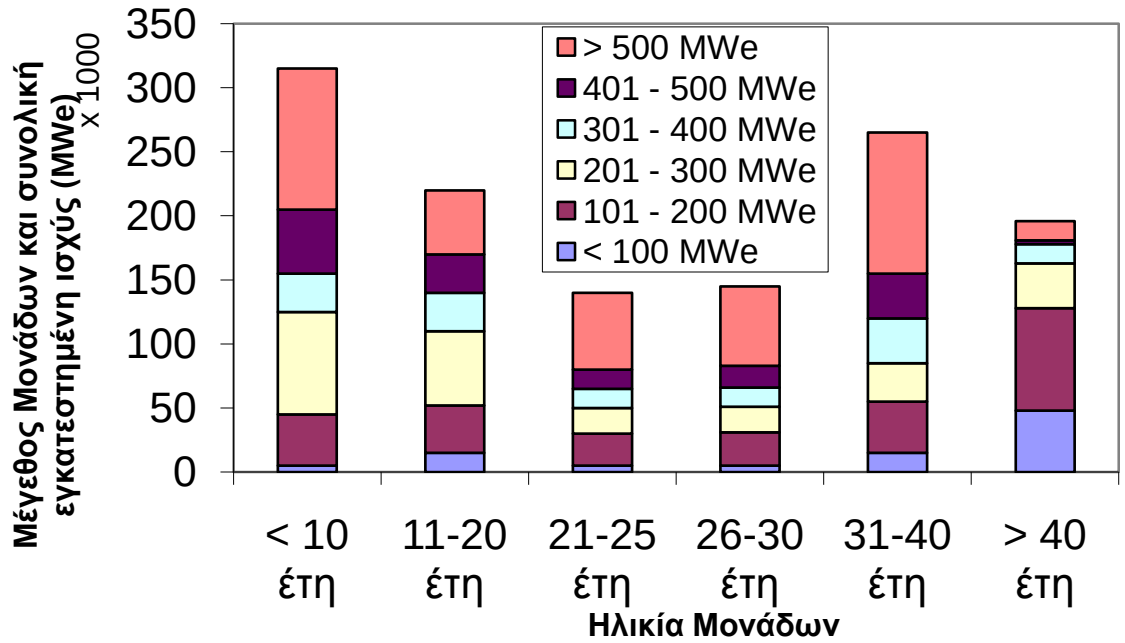

Σχήμα Π-4 :Ηλικία και εγκατεστημένη ισχύς ανθρακικών μονάδων παγκόσμια

Από τα στοιχεία που παρουσιάζονται προκύπτουν τα ακόλουθα σημαντικά συμπεράσματα :

- Περισσότερο από το μισό του συνόλου των ανθρακικών σταθμών σε παγκόσμιο επίπεδο έχει ηλικία πάνω από 25 έτη και εγκατεστημένη ισχύ μικρότερη από 300 MW_e.
- Περισσότεροι από το 80% των σταθμών που λειτουργούν έχουν υποκρίσιμα χαρακτηριστικά ατμού.
- Ο μέσος όρος του βαθμού απόδοσης των υπαρχόντων ανθρακικών σταθμών είναι 28.4%, ενώ οι βαθμοί απόδοσης που αντιστοιχούν στις βέλτιστες διαθέσιμες τεχνικές των αντίστοιχων εργοστασίων σήμερα είναι άνω του 43% για λιγνιτικές μονάδες και άνω του 48% για λιθανθρακικές μονάδες.

Η σημασία της βελτίωσης του βαθμού απόδοσης των υφιστάμενων μονάδων, προκειμένου να επιτευχθούν οι στόχοι μείωσης του CO_2, καθίσταται επομένως εμφανής.

Η πλειονότητα των υφιστάμενων μονάδων μπορεί να χωριστεί σε δύο κύριες ομάδες. Η πρώτη περιλαμβάνει πολύ παλιές μονάδες που έχουν ηλικία άνω των 30 ετών και χαμηλούς βαθμούς απόδοσης. Για αυτή την κατηγορία, όπου εκτεταμένες μετασκευές με σκοπό την αύξηση του βαθμού απόδοσης δεν είναι οικονομικά συμφέρουσες λόγω του μικρού υπολειπόμενου χρόνου λειτουργίας, υπάρχουν δύο επιλογές:
α) Διακοπή ή μόνιμη παύση λειτουργίας πολλών παλαιών και συνήθως μικρών μονάδων και αντικατάσταση της χαμένης εγκατεστημένης ισχύος, εάν είναι απαραίτητο, από σύγχρονη μονάδα με τη βέλτιστη σημερινή τεχνολογία
β) αλλαγή του σημερινού μείγματος καυσίμου και μερική υποκατάσταση μέχρι το τελικό κλείσιμο της εγκατάστασης του άνθρακα από «καύσιμα μηδενικής ή χαμηλής περιεκτικότητας σε άνθρακα», όπως η βιομάζα, και τα ανακτηθέντα καύσιμα από απορρίμματα με υψηλό βιογενές μέρος.
Η βιομάζα αποτελεί ανανεώσιμο καύσιμο με μηδενικές εκπομπές αερίων του θερμοκηπίου και γι' αυτό το λόγο η χρήση της προωθείται από την Ευρωπαϊκή νομοθεσία. Προϋπόθεση για την εφαρμογή πρακτικών υποκατάστασης του άνθρακα, είναι η δυνατότητα τεχνικής υλοποίησης της μικτής καύσης χωρίς εκτεταμένες μετασκευές στους εν λόγω λέβητες.
Η δεύτερη ομάδα περιλαμβάνει μονάδες με εναπομένουσα διάρκεια ζωής άνω των 10-15 ετών, οι οποίες έχουν χαμηλές παραμέτρους ατμού και χαμηλούς βαθμούς απόδοσης. Για την κατηγορία αυτή, η βελτίωση του βαθμού απόδοσης της εγκατάστασης και η αύξηση της συμμετοχής των ανανεώσιμων πηγών ενέργειας στο τρέχον μίγμα καυσίμου είναι η μόνη ρεαλιστική προοπτική, αν υιοθετηθούν δεσμευτικοί στόχοι για δραστική μείωση των εκπομπών αερίων του θερμοκηπίου για την περίοδο μετά τη λήξη του πρωτοκόλλου του Κιότο.
Στην παρούσα διατριβή εξετάζονται δύο διαφορετικές πρακτικές υποκατάστασης άνθρακα, οι οποίες μπορούν να βοηθήσουν στην επίτευξη των μελλοντικών στόχων μείωσης των αερίων του θερμοκηπίου και στις δύο ομάδες εργοστασίων, τόσο των παλαιότερων όσο και των νεότερων εγκαταστάσεων. Η πρώτη πρακτική επικεντρώνεται στην υποκατάσταση του άνθρακα από καύσιμα που ανακτώνται από απορρίμματα με σημαντικό βιογενές περιεχόμενο, ενώ η δεύτερη αφορά τους λιγνιτικούς σταθμούς και επικεντρώνεται στην ενοποίηση της διεργασίας προξήρανσης λιγνίτη στους υπάρχοντες

λιγνιτικούς σταθμούς και την αντικατάσταση του φυσικού λιγνίτη από ξηρό λιγνίτη προκειμένου να αυξηθεί ο βαθμός απόδοσης των μονάδων. Προκειμένου να αποσαφηνιστούν τεχνικοί όροι που χρησιμοποιούνται συχνά στην παρούσα εργασία, δίνονται παρακάτω απαραίτητοι ορισμοί.

- «Υποκατάσταση Άνθρακα» ορίζεται ως η αντικατάσταση ενός συγκεκριμένου μέρους της εισερχόμενης ποσότητας άνθρακα σε ένα σταθμό από άλλο καύσιμο, με ταυτόχρονη διατήρηση σταθερής εισερχόμενης θερμικής ισχύος.
- «Συνδυασμένη καύση ή ταυτόχρονη καύση» είναι η ταυτόχρονη καύση δύο ή περισσότερων σε καύσιμων στον ίδιο λέβητα.
- «Κύριο» καύσιμο ή καύσιμο «αναφοράς» ή «βασικό» καύσιμο είναι το καύσιμο με την υψηλότερη παροχή μάζας που χρησιμοποιείται συνήθως σε ένα σταθμό. Στην περίπτωση των θερμικών σταθμών που εξετάζονται στην παρούσα εργασία, το κύριο καύσιμο είναι λιγνίτης.
- «Εναλλακτικά καύσιμα» είναι ένας ευρύς χαρακτηρισμός που περιλαμβάνει κάθε τύπο στερεού καυσίμου που δεν είναι ορυκτό. Βιογενή καύσιμε ή καύσιμα που ανακτώνται από απορρίμματα εμπίπτουν ως εκ τούτου στον ορισμό. Η παρούσα διερεύνηση εστιάζει σε μια συγκεκριμένη ομάδα των εναλλακτικών καυσίμων, τα στερεά ανακτηθέντα καύσιμα (Solid Recovered Fuels, SRF).
- Στερεά καύσιμα με υψηλότερη θερμογόνο ικανότητα από το κύριο καύσιμο, τα οποία καίγονται μαζί με το κύριο καύσιμο προκειμένου να αυξηθεί η θερμοκρασία του θαλάμου καύσης και να υποστηριχθεί η σταθερότητα της φλόγας, χαρακτηρίζονται ως «υποστηρικτικά καύσιμα». Υποστηρικτικά καύσιμα χρησιμοποιούνται συνήθως σε λιγνιτικά εργοστάσια παραγωγής όταν ο εξορυσσόμενος λιγνίτης έχει πολύ χαμηλή θερμογόνο ικανότητα και υψηλή περιεκτικότητα σε τέφρα και υγρασία. Ο ξηρός λιγνίτης θεωρείται υποστηρικτικό καύσιμο.

Η πιθανή συμβολή μικτής καύσης SRF σε υπάρχοντες σταθμούς ηλεκτροπαραγωγής με καύση άνθρακα, στο θέμα διαχείρισης αποβλήτων αποτελεί ένα πρόσθετο επιχείρημα υπέρ αυτής της πρακτικής. Η ευρωπαϊκή κοινοτική στρατηγική για τη διαχείριση των αποβλήτων, COM (96) / 399, θέτει την ανάκτηση υλικών και την ανάκτηση ενέργειας από τα απόβλητα ως τη δεύτερη πιο αποδοτική περιβαλλοντικά λύση μετά την πρόληψη παραγωγής αποβλήτων. Υπάρχουν δύο διαφορετικές επιλογές τεχνολογιών, οι οποίες δεν θα πρέπει να θεωρούνται ανταγωνιστικές μεταξύ τους. Τόσο η αποτέφρωση σύμμεικτων αποβλήτων σε αντίστοιχες μονάδες (incineration) όσο και η μηχανική και βιολογική επεξεργασία αποβλήτων (Mechanical Biological Treatment, MBT), αποτελούν τεχνολογικές λύσεις συμπληρωματικές και απαραίτητες για μία πρακτική διαχείρισης αποβλήτων μελλοντικά πιο βιώσιμη.
Η ανάγκη για εναλλακτικές επιλογές επεξεργασίας των αποβλήτων έχει γίνει σημαντικό θέμα σε ορισμένες χώρες της Κεντρικής Ευρώπης όπως η Γερμανία, όπου η απαγόρευση της υγειονομικής ταφής των στερεών αστικών αποβλήτων τον Ιούνιο του 2005 οδήγησε σε δραματική αύξηση παραγωγής ανακτηθέντων καυσίμων και στη συνέχεια σε έλλειψη αντίστοιχου δυναμικού για ενεργειακή αξιοποίησή τους. Αυτές οι εγκαταστάσεις μπορεί να είναι α) εγκαταστάσεις αποκλειστικής καύσης - αποτέφρωσης ανακτηθέντων καυσίμων, β) ανθρακικοί σταθμοί και εργοστάσια παραγωγής τσιμέντου για μικτή καύση

- συναποτέφρωση ανακτηθέντων καυσίμων μαζί με τον άνθρακα μέχρι συγκεκριμένο ποσοστό υποκατάστασης.

Πέραν της μείωσης εκπομπών CO_2 ένα από τα ουσιαστικά κίνητρα για τη διερεύνηση της τεχνολογίας προξήρανσης λιγνίτη, είναι και η χρησιμοποίηση του ξηρού λιγνίτη ως καύσιμο υποστήριξης στους λιγνιτικούς σταθμούς. Η Ελλάδα είναι δεύτερη χώρα σε παραγωγή λιγνίτη στην ΕΕ των 27 και άνω του 50% της ελληνικής ηλεκτροπαραγωγής βασίζεται σε λιγνιτικούς σταθμούς. Η εξασφάλιση διαθεσιμότητας και ποιότητας λιγνίτη είναι, επομένως, ζήτημα πρωταρχικής σημασίας. Η χαμηλή θερμογόνος ικανότητα του ελληνικού λιγνίτη και η υψηλή διακύμανση αυτής σε κάποια ορυχεία σε συγκεκριμένες περιόδους επιβάλλουν πρόσθετους περιορισμούς στη λειτουργία των σταθμών. Η αξιοποίηση λιγνίτη εξαιρετικά χαμηλής ποιότητας μπορεί να οδηγήσει σε προβλήματα σταθερότητας της καύσης, στη μείωση της ατμοπαραγωγής και της παραγόμενης ηλεκτρικής ισχύος κάτω από τα φυσιολογικά επίπεδα ακόμη και σε «σβήσιμο φλόγας» και στη διακοπή της λειτουργίας του λέβητα.

Προκειμένου να αντιμετωπιστεί το πρόβλημα της διακύμανσης ποιότητας του λιγνίτη, λαμβάνονται δύο μέτρα: α) ομογενοποίηση των καυσίμων και β) η υποστήριξη της καύσης με ειδικά υποστηρικτικά καύσιμα. Ταυτόχρονη καύση άνθρακα με άλλα είδη όπως τον λιθάνθρακα ή τον ξυλίτη ως υποστηρικτικά καύσιμα σε συνδυασμό με το λιγνίτη αναφοράς μπορεί να ενέχει σοβαρούς κινδύνους για τη λειτουργία του λέβητα λόγω των διαφορετικών συστάσεων των καυσίμων, παρόλο που θεωρείται ως ευνοϊκή λύση από οικονομική άποψη. Η πλέον κατάλληλη λύση από τεχνική άποψη είναι η υποστήριξη με ξηρό λιγνίτη ίδιας ποιότητας με αυτή του φυσικού.

Το βασικό αντικείμενο της εργασίας στο πλαίσιο της παρούσας διατριβής είναι η αξιολόγηση και σύγκριση των δύο προτεινόμενων πρακτικών υποκατάστασης άνθρακα με βάση μία σειρά από κριτήρια. Η μείωση των εκπομπών CO_2, στους υπάρχουσες ανθρακικούς σταθμούς είναι ο κύριος στόχος των πρακτικών υποκατάστασης. Η συνολική αξιολόγηση των υπό εξέταση πρακτικών υποκατάστασης γίνεται με βάση περιβαλλοντικές, τεχνικές και οικονομικές παραμέτρους. Πειράματα, αριθμητικές προσομοιώσεις και θερμοδυναμικοί υπολογισμοί χρησιμοποιούνται ως μεθοδολογικά εργαλεία για την αξιολόγηση.

Στα πλαίσια της παρούσας εργασίας παρουσιάζονται και αξιολογούνται τα αποτελέσματα από δύο επιδεικτικές δράσεις που πραγματοποιήθηκαν σε βιομηχανικής κλίμακας λέβητες για την επίδειξη των πρακτικών υποκατάστασης λιγνίτη από εναλλακτικά και υποστηρικτικά καύσιμα. Η επιδεικτική δράση της μικτής καύσης SRF με λιγνίτη πραγματοποιείται σε γερμανικό λιγνιτικό σταθμό ισχύος 600 MW_e, ενώ δοκιμές μικτής καύσης ξηρού λιγνίτη πραγματοποιούνται σε ελληνική λιγνιτική μονάδα εγκατεστημένης ισχύος 75 MW_{th}. Πέραν των πειραματικών μετρήσεων, παρουσιάζονται και αναλύονται τα αποτελέσματα αριθμητικών προσομοιώσεων των βιομηχανικών λεβήτων, που πραγματοποιήθηκαν με χρήση της μεθόδου της Υπολογιστικής Ρευστομηχανικής (Computational Fluid Dynamics, CFD). Οι προσομοιώσεις των λεβήτων αφορούν σε τρόπους λειτουργίας που δεν μπορούν να δοκιμαστούν σε πραγματικές συνθήκες. Αυτοί σχετίζονται με την εισαγωγή των καυσίμων υποκατάστασης από διαφορετικά σημεία ή με την περαιτέρω αύξηση του ποσοστού υποκατάστασης. Προκειμένου να αξιολογηθεί η δυνατότητα εφαρμογής της τεχνολογίας προξήρανσης του λιγνίτη σε ελληνικούς λιγνιτικούς σταθμούς, πραγματοποιούνται υπολογισμοί των αντίστοιχων θερμοδυναμικών κύκλων. Συμπληρωματικά με τη

διερεύνηση στις εγκαταστάσεις βιομηχανικής κλίμακας έχουν πραγματοποιηθεί βοηθητικές διερευνήσεις σε εγκαταστάσεις μικρής κλίμακας.

Στην περίπτωση της μικτής καύσης λιγνίτη και στερεού ανακτηθέντος καυσίμου (SRF), διερεύνηση που διεξάγεται στη μικρή κλίμακα, αυτή εστιάζεται στην ανάπτυξη ενός νέου μοντέλου καύσης για σωματίδια SRF και την επιβεβαίωσή του με διαθέσιμα δεδομένα από πειραματική εγκατάσταση καύσης. Κατά την αξιολόγηση της προ-ξήρανσης η διερεύνηση που διεξάγεται στη μικρή κλίμακα, περιλαμβάνει δοκιμές ξήρανσης ελληνικού ξηρού λιγνίτη σε εργαστηριακής κλίμακας ξηραντήρα ρευστοποιημένης κλίνης και δοκιμές καύσης προξηραμένου ελληνικού λιγνίτη σε πειραματική εγκατάσταση καύσης θερμικής ισχύος 1 MW_{th}.

Στη συνέχεια παρουσιάζονται οι περιβαλλοντικές, τεχνολογικές και οικονομικές παράμετροι που χρησιμοποιούνται για την αξιολόγηση των τεχνολογιών.

Σχετικά με τους περιβαλλοντικούς δείκτες απόδοσης, οι εκπομπές CO_2 και η προβλεπόμενη μείωση τους σε κάθε ένα από τα δύο προτεινόμενα σενάρια υποκατάστασης είναι η κύρια παράμετρος που εξετάζεται μαζί με τις συμβατικές εκπομπές καυσαερίων SO_2, NO_x, CO και ιπτάμενης τέφρας. Επιπλέον για την περίπτωση μικτής καύσης λιγνίτη και SRF, αξιολογείται η περιβαλλοντική επίδοση σε σχέση με τις εκπομπές από μη συμβατικούς ρύπους, που επιβάλλεται να μετρούνται σε περίπτωση αποτέφρωσης ή συναποτέφρωσης σύμφωνα με την αντίστοιχη ευρωπαϊκή οδηγία (Πίνακας Π-1). Η αξιολόγηση με βάση τα τεχνολογικά κριτήρια περιλαμβάνει μία σειρά από παραμέτρους που σχετίζονται με την καύση και τη λειτουργία του λέβητα (Πίνακας Π-2). Η αξιολόγηση με βάση τα οικονομικά κριτήρια, περιλαμβάνει τον υπολογισμό του κόστους αποφυγής εκπομπών CO_2 για τις δύο τεχνολογίες και την αξιολογήση αντίστοιχων επενδυτικών σχεδίων για τις προτεινόμενες πρακτικές υποκατάστασης άνθρακα (Πίνακας Π-3). Σε συγκεκριμένες περιπτώσεις η επίδραση της μικτής καύσης έχει εξεταστεί για ένα από τα δύο σενάρια υποκατάστασης, δεδομένου ότι η συγκεκριμένη παράμετρος δεν έχει αξιολογηθεί ή δεν αναμένεται να μεταβάλλεται στην περίπτωση της υποκατάστασης. Στους παρακάτω πίνακες παρουσιάζονται οι μέθοδοι αξιολόγησης των εκάστοτε παραμέτρων.

Πίνακας Π-1 : Μέθοδοι αξιολόγησης των περιβαλλοντικών παραμέτρων

-		Προτεινόμενα σχέδια για υποκατάσταση λιγνίτη	
		Υποκατάσταση από SRF	Προξήρανση λιγνίτη και υποκατάσταση από ξηρό λιγνίτη (ξ.λ.)
Περιβαλλοντικές παράμετροι	Εκπομπές CO_2	Ισολογισμός μάζας από πειραματικά δεδομένα	Θερμοδυναμικοί υπολογισμοί κύκλου ατμού, ισολογισμός μάζας βάσει δεδομένων σχεδιασμού
	Εκπομπές συμβατικών αέριων ρύπων (NO_x, SO_2, CO)	Μετρήσεις	- Μετρήσεις - Υπολογιστικές προσομοιώσεις (CFD) (Προσομοιώσεις εκπομπών NO_x)
	Βαρέα Μέταλλα στα απαέρια	Μετρήσεις	μ.σ.
	HCl	Μετρήσεις	μ.σ.
	Διοξίνες – Φουράνια	- Μετρήσεις - Υπολογιστικές προσομοιώσεις (CFD) (πρόβλεψη πιθανών σχηματισμών διοξινών μέσω υπολογισμών χρόνου παραμονής σωματιδίων)	μ.σ.
	Ποιότητα τέφρας: Βαρέα Μέταλλα στην τέφρα	Μετρήσεις	μ.σ.

μ.σ. («μη συσχέτιση») επειδή η εφαρμογή της μικτής καύσης εκτιμάται ότι δεν έχει επίπτωση στη συγκεκριμένη παράμετρο, η συγκεκριμένη διερεύνηση δεν πραγματοποιείται καθώς δεν υπάρχει αντίστοιχη συσχέτιση

δ.δ. («δεν διερευνήθηκε»)Η επίδραση της μικτής καύσης στη συγκεκριμένη παράμετρο δεν διερευνήθηκε

Πίνακας Π-2 : Μέθοδοι αξιολόγησης των τεχνολογικών παραμέτρων

		Προτεινόμενα σχέδια για υποκατάσταση λιγνίτη	
		Υποκατάσταση από SRF	Προξήρανση λιγνίτη και υποκατάσταση από ξηρό λιγνίτη (ξ.λ.)
Τεχνολογικές - λειτουργικές παράμετροι	Παράμετροι λειτουργίας (Ατμοπαραγωγή, P_e)	Μετρήσεις	Μετρήσεις
	Συνολικός ενεργειακός ισολογισμός στο λέβητα	Μετρήσεις	- Μετρήσεις - Υπολογισμοί θερμικού κύκλου
	Θερμορροή στον ατμοποιητή	Υπολογιστικές προσομοιώσεις (CFD)	Υπολογιστικές προσομοιώσεις (CFD)
	Συνθήκες καύσης στην έξοδο της εστίας (θερμοκρασία, O_2)	- Μετρήσεις -Υπολογιστικές προσομοιώσεις (CFD)	- Μετρήσεις (θερμοκρασία) - Υπολογιστικές προσομοιώσεις (CFD)
	Συνθήκες καύσης στην εστία (θερμοκρασία, O_2)	Υπολογιστικές προσομοιώσεις (CFD)	Υπολογιστικές προσομοιώσεις (CFD)
	Άκαυστα	Υπολογιστικές προσομοιώσεις (CFD)	- Μετρήσεις - Υπολογιστικές προσομοιώσεις (CFD)
	Βαθμός απόδοσης λέβητα (η_{boiler}) και βαθμός απόδοσης θερμοηλεκτρικού σταθμού (η_{PP})	δ.δ.	Υπολογισμοί θερμοδυναμικού κύκλου
	Πιθανά προβλήματα λειτουργίας λόγω διάβρωσης χλωρίου	Μετρήσεις	μ.σ.
	Πιθανά προβλήματα λειτουργίας λόγω επικαθίσεων	μ.σ.	Μετρήσεις σε εγκατάσταση μικρής κλίμακας

Πίνακας Π-3 : Μέθοδοι αξιολόγησης των οικονομικών παραμέτρων

		Προτεινόμενα σχέδια για υποκατάσταση λιγνίτη	
		Ταυτόχρονη καύση SRF	Προξήρανση λιγνίτη και μικτή καύση
Οικονομικές παράμετροι	Αναμενόμενα κόστη επένδυσης και λειτουργίας	Υπολογισμοί	Υπολογισμοί
	Κόστη αποφυγής CO_2	“	“
	Οικονομικότητα της επένδυσης	“	“

Κεφάλαιο 2: Χαρακτηρισμός καυσίμων - Εναλλακτικά και υποστηρικτικά καύσιμα ως καύσιμα υποκατάστασης λιγνίτη

Στερεά ανακτηθέντα καύσιμα

Τα ανακτηθέντα από απόβλητα καύσιμα παράγονται από διάφορα κλάσματα και είδη αποβλήτων μετά από ειδικά βήματα μηχανικής ή μηχανικής και βιολογικής επεξεργασίας. Χρησιμοποιούνται ως καύσιμα υποκατάστασης λιθάνθρακα ή λιγνίτη, στον ανθρακικό βιομηχανικό τομέα, στον οποίο συμπεριλαμβάνονται οι κλίβανοι της τσιμεντοβιομηχανίας και οι ανθρακικοί θερμοηλεκτρικοί σταθμοί. Η ανάγκη για την τυποποίηση των καυσίμων που ανακτώνται από απόβλητα έχει γίνει εμφανής τα τελευταία χρόνια λόγω της ραγδαίας ανάπτυξης της αγοράς των ανακτηθέντων καυσίμων και της αύξησης της παραγωγής αυτών. Η Ευρωπαϊκή Επιτροπή, προκειμένου να συμβάλει στην περαιτέρω ανάπτυξη της αγοράς και της διασφάλισης της ποιότητας των ανακτηθέντων καυσίμων, και την αποφυγή οποιαδήποτε κακή διαχείρισης των αποβλήτων έχει ξεκινήσει τη διαδικασία για την τυποποίηση των καυσίμων που ανακτώνται από απόβλητα. Δύο Τεχνικές Επιτροπές έχουν συσταθεί για να βοηθήσουν αυτή τη διαδικασία τυποποίησης:

- Η Τεχνική Επιτροπή CEN (TC) 335, η οποία καλύπτει όλα τα καύσιμα που προέρχονται αμιγώς από "βιομάζα", όπως ορίζεται στο πεδίο εφαρμογής της οδηγίας 2000/76/EC για την αποτέφρωση αποβλήτων. Γεωργικά και δασικά κατάλοιπα περιλαμβάνονται στις δραστηριότητες της TC 335.
- Η Τεχνική Επιτροπή CEN (TC) 343, η οποία καλύπτει όλα τα άλλα μη επικίνδυνα καύσιμα που ανακτώνται από στερεά απόβλητα.

Η παρούσα εργασία επικεντρώνεται στο έργο της TC 343 σχετικά με την τυποποίηση των καυσίμων που ανακτώνται από απόβλητα, τα οποία δεν θεωρούνται ως βιομάζα, αλλά μπορεί να έχουν βιογενές περιεχόμενο. Τα αποτελέσματα της επιτροπής περιλαμβάνουν δημοσιευμένες Τεχνικές Προδιαγραφές (TS), ένα είδος προ-προτύπου, και Τεχνικές Εκθέσεις (TR). Σύμφωνα με την Τεχνική Προδιαγραφή TS 15357, ανακτηθέντα στερεά καύσιμα ορίζονται ως «στερεά καύσιμα που παράγονται από κλάσματα μη επικινδύνων αποβλήτων υψηλής θερμογόνου ικανότητας, με στόχο τη μικτή καύση αυτών μαζί με άνθρακα σε υφιστάμενες ανθρακικές μονάδες

ηλεκτροπαραγωγής και λοιπούς βιομηχανικούς κλιβάνους που χρησιμοποιούν άνθρακα». Ως εκ τούτου, ο όρος SRF αναφέρεται σε ένα ευρύ φάσμα υλικών που ανακτώνται από στερεά απόβλητα, και συμπεριλαμβάνει από κλάσματα Αστικών Στερεών Αποβλήτων (ΑΣΑ) υψηλής θερμογόνου ικανότητας έως ξηρή λυματολάσπη και τεμαχισμένα ελαστικά. Σε αντίθεση με άλλους όρους, όπως δευτερογενή καύσιμα ή RDF (Refused Derived Fuels) για το χαρακτηρισμό ενός ανακτηθέντος καυσίμου ως SRF απαιτείται μια ειδική διαδικασία χορήγησης άδειας, που ορίζεται από την επιτροπή προτυποποίησης CEN TC/ 343. Η διαδικασία παρουσιάζεται στο Σχήμα Π-5:

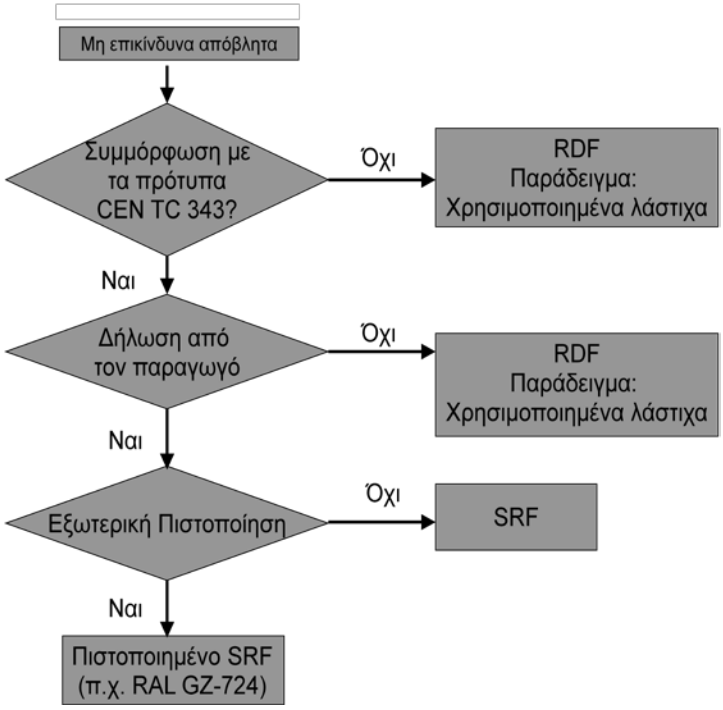

Σχήμα Π-5 : Απαιτούμενη διαδικασία για τον χαρακτηρισμό ενός ανακτηθέντος καυσίμου από απόβλητα ως SRF

Ορισμένες ευρωπαϊκές χώρες έχουν ήδη κάνει ένα βήμα παραπέρα και έχουν αναπτύξει τις δικές τους «ετικέτες ποιότητας» για το SRF, οι οποίες βασίζονται σε ορισμένα συστήματα διασφάλισης ποιότητας. Μια σύγκριση μεταξύ αυτών των συστημάτων μπορεί να βρεθεί στο έγγραφο αναφοράς (BREF) Βέλτιστων Διαθέσιμων Τεχνικών (BAT) για ανακτηθέντα στερεά καύσιμα δημοσιευμένα από την Ευρωπαϊκή Οργάνωση Ανακτηθέντων Καυσίμων (European Recovered Fuel Organisation, www.erfo.info).
Οι εργασίες της επιτροπής CEN/ TC 343 χωρίζονται σε πέντε διαφορετικές ομάδες εργασίας, που καλύπτουν διάφορους τομείς της διαδικασίας τυποποίησης.
WG1: Ορολογία και ποιοτικός έλεγχος
WG2: Ταξινόμηση καυσίμων και προδιαγραφές
WG3: Δειγματοληψία και προσδιορισμός του περιεχομένου βιομάζας του SRF
WG4: Φυσικές, μηχανικές δοκιμές
WG5: Χημικές δοκιμές

Παρακάτω παρουσιάζεται σχηματικό διάγραμμα με τις δραστηριότητες της κάθε ομάδας εργασίας (Σχήμα Π-6):

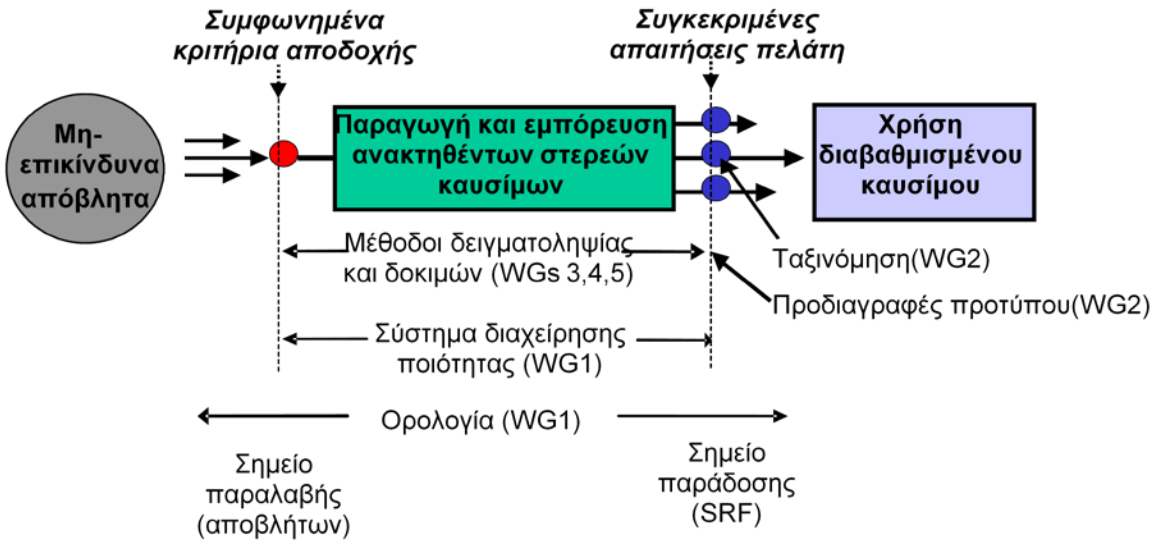

Σχήμα Π-6 : Επισκόπηση των διαδικασιών προτυποποίησης σε CEN/TC343

Ένα ευρύ φάσμα αποβλήτων μπορούν να χρησιμοποιηθούν ως ρεύματα εισόδου για την παραγωγή Ανακτηθέντων Στερεών Καυσίμων (SRF) σύμφωνα με τον Ευρωπαϊκό Κατάλογο Αποβλήτων (2000/532/EC). Οι κύριες κατηγορίες αποβλήτων, οι οποίες χρησιμοποιούνται συνήθως, είναι οι ακόλουθες:

Ομάδα 1: ξύλο, χαρτί, χαρτόνι και κουτιά από χαρτόνι,
Ομάδα 2: κλωστοϋφαντουργία και ίνες,
Ομάδα 3: πλαστικά και ελαστικά,
Ομάδα 4: άλλα υλικά (π.χ. απόβλητα μελανιών, χρησιμοποιημένος ενεργός άνθρακας),
και Ομάδα 5: υψηλά θερμιδικά κλάσματα συλλεγμένων μη επικινδύνων σύμμικτων αποβλήτων

Τα στερεά ανακτηθέντα καύσιμα παράγονται σε ειδικές μονάδες επεξεργασίας αποβλήτων. Η πλειονότητά τους χρησιμοποιεί μικτά Αστικά Στερεά Απόβλητα ως κύριο εισερχόμενο ρεύμα για την παραγωγή SRF. Άλλες κατηγορίες αποβλήτων οι οποίες χρησιμοποιούνται ευρέως είναι ογκώδη απορρίμματα και συγκεκριμένα κλάσματα εμπορικών αποβλήτων, όπως τα υλικά συσκευασίας ή παλιό χαρτί. Η διαδικασία παραγωγής του SRF μπορεί να περιλαμβάνει διάφορα στάδια, μεταξύ των οποίων τα σημαντικότερα είναι:

- Κοσκίνηση
- Τεμαχισμός, μείωση μεγέθους
- Διαχωρισμός σιδηρούχων και μη σιδηρούχων μετάλλων
- Διαχωρισμός με συμβατικές μηχανικές μεθόδους (αεροδιαχωρισμός, φυγοκεντρικός διαχωρισμός, βαλλιστικός διαχωρισμός)

- Διαχωρισμός με καινοτόμες οπτικές μεθόδους, όπως φασματοσκοπία υπερύθρου (Near Infrared, NIR)
- Θερμική ή βιολογική ξήρανση
- Πελλετοποίηση

Η μορφή του παραγόμενου SRF στο τέλος της διαδικασίας μπορεί να διαφέρει ανάλογα με την ανάγκη του αποδέκτη. Ωστόσο, τυπικές μορφές του SRF είναι μπάλες, μικρά τεμαχισμένα φύλλα (fluff) και μικρές πελλέτες. Οι μεγάλες πελλέτες συνήθως δεν χρησιμοποιούνται για SRF, σε αντίθεση με τη βιομάζα, λόγω των διαφορετικών φυσικών ιδιοτήτων του καυσίμου. Επειδή κάθε εγκατάσταση παραγωγής ανακτηθέντων καυσίμων διαφέρει στο σχεδιασμό της διεργασίας, στις συνθήκες λειτουργίας, στην ποιότητα των εισερχόμενων αποβλήτων και στην ποιότητα του παραγόμενου SRF, δεν είναι εύκολη η σαφής κατηγοριοποίηση των εγκαταστάσεων. Από μία γενική κατηγοριοποίηση βάσει των μεθόδων επεξεργασίας, προκύπτουν δύο ομάδες εγκαταστάσεων, οι μονάδες όπου εφαρμόζονται μόνο μηχανικές διεργασίες, και οι μονάδες όπου εφαρμόζονται μηχανικές και βιολογικές διεργασίες.
Μια άλλη παράμετρος κατηγοριοποίησης σχετίζεται με το σχεδιασμό της διαδικασίας διαλογής. Μια διαδικασία διαλογής μπορεί να χαρακτηριστεί ως «θετική» ή «αρνητική». Κατά την εφαρμογή θετικών μεθόδων διαλογής, προτιμάται η υψηλότερη ποιότητα του διαλεγόμενου υλικού από την ποσότητα. Ως παράμετροι ποιότητας μπορούν να χρησιμοποιηθούν η θερμογόνος ικανότητα, η συγκέντρωση σε χλώριο και βαρέα μέταλλα. Στη αρνητική μέθοδο διαλογής, επιτυγχάνεται μεγαλύτερη ροή μάζας στο ρεύμα εξόδου, διότι ξεχωρίζονται μόνο τα άχρηστα υλικά από το ρεύμα εισόδου. Παρόλα αυτά, η ομοιογένεια και η ποιότητα του ρεύματος εξόδου είναι συνήθως χαμηλότερη από αυτή που παράγεται από θετική μέθοδο διαλογής.
Σε μελέτη για τις εφαρμοζόμενες τεχνολογίες παραγωγής ανακτηθέντων καυσίμων στη Γερμανία προτείνεται η κατηγοριοποίηση των διεργασιών παραγωγής ανακτηθέντων καυσίμων σε τέσσερις κύριες ομάδες:
α. Διαχωρισμός υλικού ρεύματος
β. Μηχανική - βιολογική σταθεροποίηση με βιολογική ξήρανση
γ. Μηχανική - φυσική σταθεροποίηση με θερμική ξήρανση
δ. Μηχανική (- βιολογική) προεπεξεργασία πριν από τη θερμική επεξεργασία

Η τυποποίηση των στερεών ανακτηθέντων καυσίμων (SRF) πραγματοποιείται μέσω της κατάταξής τους σε κατηγορίες βάσει τριών παραμέτρων, οι οποίες αντιπροσωπεύονται από αντίστοιχες χαρακτηριστικές ιδιότητες του καυσίμου:

- Οικονομική παράμετρος - Θερμογόνος Ικανότητα (H_u)
- Τεχνολογική παράμετρος - Περιεκτικότητα σε Χλώριο (Cl)
- Περιβαλλοντική παράμετρος - Περιεκτικότητα σε Υδράργυρο (Hg)

Βάσει της στατιστικής κατανομής που εμφανίζει το καύσιμο για κάθε μία από τις ανωτέρω χαρακτηριστικές ιδιότητες, επιλέγεται μία ενδεικτική ποσότητα αντιστοίχως, η οποία θα αποτελέσει κριτήριο κατηγοριοποίησης όπως φαίνεται στον πίνακα Π-4. Τα

αντίστοιχα εύρη τιμών για κάθε ιδιότητα του καυσίμου βάσει των οποίων γίνεται η κατηγοριοποίηση, δίνονται στον Πίνακα 5.

Πίνακας Π-4 : Ιδιότητες καυσίμου που υπολογίζονται για την κατηγοριοποίηση

Ιδιότητα καυσίμου	Σύμβολο	Μονάδες	Στατιστική Κατανομή	Χρησιμοποιούμενη Ποσότητα	Δείκτης
Θερμογόνος ικανότητα (H_u)	Hu	MJ/kg ar *	κανονική	αριθμητικός μέσος	Οικονομικός
Χλώριο	Cl	w.t. % d **	λαμβάνεται ως κανονική	αριθμητικός μέσος	Τεχνολογικός
Υδράργυρος	Hg	mg/MJ ar *	δεξιά μετατοπισμένη	διάμεση τιμή, 80th percentile	Περιβαλλοντικός
* ar : as received (ως έχει) ** d: dry basis (επί ξηρού)					

Πίνακας Π-5 : Εύρη τιμών για κάθε προτεινόμενη τάξη των παραμέτρων κατηγοριοποίησης που λαμβάνονται υπόψη

Χαρακτηριστικό κατηγοριοποίησης	Στατιστική ποσότητα-κριτήριο	Μονάδες	Κατηγορίες (classes)				
			1	2	3	4	5
Θερμογόνος Ικανότητα (H_u)	Αριθμητικός μέσος	MJ/kg (ar)	≥ 25	≥ 20	≥ 15	≥ 10	≥ 3
Περιεκτικότητα σε χλώριο (Cl)	Αριθμητικός μέσος	% (d)	≥ 0,2	≥ 0,6	≥ 1,0	≥ 1,5	≥ 3
Συγκέντρωση σε υδράργυρο (Hg)	Διάμεση τιμή	mg/MJ (ar)	≤ 0,02	≤ 0,03	≤ 0,08	≤ 0,15	≤ 0,50
	80th percentile	mg/MJ (ar)	≤ 0,04	≤ 0,06	≤ 0,16	≤ 0,30	≤ 1,00

Το βιογενές κλάσμα είναι μια από τις σημαντικές παραμέτρους στο χαρακτηρισμό του SRF, δεδομένου ότι αντιστοιχεί στις δυνατότητες μείωσης εκπομπών CO_2 σε περίπτωση αντικατάστασης του λιθάνθρακα ή λιγνίτη από το SRF. Οι πειραματικές μέθοδοι για τον προσδιορισμό του βιογενούς κλάσματος του SRF είναι ακόμη στη διαδικασία της επικύρωσης, και εξακολουθούν να θεωρούνται ως προσχέδια ευρωπαϊκών προτύπων (preEN). Στο σχήμα Π-7 παρουσιάζεται η ειδική εκπομπής CO_2 από διάφορα καύσιμα σε kg CO_2/ GJ_{th}

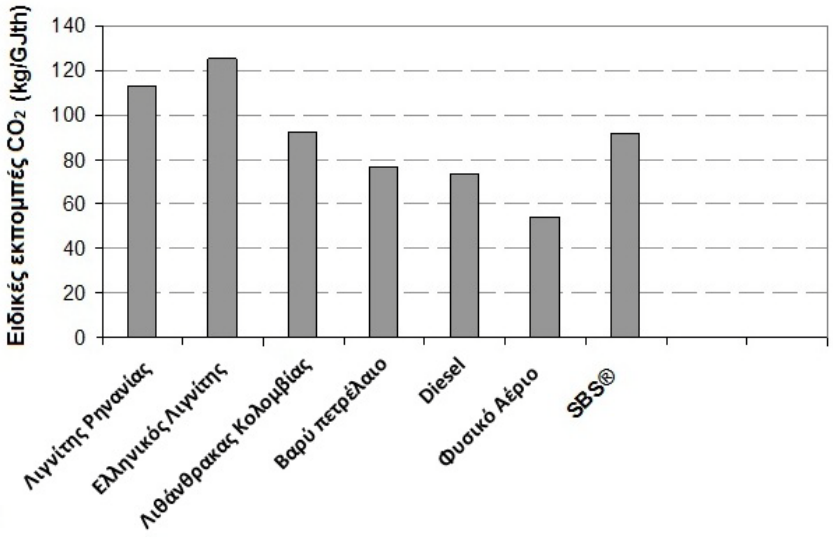

Σχήμα Π-7 : Ειδικές εκπομπές CO_2 ανά θερμική ισχύ σε kg CO_2/ GJ_{th}

Πληθώρα διαφόρων τεχνολογικών λύσεων για την μικτή καύση SRF με άνθρακα σε υφιστάμενες βιομηχανικές μονάδες βρίσκονται υπό διερεύνηση ή έχουν δοκιμαστεί σε βιομηχανική κλίμακα (Σχήμα Π-8). Οι ανθρακικοί σταθμοί ηλεκτροπαραγωγής θεωρούνται ωστόσο μια αναδυόμενη αγορά με σημαντικό δυναμικό ανάπτυξης λόγω της μεγάλης εγκατεστημένης ισχύος και των σημαντικών ποσοτήτων ανακτηθέντων καυσίμων που μπορούν να απορροφήσουν. Στις περισσότερες περιπτώσεις, η εφαρμογή της άμεσης μικτής καύσης είναι δυνατή χωρίς μεγάλες αλλαγές και επενδύσεις στις παρούσες υποδομές. Στο παρακάτω σχηματικό διάγραμμα παρουσιάζονται οι διαφορετικές χρήσεις για τη μικτή καύση του SRF.

Σχήμα Π-8 : Πιθανές τεχνολογίες αξιοποίησης SRF σε ενεργειακές και βιομηχανικές διεργασίες

Για την υλοποίηση ενός έργου μικτής καύσης SRF και άνθρακα σε ανθρακική μονάδα απαιτούνται μία σειρά από τεχνικές τροποποιήσεις και προσθήκες εξοπλισμού στις υπάρχουσες εγκαταστάσεις που αναλύονται παρακάτω:

i) Η κατασκευή - εγκατάσταση αποθηκευτικού χώρου για το ανακτηθέν καύσιμο
ii) Η εγκατάσταση συστήματος τροφοδοσίας για τα εναλλακτικά καύσιμα
iii) Τροποποίηση του συστήματος καύσης στο λέβητα, εφόσον κριθεί αναγκαίο.

Υποστηρικτικά καύσιμα

Ο λιγνίτης αποτελεί εγχώριο καύσιμο πολλών ευρωπαϊκών χωρών και ως εκ τούτου οι μονάδες ηλεκτροπαραγωγής με καύση λιγνίτη θεωρούνται αναπόσπαστο μέρος του ευρωπαϊκού συστήματος ηλεκτροπαραγωγής. Δεδομένου ότι ο τομέας ηλεκτροπαραγωγής με καύση άνθρακα είναι ο κύριος υπεύθυνος για την αύξηση των εκπομπών των αερίων του θερμοκηπίου κατά τις τελευταίες δεκαετίες, η αύξηση του βαθμού απόδοσης των υφιστάμενων και μελλοντικών ανθρακικών σταθμών ηλεκτροπαραγωγής είναι στόχος πρωταρχικής σημασίας. Μεταξύ των υπό εξέταση τεχνολογιών αναβάθμισης λιγνιτικών σταθμών για την αύξηση του βαθμού απόδοσης και τη μείωση εκπομπών CO_2 σημαντικό δυναμικό έχουν και οι τεχνολογίες προξήρανσης λιγνίτη. Οι τεχνολογίες προξήρανσης αποτελούν επίσης αναπόσπαστο τμήμα σε μελλοντικούς λιγνιτικούς σταθμούς, με τεχνολογία καύσης με καθαρό οξυγόνο και πλήρη δέσμευση των εκπομπών CO_2.

Η συμβατική διεργασία ξήρανσης στα σημερινά λιγνιτικά εργοστάσια είναι λειτουργικά ενοποιημένη με τη διεργασία κονιοποίησης και ως μέσο θέρμανσης χρησιμοποιούνται θερμά καυσαέρια που λαμβάνονται από την έξοδο της εστίας σε θερμοκρασία περίπου $1000^{o}C$. Ο υφιστάμενος τρόπος ξήρανσης έχει δύο σημαντικά μειονεκτήματα από ενεργειακή άποψη:

- Η ανακυκλοφορία θερμού καυσαερίου, σε θερμοκρασία περίπου 1000°C, προκειμένου να χρησιμοποιηθεί στην ξήρανση, οδηγεί σε υψηλές εξεργειακές απώλειες, αφού η απαιτούμενη θερμοκρασία για την ξήρανση είναι περίπου 100°C.
- Η παροχή ατμού που προέρχεται από την υγρασία του λιγνίτη που ατμοποιήθηκε δεν μπορεί να αξιοποιηθεί περαιτέρω ενεργειακά, αφού μεταφέρεται μαζί με τον ξηρό λιγνίτη και εισέρχεται στον λέβητα.

Με σκοπό την βελτίωση του βαθμού απόδοσης των λιγνιτικών μονάδων οι δύο προαναφερόμενες πτυχές πρέπει να εξεταστούν. Η τεχνολογία προξήρανσης λιγνίτη, προβλέπει τη χρήση ατμού χαμηλής θερμοκρασίας που απομαστεύεται από τον ατμοστρόβιλο και την αντικατάσταση αντίστοιχα του συστήματος ξήρανσης με θερμά καυσαέρια. Διάφορες τεχνολογίες προξήρανσης έχουν διερευνηθεί σε πειραματική και ημιβιομηχανική κλίμακα στο παρελθόν οι κυριότερες των οποίων είναι ή ξήρανση με περιστρεφόμενους ξηραντήρες αυλών, η ξήρανση με μηχανική εν θερμώ συμπίεση και η ξήρανση σε ρευστοποιημένη κλίνη. Από αυτές τις τεχνολογίες η μοναδική που έχει αναπτυχθεί έως τώρα σε βιομηχανική κλίμακα είναι η ξήρανση σε ατμοσφαιρική ρευστοποιημένη κλίνη. Ένας τυπικός σχεδιασμός ενός τέτοιου συστήματος παρουσιάζεται στο Σχήμα Π-9.

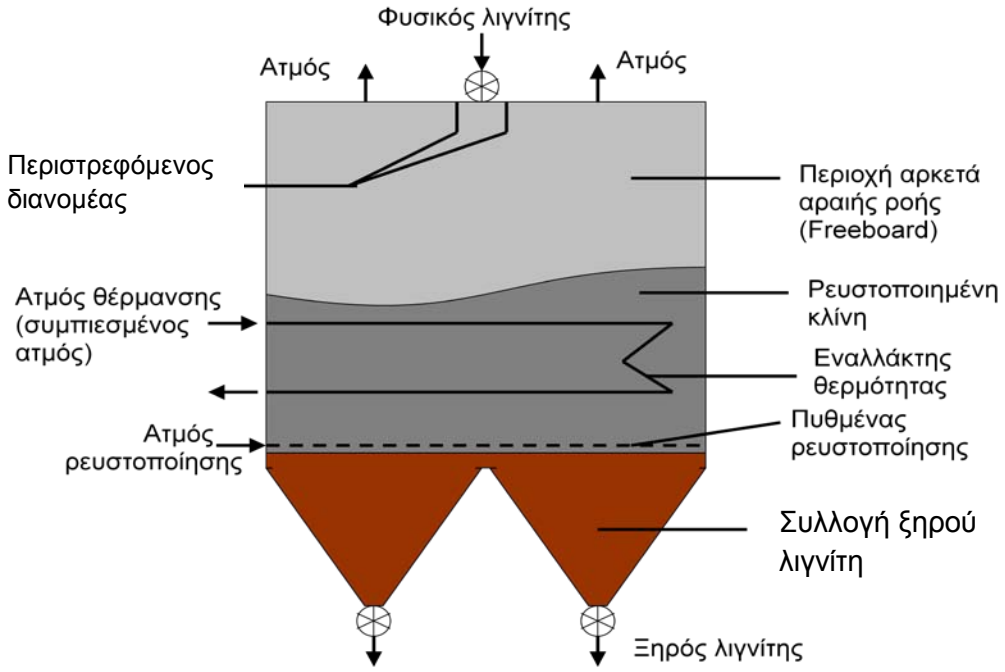

Σχήμα Π-9 : Σχηματικό διάγραμμα ξηραντήρα ρευστοποιημένης κλίνης

Η ενσωμάτωση του ατμοσφαιρικού ξηραντήρα ρευστοποιημένης κλίνης στο κύκλωμα υφιστάμενης λιγνιτικής μονάδας μπορεί να πραγματοποιηθεί με δύο διαφορετικούς τρόπους. Στο πρώτο σχέδιο, χρησιμοποιείται απομαστευμένος ατμός ως θερμαντικό μέσο στον ξηραντήρα και ο παραγόμενος ατμός από τη διαδικασία της ξήρανσης, αφού καθαριστεί σε Ηλεκτροστατικό Φίλτρο από τα σωματίδια καυσίμου που παρασύρονται, αξιοποιείται ως θερμαντικό μέσο στους προθερμαντές τροφοδοτικού νερού του λέβητα (Σχήμα Π-10). Στο δεύτερο σχέδιο, μετά το ηλεκτροστατικό φίλτρο, ο παραγόμενος ατμός συμπιέζεται σε συμπιεστή και χρησιμοποιείται ως θερμαντικό μέσο για τη διαδικασία ξήρανσης (Σχήμα Π-11).

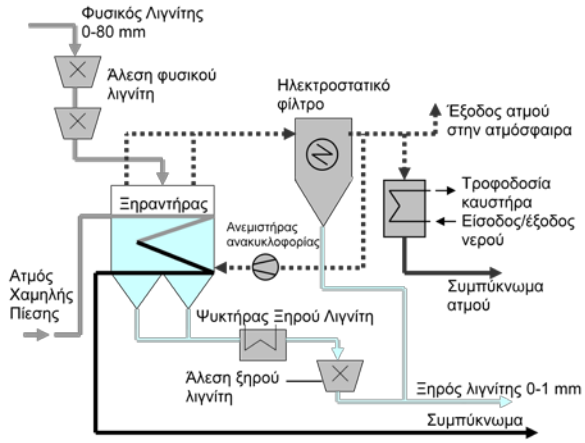

Σχήμα Π-10: Προξήρανση με χρήση αποβαλλόμενης θερμότητας για την τροφοδοσία προθερμαντών νερού

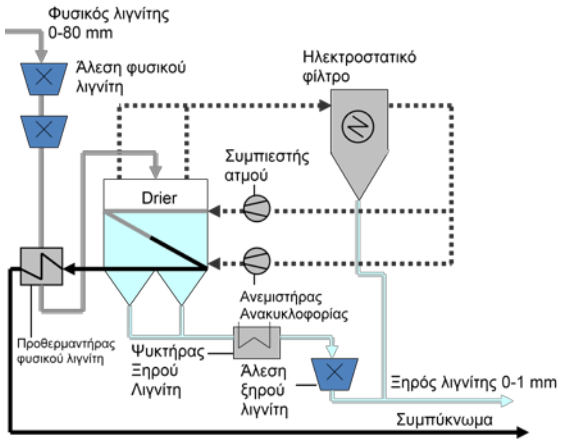

Σχήμα Π-11 : Προξήρανση με συμπίεση ατμού και χρήση αυτού ως θερμαντικό μέσο στον ξηραντήρα

Το δεύτερο σχέδιο είναι ενεργειακά ευνοϊκό δεδομένου ότι δεν χρησιμοποιείται η απομάστευση ατμού για την ξήρανση, με εξαίρεση τη λειτουργία εκκίνησης. Από την άλλη πλευρά, η προσθήκη του συμπιεστή ατμού, ενός ευαίσθητου μηχανικού μέρους, του οποίου η λειτουργία είναι απαραίτητη για τη λειτουργία του ξηραντήρα και ολόκληρης της μονάδας, οδηγεί σε ένα επιπλέον λειτουργικό κίνδυνο καθώς και σε πρόσθετες απαιτήσεις συντήρησης της εγκατάστασης.
Μια τελευταία πτυχή που σχετίζεται με τη μεταφορά θερμότητας ενός λέβητα που συναποτεφρώνει λιγνίτη, απεικονίζεται στο παρακάτω Σχήμα Π-12. Λόγω της μειωμένης υγρασίας του ξηρού λιγνίτη, η παροχή μάζας των καυσαερίων μειώνεται, και η θερμοκρασία αδιαβατικής καύσης αντίστοιχα αυξάνεται οδηγώντας σε αύξηση της ροής θερμότητας με ακτινοβολία στην περιοχή της εστίας. Αυτή η αύξηση μπορεί να μην είναι σημαντική σε υφιστάμενους λέβητες, οι οποίοι εξοπλίζονται με καυστήρες ξηρού λιγνίτη έτσι ώστε να είναι δυνατή η υποκατάσταση φυσικού λιγνίτη από ξηρό έως ένα ποσοστό 20-25% της θερμικής ισχύος. Αναμένεται όμως να επηρεάσει σημαντικά το σχεδιασμό μελλοντικών λεβήτων με καύση εξ' ολοκλήρου ξηρού λιγνίτη.

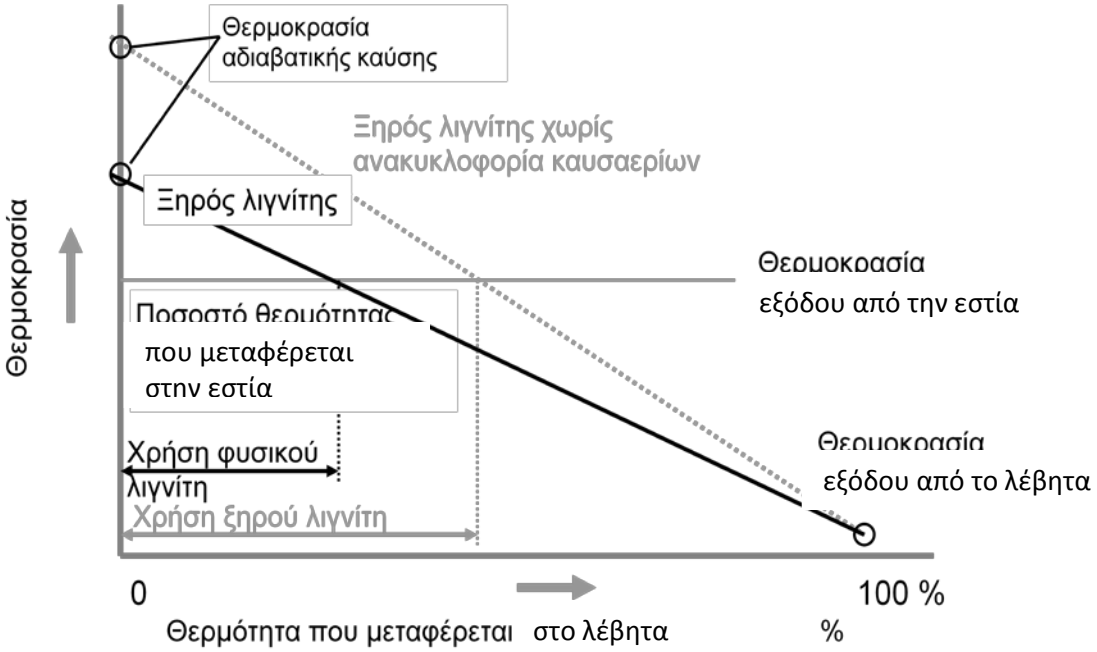

Σχήμα Π-12 : Ποιοτική παρουσίαση των διαγραμμάτων Q-T για λέβητες φυσικού και ξηρού λιγνίτη

Κεφάλαιο 3: Μικτή καύση άνθρακα και SRF – Διερεύνηση στη μικρή κλίμακα

Προκειμένου να διασφαλιστεί η επιτυχής εφαρμογή της πρακτικής μικτής καύσης στερεών ανακτηθέντων καυσίμων (SRF) και λιγνίτη σε σταθμούς ηλεκτροπαραγωγής είναι απαραίτητη η σε βάθος εξέταση παραμέτρων που σχετίζονται με την καύση του εν λόγω καυσίμου. Στις παραμέτρους αυτές συγκαταλέγονται οι φυσικές και οι χημικές ιδιότητες του καυσίμου, οι εκπομπές ρύπων που σχετίζονται με την καύσης του SRF, καθώς και η ανάλυση της ποιότητας των υπολειμμάτων (της τέφρας).
Οι κύριες κατηγορίες διερεύνησης των ιδιοτήτων των ανακτηθέντων καυσίμων περιλαμβάνουν: (α) την τυποποιημένη ανάλυση του καυσίμου στο εργαστήριο, (β) τις εργαστηριακές αναλύσεις που βασίζονται σε προηγμένες μεθόδους δημιουργημένες αποκλειστικά για το SRF, (γ) τις πιλοτικής ή ημιβιομηχανικής κλίμακας δοκιμές, και (δ) τις δοκιμές βιομηχανικής κλίμακας.
Στο πλαίσιο της διαδικασίας τυποποίησης του SRF που συντονίζεται από την CEN/TC 343, προσαρμόζονται οι υπάρχουσες εργαστηριακές μέθοδοι ανάλυσης στερεών καυσίμων ώστε να καταστεί δυνατή η συγκριτική ανάλυση των διαφόρων τύπων SRF. Οι πιο σημαντικές αναλύσεις εργαστηριακής κλίμακας που καλύπτονται από τις τεχνικές προδιαγραφές αφορούν τον προσδιορισμό μίας σειράς παραμέτρων όπως:

- Θερμογόνος ικανότητα
- Τέφρα, πτητικά και υγρασία
- Συμπεριφορά τήξης τέφρας
- Φαινόμενη πυκνότητα, πυκνότητα πελλετών και μπρικετών
- Αντοχή των πελλετών και μπρικετών
- Ιδιότητες γεφύρωσης υλικού χύδην
- Μέγεθος σωματιδίων και κατανομή μεγέθους σωματιδίων με την μέθοδο κοσκινίσματος
- Μεταλλικό αλουμίνιο
- Μέθοδο για άνθρακα (C), υδρογόνο (H), άζωτο (N)
- Μέθοδο για θείο (S), χλώριο (Cl), φθόριο (F), βρώμιο (Br)
- Κύρια στοιχεία : Al, Ca, Fe K, Mg, Na, P, Si, Ti,
- Ιχνοστοιχεία : As, Ba, Be, Cd, Co, Cr, Cu, Hg, Mo, Mn, Ni, Pb, Sb, Se, V, Zn και
- Περιεχόμενο βιομάζας με επιλεκτική διαλυτοποίηση

Στις προηγμένες μεθόδους εργαστηριακής κλίμακας, περιλαμβάνονται ως επί το πλείστον οι μέθοδοι εργαστηρίων οι οποίες έχουν αναπτυχθεί ή είναι ακόμα υπό ανάπτυξη σε πανεπιστήμια, προκειμένου να συγκεντρωθούν συμπληρωματικές πληροφορίες για τις ιδιότητες καύσης συγκεκριμένων τύπων SRF σε συγκεκριμένες συνθήκες ανάφλεξης. Ανάμεσα σε αυτές τις πληροφορίες περιλαμβάνονται :

- Ο χρόνος πλήρους καύσης των σωματιδίων SRF
- Η αεροδυναμική συμπεριφορά των σωματιδίων του SRF

- Το μέγιστο επιτρεπόμενο μέγεθος σωματιδίων SRF για την πλήρη καύση τους σε συγκεκριμένο σύστημα καύσης

Η ανάπτυξη ειδικών μοντέλων καύσης για τα στερεά ανακτηθέντα καύσιμα αποτελεί ένα σημαντικό ορόσημο για την περαιτέρω ανάπτυξη των πρακτικών καύσης SRF. Η ανάλυση των διαφόρων κλασμάτων αποβλήτων από τα οποία προέρχονται δείχνει ότι ένα ανακτηθέν στερεό καύσιμο που προέρχεται από στερεά αστικά απορρίμματα αποτελείται από περισσότερα από δύο κλάσματα που μεταξύ άλλων περιλαμβάνουν χαρτί, χαρτόνι, ύφασμα, πλαστικό φύλλα, σκληρό πλαστικό, ξύλο, κ.α.

Η μοντελοποίηση της συμπεριφοράς καύσης κάθε κλάσματος χωριστά είναι πρακτικά αδύνατη και δεν είναι επιθυμητή. Επομένως αποφασίστηκε η έρευνα να επικεντρωθεί σε δύο μεγάλα κλάσματα: στο βιογενές κλάσμα που περιλαμβάνει το χαρτί, τα χαρτόνια και το ξύλο και στο πλαστικό.

Ο μηχανισμός της καύσης για το βιογενές κλάσμα είναι παρόμοιος με εκείνον του άνθρακα, συμπεριλαμβανομένων των ίδιων βημάτων καύσης: θέρμανση, απομάκρυνση υγρασίας, καύση των πτητικών και καύση του εξανθρακώματος.

Η καύση στερεών σωματιδίων από πλαστικό εμπεριέχει διαφορετικά στάδια. Το σωματίδιο αρχικά θερμαίνεται κατά την είσοδό του στον θαλάμου καύσης και όταν επιτευχθεί μια συγκεκριμένη θερμοκρασία, αρχίζει η τήξη του σωματιδίου και η μετατροπή του σε υγρή σταγόνα. Έπεται η εξάτμιση της σταγόνας. Οι ατμοί του υδρογονάνθρακα που εξατμίστηκε καίγονται στη συνέχεια με το O_2, σύμφωνα με ένα παγκόσμιο μηχανισμό αντίδρασης. Ο μηχανισμός καύσης του πλαστικού δεν περιλαμβάνει μηχανισμό καύσης εξανθρακώματος αφού τα περισσότερα πλαστικά κατά τη θέρμανσή τους λιώνουν και στη συνέχεια ατμοποιούνται πλήρως αφήνοντας αμελητέα ποσότητα εξανθρακώματος.

Και για τα τρία πρώτα βήματα: την θέρμανση, την τήξη, την εξάτμιση της σταγόνας, η εξέλιξη της θερμοκρασίας των σωματιδίων και των συντελεστών μετατροπής από στερεό σε υγρό και από υγρό σε αέριο διέπονται από την εξίσωση του ισοζυγίου ενέργειας, η οποία ισχύει για κάθε σωματίδιο :

$$m_p c_p \frac{dT_p}{dt} = hA_p\left(T_\infty - T_p\right) + \varepsilon_p A_p \sigma\left(\theta_R^4 - T_p^4\right) + h_{source}$$

Όπου T_p : η θερμοκρασία του σωματιδίου
h_{source} : πρόσθετη πηγή

Ο συντελεστής μεταφοράς θερμότητας με συναγωγή h για την θέρμανση των σωματιδίων δίδεται από την εξίσωση:

$$h = \frac{Nu}{k_\infty d_p}$$

Και ο αριθμός Nusselt υπολογίζεται από την παρακάτω σχέση

$$Nu = 2.0 + 0.6\,\mathrm{Re}^{1/2}\,\mathrm{Pr}^{1/3}$$

Εφόσον η τήξη του πλαστικού και η εξάτμιση της αντίστοιχης σταγόνας θεωρείται διεργασία η οποία ελέγχεται από την μεταφορά θερμότητας, ο πρόσθετης όρος πηγής που χρησιμοποιείται στην εξίσωση ενεργειακής ισορροπίας εξαρτάται από το ρυθμού τήξης ή εξάτμισης ($dm_{melt/dec}/dt$) και την αντίστοιχη ενθαλπία τήξης και εξάτμισης $\Delta h_{melt/dec}$

$$h_{source} = \frac{dm_{p\_melt/dec}}{dt} \Delta h_{melt/dec}$$

Ο ρυθμός μεταβολής από την στερεά στην υγρή κατάσταση (τήξη) και από την υγρή στην αέρια, (εξάτμιση) είναι συνάρτηση της αρχικής μάζας του σωματιδίου (m_{p0}), της μεταφερόμενης στο σωματίδιο θερμότητας ($\Delta\dot{Q}$) και της συνολικής θερμότητας που απαιτείται για την πλήρη μετατροπή ($Q_{req\_melt/dec}$).

$$\frac{dm_{p\_melt/dec}}{dt} = m_{P0} \frac{\Delta\dot{Q}}{Q_{req\_melt/dec}}$$

Η απαιτούμενη θερμότητα για την τήξη ή την εξάτμιση υπολογίζεται από την παρακάτω εξίσωση.

$$Q_{req\_melt/dec} = c_{p,end} T_{end} - c_{p,start} T_{start} + \Delta h_{melt/dec}$$

Εφόσον χρησιμοποιείται μόνο η αρχική μάζα και εφόσον η συνολική μεταφερόμενη θερμότητα στο σωματίδιο ($\Delta\dot{Q}$) δεν μεταβάλλεται πολύ με τον χρόνο, ο ρυθμός τήξης και εξάτμισης αναμένεται να είναι σχεδόν σταθερός.
Τελικά, ο παραγόμενος ατμός πολυπροπυλενίου καίγεται σύμφωνα με τον καθολικό μηχανισμό αντίδρασης. Ο μηχανισμός αυτός είναι μια απλοποίηση ενός πιο πολύπλοκου μηχανισμού.

$$C_3H_6 + 3O_2 \rightarrow 3CO + 3H_2O$$

$$CO + 1/2\,O_2 \rightarrow CO_2$$

Για να αξιολογηθεί το προτεινόμενο μοντέλο καύσης, χρησιμοποιούνται πειραματικά δεδομένα από δοκιμές σε πιλοτικό καυστήρα στο Ινστιτούτο IFK του Πανεπιστημίου της Στουτγάρδης. Λόγω της ανομοιογενούς φύσης του SRF και της ποικίλης σύστασής του, δεν χρησιμοποιήθηκαν πραγματικά δείγματα SRF στις δοκιμές, αλλά έτοιμα δείγματα με γνωστή δεδομένη σύσταση τα οποία είναι χαρακτηριστικά για τα δύο κύρια κλάσματα του SRF, το βιογενές και το πλαστικό. Με αυτόν τον τρόπο η εγκυρότητα του προτεινόμενου μοντέλου κρατείται όσο το δυνατόν περισσότερο γενική και αποφεύγεται η εξάρτησή του από ένα συγκεκριμένο τύπο ανακτηθέντος καυσίμου. Τα δύο δείγματα που λαμβάνονται είναι δασική βιομάζα, η οποία αντιπροσωπεύει το βιογενές κλάσμα, και πολυπροπυλένιο, το οποίο αντιπροσωπεύει το πλαστικό κλάσμα. Επιπλέον, για λόγους σύγκρισης, δοκιμάζεται ως καύσιμο αναφοράς και λιγνίτης από την περιοχή της Βόρειας Ρηνανίας - Βεστφαλίας. Το καύσιμο αυτό προξηραίνεται σε υγρασία 8.5% ώστε να εξασφαλισθούν σταθερές συνθήκες ανάφλεξης. Στον Πίνακα Π-6 δίνονται η άμεση και η

στοιχειακή ανάλυση του λιγνίτη, του SRF, των δασικών υπολειμμάτων και του πολυπροπυλενίου.

Πίνακας Π-6 : Προσεγγιστική και στοιχειακή ανάλυση του λιγνίτη, του SRF, των δασικών υπολειμμάτων και του πολυπροπυλενίου.

	Ανάλυση	Λιγνίτης Βόρειας Ρηνανίας-Βεστφαλίας	Δείγμα SRF	Δασικά υπολείμματα	Πολυπροπυλένιο (PP)
Προσεγγιστική (%wt raw)	Υγρασία	58.40	28.00	6.0	0
	Πτητικά	20.00	55.99	82.0	100
	Καθαρός Άνθρακας	12.56	6.36	11.8	0
	Τέφρα	3.91	9.65	0.2	0
	NCV (MJ/kg)	8.171	14.78	16.83	40.19
Στοιχειακή (%wt daf)	C	67.60	59.7	57.1	85.63
	H	4.96	8.36	5.0	14.37
	O	26.30	30.10	23.68	0
	N	0.66	0.98	0.52	0
	S	0.42	0.21	0	0

Για τις προσομοιώσεις υπολογιστικής ρευστοδυναμικής (CFD) χρησιμοποιείται ο εμπορικός κώδικας Fluent 12. Κατασκευάζεται ένα διδιάστατο υπολογιστικό πλέγμα αποτελούμενο από 19.000 τετράπλευρα κελιά, το οποίο αποδεικνύεται ότι παρέχει λύσεις με ανεξαρτησία πλέγματος. Τα πειραματικά δεδομένα για την κατανομή διαμέτρων των σωματιδίων, οι αντίστοιχες κατανομές Rosin Rammler που υπολογίζονται για τα δεδομένα καθώς και οι συνθήκες λειτουργίας για όλα τα καύσιμα δίνονται παρακάτω (Πίνακας Π-7).

Πίνακας Π-7 : Φυσικές ιδιότητες καυσίμων

	Φυσικές ιδιότητες / συνθήκες λειτουργίας	Μονάδες	Λιγνίτης βόρειας Ρηνανίας - Βεστφαλίας	Δασικά υπολείμματα	Πολυπροπυλένιο (PP)
Δεδομένα κατανομής διαμέτρων	Πυκνότητα	kg/m3	1000	800	855
	Cp	J/kgK	1100	1220	2850/ 2656
	Ελάχιστη διάμετρος	μm	5	5	5
	Μέγιστη διάμετρος	“	600	1000	500
	Μέση διάμετρος	“	132	296	372
	Παράμετρος διασποράςr		2.837	1.32	3.16
Παροχή μάζας καυσίμου	Καύσιμο	kg/h			0.498
Παροχή μάζας αέρα	Κύριος αέρας	“			1.950
	Δευτερεύον αέρας	“			2.957
	Τριτογενής αέρας	“			1.371

Εφόσον για την εξάτμιση των πτητικών και την καύση του εξανθρακώματος μπορούν να ληφθούν διάφορες κινητικές σταθερές ανάλογα με το είδος των καυσίμων, πραγματοποιείται παραμετρική ανάλυση, ώστε να αξιολογηθούν οι επιλεγμένες παράμετροι σε σχέση με τα πειραματικά δεδομένα (Πίνακας Π-8).

Πίνακας Π-8 : Κινητικές σταθερές που μελετήθηκαν για τον άνθρακα και τη βιομάζα

	Κινητικές Παράμετροι	Μονάδες	Περίπτωση Άνθρακα			Περίπτωση Βιομάζας	
			A1	A2	A3	B1	B2=A2 και B3=A3
Εξάτμιση Πτητικών	Προεκθετικός συντελεστής (k)	1/s	200,000	**315,000**	315,000	Σταθερός ρυθμός 50 (1/s)	
	Ενέργεια ενεργοποίησης (E)	J/kmol	$7.4 \cdot 10^7$	$7.4 \cdot 10^7$	$7,4 \cdot 10^7$		
Απανθράκωση	Ρυθμός ελεγχόμενος από τη διάχυση μάζας	Kg/(m^2 s Pa)	$5 \cdot 10^{-12}$	$5 \cdot 10^{-12}$	$5 \cdot 10^{-12}$	$5 \cdot 10^{-12}$	
	Προεκθετικός συντελεστής ελεγχόμενος από την κινητική	1/s	6.7	6.7	**0.00208**	6.7	
	Ενέργεια ενεργοποίησης ελεγχόμενη από την κινητική	J/kmol	$1.138 \cdot 10^8$	$1.138 \cdot 10^8$	$7.9 \cdot 10^7$	$1,138 \cdot 10^8$	

Τα αποτελέσματα των προσομοιώσεων σε εργαστηριακή κλίμακα για βιομάζα και πλαστικό δίδονται στα παρακάτω Σχήματα Π12 – Π15.

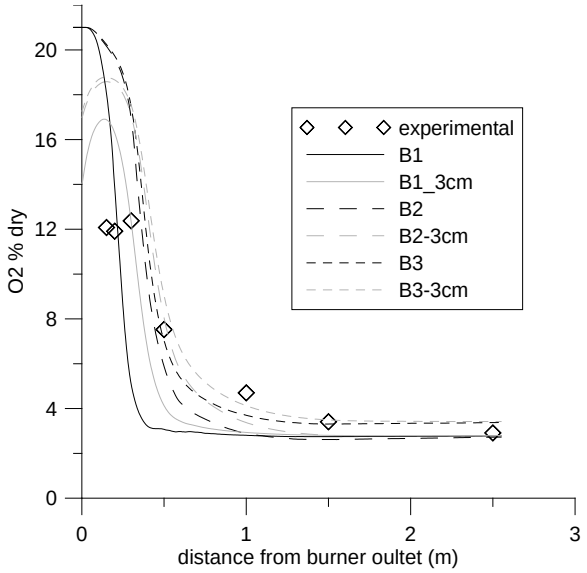

Σχήμα Π-12 : Σύγκριση των προφίλ O_2 για την περίπτωση του βιογενούς κλάσματος

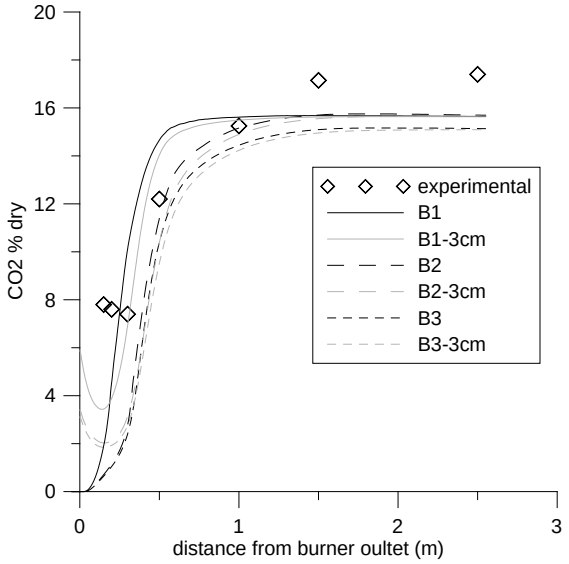

Σχήμα Π-13 : Σύγκριση των προφίλ CO_2 για την περίπτωση του βιογενούς κλάσματος

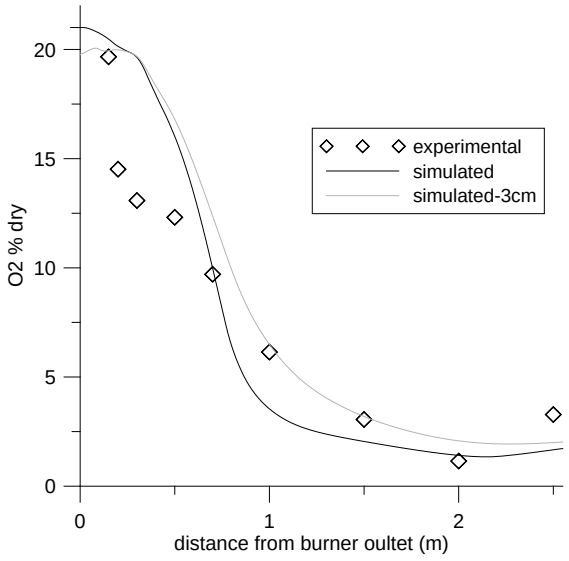

Σχήμα Π-14 : Σύγκριση των προφίλ O_2 για την περίπτωση του πλαστικού

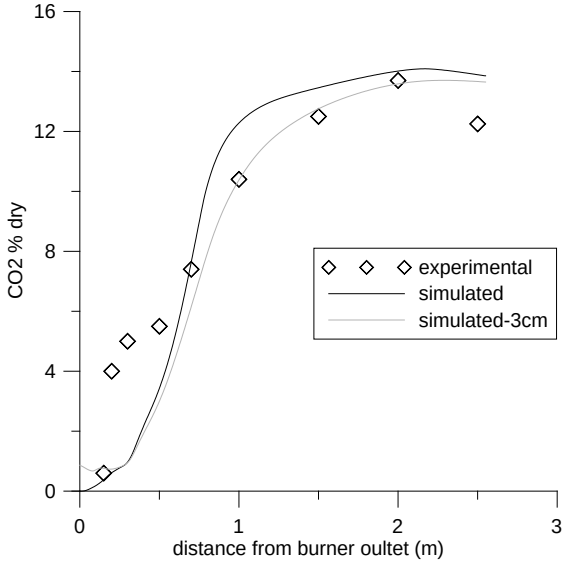

Σχήμα Π-15 : Σύγκριση των προφίλ CO_2 για την περίπτωση του πλαστικού

Η συμφωνία μεταξύ των προλέξεων του υπολογιστικού μοντέλου και των διαθέσιμων πειραματικών δεδομένων κρίνεται ως ικανοποιητική. Για την περαιτέρω μελέτη και αξιολόγηση του προτεινόμενου μοντέλου απαιτείται η ύπαρξη περισσότερων πειραματικών δεδομένων για πλαστικά με διαφορετική σύσταση και διαφορετικές φυσικές ιδιότητες. Το προτεινόμενο μοντέλο θα χρησιμοποιηθεί και στις αριθμητικές προσομοιώσεις καύσης λιγνίτη και SRF στο βιομηχανικό λέβητα.

Κεφάλαιο 4: Μικτή καύση άνθρακα και SRF – Διερεύνηση στη μεγάλη κλίμακα

Πειραματικές μετρήσεις

Στο παρόν κεφάλαιο παρουσιάζεται η διερεύνηση της μικτής καύσης SRF και λιγνίτη σε βιομηχανική κλίμακα μέσω πειραματικών μετρήσεων και υπολογιστικών προσομοιώσεων. Η επιδεικτική δράση της μικτής καύσης SRF και λιγνίτη λαμβάνει χώρα σε γερμανικό λιγνιτικό λέβητα εγκατεστημένης ισχύος 600 MW_e για χρονικό διάστημα 2 εβδομάδων. Το μέγιστο ποσοστό υποκατάστασης λιγνίτη από SRF ανήλθε στο 4% της εισερχόμενης θερμικής ισχύος. Το στερεό ανακτηθέν καύσιμο τροφοδοτείται μαζί με το λιγνίτη μέσω του υπάρχοντος συστήματος τροφοδοσίας. Στο συγκεκριμένο λέβητα μαζί με το λιγνίτη καίγεται σε συνεχή βάση και χαρτοπολτός σε θερμικό ποσοστό υποκατάστασης περίπου 2% της εισερχόμενης θερμικής ισχύος. Το μίγμα λιγνίτη χαρτοπολτού θεωρήθηκε συνεπώς ως καύσιμο αναφοράς. Στο Σχήμα Π-16 παρουσιάζεται το σύστημα τροφοδοσίας του καυσίμου αναφοράς και του SRF.

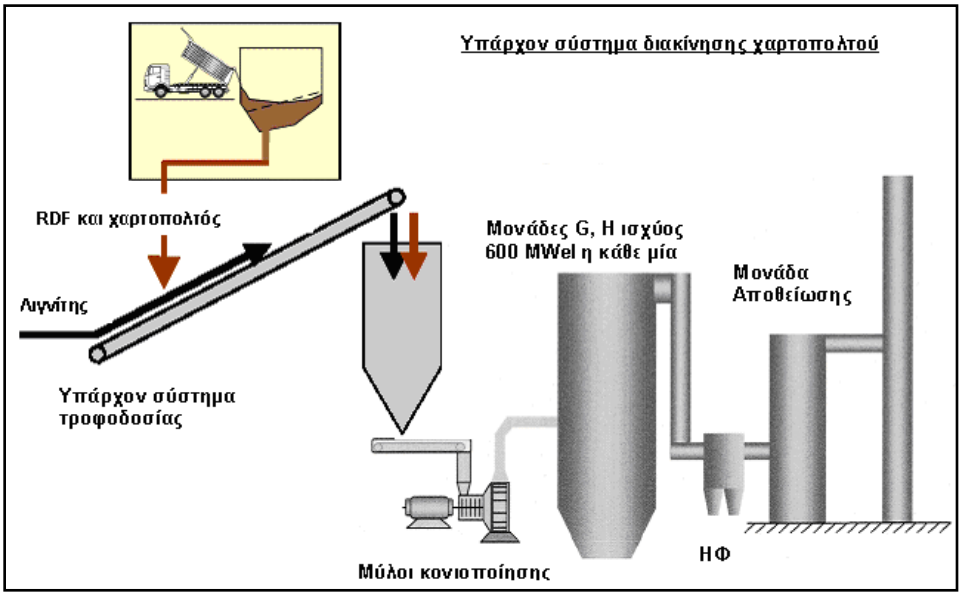

Σχήμα Π-16 : Σύστημα τροφοδοσίας SRF/χαρτοπολτού στον λέβητα

Το στερεό ανακτημένο καύσιμο που χρησιμοποιήθηκε κατά την διάρκεια των δοκιμών, παράγεται από την γερμανική εταιρία Remondis και έχει ονομασία SBS®1. Στον Πίνακα

Π-9 παρουσιάζεται η στοιχειακή και προσεγγιστική ανάλυση των διαφορετικών καυσίμων που χρησιμοποιήθηκαν.

Πίνακας Π-9 : Ανάλυση διαφορετικών καυσίμων

	Μονάδες	Λιγνίτης	Χαρτοπολτός	SBS®1	Έτοιμο καύσιμο (Άνθρακας+ Χαρτοπολτός)
C	%	25.4	13.33	37.18	25.2
H	%	1.85	1.55	5.21	1.82
O	%	9.88	13.49	20.90	9.83
N	%	0.25	0.24	0.61	0.25
S	%	0.16	0.06	0.13	0.15
Υγρασία	%	58.9	49.3	28.03	58.7
Τέφρα	%	3.6	22.0	7.93	4.1
H_u	MJ/kg	8.1	2.95	14.87	7.961

Για την αξιολόγηση της περιβαλλοντικής συμπεριφοράς και των πιθανών επιπτώσεων της ταυτόχρονης καύσης SRF, πραγματοποιήθηκαν οι ακόλουθες μετρήσεις:

- Μέτρηση της σύστασης καυσαερίων και της συγκέντρωσης HCl στο σημείο εξόδου του λέβητα πριν από τον προθερμαντήρα αέρα (LUVO)
- Μετρήσεις στην καπνοδόχο, μετά τα Η/Φ και τη μονάδα αποθείωσης. Συγκεκριμένα έλαβαν χώρα μετρήσεις συμβατικών αέριων ρύπων (CO, NO_x, SO_2, ιπτάμενη τέφρα) και μη συμβατικών αέριων ρύπων (HCl, HF, διοξίνες, φουράνια, βαρέα μέταλλα) σύμφωνα με την ευρωπαϊκή οδηγία για την αποτέφρωσης αποβλήτων και τη γερμανική νομοθεσία
- Δειγματοληψία και ανάλυση των κυριότερων καυσίμων και των στερεών παραπροϊόντων (υγρή τέφρα πυθμένα, ιπτάμενη τέφρα, γύψος). Χαρακτηρισμός των στερεών παραπροϊόντων όσον αφορά στην περιεκτικότητα σε βαρέα μέταλλα και στη δυνατότητα ταφής τους.

Επιπλέον, όσον αφορά την αξιολόγηση των τεχνικών πτυχών του λέβητα, πραγματοποιήθηκαν οι ακόλουθες μετρήσεις:

- Συνεχής παρακολούθηση και καταγραφή των κύριων λειτουργικών παραμέτρων συμπεριλαμβανομένων των θερμοκρασιών ατμού, θερμοκρασίες καυσαερίου, την παραγωγή ατμού και την παραγωγή ηλεκτρικής ενέργειας.
- Μετρήσεις και περιοδικοί έλεγχοι στους μύλους κονιοποίησης
- Επιθεωρήσεις του μηχανολογικού εξοπλισμού για την τροφοδοσία του SRF και την δοσομέτρηση

- Μετρήσεις προφίλ θερμοκρασίας και σύστασης καυσαερίων στην έξοδο του θαλάμου καύσης, με τη χρήση ειδικού ψυχόμενου πυρομέτρου
- Μετρήσεις της θερμοκρασίας καυσαερίων και σύστασης στην έξοδο του λέβητα πριν από τον προθερμαντήρα του αέρα
- Αξιολόγηση της επίδρασης της μικτής καύσης SRF στα φαινόμενα ηλεκτροχημικής διάβρωσης στις επιφάνειες εναλλακτών του λέβητα

Αρχικά αξιολογείται η επίδραση της μικτής καύσης SRF και λιγνίτη στις περιβαλλοντικές πτυχές. Οι συμβατικές εκπομπές καυσαερίων (CO, NO_x, SO_2, ιπτάμενη τέφρα), οι οποίες καταγράφονται συνεχώς, παραμένουν στα επίπεδα αναφοράς και δεν επηρεάζονται από τις συνθήκες μικτής καύσης με SRF. Σε σχέση με τη λειτουργική συμπεριφορά του λέβητα, στο χρονικό πλαίσιο των δύο εβδομάδων, δεν παρατηρήθηκε κάποια αλλαγή στη λειτουργική συμπεριφορά που να οφείλεται στη επίδραση του ανακτηθέντος καυσίμου. Η απόδοση του συστήματος τροφοδοσίας μπορεί να χαρακτηριστεί ως ικανοποιητική, αφού η ανάμειξη του ρεύματος SRF στη μεταφορική ταινία του άνθρακα πριν τους σπαστήρες οδηγεί σε ικανοποιητική ομογενοποίηση του καυσίμου. Τέλος σε σχέση με την πιθανότητα εμφάνισης φαινόμενων διάβρωσης στο λέβητα, λόγω των αυξημένων συγκεντρώσεων Cl στο ανακτηθέν καύσιμο τα πειραματικά δεδομένα δεν κατέδειξαν κάποια ισχυρή τάση. Η πιθανότητα διάβρωσης σε περίπτωση συνεχούς μακροχρόνιας λειτουργίας δεν μπορεί ωστόσο να αποκλειστεί γι΄ αυτό και απαιτείται συνεχής καταγραφή μεγεθών που σχετίζονται με αυτή μέσω ειδικών μετρητικών ληπτών.

Υπολογιστικές προσομοιώσεις

Ένα σημαντικό ζήτημα για κάθε τεχνολογία υποκατάστασης καυσίμου είναι η διατήρηση σταθερής συμπεριφοράς καύσης, εξασφαλίζοντας ταυτόχρονα την πλήρη καύση των εναλλακτικών καυσίμων. Είναι συνεπώς σημαντική η επιλογή του πιο κατάλληλου σημείου εισόδου για το εναλλακτικό καύσιμο, ώστε να επιτευχθεί πλήρης καύση και να διατηρούνται σταθερές οι άλλες λειτουργικές παράμετροι. Σε αυτό το πλαίσιο υποστηρίζεται ότι οι υπολογιστικές προσομοιώσεις (CFD) είναι ένα χρήσιμο εργαλείο για την πρόβλεψη της συμπεριφοράς των εναλλακτικών καυσίμων κατά την καύση, εφόσον υπάρχουν διαθέσιμα εξειδικευμένα μοντέλα καύσης για τα εναλλακτικά καυσιμα και αυτά ενσωματωθούν σε υπάρχοντες κώδικες υπολογιστικής ρευστοδυναμικής.

Σχετικά με την τροφοδοσία του εναλλακτικού καυσίμου μικτής καύσης σε λέβητα κονιοποιημένου καυσίμου τρεις είναι οι κύριες επιλογές (Σχήμα Π-17).

A. Η τροφοδοσία του εναλλακτικού καυσίμου πριν τους μύλους κονιοποίησης. Μέσω της διαδικασίας άλεσης, το καύσιμο ξηραίνεται και κονιοποιείται
B. Η τροφοδοσία του εναλλακτικού καυσίμου στον αγωγό του κονιοποιημένου λιγνίτη μετά το μύλο. Προκειμένου να μειωθεί η κατανομή του μεγέθους των σωματιδίων εγκαθίσταται ένας μύλος αποκλειστικά για την κονιοποίηση του εναλλακτικού καυσίμου.

C. Η εισαγωγή του εναλλακτικού καυσίμου μέσω πρόσθετων καυστήρων στο λέβητα. Ένας μύλος αποκλειστικά για το εναλλακτικό καύσιμο μπορεί να χρησιμοποιηθεί και σε αυτή την περίπτωση

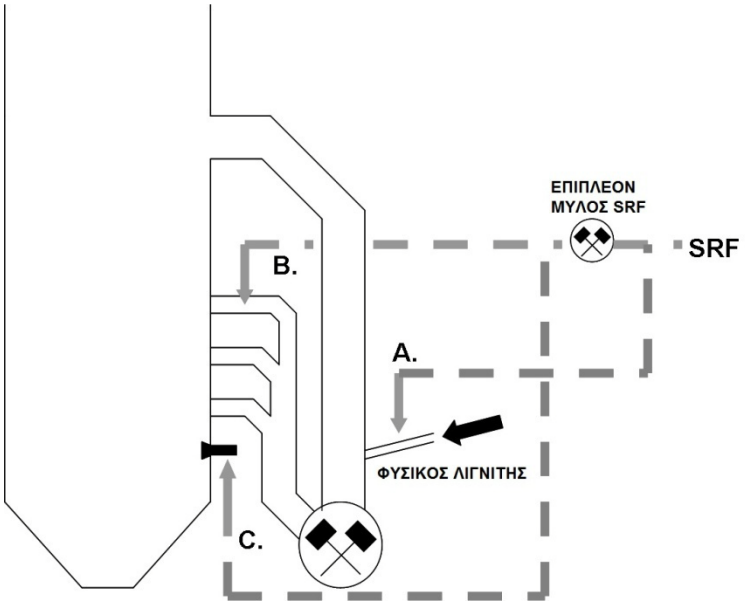

Σχήμα Π-17 : Διαφορετικά σχέδια τροφοδοσίας για εναλλακτικά καύσιμα σε λιγνιτικούς λέβητες

Μεθοδολογία

Η προσεγγιστική και στοιχειακή ανάλυση των καυσίμων που θα χρησιμοποιηθούν στις υπολογιστικές προσομοίωσεις δίνεται στον Πίνακα Π-19. Για λόγους απλοποίησης κι επειδή το SRF είναι αρκετά ανομοιογενές λαμβάνεται η θεώρηση ότι αυτό αποτελείται από 75% βιογενές κλάσμα και από 25% πλαστικό. Θεωρώντας ότι το πλαστικό έχει σύσταση πολυπροπυλενίου (PP) υπολογίστηκε η σύσταση και η θερμογόνος ικανότητα του εναπομένοντος βιογενούς κλάσματος (Πίνακας Π-11).

Πίνακας Π-10 : Προσεγγιστική και στοιχειακή ανάλυση του καυσίμου αναφοράς, του δείγματος SRF και του βιογενούς και πλαστικού κλάσματος του SRF

		Έτοιμο καύσιμο (Λιγνίτης βόρειας Ρηνανίας-Βεστφαλίας + χαρτοπολτός)	Δείγμα SRF	Βιογενές κλάσμα	Πλαστικό κλάσμα (PP)
Προσεγγιστική (%wt raw)	Υγρασία	58,70	28,11	37,49	0
	Πτητικές Ουσίες	19,95	55,99	41,14	100
	Καθαρός άνθρακας	17,25	6,36	8,46	0
	Τέφρα	4,10	9,65	12,92	0
	NCV (MJ/kg)	7,961	14,785	8,17	35,00
Στοιχειακή (%wt daf)	C	67,74	60,09	57,1	85,63
	H	4,89	8,41	5,0	14,37
	O	26,29	30,30	23,68	0
	N	0,67	0,98	0,52	0
	S	0,40	0,21	0	0

Γεωμετρία λέβητα
Το αριθμητικό πλέγμα του λέβητα που αναπτύχθηκε αποτελείται από περίπου 490.000 αδόμητα, εξαεδρικά κελιά. Στο Σχήμα Π-18 παρουσιάζεται η γεωμετρία του λέβητα που μελετήθηκε :

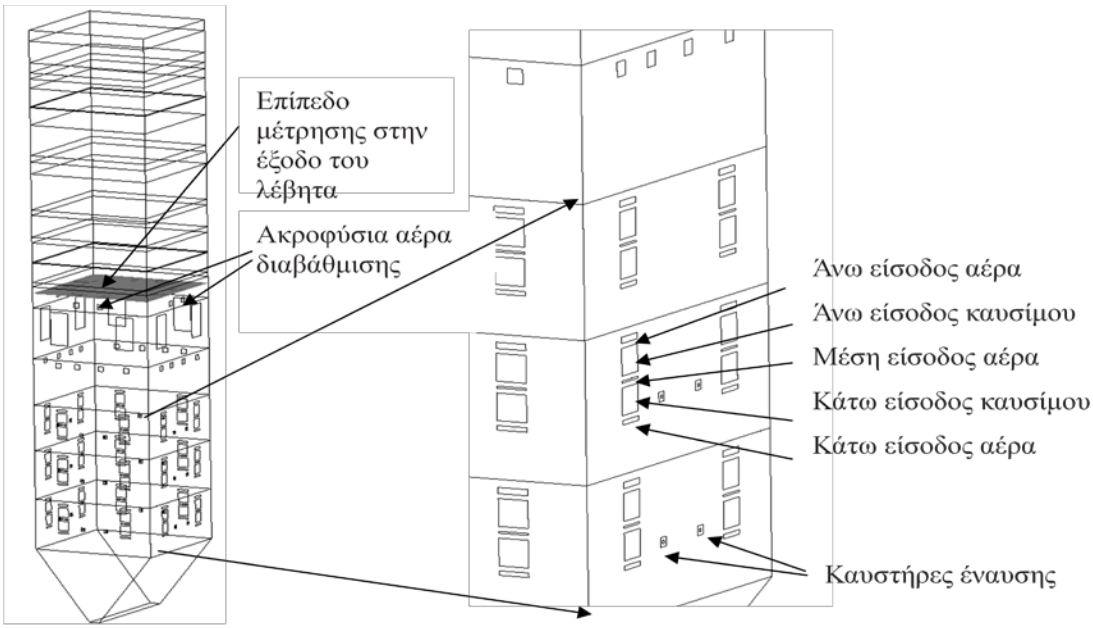

Σχήμα Π-18 : Εικόνα λέβητα προσομοίωσης και λεπτομέρεια στην περιοχή του καυστήρα

Περιπτώσεις προς διερεύνηση
Η υπολογιστική διερεύνηση επικεντρώνεται στα διαφορετικά σενάρια τροφοδοσίας του εναλλακτικού καυσίμου. Οι τρεις βασικοί τρόποι τροφοδοσίας που προαναφέρθηκαν εξετάζονται καθώς και επί μέρους περιπτώσεις αυτών.
Ο πρώτος τρόπος περιλαμβάνει την τροφοδοσία του SRF στην ταινία μεταφοράς του λιγνίτη πριν τους μύλους. Οι παρακάτω επί μέρους περιπτώσεις προσομοιώνονται:
A1. Έγχυση και στους 8 μύλους
A2. Έγχυση στους 4 από τους 8 μύλους
A3. Έγχυση στους 2 από τους 8 μύλους (τοποθετημένοι ο ένας απέναντι από τον άλλον)
Το συγκεκριμένο σχέδιο έγχυσης θεωρείται ότι απαιτεί τις λιγότερες τεχνικές μετατροπές και έχει σχετικά χαμηλό κόστος εγκατάστασης.

Ο δεύτερος τρόπος περιλαμβάνει την τροφοδοσία του SRF στο αγωγό του κονιοποιημένου λιγνίτη μετά του μύλους. Οι παρακάτω επί μέρους περιπτώσεις εξετάζονται:
B1. Έγχυση στους 8 κάτω καυστήρες, 1ο επίπεδο καυστήρων
B2. Έγχυση στους 8 μεσαίους καυστήρες, 2ο επίπεδο καυστήρων
B3. Έγχυση στους 8 πάνω καυστήρες, 3ο επίπεδο καυστήρων
Με αυτό τον τρόπο είναι δυνατό να αξιολογηθεί η επίδραση του επιπέδου τροφοδοσίας του SRF στη συμπεριφορά του λέβητα, καθώς χρησιμοποιούνται και οι 8 καυστήρες του ίδιου επιπέδου.

Το τρίτο σενάριο περιλαμβάνει την εγκατάσταση επιπλέον καυστήρων για αποκλειστική τροφοδοσία του εναλλακτικού καυσίμου. Εξετάζονται οι παρακάτω δύο περιπτώσεις :
C1. Έγχυση στους 8 κάτω καυστήρες έναυσης που είναι τοποθετημένοι στο 1ο επίπεδο καυστήρων
C2. Έγχυση στους 8 άνω καυστήρες έναυσης που είναι τοποθετημένοι στο 2ο επίπεδο καυστήρων

Στον Πίνακα Π-11 παρουσιάζονται τα σχέδια και οι διαφορετικές διάμετροι σωματιδίων που μελετώνται:

Πίνακας Π-11 : Πίνακας περιπτώσεων δοκιμών

Σχέδια μικτής καύσης		Περιγραφή	Διάμετροι σωματιδίων SRF που προσομοιώθηκαν (mm)
Έγχυση πριν τους μύλους (Α.)	A1	8 μύλοι	0.13-0.50-1.30
	A2	4 μύλοι	-//-
	A3	2 μύλοι	-//-
Έγχυση μετά τους μύλους (Β.)	B1	Κάτω επίπεδο καυστήρα	0.13-0.50-1.30-2.50
	B2	Μέσο επίπεδο καυστήρα	-//-
	B3	Άνω επίπεδο καυστήρα	-//-
Έγχυση μέσω επιπλέον καυστήρων (C.)	C1	Επιπλέον καυστήρες / κάτω επίπεδο	-//-
	C2	Επιπλέον καυστήρες / άνω επίπεδο	-//-

Κριτήρια αξιολόγησης
Τα κριτήρια σύμφωνα με τα οποία έγινε η αξιολόγηση των σεναρίων τροφοδοσίας είναι :

1. Μέση και μέγιστη θερμοκρασία στην έξοδο της εστίας. Η θερμοκρασία εξόδου είναι ένα σημαντικό τεχνικός δείκτης για τον χαρακτηρισμό της συμπεριφοράς της καύσης στον λέβητα. Υψηλότερες θερμοκρασίες στην έξοδο μπορεί να οδηγήσουν σε βελτίωση της ολικής καύσης, αλλά μπορεί να προκαλέσουν προβλήματα επικαθίσεων από τηγμένη τέφρα, ενώ χαμηλότερες θερμοκρασίες μπορεί να οδηγήσουν σε τάση αύξησης των ακαύστων. Η διακύμανση της θερμοκρασίας εντός συγκεκριμένων άνω και κάτω ορίων θεωρείται συνεπώς ως η βέλτιστη συμπεριφορά.
2. Ροή θερμότητας στα τοιχώματα της εστίας. Μια σημαντική ελάττωση της ροής θερμότητας μπορεί να οδηγήσει σε αλλαγή της θερμικής ισορροπίας του λέβητα, ακόμα και μείωση στην ατμοπαραγωγή. Σημαντική αύξηση ροής θερμότητας μπορεί να προκαλέσει υπερθέρμανση συγκεκριμένων σημείων, προκαλώντας ζημιές. Και για τη θερμοροή στα τοιχώματα της εστίας επιζητάται επομένως η ίδια συμπεριφορά όπως και για τη θερμοκρασία στην έξοδο της εστίας.

3. Άκαυστα στα βιογενή και πλαστικά σωματίδια. Για την εκτίμηση του ποσοστού των σωματιδίων που καίγονται πλήρως, αξιολογούνται δύο δεδομένα από τα αποτελέσματα των υπολογιστικών προσομοιώσεων. Το ποσοστό μάζας των σωματιδίων που διαφεύγουν από την τεφρολεκάνη λόγω βαρύτητας και τα άκαυστα στα σωματίδια που εξέρχονται από την έξοδο της εστίας. Τα αντίστοιχα κριτήρια αξιολόγησης δίνονται στον Πίνακα Π-12.

Πίνακας Π-12 : Κριτήρια αξιολόγησης

Τάξινόμηση/ Κριτήρια		Θερμοκρασία/ Ροή Θερμότητας	Ποσοστό σωματιδιών στην τεφρολεκάνη (απόλυτες τιμές)	Ολική καύση των σωματιδίων (απόλυτες τιμές)
Πολύ καλύτερα:	++	-	$0 \leq x \leq 0.25$	$99 \leq x \leq 100$
Καλύτερα:	+	-	$0.25 < x \leq 0.75$	$97.5 \leq x < 99$
Συγκρίσιμα:	0	$-5\% < x < +5\%$	$0.75 < x \leq 1.25$	$96.5 < x < 97.5$
Χειρότερα:	-	$-10\% < x \leq -5\%$ or $+5\% \geq x > +10\%$	$1.25 \leq x < 5.0$	$91 \leq x \leq 96.5$
Πολύ χειρότερα:	--	$x \leq -10\%$ or $x \geq +10\%$	$x \geq 5.0$	$x \leq 91$

Προσομοιώσεις στον λέβητα μεγάλης κλίμακας

Στο Σχήμα Π-19 παρουσιάζεται η κατανομή της θερμοκρασίας και της συγκέντρωσης O_2 στο κατακόρυφο επίπεδο και σε τρία οριζόντια επίπεδα του λέβητα:

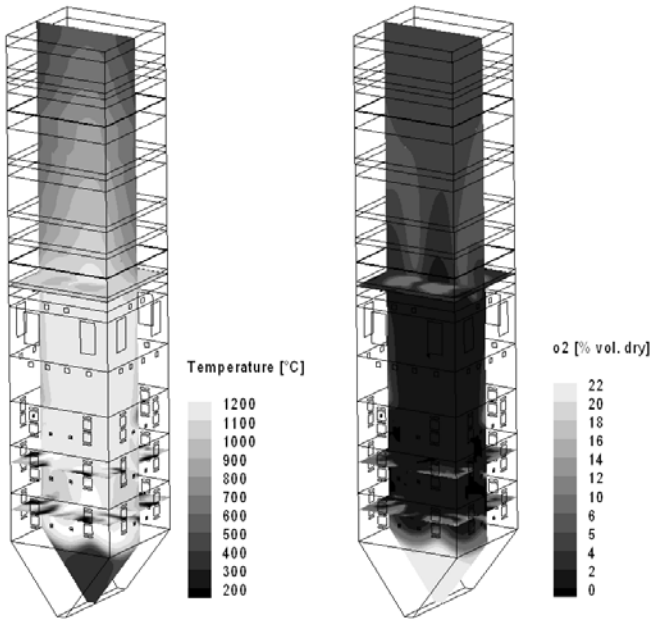

Σχήμα Π-19 : Κατανομή θερμοκρασίας και συγκέντρωσης O_2

Προφίλ θερμοκρασιών
Εφόσον ένα θερμοκρασιακό εύρος +/- 2K είναι εντός των αναμενόμενων πλαισίων ανακρίβειας των αριθμητικών λύσεων, τα αποτελέσματα των θερμοκρασιών επεξεργάζονται, ώστε να εμφανίζονται οι πραγματικές τάσεις και όχι οι αριθμητικές μεταβολές.
Τα αποτελέσματα των περιπτώσεων Α είναι συγκρίσιμα με αυτά της περίπτωσης αναφοράς. Στις περιπτώσεις Β1, Β2, Β3, το θερμοκρασιακό προφίλ αλλάζει και παρατηρείται αύξηση της μέσης θερμοκρασίας έως και 20-30K στο εκάστοτε επίπεδο τροφοδοσίας. Η πιο μεγάλη αλλαγή στην θερμοκρασία παρατηρείται στις περιπτώσεις C όπου υπάρχει αύξηση της τοπικής θερμοκρασίας, και δημιουργούνται θερμά σημεία με θερμοκρασίες περίπου 200 K μεγαλύτερες από τις αντίστοιχες που δίνονται για την περίπτωση αναφοράς.

Ροή θερμότητας στα τοιχώματα
Συγκρινόμενες με την περίπτωση αναφοράς, μέτριες αλλαγές παρατηρούνται στα σενάρια Α και Β. Η σχετική μεταβολή της συνολικής ροής θερμότητας συγκρινόμενη με την περίπτωση αναφοράς είναι κάτω από το 2% για όλες τις περιπτώσεις. Μια μεγάλη αύξηση της συνολικής ροής θερμότητας σε ένα σχετικό ποσοστό μεγαλύτερο από 5% παρατηρείται στις περιπτώσεις C1, C2.

Συμπεριφορά σχετικά με την πλήρη καύση των σωματιδίων - άκαυστα
Σύμφωνα με τις υπολογιστικές προσομοιώσεις τα βιομαζικά σωματίδια καίγονται πλήρως σε όλες σχεδόν τις εξεταζόμενες περιπτώσεις. Μόνο στις περιπτώσεις Β1 και C1, ένα μικρό ποσοστό βιομαζικών σωματιδίων μεγάλης διαμέτρου πέφτουν στην τεφρολεκάνη λόγω της χαμηλής στάθμης έγχυσης. Η εικόνα για τα πλαστικά σωματίδια είναι διαφορετική. Για τα σωματίδια μεγαλύτερα από 0.5mm περισσότερο από 10% της αρχικής παροχής μάζας πλαστικού δεν εξατμίζεται πλήρως και πέφτει στην τεφρολεκάνη υπό μορφή σταγόνας. Αυτό το ποσοστό αυξάνεται, όσο αυξάνεται και το μέγεθος των πλαστικών σωματιδίων.
Στις περιπτώσεις έγχυσης του SRF σε υψηλότερο επίπεδο του λέβητα (Β2, Β3, C2), το ποσοστό των άκαυστων σωματιδίων που πέφτει στην τεφρολεκάνη είναι μικρότερο. Με την αύξηση της διαμέτρου των σωματιδίων το ποσοστό σωματιδίων που καίγεται πλήρως μειώνεται, εφόσον ο χρόνος παραμονής των σωματιδίων δεν επαρκεί για πλήρη καύση. Η τελική αποτίμηση των εξεταζόμενων περιπτώσεων δίνεται στον Πίνακα Π-13:

Πίνακας Π-13 : Συνολική αξιολόγηση των μελετημένων περιπτώσεων μικτής καύσης σύμφωνα με τα επιλεγμένα κριτήρια αξιολόγησης

Σενάρια τροφοδοσίας		Θερμο-κρασία	Θερμορροή στα τοιχώματα	Ποσοστό σωματιδίων που πέφτει στην τεφρολεκάνη		Πλήρης καύση σωματιδίων		Ολική αποτίμηση
				Βιογενές κλάσμα	Πλαστικό	Βιογενές κλάσμα	Πλαστικό	
Τροφ/σια πριν τους μύλους (Α.)	A1	0	0	+	--	+	--	√
	A2	0	0	+	--	+	--	√
	A3	0	0	0	--	-	--	√
Τροφ/σια μετά τους μύλους (Β.)	B1	0	0	--	--	-	--	X
	B2	0	0	0	--	-	--	√
	B3	0	0	+	--	-	--	√
Τροφ/σια μέσω επιπλέον καυστήρων (C.)	C1	-	-	-	--	-	--	X
	C2	-	-	0	--	-	--	X

Σύνοψη και συνολική αξιολόγηση των κύριων περιβαλλοντικών και τεχνολογικών πτυχών σχετικά με τη μικτή καύση SRF και λιγνίτη σταθμούς ηλεκτροπαραγωγής

Πίνακας Π-14 : Αξιολόγηση των περιβαλλοντικών πτυχών μικτής καύσης SRF

		Προτεινόμενο σχέδιο υποκατάστασης άνθρακα : Μικτή καύση SRF	
		Πειραματικές Μέθοδοι	Υπολογιστικές μέθοδοι προσομοίωσης/ Ισοζύγια μάζας
Περιβαλλοντι-κές πτυχές	Εκπομπές CO_2	δ.δ.	Εξοικονόμηση περίπου 2000 t CO_2 κατά τη διάρκεια των δοκιμών δύο εβδομάδων
	Εκπομπές συμβατικών καυσαερίων (NO_x, SO_2, CO)	√	δ.δ.
	ΒΜ στα καυσαέρια	√	δ.δ.
	HCl	√	δ.δ.
	Διοξίνες - Φουράνια	√	√ (Προβλεπόμενοι χρόνοι παραμονής σε αριθμητικές προσομοιώσεις για θερμοκρασίες πάνω από 900 °C: > 5s)
	Ποιότητα τέφρας – ΒΜ στην τέφρα	√	δ.δ.

Πίνακας Π-15 : Αξιολόγηση τεχνολογικών πτυχών μικτής καύσης SRF

		Προτεινόμενο σχέδιο υποκατάστασης άνθρακα : Μικτή καύση SRF	
		Πειραματικές Μέθοδοι	Αριθμητικές μέθοδοι προσομοίωσης/ Ισοζύγια μάζας
Τεχνικές-Λειτουργικές πτυχές	Παράμετροι λειτουργίας (θερμοκρασίες ατμού, Pel)	√	δ.δ.
	Ροή θερμότητας στον ατμοποιητή	δ.δ.	√
	Ολική ισορροπία θερμότητας στον λέβητα	δ.δ.	δ.δ.
	Βαθμός απόδοσης λέβητα ($\eta_{\lambda\acute{\epsilon}\beta\eta\tau\alpha}$) Βαθμός απόδοσης σταθμού(η_{PP})	δ.δ.	δ.δ.
	Συνθήκες εξόδου από την εστία (θερμοκρασία, O_2)	√	√
	Συνθήκες καύσης στον λέβητα (θερμοκρασία και O_2)	δ.δ.	√
	Πιθανά προβλήματα λειτουργίας λόγω επικαθίσεων	δ.δ.	δ.δ.
	ανάφλεξη/ άκαυστα	√	!
	Πιθανά λειτουργικά προβλήματα λόγω διάβρωσης από χλώριο	!	δ.δ.

Κεφάλαιο 5 : Προξήρανση λιγνίτη και μικτή καύση με ξηρό λιγνίτη – Διερεύνηση στη μικρή κλίμακα

Δοκιμές ξήρανσης σε εργαστηριακής κλίμακας εγκατάσταση ξήρανσης ρευστοποιημένης κλίνης

Εφόσον τα σωματίδια λιγνίτη είναι πορώδη στερεά σωμάτια, η περιεχόμενη υγρασία δεν βρίσκεται μόνο στην μακροσκοπική τους επιφάνεια αλλά είναι δεσμευμένη με τριχοειδείς δυνάμεις στο πορώδες του σωματιδίου. Ανάλογα με το μέγεθος του πόρου, το νερό μπορεί να είναι (1) στην επιφάνεια του πόρου λόγω απλών δυνάμεων συνάφειας (2) δεσμευμένο στους πόρου μέσω τριχοειδών δυνάμενων ή (3) δεσμευμένο με μοριακές δυνάμεις σε πολύ-μοριακές δομές ως ένα εξωτερικό στρώμα αυτών. Λόγω της διαφορετικής μικροδομής των ανθράκων η διαδικασία ξήρανσης επομένως διαφέρει μεταξύ αυτών. Γι αυτό το σκοπό πραγματοποιούνται δοκιμές ξήρανσης σε εργαστηριακής κλίμακας ξηραντήρα ρευστοποιημένης κλίνης με σκοπό να αξιολογηθεί η δυνατότητα ξήρανσης του ελληνικού λιγνίτη

Περιγραφή του εργαστηριακού εξοπλισμού

Η διαδικασία ξήρανσης βασίζεται σε μια ρευστοποιημένη κλίνη συνεχούς λειτουργίας, με ενσωματωμένους εναλλάκτες θερμότητας οι οποίοι τροφοδοτούν την ρευστοποιημένη κλίνη με θερμική ενέργεια απαραίτητη για την ξήρανση. Το μέσο μεταφοράς θερμότητας είναι θερμαντικό λάδι. Ο φυσικός λιγνίτης τροφοδοτείται συνεχώς από σιλό στον ξηραντήρα. Η απομάκρυνση του ξηρού λιγνίτη από τον ξηραντήρα είναι συνεχής σε ειδικό δοχείο συλλογής ξηρού λιγνίτη. Και τα δύο δοχεία γεμίζονται και αδειάζονται με συνεχή διαδικασία. Η ρευστοποίηση στην κλίνη γίνεται με χρήση απομαστευμένου ατμού. Για την ρύθμιση των συνθηκών του ατμού ρευστοποίησης, μια βαλβίδα εκτόνωσης και ένας εναλλάκτης θερμότητας χρησιμοποιούνται μεταξύ της παραλαβής του ατμού από το δίκτυο μέχρι την είσοδό του στον ξηραντήρα. Ο ατμός μαζί με σκόνη ξηρού λιγνίτη φεύγει από την κορυφή του ξηραντήρα και οδηγείται σε κυκλώνα απ' όπου διαχωρίζεται η σκόνη από την κύρια παροχή ατμού. Έπειτα ο καθαρός ατμός μεταφέρεται εκτός εγκατάστασης μέσω της διαδρομής απαερίων του σταθμού. Η διαχωρισμένη σκόνη από τον κυκλώνα μεταφέρεται σε δοχείο παραλαβής, το οποίο αδειάζεται περιοδικά. Δείγματα λιγνίτη λαμβάνονται από το προαναφερθέν δοχείο και από το δοχείο συλλογής ξηρού λιγνίτη αλλά και από το εσωτερικό της ρευστοποιημένης κλίνης. Το σχηματικό διάγραμμα και μία φωτογραφία του ξηραντήρα δίνονται στα Σχήματα Π-20 και Π-21 αντίστοιχα

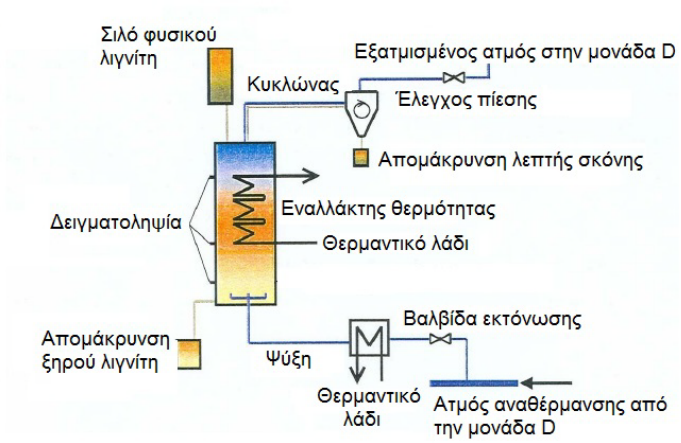

Σχήμα Π-20 : Σχηματικό διάγραμμα του ξηραντήρα ρευστοποιημένης κλίνης

Σχήμα Π-21 : Φωτογραφία του ξηραντήρα

Πειραματική διαδικασία

Πριν από κάθε μέτρηση ο λιγνίτης κονιοποιείται σε σφυρόμυλο σε μέγεθος σωματιδίων κάτω από 2mm. Στο παρακάτω διάγραμμα παρουσιάζεται το ποσοστό υγρασίας που εξέρχεται ο λιγνίτης συναρτήσει της θερμοκρασίας. Οι δύο λιγνίτες που μελετήθηκαν είναι ο ελληνικός και ο λιγνίτης της περιοχής της Βόρειας Ρηνανίας-Βεστφαλίας. Το τελικό αποτέλεσμα της πειραματικής ξήρανσης υποδεικνύει ότι ο ελληνικός λιγνίτης παρουσιάζει παρόμοια συμπεριφορά στην ξήρανση με τον αντίστοιχο γερμανικό λιγνίτη (Σχήμα Π-22).

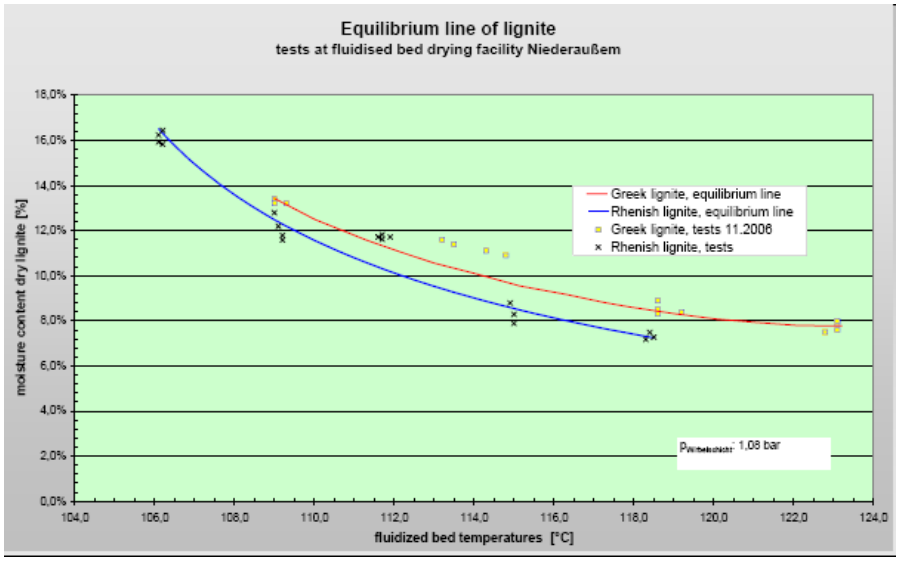

Σχήμα Π-22 : Καμπύλη ξήρανσης του ελληνικού λιγνίτη και του λιγνίτη βόρειας Ρηνανίας-Βεστφαλίας

Πειραματική διερεύνηση στην εγκατάσταση καύσης 1 MW_{th}

Τα πειράματα καύσης προξηραμένου ελληνικού λιγνίτη πραγματοποιήθηκαν σε πειραματική εγκατάσταση καύσης ημιβιομηχανικής κλίμακας με εγκατεστημένη θερμική ισχύ 1 MW_{th}. Η εγκατάσταση αποτελείται από ένα κυλινδρικό κατακόρυφο καυστήρα, έναν ενδιάμεσο οριζόντιο τμήμα με τετραγωνική διατομή και ένα δεύτερο κυλινδρικό κομμάτι ανόδου, όπου τοποθετείται και εναλλάκτης θερμότητας για την ψύξη των καυσαερίων. Ο καυστήρας έχει επένδυση από πυράντοχη πλινθοδομή και αυτή ψύχεται μέσω εναλλακτών που διαρρέονται από ψυχρό ανάθερμο ατμό. Ο λιγνίτης μεταφέρεται μέσω τροφοδοτικής ταινίας στο μύλο κονιοποίησης, όπου και κονιοποιείται και ξηραίνεται με θερμό καυσαέριο ανακυκλοφορίας. Αφού περάσει από τον μύλο και το διαχωριστή, ο ξηρός λιγνίτης διαχωρίζεται από το φέρον αέριο μέσω κυκλώνα. Αποθηκεύεται στη συνέχεια σε ενδιάμεσο σιλό και τροφοδοτείται πνευματικά μέσω του κεντρικού ανοίγματος του καυστήρα μέσα στο θάλαμο καύσης. Η ποσότητα του μίγματος απαερίων και υδρατμών που εισέρχεται στο θάλαμο καύσης ελέγχεται με βαλβίδα ελέγχου, και το υπόλοιπο οδηγείται στην καπνοδόχο. Το σχηματικό διάγραμμα της εγκατάστασης δίνεται στο Σχήμα Π-23.

1	Σιλό φυσικού λιγνίτη	12	Εναλλάκτης - ψύξη θαλάμου καύσης
2	Δοσομετρική ταινία	13	Θάλαμος καύσης
3	Διαχωριστής	14	Προθερμαντής αέρα
4	Θραυστήρας – μύλος	15	Αέρας διαβάθμισης
5	Κυκλώνας	16	Αέρας καύσης
6	Ενδιάμεσο σιλό ξηρού λιγνίτη	17	Ψύκτης καυσαερίων
7	Ψυχόμενος τροφοδοτικός κοχλίας	18	Καυστήρας έναυσης
8	Ενδιάμεσο σιλό ξηρού λιγνίτη	19	Η/Φ
9	Περιστροφικός τροφοδότης	20	Ιπτάμενη τέφρα
10	Αέριο μεταφοράς ξηρού λιγνίτη	21	Αφαίρεση τέφρας πυθμένα
11	Καυστήρας	®	Ανάλυση καυσαερίων
DI	Ξηρός λιγνίτης		

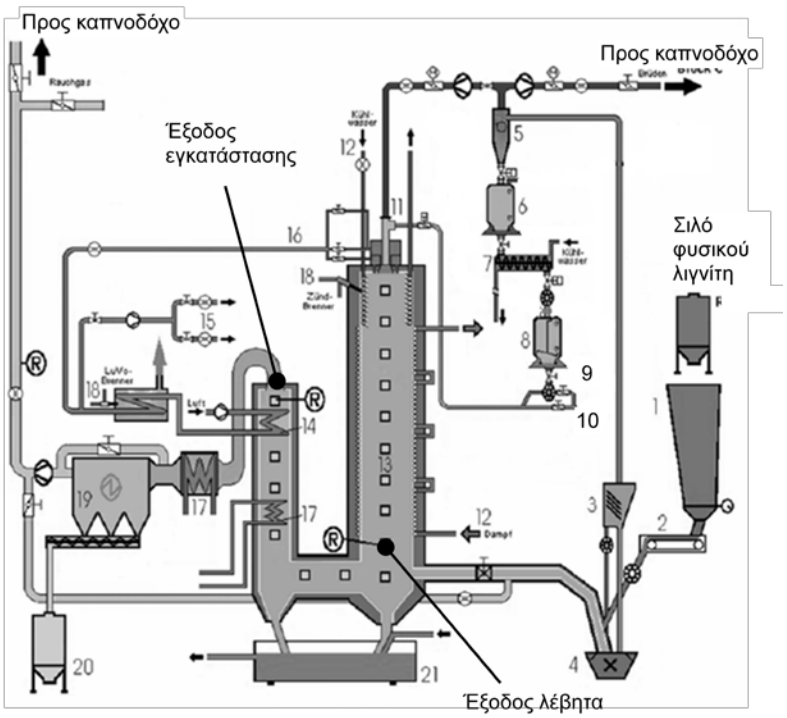

Σχήμα Π-23 : Διάταξη της εγκατάστασης καύσης 1 MWth

Περιπτώσεις προς διερεύνηση

Δύο κύριες σειρές δοκιμών Α και Β, σχεδιάζονται έτσι ώστε να αξιολογηθεί η συμπεριφορά καύσης του ελληνικού λιγνίτη, σε διάφορα επίπεδα ανακυκλοφορίας καυσαερίου. Στις συνθήκες αναφοράς, Α0 και Β0, ανακυκλοφορείται η μέγιστη δυνατή παροχή μάζας καυσαερίων πίσω στον λέβητα. Στις περιπτώσεις Α1 και Β1 το καυσαέριο

που ανακυκλοφορείται είναι περίπου το μισό και στις περιπτώσεις A2 και B2 είναι τεχνικά το ελάχιστο που μπορεί να ανακυκλοφορηθεί. Με αυτόν τον τρόπο οι περιπτώσεις A1, B1 προσομοιώνουν την μικτή καύση ξηρού λιγνίτη και οι περιπτώσεις A2, B2 προσομοιώνουν συνθήκες καύσης σχεδόν 100% ξηρού λιγνίτη.

Πίνακας Π-16 : Επισκόπηση των δοκιμών

	Σειρά πειραμάτων A	Σειρά πειραμάτων B
<u>"Περίπτωση 0" Αναφορά</u> - Παροχή μάζας καυσαερίου που ανακυκλοφορεί στο θάλαμο καύσης: 100% της μέγιστης τιμής	- Η θερμοκρασία πλησίον του καυστήρα και στο τέλος του θαλάμου καύσης προσαρμόζονται ανάλογα με τις χαρακτηριστικές τιμές των ελληνικών λεβήτων (περίπου 1000 °C) - Καθορίζεται η απαραίτητη παροχή μάζας ώστε να επιτευχθούν οι παραπάνω συνθήκες	
<u>"Περίπτωση 1"</u> - Παροχή μάζας καυσαερίου που ανακυκλοφορεί στο θάλαμο καύσης: 50% της μέγιστης τιμής	- Σταθερή παροχή ξηρού λιγνίτη - Η θερμοκρασία αναμένεται να αυξηθεί	- Η θερμοκρασία στην έξοδο του θαλάμου καύσης παραμένει σταθερή - Μείωση της ροής ξηρού λιγνίτη
<u>"Περίπτωση 2"</u> - Παροχή μάζας καυσαερίου που ανακυκλοφορεί στο θάλαμο καύσης: ελάχιστη τιμή	- Σταθερή παροχή ξηρού λιγνίτη - Η θερμοκρασία αναμένεται να αυξηθεί περαιτέρω	- Η θερμοκρασία στην έξοδο του θαλάμου καύσης παραμένει σταθερή - Μεγαλύτερη μείωση της ροής ξηρού λιγνίτη

Παρόλο που υπάρχουν συγκεκριμένες αναλογίες μεταξύ της πειραματικής εγκατάστασης και ενός τυπικού λέβητα, τα αποτελέσματα που παραλήφθηκαν δεν είναι άμεσα συγκρίσιμα με αντίστοιχα αποτελέσματα στη βιομηχανική κλίμακα και πρέπει πρώτα να αξιολογηθούν λαμβάνοντας υπόψη τις ανάλογες πειραματικές συνθήκες.

Μετρήσεις που εκτελέστηκαν:

Μετρήσεις προφίλ θερμοκρασιών
Λαμβάνεται αξονικό προφίλ στον άξονα συμμετρίας του θαλάμου καύσης. Οι θερμοκρασίες καταγράφονται για 5 λεπτά, σε κάθε θέση μέτρησης και θεωρείται μία μέση τιμή ως η τελική μετρούμενη θερμοκρασία.

Μετρήσεις εκπομπών
Οι συγκεντρώσεις του καυσαερίου (O_2, CO_2, CO, NO_x, SO_2) στην έξοδο του λέβητα μετρούνται συνεχώς κατά την διάρκεια των πειραμάτων και υπολογίζονται μέσες τιμές.

Άκαυστα και δειγματοληψία ιπτάμενης τέφρας

Λαμβάνονται δείγματα ιπτάμενης τέφρας από 8 διαφορετικά επίπεδα κατά μήκος του άξονα συμμετρίας του λέβητα και πραγματοποιούνται αναλύσεις τέφρας. Επίσης λαμβάνονται δείγματα περιοδικά και από τα ηλεκτροστατικά φίλτρα.

Έρευνες για φαινόμενα επικαθίσεων και συσσωματώσεων τέφρας
Το ζήτημα αυτό είναι αρκετά σημαντικό για τους ελληνικούς λέβητες, λόγω της υψηλής περιεκτικότητας του ελληνικού λιγνίτη σε τέφρα, και θα εξεταστεί σε 2 βήματα : το πρώτο είναι η θεωρητική εκτίμηση της τάσης για επικαθήσεις σύμφωνα με αριθμητικούς δείκτες και το δεύτερο βήμα είναι η αντίστοιχη πειραματική διερεύνηση. Ο λιγνίτης βόρειας Ρηνανίας-Βεστφαλίας χρησιμοποιείται ως καύσιμο αναφοράς και στα δύο μέρη της διερεύνησης.

Διερεύνηση μεταφοράς θερμότητας : Ενεργειακό ισοζύγιο, διαγράμματα q-T
Καταστρώνεται ένα γενικό ενεργειακό ισοζύγιο της εγκατάστασης, διαγράμματα ροής θερμότητας – θερμοκρασίας (q-T) υπολογίζονται για τα καυσαέρια. Τα τοιχώματα της εγκατάστασης ορίζονται ως ο όγκος αναφοράς για το ισοζύγιο ενέργειας, το οποίο σημαίνει ότι η ανακυκλοφορία του καυσαερίου δεν μετράται ως κλειστός βρόγχος (Σχήμα Π-24). Με άλλα λόγια, η ροή μάζας του καυσαερίου που εξέρχεται του λέβητα και χρησιμοποιείται ως θερμαντικό μέσο για την διαδικασία της ξήρανσης υπολογίζεται ξεχωριστά ως επιπλέον απώλεια καυσαερίου και δεν αντισταθμίζεται από την ροή μάζας καυσαερίου που εισέρχεται ξανά στον λέβητα.

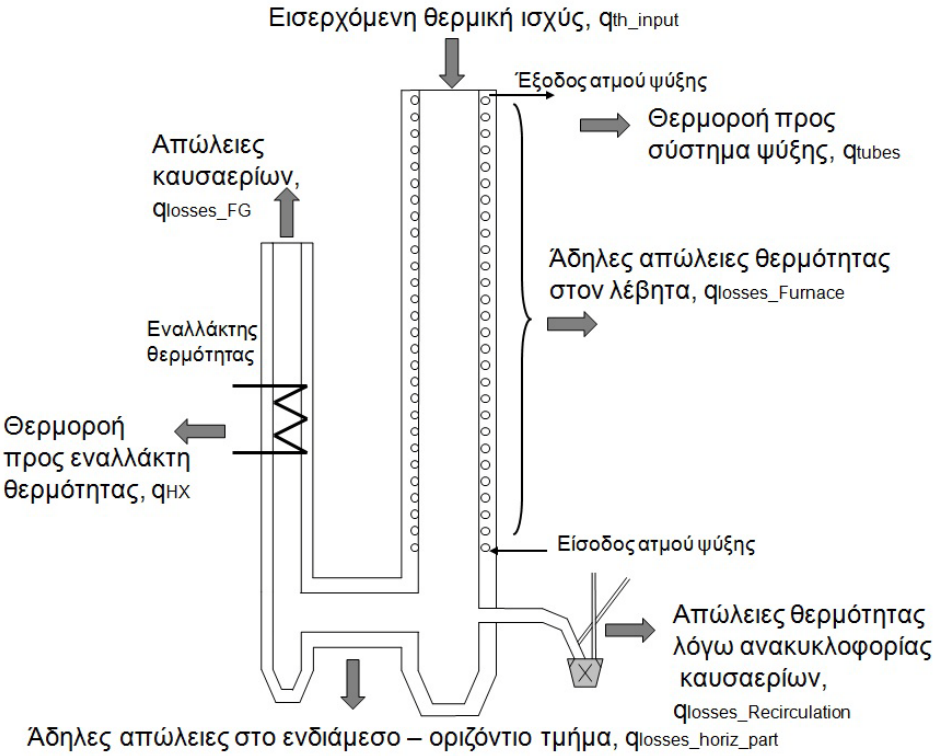

Σχήμα Π-24 : Σχηματικό διάγραμμα της VVA εγκατάστασης και οι υπολογιζόμενες ροές θερμότητας και απώλειες θερμότητας

Αποτελέσματα

Ανάλυση καυσίμου και τέφρας
Η προσεγγιστική και στοιχειακή ανάλυση του ελληνικού λιγνίτη παρουσιάζεται στον Πίνακα Π-17.

Πίνακας Π-17 : Προσεγγιστική και στοιχειακή ανάλυση του ελληνικού λιγνίτη

Προσεγγιστική ανάλυση (% ως έχει)			Στοιχειακή ανάλυση (%daf)	
	Πριν τον μύλο	Μετά τον μύλο		Μέσος όρος
Υγρασία	56.3	12.73	C	66.03
Τέφρα	13.4	24.22	H	4.65
Πτητικά	18.41	34.02	N	2.07
Fixed C	11.89	29.03	O	25.64
H_u. (MJ/kg)	6.590	16.127	S	1.62

Μετρήσεις θερμοκρασίας και χαρακτηρισμός της συμπεριφοράς των εκπομπών
Περίπτωση Α
Από τα προφίλ θερμοκρασιών που λήφθηκαν εξάγονται τα παρακάτω συμπεράσματα (Σχήμα Π-25):

- Μετρείται μια αύξηση θερμοκρασίας των 40 K στην έξοδο του λέβητα για κάθε στάδιο μείωσης της παροχής μάζας του ανακυκλοφορούντος καυσαερίου από την περίπτωση Α0 στην Α1 και από την Α1 στην Α2.
- Η αντίστοιχη αύξηση θερμοκρασίας στην περιοχή κοντά στον καυστήρα είναι έως 100 K
- Η μέγιστη θερμοκρασία μετατοπίζεται προς ανάντη κοντά στην είσοδο του καυστήρα, λόγω της γρηγορότερης έναυσης
- Οι αυξημένες τιμές των σφαλμάτων κοντά στην περιοχή του καυστήρα σηματοδοτούν μεγαλύτερη απόκλιση σε συγκεκριμένη περιοχή λόγω υψηλότερων θερμοκρασιακών διακυμάνσεων συγκρινόμενων με τις αντίστοιχες κατάντη.

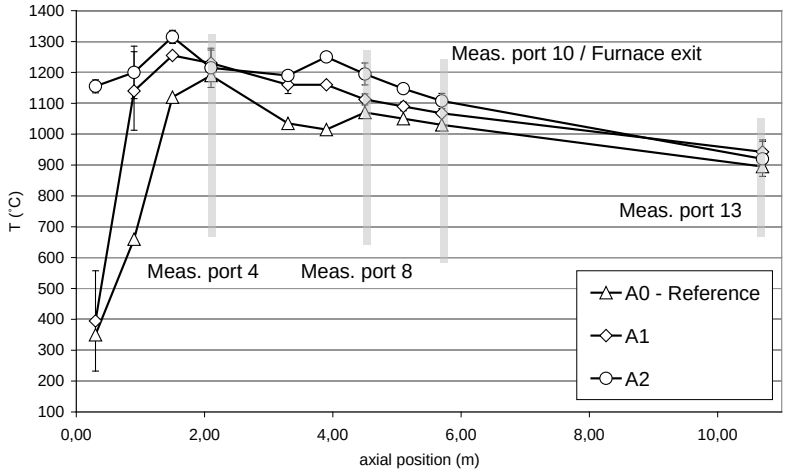

Σχήμα Π-25 : Προφίλ θερμοκρασιών της σειράς δοκιμών Α και θέσεις μέτρησης επικαθίσεων

Περίπτωση Β

Ο σκοπός των πειραμάτων Β είναι η αντιπροσωπευτική προσομοίωση της λειτουργίας ενός υφιστάμενου λέβητα για την περίπτωση όπου λαμβάνει χώρα μικτή καύση ξηρού λιγνίτη. Σε σύγκριση με την σειρά πειραμάτων Α, η παροχή μάζας ξηρού λιγνίτη συνεπώς και η συνολική φόρτιση μειώνεται με σκοπό η θερμοκρασία καυσαερίων στην έξοδο της εστίας να παραμένει σταθερή ίση με την περίπτωση αναφοράς για λόγους προστασίας των εναλλακτών θερμότητας Τα αντίστοιχα προφίλ των θερμοκρασιών παρουσιάζονται στο Σχήμα Π-26.

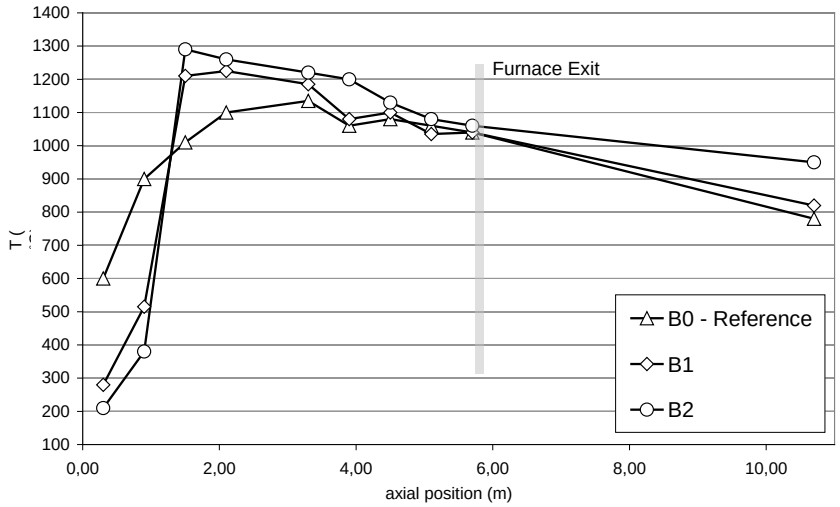

Σχήμα Π-26 : Προφίλ θερμοκρασιών της σειράς δοκιμών Β

Άκαυστα

Με την αυξανόμενη καύση ξηρού λιγνίτη παρατηρείται μείωση των ακαύστων στην ιπτάμενη τέφρα, γεγονός το οποίο αποτελεί ένδειξη για τη βελτίωση των ποσοστών πλήρους καύσης.

Διερεύνηση των επικαθίσεων του ελληνικού λιγνίτη

Η κύρια διερεύνηση επικαθίσεων πραγματοποιείται κατά την διάρκεια των πειραμάτων της περίπτωσης Α και η συνολική ώρα έκθεσης των ληπτών είναι 16h. Δεν παρατηρήθηκαν επικαθίσεις στους μετρητικούς λήπτες που είναι τοποθετημένοι στις θήρες 8 και 10. Μετά την αξιολόγηση αυτού του αποτελέσματος και ενσωματώνοντας τα αποτελέσματα των αρχικών δοκιμών, συμπεραίνεται ότι ο συγκεκριμένος ελληνικός λιγνίτης έχει χαμηλή τάση δημιουργίας επικαθίσεων σε θερμοκρασιακό εύρος από 950˚C έως 1150˚C. Αυξημένες επικαθίσεις και συσσωματώσεις παρατηρούνται στις περιπτώσεις της μικτής καύσης ξηρού λιγνίτη στην θύρα 4 που είναι κοντά στην περιοχή του καυστήρα.

Διερεύνηση της μεταφοράς θερμότητας

Τα κύρια αποτελέσματα των διαγραμμάτων q-T δίνονται παρακάτω :

- Η αδιαβατική θερμοκρασία αυξάνει κατά 70-80K από την περίπτωση Α0 στην περίπτωση Α1 και από την περίπτωση Α1 στην περίπτωση Α2, ενώ παραμένει

σχεδόν σταθερή στις περιπτώσεις B0, B1 και B2, το οποίο είναι αναμενόμενο λόγω της σχεδίασης των πειραμάτων.

- Η μεταφορά θερμότητας με ακτινοβολία στον λέβητα αυξάνει στις περιπτώσεις A1, A2 συγκρινόμενα με την αναφορά, λόγω των αυξημένων θερμοκρασιών του καυσαερίου. Η σχετική αύξηση είναι περίπου 15% μεταξύ των περιπτώσεων A0 και A1 και περίπου 22% μεταξύ των περιπτώσεων A0 και A2. Από την άλλη η μεταφορά θερμότητας με συναγωγή μειώνεται λόγω της μικρότερης παροχής μάζας καυσαερίου. Ως αποτέλεσμα το ποσοστό της μεταφοράς θερμότητας με ακτινοβολία αυξάνεται συγκρίσει του ποσού μεταφοράς θερμότητας με συναγωγή
- Μια διαφορετική εικόνα λαμβάνεται κατά την διάρκεια των πειραμάτων B, όπου η μεταφορά θερμότητας με ακτινοβολία παραμένει σχεδόν σταθερή λόγω μειωμένου φορτίου, και η μεταφορά θερμότητας συναγωγής μειώνεται σε απόλυτες τιμές. Η συνολική χρήσιμη θερμότητα μειώνεται σημαντικά σε αυτά τα πειράματα

Υπολογιστική διερεύνηση στην εγκατάσταση καύσης 1 MW_{th}

Οριακές συνθήκες

Το πλέγμα που αναπτύχθηκε αποτελείται από 350,000 εξαεδρικά κελία. Προσομοιώνονται οι περιπτώσεις του πειράματος A και τα αποτελέσματα των προσομοιώσεων συγκρίνονται με τα αντίστοιχα πειραματικά δεδομένα. Για την πραγματοποίηση των προσομοιώσεων έγιναν οι παρακάτω θεωρήσεις σε παραμέτρους που δεν είναι εξ αρχής γνωστές.

- Κατανομή θερμοκρασίας στο τοίχωμα του λέβητα
- Γωνία συστροφής ή αριθμός συστροφής του δευτερεύοντος αέρα καύσης
- Κινητικές παράμετροι του συγκεκριμένου λιγνίτη για την απελευθέρωση των πτητικών και την καύση του εξανθρακώματος

Η σύσταση του ανακυκλοφορούντος καυσαερίου, η οποία δεν μετριέται κατά την διάρκεια των δοκιμών, υπολογίζεται από το ισοζύγιο μάζας της εγκατάστασης. Οι πιο σημαντικές παράμετροι μεταξύ των οριακών συνθηκών που δεν είναι εξ αρχής γνωστές είναι οι οριακές συνθήκες τοιχώματος. Δύο διαφορετικές οριακές συνθήκες τοιχώματος υιοθετούνται και αξιολογούνται: η οριακή συνθήκη σταθερής θερμοκρασίας στο τοίχωμα και η οριακή συνθήκη σταθερής ροής θερμότητας στο τοίχωμα.

Πίνακας Π-18 : Μελετώμενες παράμετροι σχετικές με την καύση

	Θεωρούμενες παράμετροι	Τιμές προσομοίωσης	Μονάδες
Οριακές συνθήκες τοιχώματος	Σταθερή θερμοκρασία τοιχώματος	800 - 900 - 1000 - 1100	°C
	Σταθερή ροή θερμότητας τοιχώματος	0 - 10 - 20 - 14/10	kW/m2
Οριακές συνθήκες ταχύτητας εισόδου	Γωνία συστροφής δευτερεύοντος αέρα	30 - 40 - 45 - 50	°
Απελευθέρωση πτητικών και καύσης εξανθρακώματος	Προεκθετικός συντελεστής (απελευθέρωση πτητικών)	$1.5 \cdot 10^5 – 3.15 \cdot 10^5$ (τιμή αναφοράς) $– 6.0 \cdot 10^5$	1/s
	Ενέργεια ενεργοποίησης (απελευθέρωση πτητικών)	$7.4 \cdot 10^6 – 2.4 \cdot 10^7 – 7.4 \cdot 10^7$ (τιμή αναφοράς)	J/kmol
	Προεκθετικός συντελεστής (καύση εξανθρακώματος)	0.67 – 6.7 (τιμή αναφοράς) – 67	1/s
	Ενέργεια ενεργοποίησης (καύση εξανθρακώματος)	$1.138 \cdot 10^8$ (τιμή αναφοράς) $– 1.138 \cdot 10^7 – 1.138 \cdot 10^6$	J/kmol

Αποτελέσματα προσομοιώσεων

Στις αρχικές αριθμητικές διερευνήσεις εφαρμόζονται οριακές συνθήκες σταθερής θερμοκρασίας και γίνονται προσομοιώσεις για τις περιπτώσεις A0, A1 και A2. Η θερμοκρασιακή αύξηση κοντά στην περιοχή του καυστήρα και η μετατόπιση της θερμοκρασίας προς ανάντη με την αύξηση του ποσοστού ξηρού λιγνίτη προβλέπεται επιτυχώς. Ωστόσο, οι αναμενόμενες αυξημένες θερμοκρασίες σε όλο του μήκος και την έξοδο του θαλάμου καύσης δεν αναπαράγονται στις προσομοιώσεις με τις σταθερές οριακές συνθήκες. Χρησιμοποιώντας οριακές συνθήκες σταθερής ροής θερμότητας επιτυγχάνεται βελτιωμένη συμφωνία με τα πειραματικά δεδομένα.

Κεφάλαιο 6: Μικτή καύση ξηρού λιγνίτη – διερεύνηση στη μεγάλη κλίμακα

Το παρόν κεφάλαιο επικεντρώνεται στην διερεύνηση της καύσης ξηρού λιγνίτη στη βιομηχανική κλίμακα. Πραγματοποιούνται δοκιμές μικτής καύσης ξηρού λιγνίτη με φυσικό στο λέβητα ΙΙ του λιγνιτικού σταθμού Λιπτόλ εισερχόμενης θερμικής ισχύος 75 MW_{th}

Πειραματικές μετρήσεις

Περιγραφή του σταθμού
Ο λιγνιτικός σταθμός Λιπτόλ αποτελείται από δύο λέβητες σε παράλληλη λειτουργία με παραγωγή ατμού 80 t/h έκαστος. Η συνολική ατμοπαραγωγή τροφοδοτεί από κοινού δύο ατμοστροβίλους, ό ένας εκ των οποίων είναι στρόβιλος αντίθληψης και παρέχει ατμό για θερμικές καταναλώσεις (εργοστάσιο ξήρανσης - μπρικετοποίησης, τηλεθέρμανση). Στον Πίνακα Π-19 παρουσιάζονται οι λειτουργικές παράμεροι του λιγνιτικού σταθμού και στα Σχήματα Π-27 και Π-28 δίνεται μία εικόνα του σταθμού και του λέβητα ΙΙ του σταθμού.

Πίνακας Π-19 : Κύριες παράμετροι λειτουργίας του σταθμού Λιπτόλ

Παράμετροι	Μονάδες	Τιμή
Παροχή μάζας φυσικού λιγνίτη	t/h	48
Θερμογόνος ικανότητα φυσικού λιγνίτη	MJ/kg	5.6
Είσερχόμενη θερμική ισχύς ($Q_{th\text{-}input}$)	MW	75
Ατμοπαραγωγή	t/h	80
Πίεση υπέρθερμου ατμού	bar	64
Θερμοκρασία υπέρθερμου ατμού	˚C	495
Ενθαλπία υπέρθερμου ατμού	kJ/kg	3406
Θερμοκρασία τροφοδοτικού νερού	˚C	154
Ενθαλπία τροφοδοτικού νερού	kJ/kg	645
Ωφέλιμη παροχή θερμότητας (Q_{useful})	MW	61
Βαθμός απόδοσης λέβητα	%	82
Μέγιστη παροχή μάζας ξηρού λιγνίτη	t/h	2
Θερμογόνος ικανότητα ξηρού λιγνίτη	MJ/kg	14.5
Ποσοστό θερμικής υπακατάστασης για την μέγιστη παροχή μάζας ξηρού λιγνίτη	%	10

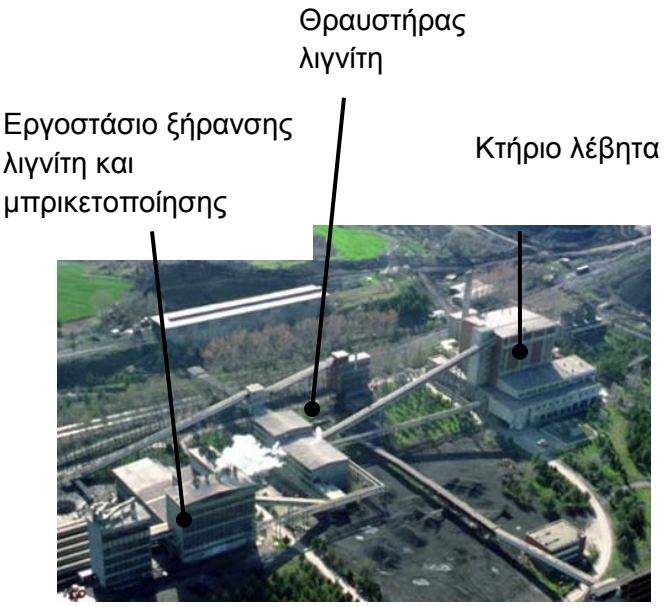

Σχήμα Π-27 : Πανοραμική εικόνα του λιγνιτκικού σταθμού Λιπτολ

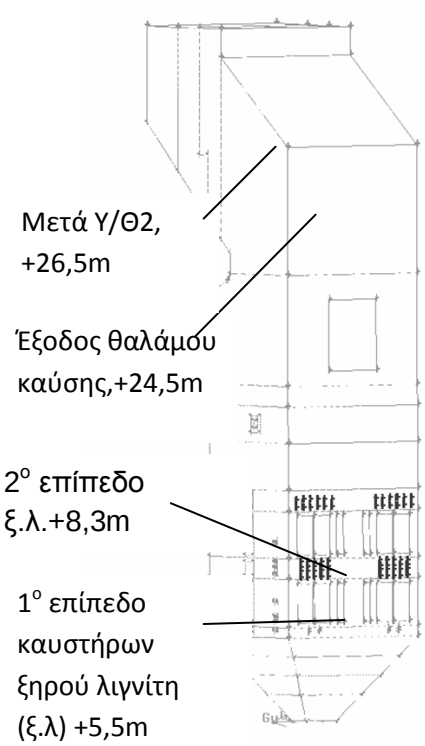

Σχήμα Π-28 : Σχεδιασμός του λέβητα ΙΙ του σταθμού Λιπτόλ

Σκοπός των δοκιμών - Πραγματοποιθείσες μετρήσεις

Ο σκοπός των μετρήσεων είναι η διερεύνηση της επίδρασης της μικτής καύσης ξηρού λιγνίτη στις παρακάτω πτυχές :

- Η λειτουργική συμπεριφορά του λέβητα. Σε αυτή συμπεριλαμβάνεται α) Η ατμοπαραγωγή, β) οι παράμετροι ατμού (πίεση, θερμοκρασία) και γ) η λειτουργία του συστήματος τροφοδοσίας για το φυσικό και ξηρό λιγνίτη
- Τα προφίλ των θερμοκρασιών στον περιοχή του υπερθερμαντή του λέβητα
- Οι εκπομπές των καυσαερίων στην καπνοδόχο
- Η ποιότητα της τέφρας

Συνεχείς καταγραφές της θερμοκρασίας καυσαερίων λαμβάνονται από θερμοστοιχεία τοποθετημένα στο εσωτερικό του λέβητα πλησίον των τοιχωμάτων. Κατά την διάρκεια των κυρίων πειραμάτων, η παραγόμενη ηλεκτρική ισχύς και η ατμοπαραγωγή, καταγράφονται στο κεντρικό σύστημα ελέγχου του λέβητα. Το σημείο μέτρησης, το οποίο είχε αρχικά αποφασιστεί για τη μέτρηση του προφίλ θερμοκρασιών είναι το επίπεδο στην έξοδο του θαλάμου καύσης. Επειδή ωστόσο δεν υπήρχε κατάλληλη οπή μέτρησης επιλέχθηκε το αμέσως ανώτερο επίπεδο. Η μέτρηση των καυσαερίων στην καπνοδόχο πραγματοποιείται με φορητό αναλυτή καυσαερίων.

Χαρακτηρισμός της συμπεριφοράς λειτουργίας

Δοκιμές αναφοράς
Διαπιστώνεται ότι λόγω της χειροτέρευσης της ποιότητας λιγνίτη λαμβάνει χώρα συνεχής μικτή καύση με ξηρό λιγνίτη σε θερμικό ποσοστό υποκατάστασης περίπου 1-2% με σκοπό την υποστήριξη της φλόγας.

Δοκιμές μικτής καύσης
Τα σημεία λειτουργίας που εξετάστηκαν είναι :
- Μικτή καύση για ποσοστό θερμικής υποκατάστασης ξηρού λιγνίτη 6%
- Μικτή καύση για ποσοστό θερμικής υποκατάστασης ξηρού λιγνίτη 6%
- Καύση φυσικού λιγνίτη, η οποία έχει σύντομη διάρκεια λόγω της παρατηρούμενης αστάθειας φλόγας

Στις δεδομένες καταγραφές παρατηρείται ότι διακύμανση της θερμοκρασίας του ατμού σε μερικές περιόδους της ημέρας ξεπερνά τους 30 K. Η καύση ξηρού λιγνίτη μαζί με φυσικό, παρουσιάζεται να μην έχει άμεση επίπτωση στην λειτουργία της εγκατάστασης όσο η διακύμανση της θερμοκρασίας που εξετάζεται παραμένει εντός συγκεκριμένων ορίων κατά την διάρκεια της μέρας και δεν επηρεάζεται από τις δοκιμές μικτής καύσης.

Μετρήσεις προφίλ στην περιοχή των υπερθερμαντών

Δοκιμές μικτής καύσης
Κατά τις περιπτώσεις μικτής καύσης ξηρού λιγνίτη μετρούνται μειωμένες θερμοκρασίες καυσαερίων σε σχέση με την περίπτωση αναφοράς, ενώ οι διακυμάνσεις των μετρούμενων θερμοκρασιών είναι υψηλές. Αιτία για αυτά τα αποτελέσματα είναι πιθανώς η παλαιότητα του συστήματος καύσης και του συστήματος ελέγχου του λέβητα.

Μετρήσεις εκπομπών στην καπνοδόχο
Οι μέσες τιμές των εκπομπών καυσαερίου παρουσιάζονται στον Πίνακα Π-20

Πίνακας Π-20 : Σύσταση καυσαερίου Μέσες τιμές και τυπική απόκλιση

		Περίπτωση αναφοράς	Μικτή καύση 3%	Μικτή καύση 6%
O_2 (% κ.ο. επί ξηρού)	Μέση τιμή	6.13	7.05	6.44
	τυπική απόκλιση	0.62	0.73	0.39
NOx (mg/Nm3 επί ξηρού)	Μέση τιμή	290	319	340
	τυπική απόκλιση	11.0	18.4	14.7
CO (mg/Nm3 επί ξηρού)	Μέση τιμή	60	67	58
	τυπική απόκλιση	4.9	4.1	3.4
SO_2 (mg/Nm3 επί ξηρού)	Μέση τιμή	984	1040	991
	τυπική απόκλιση	82.3	134.3	64.9

Υπολογιστικές προσομοιώσεις (CFD) για μικτή καύση ξηρού λιγνίτη

Οι πιο σημαντικές τεχνικές παράμετροι που υπολογίζονται και αξιολογούνται στις προσομοιώσεις είναι τα προφίλ θερμοκρασιών, οι εκπομπές NO_x, τα άκαυστα και η μεταφορά θερμότητας στα τοιχώματα της εστίας.

Μεθοδολογία

Μοντελοποίηση του μεγάλης κλίμακας λέβητα – Αριθμητικό πλέγμα και οριακές συνθήκες

Η τελική έκδοση του πλέγματος αποτελείται από 357,000 εξαεδρικά κελιά. Η προσεγγιστική και η στοιχειακή ανάλυση του ξηρού λιγνίτη που χρησιμοποιήθηκε στις προσομοιώσεις δίνεται στον Πίνακα Π-21:

Πίνακας Π-21 : Προσεγγιστική και στοιχειακή ανάλυση του ελληνικού λιγνίτη

Άμεση ανάλυση (% a.r.)		Στοιχειακή ανάλυση (%daf)	
	Πριν τον μύλο		Μέσος όρος
Υγρασία	56.25	C	63.81
Τέφρα	13.35	H	4.87
Πτητικά	18.33	N	2.07
Fixed C	12.07	O	27.60
H_u (MJ/kg K)	5.656	S	1.68

Οι ταχύτητες του πρωτεύοντος και δευτερεύοντος ρεύματος αέρα καύσης δίνονται στον Πίνακα Π-22:

Πίνακας Π-22 : Τιμές ταχύτητας του κυρίου και δευτερεύοντος ρεύματος αέρα

		Ταχύτητες αέρα καύσης (m/s)			
		Περίπτωση αναφοράς	Ξηρός λιγνίτης 5%	Ξηρός λιγνίτης 10%	Ξηρός λιγνίτης 20%
Πρωτεύων αέρας (αέρας μεταφοράς)		6.1	5.7	5.4	4.6
Δευτερεύον αέρας	Εμπρόσθιο τοίχωμα λέβητα	42.4	42.4	42.4	35.5
	Αριστερό-δεξιό τοίχωμα	24.9	24.9	24.9	20.9
	Πίσω τοίχωμα	13.5	13.5	13.4	11.3
	Τεφρολεκάνη	2.2	2.2	2.2	1.9

Προφίλ θερμοκρασιών και O_2

Στη χαμηλή στάθμη των καυστήρων φυσικού και ξηρού λιγνίτη, υπολογίζεται μια αύξηση της μέσης θερμοκρασίας στις περιπτώσεις καύσης ξηρού λιγνίτη έως 100 K συγκρινόμενη με την περίπτωση αναφοράς. Στην άνω στάθμη των καυστήρων λιγνίτη, η θερμοκρασία αυξάνεται περίπου κατά 50 K. Στην έξοδο του θαλάμου καύσης η μέγιστη θερμοκρασιακή διαφορά μεταξύ της περίπτωσης αναφοράς και της περίπτωσης μικτής καύσης 20% είναι περίπου 30K. Ακόμη οι μέγιστες τιμές θερμοκρασίας αυξάνονται στην περιοχή των καυστήρων και μειώνονται στην περιοχή πάνω από την ζώνη καύσης. Με τη αύξηση του ποσοστού υποκατάστασης ξηρού λιγνίτη η μέση συγκέντρωση O_2 στην περιοχή του κύριου καυστήρα μειώνεται. Αυτό δικαιολογείται από την ταχύτερη ανάφλεξη του καυσίμου και ταχύτερη κατανάλωση οξυγόνου από τον ξηρό λιγνίτη

αντίστοιχα. Συνολικά το ποσοστό ακαύστων στην περίπτωση του ξηρού λιγνίτη μειώνεται και για αυτόν τον λόγο η μέση συγκέντρωση οξυγόνου στην έξοδο του λέβητα επίσης μειώνεται.

Άκαυστα
Στην περίπτωση υποκατάστασης ξηρού λιγνίτη στο μέγιστο ποσοστό, 20% το ποσοστό ακαύστων υπολογίζεται ότι μειώνεται περίπου στο μισό της αντίστοιχης τιμής της περίπτωσης αναφοράς.

Μεταφορά Θερμότητας
Η ολική θερμοροή στα τοιχώματα του λέβητα αυξάνεται, με την αύξηση του ποσοστού υποκατάστασης, ωστόσο οι μεταβολές αυτές είναι μικρές. Συγκεκριμένα για την περίπτωση υποκατάστασης 20% ξηρού λιγνίτη η αύξηση της θερμοροής σε σχέση με την περίπτωση αναφοράς είναι μικρότερη από 4%. Επιπλέον ο λόγος της μεταφοράς θερμότητας με ακτινοβολία προς την ολική μεταφορά θερμότητας παραμένει σταθερός, καταδεικνύοντας ότι η μικτή καύση ξηρού λιγνίτη δεν επηρεάζει εκτενώς το μηχανισμό μεταφοράς θερμότητας στον συγκεκριμένο λέβητα.

Προβλεπόμενες εκπομπές NO_x
Με την αύξηση του ποσοστού υποκατάστασης φυσικού λιγνίτη από ξηρό παρατηρείται μια σαφής τάση αύξησης των συγκέντρωσεων NO_x σε όλο το ύψος του λέβητα, με αποτέλεσμα να αυξάνονται και οι τελικές εκπομπές NO_x.

Θερμοδυναμικοί υπολογισμοί για την ενσωμάτωση κύκλου προξήρανσης σε υφιστάμενο λιγνιτικό σταθμό

Σκοπός της διερεύνησης
Η παρούσα ανάλυση επικεντρώνεται στη θερμοδυναμική προσομοίωση του κύκλου ατμού ενός λιγνιτικού ατμού σε συνθήκες αναφοράς και σε συνθήκες μικτής καύσης με ξηρό λιγνίτη που παράγεται σε ξηραντήρα ενσωματωμένο στον κύκλο ατμού. Με τους υπολογισμούς αυτούς εκτιμάται η αύξηση του βαθμού απόδοσης Ο υπολογισμός αυτός είναι απαραίτητος για την περαιτέρω εξέταση της οικονομικής βιωσιμότητας του σεναρίου ενσωμάτωσης κύκλου προξήρανσης σε υφιστάμενους λιγνιτικούς σταθμούς Υπολογίζεται επίσης και η μεταβολή στο ισοζύγιο θερμότητας του λέβητα καθώς και όλες οι θερμοδυναμικές παράμετροι του κύκλου.

Μεθοδολογία – Μελέτη πιθανών ρυθμίσεων
Τα θερμικά ποσοστά υποκατάστασης φυσικού λιγνίτη από ξηρό που μελετώνται είναι 10%, 20% και 30%. Επειδή στο εργαλείο υπολογισμού μπορεί να δοθεί ένα μόνο στερεό καύσιμο υπολογίζεται για τις περιπτώσεις μικτής καύσης ένα ισοδύναμο καύσιμο που αντιστοιχεί στο μίγμα φυσικού και ξηρού λιγνίτη τόσο στη σύσταση όσο και στη θερμογόνο ικανότητα. Τα δεδομένα δίνονται στον Πίνακα Π-23:

Πίνακας Π-23 : Ανάλυση του φυσικού και ξηρού λιγνίτη και του ισοδύναμου καυσίμου

Ανάλυση	Μον άδες	Καύσιμο αναφοράς	Προ-ξηραμένος λιγνίτης, 12% υγρασία	θερμικό ποσοστό υποκατάστασης 10%	θερμικό ποσοστό υποκατάστασης 20%	θερμικό ποσοστό υποκατάστασης 30%
C	% w.	18.00	34.43	18.75	19.61	20.58
H	“	1.45	2.77	1.51	1.58	1.66
N	“	3.00	0.96	0.52	0.54	0.57
O	“	8.50	16.26	8.86	9.26	9.72
S	“	0.44	0.84	0.46	0.48	0.50
υγρασία	“	54.00	12.00	52.08	49.90	47.40
τέφρα	“	14.60	27.93	17.83	18.64	19.56
H_u	MJ/kg	5.464	12.682	5.794	6.169	6.597

Ο συγκεκριμένος κύκλος ατμού έχει 2 προθερμαντές νερού χαμηλής πίεσης και 4 υψηλής πίεσης. Για τη διατήρηση των θερμοκρασιών ατμού υψηλής και μέσης πίεσης κάτω από το όριο των 540 ^{o}C, χρησιμοποιούνται δύο ψυκτήρες ατμού στο τμήμα της υψηλής πίεσης και ένας στο τμήμα της μέσης πίεσης. Η θερμοκρασία του νερού ρυθμίζεται αντίστοιχα με την έγχυση νερού τροφοδοσίας.

Αποτελέσματα

Η συνολική επίδραση μικτής καύσης ξηρού λιγνίτη στον όλο θερμοδυναμικό κύκλο συνοψίζεται παρακάτω:

- Ο βαθμός απόδοσης του λέβητα αυξάνεται κατά 1.5 ποσοστιαία μονάδα από την περίπτωση αναφοράς στην περίπτωση υποκατάστασης 30% λόγω της μείωσης των απωλειών καυσαερίων.
- Ο καθαρός βαθμός απόδοσης του σταθμού αυξάνεται κατά 0.8 ποσοστιαίες μονάδες από την περίπτωση αναφοράς στην περίπτωση υποκατάστασης 30%.
- Η αυξητική αυτή τάση στα μεγέθη μπορεί να διαφέρει σε διαφορετικό κύκλο ατμού και εξαρτάται από την επίδραση της ενσωμάτωσης της προξήρανσης στον κύκλο και την επίδραση της αύξησης των αναγκαίων παροχών νερού στους ψυκτήρες ατμού. Οι δύο αυτές μεταβολές έχουν αντικρουόμενα αποτελέσματα όσον αφορά το βαθμό απόδοσης.

Περίληψη και αξιολόγηση των διερευνήσεων μεγάλης κλίμακας στην ξήρανση λιγνίτη και στη μικτή καύση ξηρού λιγνίτη

Ικανοποιητικά αποτελέσματα λαμβάνονται σε σχέση με την περιβαλλοντική επίδοση του σταθμού για την περίπτωση υποκατάστασης φυσικού λιγνίτη από ξηρό. Εφόσον ο ξηρός λιγνίτης που αναφλέγεται είναι της ίδιας ποιότητας όπως το κύριο καύσιμο, μετρούνται μόνο συμβατικές εκπομπές αερίων και δεν αναμένονται μη συμβατικοί ρύποι όπως HCl. Παρατηρήθηκε πειραματικά η τάση αύξησης των εκπομπών NO_x λόγω υψηλότερων θερμοκρασιών φλόγας. Η τάση αυτή προβλέφθηκε και από τις υπολογιστικές προσομοιώσεις. Θα πρέπει συνεπώς να ληφθεί υπόψη η ανάγκη μείωσης των εκπομπών NO_x με μέτρα διαβάθμισης αέρα στην περίπτωση λεβήτων, όπου πρόκειται να πραγματοποιηθούν μετασκευές για την υλοποίηση μικτής καύσης ξηρού με φυσικό λιγνίτη. Στον Πίνακα Π-24 παρουσιάζονται οι περιβαλλοντικές πτυχές της μικτής καύσης ξηρού λιγνίτη.

Πίνακας Π-24 : Πίνακας αξιολόγησης των περιβαλλοντικών πτυχών της μικτής καύσης ξηρού λιγνίτη

		Προτεινόμενο σχέδιο υποκατάστασης λιγνίτη: μικτή καύση ξηρού λιγνίτη	
		Πειραματικές μέθοδοι	Υπολογιστικές μέθοδοι προσομοίωσης/ ισοζύγιο μάζας
Περιβαλλοντικές πτυχές	Εκπομπές CO_2	δ.δ.	Μείωση ετήσιων εκπομπών CO_2 κατά 208,000 t CO_2 σε περίπτωση υποκατάστασης με ποσοστό 20%
	Εκπομπές συμβατικών καυσαερίων (NO_x, SO_2, CO)	!	!
	Βαρεά Μέταλλα στα καυσαέρια	μ.σ.	μ.σ.
	HCl	μ.σ.	μ.σ.
	Διοξίνες – Φουράνια	μ.σ.	μ.σ.
	Ποιότητα τέφρας: ΗΜ στην τέφρα	μ.σ.	μ.σ.

Στον Πίνακα Π-25 παρουσιάζεται η αξιολόγηση των τεχνικών παραμέτρων.

Πίνακας Π-25 : Πίνακας αξιολόγησης των τεχνολογικών πτυχών της μικτής καύσης SRF

		Προτεινόμενο σχέδιο υποκατάστασης λιγνίτη: μικτή καύση ξηρού λιγνίτη	
		Πειραματικές μέθοδοι	Υπολογιστικές μέθοδοι προσομοίωσης/ ισοζύγιο μάζας
Τεχνολογικές – λειτουργικές πτυχές	Παράμετροι λειτουργίας (θερμοκρασίες ατμού, P_e)	√	δ.δ.
	Μεταφορά θερμότητας στον ατμοποιητή	δ.δ.	!
	Ολική ισοζύγιο θερμότητας στον λέβητα	δ.δ.	!
	Βαθμός απόδοσης λέβητα (η_{boiler}) Βαθμός απόδοσης ηλεκτρικού σταθμού (η_{PP})	δ.δ.	√
	Συνθήκες εξόδου από την εστία (θερμοκρασία, O_2)	√	√
	Συνθήκες καύσης στον λέβητα (θερμοκρασία και O_2)	δ.δ.	√
	Πιθανά λειτουργικά προβλήματα λόγω επικαθίσεων	! (Μελέτες στην εγκατάσταση μικρής κλίμακας)	√
	Ανάφλεξη και άκαυστα	√	√
	Πιθανά λειτουργικά προβλήματα λόγω διάβρωσης από χλώριο	μ.σ.	μ.σ.

Κεφάλαιο 7 : Οικονομική αξιολόγηση

Οι δύο περιπτώσεις υποκατάστασης λιγνίτη παρουσιάζονται και αξιολογούνται ανάλογα με την οικονομική τους βιωσιμότητα. Περιγράφονται και συγκρίνονται τα αναμενόμενα πρόσθετα κόστη και έσοδα στην περίπτωση της υλοποίησης των σεναρίων υποκατάστασης πέραν αυτών που αντιστοιχούν στη λειτουργία του υφιστάμενου σταθμού. Τα δεδομένα για τα απαιτούμενα κόστη επένδυσης και κόστη λειτουργίας των εγκαταστάσεων έχουν ληφθεί μετά από έρευνα αγοράς και μέσα από προσωπική επαφή με προμηθευτές στη βιομηχανία. Η δυσκολία στην συλλογή αυτών των δεδομένων έγκειται στην έλλειψη συγκεκριμένων δοκιμασμένων τεχνικών λύσεων για τα προτεινόμενα σχέδια αποκατάστασης άνθρακα, αφού αυτά βρίσκονται ακόμα σε στάδιο εξέλιξης. Τέλος, η οικονομική επίδοση και των δύο τεχνολογιών υποκατάστασης αξιολογείται με βάση ένα ρεαλιστικό σενάριο υποκατάστασης σε ελληνικό λιγνιτικό σταθμό.

Για την εκτίμηση των τεχνολογιών υποκατάστασης, τα αναμενόμενα πρόθετα κόστη και έσοδα που προκύπτουν δίνονται βάσει υπολογισμών και από βιβλιογραφικά δεδομένα. Επισημαίνεται ότι η μείωση των εκπομπών CO_2 επιτυγχάνεται με διαφορετικούς τρόπους σε κάθε τεχνολογία. Με την υποκατάσταση του φυσικού λιγνίτη από SRF μειώνεται η κατανάλωση φυσικού λιγνίτη και έτσι επιτυγχάνεται και η μείωση των εκπομπών CO_2, εφόσον το SRF είναι καύσιμο με υψηλό βιογενές μέρος. Για τους συγκεκριμένους υπολογισμούς λαμβάνεται υπόψη ένα εναλλακτικό καύσιμο με βιογενές μέρος 50%. Αυτή είναι μια ρεαλιστική τιμή για εναλλακτικά καύσιμα που ανακτώνται από αστικά απορρίμματα. Από την άλλη πλευρά, με την ενσωμάτωση ενός συστήματος προξήρανσης λιγνίτη σε υφιστάμενο σταθμό η μείωση των εκπομπών CO_2 επιτυγχάνεται μέσω της αύξησης του βαθμού απόδοσης και της υποκατάστασης λιγνίτη από καύσιμο με υψηλότερη θερμογόνο ικανότητα, συνεπώς τη μείωση της παροχής μάζας του καυσίμου στο ρεύμα υποκατάστασης. Μια σύγκριση των κατηγοριών κόστους και εσόδων που αναμένονται σε περίπτωση εφαρμογής πρακτικών υποκατάστασης παρουσιάζεται στον Πίνακα Π-26.

Πίνακας Π-26 : Κατηγορίες κόστους για τα διερευνούμενα σχέδια υποκατάστασης λιγνίτη

			Μονάδες	1. Μικτή καύση εναλλακτικών καυσίμων		2. Ξήρανση και μικτή καύση ξηρού λιγνίτη
				a) Στερεά βιοκαύσιμα(αγροτικά, δασικά υπολείμματα)	b) Στερεά ανακτηθέντα καύσιμα (SRF)	
Κατηγορίες κόστους	Κόστος επένδυσης	Σύστημα αποθήκευσης και διαχείρισης εναλλακτικού καυσίμου	€/ kW_e ισχύος που αντιστοιχεί στη θερμική ισχύ του καυσίμου υποκατάστασης	55-85	55-85	-
		Σύστημα προξήρανσης λιγνίτη, σύνδεση με λέβητα και ατμοστρόβιλο, μετασκευή συστήματος καύσης	“	-	-	270-290
	Κόστος λειτουργίας και συντήρησης	Σταθερά κόστη λειτουργίας και συντήρησης	€/ kW_e ισχύος που αντιστοιχεί στη θερμική ισχύ του καυσίμου υποκατάστασης	30	30	30
		Μεταβλητά κόστη λειτουργίας και συντήρησης	€/ MWhe από το καύσιμο υποκατάστασης	1.2	1.2	1.2
	Κόστος καυσίμου	Στερεά βιοκαύσιμα	€/t	50-150	-	-
		SRF (gate fee)	€/Mg SRF	-	0-60	-

		Φυσικός λιγνίτης (εξοικονόμηση)	€/GJ - €/t	2.6 - 14
	Κόστος CO_2	Κόστος δικαιωμάτων CO_2 allowances (εξοικονόμηση)	€/ t CO_2	15

Πίνακας Π-27 : Έσοδα για τα διερευνούμενα σχέδια υποκατάστασης λιγνίτη

		Μονάδες	3. Μικτή καύση εναλλακτικών καυσίμων		4. Ξήρανση και μικτή καύση ξηρού λιγνίτη
			c) Στερεά βιοκαύσιμα(αγροτικά, δασικά υπολείμματα)	d) Στερεά ανακτηθέντα καύσιμα (SRF)	
Έσοδα	Επιδοτούμενη τιμή ηλεκτρισμού	€/ MWhe από το καύσιμο υποκατάστασης	55-85	55-85	-
	Μέση τιμή πώλησης ηλεκτρικής ενέργειας	€/ MWhe			

Δυνατότητες εξοικονόμησης εκπομπών CO_2 από τα προτεινόμενα σχέδια μικτής καύσης

Για να εκτιμηθεί η δυνατότητα εξοικονόμησης εκπομπών CO_2 από τις προτεινόμενες τεχνολογίες ένα ποσοστό θερμικής υποκατάστασης της τάξης του 5% θεωρείται και για τις δύο τεχνολογίες μικτής καύσης. Το συγκεκριμένο ποσοστό είναι κανονικά πολύ μικρό για να είναι οικονομικά εφικτό για την τεχνολογία προξήρανσης. Σκοπός αυτού του υπολογισμού ωστόσο είναι μόνο ο υπολογισμός του δυναμικό μείωσης των εκπομπών CO_2 με το ίδιο ποσοστό υποκατάστασης.
Η μονάδας V του ατμοηλεκτρικού σταθμού του Αγίου Δημητρίου λαμβάνεται ως μονάδα αναφοράς για τη σύγκριση. Τα δεδομένα αναφοράς για τη μονάδα Άγιος Δημήτριος V δίνονται στον Πίνακα Π-27. Το ποσοστό υποκατάστασης είναι σταθερό για όλα τα σενάρια και ίσο με 5% της εισερχόμενης θερμικής ισχύος. Επιπλέον, για τον υπολογισμό αύξησης του βαθμού απόδοσης μέσω της ενσωμάτωσης της τεχνολογίας προξήρανσης απαιτούνται θερμοδυναμικοί υπολογισμού του κύκλου ατμού του σταθμού. Για το σκοπό αυτό λαμβάνονται τα αποτελέσματα του κεφαλαίου 6. Τα αποτελέσματα των υπολογισμών παρουσιάζονται στον Πίνακα Π-28. Η υποκατάσταση από βιομάζα έχει το μεγαλύτερο δυναμικό μείωσης των εκπομπών CO_2. Η υποκατάσταση 5% της εισερχόμενης θερμικής ισχύος από βιομάζα οδηγεί σε μείωση των εκπομπών CO_2 κατά 5% ενώ για τις περιπτώσεις του SRF και του ξηρού λιγνίτη, οι τιμές αυτές είναι περίπου 3.05% και 1.49% αντίστοιχα.

Πίνακας Π-27 : Παράμετροι σταθμού ηλεκτροπαραγωγής για την περίπτωση αναφοράς

Δεδομένα αναφοράς για την μονάδα Αγίου Δημητρίου V		
P_e	375	MW_e
Καθαρός βαθμός απόδοσης σταθμού ($\eta_{pp,\ net}$)	35.4	%
H_u. (φυσικού λιγνίτη)	5.418	MJ/kg
Υγρασία φυσικού λιγνίτη	55.3	% w.t.
Ειδικές εκπομπές CO_2 καυσίμου (μ_{CO2})	0.677	kg CO_2 / kg fuel
Ετήσιες εκπομπές CO_2	3,811,025	t CO_2 / a

Πίνακας Π-28 : Αναμενόμενη μείωση CO_2 μέσω πρακτικών μικτής καύσης

	Μικτή καύση βιομάζας	Μικτή καύση SRF	Προξήρανση λιγνίτη και μικτή καύση ξηρού λιγνίτη	Μονάδες
Μείωση εκπομπών CO_2	190,551	116,241	56,811	t CO_2 / a
Ποσοστό μείωσης εκπομπών CO_2 συγκριτικά με την περίπτωση αναφοράς	5.00	3.05	1.49	%

Υπολογισμός κόστους αποφυγής CO_2

Το κόστος αποφυγής του CO_2 (C_{avoid} σε €/t CO_2) δίνεται από την παρακάτω έκφραση :

$$C_{avoid} = (C_{CO2} - C_{ref.}) / (em_{ref.} - em_{CO2})$$

Όπου :
$C_{ref.}$: Το κόστος παραγωγής ηλεκτρικής ενέργειας στην περίπτωση αναφοράς (€/kWh)
C_{CO2} : Το κόστος παραγωγής ηλεκτρικής ενέργεια κατά την πρακτική υποκατάστασης (€/kWh)
em_{ref} : Ειδικές εκμπομπές CO_2 στην περίπτωση αναφοράς (t CO_2/kWh)
em_{CO2}: Ειδικές εκπομπές CO_2 κατά την πρακτική υποκατάστασης (t CO_2/kWh)

Στην παρούσα ανάλυση η προαναφερθείσα έκφραση απλοποιείται. Αντί να υπολογίζονται τα κόστη παραγωγής ηλεκτρικής ενέργειας για όλο το εργοστάσιο στην κατάσταση αναφοράς και στις δύο περιπτώσεις μικτής καύσης, μόνο τα επιπλέον κόστη και έσοδα που εμφανίζονται από την εγκατάσταση των συστημάτων μικτής καύσης λογίζονται και συγκρίνονται. Η συγκεκριμένη μεθοδολογία ακολουθείται, αφού δεν είναι διαθέσιμα αναλυτικά στοιχεία για την αναλυτική κατανομή του κόστους παραγωγής της ηλεκτρικής ενέργειας σε υφιστάμενους σταθμούς.

Η διαφορά στο κόστος παραγωγής ηλεκτρικής ενέργειας επηρεάζονται από :
- Τα επιπλέον κόστη λειτουργίας του εργοστασίου, λόγω της συνεχούς λειτουργίας των συστημάτων μικτής καύσης. Σε αυτά τα κόστη συμπεριλαμβάνεται α) Το κόστος επένδυσης των εγκαταστάσεων ανηγμένο στην ετήσια λειτουργία αυτών β) Η διαφορά στο κόστος καυσίμου, λόγω της αλλαγής του καυσίμου γ) τα επιπλέον κόστη προσωπικού δ) τα επιπλέον κόστη λειτουργίας και συντήρησης και ε) επιπλέον κόστη για αναλύσεις καυσίμου και ποιοτικό έλεγχο και μετρήσεις ρύπων
- Τα επιπλέον εσοδα που εμφανίζονται από την λειτουργία των συστημάτων μικτής καύσης. Αυτά περιλαμβάνουν α) τα αυξημένα έσοδα από την παραγωγή ηλεκτρικής ενέργειας, λόγω της επιδοτούμενης τιμής της ηλεκτρικής ενέργειας, όταν πραγματοποιείται καύση βιομάζας ή SRF β) τα έσοδα από gate fee, όταν πραγματοποιείται μικτή καύση στερεών ανακτηθέντων καυσίμων γ) τα έσοδα από την εξοικονόμηση των εκπομπών CO_2.

Τα συνολικά δεδομένα των περιπτώσεων δίνονται στον Πίνακα Π-29. Γίνονται υποθέσεις για συγκεκριμένες τιμές όπως για την τιμή της ηλεκτρικής ενέργειας, την τιμή των δικαιωμάτων CO_2, την τιμή της βιομάζας και την τιμή του λιγνίτη. Ανάλυση ευαισθησίας πραγματοποιείται στη συνέχεια με σκοπό την αξιολόγηση της διακύμανσης αυτών των τιμών και την επίδραση αυτών στο κόστος αποφυγής CO_2.

Πίνακας Π-29 : Υποθέσεις για υπολογισμούς

Παράμετροι	Μονάδες	Μικτή καύση εναλλακτικών καυσίμων		Προξήρανση και μικτή καύση ξηρού λιγνίτη
		Στερεά βιοκαύσιμα	SRF	
Θερμικό ποσοστό υποκατάστασης	%	5	5	25
Προβλεπόμενη διάρκεια ζωής	έτη	20	20	20
Ώρες λειτουργίας	h/a	6000	6000	7500
Κόστος βιομάζας	€/ t	100	-	-
SRF Gate fee	€/Mg	-	0	-
Κόστος λιγνίτη	€/ GJ	-	-	2.6
Μέση τιμή πώλησης ηλεκτρικής ενέργειας	€/MWh	55	55	55
Επιδοτούμενη τιμή ηλεκτρισμού	€/MWh	150	87.75	-

Βασισμένο στις υποθέσεις που παρουσιάστηκαν προηγουμένως, οι ειδικές εκπομπές CO_2 υπολογίζονται για τις περιπτώσεις αναφοράς και μικτής καύσης (Σχήμα Π-29). Στις περιπτώσεις μικτής καύσης βιομάζας και SRF οι ειδικές εκπομπές CO_2 μειώνονται κατά 3.75% και 2.29% αντίστοιχα, ενώ η συνολική μείωση για το σενάριο της μικτής καύσης ξηρού λιγνίτη ανέρχεται στο 5.5%. Περίπου 2% από αυτή την τιμή προέρχεται από την αύξηση της απόδοσης του εργοστασίου και περίπου 3.5% προέρχεται από την αλλαγή καυσίμου και την μείωση της παροχής μάζας του λιγνίτη λόγω της αυξημένης θερμογόνου ικανότητας του ξηρού λιγνίτη.

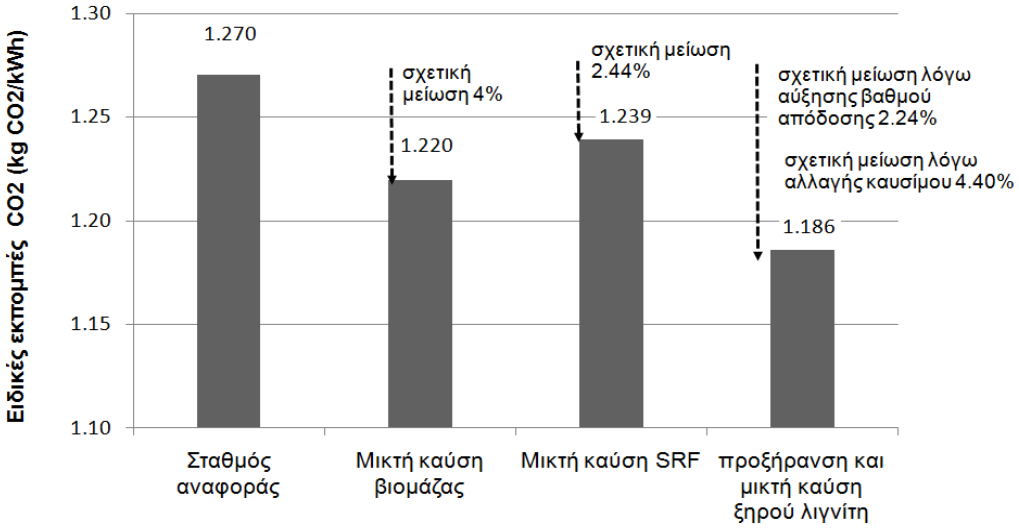

Σχήμα Π-29 : Μείωση των ειδικών εκπομπών CO_2 από τα προτεινόμενα σενάρια μικτής καύσης

Τα προβλεπόμενα ετήσια κόστη λειτουργίας (σε M €/ a) που εμφανίζονται στην εγκατάσταση και λειτουργία των συστημάτων υποκατάστασης περιλαμβάνουν : α) το μειωμένο κόστος επένδυσης στην ετήσια λειτουργία του εργοστασίου β) την διαφορά του κόστους καυσίμων μεταξύ της μικτής καύσης και της κατάστασης αναφοράς γ) τα επιπλέον κόστη προσωπικού δ) τα επιπλέον κόστη συντήρησης και ε) τα επιπλέον κόστη για αναλύσεις και την παρακολούθηση ποιότητας. Στον Πίνακα Π-30 οι τιμές αυτές εκφράζονται σε €/ MWh της ηλεκτρικής ενέργεια που παράγεται από υποκατάστατο καύσιμο και παρουσιάζονται μαζί με το υπολογιζόμενο κόστος αποφυγής CO_2.

Πίνακας Π-30 : Κόστη αποφυγής CO_2 ανάλυση του πρόσθετου λειτουργικού κόστους για τις περιπτώσεις μικτής καύσης συγκρινόμενες με την περίπτωση αναφοράς (€/ MWh ηλεκτρικής ενέργειας από καυσίμο υποκατάστασης)

	Μονάδες	Μικτή καύση εναλλακτικών καυσίμων		Προξήρανση λιγνίτη και μικτή καύση ξηρού λιγνίτη
		Μικτή καύση βιομάζας	Μικτή καύση SRF	
Κόστος επένδυσης	M €/ a	0.278	0.278	4.70
Κόστος καυσίμου	“	3.76	-2.98	-4.85
Σταθερό κόστος λειτουργίας και συντήρησης	“	0.61	0.61	2.97
Μεταβλητό κόστος λειτουργίας και συντήρησης		0.14	0.14	0.82
Σύνολο	“	4.78	-1.95	3.65

Τα αναμενόμενα έσοδα από την υλοποίηση των σεναρίων μικτής καύσης δίνονται στον Πίνακα Π-31 και εκφράζονται σε M€/. Εφόσον τα πρόσθετα έσοδα είναι μεγαλύτερα από το πρόσθετο κόστος λειτουργίας σε όλα τα σενάρια υποκατάστασης, συμπεραίνεται ότι η εφαρμογή κάθε μίας από τις εξεταζόμενες πρακτικές υποκατάστασης οδηγεί σε πρόσθετα ετήσια έσοδα. Με άλλα λόγια η εφαρμογή ενός σχεδίου υποκατάστασης φαίνεται να είναι επικερδής επένδυση σύμφωνα με αυτή την αρχική ανάλυση.

Πίνακας Π-31 : Αναμενόμενα συνολικά έξοδα σταθμού από την εφαρμογή των προτεινόμενων σχεδίων μικτής καύσης, σε M €/ έτος

Annual costs	Μονάδα	Σταθμός αναφοράς	Μικτή καύση εναλλακτικών καυσίμων		Προξήρανση λιγνίτη και μικτή καύση ξηρού λιγνίτη
			Μικτή καύση βιομάζας	Μικτή καύση SRF	
Κόστος επένδυσης	M €/ a		0.278	0.278	4.70
Κόστος καυσίμου	“	74.36	78.12	71.39	69.52
Σταθερό κόστος λειτουργίας και συντήρησης	“	12.15	12.76	12.76	15.12
Μεταβλητό κόστος λειτουργίας και συντήρησης		3.38	3.51	3.51	4.20
Μεταβλητό κόστος CO_2 (μετά 2013)		53.59	51.45	52.28	50.03
Σύνολο	“	143.68	146.11	140.22	143.57

Οικονομική βιωσιμότητα των προτεινόμενων σχεδίων υποκατάστασης λιγνίτη

Στην παρούσα ενότητα συγκρίνονται τα προτεινόμενα σχέδια υποκατάστασης σε σχέση με την οικονομική τους επίδοση. Οι υποθέσεις των προηγούμενων σεναρίων λαμβάνονται υπόψη στην παρούσα ανάλυση: α) θερμικό ποσοστό υποκατάστασης 5% στην μία μονάδα στις περιπτώσεις υποκατάστασης βιομάζας και SRF και β) θερμικό ποσοστό υποκατάστασης 20% σε δύο μονάδες στην περίπτωση εφαρμογής προξήρανσης λιγνίτη και υποκατάστασης ξηρού λιγνίτη. Τρεις οικονομικοί δείκτες υπολογίζονται για την αξιολόγηση των υπό εξέταση επενδυτικών σεναρίων : η καθαρή παρούσα αξία (ΚΠΑ), ο εσωτερικός βαθμός απόδοσης (IRR), και ο χρόνος αποπληρωμής της επένδυσης. Στον Πίνακα Π-33 παρουσιάζονται οι οικονομικοί παράμετροι των υπολογισμών.

Πίνακας Π-33 : Οικονομικές παράμετροι υπολογισμών

	Μικτή καύση εναλλακτικών καυσίμων (biomass/ SRF)	Προξήρανση λιγνίτη και μικτή καύση ξηρού λιγνίτη
Θερμικό ποσοστό υποκατάστασης	5	20
Χρόνος ανάπτυξης και κατασκευής προγράμματος	2	3
Χρόνος ζωής επένδυσης (έτη)	20	20
CAPEX (M €)	2.4	61.2
% επένδυσης που καλύπτεται από ίδια κεφάλαια	70	50
% επένδυσης που καλύπτεται από δανεισμό	30	30
% επένδυσης που καλύπτεται από επιδότηση	0	20

Τα δύο διαφορετικά σχέδια μικτής καύσης παρουσιάζουν μία εξαιρετικά θετική οικονομική απόδοση. Οι υπολογισμένοι εσωτερικοί βαθμοί απόδοσης (IRR) είναι πολύ υψηλοί και η περίοδος αποπληρωμής τελειώνει μέσα στον πρώτο χρόνο λειτουργίας της εγκατάστασης. Η συγκεκριμένη επένδυση μπορεί να είναι τόσο επικερδής, λόγω της χρήσης του υπάρχοντος εξοπλισμού του εργοστασίου (λέβητα, ατμοστρόβιλος, γεννήτρια, σύστημα καθαρισμού απαερίων), της πολύ μικρή πρόσθετης υποδομής που απαιτείται και της επιδοτούμενης τιμής ηλεκτρικής ενέργειας. Από την άλλη πλευρά, ένα έργο για την ενοποίηση της τεχνολογίας προξήρανσης υφιστάμενο κύκλο ατμού αποτελεί μεγάλης έκτασης επένδυση με μεγάλη περίοδο αποπληρωμής, 19 έτη και χαμηλό εσωτερικό βαθμό απόδοσης (IRR). Με άλλα λόγια μπορεί δύσκολα να θεωρηθεί ως βραχυπρόθεσμο ή μεσοπρόθεσμο έργο για την μείωση των εκπομπών CO_2 σε υπάρχοντα εργοστάσια ηλεκτρικής ενέργειας με περιορισμένο εναπομείναντα χρόνο ζωής. Η προξήρανση ως πρακτική μείωσης εκπομπών CO_2 είναι συνεπώς περισσότερο εφαρμόσιμη σε περιπτώσεις νέων μονάδων ή και νέων έργων που βρίσκονται ακόμα στο στάδιο του σχεδιασμού. Εάν σε αυτό το στάδιο γίνει ακριβής σχεδιασμός της ενοποίησης του

ξηραντήρα στον κύκλο ατμού του σταθμού, τότε μπορούν να επιτευχθούν σημαντικές μειώσεις του πρόσθετου κόστος επένδυσης για τον ξηραντήρα. Στον Πίνακα Π-34 παρουσιάζεται η καθαρή παρούσα αξία, ο εσωτερικός βαθμός απόδοσης και ο χρόνος αποπληρωμής για τα εξεταζόμενα σενάρια υποκατάστασης, και στο Σχήμα Π-30 δίνονται οι αθροιστικές χρηματοροές.

Πίνακας Π-33 : Υπολογιζόμενη καθαρή παρούσα αξία, εσωτερικός βαθμός απόδοσης και χρόνος αποπληρωμής

	Μικτή καύση βιομάζας	Μικτή καύση SRF	Προξήρανση λιγνίτη και μικτή καύση ξηρού λιγνίτη
Καθαρή παρούσα αξία (Μ €)	25.02	23.81	7.69
Εσωτερικός βαθμός απόδοσης (IRR) (%)	116.5	95.6	9.2
Χρόνος αποπληρωμής (έτη)	2	2	18

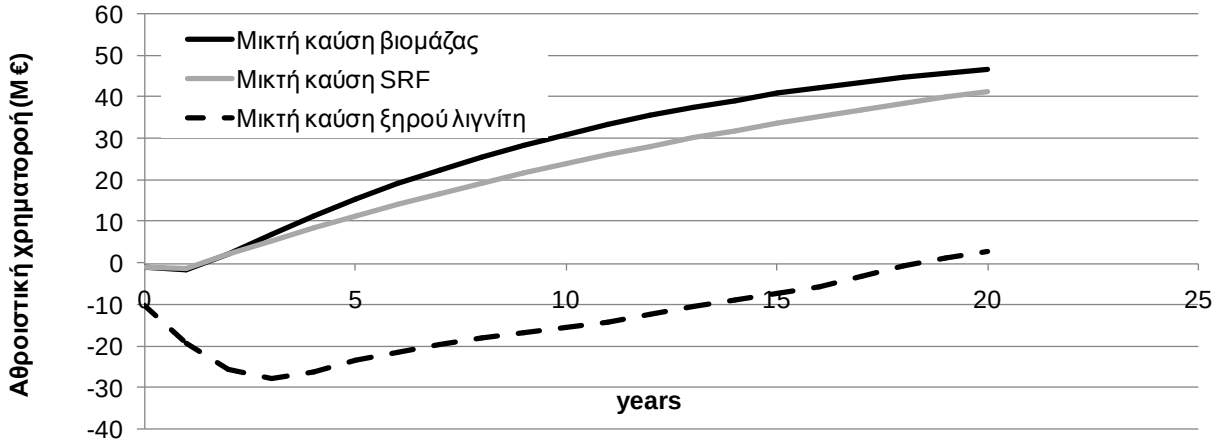

Σχήμα Π-30 : Αθροιστικές χρηματοροές για τα εξεταζόμενα σχέδια υποκατάστασης

Κεφάλαιο 8 : Σύνοψη και συμπεράσματα

Η υποκατάσταση φυσικού λιγνίτη από άλλα είδη καυσίμου θεωρείται ως η κύρια τεχνολογική επιλογή σε αυτή την διερεύνηση. Στο πρώτο σενάριο υποκατάστασης εξετάζεται η υποκατάσταση του λιγνίτη από εναλλακτικά καύσιμα με υψηλό βιογενές περιεχόμενο, ενώ στο δεύτερο η εφαρμογή της τεχνολογίας προξήρανσης λιγνίτη και η υποκατάσταση του φυσικού λιγνίτη από ξηρό. Περιβαλλοντικές, τεχνολογικές και οικονομικές παράμετροι χρησιμοποιούνται ως δείκτες απόδοσης για την ανάλυση, ενώ τα θεωρούμενα εργαλεία ανάλυσης είναι οι πειραματικές μετρήσεις, οι αριθμητικές προσομοιώσεις και οι θερμοδυναμικοί υπολογισμοί. Επιπλέον διερεύνηση σε μικρής κλίμακας εγκαταστάσεις διενεργείται, ως υποστηρικτική δράση για την αξιολόγηση των πρακτικών υποκατάστασης στη βιομηχανική κλίμακα.

Αξιολόγηση των περιβαλλοντικών και λειτουργικών παραμέτρων

Για την αξιολόγηση του δυναμικού εξοικονόμησης εκπομπών CO_2 από τις δύο εξεταζόμενες τεχνολογίες λαμβάνεται υπόψη συγκεκριμένος ελληνικός λέβητας και θεωρείται ποσοστό θερμικής υποκατάστασης 5%. Προκύπτει ότι το δυναμικό μείωσης των εκπομπών CO_2 είναι μεγαλύτερο στην περίπτωση της μικτής καύσης με εναλλακτικά καύσιμα. Η περιβαλλοντική επίδοση των δύο τεχνολογιών σε σχέση με τους δεδομένους περιβαλλοντικούς δείκτες παρουσιάζεται στον Πίνακα Π-35:

Πίνακας Π-35 : Αξιολόγηση και σύγκριση των περιβαλλοντικών παραμέτρων στα προτεινόμενα σχέδια υποκατάστασης

		Προτεινόμενα σχέδια υποκατάστασης λιγνίτη	
		Μικτή καύση SRF	Προξήρανση λιγνίτη και μικτή καύση ξηρού λιγνίτη
Περιβαλλοντικές πτυχές	Εκπομπές CO_2	√ (++)	√ (+)
	Εκπομπές συμβατικών ρύπων (NO_x, SO_2, CO)	√	!
	Βαρεά Μέταλλα στα καυσαέρια	√	δ.δ.
	HCl	√	δ.δ.
	Διοξίνες - Φουράνια	√	δ.δ.
	Ποιότητα τέφρας : ΗΜ στην τέφρα	√	δ.δ.

Γίνεται η εκτίμηση αρκετών παραμέτρων που σχετίζονται με την λειτουργική συμπεριφορά των λεβήτων και την ανάλογη επίπτωση της μικτής καύσης σε αυτούς. Μια ποιοτική εικόνα δίνεται από παρακολουθούμενες παραμέτρους, μεταξύ των οποίων είναι οι θερμοκρασίες του ατμού και των καυσαερίων και η παραγόμενη ενέργεια. Δεν βρέθηκαν δεδομένα που να δείχνουν μία σαφή επίδραση της μικτής καύσης στην λειτουργία του λέβητα. Η επισκόπηση της αξιολόγησης των τεχνολογιών υποκατάστασης με βάση τις τεχνολογικές πτυχές δίνεται στον παρακάτω πίνακα :

Πίνακας Π-36 : Αξιολόγηση και σύγκριση των τεχνολογικών παραμέτρων στα προτεινόμενα σχέδια υποκατάστασης

		Προτεινόμενα σχέδια υποκατάστασης λιγνίτη	
		Μικτή καύση SRF	Προξήρανση λιγνίτη και μικτή καύση ξηρού λιγνίτη
Τεχνολογικές –λειτουργικές πτυχές	Παράμετροι λειτουργίας(θερμοκρασία ατμού, P_e)	√	√
	Θερμική ισορροπία στο λέβητα	δ.δ.	!
	Απόδοση λέβητα(η_{boiler}) Απόδοση εργοστασίου (η_{PP})	δ.δ.	√
	Συνθήκες εξόδου από την εστία (θερμοκρασία, O_2)	√	√
	Συνθήκες καύσης στον λέβητα (θερμοκρασία, O_2)	√	√
	Πιθανά λειτουργικά προβλήματα λόγω επικαθίσεων	δ.δ.	!
	Ανάφλεξη/άκαυστα	!	√
	Πιθανά λειτουργικά προβλήματα λόγω διάβρωσης από χλώριο	!	μ.σ.

Επιπλέον λειτουργικές παράμετροι

Η εφαρμογή και των δύο τεχνολογιών υποκατάστασης λιγνίτη απαιτούν έναν αριθμό μετασκευών στον λέβητα και ενδεχομένως και σε άλλα σημεία του σταθμού. Για την πραγματοποίηση ενός σχεδίου μικτής καύσης SRF και λιγνίτη σε ήδη υπάρχον σταθμό, πρέπει να εγκατασταθεί μία περιοχή παράδοσης και αποθήκευσης του SRF. Η τροφοδοσία του SRF μπορεί να γίνει είτε με πνευματική μεταφορά, είτε με χρήση του υπάρχοντος συστήματος μεταφοράς για τη μεταφοράς του SRF μαζί με το λιγνίτη. Για την ενσωμάτωση ξηραντήρα λιγνίτη ρευστοποιημένης κλίνη σε ήδη υπάρχον κύκλο ατμού, η κατασκευή νέων συνδέσεων σωληνώσεων μεταξύ του κτιρίου του ατμοστροβίλου και του ξηραντήρα είναι απαραίτητα για : α) την απομάστευση ατμού για την διαδικασία της ξήρανσης β) την χρήση του ατμού που παράγεται από την ξήρανση ως μέσου θέρμανσης αντί αντίστοιχων απομαστεύσεων στους αρχικούς προθερμαντήρες τροφοδοτικού νερού. Επιπλέον απαιτείται η κατασκευή ενός πρόσθετου συστήματος πνευματικής μεταφοράς για ξηρό λιγνίτη και η εγκατάσταση ειδικών καυστήρων ξηρού λιγνίτη.

Αξιολόγηση των οικονομικών δεδομένων

Η αξιολόγηση των οικονομικών πτυχών δείχνει ότι τα προτεινόμενα σχέδια αντιστοιχούν σε διαφορετικές πρακτικές επένδυσης. Η εφαρμογή συναποτέφρωσης εναλλακτικών καυσίμων θεωρείται ως επένδυση μεσοπρόθεσμη, με χαμηλό κόστος επένδυσης και σημαντικά έσοδα, λόγω της επιδοτούμενης τιμής ηλεκτρικής ενέργειας για την μικτή καύση βιομάζας ή SRF. Η περίοδος αποπληρωμής είναι πολύ μικρή και η συγκεκριμένη επένδυση χαρακτηρίζεται ως πολύ επικερδής.

Τα αποτελέσματα της οικονομικής εκτίμησης δίνονται περιληπτικά στον παρακάτω πίνακα. Όλοι οι οικονομικοί δείκτες είναι θετικοί στην περίπτωση συναποτέφρωσης εναλλακτικών καυσίμων, ενώ στην περίπτωση προξήρανσης και μικτής καύσης λιγνίτη το μεγάλο κόστος επένδυσης με τα περιορισμένα οικονομικά έσοδα, λόγω έλλειψης επιδοτήσεων στην παραγωγή ηλεκτρικής ενέργειας, οδηγούν σε επενδύσεις με οριακό κέρδος.

Πίνακας Π-37 : Αξιολόγηση και σύγκριση των οικονομικών παραμέτρων στα προτεινόμενα σχέδια υποκατάστασης

		Προτεινόμενα σχέδια υποκατάστασης λιγνίτη	
		Μικτή καύση SRF	Προξήρανση λιγνίτη και μικτή καύση ξηρού λιγνίτη
Οικονομικές πτυχές	Αναμενόμενα κόστη επένδυσης και λειτουργίας	√	!
	Κόστη αποφυγής CO_2	√	√
	Βιωσιμότητα αντίστοιχης επένδυσης (δείκτες NPV, IRR, χρόνος αποπληρωμής)	√	!

Συμπεράσματα και μελλοντικές προοπτικές

Στα πλαίσια της παρούσας εργασίας αναλύθηκε και αξιολογήθηκε πληθώρα θεμάτων, για πολλά από τα οποία υπάρχει σημαντικό περιθώριο μελλοντικής έρευνας. Ακριβή μοντέλα για την περιγραφή της κίνησης και καύσης των σωματιδίων SRF αποτελούν αντικείμενο μελλοντικής έρευνας. Ακόμη η διερεύνηση των φαινομένων διάβρωσης από Cl με σκοπό την παρακολούθηση και τον έλεγχό τους αποτελεί έναν επιπλέον ερευνητικό στόχο για την αντιμετώπιση τεχνολογικών ζητημάτων κατά τη μικτή καύση στερεών ανακτηθέντων καυσίμων (SRF) με λιγνίτη. Σε σχέση με την τεχνολογία προξήρανσης και υποκατάστασης φυσικού λιγνίτη από ξηρό, η αντιμετώπιση της αναμενόμενης αύξησης των εκπομπών NO_x με μέτρα διαβάθμισης του αέρα καύσης αποτελεί σημαντικό ζήτημα μελλοντικής έρευνας. Επιπλέον η έρευνα για την επίδραση της καύσης με ξηρό λιγνίτη στην τάση για δημιουργία επικαθίσεων και συσσωματώσεων στις επιφάνειες συναλλαγής αλλά και στις μεταβολές του ισοζύγιου θερμότητας του λέβητα αποτελούν σημαντικά τεχνικά ζητήματα που πρέπει να διερευνηθούν σε περίπτωση μελλοντικής βιομηχανικής εφαρμογής της τεχνολογίας αυτής σε ελληνικούς λέβητες.

Σχετικά με την επιλογή μίας εκ των δύο τεχνολογιών θα πρέπει να επισημανθεί η ύπαρξη ενός πλήθους μη τεχνολογικών παραμέτρων, οι οποίες διαδραματίζουν εξίσου σημαντικό ρόλο στην αξιολόγηση των τεχνολογιών και στη λήψη απόφασης υπέρ ή κατά αυτής. Η διαθεσιμότητα των εναλλακτικών καυσίμων, η εφοδιαστική, η οικονομική δυνατότητα για επένδυση, το

επιχειρησιακό πρόγραμμα της εταιρείας ηλεκτροπαραγωγής, ακόμα και οι περιβαλλοντικές ανησυχίες των πολιτών μπορεί να επηρεάσουν ή ακόμα και να καθορίσουν την διαδικασία λήψης της απόφασης. Η παρούσα διατριβή αναφέρεται σε θέματα που σχετίζονται με την περιβαλλοντική, τεχνική και οικονομική επίδοση των δύο πρακτικών υποκατάστασης. Το σημαντικό αποτέλεσμα είναι ότι από τεχνολογικής σκοπιάς η εφαρμογή των δύο αυτών σχεδίων υποκατάστασης είναι εφικτή στη βιομηχανική κλίμακα σε βραχυπρόθεσμη προοπτική. Αυτό το μήνυμα θα πρέπει συνεπώς να θεωρηθεί ως ένα επιπλέον κίνητρο για τις εταιρείες ηλεκτροπαραγωγής προκειμένου να δράσουν και να αναλάβουν σοβαρές πρωτοβουλίες για την μείωση εκπομπών CO_2 σε υφιστάμενους λιγνιτικούς σταθμούς.

1 Introduction

1.1 Key facts related with electricity production

Electricity supply and the availability of the respective energy sources are regarded as two of the main issues, which most countries shall be confronted with in the coming decades. In the entire period following the industrial revolution and until the end of the 20th century the key criteria for the selection of power production systems and respective energy sources have been, apart from economic viability, the security and quality of electricity supply. Within this framework centralised energy systems such as large-scale power plants based on fossil fuels – primarily hard coal or brown coal – were constructed and operated in the industrialised countries in the years after the Second World War in order to cover the increased electricity demands resulting from high economic growth. The first doubts and criticism on the approach followed regarding electricity supply appeared in the 1970s and 1980s, when air pollution problems from power plants increased, primarily in regions of intense industrialisation. Social concerns led to the development of pollution abatement technologies, which are nowadays capable of radically reducing the respective flue gas emissions, mainly SO_2, CO, NO_x and fly ash.

By means of these technological improvements coal along with oil and natural gas continued to play a major role in the world's energy mix and electricity generation (Figure 1.1) during the entire post-war period [I-1]

In particular, regarding the role of coal, its contribution to the overall energy mix remained at the same level between 1970 and 2000 despite the fact that the primary energy supply almost doubled during this period (Figure 1.2). In the same period electricity generation almost tripled and coal continued to play a dominant role, while a significant part of power production based on oil was replaced by natural gas and nuclear power (Figure 1.3). From another perspective, the available data illustrates the high dependency of the existing electricity production system on centralized structures and primarily on coal as the main fuel. In addition, it appears that to date alternative energy sources seem to play only a minor role in the current fuel mix.

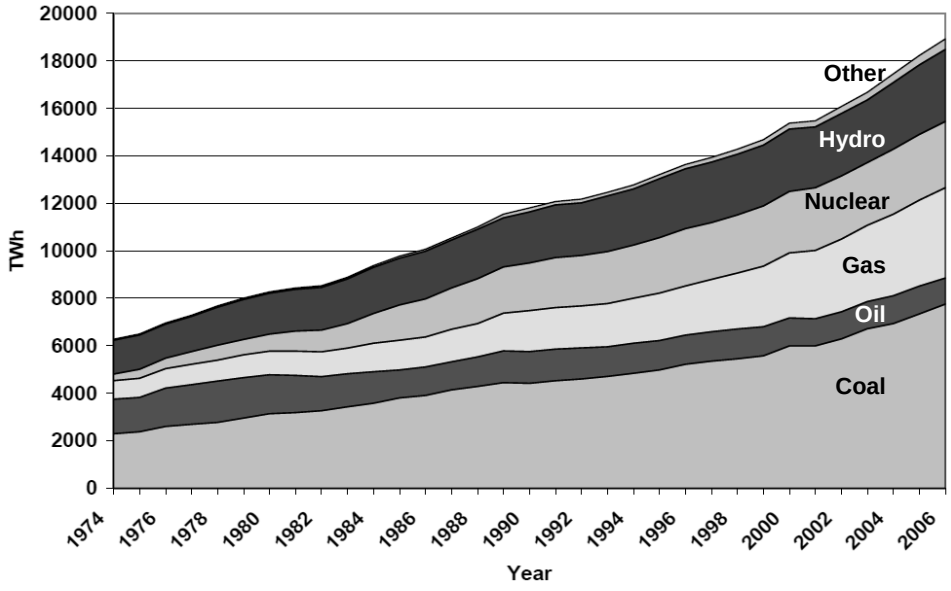

Figure 1.1 Evolution from 1971 to 2006 of world electricity generation by fuel (TWh)

(*) Other includes geothermal, solar, wind, combustible renewables & waste, and heat

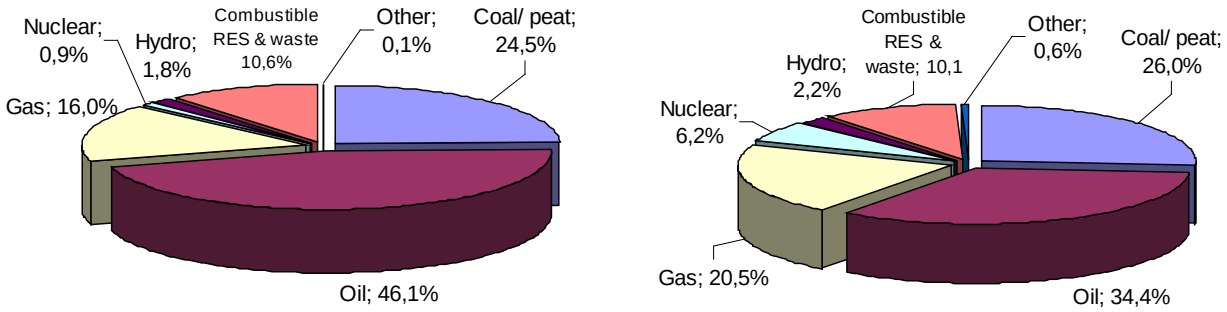

Year 1973: Total primary energy supply 2,6 10^8 TJ Year 2006: Total primary energy supply 4,9 10^8 TJ

Figure 1.2 Total primary energy supply and respective fuel shares in years 1973 and 2006

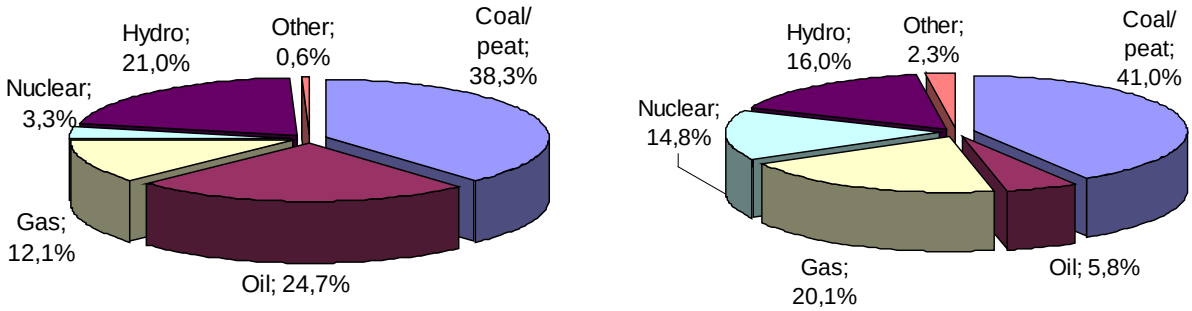

Year 1973: Total electricity generation 2,2 10^7 TJe Year 2006: Total electricity generation 6,8 10^7 TJe

Figure 1.3 Total electricity generation and respective fuel shares in years 1973 and 2006

At the end of the 20th century, the significance of another global environmental issue became prominent. According to the findings of the Intergovernmental Panel on Climate Change (IPCC), global warming is an ongoing phenomenon which is monitored by means of various observations of the earth's climate parameters, such as the widespread melting of snow and ice, the rise of the global average sea level and more significantly, the increase of the global average air and ocean temperatures. Based on recent research findings, the fourth assessment report of IPCC, published in 2007 [I-2] describes the physical science basis of the observed changes and relates them with anthropogenic gas emissions to an increased level of confidence compared to the previous IPCC Report. These gases are characterised as Green House Gases (GHG), and the most important of them, resulting from human activities are CO_2, CH_4 and N_2O.

Potential impacts of the climate change on natural and human systems, as assessed by the study, are related with fresh water resources, food and forest products, coastal systems and health. The specific influence of global warming on the aspects mentioned cannot be accurately simulated due to the large amount of unspecified parameters. However, the risk of disregarding these findings and not taking any particular measures to reduce anthropogenic green house gas emissions is too high to be ignored [I-3]. In this framework, the Kyoto Protocol was adopted in 1997 and entered into force in 2005 after being ratified by 187 UN member countries [I-4]. Since developed countries are primarily responsible for the increase of GHG values through their industrial activities of over 150 years, the Protocol places a heavier burden on them under the principle of "common but differentiated responsibilities". Specific targets are set to the European Union and 37 industrialised countries for reducing GHG emissions until 2012 to an average of 5% against 1990 levels. There are three main mechanisms defined by the Protocol in order to achieve the GHG reduction targets: the Emissions Trading Scheme (ETS), the Clean Development Mechanism (CDM) and Joint Implementation (JI). Through the Kyoto Protocol a new stock market has been developed in the

form of GHG emission reduction or removals. Since CO_2 is the main green house gas produced by industrial activities, and carbon found in fossil fuels is primarily responsible for the global CO_2 emission increase, the new stock market is called "carbon market". In the framework of the Kyoto protocol EU is committed to a relative CO_2 emission reduction of 8% until 2012 based on the 1990 levels and this target has been adopted by all EU member states.
According to statistical data [I-6], the main sectors responsible for the increase of GHG emissions are, in decreasing order, power generation, transportation, the residential sector, and the manufacturing industry and constructions. The detailed breakdown is given in Table 1.1 [I-4]

Table 1.1: EU-27 Greenhouse Gas Emissions in 2006 by Sector

Sector	(%) of total
Power Generation	30.9
Manufacturing Industries and Construction	12.9
Transport	19.3
Fugitive Emissions from fuels	1.7
Residential Sector	14.8
Industrial Processes (Non-Energy Related)	8.1
Agriculture	9.2
Waste	2.9
Other (Non-Energy Related)	0.1

Since recording of the existing GHG emissions sources and the determination of specific reduction targets is more feasible in centralised sectors like power generation and the manufacturing industry, the GHG reduction goals imposed by the Kyoto protocol have affected the two sectors mentioned above to date. This group of industries includes the following plants and production processes: coal power plants, refineries, cement-, lime-, steel production plants and chemical industries. Coal power plants, due to their large scale, represent the major percentage of the total installed thermal power in the fossil-fuel-based industrial sector. Therefore, the coal power sector has the major contribution in the increase of GHG emissions in this industrial category, although it may not have the greatest number of plants compared to the other industrial categories. *Thus, the reduction of CO_2 emissions in existing and new coal power plants remains as one of the top priorities, in order to reach the Kyoto targets*. In other sectors like buildings and transportation, which also contribute to GHG emissions, no Emissions Trading System is applied. In these sectors the effort is focused on increasing overall energy conversion efficiency, such as the efficiency of vehicle engines and the energy performance of buildings.
The first commitment period of Kyoto Protocol ends in 2012 and further actions have to be taken in the post-Kyoto era, in order continue the efforts on reducing GHG emissions globally and combat climate change. For this scope a future global climate agreement has to be prepared and signed by the countries, which are the biggest GHG emitters, until 2013. Although the expectations on reaching the global climate change agreement in the Copenhagen Congress in 2009 were not fulfilled, the Copenhagen Accord represents a step forward towards such an agreement.
EU has already decided upon ambitious goals in a defined road map until 2020 [I-7]. The following goals have been set in this framework:

- 20% reduction of Green House Gases compared to the 1990 levels. The reduction target will be increased to 30%, in case that comparable emission reduction targets are decided between developed countries.
- 20% increase of overall energy efficiency in the EU
- 20% share of Renewable Energy Sources (RES) in the overall energy consumption

In the long term, however, and beyond the goals to be set in a future climate agreement, more drastic changes in the energy sector are needed in order to mitigate climate change. According to IPCC, a decrease of atmospheric CO_2 concentration to 450 ppm, which corresponds to the

according concentration in the 1990's, is necessary in order to avoid future impacts of climate change. The International Energy Agency (IEA) has prepared a specific scenario on how to achieve this ambitious goal [I-8[I-9]. In the specific study the contribution of OECD and non-OECD member countries, primarily China, India, Russia and the Arabic countries, to GHG emissions is considered separately due to the different roles and responsibilities of developed and developing countries in the mitigation of climate change. The "Business As Usual Scenario" is initially analysed, according to which global GHG emissions will continue to rise at an almost steady pace from the levels of 27Gt CO_{2eq} in year 2008 to more than 40 Gt CO_{2eq} in 2030 (Figure 1.4). The "450ppm stabilization scenario" foresees a peak of global GHG emissions in the years around 2020 and then a decline of more than one third until 2030 so as to reach the target of 26 Gt CO_{2eq} (Figure 1.45). In order to achieve this, a radical change in the structure of the current electricity production system is necessary. The reduction goals are expected to be reached by means of the following three major targets:

- Improvement of energy efficiency in power production and consumption
- Increase of Renewable Energy Sources (RES) and biofuels
- Development and application of Carbon Capture and Storage Technologies (CCS) in the new generation of coal power plants

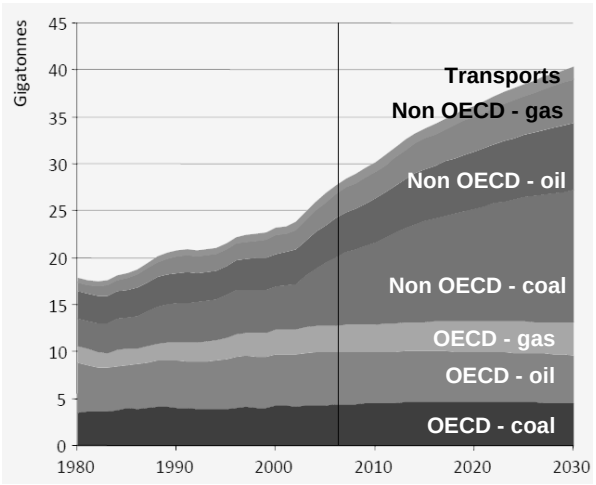

Figure 1.4: Energy related CO_2 emissions in the Business As Usual Scenario

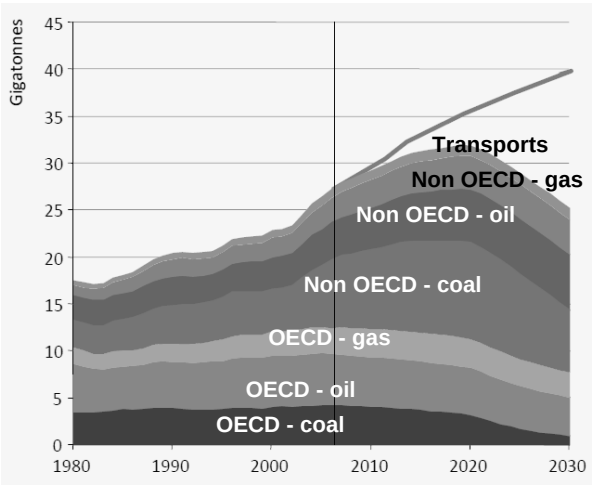

Figure 1.5: Energy related CO_2 emissions in the 450 stabilisation scenario

The break down of the expected reduction achievements by adopting the proposed measures is given in Figure 1.6. The CO_2 emission reduction potential is reported to be higher in the developing countries, due to the higher potential for improving power production efficiency. It is also stressed out that the drastic reduction of GHG emissions to the 1990 levels will not be possible without keeping constant or even slightly increasing the power production from nuclear power plants. The necessary change in the electricity generation mix until 2030 is given in Figure 1.7. An increase of the share of Renewable Energy Sources in the electricity generation mix up to 40% is set as a target, while a decrease of the share of coal to about 20% has to be achieved.

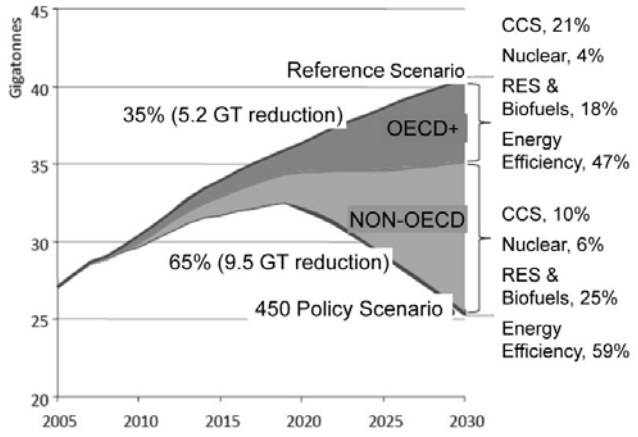

Figure 1.6: Reduction in energy related CO_2 emissions according to the "450 stabilisation scenario"

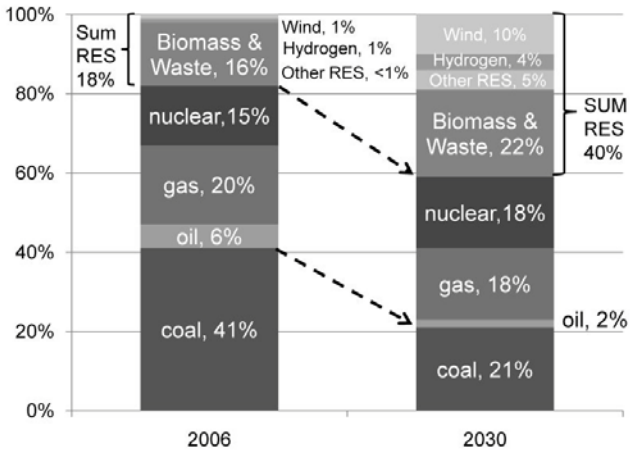

Figure 1.7: Breakdown of the electricity generation mix according to the "450 stabilisation scenario"

Apart from the GHG reduction goals mentioned, the other two conditions which are indispensable in any electricity production system in present or future time, and have to be fulfilled every time [I-10] are a) the security of electricity supply and b) the economic competitiveness and social development for the future energy mix. In order to reach all targets given, which are even counteracting at times, a combination of various measures is required, which have to be taken by the developed and developing countries. In any case, the contribution of the coal power sector to the achievement of these reduction targets is indispensable, and future as well as existing coal power plants have to play a key role in this.

1.2 Motivation for the present work

1.2.1 The role of "coal substitution practices" in existing coal power plants towards reducing GHG emissions

The role of large-scale coal plants in meeting the GHG reduction targets becomes clear by the previous analysis. An overview of the average age, size and operating efficiency of the world coal power plant fleet is given in Figure 1.8. The following important results are drawn from the data presented:

- More than a half of the coal plants globally are more than 25 years of age and their unit size is less than 300 MW_e.
- More than 80% of the operating plants are sub-critical.
- The average plant efficiency of the existing coal fleet is 28.4% while the current state-of-the-art efficiency is more than 43% for brown coal plants and more than 48% for hard coal plants.

The importance of efficiency improvement in existing power plants, in order to meet the CO_2 reduction targets, becomes apparent by the presented data. For this reason efficiency improvement is also characterised as the first priority in the road map of the "Stabilisation Scenario". The second action proposed, the increase of Renewable Energy Sources (RES) is realised in existing coal power plants through the substitution of coal by biogenic fuels. This substitution practice leads to fossil fuel savings and respectively to CO_2 emissions' reduction.

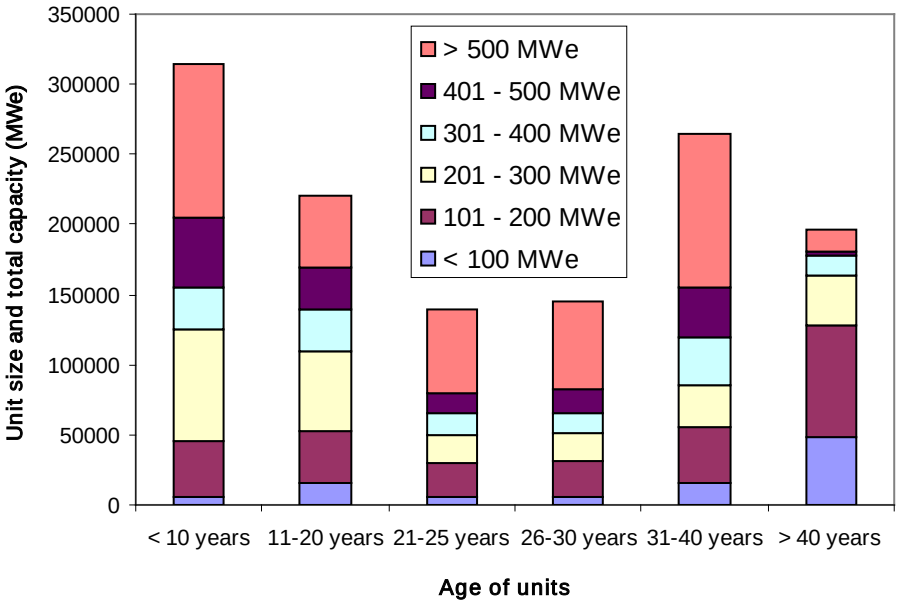

Figure 1.8: Age, size and operating efficiency of the coal power plant fleet worldwide

The third action proposed is the implementation of Carbon Capture and Storage (CCS) technologies in coal power plants. Although CCS technologies constitute an important technological milestone and may greatly assist towards meeting the set GHG reduction targets, it is not expected that they will be commercially available in the large scale before 2015 [I-11]. Furthermore, high investment costs are expected for this new technology, at least during the first period of demonstration, and, therefore, only a very small percentage of the worlds' existing coal power plant fleet is expected to be retrofitted with post-combustion CO_2 capture technologies, in order to mitigate CO_2 emissions.
The majority of the existing plants can then be divided into two main groups. The first one includes very old plants of an age of more than 30 years and low plant efficiency. For this category, in which retrofitting in order to increase plant efficiency is not marketable, there are two remaining options: a) *mothballing or permanent shutting down* of several old and usually small size units and replacing the missing capacity, if required, by a larger size and state of the art unit and b) *changing the current fuel mix* and co-utilizing "zero carbon fuels" like biomass, or "low carbon fuels" like fuels deriving from waste with a high biogenic content, in the remaining time until the final plant shut down. Biomass is considered as a fuel with zero GHG emissions since the amount of carbon dioxide produced during its combustion has been absorbed from the atmosphere over its lifetime, and for this reason the increase of the use of biomass as a renewable energy source in the current electricity sector is also promoted by European legislation [I-12]. The condition for the implementation of such a coal substitution practice is the technical feasibility of co-firing without extensive technical reconstruction works in the boiler. For both perspectives the prices of GHG allowances and of renewable fuels to be co-fired are the main factors, based on which the decision for the future plant operation is taken [I-13]. If no co-firing scenario is feasible and the operating costs overcome the estimated operating revenues, due to low plant efficiency and high prices for GHG allowances, the perspective of a planned shut down is usually the only viable option.
The second group includes plants with an expected remaining lifetime of more than 10 years, which have low steam characteristics and low efficiency rate. For this category the option of *improving plant efficiency* and *increasing the renewable energy share in the current fuel mix* is the only realistic perspective, if binding targets for drastic reduction of GHG emissions are adopted in the post-Kyoto era. The increase of the renewable energy share may be achieved by implementing co-firing practices with biogenic or low carbon fuels, as previously mentioned. The increase of plant

efficiency in an aged boiler can be achieved either by small-scale retrofitting works or by more extensive repowering works. Smaller-scale technical modifications in the boiler or the steam cycle are characterised as retrofitting, while repowering is the complete change of a boiler in order to increase steam characteristics and boiler efficiency.
The following technical modifications are regarded as retrofitting among others:

- Improving cold end efficiency by refurbishment of the condenser or the cooling tower. This is achieved by reconstruction works in the condenser in order to have it operate at a lower pressure and replacing the filling material in the cooling tower in order to improve heat transfer characteristics.
- Installing additional heat exchanger surfaces, such as additional water pre-heaters, at the end of the flue gas path in order to increase the plant net efficiency rate.
- Reducing false air by proper reconstruction works at the boiler.
- Installation of coal pre-drying systems in the case of utilization of low rank coals with high moisture content.

The economics of various retrofitting options have been evaluated in the past by IEA [I-14], while specific refurbishment options in non-OECD countries like Russia can be also found in the literature [I-15].
In the present thesis two different coal substitution practices are examined, which may assist towards the achievement of future GHG reduction targets in both groups of plants, both the older and the newer plants. *The first concept focuses on the substitution of coal by waste recovered fuels with considerable biogenic content, while the second concept focuses on coal pre-drying and the substitution of raw brown coal by dry brown coal as a retrofitting option, in order to increase plant efficiency*.
Waste recovered fuels derive from mechanical processing of Municipal Solid Waste (MSW), and are biogenic to a high percentage since they include paper and cardboard to 40-70% w.t. For the specific waste recovered fuels, which are in agreement with the specifications of the European Standardisation Committee (CEN), the term Solid Recovered Fuels (SRF) may be used. The thermal utilization of SRF will be addressed in detail in the following chapters. Depending on the SRF biogenic content and the coal quality, the substitution of 1 kg lignite by SRF may bring savings of more than 1 kg CO_2 [I-16], [I-17].
Regarding the second concept examined in the present thesis, although dry brown coal is fossil fuel, as raw brown coal, the substitution of raw brown coal by dry brown coal through the integration of a coal pre-drying system in an existing steam cycle leads to savings of CO_2 emissions. This is achieved through a) the reduced mass flow of the supporting fuel co-fired compared to the raw fuel mass flow, owed to the increased heating value of the supporting fuel and b) the overall plant efficiency increase through the improvement of the drying process and the minimization of the respective energy losses. Such an integration of a pre-drying concept in an existing Greek power plant is investigated in the present work by thermal cycle calculations as well as by experimental activities and numerical simulations. The expected plant efficiency increase is predicted by thermal cycle calculations. The influence of dry coal co-firing on the combustion and behavior and operation of the boiler is assessed by experimental measurements in small scale and industrial scale facilities as well as by respective numerical simulations of these facilities.
In order to clarify important terms that are often used in the present thesis, proper definitions are given.

- “Coal substitution” is defined as the replacement of a specific fraction of the coal input of a power plant by another fuel by keeping the thermal input constant at the same time.
- “Co-firing or co-combustion” is the simultaneous firing of two - or more than two - fuels in the same furnace.

- "Main" or "reference" or "base" fuel is the fuel with the highest mass flow. In the case of the large-scale Thermal Power Plants (TPPs) considered in the present work, the main fuel is usually brown coal.
- "Alternative fuel" is a broad characterization, which includes every type of fuel that is not considered as fossil fuel. Biogenic fuels or fuels derived from waste are, therefore, included in the definition. The present investigation focuses on a specific group of alternative fuels, the Solid Recovered Fuels (SRF). Specific definitions of the terms "Waste Derived Fuels", "Refused Derived Fuels (RDF)" and "Solid Recovered Fuels, (SRF)" and the difference between each other are given in the next chapter.
- Solid fuels with higher heating value than the main fuel, which are co-fired together with the main fuel in order to increase furnace temperatures and support flame stability, are characterized as "supporting fuels". Supporting fuels are usually needed in power plants firing low rank lignites with high ash and moisture content. Dry brown coal is considered as a supporting fuel.

In the following sections additional argumentation is given, which supports the further spread of coal substitution in large scale power plants, as a practice which may bring further environmental, operational and economic benefits.

1.2.2 The need for sustainable waste management strategy as additional motivation for SRF co-utilisation in existing thermal power plants

The potential contribution of SRF co-utilisation in existing coal power plants in the waste management issue is an additional argument speaking in favour of this co-combustion practise and is in detail addressed in the present section. Waste treatment practices in EU member countries undergo a transition period in the present years. The reduction of the waste amount disposed at landfills and the promotion of more sustainable waste treatment methods are considered as key elements in the future European waste management policy. The European Community Strategy for Waste Management, COM (96)/399, sets materials and energy recovery from waste as the second most favourable option after the prevention of waste production, and the European Waste Landfill Directive (1999/31 EC) sets specific reduction targets for the biodegradable waste quantities disposed at landfills (Figure 1.9). In this framework, the mechanical treatment of waste and the thermal utilisation of waste derived fuels become technological options of prime importance [I-18], [I-19].

Additionally, mass burn incineration of mixed MSW without any pre-treatment stage constitutes an alternative waste treatment concept applied in many European countries. Current waste treatment practices in the European countries are presented in Figure 1.10. It is noted that in countries with increased incineration capacities (>25% of the waste stream) materials' recovery is also a favoured waste treatment practice. Therefore, these two different technological options should not be considered as competitive to each other. In other words, both incineration and waste treatment facilities are needed as two supplementary factors for a more sustainable future waste treatment policy.

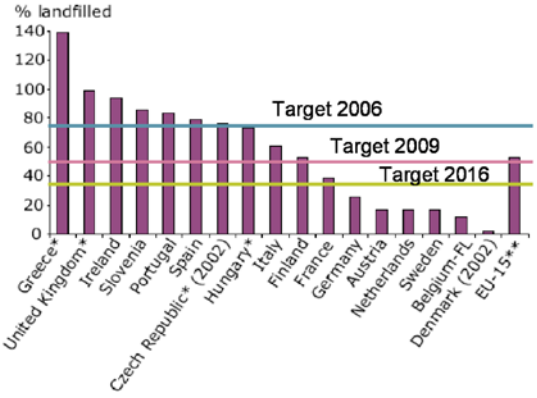

Figure 1.9: Biodegradable waste landfilled in 2003 and set reduction targets, Source: European Environment Agency

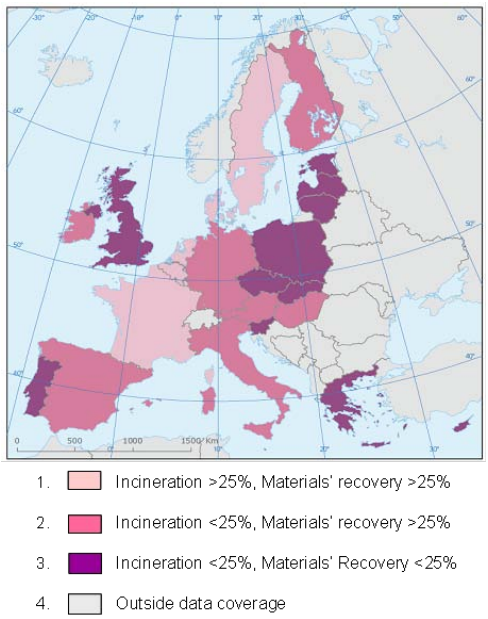

Figure 1.10: Country grouping according to the current waste management practices, Source: European Environment Agency

The need for alternative waste treatment options has become prominent in some countries fo central Europe like Germany, where the prohibition of land filling of MSW in June 2005 led to a drastic increase of waste derived fuels produced in waste treatment plants and subsequently to a lack of respective capacities for their energetic utilisation. These capacities can be a) dedicated mono-combustion plants for their incineration, b) coal and cement plants for their co-incineration together with coal up to a definite thermal share.

In Figure 1.11 the production of waste derived fuels in Germany is presented along with the available utilisation capacity since 2005. A prediction for the development of these values until 2020 is also given. The lack of treatment capacities in the years 2005-2009 can be noticed. This shortage was covered by increasing the incineration and co-incineration capacities, either by spreading the co-firing practices in cement and coal plants in Germany or by building new incineration plants dedicated for the incineration of the waste derived fuels. Performed studies [I-19],[I-20],[I-21] indicate that no capacity problems for the utilisation waste derived fuels are expected for the forthcoming years in Germany. It should be however pointed out that the particular market has been stabilised after undergoing a long transition period of high capacity shortages. It is therefore expected that many European countries will also undergo this transition period in the coming years, and increase their thermal utilisation capacities for waste derived fuels, in order to comply with the new European standards and practices for waste treatment. Co-combustion of waste recovered fuels in existing cement kilns and utility boilers may play a key role at this point. Due to the large scale of the particular plants, partial substitution even in a low thermal share of 5% can effectively assist in covering capacity limitations.

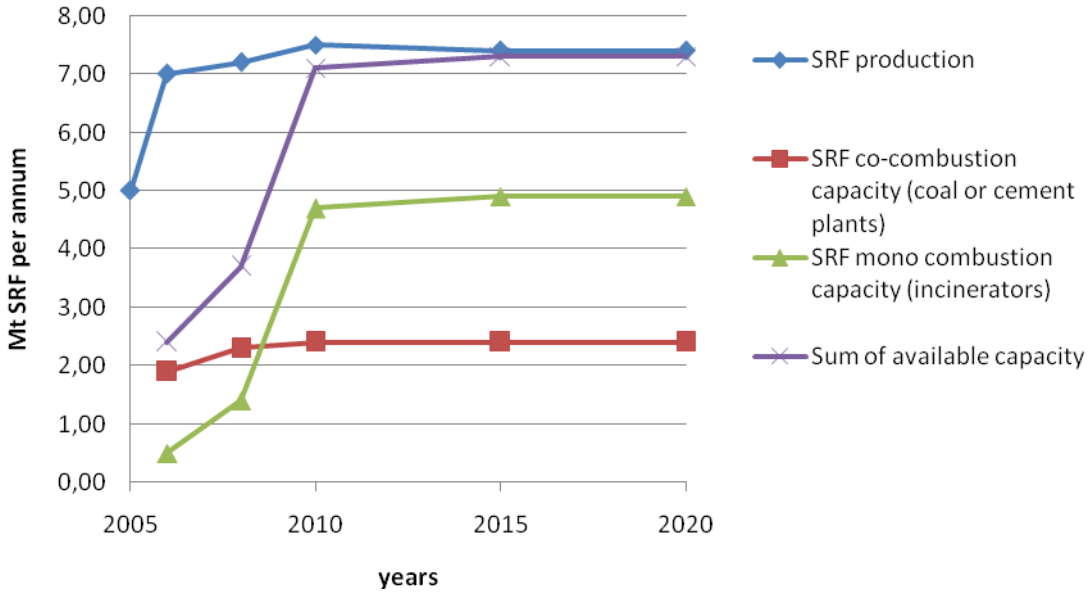

Figure 1.11 Market study on the development of SRF production quantities and incineration capacities in Germany, Source: Prognos AG [I-20]

1.2.3 The utilization of supporting fuels in Greek power plants as additional motivation for the implementation of lignite pre-drying in existing units

An additional reason for the investigation of lignite pre-drying technologies, apart from the potential plant efficiency increase, is the utilization of dry lignite as a supporting fuel in Greek power plants. Greece is the second largest lignite producer country in EU 27 and more than 50% of the Greek electricity production is based on large-scale lignite power plants [I-22],[I-23],[I-24]. Securing lignite availability and quality is, therefore, of prime importance. The poor quality and high variation of the Greek lignite feed [I-25] imposes additional restrictions on power plant operation. Firing of extremely low quality lignite may lead to combustion stability issues to a decrease of produced power below nominal levels and even further on to unexpected outages of lignite boilers.

In order to deal with the problem of the varying lignite quality, two measures are taken [I-26]: a) fuel homogenisation and b) support of combustion with dedicated supporting fuels. Following fuels are considered as supporting fuels in Greek power plants and have been used in the past: diesel, hard coal [I-27], xylite and dried lignite dust [I-28]. Flame supporting by using the start-up burners and firing liquid fuels is an extremely costly option, although it provides great flexibility in the combustion control by using the existing start-up firing system. Co-firing other coal types like hard coal or xylite as supportive fuels together with the reference lignite may impose significant risks on boiler operation, although it is considered as a favourable option from a financial point of view. The difference in the ash chemistry between the reference and the supporting fuels may lead to unexpected low melting eutectic points in the ash, which may cause slagging problems in the furnace and the superheater surfaces. The most appropriate solution from a technical point of view is, therefore, the flame support by using the same lignite quality used in the plant after drying a specific mass flow of raw lignite in an external drying facility [I-29]. Several pre-drying systems, which are available in the industrial scale and can be integrated in existing power plants, are described in the next chapter. The integration of a dedicated pre-drying system in an existing steam cycle would therefore, assist the operational availability of the boiler in addition to the expected plant efficiency increase.

1.3 Scope of work, methodology and approach

The main scope of work in the present thesis is the evaluation and comparison of the two proposed coal substitution practices on the basis of specific criteria. The main motivation for both concepts is CO_2 emissions' reduction in existing coal power plants. A number of additional environmental, technical and economical aspects, necessary for the overall comparison of the two concepts, are also considered. Experimental activities, numerical simulations and thermodynamic calculations are used as methodological tools for the evaluation of the proposed co-firing concepts. Two measurement campaigns in utility boilers are planned, carried out and evaluated during the large scale experimental investigations. The demonstration of SRF co-firing is carried out in the 600 MW_e German power plant, while the dry lignite co-firing tests take place in a 75 MW_{th} Greek power plant. Numerical simulations of the industrial boilers based on Computational Fluid Dynamics (CFD) simulation tools are further carried out for operational modes, which cannot be tested in real conditions. In order to evaluate the applicability of the lignite pre-drying technology in Greek power plants, respective thermal cycle calculations are carried out. The integration of a modern fluidized bed lignite dryer in an existing lignite power plant has not been realised yet in the large scale and therefore, the evaluation of this concept is based on calculations.

Small-scale investigations are performed as supporting activities for the evaluation of the large-scale co-firing concepts. In the case of SRF co-firing, the performed small-scale investigations focus on the development of a new combustion model for SRF particles and its validation with available experimental data from a lab scale combustor. In the evaluation of the pre-drying concept the small-scale investigations include drying tests of Greek dry lignite at a laboratory-scale fluidised bed dryer and combustion tests of pre-dried Greek lignite at a 1MW_{th} experimental combustion facility. During the combustion tests several parameters are examined concerning, among others the combustion behavior of pre-dried lignite, the emissions and the slagging and fouling tendency. Numerical simulations of the performed combustion tests based on a CFD simulation tool are also carried out, in order to define a model setup, based on which the combustion behaviour of pre-dried lignite is accurately predicted. The particular model setup is then used in the large-scale simulations.

The environmental, technical and economic parameters which are used as performance indices for the evaluation of the examined concepts are given in Tables 1.2, 1.3, 1.4, while the analysis tools used for the evaluation are also presented in each cell. Regarding the environmental performance indices, CO_2 emissions and their predicted reduction by each of the two proposed concepts is the main parameter considered together with the conventional flue gas emissions SO_2, NO_x, CO and dust, for which respective emission limits are set by the European Large Combustion Plant Directive (LCPD) [I-30]. However, since Solid Recovered Fuels are considered as waste according to European legislation, their thermal co-utilisation in existing coal plants is subject to the Waste Incineration Directive (WID) [I-31]. Periodic measurements of additional non-conventional flue gas emissions including HCl, Dioxins - Furans and Heavy Metals are required by the WID, and these measurements are performed during the large-scale SRF co-firing campaign. The non conventional flue gas emissions are therefore also included in the list of the environmental performance indices.

Securing a stable, reliable and efficient boiler operation without unexpected knock outs is the main target regarding the technical aspects. A number of technical parameters can be used as performance indices for this evaluation; the flue gas temperature at the furnace exit, the ignition and burnout behaviour of the fuel, the heat flux to the evaporator wall, the boiler efficiency and the slagging and fouling tendency of the fuel or the corrosion tendency due to chlorine are regarded as the main technical parameters considered in the particular investigations.

The evaluation based on the economic criteria includes the CO_2 avoidance cost for both technologies and the evaluation of both concepts, after taking into account the necessary investment costs and the expected revenues due to the CO_2 emissions' reduction.
Regarding the experimental investigations performed in the large scale, it is noted that these measurement campaigns require the simultaneous contribution of working groups with different specialisations rather than single researchers. In particular, the measurement campaign performed in the German power plant is carried out by a large team of engineers divided in different working groups. Some of the results presented are, therefore, not only part of the author's work, but part of the work of a whole working group. For reasons of completeness and because the work of all groups is published as a common result in scientific journals, it is shown in the present thesis and marked in Tables 1.2, 1.3 with an asterisk (*). Moreover, some technical or environmental aspects are examined for only one of the two concepts, since no effect on the particular parameter is expected or can be measured in the case of the other concept. For example, co-firing dry lignite with raw lignite is not expected to lead to increased heavy metal or dioxine concentration in the flue gas, since dry lignite is produced from raw lignite and has the same quality. In this case the particular analysis is considered as "not relevant" and "n.r." is written in Tables 1.2, 1.3. In other cases, some examinations, which are not carried out, due to different scheduling, are characterized as "not investigated", and "n.i." is written in the Tables 1.2, 1.3

Table 1.2: Analysis tools used for the evaluation of the environmental aspects

		Proposed brown coal substitution concepts	
		SRF co-firing	Lignite pre-drying and dry lignite co-firing
Environmental aspects	CO_2 emissions	Mass balance based on experimental data	Thermodynamic steam cycle calculations, mass balance based on experimental and plant design data
	Conventional flue gas emissions (NO_x, SO_2, CO)	Measurements	- Measurements - CFD simulations (NOx emission simulations)
	HM in the flue gas	Measurements (*)	n.r.
	HCl	Measurements	n.r.
	Dioxins – Furans	- Measurements (*) - CFD simulations (prediction of potential PCCD formation through particle residence time calculations)	n.r.
	Ash quality: HM in the ash	Measurements (*)	n.r.

Table 1.3: Analysis tools used for the evaluation of the technological aspects

		Proposed brown coal substitution concepts	
		SRF co-firing	Lignite pre-drying and dry lignite co-firing
Technological - operational aspects	Operational parameters (steam temperatures, Pel)	Measurements (*)	Measurements
	Overall boiler heat balance	n.i.	- Measurements - Thermal cycle calculations
	Heat Flux to Evaporator	CFD simulations	CFD simulations
	Boiler Efficiency (η_{boiler}) Power plant efficiency (η_{PP})	n.i.	Thermal cycle calculations
	Combustion conditions at furnace exit (temperature, O_2)	- Measurements - CFD simulations	- Measurements (temperature) - CFD simulations
	Combustion conditions in the furnace (temperature, O_2)	CFD simulations	CFD simulations
	Risk of potential operational problems due to slagging and fouling	n.i.	Measurements at the small-scale facility
	Ignition/ Burnout	CFD simulations	- Experimental - CFD simulations
	Risk of potential operational problems due to chlorine corrosion	Measurements (*)	n.r.

Table 1.4: Analysis tools used for the evaluation of the economic aspects

		Proposed brown coal substitution concepts	
		SRF- co-firing	Lignite pre-drying and dry lignite co-firing
Economic aspects	Expected investment and running costs	calculations	calculations
	CO_2 avoidance costs	"	"
	Feasibility of investment	"	"

Index

"nr": no change is anticipated for the specific parameter and, therefore, it is considered as "not relevant" for the examination

"ni": the specific parameter is "not investigated"

(*): data obtained from the overall working team and not exclusively from the author's work

The final evaluation of the parameters considered is carried out by the comparison of the respective parameter values in the reference and the co-firing cases. The results of the respective analyses are presented in a qualitative way by the following signs:

"√" The tick mark implies that no drastic change is noticed between the baseline and the co-firing operation for the considered parameter. The parameter remains in the normal and expected range and its behaviour is, therefore, regarded to be within "accepted" limits.

"!" The exclamation mark implies that the examined parameter is affected by the proposed co-firing practice and the particular change should be closely addressed, since in the future it may risk the efficient and reliable performance of the plant in technical or environmental terms. The parameter is, therefore, considered as "accepted with reservations".

"x" The x character implies that the examined parameter is negatively influenced by co-firing and lays outside of the accepted limits, it is therefore considered as "not accepted". The investigation of alternative options, through which the present behaviour may be improved is, therefore, required.

The respective limits for each of the signs mentioned are given at this point. The limits of the environmental performance indices derive from the legislative limits of the LCP Directive and the Waste Incineration Directive. Any value of the environmental parameters, which is above legislative limits cannot be accepted. Modifications in the combustion process are reqired, so that the particular parameters will comply with the environmental limits in the future.

The evaluation of the technical parameters is more complex. No certain operational limits apply for most of the technical parameters, and for this reason a comparison with the reference case scenario is used. The relative difference (Δx) of the operational values between the baseline and the co-firing mode should be within certain limits as described in Table 1.5. The relative difference is calculated according to Equation 1.1, where $x_{co\text{-}firing}$ and $x_{reference}$ are the according values in reference and co-firing conditions.

$$\Delta x = \frac{x_{co-firing} - x_{reference}}{x_{reference}} \cdot 100\% \qquad \text{(Eq. 1.1)}$$

The particular limits depend on the specific parameter. In the case of the furnace exit temperature, for example, a high increase could lead to slagging and fouling phenomena in the superheater section, while a significant decrease could lead to reduced steam production and, subsequently, to a power loss. Keeping the furnace temperature within a certain variation range is, therefore, required. The same applies to the evaporator heat flux, while on the other hand, a decrease of NO_x emissions and unburned carbon in ash is favored. NO_x emissions are also regarded as a technical parameter since their increase or decrease trend is also important in addition to keeping the respective legislative limits. An increase of the particle residence time in the furnace is favored, particularly in the case of SRF co-combustion, in order to ensure the destruction of dioxins and furans, while an increase of the plant efficiency rate in the case of the implementation of lignite pre-drying is also required. Finally, no qualitative evaluation criteria are used for the evaluation of the economic aspects since the economic data presented are indicative and are not complete financial scenarios.

Table 1.5: Criteria for process evaluation

Rank/ Criteria		Temperature / Evaporator Heat Flux	Residence time	NO_x emissions / unburned C(s)	Efficiency rates (percentage units)
Accepted:	√	-5% ≤ x ≤ +5%	x > 0	x < 0	x > 0
Accepted with reservations:	!	-10% ≤ x ≤ -5% or +5% ≥ x ≥ +10%	-10% ≤ x ≤ 0	0 ≤ x ≤ 10%	-
Not accepted, modifications necessary:	X	x < -10% or x > +10%	x < -10%	x > 10%	x < 0

2 Fuel characterisation: Alternative and supporting fuels used as substitute fuels for raw brown coal

Summary
The present chapter focuses on the presentation, characterisation and comparison of the different fuel types which are investigated as possible substitute fuels for brown coal. Regarding Solid Recovered Fuels, a definition is given according to the European Standardisation Committee, the waste fractions used as input streams are considered and the main stages of their production process are briefly explained. The current CEN standardization activity for SRFs is also mentioned and the proposed classes for SRF classification are presented. The biogenic fraction of SRF and the respective determination methods are also presented. The second part of the chapter includes the available fuel retrofitting concepts in existing brown coal power plants in order to increase their plant efficiency. The integration of brown coal pre-drying in existing steam cycles is one of the most promising concepts for the further efficiency increase in lignite power plants. Already available lignite pre-drying processes are presented, while the Fluidised Bed Drying Concept with internal Waste Heat Utilisation, the "WTA Concept" is closely examined. In the last part the two coal substitution concepts are compared in terms of their economic performance. The expected additional costs and revenues are analysed for both concepts and according investment scenarios are developed and evaluated.

2.1 Solid Recovered Fuels (SRF) - an introduction

2.1.1 Definition, specifications, quality assurance

Waste recovered fuels are produced from various waste fractions after specific mechanical, or mechanical and biological processing steps. They are used as substitute fuels for hard coal or brown coal, in the coal based industrial sector, including primarily cement kilns and coal power plants. The production and thermal utilisation of these fuels date back to the time of the oil crisis; since then waste treatment technologies have gradually developed and improved, and the production capacity has steadily increased in all EU member states.

The need for standardisation of waste recovered fuels became apparent in recent years, when a high increase of the fuel production led to the development of a competitive market for the thermal utilization of waste recovered fuels in industrial facilities like cement kilns and thermal power plants. The European Commission, aiming to contribute to the further development of this market, to ensure the quality of the traded fuels, and avoid any unwanted mishandling of waste, such as the dilution of hazardous waste in waste recovered fuel streams, has issued a mandate on the standardisation of waste recovered fuels. Two Technical Committees have been formed in order to assist this standardisation process:

- The CEN Technical Committee (TC) 335, which covers all fuels purely derived from "biomass" as defined in the scope of the Waste Incineration Directive 2000/76/EC [II-1]. Agricultural and forest residues are included in the activities of TC 335.
- The CEN Technical Committee (TC) 343, which covers all other non hazardous solid waste recovered fuels [II-2].

The present thesis focuses on the work of TC 343 on the standardization of waste recovered fuels, which are not considered as biomass but may have biogenic content. CEN/ TC 343 started work in the beginning of 2003. The results of the Committee include published Technical Specifications (TS), a kind of a pre-standard, and Technical Reports (TR). These

Technical Specifications are regarded as Pre Norms (prENs) and after their validation, they are expected to be reviewed and upgraded to EN standards in 2011.
According to Technical Specification 15357, Solid Recovered Fuels are defined as "solid fuels prepared from high calorific fractions of non-hazardous waste materials intended to be fired in existing coal power plants and industrial furnaces" [II-3]. Therefore, the term SRF refers to a wide range of solid waste recovered materials ranging from high calorific fractions of Municipal Solid Waste (MSW) to sewage sludge and shredded tyres.
In contrast to other terms such as "Secondary Fuels" or "Waste Recovered Fuels" or "Waste Derived Fuels" or "Refused Derived Fuels, RDF" or "Alternative Fuels and Raw materials, AFR", a specific permission procedure, defined by CEN TC/ 343, has to be followed for the characterisation of a fuel as "SRF" (Figure 2.1). The necessary steps include: a) the compliance of the fuel producer with the standards of TC/ 343 on fuel specifications and classes, currently under development [II-4], and b) the self declaration of the produced fuel as SRF. In this way, the term "SRF" becomes a quality label indicating that specific quality criteria apply to the particular fuel characterised as SRF.
Some European countries have already taken a step further and have developed their own quality labels for SRF, which are based on certain quality assurance systems. The German RAL GZ-723 developed by the BGS [II-5], the Austrian quality label developed by ÖG-SET and the Finnish label SFS 5875, proposed by the Finnish authorities, are some examples of SRF quality labels. A comparison between these systems can be found in the Best Available Techniques (BAT) Reference Document (BREF) on Solid Recovered Fuels published by the European Recovered Fuel Organisation [II-6]. Furthermore, Technical Specification TS 15358 provides the framework for the application of quality management systems in the SRF production process [II-7].

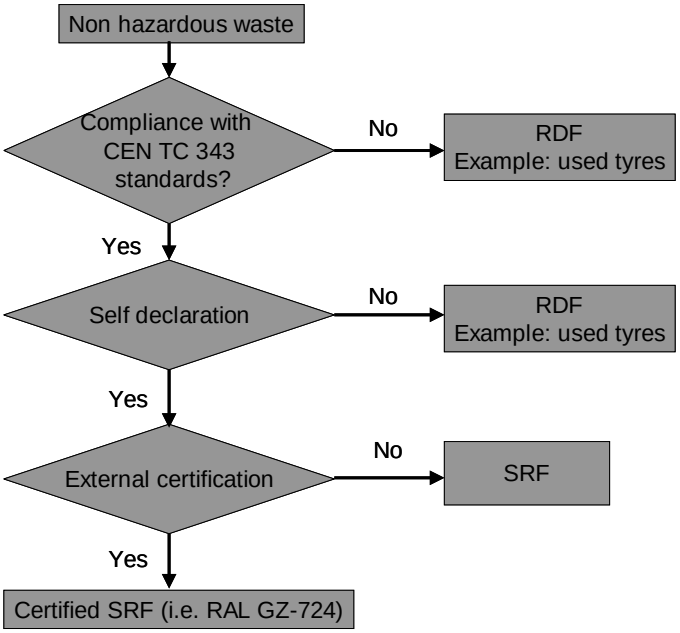

Figure 2.1 Required procedure for the characterisation of a waste recovered fuel as SRF, Source: [II-8]

The work of TC 343 is devided in five different working groups covering different areas of the standardisation procedure.

WG1: Terminology and quality management
WG2: Fuel classification ad specification

WG3: Sampling and Determination of the biomass content of SRF
WG4: Physical, mechanical tests
WG5: Chemical tests

A schematic diagram with the activities of each working group is presented in Figure 2.2.

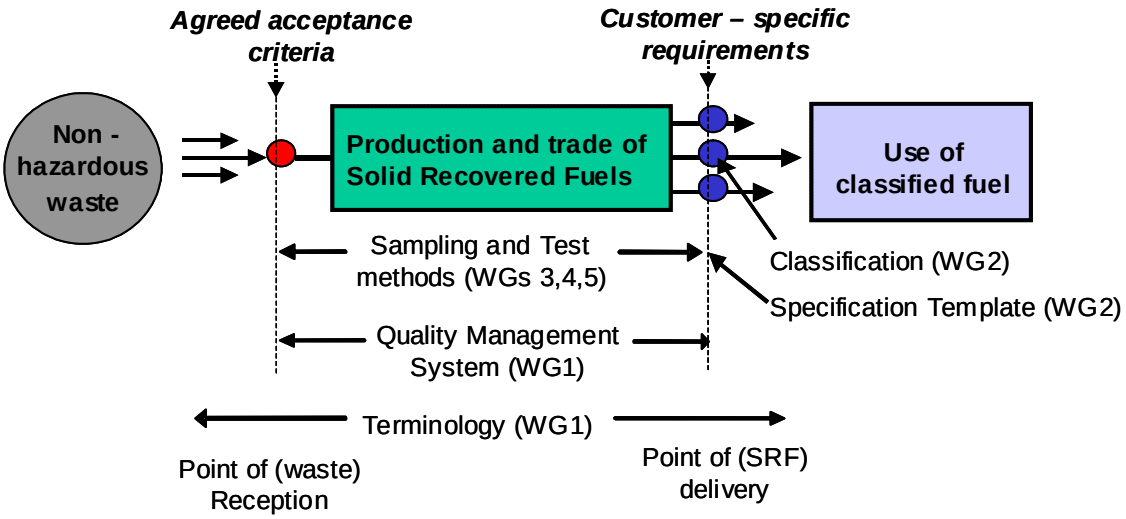

Figure 2.2: Overview of the standardisation activities in CEN/ TC 343, Source: [II-3]

A broad range of waste can be used as input streams for the production of Solid Recovered Fuels according to the European Waste Catalogue (2000/532/EC) [II-9]. The main waste categories, which are commonly used, are given below:
Group 1: wood, paper, cardboard and cardboard boxes,
Group 2: textiles and fibres,
Group 3: plastics and rubber,
Group 4: other materials (e.g. waste ink, used absorbers, spent activated carbon), and
Group 5: high calorific fractions from non-hazardous mixed collected wastes.

2.1.2 Waste Treatment methods

SRFs are produced in specific waste treatment facilities. The majority of them utilise mixed Municipal Solid Waste fractions as the main input stream for SRF production. Other waste streams which are also commonly utilized are bulky waste and specific fractions of commercial waste, such as packaging material or old paper. The production process of SRF may include various steps. Among them the most significant are:

- Screening
- Size reduction
- Ferrous and non ferrous metal separation
- Classification based on conventional mechanical methods like air or centrifugal or ballistic classification
- Classification based on novel optical methods like Near Infrared Spectroscopy (NIR)
- Thermal or biological drying
- Compacting, pelletising

The form of the produced SRF at the end of the process may differ according to the market demand; nevertheless, typical forms of SRF are bales, fluff and soft pellets. Hard pellets are not usually applicable for SRF, in contrast to biomass, due to the different physical properties of the fuel. More information on the available process technologies and the corresponding

Best Available Techniques in Waste Treatment Plants is provided in the European Reference Document (BREF) for Waste Treatment Industries [II-10].

The process design in waste treatment plants varies significantly among different plants, and no categorizations can be easily established. Different technological solutions are proposed for each plant, depending on the type and quality of the waste input stream and the specifications for the SRF to be produced. No standardised concepts are, therefore, available. According to a first categorization based on the treatment method, waste treatment processes can be divided in two major groups: the plants where only mechanical processes are applied, and the plants where the waste streams undergo mechanical and biological processes.

Another categorisation parameter is also related with the design of the sorting procedure. A sorting procedure can be characterised as “positive” or “negative”. When applying positive sorting methods, the high quality of the sorted out material is preferred over quantity. The average values and the standard deviation of specific fuel characteristics like the heating value or the chlorine and heavy metal content, can be used as quality parameters. As a result, a small fraction, less than 50% of the main inlet stream is usually taken out for further treatment in the positive sorting procedures. The positively sorted stream is, however, more homogeneous and may have better physical characteristics, eg. high heating value, low chlorine content. On the other hand, in a negative sorting procedure only the unwanted materials are sorted out from the inlet stream. In this way, a higher outlet stream mass flow is achieved; nevertheless, the quality and homogeneity of the outlet stream is usually lower than that of the stream produced by a positive sorting process. After having collected and evaluated data on the design and operation of most of the German waste treatment plants, Thiel [II-11] has proposed the categorization of the waste treatment concepts into four main groups:

a. Material stream separation
b. Mechanical - biological stabilization with biological drying
c. Mechanical - physical stabilization with thermal drying
d. Mechanical (- biological) pre-treatment before the thermal treatment

In the first group, a high calorific fraction is separated from the main waste stream through consecutive mechanical processes (Figure 2.3a). SRF derives from this high calorific fraction. The remaining waste stream undergoes a biological drying process, during which the moisture content is reduced, and is then disposed to landfills. A second mechanical treatment process where additional stabilised high calorific fractions are recovered from the waste stream is optional and is installed in some cases. The second and third groups of waste treatment plants include a drying step as a key process step, which is either biological (group b, Figure 2.3b) or thermal (group c, Figure 2.3c). By reducing the water content of the input waste stream a higher calorific value is achieved for the recovered high calorific fractions. Finally, the fourth concept includes a main mechanical process step, in which the high calorific fraction is recovered from the inlet waste stream (Figure 2.3d). The remaining waste stream goes to incineration facilities either directly or after undergoing a biological drying and a last mechanical treatment step where an additional high calorific fraction is recovered from the stabilised waste stream. The particular treatment process is adopted for the production of the Solid Recovered Fuel SBS® by the German company Remondis. The demonstration of SBS® co-firing together with Rhenish brown coal in a large scale power plant is presented in one of the next chapters.

Finally, it has to be stressed that the particular categorisation is based on the experience in German waste treatment plants. Since source separation of waste is applied to a high extent in households in Germany, the organic waste, like food residues, is usually not included in the MSW and for this reason the organic content of German MSW is usually low. In other European countries, like Greece, where organic waste is not separated from the main waste

stream, MSW composition is different and, therefore, the waste treatment concepts are also differentiated. In this case, an additional composting step may be included in the process so that the remaining waste fraction with high organic content can be recovered. Nevertheless, due to mixing of the organic content with the main waste stream, the produced compost is not of a quality comparable to the products derived from separate composting processes because of the higher content in heavy metals. The layout of the waste treatment facility operated in Athens is presented in Figure 2.4 as an example of a waste treatment process which integrates a composting step.

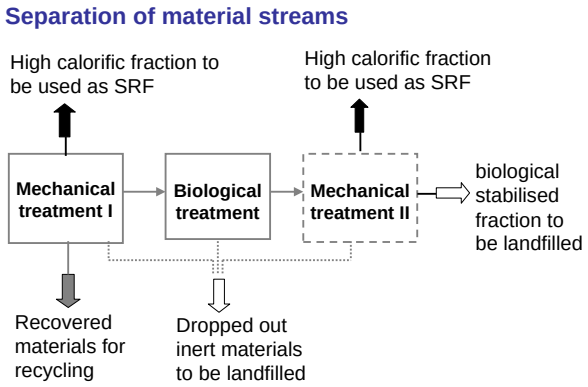

Figure 2.3a: Waste treatment concept a

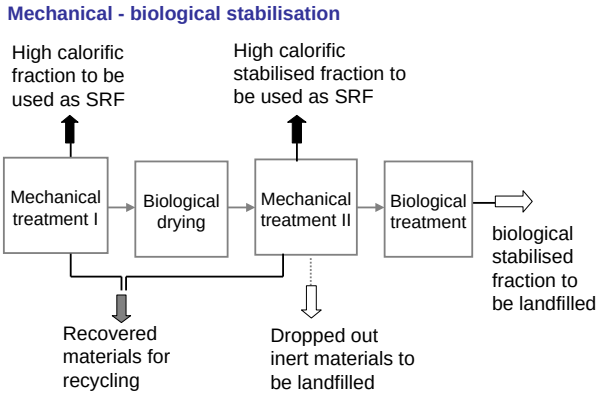

Figure 2.3b: Waste treatment concept b

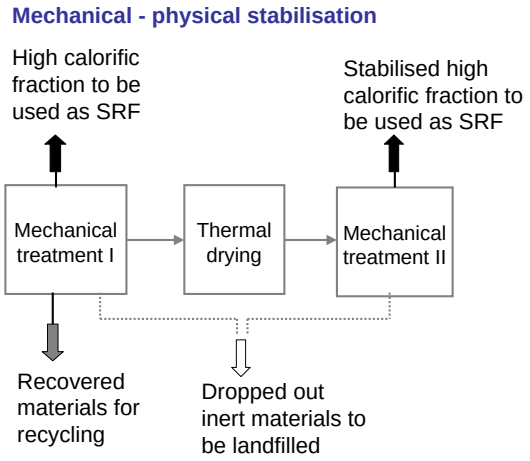

Figure 2.3c: Waste treatment concept c

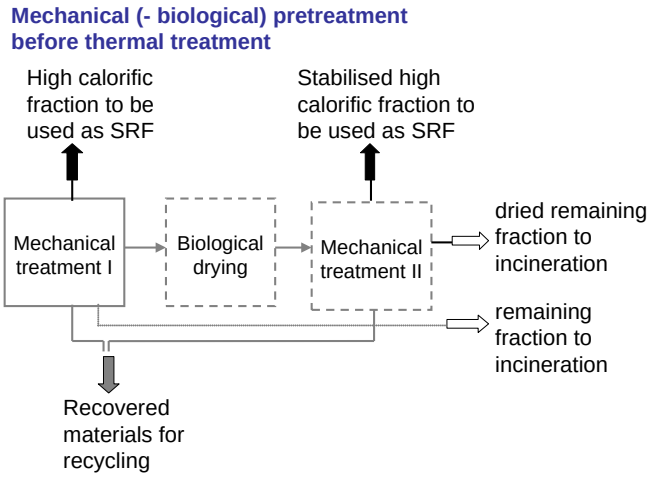

Figure 2.3d: Waste treatment concept d

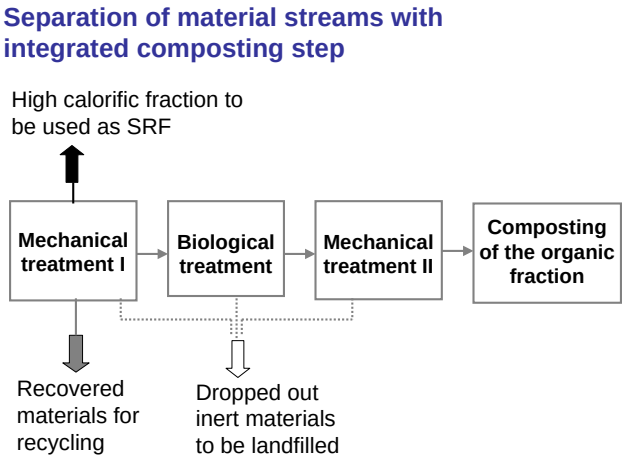

Figure 2.4: Waste treatment concept with integrated composting step

2.1.3 Classification of Solid Recovered Fuels

In order to categorise the Solid Recovered Fuels available in the market on the basis of their specification, a number of classification parameters is adopted by CEN. Technical Specification 15359 defines three parameters: a) Net Calorific value, which is considered as an economical index, b) Chlorine content, which is considered as a technological index, and c) Mercury concentration, which is considered as an environmental index. An overview of the proposed parameters as well as the classes considered for each one of them is given in Tables 2.1, 2.2.

Table 2.1: Fuel properties taken into account in classification

Fuel parameter	Symbol	Unit	Statistical distribution	Statistical measure	Index
Net calorific value	Hu	MJ/kg ar *	Normal	Mean value	Economical
Chlorine	Cl	w.t. % d **	Assumed as normal	Mean value	Technological
Mercury	Hg	mg/MJ ar *	Translated to right	Median, 80th percentile value	Environmental

*ar : as received, **d: dry basis

Table 2.2: Ranges of values for each proposed class of the classification parameters considered

Classification property	Statistical measure	Unit	Classes				
			1	2	3	4	5
Net Calorific value (Hu)	Mean value	MJ/kg (ar)	≥ 25	≥ 20	≥ 15	≥ 10	≥ 3

Classification property	Statistical measure	Unit	Classes				
			1	2	3	4	5
Chlorine (Cl)	Mean value	% (d)	≤ 0,2	≤ 0,6	≤ 1,0	≤ 1,5	≤ 3

Classification property	Statistical measure	Unit	Classes				
			1	2	3	4	5
Mercury (Hg)	Median value	mg/MJ (ar)	≤ 0,02	≤ 0,03	≤ 0,08	≤ 0,15	≤ 0,50
	80^{th} percentile	mg/MJ (ar)	≤ 0,04	≤ 0,06	≤ 0,16	≤ 0,30	≤ 1,00

In order to obtain a representative sample from an SRF production process, a specific procedure defined in Technical Specifications 15540 and 15443 has to be followed [II-12], [II-13]. Weekly production is divided in groups of 1500 t at maximum defined as "lots", and an analysis of a representative fuel sample for each lot is carried out. This representative fuel sample is obtained by mixing at least 24 increments sampled regularly during the production of the particular lot. For the SRF classification at least 10 lots are required for a production period of several months, during which the set up of the production process remains constant. The values which are taken into account for classification represent the 95% confidence level of the normal distributions obtained from the Hu, Cl and Hg values of each lot, and are calculated from the equation below.

$$X = \overline{X} \pm 1,96 \times \frac{s}{\sqrt{n}} \quad \text{(Eq. 2.1)}$$

where

X	The upper or lower limit of the 95% confidence level
$\overline{X}$	Average value of the obtained analyses of each lot
1,96	Characteristic constant for the normal distribution
s	Standard deviation
n	Number of values

The upper limit of the 95% confidence level is taken into account for the heating value, while the lower limit is used for chlorine. In the case of mercury, the highest value between the median and the 80^{th} percentile value is used for classification. After correlating the correct class code to each of the three classification properties, the particular SRF is characterized by the class codes of the three parameters.

In order to have a comparison on the basis of different waste recovered fuels and their proposed class codes, the classification of the Solid Recovered Fuel SBS® produced by the German company Remondis is attempted parallel to the Refused Derived Fuel produced in the Athens waste treatment plant. Since the standardisation process for the fuel produced in the Athens waste treatment plant has not initiated yet, the term SRF cannot be used for the particular fuel. A comparison of the heating value, the moisture content, the chlorine and the mercury between both fuels is presented in Table 2.3 SBS® has a slightly higher heating value and lower moisture content. The Chlorine content and Mercury concentration are comparable; however, the major difference between both fuels lies in the standard deviations of the presented parameters. The standard deviations of the values considered for the RDF produced in the Athens plant are about double the respective values of SBS®. This difference is associated with the particular waste treatment processes applied, and primarily with the optical sorting methods used in the production process of SBS®. Through the applied Near Infrared sorting method (NIR) increased homogeneity of the high calorific fraction sorted out from the main waste stream is achieved.

The proposed classification for both fuels would be (Hu, Cl, Hg): (4, 2, 1). At this point it should be pointed out that SBS® is utilized in brown coal power plants due to its medium heating value. Other industries which utilize hard coal, like cement kilns or hard coal power plants, would require SRFs with higher heating value, about 20-22 MJ/kg, in order to have

comparable thermal input to that of hard coal. Co-firing of SRF with lower heating values in these plants would require higher fuel mass flows, which could present difficulties from a technical point of view.

Table 2.3: Fuel parameters of Athens RDF and SBS® (production year 2007)

	Athens RDF				SBS®1 (2007)			
	Hu (MJ/kg ar)	Water (%)	Cl (% ds)	Hg (mg/kg ds)	Hu (MJ/kg ar)	Water (%)	Cl (% ds)	Hg (mg/kg ds)
Minimum	7,95	10,4	0,08	0,12	9,92	7,20	0,20	0,20
Maximum	21,72	49,9	1,37	1,30	18,6	23,10	0,80	0,80
Mean	13,62	27,1	0,34	0,36	14,15	21,50	0,44	0,31
St. dev.	2,80	5,8	0,27	0,29	1,25	4,06	0,13	0,15
Median				0,31				0,30
80% percentile				0,38				0,30
Nr. samples	61	61	57	15	79	79	79	14

2.1.4 Biogenic content of Solid Recovered Fuels

The biogenic content is one of the important aspects in the characterisation of SRF since it corresponds to the CO_2 emission reduction potential in the case of substitution of hard coal or brown coal by SRF. The experimental methods for the determination of the biogenic content of SRF are still in the process of validation, and are still regarded as pre European Norms (pre ENs). The standard determination methods are based on selective dissolution procedures followed by further analytical steps, and are described in Technical Specification 15440 [II-14]. Alternative techniques such as the ^{14}C method are still under development, while a Technical Report on them is also available by CEN/ TC 343 [II-15]. A representative value for the biogenic content of most SRF derived from MSW is 40 - 60% w.t. The energy specific CO_2 emissions of different fossil fuels in comparison with SBS®1 are presented in Figure 2.5. The CO_2 emissions of SBS®1 after subtracting the emissions of the biogenic share, which have to be excluded from the calculation, are also estimated.

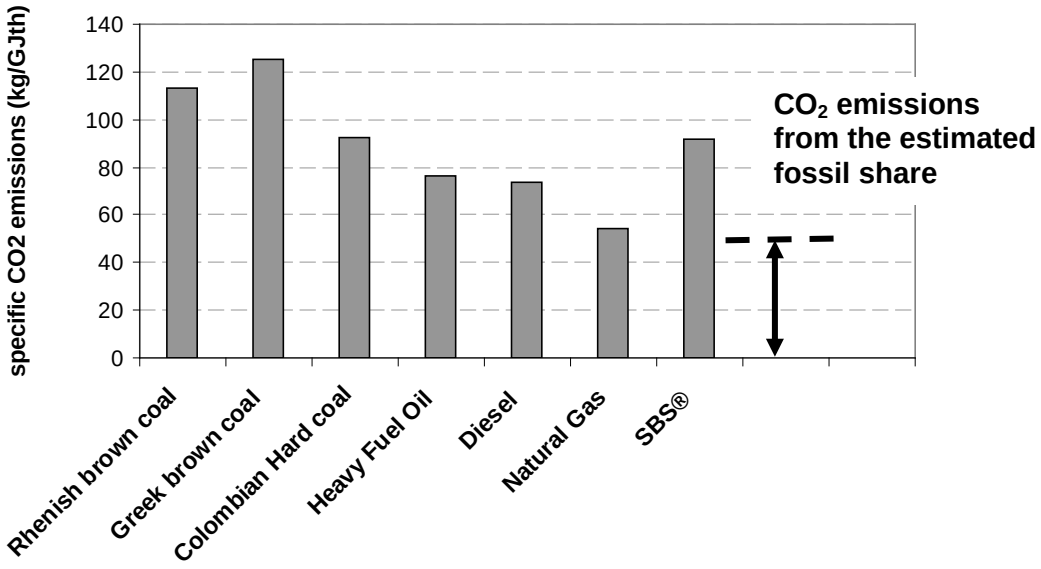

Figure 2.5: Energy specific CO_2 emissions in kg CO_2/ GJ_{th}

2.1.5 The experience from successful SRF co-combustion projects

Many different technological concepts for SRF co-utilisation in existing thermal power plants or industrial facilities are available and have been tested in the industrial practice (Figure 2.6). As mentioned in Chapter 1, the most successful SRF co-utilization projects to date can be found in the cement and lime industry. Nevertheless, the coal power sector is considered as an emerging market with considerable potential. In most cases the implementation of direct co-combustion is possible without major changes and investments in existing infrastructure, and provides a cost effective alternative for the increase of the renewable energy share in existing large-scale facilities firing fossil fuels.

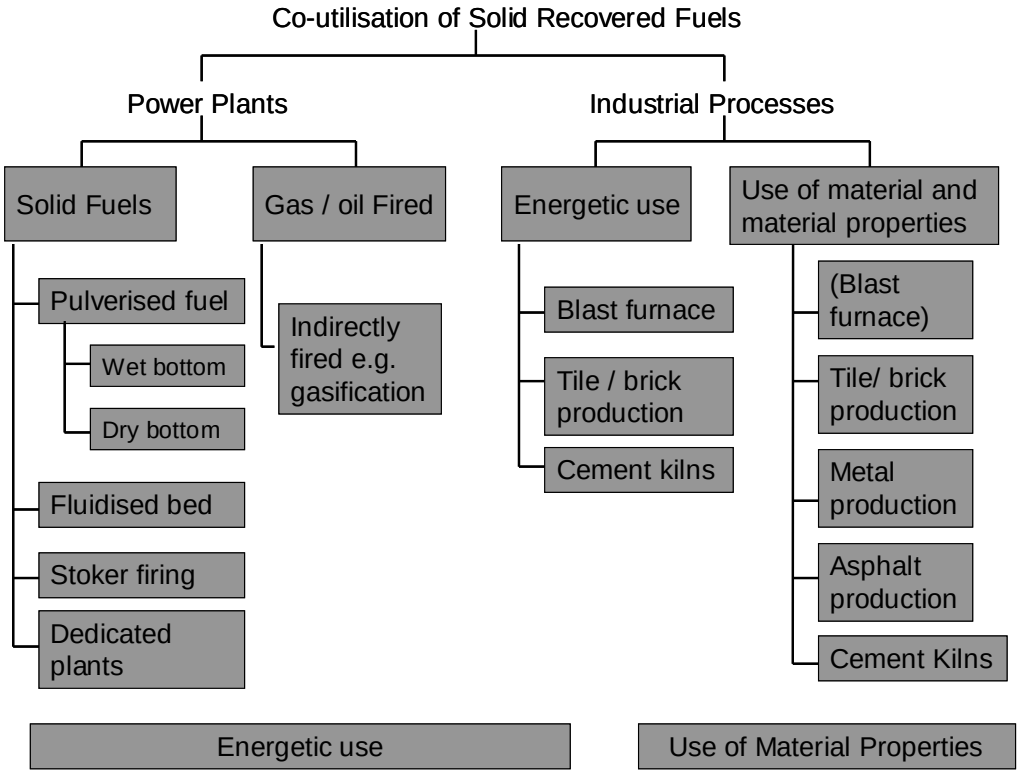

Figure 2.6 Possible means of SRF co-utilization in power plants and industrial processes

Several examples of SRF co-combustion practices in coal power plants which have been successfully realised and are still in operation, can be found in Table 2.4. [II-16], [II-17], [II-18].

Table 2.4: Coal power plants, where co-firing has been successfully demonstrated

Power plant name	Company	Boiler type	Fuel type	Installed power (MW_e)	Substitute Fuel	Capacity (10^3 t/ a)
Boxberg III	Vattenfall	Pulverised Fuel (PF)	Brown coal	900	Sewage sludge/ MBM	160/ 35
Jaenschwalde	“	“	Brown coal	4 x 300	SRF from MSW	400
Lippendorf	Vattenfall, E.ON, ENBW	“	Brown coal	2 x 920	Sewage sludge	385
Schwarze Pumpe	“	“	Brown coal	2 x 800	Mixed derived fuel / paper sludge	360/ 100
Werdohl-Elverlingsen	Mark E	Pulverised Fuel, Wet Bottom (PF - WB)	Hard coal	637	SRF from MSW, MBM	n.a.
Ensdorf - Saar	VSE AG	“	Hard coal	430	SRF from commercial waste, sludge, MBM	n.a.
Gersteinwerk	RWE-Power	PF	Hard coal	750	SRF from MSW, MBM, commercial waste	n.a.
Hamm-Westfalen	“	PF - WB	Hard coal	588	SRF from MSW	n.a.
Weisweiler	“	PF	Brown coal	2 x 600	Paper sludge	n.a.
Ville/ Berrenrath	“	Circulating Fluidised Bed (CFB)	Brown coal	107	SRF from MSW	n.a.
Flensburg	Stadtwerke Flensburg	“	Hard coal	170	SRF from MSW, commercial waste	n.a.

n.a.: not available

2.1.6 Main parts of SRF co-firing systems in coal power plants

Considering the realisation of these SRF co-firing projects in large scale coal power plants and the technical modifications required in the existing sites, following aspects have to be considered. The installation of an additional storage and handling system for the alternative fuels and the modification of the boiler’s firing system, in order co-fire SRF are the major technical challenges for the implementation of SRF co-firing in an existing coal power plant. Regarding the fuel handling system for SRF it is composed of following parts:

a) Unloading station and intermediate storage area.

An area, where the fuel is delivered and unloaded from the transportation tracks is regarded in every co-firing application. The particular area is inside the power plant site and is located as closer as possible to the boiler house. An area for the intermediate storage of the fuel is

usually also located nearby the unloading site. The unloading station and storage area can be at open site like the unloading station at the RWE's 600 MW_e Weisweiler power plant [II-19] , where the SRF co-firing tests to be analysed in the following chapters took place. Another alternative is to place the unloading station and intermediate storage area of SRF in a closed building as described in other successful co-combustion projects [II-18]. The feeding of the fuel into the main fuel transport system may be realized manually by a bucket excavator working in shifts and loading the fuel from the intermediate storage area to a dedicated hopper, below which the main feeding screw is placed. The alternative would be a more sophisticated system, including an automatic walking floor, where the fuel is directly unloaded from the transportation trucks. The walking floor may be then controlled by the plant's main control room and the standards operating personnel or by an additional control room and additional personnel. Through this walking floor the feeding rate of the alternative fuel through the hopper and the main feeding screw to the boiler may be scheduled and controlled.

b) Feeding and dosing system for SRF

The feeding and dosing system is mainly responsible for the transportation of the alternative fuel from the storage area into the boiler. Depending on the fuel specifications three concepts may in general be followed: i) The option is to use the existing transport system for the main fuel, i.e. the coal conveyor belts. SRF is then transported together with coal into the existing milling system, where it is dried and milled with coal and finally enters the boiler furnace through the existing coal burners. ii) The second option is the installation of an additional transport system dedicated for the feeding of the alternative fuel. A pneumatic transport system is usually applied in this case and additional mills may be installed to reduce the fuel's Particle Size Distribution depending on the characteristics of the fuel to be delivered and the required characteristics in the boiler for a complete fuel burn out. SRF enters then the furnace through additional burners, which are extra installed to assure a complete burnout of the alternative fuel. iii) The third option is a combination of the two options presented above. An additional pneumatic transportation system may be then used for the transportation of the alternative fuel to the boiler. An additional milling system may be also installed, if this is proven as necessary due to the particular fuel specifications. The alternative fuel is then injected into the main coal duct after the mills and enters the boiler through the existing coal burners. In this way significant savings in investment costs are possible, since expensive modifications of the boiler's firing system are avoided.

After SRF is injected into the boiler it follows exactly the same path as the raw fuel. It is combusted in the furnace section and the flue gas and ash particles pass through the boiler's convective section and the Air Preheater to the flue gas cleaning system. In brown coal power plants this is usually composed of the Electrostatic Precipitator (ESP) and the Flue Gas Desulphurisation Unit (FGD). No additional equipment is therefore required for handling the alternative fuels - or their by-products - after being injected into the boiler.

2.2 Brown coal pre-drying concepts

2.2.1 Overview of the pre-drying systems currently under development

Brown coal is a domestic fuel for many European countries, and its efficient and cost effective utilisation in the power generation sector supports the stability of European electricity grids, enhances energy security and reduces the dependency of the European energy sector on energy imports like oil and natural gas. Brown coal power plants are, therefore, still considered as an indispensable part in the electricity generation mix in the coming decades. However, since the coal power sector bears the main responsibility for the increase of the GHG emissions in the last decades, the efficiency increase in existing and future coal power plants is of prime importance. Among other retrofitting options presented in the first chapter, the potential optimization of the drying process in brown coal power plants is considered as one of the most interesting options from a technical and a financial point of view [II-20], [II-21]. Besides, another motivation for the development of brown coal pre-drying systems is the implementation of oxy fuel firing in future brown coal power plants, for which brown coal pre-drying is considered as an indispensable part. Such future steam cycles for thermal plants firing low rank lignites have already been studied and are available in the literature, [II-22], [II-23], [II-24].

Brown coal has a moisture content of more than 50% w.t. and the current drying systems, despite their high reliability, show a significant potential for further efficiency increase. The drying process in the current plants is integrated with the milling system, and hot recirculated flue gas taken at the furnace exit level at a temperature of about 1000°C is utilised as a heating medium. The main argument in favour of this configuration is its operational reliability and the large industrial experience on the particular process. However, two main energetic drawbacks can be found in the particular system:

- The recirculation of hot flue gas, at a temperature of about 1000 °C, to be used as heating medium for drying, where an amount of heat at about 100 °C would be sufficient, results in high exergy losses.
- The evaporated moisture cannot be further energetically utilised, since it is transported together with dried brown coal dust through the coal duct into the boiler. In this way, the mass flow which enters the boiler and consequently, the flue gas mass flow is increased resulting in increased flue gas losses and reduced boiler efficiency.

Thus, for efficiency improvement in brown coal plants the two aforementioned aspects have to be considered. Lignite pre-drying systems, which utilise low temperature steam bleed from the steam turbine and avoid hot flue gas recirculation, are currently developed with the ultimate goal of being implemented in the large industrial scale. Different technologies are considered, most of which are thermal processes, where lignite drying takes place in fluidised bed conditions. An additional lignite drying technology implemented since the beginning of the 20th century in lignite drying and briquetting plants is based on tubular dryers operating with low temperature steam as a heating medium. Moreover, another technology, developed in recent years and demonstrated in pilot scale, incorporates the combination of a mechanical process, by means of which a fraction of the surface moisture is set free only by mechanical pressure while the rest by thermal drying. The particular process is called Mechanical Thermal Dewatering (MTE).

A comparison of the most developed pre-drying concepts including the tubular dryers, the MTE, and the atmospheric and pressurized fluidised bed drying process can be found in the literature [II-25]. According to the study, the implementation of each of the processes considered as a main drying system substituting conventional mill drying and flue gas recirculation to 100% would lead to an efficiency increase of 3 to 6 percentage points. The

highest increase is calculated for the MTE process, while fluidised bed drying shows comparable potential. Beyond the thermodynamic aspects, however, the operational aspects and the minimisation of risks in the long-term operation are also decisive factors for the selection of a technology to be applied in the large industrial scale. In this aspect fluidised bed drying systems have a certain advantage due to their lack of main mechanical systems such as moving or rotating parts, which usually have higher maintenance requirements.
Two fluidised bed drying systems currently under development utilise low temperature steam as heating and fluidising medium, and the difference between them lies on the operating pressure. The fine grain Fluidised Bed system with internal waste heat utilisation developed by RWE ("Wirbelschichttrocknung mit Abwaermenutzung" – fine grain WTA) operates at a low pressure ranging from atmospheric conditions up to 3 bar [II-26], [II-27], , while the Pressurised Fluidised Bed system developed by Vattenfall ("Druckaufgeladene Dampfwirbelschichttrocknung" DDWT has a design pressure of up to 10 bar [II-28]. Additionally, another fluidised bed drying concept utilising waste process heat as heating medium is developed and demonstrated by a power plant operator in the USA [II-29]. No further design data on the particular drying concept are, however, available.
Between the two fluidised bed drying systems initially mentioned the atmospheric concept has been further developed to date. It has been successfully demonstrated for about ten years in a pilot plant in Frechen, Germany with a dry lignite production capacity of up to 15 t/h. The industrial scale up integrated in a 1000 MW_e unit is now in commissioning phase. On the other hand, the pressurised fluidized bed drying concept has been demonstrated in a pilot plant with a drying capacity of up to 5 t/h dry lignite and an operating pressure of up to 6 bar for one year, while the scale up of the dryer is planned to be constructed until 2015 as a main part of the 250 MW_e oxyfuel lignite fired boiler announced by Vattenfall.

2.2.2 The fine grain fluidised bed drying concept (fine grain WTA)

A typical design of a fluidized bed drying system for lignite is presented in Figure 2.7. Raw lignite, which is already milled to its final particle size distribution, enters the dryer from the top through a dedicated distributing mechanism. The main part of the dryer is covered by the heat exchanger. Low temperature steam flows in the inner side of the tubes and heats up the raw lignite up to the moisture evaporation temperature. A small fraction of steam is also used as a fluidising medium. Lignite drying leads to shrinkage of the porous structure of lignite particles. The particle density increases, therefore, and the dried lignite falls into the hopper section, where it is collected and transported by cooled screw conveyors.

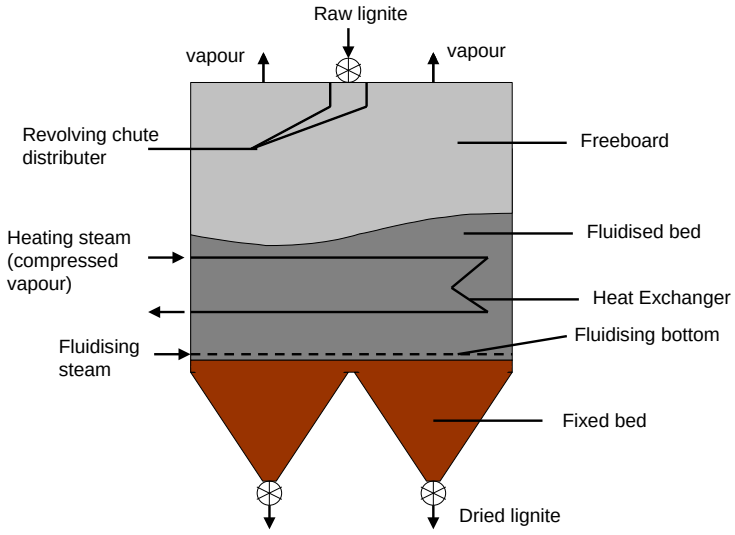

Figure 2.7: Schematic diagram of a fluidised bed dryer, Source: RWE-Power

The integration of the atmospheric fluidised bed dryer into an existing power plant cycle may be implemented in two different ways according to literature [II-30]. In the first concept (Figure 2.8), a steam bleed is used as heating medium in the dryer and the produced vapor from the drying process, after being cleaned from fine coal dust, is utilised as heating medium in the boiler feed water pre-heaters. In the second concept, after the removal of the fine coal particles, the evaporated moisture is compressed by a vapor compressor and is used as heating medium for the drying process (Figure 2.9). The particular concept is energetically favorable since no steam bleed is used for drying, with the exception of the start-up time. On the other hand, the addition of the vapor compressor, a mechanical part which is indispensable for the operation of the dryer and of the entire plant, leads to an extra operational risk and additional maintenance requirements in the facility.
In the integration of the first full industrial scale dryer into the 1000MW_e unit the first concept is followed. The prototype has a drying capacity of 120 t/h of lignite moisture and accordingly a dry lignite production capacity of 110 t/h. The produced dried lignite is pneumatically transported to the boiler and fired through dedicated swirl burners. The nominal thermal share of the dry lignite is up to 30% of the boiler's total thermal input. The vaporised coal moisture produced from the drying process is utilised as heating medium for feeding water in the boiler water pre-heaters so that corresponding steam bleeds from the low pressure steam turbine can be saved for the two initial low pressure water pre-heaters.

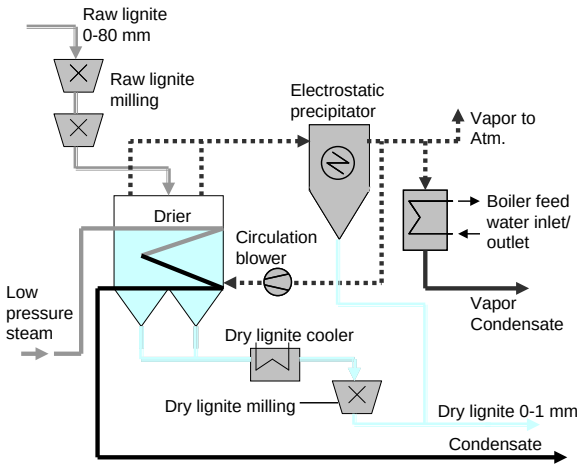

Figure 2.8: WTA concept with waste heat utilisation in the feed water preheaters

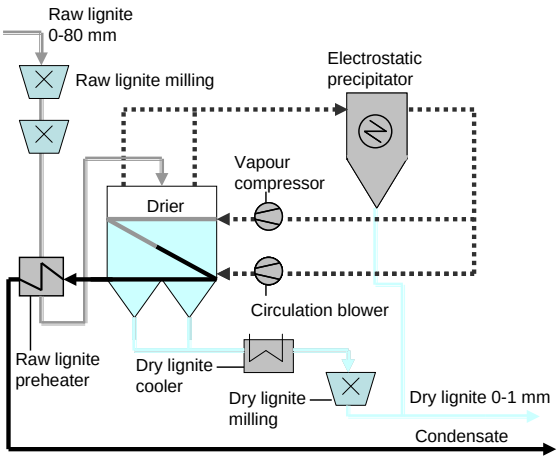

Figure 2.9: WTA concept with vapor compression and utilisation of the evaporated moisture as heating medium in the dryer

2.2.3 Influence of dry lignite co-firing on heat transfer

One last aspect related with the heat transfer of a boiler co-firing dry lignite, is illustrated in Figure 2.10. Due to the reduced moisture content of dry lignite, the flue gas mass flow decreases, and adiabatic combustion temperature increases respectively resulting in a rise of the radiative heat flux to the evaporator. This increase may be slightly noticed in current lignite boilers being modified to co-utilise dry lignite up to a thermal share of 20 or 30%; however, it will considerably influence the design of future lignite boilers firing 100% dry lignite. The total surface of the furnace section in dry lignite boilers is expected to increase so that a higher fraction of the total heat compared to raw lignite firing can be transferred to the evaporator walls up to the furnace exit. The reason is that furnace exit temperature, which is a design parameter should not change in future boilers, since it is usually determined by the ash properties of the particular lignite fired and the available superheater materials. One additional measure considered, to avoid very high flame temperatures and possible overheating of

furnace walls, is cold flue gas recirculation from a level at the boiler exit, before the air pre-heater. Regarding the convective section, the convective heat flux is expected to decrease due to the lower flue gas mass flow. Furthermore, in order to keep similar flue gas velocities with the raw coal case in the convective section, the boiler cross-section is expected to decrease. As a result, future dry brown coal boilers are expected to have a smaller cross-section and an increased furnace height resulting in increased total height.

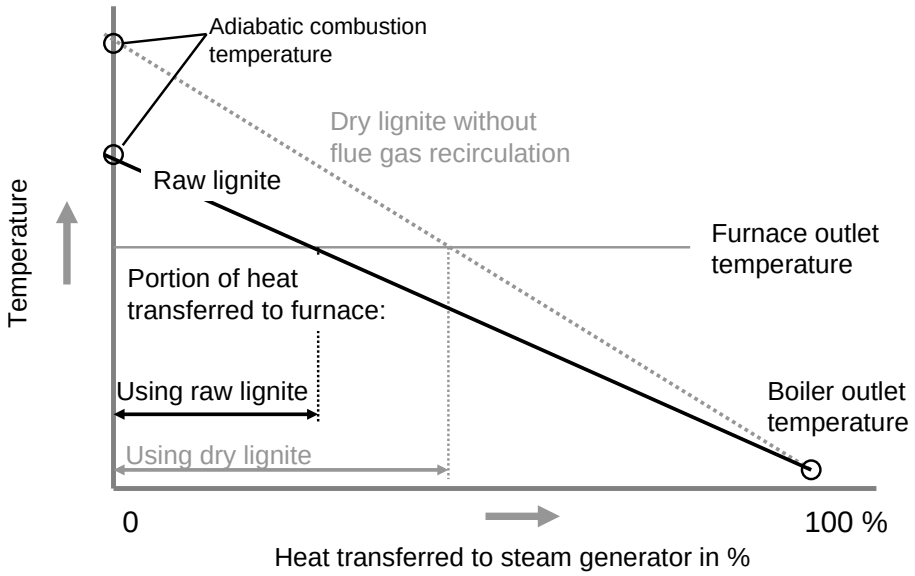

Figure 2.10: Qualitative presentation of the Q-T diagrams of a raw lignite and a dry lignite boiler

2.3 Comparison of the proposed coal substitution concepts in respect with their CO_2 emissions' reduction potential

As explained in the first chapter both co-firing concepts are compared in terms of several parameters representing environmental, technical and economic aspects. The first environmental aspect to be investigated is the potential on CO_2 emissions' reduction. In order to evaluate this potential, a realistic co-firing scenario is examined based on available data of a Greek power plant. The 375 MW_e Agios Dimitrios V unit is considered for this investigation. In both co-firing concepts investigated and compared the co-firing thermal share regarded is 5%, while it is assumed that co-firing is continuous for the whole annual hours of operation. The particular co-firing share may be too low to be economically feasible for the pre-drying technology. Scope of this calculation is however, the comparison of the technology related aspects of the two coal substitution concepts, which determine the CO_2 emissions' reduction potential.

The parameters used for the calculations are given in Tables 2.5, 2.6. Apart from the data of the particular plant, data of the substitute fuels is also used including the heating value, and specific CO_2 emissions. Regarding the substitution concept of coal by alternative fuels a second type of alternative fuels is also evaluated apart from Solid Recovered Fuels (SRF), the Solid Biofuels. Solid Biofuels derive from biomass such as agricultural or forrest residues and are fully biogenic. They are often used as substitute of coal in large scale power plants and for this reason they are included in the investigation.

In order to calculate the expected CO_2 emissions reduction by the integration of the lignite pre-drying technology complete thermal cycle calculations of the considered power plant are required, in order to evaluate the expected net plant efficiency increase by the application of lignite pre-drying The particular calculations have been performed for Agios Dimitrios V unit in the framework of this thesis and the according results for three dry lignite co-firing thermal shares are given in Table 2.7. The methodology and calculation procedure, as well as the detailed results of the thermal cycle calculations are presented in detail in Chapter 6.

Table 2.5: Power Plant parameters in the reference case

Reference data for Agios Dimitrios V unit		
P_e	375	MW_e
Net plant efficiency ($\eta_{pp,\ net}$)	35.4	%
Hu (raw lignite)	5.418	MJ/kg
Raw lignite moisture content	55.3	% w.t.
Fuel specific CO_2 emissions (μ_{CO2})	0.677	kg CO_2 / kg fuel
Annual hours of operation	7,500	h
Annual CO_2 emissions	3,811,025	t CO_2 / a

Table 2.6: Fuel related - and plant parameters in the co-firing cases

Data for biomass/ SRF co-firing			Data for lignite pre-drying and dry lignite co-firing		
Thermal share of substitution	5	%	Thermal share of substitution	5	%
SRF biogenic share	50	%	Dry lignite moisture	12	%
Biomass biogenic share	100	%	Hu dry lignite	13.03	MJ/kg
LHV SRF	14	MJ/kg	Fuel specific CO_2 emissions (μ_{CO2})	1.335	kg CO_2 / kg fuel
LHV biomass	17	MJ/kg	Predicted net efficiency increase for dry coal co-firing thermal share 5%	0.2	Δ(%)
Fuel specific CO_2 emissions (μ_{CO2}) after considering the biogenic share of SRF	0.682	kg CO_2 / kg fuel	Predicted net efficiency increase for dry coal co-firing thermal share 10%	0.4	Δ(%)
			Predicted net efficiency increase for dry coal co-firing thermal share 20%	0.7	Δ(%)

The results are presented in Table 2.7. For a co-firing share of 5% a reduction of CO_2 emissions of about 3% is feasible in the case of SRF, due to the biogenic content of SRF, which is taken as 50% in the particular calculation. In the case of co-firing Solid Biofuels, which are fully biogenic, the expected reduction rate is then 5%. Dry lignite co-firing with the same thermal share leads to a relative CO_2 emissions' reduction of about 1.5 %. This reduction rate is related with a) the increase of the plant efficiency through the integration of

the dryer and b) the decreased dry lignite input, when substituting raw lignite by dry lignite, because of the increased heating value of dry lignite. Summing up, the substitution of coal by Solid Biofuels, which are fully biogenic brings the highest potential to decrease CO_2 emissions in existing power plants. The percentage of decrease is equal with the thermal share in the case of biomass, since no CO_2 emissions are accounted for 100% biogenic fuels. It has to be further mentioned that biomass co-firing in coal power plants has been successfully demonstrated also for higher thermal shares up to 10%. Savings of CO_2 emissions may therefore further increase, when increasing the co-firing share, which denotes the high CO_2 reduction potential of the biomass co-firing concept.

Substitution of coal by SRF may also bring considerable savings. A higher substitution thermal share for SRF co-firing, above 5%, cannot be easily realised in pulverised coal power plants, due to technological aspects such as the risk of chlorine corrosion. The CO_2 emissions reduction potential of the SRF co-firing concept is therefore considerable, nevertheless lower than the one of biomass co-firing.

The lowest CO_2 emissions reduction is achieved by the pre-drying concept. This is reasonable, since the substitute fuel in the pre-drying concept is dry lignite, which is still a fossil fuel. It should be however underlined that the pre-drying and dry lignite co-firing is usually applied for higher thermal shares up to 25-30%, where the decrease of CO_2 emissions is much higher. According to calculations a pre-drying and dry lignite co-firing concept of a thermal share of 25% may lead to a relative reduction of annual CO_2 emissions up to 6.5%. The potential CO_2 emissions reduction is therefore higher than initially regarded, since the typical substitution thermal share applied for dry lignite co-firing is much higher than 5%, usually 25-30%.

Table 2.7: Expected CO_2 reduction through co-firing practices

	Unit	Alternative fuels' co-firing		Lignite pre-drying and dry lignite co-firing
		Biomass co-firing	SRF co-firing	
Reduction of CO_2 emissions	t CO_2 / a	178,642	108,976	53,260
Percentage of CO_2 emissions' reduction compared to reference case	%	5.00	3.05	1.49

3 SRF co-firing: Investigations in the small scale

Summary
Under the scope of the evaluation of the SRF co-firing technology in the large scale, small-scale investigations are used as support work for the research work in the large scale. An overview on the current laboratory analysis techniques for the characterisation of SRF combustion behaviour is presented in the first part of the chapter. A literature review is carried out on the most important research work ongoing in this field. The second part focuses on the description of the developed model for SRF particle combustion, the implementation of the particular model in a commercial CFD code and its validation based on available experimental data. Given the fact that satisfying results are obtained, the proposed model will be further used in the evaluation of different SRF co-firing modes by large-scale boiler simulations. The last part of the chapter includes a discussion of the obtained simulation results and propositions for further research work in the field of SRF particle combustion modeling.

3.1 Lab-scale investigations on fuel properties and combustion behaviour of SRF – Literature overview

In order to ensure the successful implementation of the direct SRF co-firing practice in power plants and assist its future spread in more industrial facilities, an in depth examination of the combustion related parameters of SRF is required. These parameters include the physical and chemical properties of the fuel, the combustion and emission behaviour related to SRF, and the analysis of the residue quality. Since a broad range of investigation methods is available for solid fuels ranging from fuel analysis and lab scale tests to semi-industrial scale tests, their evaluation and categorization into main groups is a necessary step towards the development of an analysis procedure that can be followed by any SRF. Such a categorization is proposed by CEN/ TC 343 [III-1], [III-2] and the respective scheme is presented in Fig. 3.1. The main analysis categories are (a) the standard laboratory fuel analysis, (b) the laboratory analysis based on advanced methods exclusively developed for SRF, (c) the pilot or semi-technical scale tests, and (d) the full scale tests. Through the proposed analysis procedure an overall characterization of SRF combustion behaviour at multiple levels and firing systems is possible.
In the framework of the standardisation procedure for SRF coordinated by CEN/ TC 343 the existing lab scale methods for solid fuel analysis are adapted to enable a comparable analysis of varying SRF types. The most important lab-scale tests covered by the technical specifications are the determinations of:

- Calorific value,
- Ash, volatile and moisture content,
- Ash melting behaviour,
- Bulk density, Density of pellets and briquettes,
- Durability of pellets and briquettes,
- Bridging properties of bulk material,
- Particle size and particle size distribution by screen method,
- Metallic aluminium,
- Method for Carbon (C), Hydrogen (H), Nitrogen (N),
- Method for Sulphur (S), Chlorine (Cl), Fluorine (F), Bromine (Br),
- Major Elements: Al, Ca, Fe, K, Mg, Na, P, Si, Ti,

- Trace elements: As, Ba, Be, Cd, Co, Cr, Cu, Hg, Mo, Mn, Ni, Pb, Sb, Se, V, Zn, and
- Biomass content by selective dissolution.

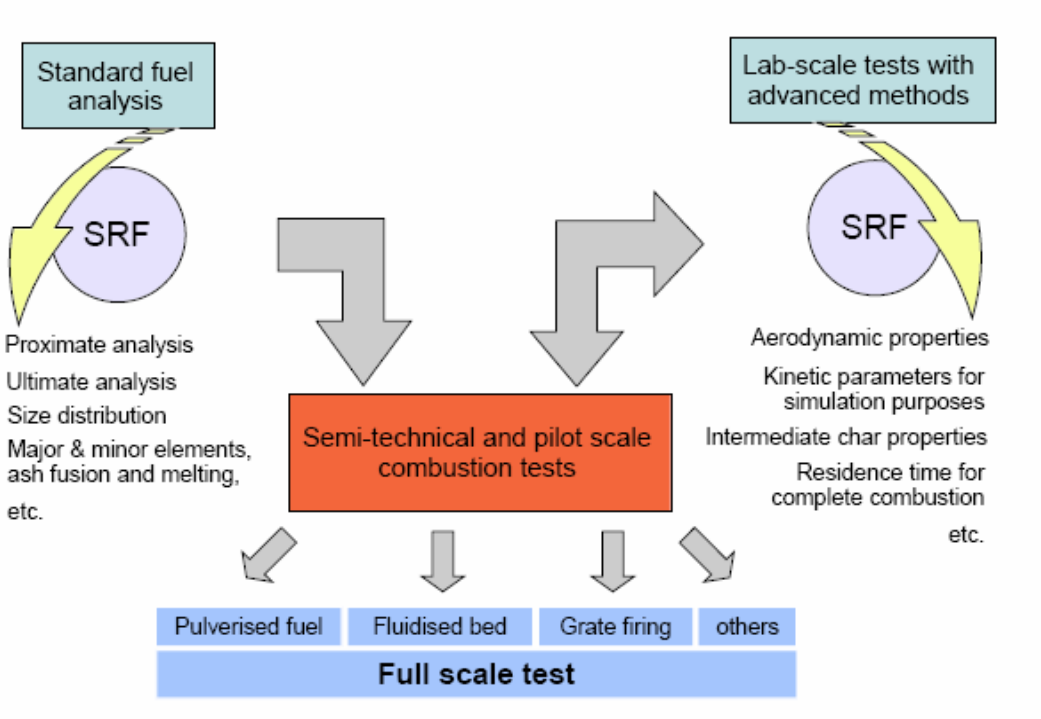

Fig. 3.1 Proposed categorization for the determination of SRF combustion behaviour

The second category, of the advanced lab-scale methods, includes mostly laboratory methods which have been developed or are still under development by universities in order to acquire additional information for the combustion properties of specific SRF types in particular firing conditions.

Since standard analyses require dedicated fuel preparation in order to produce a laboratory sample in similar form in all cases, eg. pressed pellet or fine dust, specific fuel preparation steps are often required, such as grinding, milling or screening. During these preparation steps the particle shape, which is a decisive factor of the combustion behaviour, is lost. Standard analyses may provide, therefore, a large amount of information on the general combustion properties of SRF; they cannot, however, give much information on the combustion properties of a specific SRF type and its behaviour when combusted in a real firing system. This kind of information would include among others

- The burnout time of untreated SRF particles
- The aerodynamic behaviour of SRF particles
- The maximum particle size allowed for complete combustion in a given firing system.

Lab-scale experimental methods for the investigation of the above mentioned fuel parameters are proposed by Maier and Dunnu [III-3], [III-4]. Another current research subject, which is part of the advanced lab-scale measurements, is the determination of kinetic parameters for SRF particles. In the past many researchers studied the kinetics of municipal solid waste, either in the form of received fuel [III-5] or in the form of prepared mixtures of specific prepared fractions [III-6]. According to the results, the most important fractions of MSW which characterize its combustion behaviour and kinetics are the biogenic and the plastic fraction. Since the current focus is on Solid Recovered Fuels, similar investigations performed by Grammelis et al. [III-7] show that the same behaviour is also found in SRF. In this way it is shown that an accurate description of the combustion behaviour of SRF requires both

mentioned fractions, the biogenic as well as the plastic one, to be taken into account. Moreover, other research activities in the category of advanced lab-scale experimental methods include the characterization of the devolatilisation behaviour [III-8] and the ignition and burnout [III-9], [III-10] of SRF particles.
The third category of the experimental analysis of SRF combustion behaviour includes investigations in pilot and semi-industrial-scale facilities. Only a view research work is carried out in the particular field due to the increased technical difficulties related with the realisation of SRF combustion or co-combustion tests at pilot or semi-technical scale. The published investigations to date focus on the environmental aspect and the expected effect of SRF co-firing on the trace element and HCl emissions [III-11], [III-12].

3.2 Model development and validation based on lab-scale data

3.2.1 Introduction

Apart from the analytical and experimental test methods, the development of specific combustion models for Solid Recovered Fuels, is an important milestone for the further development of SRF combustion practices. By incorporating these combustion models in comprehensive CFD codes, either commercial or university-owned, the simulation and optimization of SRF combustion or co-combustion at real, industrial-scale conditions is feasible. Therefore, the present work proposes a dedicated model for SRF combustion.
The analysis of the different waste fractions in SRF presented in the previous chapter indicates that a Solid Recovered Fuel deriving from MSW is composed of more than two fractions including paper, cardboard, textile, plastic foils, hard plastic, wood, etc. However, modeling the combustion behaviour of each fraction is practically impossible and not desirable, since the general applicability of the model for as many SRF types as possible will be lost. It is, therefore, decided to focus on the investigation of the two major fractions: the biogenic one which includes the paper, the cardboard and the wood materials, and the plastic one.
The combustion mechanism for the biogenic fraction is similar to the one of coal, including the same successive combustion steps: inert heating, moisture evaporation, devolatilisation and char combustion. Devolatilisation is modeled by a single rate Arhenius type expression, and char combustion by the kinetics/ diffusion limited reaction model. A detailed description of the models applied for coal/ biomass combustion is given in Annex A.3. On the other hand, the plastic part combustion includes successive steps of inert heating, melting, decomposition and combustion of hydrocarbon vapours. The aforementioned steps are explained in more detail in the next paragraph.

3.2.2 Modelling approach

In contrast to the already existing models for coal and biomass particle combustion, the combustion of a solid plastic particle undergoes different steps. The particle is initially heated when entering the combustion chamber and when melting temperature is reached, the melting of the particle and its conversion to a liquid droplet begins. After the completion of the melting step, the evaporation of the liquid droplet starts. The evaporated hydrocarbon vapor is afterwards combusted with O_2 following a global reaction mechanism similar to coal volatiles' combustion. No char combustion is considered in the specific mechanism. The reason is that the reference plastic used for validation purposes, Polypropylene, has no char content. Most of the plastics with the exception of PVC have no char content.

For all three initial steps, inert heating, melting, decomposition, the evolution of particle temperature and the conversion rates from solid to liquid and from liquid to gas phase are governed by the standard energy balance equation, which applies to each particle (Equation 3.1)

$$m_p c_p \frac{dT_p}{dt} = hA_p\left(T_\infty - T_p\right) + \varepsilon_p A_p \sigma\left(\theta_R^4 - T_p^4\right) + h_{source} \tag{3.1}$$

where T_p is the particle temperature and h_{source} is the corresponding source term for each step. The convective heat transfer coefficient for particle heating h is given by the expression

$$h = \frac{Nuk_\infty}{d_p} \tag{3.2}$$

where the Nusselt number of the particle is calculated by the expression of Ranz and Marshall [III-13] (Equation 3.3)

$$Nu = 2.0 + 0.6\,\mathrm{Re}^{1/2}\,\mathrm{Pr}^{1/3} \tag{3.3}$$

Since plastic melting and decomposition is considered as a heat transfer controlled process, the respective source term is described as a product between the rate of melting or decomposition ($dm_{melt/dec}/dt$) and the corresponding enthalpies for melting or decomposition $\Delta h_{melt/dec}$ (Equation 3.4).

$$h_{source} = \frac{dm_{p\_melt/dec}}{dt}\Delta h_{melt/dec} \tag{3.4}$$

For the calculation of the melting and decomposition rate the approach of Deeg et al. [III-14] is followed. This approach has been also successfully adopted for the description of the decomposition processes of liquid tar droplets [III-15] as well as for the description of the devolatilisation process of specific biomass species [III-16]. According to this, the rate of transformation from the solid to the liquid face (melting) and from the liquid to the gas phase (decomposition) for the plastic particle is a function of the initial particle mass (m_{p0}) of the heat transferred to the particle (ΔQ) and of the total heat required for the full transformation ($Q_{req\_melt/dec}$) (Equation 3.5).

$$\frac{dm_{p\_melt/dec}}{dt} = m_{P0}\frac{\Delta\dot{Q}}{Q_{req\_melt/dec}} \tag{3.5}$$

where $\Delta\dot{Q}$ is equal to $\Delta\dot{Q} = m_P c_p \frac{dT_p}{dt}$

The required heat for melting or decomposition is then calculated from the following expression

$$Q_{req\_melt/dec} = c_{p,end}T_{end} - c_{p,start}T_{start} + \Delta h_{melt/dec} \tag{3.6}$$

The temperatures for the start and the end of the melting and decomposition process are obtained from Deeg [III-14], while the corresponding thermal capacities and the enthalpies for melting and decomposition can be found in the recent literature [III-17]. The respective values are given in Table 3.1.

Finally the produced polypropylene vapour, which is the only gaseous species released by the decomposition of PP, is burning according to the two-step global reaction mechanism presented by Equations 3.4 and 3.5. This mechanism is a simplification of a more complex mechanism proposed by Deeg [III-14].

(3.7)

$$C_3H_6 + 3O_2 \rightarrow 3CO + 3H_2O$$
$$CO + 1/2\,O_2 \rightarrow CO_2 \quad (3.8)$$

Nevertheless, one could incorporate the release of further intermediate gaseous species like C_2H_4, H_2 in the case of further char-bounded plastic materials but their further oxidation would mainly lead to the same final gaseous products, i.e CO_2 and H_2O. Such plastic materials are not incorporated in the presented model. The models describing the rates of melting and decomposition for the plastic part of the SRF particles have been implemented in the Fluent platform via house-built UDF (User Defined Function) subroutines. For the calculation of motion of plastic particles and droplets in the gas phase a spherical assumption is adopted for their shape, since no detailed data on their real shape is available.

Table 3.1: Physical data of plastic for the melting and the decomposition step

Physical data		Plastic melting	Plastic decomposition
T_{start}	K	413	513
T_{end}	K	513	-
$Cp_{droplet}$	J/kgK	2850	2850
Δh (melting/ decomposition)	J/kg	71,405	469,000

3.2.3 Model validation - Methodology

The validation of the proposed combustion model for plastic is based on experimental data available from combustion tests performed at a pilot combustor at IFK, University of Stuttgart [III-18]. Due to the inhomogeneous nature of SRF and its varying composition, no real SRF samples are used for the validation purposes, but rather prepared samples which are representative of the two main SRF fractions considered, the biogenic and the plastic one. In this way the validity of the proposed combustion model is kept as general as possible and its dependence on a particular SRF type is avoided. Different Solid Recovered Fuels with different compositions can then be simulated by setting the correct mass composition of the biogenic and the plastic fraction and the respective proximate and ultimate analysis of both fractions. The two prepared samples used are woody biomass representing the biogenic fraction, and Polypropylene representing the plastic fraction. Additionally, Rhenish brown coal is fired for reasons of comparison.

The pilot combustor - named “BTS” - is a cylindrical drop tube vertically placed, with a diameter of 200mm and a total height of 2.500mm. The burner of the facility has a central clearance, where the fuel is injected together with the carrier air, and two angular clearances, the secondary and the tertiary. Through dedicated guide vanes the secondary and tertiary air mass flows can be injected with a specific swirl. The current tests are, however, performed without swirl. The furnace walls are ceramic and are electrically heated by ohmic resistances. In this way a constant temperature profile can be set along the whole furnace wall. The wall temperature during the tests was set at 1300 °C. A detailed facility description can be found in the literature [III-19]. Axial profiles of O_2 and CO_2 are taken during the tests. No temperature profiles can be measured in the particular facility because, due to its small dimensions, the cooling effect of the water cooled measuring probe would affect the measured temperature.

The proximate and ultimate analysis for all fuels tested is given in Table 3.2. The fired Rhenish lignite is pre-dried to moisture of 8.5%w. in order to ensure stable ignition conditions. Additionally, the analysis of a typical SRF sample derived from high calorific fractions of MSW and bulky waste is presented.

Table 3.2: Proximate and ultimate analysis of Rhenish brown coal, SRF and woody biomass

	Analysis	Rhenish browncoal	SRF sample	Forest Residues	Polypropylene (PP)
Proximate (%wt raw)	Moisture	58.40	28.00	6.00	0.00
	Volatile Matter	20.00	55.99	82.00	100.00
	Fixed Carbon	12.56	6.36	11.80	0.00
	Ash	3.91	9.65	0.20	0.00
	NCV (MJ/kg)	8.17	14.78	16.83	40.19
Ultimate (%wt daf)	C	67.60	59.7	57.10	85.63
	H	4.96	8.36	5.00	14.37
	O	26.30	30.10	23.68	0.00
	N	0.66	0.98	0.52	0.00
	S	0.42	0.21	0.00	0.00

For the Computational Fluid Dynamics (CFD) simulations the commercial package Fluent 12 is used. A 2D computational mesh composed of about 19,000 quadrilateral cells is constructed, which was proven to provide grid independent results. The grid independence study performed includes refined grids with a size up to 90,000 cells and the respective results are given in Annex B1. A picture of the 2D numerical mesh at the near burner region of the combustor is given in Figure 3.2

The SIMPLE scheme is used for the pressure velocity coupling and the standard k-e model is adopted for the turbulence modelling. As far as the discretisation scheme is concerned, a second order upwind discretisation scheme is finally used in all simulations after obtaining convergence with the initial first order discretisation sheme. The Discrete Ordinates model is applied for radiation. Particle trajectories are calculated by integrating the force balance of the particles in a Lagrangian reference frame. One discrete phase calculation and update of the discrete phase source terms is performed every 25 continuous phase calculations. An overview of the standard models applied in a comprehensive combustion code, like Fluent, is given in Appendices A1-6.

Physical properties, which are important boundary conditions, are given in Table 3.3. These are density, thermal capacity and Particle Size Distribution (PSD). A Rosin Rammler Distribution of the form $Y_d = e^{-(d/dmean)^{\wedge}n}$ is fitted to the available data for all three fuels tested. The calculated mean diameter d_{mean}, spread parameter n, and the minimum and maximum diameters accounted are given in Table 3.3, too. The experimental data of PSD, the fitted Rosin Rammler distributions as well as the operating conditions for all fuels are given in Figure 3.3.

Table 3.3: Physical properties

	Physical properties / operating conditions	unit	Rhenish browncoal	Forest Residues	Polypropylene (PP)
PSD data	Density	kg/m^3	1000	800	855
	Cp	J/kgK	1100	1220	2850/ 2656
	Min diameter	µm	5	5	5
	Max diameter	“	600	1000	500
	Mean diameter	“	132	296	372
	Spread Parameter	“	2.837	1.32	3.16
Fuel mass flows	Fuel	kg/h			0.498
Air mass flows	Primary air)	“			1.950
	Secondary air	“			2.957
	Tertiary air	“			1.371

Since various kinetic constants are available in the literature for modelling devolatilisation and char combustion of solid fuel particles like brown coals and biogenic fuels, specific sets of kinetics are tested during the simulations in order to evaluate the agreement of the chosen parameter sets with the experimental data.
For coal combustion, parameter set A1 is a typical value [III-20] while parameter set A3 is used by Deeg et al [III-14]. Since the two sets differ in the pre-exponential factors of devolatilisation and char combustion, the intermediate case A2 is defined and simulated in order to separately evaluate the effect of each one of the pre-exponential factors. It can be noted at this point that the difference in the activation energy of the char combustion step between the two cases (1,13810 ^{8} J/kmol versus 7,9·10^{7} J/kmol) is proven by simulations not to have a visible influence on the predicted O_2 and CO_2 profiles. Furthermore, an additional parametric evaluation covering an extended range of values for the accounted pre-exponential factors is performed and presented in Annex B1.2.
A similar comparative study is performed in the case of the biogenic fuel. Since biomass has a higher volatile content and a lower char content, a constant devolatilisation rate 50 1/s is tested in order to account for the higher reactivity of biomass. Additional parametric investigations covering an extended range of devolatilisation pre-exponential factors are also carried out and can be found in Annex B1.3. All values used are given in Table 3.3 together with the respective literature sources [III-21], [III-22].

Table 3.3: Investigated sets of kinetic constants

	Kinetic Parameters	Unit	Coal case			Biomass Case	
			A1	A2	A3	B1	B2=A2 and B3=A3
Devolatilisation	Pre-exp. factor (k)	1/s	**200,000**	**315,000** [III-20]	315,000	Constant rate 50 (1/s)	
	Activation energy (E)	J/kmol	7.4·10^{7} [III-20]	7.4·10^{7}	7.4·10^{7}		
Char Combustion	mass diffusion limited rate	Kg/(m^{2} s Pa)	5·10^{-12} [III-21]	5·10^{-12}	5·10^{-12}	5·10^{-12}	
	kinetics limited pre-exp. factor	1/s	6.7 [III-21]	**6.7**	**0.00208**	6.7	
	kinetics limited activation energy	J/kmol	1.138·10^{8} [III-21]	1.138·10^{8}	7.9·10^{7}	1.138·10^{8}	

3.2.4 Model validation - Results

The results of the lab-scale simulations for brown coal, biomass and plastic are given in Figures 3.4 – 3.6. In order to account for the suction effect of the measuring probe, the values at the horizontal line with an offset of 3cm from the centreline are also given. A good agreement with the experimental data is achieved for most of the examined cases.
By increasing the devolatilization or char combustion pre-exponential factor a faster ignition and char combustion is predicted for the coal and the biomass case as well, illustrated by the higher slope of the O_2 and CO_2 profiles. The constant devolatilisation rate tested for the case of biomass leads to very fast devolatilisation which is not measured in the experiments and

does not represent, therefore, a realistic trend. All other chosen parameter sets are, however, in satisfying agreement with the experimental data indicating that more than one set of kinetic constants may provide satisfying results in this lab-scale investigation.
The proposed model for plastic melting and decomposition succeeds in reproducing the experimental tendency. The melting and decomposition rates are slightly under predicted in the beginning, indicating that rates which are not constant through the whole conversion steps can be tested in future investigations.

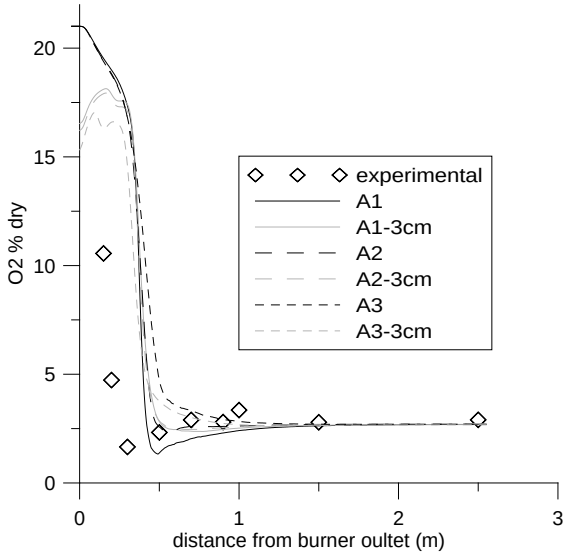

Figure 3.4a: Comparison of O_2 profiles for the coal case

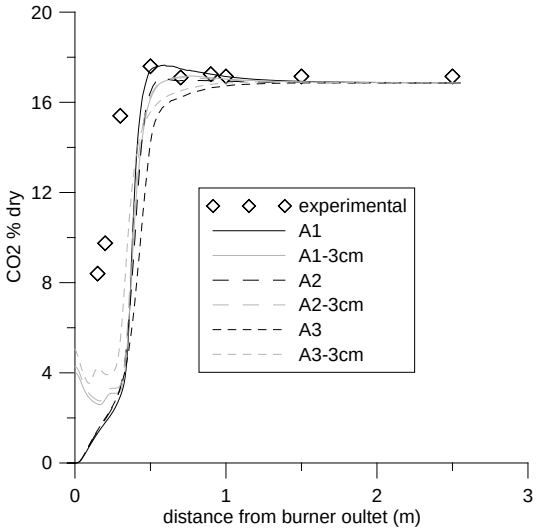

Figure 3.4b: Comparison of CO_2 profiles for the coal case

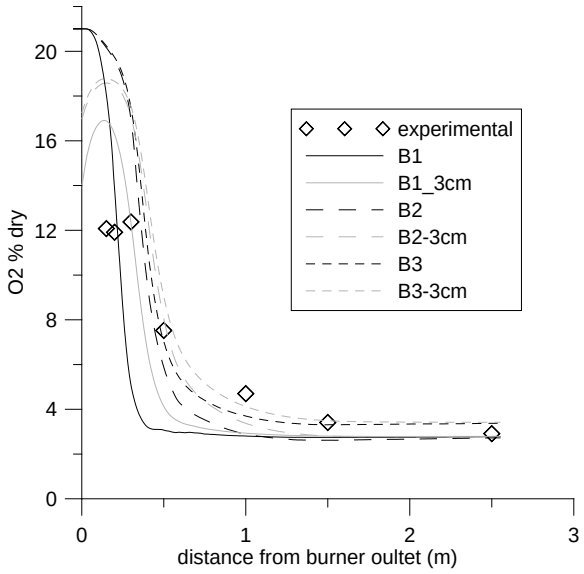

Figure 3.5a: Comparison of O2 profiles for the biogenic case

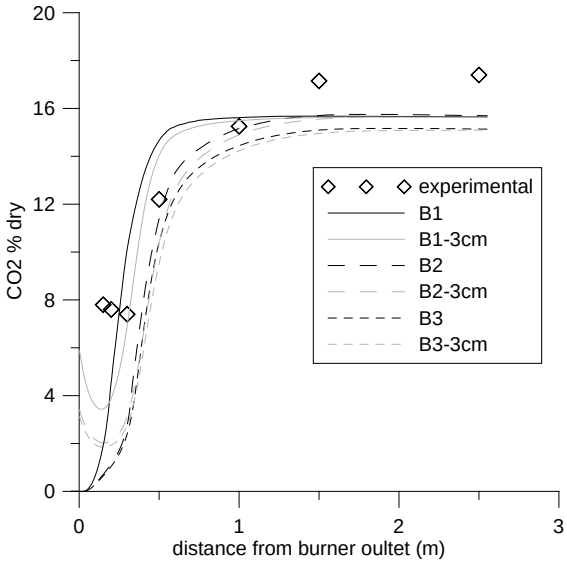

Figure 3.5b: Comparison of CO2 profiles for the biogenic case

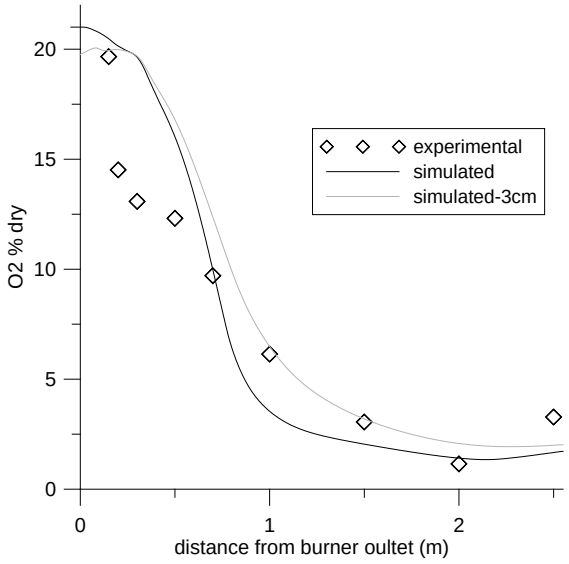

Figure 3.6a: Comparison of O_2 profiles for the plastic case

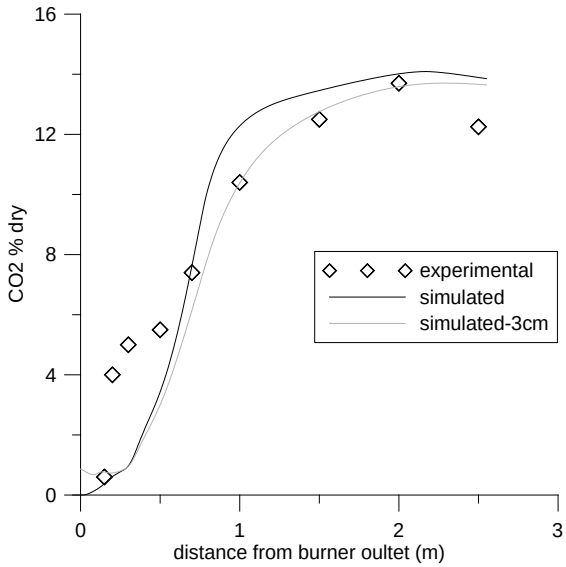

Figure 3.6b: Comparison of CO_2 profiles for the plastic case

3.2.4. Discussion – further research work

A modeling approach for the combustion of Solid Recovered Fuel particles is presented in the second part of this chapter. The assumption that SRF is mainly composed of a biogenic and a plastic fraction is made. New submodels for the melting and decomposition of plastic are developed and integrated in a commercial CFD code, and are validated with available experimental data for prepared biogenic and plastic samples and for brown coal [III-23]. A good agreement of the simulated results with the available experimental data is achieved for all considered fuels. In order to obtain further results on the behaviour of the numerical model in the industrial scale, it is also used in the large boiler SRF co-firing simulations presented in the next chapter.

Future research work in the particular field should focus on the accurate description of the motion and the combustion behaviour of irregular shaped particles. Most of the Solid Recovered Fuels prepared from MSW are produced in the form of fluff containing to a great percentage paper or plastic foils with average diameters between 5-30mm. After being milled, either in a brown coal mill or in a dedicated mill for SRF, their Particle Size Distribution is reduced down to the millimetre size. Under these conditions the spherical assumption for the considered particles is valid and therefore, the model validation with prepared biomass and plastic fractions, whose particles are almost spherical, is justified. However, if no milling step applies, the spherical assumption for SRF particles is not valid. The aerodynamic drag increases in the case of irregular, non-spherical particles resulting in increased particle residence times in the furnace. The available surface of non-spherical particles compared to their volume also increases resulting in increased heat transfer rates. Therefore, non-spherical particles like SRF foils are expected to have a satisfying burnout despite their larger size compared to milled SRF particles, and this is also proven by experience during the large-scale tests.

In particular, the motion of irregular particles in the continuum is governed by a new expression of the particle force balance, which incorporates the aerodynamic lift and drag of non-spherical particles as also rotation. These forces are dependent on the particle orientation

and have to be calculated in a relative reference frame for each time step [III-24]. Furthermore, in order to describe heating, devolatilisation and char combustion of non-spherical particles the currently available laws for spherical particles have to be modified. Some efforts are already being made by other researchers [III-25], [III-26], [III-27]; however, without accurate experimental data covering different particle shapes and diameter classes, the validation of the proposed models is not possible. This kind of data have to be provided initially by laboratory furnaces, modified for SRF particle combustion as performed by Dunnu [III-4], and subsequently be applied in pilot or semi-technical scale combustion furnaces which will be able to fire fluffy SRF material.

4 SRF co-firing: Investigations in the large scale

Summary
The investigations of direct SRF co-firing in the industrial scale through experimental activities and numerical simulations are discussed in the present chapter. The results of the measurement campaign performed during a two-week demonstration of SRF direct co-firing in a 600 MWel pulverized brown coal boiler are presented in the first part. The overall results indicate that large scale co-firing up to a thermal share of 4% is feasible without any environmental impacts and without seriously endangering the standard boiler operation. The second part focuses on the evaluation of different injection concepts for SRF through numerical simulations. Testing different SRF injection concepts in the large scale cannot be easily realized and requires extensive boiler modifications. At this point CFD analysis is a useful tool for the initial evaluation of the proposed injection modes and the determination of the optimum ones that have to be further considered for a real scale implementation. In this framework the same boiler is simulated and different co-firing concepts are modeled and evaluated based on specific criteria related with the combustion behaviour.

4.1 SRF co-firing: Demonstration in the large scale

4.1.1 Introduction

To date co-utilisation of Solid Recovered Fuels has been up to now a common practice only in few plants of the cement and the lime industry in Europe [IV-1]. However, co-firing of SRF in large scale hard coal or brown coal power plants has not been tested until recently due to a number of reasons. The most important ones are:
a. the reluctance of the boiler operators to co-fire different fuel types from their main guaranteed fuels due to potential technical risks,
b. the necessary administrative work for the authorisation of SRF co-firing in existing power plants since SRFs are produced from waste fractions and are considered as waste,
c. the reluctant public acceptance of the particular fuel and its co-firing in existing power plants with conventional flue gas cleaning technologies.
In this framework, the scope of the performed SRF co-firing campaign - co-funded by the EU Demonstration Project Recofuel [IV-2] – was, firstly, the proof of concept without the appearance of any technical knock out criteria, and, secondly, the demonstration that no negative environmental impacts are expected by the particular co-utilisation practice. Two 600 MW_e brown coal boilers at RWE's Weisweiler power plant were used for this scope. Large-scale measurements took place in one of them, Boiler H.
During the two-week demonstration the share of SRF in the overall thermal input was adjusted to approximately 2% resulting in a feeding rate of about 25 tons per hour and per boiler while an increased share of 4% was tested for some days. The extensive measurement campaign performed by a large team of engineers from universities, research institutes and industrial partners focused on environmental and technical aspects. The evaluation concerning the environmental aspects includes the measurement of flue gas emissions, solid by-products and other potential impacts to the environment, whereas the evaluation of the technical aspects includes the measurement of various technical parameters related with the boiler operation and the respective effect of SRF

co-firing. The overall results of the measurement campaign are also published in international scientific journals [IV-3], [IV-4], [IV-5].

4.1.2 Measurement methods

Description of the power plant site and the feeding system
RWE's Weisweiler power plant consists of six units with total installed capacity of about 2060 MW_{el}. The tests took place in Units G and H, with a nominal capacity of 600 MW_{el} each, which co-fire paper sludge at a standard operation mode in a thermal share of about 2%. The feeding schema for both secondary fuels is presented in Figure 4.1. In particular, paper sludge and SRF are transported with lorries and unloaded in a dedicated unloading station. This consists of a twin 180m^3 and a single 90m^3 bunker together with two intermediate storage areas summing up to 4000 tons. The feeding capacity of the three screw feeders amounts to 125 m^3/h each, resulting in a feeding capacity of 62.5 Mg/h for paper sludge and 25 Mg/h for SRF. From the intermediate bunkers of the unloading station both secondary fuels are transported through screw feeders and conveyor belts to the main coal conveyor belt and mixed with brown coal. The mixed ready fuel composed of brown coal, paper sludge and SRF enters then the crushing unit, where it is downsized, mixed and homogenized. After the crushing step, the fuel mix enters the coal bunkers from which it is further fed through chained conveyor belts into the coal mills. In this way it is possible to ensure that the SRF mass flow is equally divided to all operating mills - seven or eight – and that SRF inserts the furnace through all burner levels of each mill. The thermal share of 2% corresponds to an SRF mass flow of 12.5 Mg/h per boiler. The total feedstock consumption for both units during the two-week co-firing tests was 4200 Mg SRF, 13.300 Mg paper sludge and 345.000 Mg brown coal.

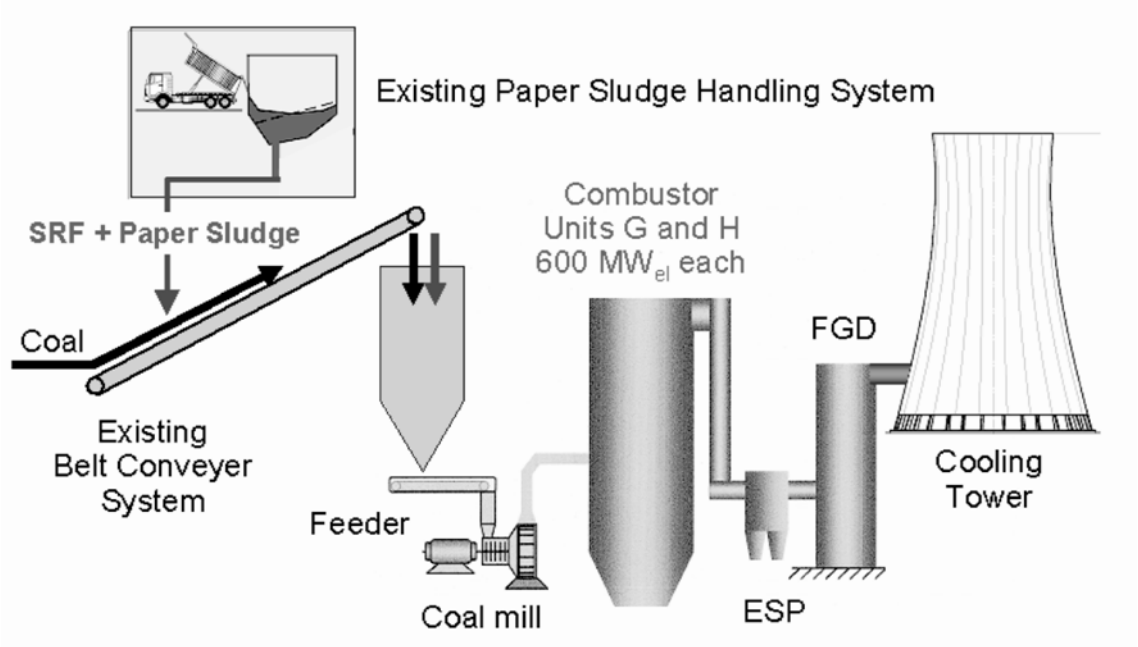

Figure 4.1. SRF/ paper sludge supply system to the boiler, Source: RWE Power AG

Fuel characterisation
The Solid Recovered Fuel utilised during the tests is produced by the German company Remondis and bears the trademark SBS®1 ("Substitutbrennstoff" in German nomenclature). It derives from mixtures of High Calorific Fractions (HCF) of Municipal

Solid and Bulky Waste. Its production is based on positive sorting methods, by means of which only a small amount, about 30 wt.-% of the MSW input stream – mainly the paper fraction, the biogenic fibre material and some plastic – is sorted out positively by Near Infra Red (NIR)-technology as high calorific fraction [IV-6]. The analysis of the raw fuels, lignite, paper sludge, SBS®1 and of the ready-fuel, which is the mixture of coal and paper sludge fired at a normal operation mode, is given in Table 4.1. The values presented are averages of all daily samples collected during the two-week co-firing campaign.

Table 4.1: Analysis of the different fuels, Source: RWE-Power

	unit	Lignite	Paper Sludge	SBS®1	Readyfuel (coal+paper sludge)
C	%	25.40	13.33	37.18	25.20
H	%	1.85	1.55	5.21	1.82
O	%	9.88	13.49	20.90	9.83
N	%	0.25	0.24	0.61	0.25
S	%	0.16	0.06	0.13	0.15
Moisture	%	58.9	49.30	28.03	58.7
Ash	%	3.60	22.00	7.93	4.10
H_u (raw)	MJ/kg	8.10	2.95	14.87	7.961

Furthermore, mean values of chlorine, fluorine and heavy metals concentration of the three different fuels are presented in Annex B2, in Table B2.1, as well as respective maximum measured values of SBS®1 and typical values of coal. The high chlorine values of SRF - about an order of magnitude greater than the chlorine value of lignite - have to be discussed. Considering the heavy metal concentrations of SRF presented in mg/kg, increased values are observed compared to the ones of paper sludge. However, for the correct comparison of the concentrations of different fuels, the energy-specific concentrations (mg/MJ) have to be calculated and compared according to CEN/ TC 343. After the appropriate conversion, the differences between the values of the two alternative fuels become minimal indicating that there is no remarkable difference in the heavy metal concentration of SBS®1 and paper sludge.
The biogenic content of SRF is also of high importance for the characterization of the specific fuel due to its correlation with the estimated CO_2 emission reduction potential. The respective biomass determination methods are, however, still under development. They are mainly based on a selective dissolution procedure followed by further analytical steps. Alternative techniques such as the ^{14}C method are still under development [IV-7]. The mean biomass content of the considered SRF is around 64% according to the weight determination, about 62% according to the calorific value determination and about 60% according to the total carbon content determination. In order to have a complete picture regarding the fuel parameters of SRF, its main ash components compared with the ones of Rhenish lignite are given in Annex B2, in Table B2.2. The increased Al_2O_3 and CaO concentration in the SBS® ash compared with the lignite ash has to be pointed out for the subsequent interpretation of results.

Performed measurements

In respect of the evaluation of the environmental behaviour and the potential impact of SRF co-firing on it, the following measurements are performed:

- Measurement of standard flue gas composition and of HCl concentration at the boiler outlet before the air preheater
- Complete flue gas measurements at the stack, after the ESPs and the desulphurisation unit including conventional emissions (CO, NOx, SO_2, dust) and non-conventional flue gas emissions (HCl, HF, dioxins-furans, heavy metals) according to the Waste Incineration Directive and German legislation
- Sampling and analysis of the main fuel and the solid by-products (wet bottom ash, fly ash, gypsum). Characterisation of the solid by-products in respect of their heavy metal content and the possibility to be landfilled.

Furthermore, as regards the evaluation of the boiler technical aspects, the following investigations are performed:

- Continuous monitoring and recording of the main operational parameters including steam temperatures, flue gas temperatures, steam production, electric power production.
- Mill measurements and periodic mill inspections
- Inspections of the mechanical equipment for SRF feeding and dosing including mainly conveyor belts and screw feeders
- Profile measurements of the flue gas temperature and composition at the furnace exit, Figure 4.2a, location (i), by using a dedicated water cooled measurement probe
- Measurements of flue gas temperature and composition at the boiler outlet before the air pre-heater, Figure 4.2a, location (ii)
- Evaluation of the expected effect of SRF on the boiler corrosion potential

Three different operation modes are tested: the standard operation, at which lignite and paper sludge is fired as reference fuel, and the 2% and 4% co-combustion modes, at which SRF is also co-combusted in thermal shares of 2% and 4% respectively. Regarding the profile measurements at the furnace exit, a distinction between the eight-mill symmetrical operation and the seven-mill operation has to be made due to the different flow field and combustion conditions in each case. Profile measurements from the front and the rear boiler side are taken, as presented in Figure 4.2b in order to have a more complete picture of the variation of temperature and flue gas composition at the entire furnace cross-section. Measurement points are taken in 0.2m steps up to a total depth of 5m. The sampling time of five minutes is set for each measurement point. The measurement plan of the investigation performed at the furnace outlet is presented in Table 4.2.

Apart from the profile measurements, dedicated corrosion probes for the monitoring of the corrosion potential are also installed at the furnace exit level as shown in Figure 4.2b. Two different measurement probes are installed at the front and the rear boiler walls, an electrochemical corrosion monitoring probe and a deposition probe. The operating temperature of both probes is set at 475 °C and controlled by active cooling so that intense slagging effects are avoided. The electrochemical corrosion probe continuously monitors the developed electrochemical potential on the probe surface by

two different measurement techniques, the Linear Polarisation Resistance (LPR) and the Electrochemical Noise (EN) method. The relative change of the electrochemical potential is an index for the increase or decrease of the corrosion rate. The second probe installed is a tubular corrosion probe consisting of three cylindrical material samples, welded to each other and to the probe body, which are similar to those used in the furnace and super heater sections of the boiler. After the removal of the probe, the analysis of the interaction of the ash particles on the metallic surface and its different layers through electronic microscopy gives valuable information on the potential corrosion phenomena. The corrosion investigations are performed by two different institutions and are not part of the investigations of this thesis. They are, however, mentioned as literature sources, in order to have a complete picture of the investigations performed and the results obtained during the large-scale tests.

Table 4.2: Performed profile measurements at the furnace exit level

	Symmetrical operation (8mills)	7 mills operation
Baseline	measurements at the front and rear side	-
2% SRF co-combustion	measurements at the front side	measurements at the front and rear side, mill nr. 7 in planned revision
4% SRF co-combustion	-	measurements at the rear side, mill nr. 7 in planned revision

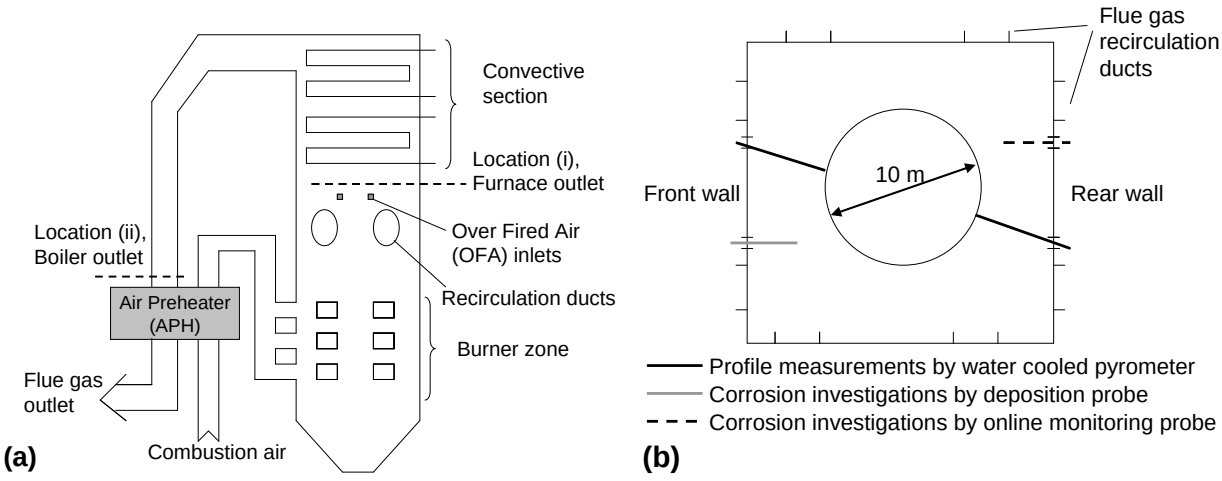

Figure 4.2 (a) boiler measurement locations, (b). measurement locations at furnace exit

As regards the measurements of HCl concentration at the boiler outlet, before the air pre-heater, a dedicated glass probe is used and the analysis is performed according to the German VDI guideline 3480 [IV-8]. The overall assembly of the sampling line is presented in Figure 4.3. Flue gas is sucked through the whole measurement installation at a constant volume flow. The probe itself is heated to avoid condensation. In front of the bubbling bottles a heated fly ash filter removes the particle load. The bottles - filled with distilled water - are situated in a cooler to achieve a constant solvent temperature

of approx. 10°C. Hydrogen chlorine dissolves almost totally in water, whereas the flue gas moisture condensates in the bottle. The flue gas moisture can be calculated from the difference between the initial water volume and the determined condensed volume. The chlorine content is afterwards analysed in the laboratory by ion-chromatography.

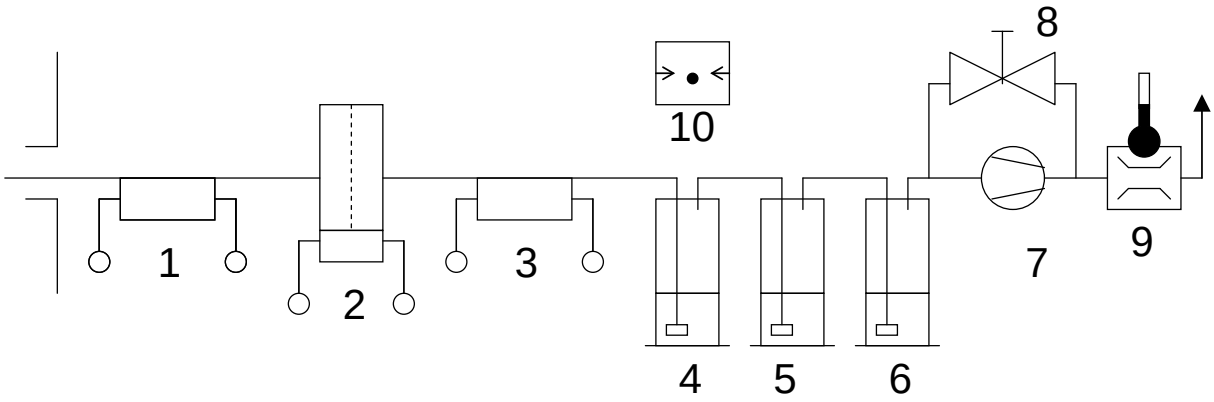

Figure 4.3 Sampling assembly of the HCl measurement equipment, Source [IV-6]

Index

1	Heated sampling probe	7	Pump
2	Heated quartz wool filter	8	Overflow valve with flow control valve
3	Heated sampling duct	9	Gas meter with thermometer
4, 5	Absorption vessels	10	barometer
6	Droplet separator		

4.1.3 Results and discussion

Evaluation of the environmental impact of SRF co-firing

The effect of SRF co-firing on environmentally related aspects is initially evaluated. Conventional flue gas emissions (CO, NOx, SO_2, dust), which are continuously monitored, remain in the previous variation range and are not affected by the co-combustion tests. In particular, SO_2 emissions which are more related with the composition of the inlet fuel also remain in the normal range since the sulphur content of SRF is comparable with that of coal, according to the ultimate analysis of all fuels presented in Table 4.1.

The results of the discontinuous emission measurements performed at the stack are given in Table 4.3. Two measurements are performed, one in the baseline and one in the SRF co-firing mode to enable a comparison between them. The respective limits set by German legislation, 17. BlmSchV, and the stricter limits set by the local German authorities for the particular co-firing demonstration are also presented.

No influence of SRF co-combustion is visible on all pollutants considered, including HCl, HF, heavy metals and dioxins-furans. Although the heavy metal content of SRF is higher compared to that of brown coal as also noticed in Table B2.1, the low thermal share and the even lower mass share of SRF to the overall fuel flow leads to very small changes of the heavy metal content in the flue gas, which are within the variation range. The increased Chlorine level of SRF does not seem to have any influence on the HCl concentration of flue gas at the stack indicating that the additional Chlorine is removed

by the scrubbing process at the desulphurisation unit. Regarding the potential increase of dioxin and furan emissions, due to the higher content of plastic in Solid Recovered Fuels such behaviour is not confirmed. The adequate residence time of SRF particles in the high temperature region – over 800°C – is expected to be the main reason for the destruction of potential PCDD/F emissions. This residence time is estimated by numerical simulations presented in section 4.2 to be more than 5s.

Table 4.3: Emission measurement according to legislation, Source: RWE-Power

Component	Unit	Baseline (lignite and paper sludge)	SRF co-combustion	Permitted Emission	German legislation 17. BlmSchV
Dust	mg/Nm^3	3.0	1.5	10	10
Total Carbon	"	0.3	0,5	8.4	10
HCl	"	0.3	<0.1	20	20
HF	"	<0.1	<0.1	1	1
Σ Cd-Ti	"	<6.3	<7.0	11	50
Hg	"	9	7	16	20
Σ As-Sn	"	<65.7	<64.8	500	500
PCDD/F	"	<0.001	<0.001	0.026	0.1

A more complete picture on the influence of the SRF Chlorine content on the HCl concentration in the flue gas is given by evaluating the HCl measurement results in the boiler outlet before the air preheater. The baseline chlorine concentration at the boiler outlet ranges between 53 and 57 mg/m^3_N (Figure 4.4). A difference can be observed between the measured HCl values and the calculated values according to a simple mass balance. The amount of chlorine not diluted in the flue gas and bound in the fly ash is probably the reason for this. A linear dependency between the SRF co-firing share and the HCl concentration in the flue gas is also detected, as expected by the mass balance. No increased HCl concentration was, however, observed in the stack measurements after the flue gas desulphurisation unit indicating an adequate removal of HCl in the Flue Gas Desulphurisation system.

The last point to be investigated in respect of environmental behaviour is the residue quality. In order to evaluate the leaching behaviour and stability of the combustion residues consisting of ESP ash, wet bottom ash and FGD gypsum, which are dumped on the Inden ash landfill, specific mixed samples were prepared and analysed. The results of the leaching values of the mixed fly and bottom ash samples together with the subsequent permission limits for a storage time period of 28 days are presented in Annex B2, in Table B2.3. The values do not exceed permission limits, and no significant difference is observed between the reference case samples and the samples taken during SRF co-combustion. Finally, the heavy metal analysis of the fly ash samples taken during the reference and the SRF co-combustion period is given in Table B2.4. Daily samples composed of respective 1 hour samples were analysed. Slightly higher mean values can be found for some components, while the range of the measured values remains for most components the same.

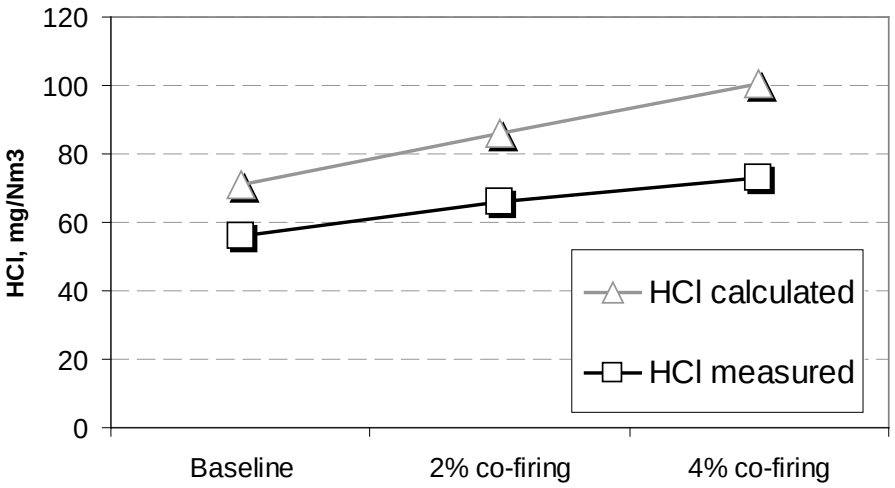

Figure 4.4. Measured and calculated HCl concentration in front of air pre-heater (APH)

Evaluation of SRF co-firing effects on the boiler technical parameters

Operational behaviour

Regarding the evaluation of the boiler operational behaviour during the two-week co-combustion trials, the general and most significant result is that the normal operation of the plant continued without any technical knock out caused by co-firing [IV-9]. Main operational parameters, such as steam temperatures and pressures, steam and electricity production, were monitored during the entire demonstration period. No negative influence of SRF co-firing on the operational parameters is observed and all values remain in the normal variation range.

Feeding system

The performance of the feeding system is characterised as satisfying. Mixing the SRF stream into the coal conveyor belt before the pre-crushers secured satisfying fuel homogenization as expected. No false alarms were observed in the metal and fire detectors. Furthermore, the tests indicated the need for special housing of the fuel unloading station and sealing of specific places of the coal feeding system, such as the SRF and coal mixing point in order to avoid spoiling of outside and inside spaces. For this reason a separate pneumatic system for SRF transportation combined with a dedicated unloading station has to be considered as an alternative for permanent operation.

Profile measurements at the furnace exit

An overview of the results obtained by the profile measurements at the furnace exit is given in this section. Slightly increased exit temperatures (approx. 20K) are observed in some co-combustion cases, although this tendency is not verified for all profiles. This increase is also in the range of the standard deviation of the temperature measurements performed (±20-30K). No clear tendency for SO_2 and CO is visible, while the nitrogen oxides are slightly lower in co-combustion operation. The standard deviation of the flue gas measurements is in all cases lower than 10% of the respective values. The

measurement error of the equipment used during the tests is 10K for the specific thermoelement type, 0,01% for the O_2 and CO_2 analysers and approximately 10ppm for CO, NO_x, and SO_2 analysers. In order to have a complete picture of the boiler operation conditions, symmetrical and non-symmetrical conditions in the furnace are measured and evaluated. The seven-mill operation leads to a shift of the flame to the particular boiler site where the mill is out of operation as a result of the missing impulse. As a direct consequence, the shape of the oxygen profiles changes and high CO levels in the near-wall atmosphere are measured.
A direct comparison between symmetrical - 8 mills in operation - and non-symmetrical - 7 mills in operation - flame conditions is not possible, as the effects of co-combustion interfere with the altered flow conditions. Therefore, the results will be evaluated separately for the seven- and eight-mill operation. In order to reduce the data set (profiles taken in 0,20m steps from 0 up to 5,0m depth) and to achieve clearer diagrams, mean values are calculated for sections (1,0 – 2,0); (2,0 – 3,0); (3,0 – 4,0) and (4,0 – 5,0) meters. Section (0 – 1,0) is afterwards omitted as the results are highly influenced by false air introduction via the measurement port. The discussion and evaluation focuses on the following parameters: (a) Temperature (in °C), (b) Oxygen concentration (in % vol. dry), (c) Carbon monoxide (CO, mg/m^3_N dry), (d) Nitrogen oxide (NO_x, mg/m^3_N), and (e) Sulphur oxide (SO_2, mg/m^3_N). The CO, NOx and SO_2 values presented are corrected to a reference O_2 value of 6%.

(a) Temperature profiles (Figure 4.5)
For both 7- and 8-mill operation differences are determined between the boiler front side (measurement BL_V) and rear side (measurement BL_R). Nevertheless, satisfying matching is observed between the profiles taken at the same position (BL_R vs. 2%_R and 2%_R vs. 4%_R). The temperature level during co-combustion is slightly reduced for both cases investigated.

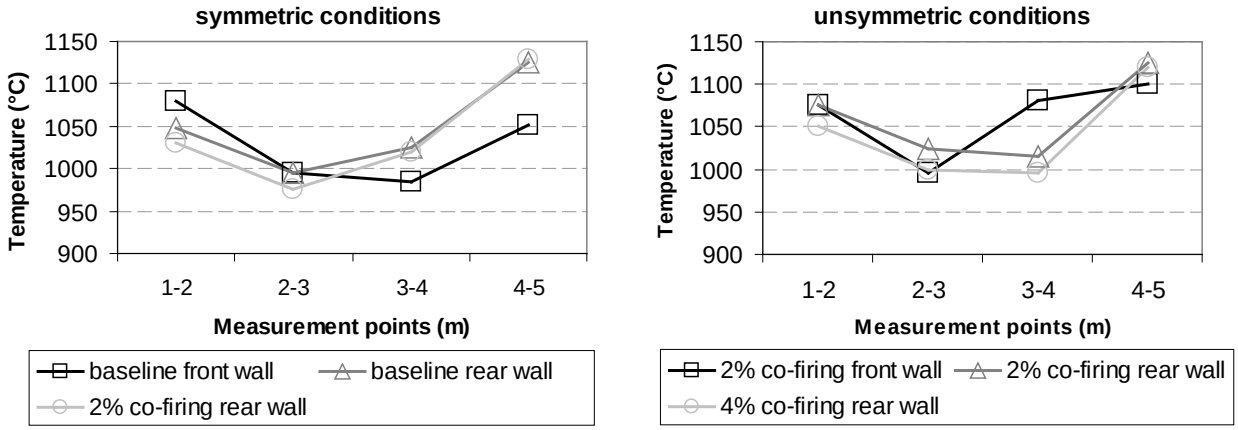

Figure 4.5: Furnace exit temperature (°C): (a) symmetrical conditions, (b) unsymmetrical conditions

(b) Oxygen concentration (Figure 4.6)
During the 8-mill operation the oxygen level increases at the furnace wall and decreases deeper inside the boiler during co-combustion operation. Both baseline measurements on the boiler front and rear side are comparable. Considering the 7-mill operation and

the increased thermal share from 2% to 4%, no differences could be determined. However, differences are observed for non-symmetric combustion conditions comparing a thermal share of 2% on the boiler front and rear side.

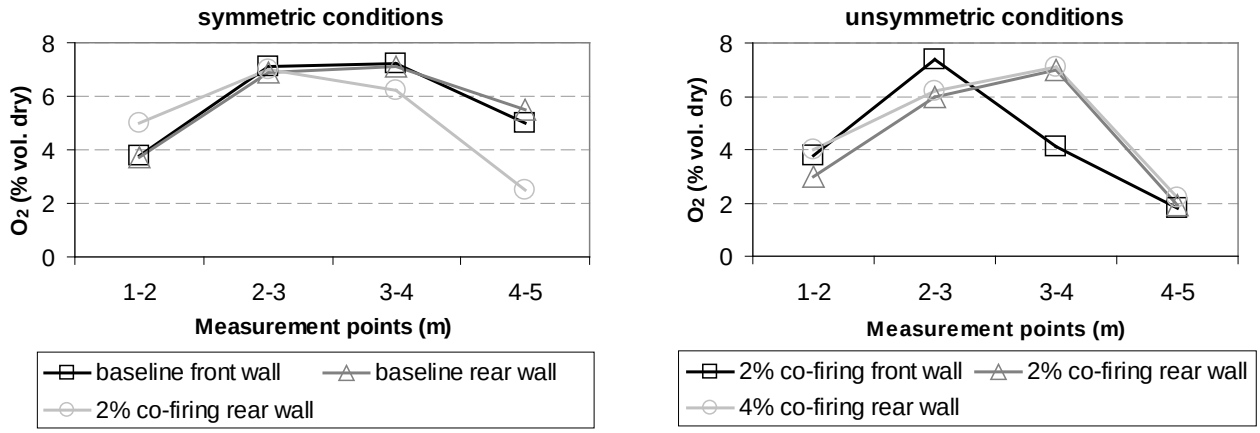

Figure 4.6: O_2 concentration (% vol. dry): (a) symmetrical conditions, (b) unsymmetrical conditions

(c) Carbon monoxide (Figure 4.7)
Carbon monoxide levels are slightly increased comparing BL-2% and 2%-4%. Differences between boiler front and back side are again observed. Due to the nature of the co-combusted material, slightly increased CO levels can be expected at the furnace exit as the material may need more time for a complete burnout due to the average larger diameter distribution.

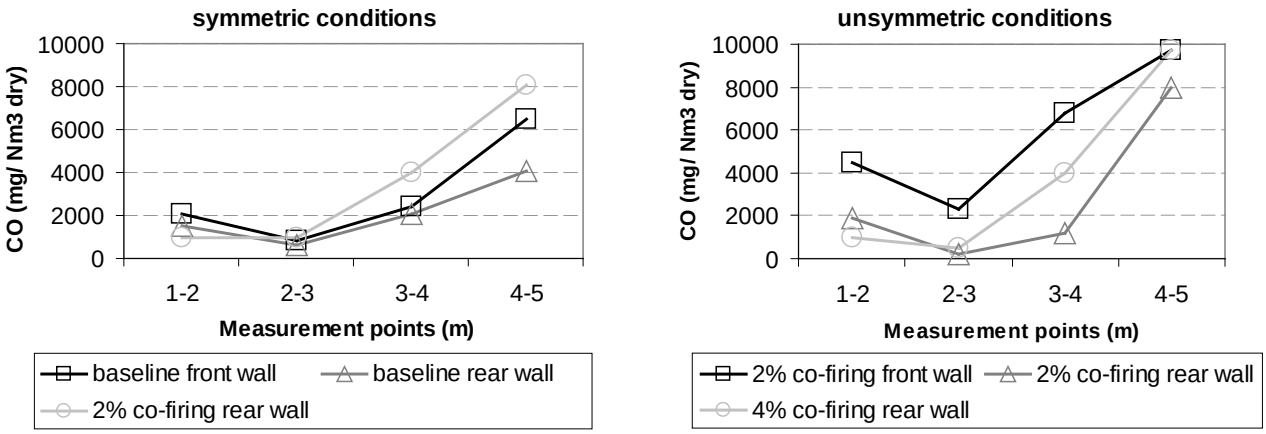

Figure 4.7: CO concentration (% vol. dry): (a) symmetrical conditions, (b) unsymmetrical conditions

(d) Nitrogen oxides (Figure 4.8)
Profiles for the 8-mill operation show slightly lower NO_x levels during co-combustion. Deviations between boiler front and back side are negligible in the case of nitrogen oxides. Considering the increase from 2% to 4%, the emission profile remains

comparable. As the nitrogen content of SRF is higher compared to that of lignite and paper sludge, increased emissions could be expected. The continuous flue gas measurement at the stack did not show, however, such a behaviour which is a positive result for the co-combustion practice.

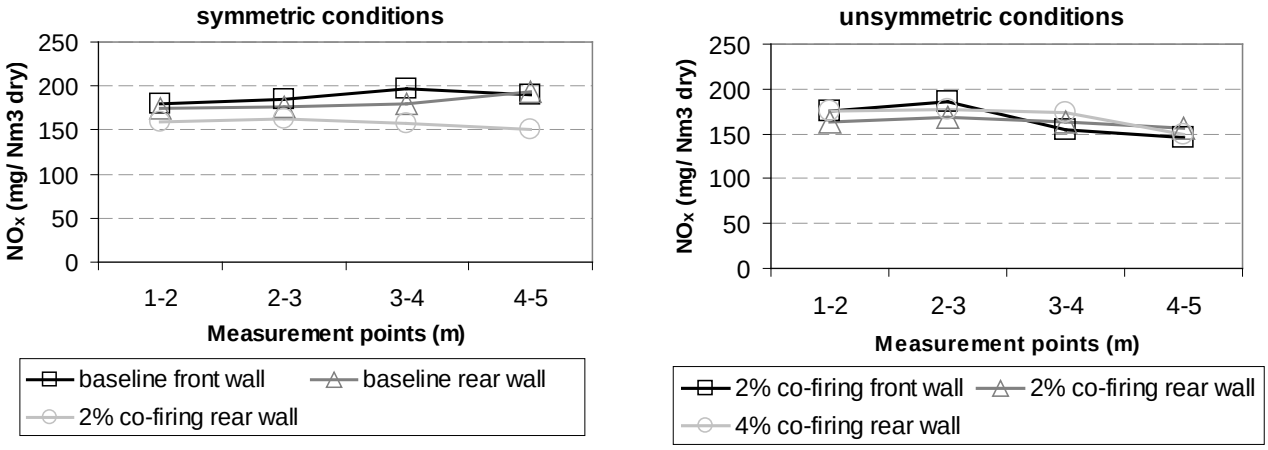

Figure 4.8: NOx concentration (% vol. dry): (a) symmetrical conditions, (b) unsymmetrical conditions

(e) Sulphur oxides (Figure 4.9)
A comparison of baseline and a thermal share of 2% indicate lower SO_2 concentrations for the measured profiles, although the baseline profiles measured at the boiler front and rear side differ extensively. The profiles for non-symmetric conditions (H7-) indicate no clear tendency. For both cases the results remain uncertain. Generally, the lower amount of sulphur in the co-combusted SRF should lead to lower SO_2 emissions.

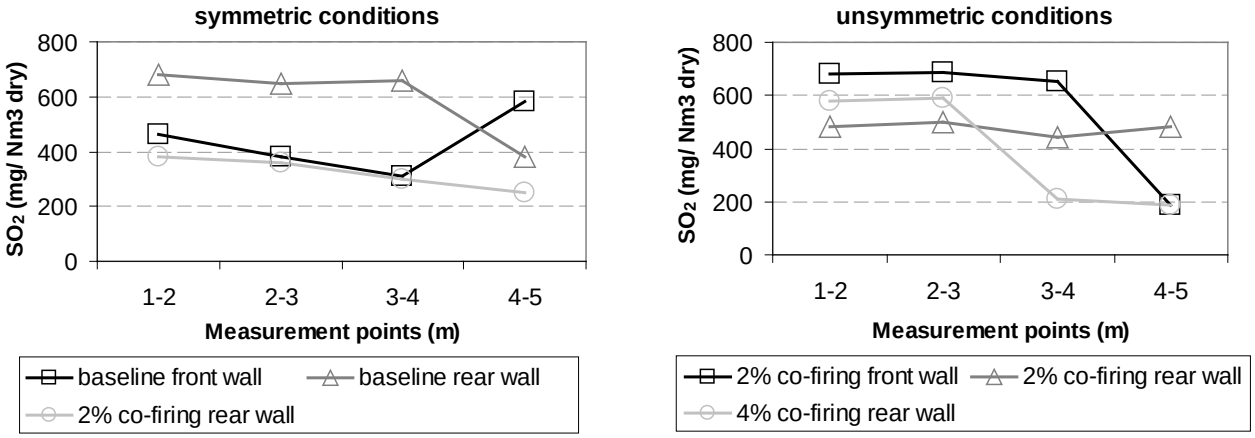

Figure 4.9: SO_2 concentration (% vol. dry): (a) symmetrical conditions, (b) unsymmetrical conditions

Evaluation of the boiler corrosion potential
The corrosion data obtained during the measurements at the Weisweiler power plant are filtered and synchronised with the recorded boiler process data. The correlation coefficient is calculated between the corrosion data and each of the process parameters.

No significant correlation is established between corrosion and the recorded data series indicating no significant influence of the operation mode on corrosion. The data set is afterwards separated according to the SRF thermal share (0%, 2 or 4%) and corrosion rates are determined. The latter are constant for 0% and 2% applied and increase slightly for the 4% co-firing share. All the changes are, however, less than the standard deviation indicating no clear influence of SRF co-firing on corrosion. Regarding the analysed samples from the deposition probe, the major phase detected is Fe-oxide (aside from the resin), whereas the rest of the sample is a mixture of Fe-silicates, -sulphates, Ca-sulphate, CaMg-sulphate. The deposit consists mainly of Fe-oxide and ash particles coming from the lignite and no trace of unburned SRF is detected. The external oxide layers of the material samples collected showed enrichment in Calcium, Silicon and Aluminium. It is also possible to note the presence of sulphur into the oxide both in the more external layer and at the interface with the base material. No chlorine presence is detected in the oxide layers for all three samples, which indicates that the metal oxides are stable at high temperatures. Summing up, as far as the experimental investigations on potential corrosion risks during SRF co-firing are concerned, it can be stated that the experimental measurements could not indicate a clear effect of SRF co-firing on corrosion. It should, however, be pointed out that by measuring in only one location and for a short period of time, no clear picture of the corrosion phenomena inside the whole boiler can be observed. The results are, therefore, regarded as a first impression only and long-term tests in multiple locations are needed in order to have a more comprehensive and reliable picture on the corrosion potential and the influence of SRF co-firing.

4.1.4 Conclusions – Further outlook

Co-firing of Solid Recovered Fuels derived from Municipal Solid and Bulky Waste is demonstrated in a pulverised brown coal power plant in the Rhenish region in Germany for a continuous period of two weeks. During this period the co-combustion thermal share is kept constant at 2% and increases up to 4% for shorter time periods. An extensive study on the possible impact of SRF co-firing on the environmental performance of the plant and the technical parameters related with the boiler operation is carried out. The performed measurements show that all emission limits for conventional and non-conventional pollutants determined by German legislation [IV-10] and the Waste Incineration Directive [IV-11] are observed. Clear indications of a definite impact of SRF co-firing on the boiler operation are not found during the two-week demonstration. The most important aspect which has to be further investigated is the potential of chlorine corrosion at the first superheater surfaces. Although the measurement campaign did not show any specific trend on increased corrosion rates caused by SRF, the decision for the realisation of a second co-firing campaign with a long-term perspective of several months has not been taken by the plant operator. The risk of causing permanent damage to the super heater section after a long-term co-firing operation without being able to monitor and accurately predict the corrosion progress, is considered as too high by the operator. On the other hand, other pulverised brown coal power plants in Germany with different coal quality, successfully apply SRF co-combustion in continuous operation mode [IV-12]. The detailed investigation of the increased HCl levels on the corrosion potential in large-scale conditions is, therefore, recommended.

This kind of large-scale investigations is performed in a Circulating Fluidised Bed (CFB) boiler co-firing Rhenish brown coal, sewage sludge and SRF [IV-13]. Online

corrosion monitoring probes and deposition probes are installed in the superheater section of the fluidized bed boiler and the HCl levels are continuously measured by an innovative online HCl measurement method. The overall results of the large-scale campaign in the CFB boiler indicate the necessity for control of the chlorine content in SRF through a dedicated Quality Assurance System in the SRF production process. Sulphur to Chlorine (S/Cl) Ratio in the flue gas is a significant parameter which influences corrosion rates. In particular, the measurements at the CFB plant showed that co-firing sewage sludge with high sulphur content reduces the introduction of chlorine into fly ash and the respective deposits in the heat exchanger surfaces preventing, in this way, the increase of the corrosion related phenomena. In this sense, online determination of S/Cl ratio in the flue gas through dedicated online HCl measurements and the evaluation of the relative increase or decrease tendencies is a useful tool for the estimation of specific changes in the corrosion rates.

4.2 Large scale CFD simulations on SRF co-firing

4.2.1 Introduction

One important issue for every co-firing project is keeping combustion behaviour stable, while ensuring the complete burnout of the alternative fuel. In the case of Solid Recovered Fuels this constitutes a challenging task due to their inhomogeneous nature and their large particle size distribution since they are delivered at the plant site in the form of fluff. Choosing the most capable injection concept in order to ensure complete burnout, while keeping other combustion related parameters - like the furnace exit temperature and the wall heat flux - constant is, therefore, of high importance. However, an examination on the different injection modes of the alternative fuel into the boiler cannot be easily performed in the industrial scale by means of measurements due to the extensive technical modifications required. In order to overcome this problem the same research groups presented in Chapter 3.1 focus on the characterisation of SRF combustion behaviour through lab-scale analysis and kinetic evaluation [III-5 - 8], while other research groups try to extrapolate the information gained from the lab-scale data in the large-scale boilers and predict in this way the burnout of SRF particles [III-4].

In this framework it can be argued that CFD simulations are a useful tool towards predicting SRF combustion behaviour if dedicated models for SRF are developed and incorporated in existing CFD codes. In this way different co-firing concepts can be simulated in advance, without the necessity of their being tested in the large scale. After the evaluation of the simulation results, some of the initially proposed scenarios can be excluded and the ones showing the most satisfying results are considered as candidate solutions to be implemented at the site.

According to literature and available technical experience from realised large-scale co-firing projects [IV-12], there are three main feeding options for the alternative fuel in the case of direct co-firing into a pulverised coal boiler (Figure 4.10):

A. Feeding the alternative fuel upstream the coal mills. Through the milling process the fuel is dried and the mean particle size is reduced.
B. Feeding the alternative fuel into the coal ducts, downstream the mill. The fuel enters the boiler through the main coal burners. In order to reduce the particle size distribution a dedicated mill for the substitute fuel is usually installed.
C. Injecting the alternative fuel through dedicated burners into the boiler. A dedicated mill for reducing the particle size distribution may be used in this concept, too.

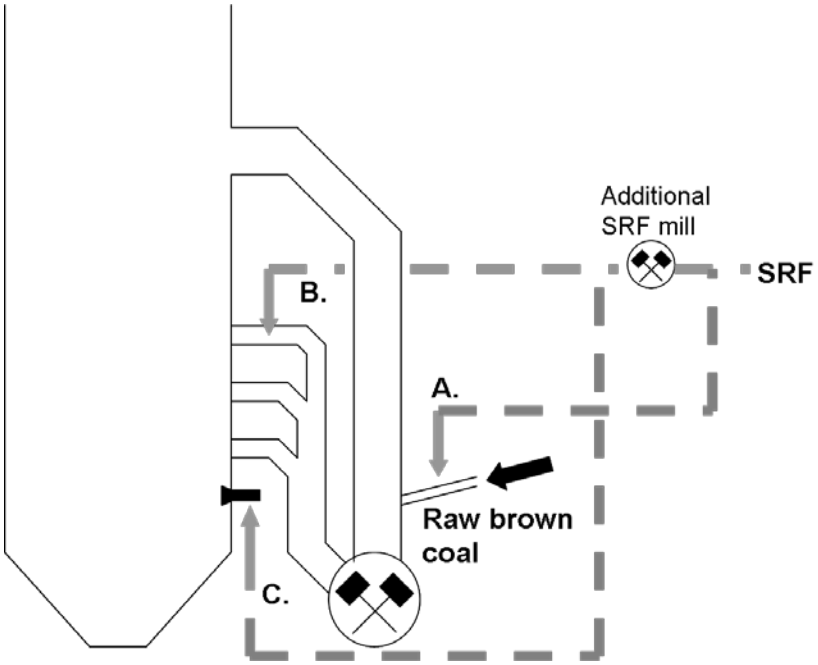

Figure 4.10: Different injection concepts for alternative fuels in lignite boilers

The work in the present section focuses on the evaluation of these three different co-firing concepts on the particular case of Boiler H of the Weisweiler power plant, where the large-scale measurements are performed. For this scope the developed and validated combustion model for SRF presented in chapter 3 is integrated in the commercial Fluent code and Boiler H is simulated under three different SRF co-firing modes. The same assumption for SRF composition is adopted, namely that it consists of a biogenic and a plastic fraction with each fraction undergoing a different combustion mechanism. The influence of the SRF particle size on the combustion behaviour is evaluated by performing simulations for different particle diameters. Specific parameters post-processed from the simulation results are used as performance indices for judging combustion behaviour. The most important among them are the average and maximum furnace outlet temperature, the total heat flux to the evaporator and the burnout of SRF particles. Based on these evaluation criteria, the simulated cases showing the best results then become the most probable scenarios to be applied in real conditions.

4.2.2 Methodology

Fuel Characterisation

The considered SRF which is co-fired during the large-scale tests derives from high calorific fractions of MSW and bulky waste, and a picture of a typical fuel sample is given in Figure 4.11a. After following a manual sorting procedure, different fuel fractions can be recognised. The same SRF type is analysed by Dunnu et.al. [III-3] and the results of the performed manual sorting are presented in Figure 4.11b. The large number of different fuel fractions recognised has to be stressed, which is a proof of the increased variance of the input streams of waste recovered fuels. Since it is not possible to model the combustion behaviour of each fraction, it has been decided to focus on the most significant among them, the paper/ cardboard and the plastic fraction, with the same argumentation as in the previous chapter.

Fig. 4.11a: Typical SRF sample from MSW

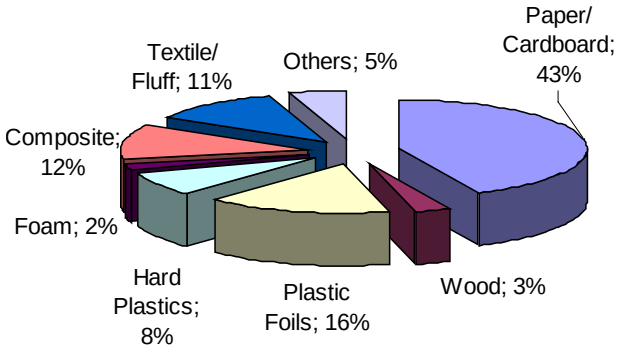

Fig. 4.11b: SRF fractions after manual sorting

The proximate and ultimate analysis of the SRF and the reference fuel (Rhenish lignite and paper sludge) used for the simulations are given in Table 4.4. SRF has relatively high water content and low ash and carbon content. Despite its high water content, its calorific value is almost double that of the Rhenish lignite, which is justified by the presence of the plastic fraction in the fuel. Plastic is usually found in the form of foils in the fluffy material, and possible plastic types are PP, LDPE, HDPE and PVC. The assumption that the plastic fraction of the considered SRF accounts for 25% of its mass is made. This value corresponds to about the sum of the hard plastics and the plastic foils presented in Figure 4.11b. Polypropylene is taken as a representative plastic sample, and its proximate and ultimate analysis is also given in Table 4.4. The proximate and ultimate analysis of the remaining fraction, the biogenic one, is calculated, from the mass balance of the regarded elements C, H, N, O, S and the energy balance as given by the heating value of the fuels. In this way the weighted mixture of the two considered fractions will meet the initial proximate - ultimate analysis and net calorific value of the SRF sample. This procedure allows the influence of the combustion of plastics that do not undergo the same steps as the biogenic fraction, to be incorporated, while the overall fuel analysis of the SRF considered remains constant.

Table 4.4: Proximate and ultimate analysis of the reference fuel, SRF and the SRF biogenic and plastic fraction

		Ready fuel (Rhenish brown coal + paper sludge)	SRF sample	Biogenic Fraction	Plastic Fraction (PP)
Proximate (%wt raw)	Moisture	58.70	28.11	37.49	0
	Volatile Matter	19.95	55.99	41.14	100
	Fixed Carbon	17.25	6.36	8.46	0
	Ash	4.10	9.65	12.92	0
	NCV (MJ/kg)	7.961	14.785	8.17	35.00
Ultimate (%wt daf)	C	67.74	60.09	57.1	85.63
	H	4.89	8.41	5.0	14.37
	O	26.29	30.30	23.68	0
	N	0.67	0.98	0.52	0
	S	0.40	0.21	0	0

For the determination of the Particle Size Distribution coal dust samples are taken from after the mills. 4 sieves are used. The results of the sieving process are given in Table

4.5 together with the proposed parameters of the fitted Rosin Rammler distribution, while the respective plot is presented in Figure 4.12.

Table 4.5: Particle size distribution data

d	PSD passing (%)	Yd
90	69.2	0.308
200	82.7	0.173
1000	96.5	0.035
1500	99.5	0.005
dmean	63	
n	0.47	

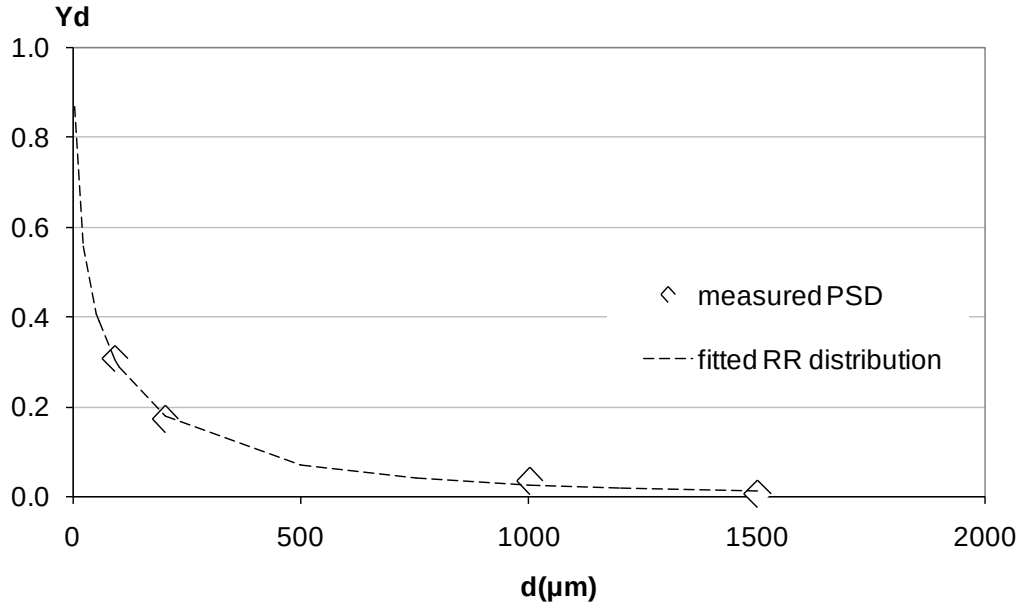

Fig. 4.12 Measured PSD and fitted Rosin Ramler distributions

Overview of the modeling approach

The commercial package Fluent is used for the combustion simulations. An overview of the standard models applied in a comprehensive combustion code like Fluent is found in Appendices A1-6. P1 model is applied to radiation modelling and the standard k-e model for turbulence modelling. Particle trajectories are calculated by integrating the particle force balance in a Lagrangian reference frame. Since SRF is considered as a mixture of biogenic and plastic fractions, the combustion mechanisms presented in section 3.2 are used. In particular, for the reference fuel and the biogenic fraction the common single rate mechanism is considered for devolatilisation and the kinetics/ diffusion limited model is considered for char combustion. The adopted kinetic parameters for the reference fuel and the biogenic fraction of SRF are presented in Table 4.6. The second order upwind discretisation scheme is used in all simulations after initially obtaining convergence with the first order one.

Table 4.6: Adopted kinetic constants for the reference fuel (brown coal and paper sludge) and the biogenic fraction of SRF

	Kinetic Parameters	Unit	Brown coal	Biogenic fraction
Devolatilisation	Pre-exp. factor (k)	1/s	315,000	Constant rate
	Activation energy (E)	J/kmol	$7.4 \cdot 10^{7}$	50 (1/s)
	mass diffusion limited rate	kg/(m^2 s Pa)	$1 \cdot 10^{-11}$	$1 \cdot 10^{-11}$
Char Combustion	kinetics limited pre-exp. factor	1/s	6.7	6.7
	kinetics limited activation energy	J/kmol	$1.138 \cdot 10^{8}$	$1.138 \cdot 10^{8}$

Boiler geometry

The developed numerical grid of the boiler furnace is composed of about 490.000 unstructured, hexaedral elements. The results obtained by the particular grid are grid independent according to the performed grid independence study presented in Annex B3. The boiler convective section is also simulated as a second step by modeling the heat exchanger surfaces as heat sinks. By means of this overall boiler simulation the verification of the complete boiler mass and energy balance is feasible. Boundary conditions are obtained by the records during the large-scale measurements. Overall boundary conditions including primary - secondary air, fuel mass flows are given in Table 4.7. Regarding wall boundary conditions a constant wall temperature of 400 °C is set for the lower half of the furnace wall, while a temperature of 450 °C is set for the upper half of the furnace wall. The particular temperature value is calculated from the steam temperature of the evaporator after the addition of ΔT value, corresponding to the total thermal resistance of walls.

Table 4.7: Boundary conditions for the large-scale boiler simulations

		Air/ fuel mass flows	Gas composition (%w.t.)			
		kg/s	O_2	N_2	H_2O	CO_2
Hopper		112.22	0.23	0.67	-	-
1st burner level	Primary air (carrier gas)	498.16	0.05	0.56	0.12	0.26
	Secondary air	114.51	0.23	0.67	-	-
	coal	71.1	-	-	-	-
2nd burner level	Primary air (carrier gas)	223.31	0.05	0.56	0.12	0.26
	Secondary air	114.51	0.05	0.56	0.12	0.26
	coal	38.67	0.23	0.67	-	-
3d burner level	Primary air (carrier gas)	137.42	0.05	0.56	0.12	0.26
	Secondary air	114.51	0.23	0.67	-	-
	coal	14.97	-	-	-	-
OFA		181.50	0.23	0.67	-	-
Recirculation ducts		-511.35	0.03	0.63	0.13	0.21

The reference case is initially simulated and the predicted furnace exit temperatures and O_2 concentrations are compared with available measurement data obtained by the suction pyrometer measurements at the boiler furnace exit, Figure 4.13. As also mentioned in chapter 4.1, two different data series are available from two opposite

boiler sites, the front and the rear side. The reference case simulations are based on the boundary conditions of the “8-mill operation”, and not the “7-mill operation”, which is the standard operation mode of the particular boiler in order to get a symmetric flow and temperature field. In all simulations the 8-mill operation is considered so that a comparison with the reference case is possible. The average temperature at the boiler outlet, downstream the economizer section, is also compared with the available temperature records.

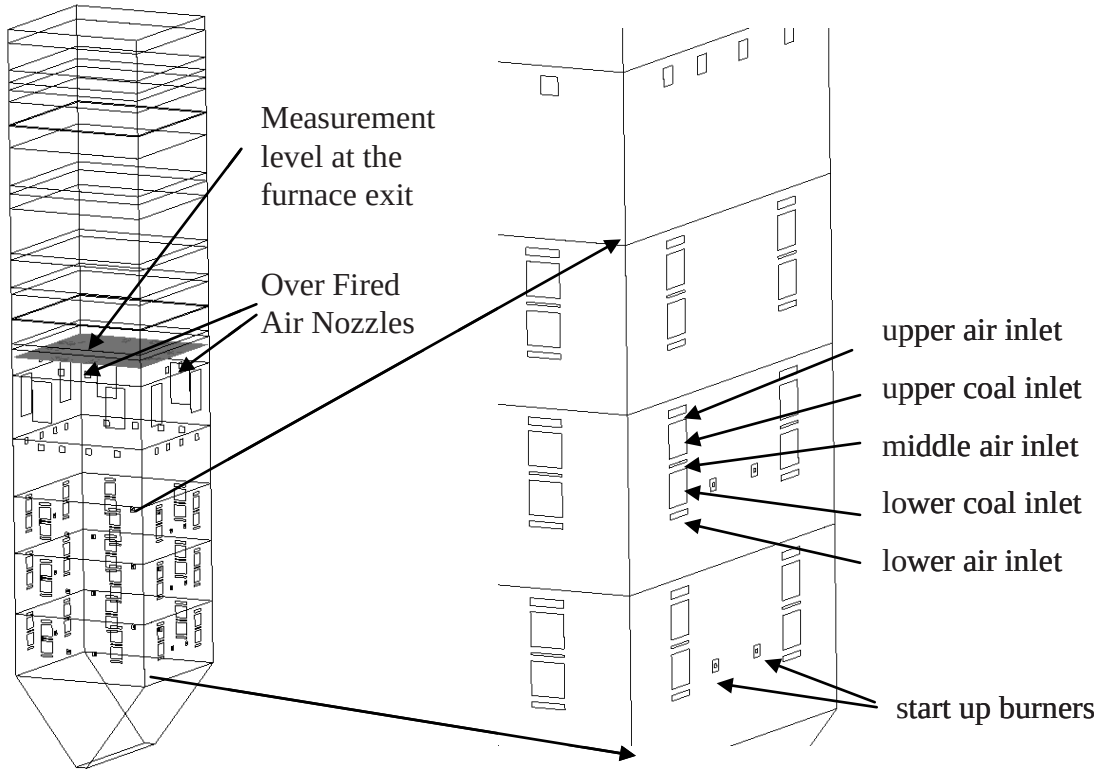

Figure 4.13: Overview of the simulated boiler and detail of the burner region

Investigated cases

In the framework of the numerical investigations on SRF co-combustion in large-scale boilers preliminary work is carried out with reference to the effect of the co-firing share and SRF particle diameter, moisture and shape on the combustion behaviour [IV-14]. However, the main work to be presented in this thesis focuses on the investigation of different injection concepts and their evaluation on the basis of different combustion related parameters. The parameters which are kept constant are the total thermal input into the boiler and the co-firing thermal share, which is 5% in all cases. A thermal share higher than 5% was not investigated in the particular boiler even during the large-scale SRF co-combustion campaign for two main reasons; the first reason is the limitations in the logistic and supply chain, due to the very high amounts of SRF which have to be delivered “just in time” at the site. The second reason is the increased risk for chlorine corrosion on the heat exchanger surfaces of the boiler caused by the high chlorine content of SRF.

All co-firing modes considered in the simulations are going to be presented following the categorisation of the three different direct co-firing modes mentioned in the introduction. In the first co-firing mode (A), where SRF is injected into the coal conveyor belt, upstream the mill, the following parametric subcases are simulated.

A1. Injection into all 8 mills

A2. Injection into 4 out of 8 mills
A3. Injection into 2 out of 8 mills (oppositely located)
The injection concept A is considered as the one, where minimum technical modifications are required and respectively low installation costs. By utilizing the existing milling equipment for milling the alternative fuel no extra milling equipment is required. Nevertheless, it should be mentioned that ordinary fan beater mills with or without prebeaters, used for brown coal, are theoretically not suitable for milling soft materials such as SRF fluff. Nevertheless, the experience of the large-scale tests - where SRF was fed into all 8 mills - showed that SRF particle size distribution is adequately reduced below millimeter size during milling. This effect cannot be justified by the efficiency of the mill itself, but rather by the interaction of the soft SRF paper or plastic foils with the dense and high velocity coal particle stream during their passing through the mill.
Since, after the mill, SRF is mixed in the coal stream, the determination of its particle size distribution is not possible. For this reason it has been decided that SRF injections will be modeled with a uniform diameter and its effect will be evaluated through parametric investigation. In this framework three different diameters - 0,13m, 0,50mm and 1,30mm - are examined. These are also used in the analysis of Deeg et.al. [III-13]. The option of reducing the number of mills in which SRF is fed either to four and or to two mills can be regarded as an alternative solution that may bring additional savings of installation and maintenance costs.
Regarding the second concept, the alternative fuel is fed into the coal ducts after the mills. The following scenarios are considered.
B1. Injection into the 8 lower burners, 1st burner level
B2. Injection into the 8 middle burners, 2nd burner level
B3. Injection into the 8 upper burners, 3^{d} burner level
In this way it is possible to evaluate the effect of the SRF injection level on the boiler operation, while all 8 coal burners of the same level are used. For this injection scenario the operation of a separate mill for SRF is required. For the scope of the simulations SRF is assumed to have a uniform diameter distribution. Four diameters are tested in total, i.e. the previous three and a larger one equal to 2,5mm, which accounts for coarser particles that can be expected when using an additional mill for SRF.
The third injection concept investigated includes the installation of extra dedicated burners for the alternative fuel. The necessary combustion air for SRF enters then then through the additional burners and not through the existing coal burners. The existing start-up burners are chosen as the locations for the additional SRF burners. The reason is that a replacement of the start-up burners by new burners equipped with an oil firing system for start up and an alternative fuel firing system for permanent operation is feasible, without any further technical modifications in the furnace membrane walls. The installation of the additional burners in any other location of the furnace would require cutting of membrane walls and therefore, significant reconstruction works. The particular boiler is equipped with 16 start-up burners in total, divided in two rows and located at the same heights as the lower and the middle coal burners level (Figure 4.13b). Two cases are simulated:
C1. Injection into the 8 lower start-up burners, at the 1st coal burner level
C2. Injection into the 8 upper start-up burners, at the 2nd coal burner level
Since extra milling equipment is also required for this case, four different diameters are also investigated. An overview of all cases investigated is given in Table 4.8

Table 4.8: Test cases' matrix

Co-firing concepts		Description	SRF particle diameters simulated (mm)
Injection upstream of mills (A.)	A1	8 mills	0.13-0.50-1.30
	A2	4 mills	-//-
	A3	2 mills	-//-
Injection into coal ducts downstream of mills (B.)	B1	Lower burner level	0.13-0.50-1.30-2.50
	B2	Middle burner level	-//-
	B3	Upper burner level	-//-
Injection through additional burners (C.)	C1	Additional burners / lower level	-//-
	C2	Additional burners / upper level	-//-

Evaluation criteria

In order to compare and evaluate the numerical results of the proposed scenarios, the following parameters are used as main performance indices:

1. Average and maximum temperature at furnace exit:

The furnace exit temperature is an important technical index for the characterisation of the boiler combustion behaviour. Higher furnace exit temperature may lead to an improvement of the fuel burnout, but may also cause slagging and fouling problems at the first superheater stages, and even accelerate the chlorine corrosion mechanisms in the case of firing alternative fuels with increased Chlorine content such as SRF. Lower furnace exit temperatures, on the other hand, are a sign of reduced burnout. Comparable values of furnace exit temperature are, therefore, required. More specific, a temperature difference between the investigated cases and the reference of less than +/- 50K is favorable. For a furnace outlet value of about 1000 °C, a temperature difference of +/- 50K corresponds to a relative change of +/- 5% and this value is set in Table 4.9 presenting the overall evaluation criteria.

2. Heat flux to the furnace walls:

The same logic applies to the case of the wall heat flux. A significant decrease of heat flux may lead to a change in the boiler heat balance and even a decrease in steam production, while significant increase of the heat flux above the normal operation values may cause overheating at certain spots in the membrane wall resulting in the damage of the finned steam tubes. The respective values used for the evaluation of the changes of the calculated heat flux to the furnace are presented in Table 4.9.

3. Burnout of biogenic and plastic particles:

In order to assess the burnout of particles two different values are calculated and taken into consideration. Firstly, the mass fraction of plastic and biogenic particles which fall into the furnace's hopper due to gravity and secondly the burnout of particles exiting the furnace. In the case of plastics no burnout value can be directly calculated since the considered plastic fraction does not have char content. For this reason another value is considered as an index for the completeness of the combustion process of plastic particles. That is the percentage of the liquid plastic fraction completely decomposed compared to the initial plastic fraction. A value of percentage equal to 100% reveals a complete decomposition.

The burnout of coal particles leaving the furnace is calculated to about equal to 97% in the reference case, whilst the percentage of the coal particles mass flow falling into

hopper is equal to 1% of the initial particles mass flow entering the boiler. In order to get a comparison measure between the SRF co-firing cases and the reference case, the range of 96.5% to 97.5% as regards SRF particles' burnout is considered to be comparable with the coal particles' burnout value in the reference case, i.e. 97%. Moreover, the range of 0.75% to 1.25% as regards the fraction of SRF mass flow falling into hopper is considered as comparable with the predicted fraction of coal mass flow falling into hopper in the reference case, i.e. 1%. The proposed ranges of these evaluation parameters are presented in Table 4.9.

Additionally, a fourth and more qualitative parameter, which is not included in the evaluation table but should qualitatively be considered in the evaluation process, is the appearance of temperature hot spots in the furnace. Temperature hot spots may influence NO_x formation and may lead to increased NO_x emissions. Moreover, increased flue gas temperatures near boiler' walls may induce ash slagging problems if the ash melting temperature is reached. For these reason the appearance of temperature hot spots is an additional qualitative index that should be taken into consideration in the evaluation of the SRF co-firing simulations.

The overall evaluation of the investigated concepts is presented in Table 4.10. The following marks are used in the evaluation table

"√" The tick mark implies that no drastic change is noticed between the baseline and the particular co-firing case. The combustion behaviour in the examined co-firing case is therefore regarded to be within the "accepted" limits.

"x" The "x" character denotes that the overall combustion behaviour at the particular co-firing case deteriorates and falls within the range considered as "not accepted".

Table 4.9: Evaluation criteria

Rank/ Criteria		Temperature/ Heat Flux (relative difference)	Mass fraction to hopper (percentage points)	Burnout of particles (percentage points)
much better:	++	not applicable	$0 \leq x \leq 0.25$	$99 \leq x \leq 100$
better:	+	not applicable	$0.25 < x \leq 0.75$	$97.5 \leq x < 99$
comparable:	0	$-5\% < x < +5\%$	$0.75 < x \leq 1.25$	$96.5 < x < 97.5$
worse:	-	$-10\% < x \leq -5\%$ or $+5\% \geq x > +10\%$	$1.25 \leq x < 5.0$	$91 \leq x \leq 96.5$
much worse:	--	$x \leq -10\%$ or $x \geq +10\%$	$x \geq 5.0$	$x \leq 91$

4.2.3 Results – Discussion

4.2.3.1 Large-scale boiler simulations: Reference case

In Figure 4.14 the temperature and O_2 contours on a boiler's symmetry plane for the reference case are presented.

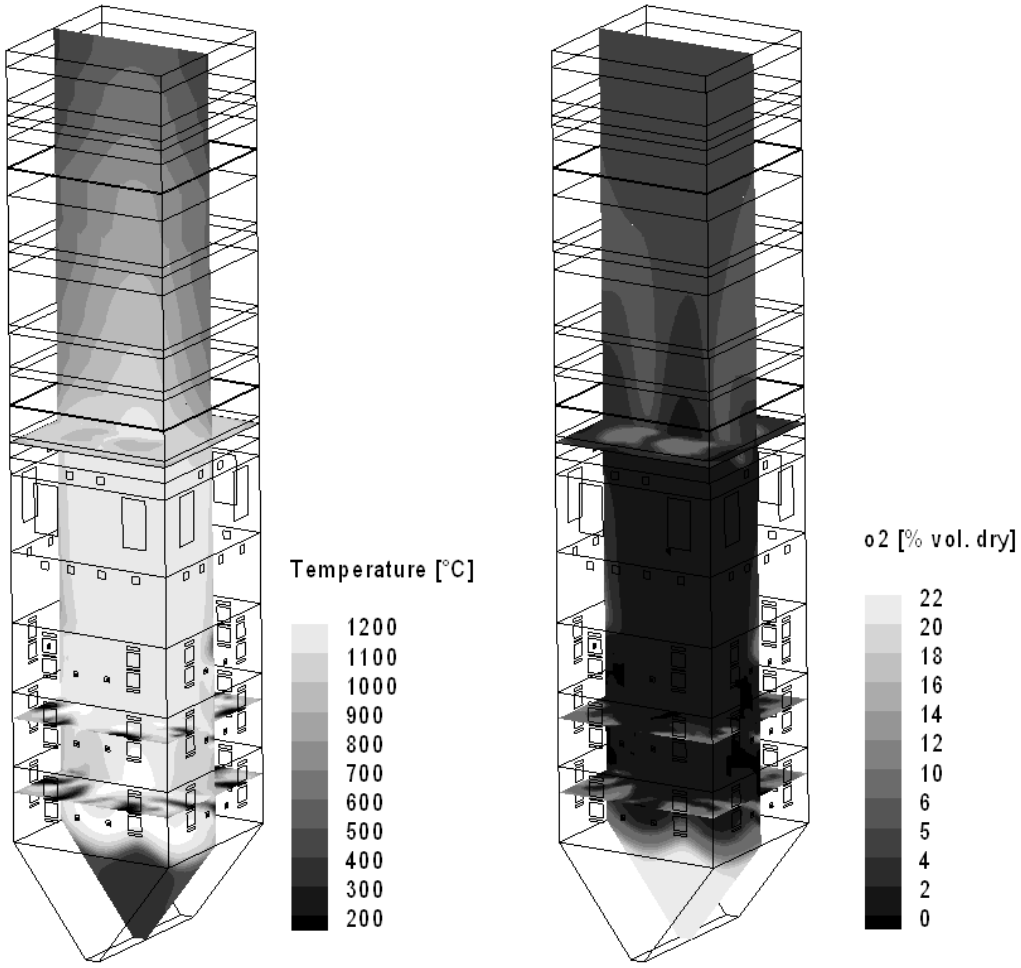

Figure 4.14: Temperature and O_2 contours in the large-scale boiler

The comparison between the numerically predicted and the measured temperature and O_2 profiles are presented Figure 4.15a,b. In order to account for the given inaccuracy of the measuring probe position in relation to the boiler volume and dimensions, a specific post-processing procedure is followed. Instead of reading the temperature and O_2 values on the points of the line that refers to the estimated position of the measuring probe, concentric circles with a radius of 0.5m are made on this line and the minimum, maximum and average values on these circles are recorded. In this way the simulated temperature and O_2 values at the vicinity of the measurement probe are taken into account. The agreement between simulated and experimental values is considered as satisfying taking into account a) the inaccuracy of the position of the measuring probe in relation to the total boiler volume and b) the specific region where the measurements are taken, which is namely close to the Over Fired Air nozzles, where ongoing combustion phenomena take place and large temperature and species concentrations gradients are expected.

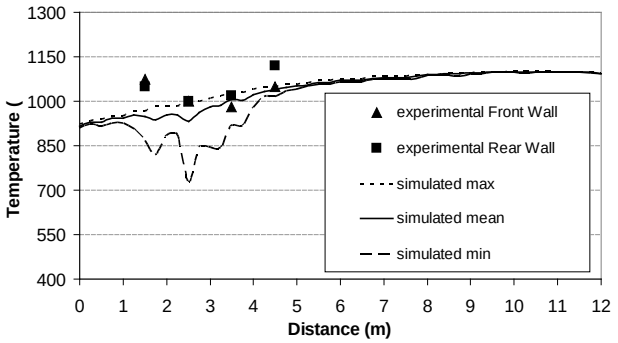

Figure 4.15a: Comparison simulated - measured Temperature profiles

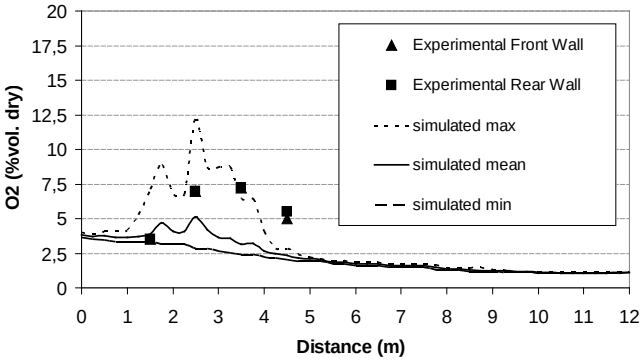

Figure 4.15b: Comparison simulated - measured O_2 profiles

4.2.3.2 Large-scale boiler simulations: Evaluation of proposed injection modes

For the evaluation of the considered SRF injection concepts the following combustion related parameters are used: temperature at the furnace exit, total heat flux and SRF particles burnout. The detailed results are given below.

Temperature profiles

The calculated average and maximum furnace exit temperatures for all simulated cases are presented in Figure 4.16a, b. The simulation results for each case include 3 to 4 temperature values corresponding to the number of SRF diameters simulated. For means of comparison the furnace exit temperature of the reference case is also given, where no SRF is co-fired. The simulated temperature results are presented after post processing. They are categorised in temperature classes, in order to allow significant temperature trends to be noticed and avoid evaluating small temperature differences of 1-2 K, which are in the inaccuracy range of the numerical methods. Each simulated temperature is rounded to the closest value with an ending digit "0" or "5". As a result, the mean values of the obtained temperature classes end in "0" or "5" and their range is +/- 2.5 K. Based on this post processing following conclusions are drawn from the simulation results:

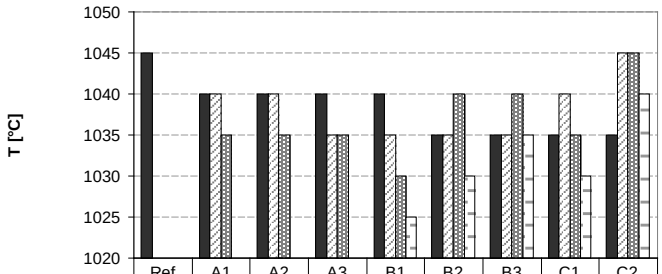

	Ref	A1	A2	A3	B1	B2	B3	C1	C2
diam. 0.13mm	1045	1040	1040	1040	1040	1035	1035	1035	1035
diam. 0.5mm		1040	1040	1035	1035	1035	1035	1040	1045
diam. 1.3mm		1035	1035	1035	1030	1040	1040	1035	1045
diam. 2.5mm					1025	1030	1035	1030	1040

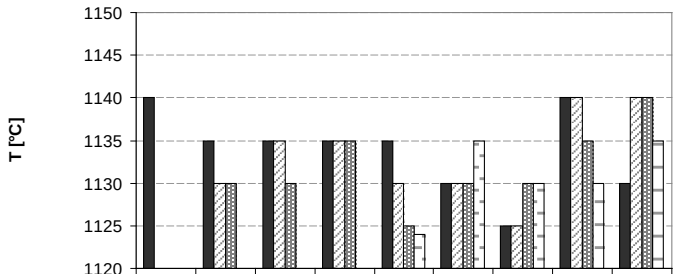

	Ref	A1	A2	A3	B1	B2	B3	C1	C2
diam. 0.13mm	1140	1135	1135	1135	1135	1130	1125	1140	1130
diam. 0.5mm		1130	1135	1135	1130	1130	1125	1140	1140
diam. 1.3mm		1130	1130	1135	1125	1130	1130	1135	1140
diam. 2.5mm					1124	1135	1130	1130	1135

Figure 4.16: Furnace exit temperatures in all simulated cases: (a) Average values, (b) Maximum values

On the basis of this post-processing the following conclusions are drawn from the simulation results:

- A moderate decrease of the average and the maximum temperature, in the range of 5 to 10K (0.95% in dimensionless form) compared to the reference case is predicted for most of the cases, probably due to the lower burnout of SRF particles. Burn-out of SRF particles is computed in terms of decomposition for the plastic part and char combustion for the biogenic one.
- An influence of the SRF particle diameter on the predicted temperatures is noticed. Most cases with a uniform SRF diameter of 130μm, which is about double than the mean coal diameter, give comparable results with the reference case.
- By increasing the SRF particle diameter the average and maximum furnace exit temperature slowly decrease in cases A, where SRF is fired from all three burner levels. In cases B and C, where SRF is fired in each case from a different burner level, lower temperatures are predicted, for SRF diameters equal to 0.13 and 0.5mm, in comparison with case A. In the case of a SRF diameter equal to 1.3mm the opposite trend is predicted, because of the fact that the burnout of this size class takes place closer to the furnace's exit. In the case of a SRF diameter equal to 2.5mm a smaller fraction of particles is completely burnt lowering significantly the furnace outlet temperature. This non monotonic behaviour of the furnace exit temperature is attributed to the different paths and burning rates the SRF particles exhibit, due to their different injection points and initial diameters.
- In cases B1 and C1, in which SRF is fired from a lower injection point, a higher dependence of the furnace exit temperature on the SRF diameter is observed.
- In C cases, where SRF is injected from dedicated injection nozzles, high furnace exit temperatures are obtained for specific diameters.

In order to have a more detailed picture of the temperature variation along the furnace height respective profiles of the average and the maximum temperature are presented in Figure 4.17a, b, c.

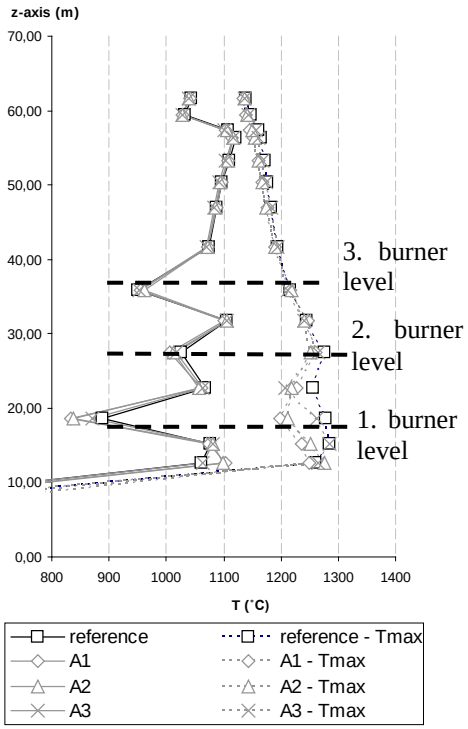

Figure 4.17a: case A

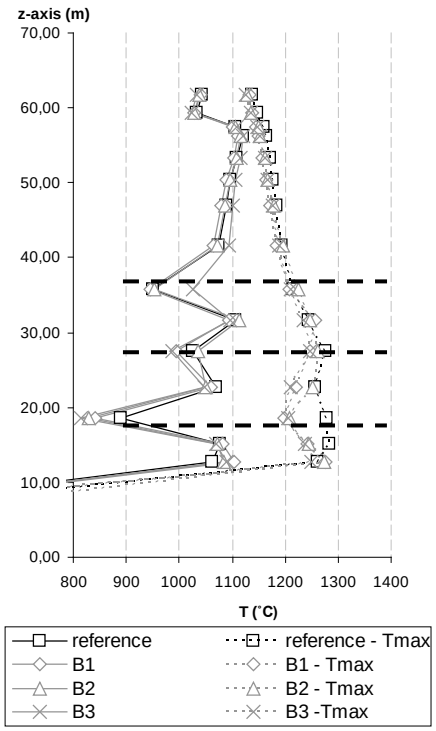

Figure 4.17b: case B

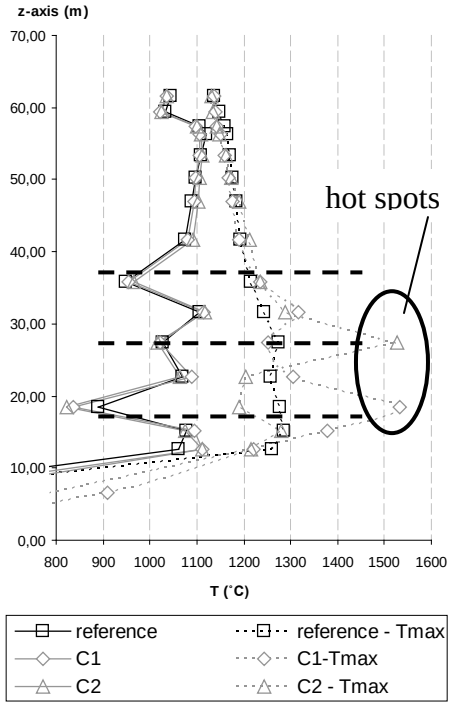

Figure 4.17c: case C

The results of the A-cases, in which SRF is fired from all three burner levels are comparable with each other and with the reference case. By injecting SRF from one of the three burner levels, as in cases B1, B2, B3, the temperature profile changes and an increase of the average temperature up to 20-30K is observed at the respective injection level of each case. The most drastic change in the temperature behaviour is noticed, when firing through the dedicated SRF burners (co-firing mode C). In this case SRF enters the furnace in an area with already high temperature. As a result, the local temperature increases further through firing of the alternative fuel and a local hot spot with a temperature of about 200K higher than the respective of the reference case is predicted. Comparing the temperature contours of the reference case with those of cases C1 and C2, (Figure 4.18a, b, c) the local temperature peaks are clearly visible, despite the fact that the corresponding area of the predicted hot spots is not large. Although average temperature along the furnace height is not highly affected, these high temperature peaks may be considered as negative outcome. The reason is that a drastic temperature increase at specific locations in the furnace could lead to overheating of the furnace walls or even to ash slagging problems, if the ash melting temperature is reached. In addition, NO_x formation mechanisms may be affected by the increased flue gas temperatures. The qualitative evaluation of the temperature results according to the criteria of Table 4.9 shows that all cases have comparable behaviour regarding the predicted furnace exit temperature. Only the behaviour of cases C1, C2 is characterised as “worse” than that of the reference case because of the predicted temperature hot spots, which impose a risk in the boiler’s efficient operation (Table 4.10).

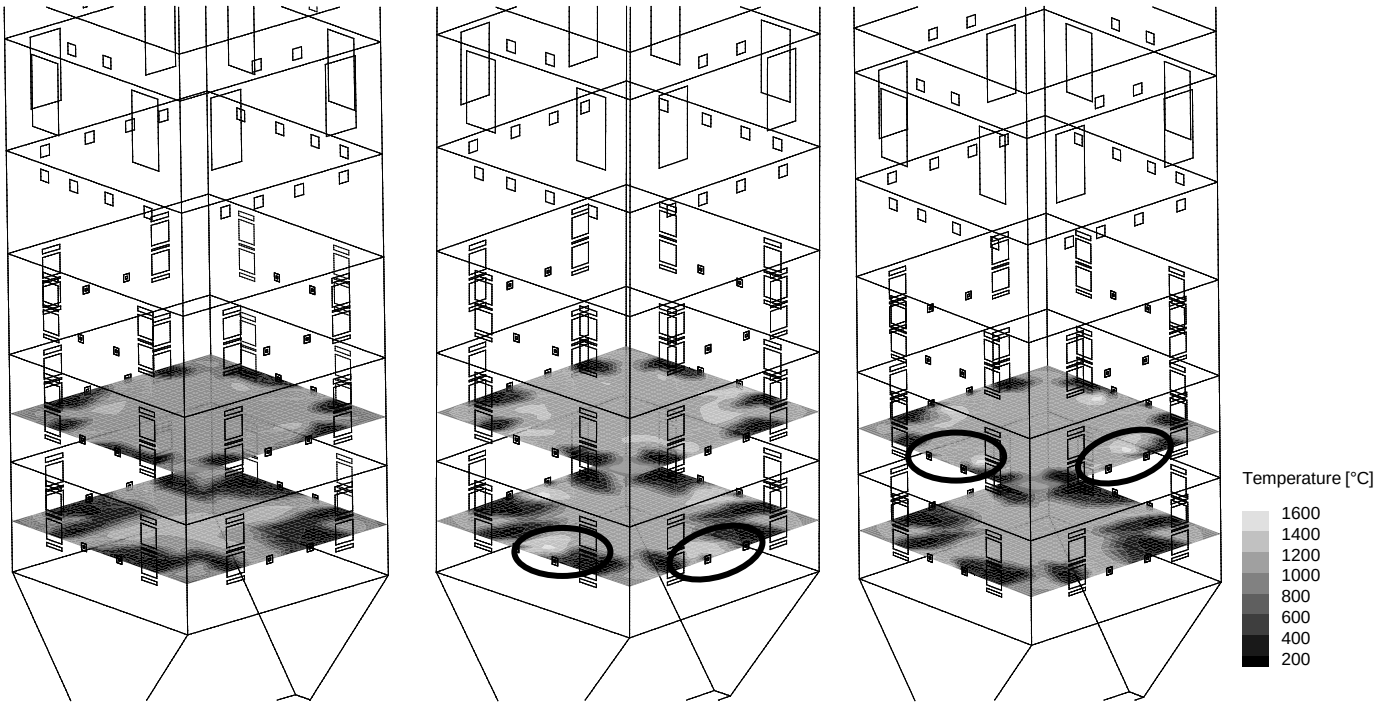

Figure 4.18: Temperature contours at the levels of the start up burners: (a) Reference, (b) case C1, (c) case C2

Wall heat flux

The predicted total wall heat flux to the evaporator is presented in Figure 4.19 while the respective profiles of the wall heat flux along the furnace height are given in Figure 4.20 a, b, c. The same post-processing procedure as the one followed in the furnace outlet temperatures (Figure 9a,b) is also followed for the total heat flux values of Figure 10. A similar picture to the one obtained by the evaluation of the predicted temperature fields

is seen. Moderate diferences compared to the reference case are observed in A and B scenarios. The relative change of the total heat flux compared to the baseline is below 2% for all cases. The influence of the injection of SRF at a specific level in cases B1-B3 is also shown in the according profile of Figure 17b. A drastic increase of the total wall heat flux to a relative percentage of more than 5% is noticed in cases C1, C2. The large temperature peaks observed in the specific cases are probably the reason for this behaviour. In the overall evaluation of the co-firing cases in terms of their predicted furnace heat flux, similar results are obtained to the evaluation in terms of the temperature fields (Table 4.10).

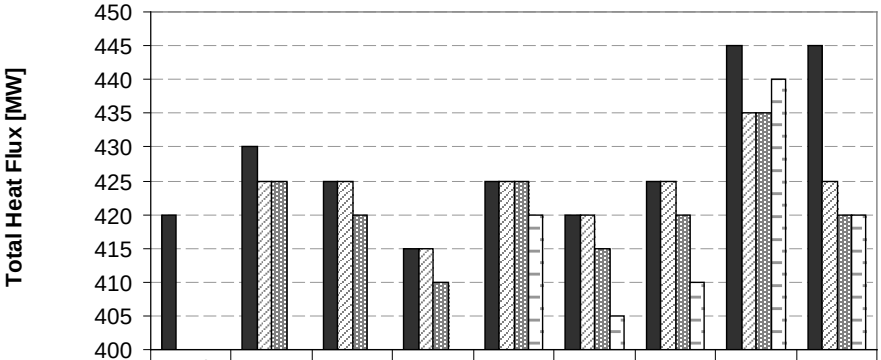

	Ref	A1	A2	A3	B1	B2	B3	C1	C2
diam. 0.13mm	420	430	425	415	425	420	425	445	445
diam. 0.5mm		425	425	415	425	420	425	435	425
diam. 1.3mm		425	420	410	425	415	420	435	420
diam. 2.5mm					420	405	410	440	420

Figure 4.19: Calculated total heat flux to the evaporator in all simulated cases

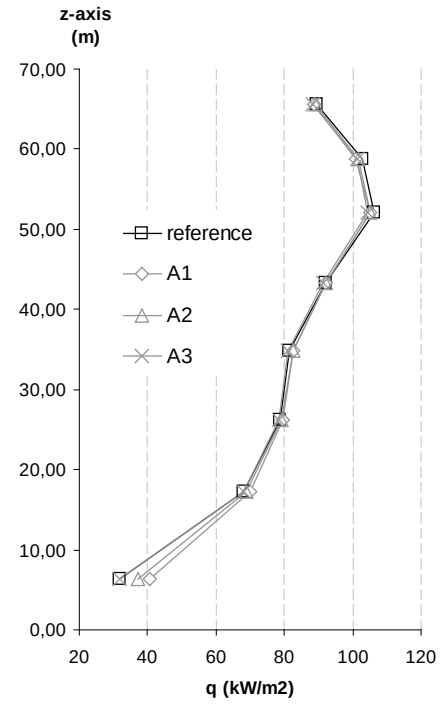

Figure 4.20a: case A

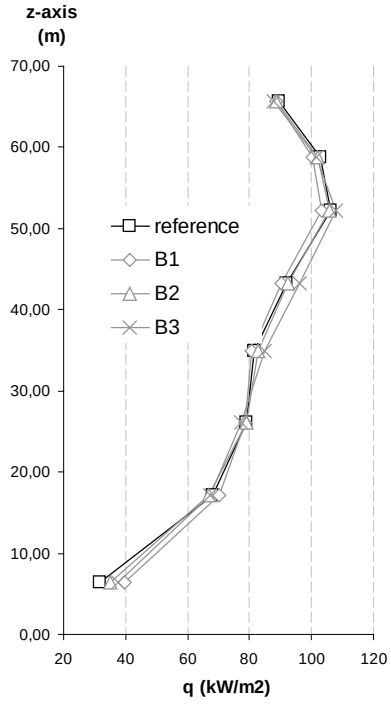

Figure 4.20b: case B

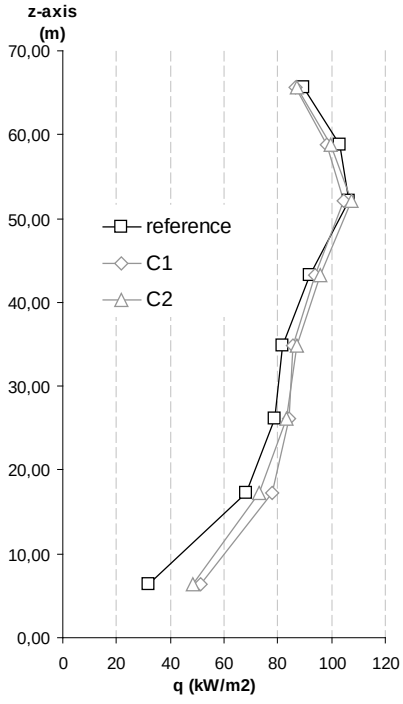

Figure 4.20c: case C

Figure 4.20: Average Heat Flux profile over furnace height

Burnout behaviour

In the evaluation of the burnout behaviour a difference of one or two percentage points is considerable and should not be disregarded by rounding the particular results to the closest decade. For this reason no rounding is performed as a post processing step in the results for particles' burnout. The fraction of particles that fall into the hopper due to gravity is presented in Figure 4.21a, b for the biogenic and the plastic SRF particles respectively. For means of comparison the mass fraction of the initial coal mass flow falling into the hopper in the reference case is given, which is 1%. Almost zero biogenic particles fall into hopper in the considered cases and diameter classes, with the exception of cases B1 and C1, where an increased percentage of particles of the high diameter class falls into hopper, due to the low injection level. A different picture is observed in the case of plastics. For particle diameter classes above 0.5mm a high percentage, over 10% of the initial plastic mass flow, does not completely decompose and falls into the hopper in form of droplets. This fraction increases in the higher diameter classes and reaches very high values in the case of 2.5mm particle diameters, where almost the whole plastic mass flow falls into hopper without having completely decomposed. These particular results may be considered as an over prediction in comparison with the real conditions, where the fired SRF particles with an irregular shape have a higher aerodynamic drag coefficient and therefore higher residence times in the furnace and higher burnout. Nevertheless, the effect of the injection location on the investigated parameter is correctly reproduced by the numerical simulations. Namely, in the case of SRF injections at a higher furnace level, such as B2, B3 and C2, lower mass fractions of unburned fuel falling into hopper, are calculated.

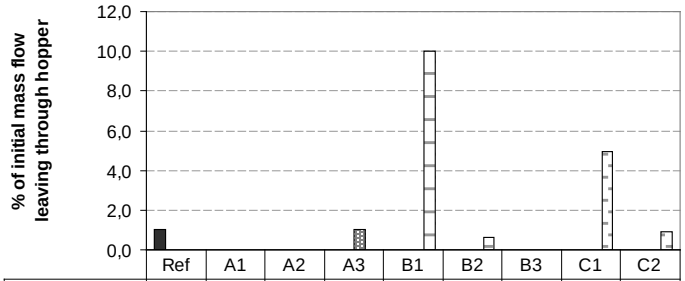

	Ref	A1	A2	A3	B1	B2	B3	C1	C2
diam. 0.13mm	1,0	0	0	0	0	0	0	0	0
diam. 0.5mm		0	0	0	0	0	0	0	0
diam. 1.3mm		0	0	1	0	0	0	0	0
diam. 2.5mm					10	1	0	5	1

Figure 4.21a: Percentage of initial biogenic mass flow falling to the hopper

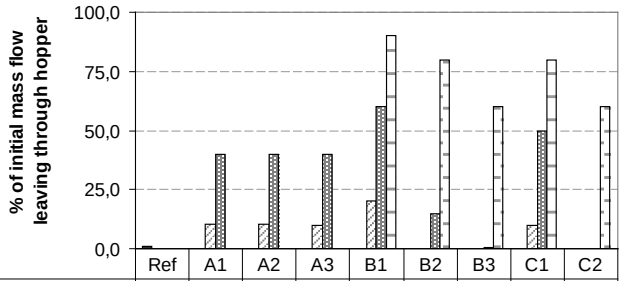

	Ref	A1	A2	A3	B1	B2	B3	C1	C2
diam. 0.13mm	1,0	0	0	0	0	0	0	0	0
diam. 0.5mm		10	10	10	20	0	0	10	0
diam. 1.3mm		40	40	40	60	15	0	50	0
diam. 2.5mm					90	80	60	80	60

Figure 4.21b: Percentage of initial plastic mass flow falling to the hopper

The burnout of particles leaving through the furnace outlet is given in Figure 4.22a, b. Like in the previous analysis the respective burnout value for coal of 97.2 % is taken as a reference. Regarding the biogenic fraction of SRF, satisfying burnout behaviour is predicted in all cases for diameter classes of 0.13 and 0.5mm, i.e from 95% to 100%. By increasing particles' diameter the burnout decreases since the existing particles' residence time is not enough for a complete burnout. Primarily, B2, B3 and C2 cases, where SRF is injected at higher furnace levels seem to be further affected, due to the reduced distance from the furnace exit exhibiting lower burnout. A similar picture is noticed for the plastic particles, which differs however from the biogenic fraction in absolute values. Lower conversion is noticed for all cases of plastic particles. The zero values observed for the results of larger SRF particles, mainly in cases B1 and C2 indicate that a very low percentage of plastic, less than 5% leaves through the furnace

top in these simulated cases. The evaluation of the burnout behaviour of the biogenic and plastic SRF fraction is given separately for each fraction in Table 8. The specific model setup for plastic does not allow high burnout, thus this behaviour is characterised as “much worse” compared to the reference for all cases. However qualitative differences between the cases are pointed out in the presented analysis.

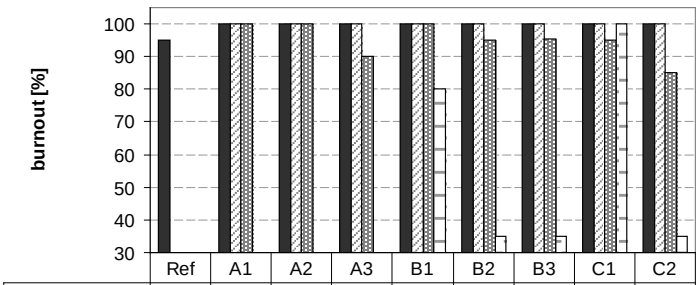

	Ref	A1	A2	A3	B1	B2	B3	C1	C2
diam. 0.13mm	95	100	100	100	100	100	100	100	100
diam. 0.5mm		100	100	100	100	100	100	100	100
diam. 1.3mm		100	100	90	100	95	95	95	85
diam. 2.5mm					80	35	35	100	35

Figure 4.23a: Burnout of biogenic SRF particles

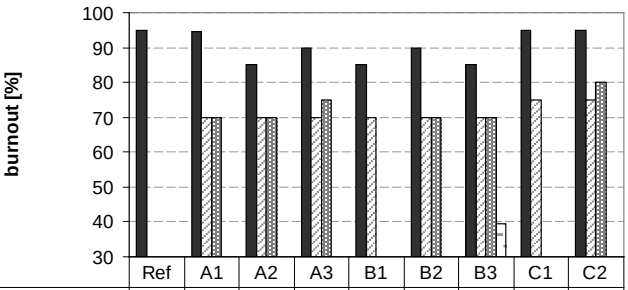

	Ref	A1	A2	A3	B1	B2	B3	C1	C2
diam. 0.13mm	95	95	85	90	85	90	85	95	95
diam. 0.5mm		70	70	70	70	70	70	75	75
diam. 1.3mm		70	70	75	0	70	70	0	80
diam. 2.5mm					0	0	40	0	0

Figure 4.23b: Burnout of plastic SRF particles

Finally, in order to visualise the SRF particle motion in the furnace, the particle tracks of the plastic fraction are calculated for the cases considered. In Figures 4.24a-h the particle tracks are plotted during the melting process. Particles trajectories are coloured according to the fraction of the already melted mass to the initial plastic mass. A value of 1 for this parameter indicates the completed melting process. It is noticed that in all cases particle melting is completed in a very short time after particle injection inside the boiler. In a similar way, the particle tracks during the plastic decomposition step are presented in Figures 4.25a-h. The fraction of particle mass decomposited to the initial particle mass is used as a colour map in this figure. The set particle diameter for all particle track calculations is 1.3mm, in order to visualise the trajectories of the particles that fall into the hopper and have a comparable picture in all cases. The overall results of the particle tracks presented confirm the aforementioned results regarding the burnout of SRF particles.

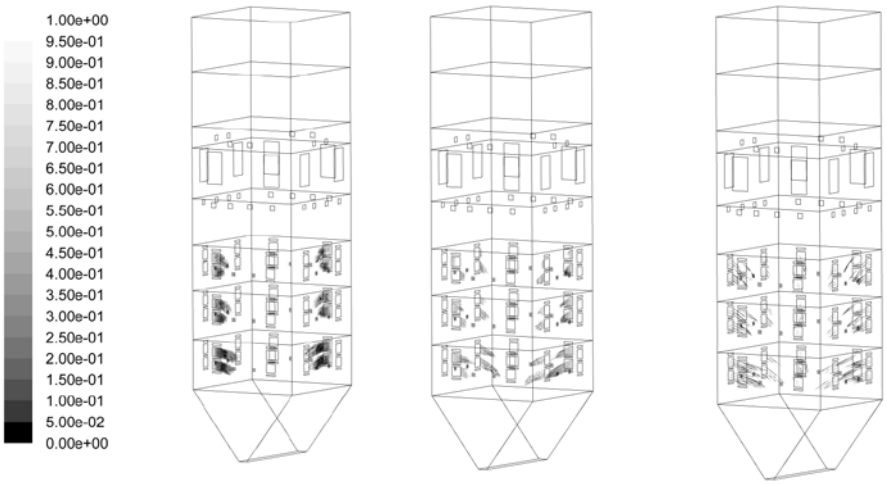

a) case A1 b) case A2 c) case A3

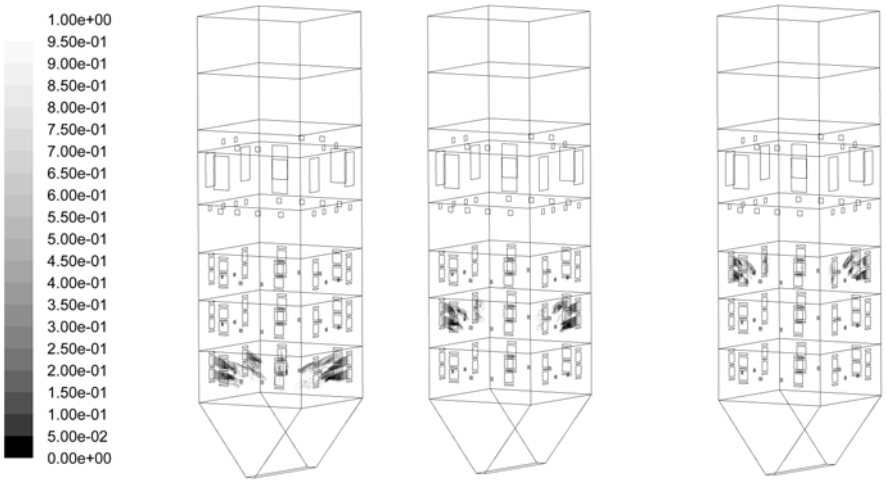

d) case B1 e) case B2 f) case B3

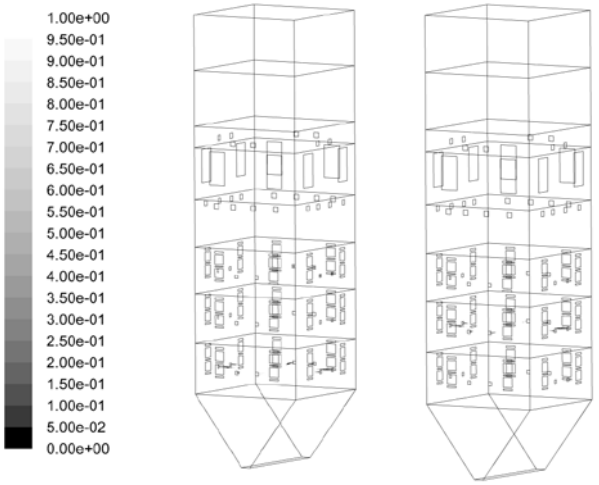

g) case C1 h) case C2

Figure 4.24 a-h: Particle trajectories of the plastic fraction coloured by the percentage of the initial mass melted, all cases

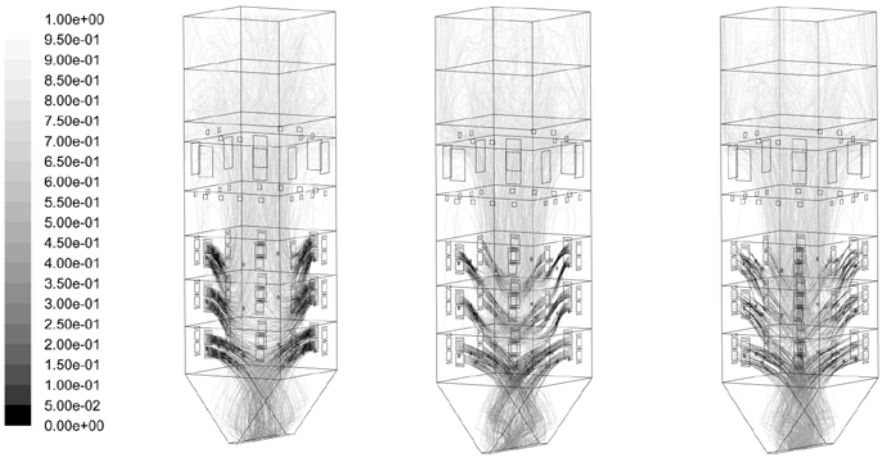

a) case A1 b) case A2 c) case A3

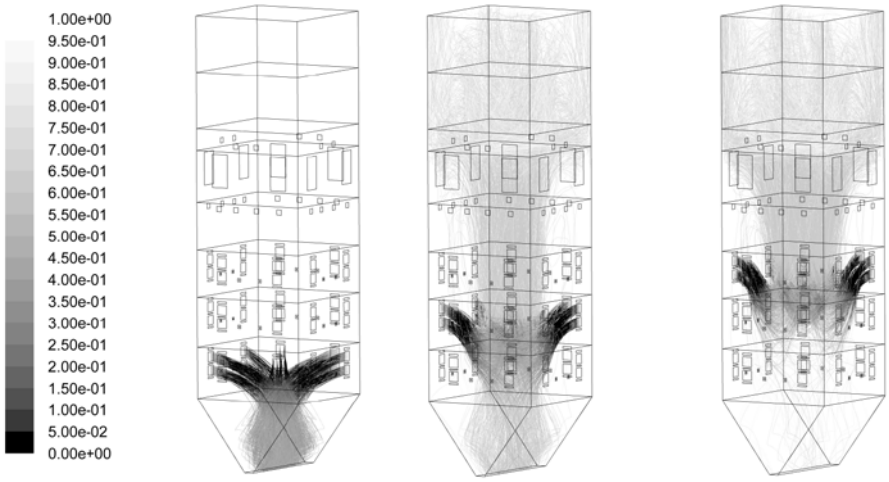

d) case B1 e) case B2 f) case B3

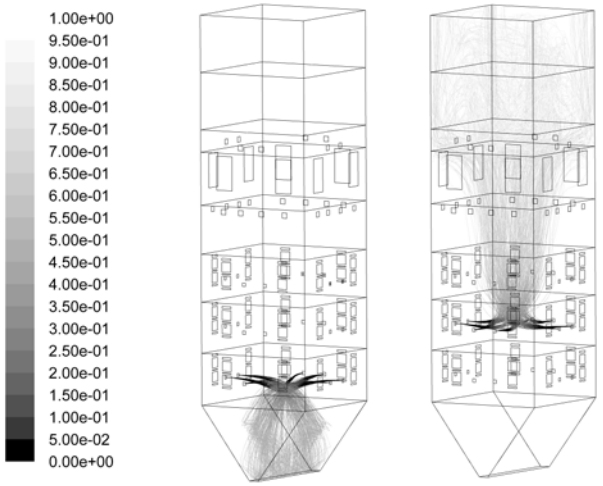

g) case C1 h) case C2

Figure 4.25 a-h: Particle trajectories of the plastic fraction coloured by the percentage of the initial mass decomposited

4.2.4 Overall Evaluation

The overall evaluation of all cases is given in Table 4.10. The present chapter aims at the evaluation of possible co-firing concepts on the basis of specific quantitative parameters, as a result of which the co-firing cases that do not meet the minimum criteria are found and excluded from further analysis. These are cases B1, C1 and C2 in the investigations performed. For both C cases the decisive factor are the changes in the predicted temperature field, while for case B1the most influencing parameter is the low burnout compared to the other cases, B2, B3. The remaining co-firing concepts have to be further evaluated by other methods and criteria, such as short term industrial tests on site, and overall technical and financial feasibility studies. Based on these results and the respective industrial experience the optimum solution for a long term demonstration will be chosen.
Finally, it should be stressed out that the particular results are dependent on the geometry and boundary conditions of the particular boiler and cannot be generalised for any other configuration of pulverised fuel boilers. For example, by modifying and optimising the location of the additional SRF burners or the specific burner geometry, a further improvement of the corresponding results of the C cases could be expected.

Table 4.10: Overall evaluation of the considered co-firing cases based on the chosen evaluation criteria

Co-firing concepts		Temperature	Wall Heat Flux	Percentage of particles falling to hopper		Particles' Burnout		Overall evaluation
				biogenic fraction	plastic fraction	biogenic fraction	plastic fraction	
Injection upstream of mills (A.)	A1	0	0	+	--	+	--	√
	A2	0	0	+	--	+	--	√
	A3	0	0	0	--	-	--	√
Injection into coal ducts downstream of mills (B.)	B1	0	0	--	--	-	--	X
	B2	0	0	0	--	-	--	√
	B3	0	0	+	--	-	--	√
Injection into additional burners (C.)	C1	-	-	-	--	-	--	X
	C2	-	-	0	--	-	--	X

4.2.5 Conclusions – Further work

The simulation of different concepts for the direct co-firing of Solid Recovered Fuels in existing pulverised brown coal boilers is investigated in this section. The SRF combustion models presented in Chapter 3 are incorporated in a commercial CFD code and the 600MWe brown coal boiler is simulated in various co-combustion conditions so that the proposed co-firing concepts are evaluated according to criteria such as the furnace outlet temperature, the total furnace heat flux and the particle burnout behaviour. Based on the simulation results and additional post-processing, the simulated cases showing a moderate performance are excluded from further analysis. These are the cases corresponding to SRF injection from lower levels and the cases corresponding to SRF injection through additional burners. By means of this qualitative evaluation extensive time and effort is saved, which would be required for the investigation of the

particular co-firing concepts in large-scale conditions. CFD simulations are, therefore, a useful tool in the analysis and further optimisation of possible co-firing concepts in existing pulverised fuel boilers.
Further work on the numerical simulation of SRF combustion is closely related with further model development of the combustion behaviour of irregular, non-spherical particles. Accurate models describing the combustion of real SRF particles will allow more accurate predictions of the boiler operational behaviour when co-firing SRF, even in cases in which no additional mills are installed and coarse SRF particles are co-fired.

4.3 Sum up and evaluation of the large-scale SRF co-firing investigations

The results of the experimental and numerical SRF co-firing investigations are summarised and evaluated in this part. The main result of the experimental measurement campaign was the proof of concept for the particular co-firing practice. SRF co-combustion in existing brown coal power plants is namely feasible without any expected negative impacts on environmental or technical aspects. The environmental performance was examined through dedicated measurements. Conventional flue gas emissions (CO, NO_x, SO_2, dust) were continuously monitored during the tests and measurements of additional compounds, which may be present in waste incineration, including HCl, heavy metals and dioxins-furans, were carried out according to the Waste Incineration Directive. Finally, fly ash, bottom ash and gypsum samples were collected and examined by according leaching tests. An overall satisfying environmental performance is observed, since the respective legislative limits are kept for all measurements carried out. Particularly, regarding the expected dioxins and furans emissions, the measurements carried out did not indicate any specific increase trend, while the performed numerical simulations imply that there is sufficient residence time in the high temperature region of the furnace, during which dioxins and furanes are expected to be destroyed. The overview performance table of the environmental aspects on SRF co-firing is given in Table 4.11.

Table 4.11: Evaluation table on the environmental aspects of SRF co-firing

		Proposed coal substitution concept : SRF co-firing	
		Experimental methods	Numerical simulation methods/ mass balances
Environmental aspects	CO_2 emissions	n.i.	savings of about 2000 t CO_2 during the co-firing tests
	Conventional flue gas emissions (NO_x, SO_2, CO)	√	“not investigated” - n.i
	HM in the flue gas	√	n.i.
	HCl	√	n.i
	Dioxines – Furans	√	√ (predicted residence times in numerical simulations in temperatures higher than 900 °C: > 5s)
	Ash quality: HM in the ash	√	n.i

The technical and operational aspects were also examined through experimental activities and simulations. Overall qualitative results of the examination are presented in Table 4.12. No incidents, which could lead to boiler tripping or any kind of technical knockout, were noticed during the tests. This is also supported by the stable behaviour of all monitored plant operational parameters. The conditions at the furnace exit including temperatures and flue gas concentration profiles were also measured and numerically simulated. No clear influence of SRF co-firing on the furnace exit temperature was experimentally observed, while according to the numerical simulations, a small increase of the furnace exit temperature could be expected. Constant behaviour is also predicted for the radiative heat flux to the evaporator based on the simulations performed. Regarding the burnout of SRF particles, no indications of increased unburned material could be found during the measurements implying sufficient burnout. The after-burning grid installed in the particular boiler, where the tests took place, should have contributed to this result. Larger SRF particles, which would fall into the hopper, stay on the after burning grid and so their combustion time is prolonged. In the performed simulations however, an increased percentage of unburnt SRF particles is generally noticed. This is mainly predicted for the plastic particles, which fall into the hopper before being completely evaporated and burnt. The lack of modeling of the after burning grid in the numerical simulations is one reason for this discrepancy. Finally, the main technical aspect, which may have a negative impact on the boiler operation and has to be investigated in detail in future examinations, is the potential chlorine corrosion risk, due to the increased chlorine content in SRF. The measurements performed indicated that this risk is not negligible and has to be considered in future investigations.

Table 4.12: Evaluation table on the technical aspects of SRF co-firing

		Proposed coal substitution concept: SRF co-firing	
		Experimental methods	Numerical simulation methods/ mass balances
Technological - operational aspects	Operational parameters (steam temperatures, Pel)	√	n.i.
	Heat flux to evaporator	n.i.	√
	Overall boiler heat balance /	n.i.	n.i.
	Boiler Efficiency (ηboiler) Power plant efficiency (ηPP)	n.i.	n.i.
	Furnace exit conditions (temperature, O2)	√	√
	Combustion conditions in the furnace (temperature and O_2)	n.i.	√
	Risk of potential operational problems due to slagging and fouling	n.i.	n.i.
	Ignition/ Burnout	√	!
	Risk of potential operational problems due to chlorine corrosion	!	n.i.

5 Lignite drying and dry lignite co-firing: Investigations in the small scale

Summary
As presented in the second chapter, pre drying of lignite and dry lignite firing in pulverised boilers is an important technology which will play a key role in future lignite-fired power plants. An efficiency increase of 4 to 5 percentage points is feasible in the next generation of lignite power plants to be built after 2015 [II-26, II-27] if the conventional lignite milling and drying system with hot flue gas can be replaced by newly developed fluidised bed drying concepts using steam bleed as a heating medium, and energetically utilising the waste heat from the evaporated lignite moisture. Since this radical change of the conventional milling and drying systems to an innovative fluidised bed drying concept is followed by additional risks to the operation of the new plants, a step by step development process has been decided by boiler manufacturers and plant operators. The installation and integration of an industrial-scale fluidised bed dryer in an existing large-scale plant, and the replacement of the boiler thermal input up to 30% by dry lignite is decided as the necessary intermediate step towards the further development of the 100% dry coal firing technology. Furthermore, it should be pointed out that, since drying is a physical process which depends on the physical parameters of the material to be dried, the design of the fluidised bed drier is exclusively based on the lignite type applied. Up to now the constructed industrial-scale atmospheric fluidised bed dryers are designed for German brown coal of the Rhenish area, while a pressurised fluidised bed drying concept, which is still under development, is designed for the German brown coal of the Lausitz mine in the Brandenburg area.
In order to prepare and assess a future demonstration of the fluidised bed drying and dry coal firing technology in Greek lignite power plants, the present thesis focuses on specific aspects of these technologies, which are fuel related and have to be carefully addressed when redesigning the particular processes for different fuel types. In this framework experimental tests on the drying behaviour of Greek lignite are performed in a lab-scale fluidised bed dryer. Furthermore, considering the combustion behaviour of Greek dried lignite, an extensive experimental campaign is carried out at a 1MWth semi-industrial-scale combustion facility. Based on the experimental data obtained and in order to draw further conclusions on the expected behaviour of a Greek large-scale boiler when co-firing dry lignite, the thermal balance of the facility is performed and respective heat flux - temperature plots (Q-T plots) are derived. In the third part of this chapter the furnace of the 1MWth facility is numerically simulated by means of Computational Fluid Dynamics. The accurate simulation of dry lignite combustion conditions at the experimental scale and the correct reproduction of the observed trends at this scale are important steps towards the further use of CFD modelling as a design tool for large-scale boilers co-firing dry lignite. In other words, by evaluating the experimental results at the semi-industrial scale, key information regarding the combustion behaviour of Greek dried lignite is obtained. This information is then used for the prediction of the operational behaviour of an existing Greek boiler when co-firing dry lignite. CFD is an important tool in this analytical procedure since various combustion conditions can be simulated and evaluated, either in the small or in the industrial scale, and need not be tested in reality.

5.1 Lab-scale lignite drying tests at the experimental fluidized bed dryer

5.1.1 Introduction

In the present section the drying investigations of Greek lignite performed at a lab-scale fluidised bed drying facility in Germany are presented and analysed. Drying high moisture brown coals and lignites has been a matter of experimental investigations for many decades. Already in the 70's Evans et. al. investigated the effect of the drying temperature and pressure on the drying behaviour of Australian brown coals [V-1], [V-2], [V-3]. Bongers et.al. focused on the drying behaviour of Australian brown coal at elevated pressures between 10 and 25 bar by using a heated lab-scale pressure vessel [V-4], [V-5]. Furthermore, Agarwal et. al. developed a semi-empirical model on the description of the heat transfer on a coal particle which is dried in a steam atmosphere [V-6], and extended the particular model in order to describe the steam drying behaviour of coal particles in fluidised bed conditions [V-7].

Since brown coal particles are porous solid particles, their water content is not only located on their macroscopic surface but is also bound by capillary forces in pore structures in the inner side of particles. Depending on the pore size, the water found in them may be (1) located on the pore surface due to simple adhesion forces, (2) bound in pores through capillary forces or (3) bound by molecular forces on multi-molecule structures as an outer layer of them. It is further observed that in order to vaporise the water amount bound by capillary forces in pores, an increased heat input is required which exceeds the vaporisation enthalpy of water. The distribution of water in the different particle levels is determined by Allardice [V-8] for an Australian brown coal with an initial water content of 67% as follow: (a) 43% surface water, (b) 19% water bound in pores by capillary forces, (c) 3% water bound on multi-molecule structures, (d) 2% water bound in molecules. The respective heat needed for the complete vaporisation of the water content of a typical brown coal is given in Figure 5.1.

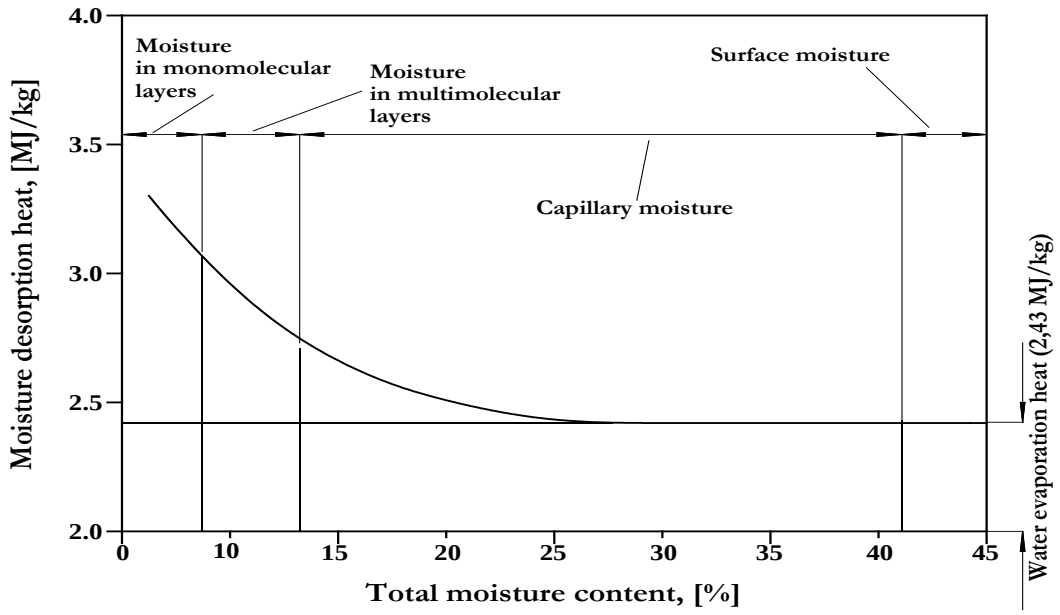

Figure 5.1 Typical moisture desorption heat of a brown coal in function of the total moisture content [V-8]

As shown in Figure 5.1 the required vaporisation heat for water in a coal particle increases exponentially when decreasing targeting to very low water content levels. In an energy efficient coal drying process the minimum moisture content which has to be determined should allow a positive energy balance between the thermal efficiency gain obtained by firing dried brown coal and the required heat input for coal drying up to the given moisture content. This value is usually between 10 and 20% for most brown coals.
The drying tests with Greek lignite are performed in a lab-scale fluidised bed dryer. Extensive investigations have been performed in the past in the particular facility to study the effect of process related parameters, like the operating temperature and pressure, the fluidisation velocity, the residence time in the bed and the particle size distribution on heat transfer and the total heat transfer coefficient (α [W/m^{2}K]) [V-9]. Nevertheless, the performed tests did not focus on an extensive investigation of the drying behaviour of Greek lignite by varying all possible process parameters. The experimental conditions at the particular facility, due to its lab-scale, are namely not fully comparable with those of an industrial-scale dryer and in this way no specific conclusions on the drying behaviour of Greek lignite at industrial-scale conditions can be drawn through these tests. This information can be only obtained by large-scale drying tests, during which a great quantity of Greek lignite has to be dried at the industrial scale bed dryer in Germany. These tests have been planned for the near future and are not included in the current investigations. The tests performed at the lab scale are, therefore, considered as indicative and may give qualitative information regarding the drying behaviour of Greek lignite compared to Rhenish brown coal used as a reference fuel. In particular, equilibrium curves for the Greek lignite are determined during the lab-scale campaign and compared with the Rhenish brown coal. In the equilibrium curves the remaining moisture content of the dried lignite is presented over the drying temperature, and in this way useful information on the required heat for the drying process is obtained.

5.1.2 Experimental methods

Description of the experimental equipment

The lab-scale fluidised bed drying facility is located at RWE's premises in the lignite-fired power station Niederaussem, Germany. It is installed in the boiler house close to a boiler unit; thus, the supply and discharge of consumables is ensured by the infrastructure of the large-scale boiler. The drying process is based on the principle of a continuously operated, stationary fluidized bed with integrated heat exchangers which supply the fluidized bed with the heat energy necessary for drying (Figure 5.2a,b). The heat transfer medium used is thermo oil. The raw lignite is fed continuously from the coal silo into the drier. Discharge of the dried lignite also occurs continuously from the drier into a dry lignite discharge vessel. Both vessels are filled and emptied discontinuously. The bed is fluidized using steam extracted from the steam main of the power station unit. In order to adjust the condition data (pressure and temperature) of the fluidizing steam to the requirements of drying, a pressure relief valve and a heat exchanger are provided between extraction from the steam network and entry into the drier. The dust-laden vapour leaving the drier (fluidizing steam and water liberated from the lignite) is withdrawn at the top of the drier and conducted to a cyclone where the entrained dust from the fluidized bed is separated. The cleaned vapour is, then, carried off via the flue gas path of the power station. The dust separated in the cyclone is transported to a receiving tank which is emptied discontinuously. Lignite samples can be taken from the described bin or receiving tank or directly from the fluidized bed by using sampling connections which are provided laterally at the drier wall.

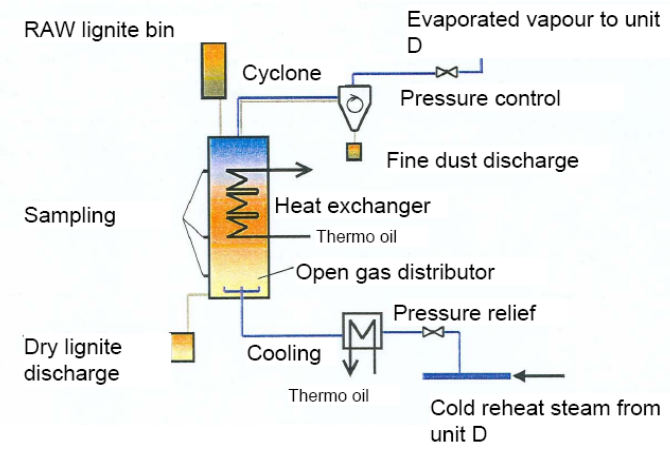

Fig. 5.2a: Schematic drawing of the fluidised bed dryer

Fig. 5.2b: Photo of the dryer

Experimental procedure

Before the drying tests, the raw lignite to be dried is crushed in a hammer mill to a particle size below 2mm in order to allow handling of the fuel in the test plant, and to ensure that fluidisation conditions of the lab-scale fluidised bed dryer are comparable with the conditions in the industrial-scale fine grain fluidised bed dryer (WTA2-dryer).

During the tests the temperature in the fluidised bed is set at a constant level by controlling the mass flow of the heating medium, and after reaching thermodynamic equilibrium conditions, a fuel sample is taken and its moisture content is determined. Four different bed temperatures are set during the tests, and the bed pressure is adjusted to 1.08 bar during the entire period of the investigations. For the determination of lignite moisture four samples of dry lignite are taken directly from the drier and analysed. Additionally, the temperature of the dried lignite sample is measured directly after sampling by immersing a thermometer into the sample vessel.

5.1.3 Results – Discussion – Further work

In Figure 5.3 the particle size distribution (PSD) of different samples is presented. These have been taken (a) before the tests (wet lignite sample), (b) after the tests in the dryer and (c) after the test in the cyclone.

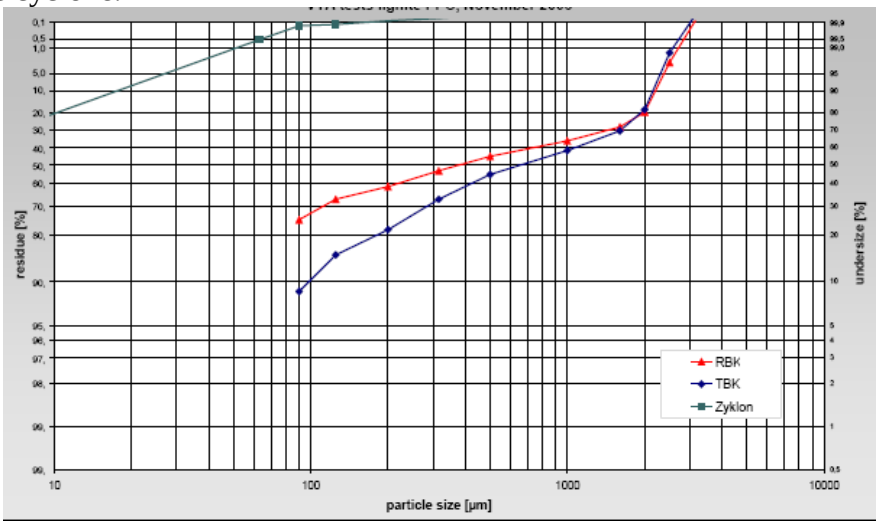

Figure 5.3: PSD of samples taken: (a) before the tests (“RBK”), (b) after the tests in the dryer (“TBK”) and (c) after the tests in the cyclone (“Zyklon”)

The equilibrium line of the Greek lignite together with the equilibrium line of the Rhenish lignite, are presented in Figure 5.4. Higher equilibrium temperatures than the ones applied for the Rhenish lignite are necessary for drying the Greek coal. This difference is up to 1K for the target remaining moisture of 12%. Although the required higher temperatures will affect the energetic efficiency of the drying process, it is estimated that this “energetic loss” will be counterbalanced by the higher moisture content of the raw Greek coal, thus by the higher efficiency gain after integrating the dryer in a steam power plant and utilising its evaporated moisture in the first water preheater stages.
Although the performed drying tests are considered as indicative and only basic drying related parameters are examined, qualitative remarks on the drying behaviour of Greek lignite compared to the Rhenish may be done. The overall results of the experimental drying investigations imply that Greek lignite shows a similar drying behaviour to Rhenish lignite. Therefore, a realisation of a more detailed campaign in the large-scale WTA prototype of RWE would be feasible as well as a future application of the WTA drying concept in one of the Greek power plants.

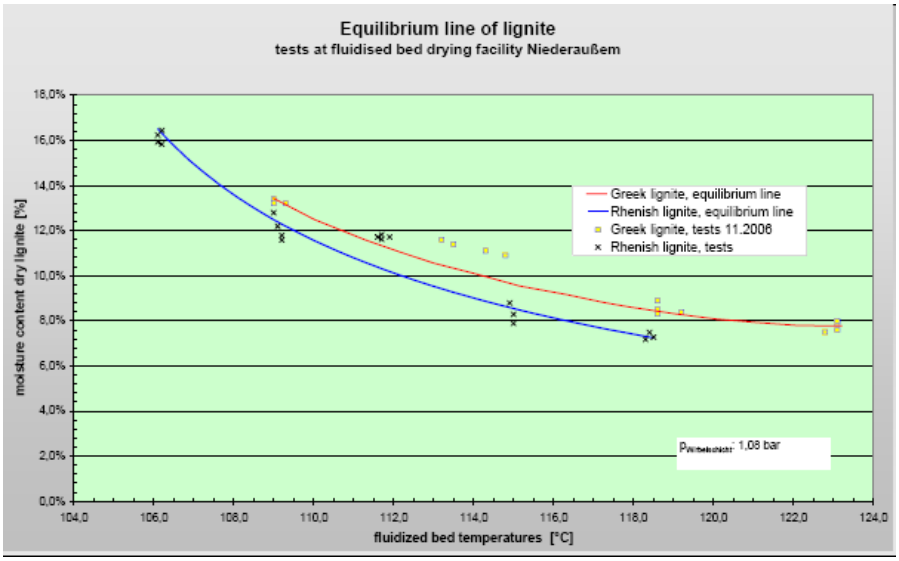

Figure 5.4: Equilibrium line of the Greek and the Rhenish lignite

5.2 Experimental investigations at the 1 MW_{th} combustion facility

5.2.1 Introduction

As mentioned earlier dry lignite co-combustion in existing or new pulverized lignite boilers is the necessary intermediate step for the further development of the 100% dry lignite boilers. However, retrofitting a conventional lignite boiler of the current state of the art in order to co-fire dry lignite up to a thermal share of 20 or 30% is not a trivial step. A change of the boiler standard operational behaviour can be expected. Although the thermal input remains constant, when co-firing dry lignite together with raw lignite, the temperature fields in the furnace and the convective section may change. Higher temperatures can be expected in the furnace region due to the reduced flue gas volume flow, and these may result in an increase of the radiative heat flux to the evaporator. On the other hand, the reduced flue gas volume flow may influence the heat exchange in the convective part of the boiler and thus lead to decreased heat fluxes in the convective heat exchanger section. The range of impact of these

potential effects on the real boiler behaviour cannot be generally estimated and depends on the particular boiler examined in each case. The governing parameters are the boiler geometry and firing system and the specific fuel fired. A detailed investigation of the expected effects of co-firing by experimental and simulation means is, therefore, advisable before implementing the proposed concept in the large scale.
For this reason it has been decided that combustion investigations are going to be carried out in a small-scale facility so that different combustion related parameters can be examined. The particular facility, despite its experimental function, shows similar behaviour to that of industrial-scale boilers as regards temperature fields, emissions and particle residence time due to its rather large scale, 1 MW_{th}, compared to normal experimental combustors. For this reason it is considered as a semi-industrial-scale facility and not a laboratory or a pilot scale one.
The scope of the experimental campaign performed at the 1 MW_{th} semi-industrial-scale facility campaign is the investigation of the combustion behaviour of Greek lignite i.e. temperature fields, ignition, burnout, emissions, as well as slagging and fouling tendency, while firing with varying levels of recirculated flue gas. Additionally, the heat transfer in the particular facility is evaluated by performing an overall energy balance and by post-processing the measurement results in order to obtain respective Q-T diagrams. Dry coal co-firing conditions in a large-scale boiler are simulated by adjusting the volume flow of the recirculated flue gas. Two test series representing different boiler operation modes have been planned and carried out. A detailed measurement set is carried out including temperature profiles, emissions, fuel, fly ash sampling and slagging and fouling investigations through the installation of dedicated deposition probes.

5.2.2 Methodology

5.2.2.1 Description of the experimental facility
Combustion tests were carried out at the 1MW_{th} VVA combustion facility and about 100 tons of Greek lignite were burnt for the scope of the investigations. The facility consists of a top fired vertical cylindrical furnace (radiative part), an intermediate horizontal part with square cross section and a second vertical cylindrical part (Figure 5.5), where a heat exchanger is placed (convection part). The furnace is refractory lined and cooled with cold reheated steam. The facility operates with raw brown coal with a moisture content range from 50 to 59% wt, and the maximum thermal output is 1,0 MWth corresponding to a raw coal mass flow of 300 kg/h with Rhenish brown coal as reference fuel. The drying concept is similar to the large-scale technology. Pre crashed raw brown coal is transported through a dosing belt conveyor (Fig. 5.5, [2]) to the beater fan mill (Fig. 5.5, [4]). Brown coal is milled and dried with hot recirculated flue gas while the remaining moisture content in the coal after milling varies between 12 and 17% wt. After passing through the mill and the classifier (Fig. 5.5, [3]), dried coal dust is separated from the carrier gas in a dedicated cyclone (Fig. 5.4, [5]). The coal dust is afterwards stored in two consecutive intermediate bunkers (Fig. 5.5, [6,8]) and fed pneumatically through the central burner clearance into the furnace (Fig. 5.5, [11]). The amount of recirculated flue gas entering the furnace is controlled with a control valve, and the remaining quantity is directed to the stack. A more detailed description of the VVA facility can be found in the literature [V-10].

1	Raw lignite bunker	12	Combustion chamber cooler
2	Proportioning belt weigher	13	Combustion chamber
3	Coal classifier	14	Air heater
4	Beater – fan mill	15	Burnout air
5	Cyclone	16	Burner air
6	DI intermediate bunker	17	Flue gas cooler
7	Cooling screw conveyor	18	Ignition Burner
8	DI intermediate bunker	19	ESP
9	Rotary feeder	20	Ash
10	DI carrier gas	21	Wet Ash removal
11	Burner	®	Flue gas analysis
DI	Dry lignite		

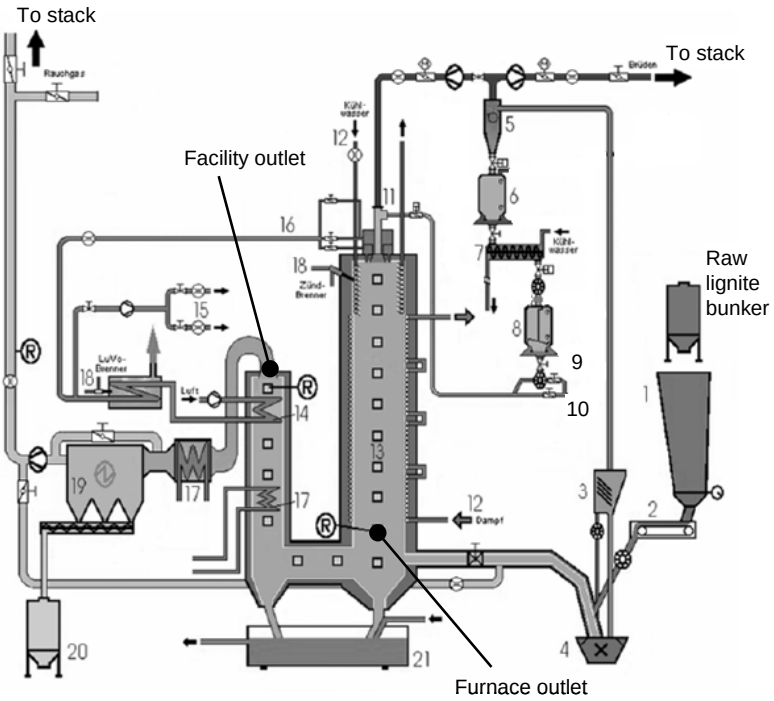

Figure 5.5: Layout of the 1MWth combustion facility

Different operation modes from “raw coal” firing up to “dry coal” firing can be simulated by controlling the amount of recirculated flue gas. This amount would correspond to the carrier gas mass flow in the industrial conditions. However, neither 0% nor 100% flue gas recirculation is possible for reasons of flame stability. The minimum required volume flow of recirculated flue gas is about 80Nm^3/h while the maximum allowed is about 380 Nm^3/h depending on the coal quality. These operation conditions are defined as “dry coal firing” and “raw coal firing” respectively.
Combustion air is preheated in a heat exchanger and adjusted to a final temperature of about 300 °C by a propane gas burner. In the case of staged combustion conditions, a fraction of the combustion air is inserted in the furnace as over-fired air (OFA) through downstream located nozzles. Temperature, emission measurements and fly ash sampling can be performed in 16 levels along the furnace axis, while slagging and fouling investigations are conducted with the use of dedicated deposition probes in four levels along the furnace axis.

5.2.2.2 Test matrix

Two main test series, “A” and “B”, are planned in order to evaluate the combustion behaviour of Greek lignite at varying levels of recirculated flue gas. The overall test matrix is given in Table 5.1. In the reference cases, A0 and B0, the maximum possible flue gas mass flow is recirculated into the furnace. The temperature at the furnace exit is initially set to about 1000°C, which is representative of the combustion conditions in Greek boilers, and the dry coal mass flow is then adjusted accordingly. Although both A0 and B0 represent the reference case, the applied boundary conditions including fuel, air and flue gas mass flows are not the same between A0 and B0, since A and B test series were performed at different periods with different facility loads. In other words, only comparison between cases of the same test series is possible. The recirculated flue gas is decreased to about half of the reference value in cases A1, B1, and in cases A2, B2 to the technically achievable minimum value. In this way A1, B1 cases simulate dry coal co-firing conditions, and A2, B2 cases simulate almost 100% dry coal firing conditions.

Series “A” differs from series “B” in the following aspect; in series “A” the dry coal mass flow is kept constant and the increase of the furnace temperature is recorded due to the constant thermal input and the reduced flue gas mass flow. The maximum temperature rise is an indication of the expected effect of dry coal combustion on the flue gas temperatures. In series “B” the dry coal mass flow is also decreased when decreasing recirculated flue gas in order to keep the furnace exit temperature constant and equal to the reference value. This operation mode is considered as more realistic and closer to the operation of large-scale boilers, where an increase of the furnace exit temperature above the reference values is not allowed due to limitations in the superheater materials. The expected fuel mass flow reduction and respective thermal input reduction required to keep the furnace outlet temperature constant, is determined in series “B”. In the case of a large-scale boiler this fuel input reduction corresponds to lower steam and electricity production.

Table 5.1: Overview of the test matrix

	Test series A	Test series B
“Case 0” Reference - Recirculated flue gas mass flow into the furnace: 100% of the maximum value	- Temperature at the near burner region and at furnace exit adjusted according to representative values of Greek boilers (about 1000 °C) - The necessary mass flow in order to achieve the above mentioned conditions is registered	
“Case 1” - Recirculated flue gas mass flow into the furnace: 50% of the maximum value	- Constant dry coal mass flow - Temperature is expected to increase	- Keeping temperature at furnace exit constant - Decrease of dry coal mass flow
“Case 2” - Recirculated flue gas mass flow into the furnace: minimum value	- Constant dry coal mass flow - Temperature is expected to increase further	- Keeping temperature at furnace exit constant - Further decrease of dry coal mass flow

It can be noted at this point that although specific analogies exist between the experimental facility and a typical utility boiler, the results obtained cannot be directly extrapolated to the large scale and have to be firstly evaluated by taking into account the given experimental conditions. In particular, due to flame stability requirements, the fraction of the flue gas mass flow recirculated and the fraction of the flue gas inserted again into the experimental furnace are not fully representative of the large-scale conditions. A reduction of the recirculated flue gas to 50% is, in other words, considered as very high for the industrial scale since it would correspond to a very high co-firing thermal share not feasible for existing boilers.
In order to estimate this thermal share combustion calculations are performed for a typical Greek boiler. The boiler considered is the 330 MW_e Agios Dimitrios V unit. A comparison between experimental and large scale conditions is attempted. The flue gas mass flow reduction measured at the experimental facility, when firing dry coal, is correlated with the expected flue gas reduction at the Agios Dimitrios V unit in the hypothetical case of dry coal co-firing. The dry coal co-firing thermal share in the large-scale boiler, which would result to the same relative flue gas reduction as in the experimental scale, is calculated for this scope. Although such a co-firing scenario is not currently feasible in Greek power plants with the

current firing systems, it is investigated as a possible retrofitting option. The moisture content of raw lignite is set at 54% based on the fuel analysis available, while the respective value of dry lignite is set at 12%.

5.2.2.3 Performed Measurements

The measurements performed during the tests are given below:

Measurements of temperature profile

The effect of dry coal co-firing on the obtained temperature fields in the facility is investigated. Temperature profiles are recorded at 9 different levels of the radiative part along the central vertical axis. The 10^{th} measuring point is placed in the vertical flue gas up-going path before the facility outlet. A dedicated water cooled suction pyrometer is used for the temperature measurements. A cylindrical ceramic shield is placed on the pyrometer top at the measuring junction of the thermoelement in order to reduce the radiation error. The estimated measurement error of the overall system is about 10K. Temperatures are recorded for 5 min in each measurement position and the average value is considered as the final measured temperature. During the "A-series" tests two consecutive temperature measurements are performed for each of the points A0, A1 and A2 in order to test the operation of the facility milling, feeding and dosing system. The variation of temperature values is expected to be low as long as the combustion conditions remain the same during each measurement point and coal quality does not vary to a large extent.

On-line emission measurements

The flue gas concentration (O_2, CO_2, CO, NOx, SO_2) at the furnace exit is continuously measured during the tests and average values are calculated.

Burnout and fly ash sampling

Fly ash samples are collected by isokinetic sampling with a dedicated sampling probe from eight different levels along the furnace axis, and ash analyses are performed for the obtained samples. ESP ash samples are also periodically collected during the tests.

Slagging and fouling investigations

One of the important aspects in the characterisation of Greek lignite at dry coal firing conditions is the investigation of its slagging and fouling behaviour. The main question to be clarified is whether the elevated temperatures during dry coal firing approach the ash melting temperatures of the Greek lignite. In case that this assumption is confirmed, significant slagging and fouling problems can be expected in future Greek boilers firing or co-firing dried lignite. This aspect is, therefore, of particular importance for future dry lignite boilers in Greece and will be examined in two steps; the first is the theoretical evaluation according to calculated slagging indices, and the second step is the experimental investigation using dedicated deposition probes. Rhenish brown coal is used as reference fuel in both parts of the examinations. In the theoretical evaluation, literature data of three different Rhenish brown coals is used, and the respective indices for the Greek and the Rhenish coals are calculated and compared. In the experimental activities the experience of the facility operating personnel on the deposition behaviour of Rhenish brown coals is utilized, and a comparison with the new results for the Greek lignite case is attempted. The first part of the investigation includes a literature survey on available indices which characterise the deposition behaviour of coals,

and the calculation of the respective values for the examined coals. Depending on the coal ash type, different expressions of slagging indices are used. Coal ash types are categorised in bituminuous and lignitic ones according to the relations proposed by Unswort [V-11]
Bituminous : $(CaO + MgO) < Fe_2O_3$
Lignitic : $(CaO + MgO) > Fe_2O_3$
All coal ashes examined are classified under the lignitic type. The following slagging indices of the Greek lignite are calculated and compared with equivalent data of the Rhenish brown coals.

Basic to acid ratio

$$B/A\_R = \frac{Fe_2O_3 + CaO + MgO + K_2O + Na_2O}{Al_2O_3 + SiO_2 + TiO_2} \tag{5.1}$$

Characteristic Alkali Number

$$A = Na_2O + 0.659 \cdot K_2O \tag{5.2}$$

Fouling Index

$$Fu = B/A\_R \cdot (Na_2O + K_2O) \tag{5.3}$$

Iron Oxide in the coal ash

$$Fe_2O_3 \tag{5.4}$$

Iron to Calcium oxides Ratio

$$Fe/Ca\_R = \frac{Fe_2O_3}{CaO} \tag{5.5}$$

Silica to Alumina Ratio

$$Si/Al\_R = \frac{SiO_2}{Al_2O_3} \tag{5.6}$$

Silica Ratio

$$Si\_R = \frac{SiO_2}{SiO_2 + Fe_2O_3 + CaO + MgO} \tag{5.7}$$

The work of many researchers including Bryers and Barosso [V-12], [V-13] concludes that the calculated slagging indices may give some tendencies on the expected deposition behaviour of coals, but occasionally fail to predict the correct - experimentally proofed - deposition behaviour. Therefore, the theoretical results have to be confirmed by experimental data. An overview of the indices considered together with the specific regions representing different slagging tendencies is given in Table 5.2. Since different ranges are found in the literature for the same slagging behavior [V-14-[V-17], more than one proposed values are included in the table wherever needed.

Table 5.2: Overview of the slagging indices combined with the respective regions representing different deposition tendencies

Index		low deposition tendency (+)	medium deposition tendency (++)	high deposition tendency (+++)	Source
Basic to Acid Ratio	B/A_R	<0,2 <0,5	0,2-1,0 0,5-1,0	>1,0 1,0-1,75	Zelkowski [V-14] Couch [V-15]
Characteristic Alkali Number	A	<0,5	0,5-2,5	>2,5	Zelkowski [V-14] Unsworth [V-16]
Fouling Index	Fu	<0,6	0,6-40	>40	Zelkowski [V-14]
Iron Oxide	Fe_2O_3	3-8	8-15	15-23	Raask [V-16]
Fe to Ca Ratio	Fe/Ca_R	<0,3 and >3,0		0,3-3,0	Bryers [V-12], Couch [V-17]
Silica to Alumina Ratio	Si/Al_R	<1,4	1,4-2,8	>2,8	Winegartner [V-15] Barroso [V-13]
Silica Ratio	Si_R	>0,72 0,8-0,72	0,65-0,72 0,72-0,65	<0,65 0,65-0,5	Zelkowski [V-14] Raask [V-16]

Dedicated deposition probes are used for the investigation of slagging and fouling behaviour. The probes are installed during test series A, where the fuel mass flow is kept constant during the three different cases and a temperature rise is expected. Four different probes are installed in different levels along the vertical axis, which are representative of different boiler regions. The first probe is installed in the near burner region, at measuring port nr. 4, 2.10 m from the burner outlet. The second probe is installed after the OFA, at measuring port nr. 8, 4.50 m from the burner outlet. The third probe is installed at the furnace exit, at measuring port nr. 10, 5.70 m from the burner outlet. The fourth probe is installed in the second vertical flue gas (convective) section before the heat exchanger, at port nr. 13 (Fig.5.5, [17]).
The probes consist of a metallic and a ceramic part. The metallic part is air cooled so that its surface temperature is adjusted to about 500˚C corresponding to an average tube temperature. The ceramic part is not cooled and therefore, its surface temperature is higher and may approach the flue gas temperature. As a result, intense deposition phenomena may be observed, and thus the deposition behaviour of a “fouled tube” is simulated. This behaviour is not representative of regular operation conditions in large-scale boilers, but may be an indication of the estimated deposits at extreme conditions. The total exposure of the probes is set at 16 hours during the main deposition investigations.

Investigation of heat transfer: Energy balance, q-T diagrams
Further information on the heat transfer in the facility and the radiative and convective heat fluxes is obtained by using the operational data and the profile temperature values. An overall energy balance for the facility is attempted and Heat Flux - Temperature plots (q-T plots) are calculated for the flue gas side. The facility walls are defined as the reference volume for the energy balance, which means that flue gas recirculation is not accounted as a closed loop. In other words, the flue gas mass flow leaving the furnace and used as a heating medium for the drying process is calculated separately as additional flue gas loss and is not counterbalanced by the flue gas mass flow inserted again into the furnace through the burner. This methodology leads to overpredicted values of flue gas losses; however, it enables a clear balance of all inserting and outgoing gas flows in the furnace. All required heat fluxes for the energy balance of the facility are obtained either by direct calculation from operational data or by further post-processing and utilization of data derived from combustion calculations (eg.

the adiabatic flame temperature). In Table 5.3 the heat fluxes and heat losses which form a part of the energy balance are given together with the respective calculation methods. For the calculation of the heat losses the methodology presented in the literature [V-19], [V-20] is followed. The final closure of the energy balance is performed after summing all heat losses and heat fluxes, and comparing with the value of the initial thermal input.

$q_{th\_input} = q_{tubes} + q_{losses\_Furnace} + q_{losses\_Recirculation} + q_{losses\_horiz.\ part} + q_{HX} + q_{losses\_FG}$

Table 5.3: Heat fluxes and heat losses considered in the energy balance

Parameter	Symbol	Calculation method
Thermal input	q_{th_input}	$q_{coal} + q_{secondary\ air} + q_{carrier\ air} + q_{OFA} + q_{recirculated\ FG}$
Heat Flux to cooling tubes	q_{tubes}	$m_{steam}\ (h_{steam\_out} - h_{steam\_in})$
Thermal power of the flue gas leaving furnace exit	$q_{FG\_Furnace\ exit}$	$m_{FG}\ cp_{FG}\ (T_{G\_Furnace\ exit} - T_{ambient})$
Total heat flux to furnace	$q_{Furnace}$	$m_{FG}\ cp_{FG}\ (T_{G\_adiabatic} - T_{G\_Furnace\ exit})$ or $q_{th\_input} - q_{FG\_Furnace\ exit}$
Heat losses at furnace	$q_{losses\_Furnace}$	$q_{Furnace} - q_{tubes}$
Heat losses due to Flue Gas (FG) recirculation (*)	$q_{losses\_Recirculation}$	$m_{Rec}\ cp_{FG}\ (T_{G\_Furnace\ exit} - T_{ambient})$
Heat losses at the facility intermediate horizontal part	$q_{losses\_horiz.\ part}$	$(m_{FG} - m_{Rec})\ cp_{FG}\ (T_{G\_Furnace\ exit} - T_{G\_upstream\ HX})$
Heat Flux to the convective heat exchanger (HX)	q_{HX}	$(m_{FG} - m_{Rec})\ cp_{FG}\ (T_{G\_upstream\ HX} - T_{G\_downstream\ HX})$
Flue gas losses	q_{losses_FG}	$(m_{FG} - m_{Rec})\ cp_{FG}\ (T_{G\_out} - T_{ambient})$

(*)The heat losses in the intermediate part include, apart from the respective radiation losses, the burnout losses due to the unburnt carbon falling into the hopper.

A schematic representation of the facility and the heat fluxes and the respective heat losses is given in Figure 5.6

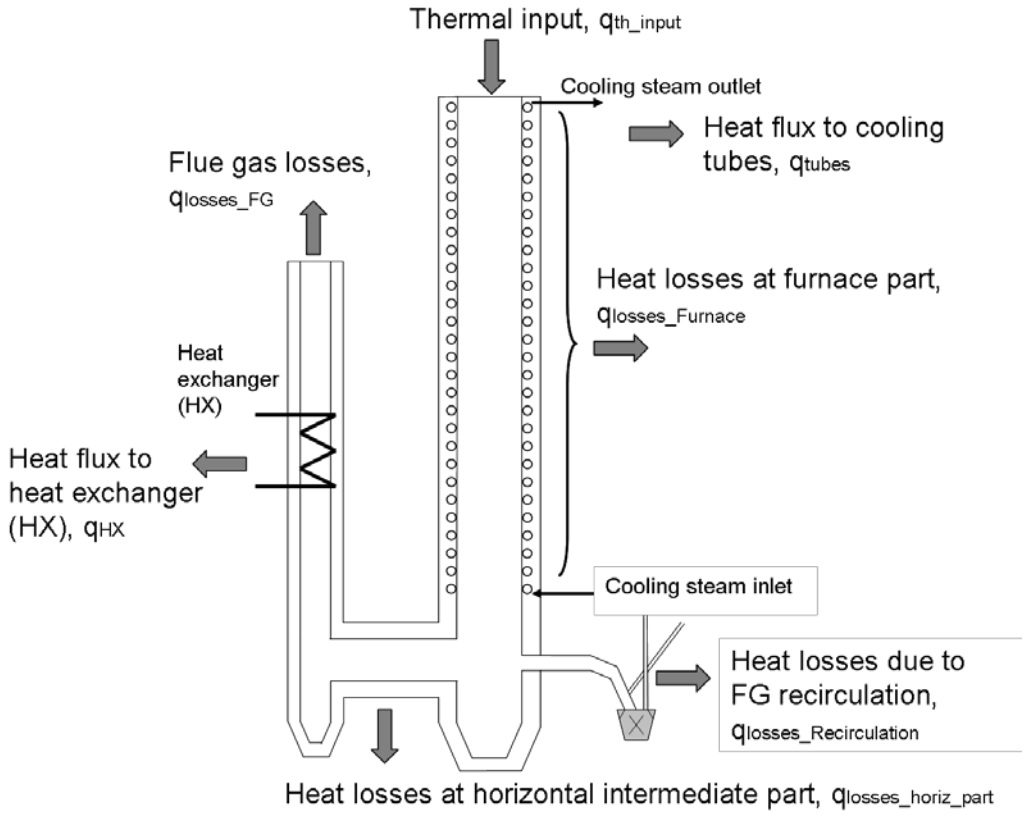

Figure 5.6: Schematic drawing of the VVA facility and the estimated heat fluxes and heat losses

For the calculation of the q-T plots the respective temperatures upstream and downstream each heat exchanger as well as the heat flux to the particular heat exchanger are calculated. The furnace section is also regarded as a heat exchanger and the adiabatic temperature is used as its inlet temperature. Taking into account that the particular combustion facility consists of the furnace (radiative part) and only one heat exchanger bundle (convective part), three locations are defined for which temperature measurements are required: the furnace exit, and the points upstream and downstream the heat exchanger. The temperature at the fourth point, the furnace inlet, is the adiabatic combustion temperature. The y-coordinates of the q-T plot are, therefore, determined by these three temperature records and the calculated adiabatic temperature. The x-coordinates correspond to the heat fluxes in the facility radiative and convective part. Since the considered q-T plots refer only to the flue gas side and not to the steam side, the heat fluxes at the radiative and the convective part are obtained from the energy balance.

In the initial calculation methodology of the q-T plots, as published in previous work [V-20], the heat transfer to the radiative part is calculated only by the steam data of the cooling tubes. These parameters remained constant through the tests, namely:

Steam mass flow: ~1.1 t/h

Steam inlet/ outlet temperature: 307°C/ 390°C

Steam inlet/ outlet pressure: ~40bar

From the given data the heat flux to the cooling tubes is calculated, $q_{tubes} = 77.5\ kW_{th}$.

However, this value almost remains constant during all the test cases and is much lower than the total heat flux transferred to the furnace walls through radiation. This implies that high

radiation losses are apparent in the particular facility, which can be expected, because the particular combustor is designed for experimental purposes and not for heat or power production. In order to account for the total heat flux transferred from the flue gas to the furnace wall, and not only for the amount transferred to the cooling tubes, the overall heat flux to the furnace walls obtained by the heat balance is used.

5.2.3. Results - Discussion

The results of the experimental activities, which are presented in parts in the present section, include (a) the fuel and ash analyses, (b) the temperature and emissions measurements, (c)the evaluation of the fuel burnout and ignition behaviour, (d) the examination of the slagging and fouling tendency of the Greek lignite and (e) the overall heat balance of the facility and the corresponding q-T plots. A more detailed examination of the particular experimental results can be found in the literature [V-21].

5.2.3.1 Fuel, ash and mineral phase analysis

Proximate and ultimate analysis of the Greek lignite from the "Mavropigi" mine, which is fired in the facility, are given in Table 5.4. The specific lignite is characterised by its high ash content and its low calorific value.

Table 5.4: Proximate and ultimate analysis of the Greek lignite

Proximate analysis (% a.r.)			Ultimate analysis (%daf)	
	Before mill	After mill		Mean
Water	56.3	12.73	C	66.03
Ash	13.4	24.22	H	4.65
Volatiles	18.41	34.02	N	2.07
Fixed C	11.89	29.03	O	25.64
Hu (kJ/kg K)	6,590.7	16,127.4	S	1.62

In Table 5.5 the oxide analysis of the Greek lignite is given. For reasons of comparison the analysis of a second Greek lignite extracted from the "Kardia" mine is also given. The two coals show similar ash compositions and the main oxides present are CaO, Al_2O_3 and SiO_2. Additionally, oxide analyses of three different Rhenish brown coal types are obtained from the literature [V-10]. It is experimentally proven that the three specific Rhenish brown coals show different deposition behaviours ranging from low to increased deposition tendency. The following results are drawn by the comparison between Greek and Rhenish coals:

- Fairly increased portions of potassium are observed in the analysis of Greek lignites.
- Elevated portions of aluminium and silicon and lower sodium and sulphur content are measured in the Greek lignites compared to the Rhenish ones.

Judging from this first ash analysis, it is assumed that moderate deposition behaviour is expected for the case of the Greek lignite as the high concentration of acid oxides in the ash (Al_2O_3 and SiO_2) does not allow the formation of low temperature melting points. On the other hand, elevated alkali concentrations, like sodium and potassium, could lead to fouling problems in the convection part of a boiler according to the mechanism described by W. Bryers [V-12]. For the activation of this mechanism, however, increased sulphur concentration in the ash is required, which is not the case for the Greek lignite. No severe fouling problems are, therefore, expected for the Greek lignite based on these initial results derived from the ash characterisation.

Table 5.5: Oxide analysis of lignite ash, compared with the oxide analysis of Rhenish brown coals

	Na_2O	K_2O	CaO	MgO	Al_2O_3	SiO_2	Fe_2O_3	TiO_2	SO_3
Greek lignite ("Mavropigi" mine)	0.25	0.71	33.27	3.88	11.80	25.34	6.10	0.57	7.35
Greek lignite ("Kardia" mine)	0.28	0.39	45.24	4.65	11.22	22.91	8.41	0.66	5.57
Rhenish brown coal (high fouling tendency)	4.5	0.5	30	15	5	10	15	0.4	20
Rhenish brown coal (medium fouling tendency)	2.5	0.5	20	10	5	35	10	0.5	15
Rhenish brown coal (low fouling tendency)	0.5	<0.5	20	5	10	35	15	1	15

A qualitative classification of the different coal ashes based on their chemical composition is also found in the Altmann's triangle, shown in Figure 5.7. Each side of the triangle represents the summations below, following counter-clockwise direction:
Oxides : $SiO_2+Al_2O_3+TiO_2$
Calcic : $CaO+MgO+Na_2O+K_2O$
Ferric : $Fe_2O_3+SO_3$
The marks on the ternary diagram for each category are calculated as the sums of the equivalent oxides for the five available coal ashes. Depending on the chemical composition of each ash, a number of intermediate subgroups is formed, including ferrosialic, calsialic, ferrocalsialic ferric, calcic and rarely, ferrocalcic ash types. The results obtained from this triangle are informative and are regarded as a useful tool for the comparison between the different coal types, as described in the work of Goodarzi et al. [V-22]. Greek lignite ashes are classified under the calcic type, while German brown coals fall under the ferric and ferrocalcic subgroups due to their high content in ferric oxides.

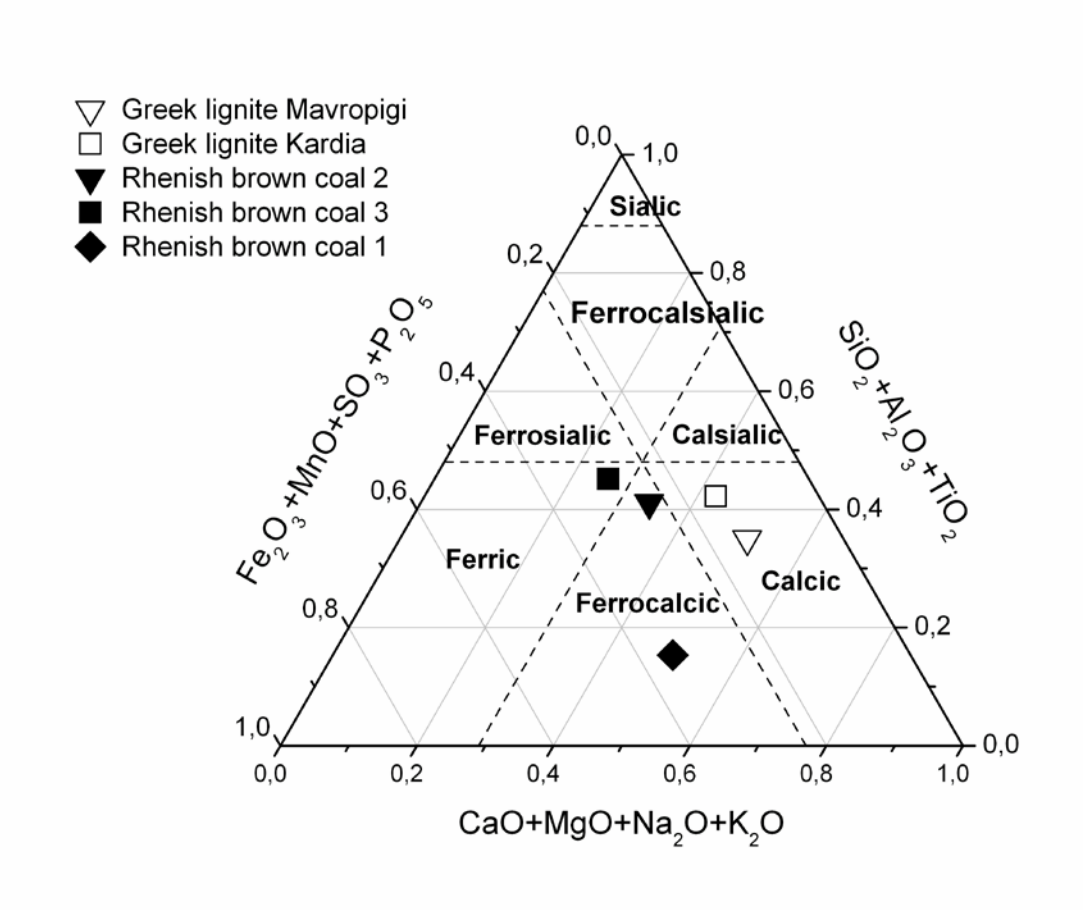

Figure 5.7: Classification of the available coals on Altmann's triangle based on the major oxides

As a last point in the fuel and ash characterization, the mineral phase analysis of the "Mavropigi" lignite is given in Table 5.6. It can be noted that calcium is present mainly as calcite and less as anhydrite, while silicon is present in the form of silica. Finally, as regards the form of alkalis in the minerals, potassium is mainly present in the combined state, in muscovite [$KAl_2(OH,F)_2AlSi_3O_{10}$].

Table 5.6: Mineral phase analysis of the Greek lignite as received

Greek coal	Calcite $CaCO_3$	Mica (Muscovite) $KAl_2(OH,F)_2AlSi_3O10$	Silica SiO_2	Magnetite,Maghemite Fe_3O_4,Fe_2O_3	Tricalciumaluminate $Ca_3Al_2O_3$	Anhydrite $CaSO_4$	Roentgen amorphous part
sample 1	49.0	19.0	6.0	1.0	1.0	8.0	16.0
sample 2	36.0	10.0	4.0	2.0	-	6.0	42.0

5.2.3.2 Temperature measurements and characterisation of the emission behaviour

Test series A

In the test series A the maximum temperature increase is measured by keeping the load constant and reducing the recirculated flue gas amount. Although this operational mode can hardly be realised in an existing boiler co-firing dry coal, due to the limitations on the furnace exit temperature, the particular investigation is performed in order to record the maximum achievable temperatures and their effect on the emissions and the slagging and fouling behaviour. From the obtained temperature profiles (Figure 5.8) the following conclusions are drawn:

- A temperature increase of 40K at the furnace exit is measured for each reduction step of the carrier gas mass flow, from A0 to A1 and from A1 to A2.
- The equivalent temperature increase in the near burner region is up to 100K
- A shift of the maximum temperature upstream, closer to the burner inlet, is noticed imposing earlier flame ignition.
- The increased values of error bars in the near burner region indicate higher standard deviation in the specific location due to higher temperature fluctuations compared to downstream.

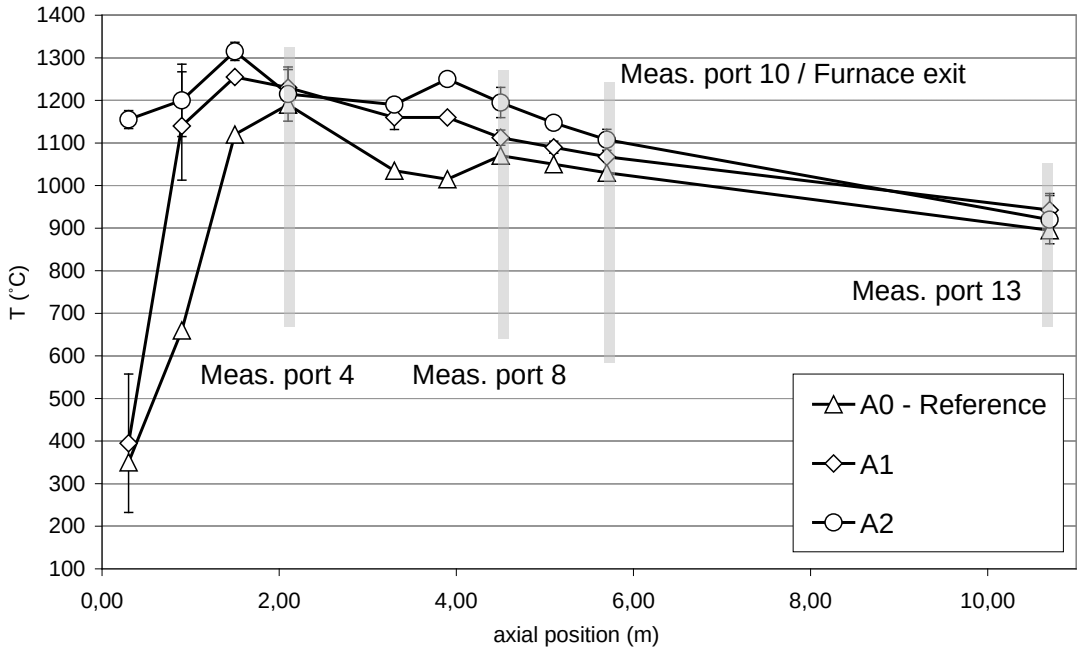

Figure 5.8: Temperature profiles of test series A and measurement locations of the deposition probes

The operational parameters of test series A and B including coal, carrier gas and total flue gas mass flows are given in Table 5.7 together with the respective variation of the values in %. A decrease of the carrier gas mass flow to 41% and to 75% is recorded during tests A1 and A2. In order to keep the air to fuel ratio constant, when decreasing the carrier gas mass flow, the combustion air mass flow increases. As a result, the total flue gas mass flow decreases to a percentage lower than the carrier gas, namely to 4% and 14% in cases A1 and A2 respectively.

An important remark regarding the comparison of the experimental results with the industrial scale and their potential transferability is also presented in the last row of Table 5.7. Based on

the combustion calculations, the equivalent dry coal co-firing share in a large-scale power plant which would give the same relative decrease of the flue gas mass flow is calculated. The reference data is taken by PPC's Agios Dimitrios V boiler firing lignite with 54% moisture content. The substitution of raw lignite by dry lignite with 12% moisture is assumed. According to the calculations, a thermal share of substitution of 17% and 59% would be required in order to reach the flue gas mass flow reduction of tests A1, A2. These high and unrealistic values of substitution indicate that the relative flue gas mass flow reductions of 4 and 14 % are rather high values which cannot be reached in large-scale plants. Therefore, the application of lower dry coal co-firing shares in industrial-scale boilers will also lead to lower temperature peaks than the ones observed during the experimental tests.

Table 5.7: Overview of the operational parameters and their relative variations during the tests

	Parameters	A0	A1	A2	B0	B1	B2
Thermal input	kWth	673	688	662	764	678	560
	variation (%)	0 (Ref.)	+2.2	-1.6	0 (Ref.)	-11.3	-26.7
Coal mass flow	kg/h	154	157	152	174	155	126
	variation (%)	0 (Ref.)	+1.9	-1.3	0 (Ref.)	-10.9	-27.6
Carrier gas mass flow	kg/h	342	216	88	447	228	85
	variation (%)	0 (Ref.)	-41	-75	0 (Ref.)	-50	-76
Total flue gas mass flow	kg/h	1296	1246	1119	1574	1308	1141
	variation (%)	0 (Ref.)	-4	-14	0 (Ref.)	-17	-28
Equivalent co-firing thermal share in a typical Greek boiler (%)		0	17	59	-	-	-

The results of CO, NOx and SO_2 emissions (Table 5.8) do not provide a clear picture on the emission behaviour which can be confirmed by the work of other researchers. High variations are observed for SO_2 emissions, while CO, NOx levels tend to decrease by increasing the dry coal co-firing share. The slight decrease is reasonable in the case of CO due to the improved burnout; however, it cannot be justified in the case of NOx, where an increase, due to the higher temperature levels, is expected as described in the work of Maier et al. [V-23], [V-24], [V-25], [V-26]. The control of NO_x emissions can be then achieved by the variation of two combustion related parameters: a) The stoichiometry in the reduction zone, and b) the coal particle residence time in the reduction zone, or, in other words, the length of the zone.

Table 5.8: Average emission values of the "A" series tests

emissions		units	A0	A1	A2
CO (dry, 6% ref.)	average	mg/Nm^3	33.6	30.4	29.2
	st. deviation	"	1.3	0.9	7.2
NOx (dry, 6% ref.)	average	"	434.3	407.3	382
	st. deviation	"	24.1	21.7	43.7
SO_2 (dry, 6% ref.)	average	"	243.6	252.71	219.56
	st. deviation	"	58.5	52.09	62.08

Test series B

The scope of test series B is the simulation of a combustion mode representing the operation of an existing large-scale boiler co-firing dry coal. In contrast to series A, where the furnace exit temperature increases up to 40-50 K due to the constant fuel input, a realistic boiler operation strategy does not allow such a temperature rise at the furnace exit due to the already given flue gas upper temperature limits for the superheater section. Therefore, the option of reducing the load during co-firing dry coal in order to keep the exit temperature constant is examined in these tests. However, it has to be further examined to what extent the reduced coal and flue gas mass flow will lead to a decrease of the heat flux in the boiler convective section, and influence the boiler balance. Such an operation mode is particularly interesting in the case of power plants firing extremely low rank lignites and facing capacity problems at the mills when trying to keep the maximum load constant. Dry coal co-firing in this situation will help to reach higher combustion temperatures in the furnace and cover the load demand with lower coal mass flows.

The temperature profiles of test B are presented in Figure 5.9. A temperature rise of more than 200K in the near burner region is observed between reference case B0 and case B2 with the minimum carrier gas mass flow. No temperature variation is observed, however, at the furnace exit where the temperature value remains about 1050°C in all cases. Furthermore, lower temperatures are noticed in the near burner region for cases B1, B2 compared to reference B0 indicating delayed ignition. The reason for this is probably the reduction of the air and fuel mass flow and the changes in the burner aerodynamics leading to a shift of the ignition downstream. The achieved decrease of the inserted dry coal mass flow from 174kg/h to 126kg/h corresponds to a load decrease of up to 27%. This fuel input decrease will also influence the produced useful heat and the produced electricity in case of a large-scale plant. It is, however, argued that similar to the “A series” tests, a very high dry coal combustion share, not feasible for large-scale conditions, would be necessary in order to achieve a flue gas mass flow reduction of 28% in existing plants. A moderate flue gas mass flow decrease and accordingly, a moderate load reduction towards keeping the furnace outlet temperature constant is, therefore, expected by the implementation of dry coal substitution practices in existing pulverised brown coal boilers.

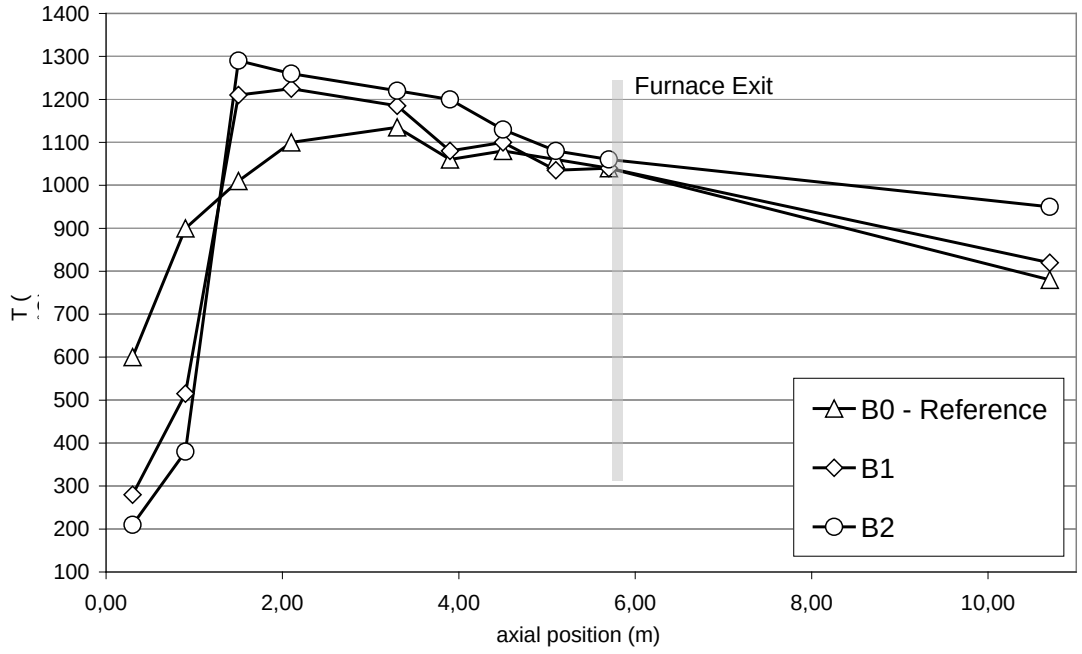

Figure 5.9: Temperature profiles of test series B

5.2.3.3 Investigations of burnout

For the evaluation of burnout when firing dry coal, fly ash and ESP ash samples at different levels along the furnace central axis are taken. Total Organic Carbon (TOC) is measured in the obtained ash samples and the results are presented in Figure 5.10a,b. A decrease of the unburned carbon in ash when firing dry coal can also be noticed, especially in the ESP ash, which is a clear indication of the improved burnout.

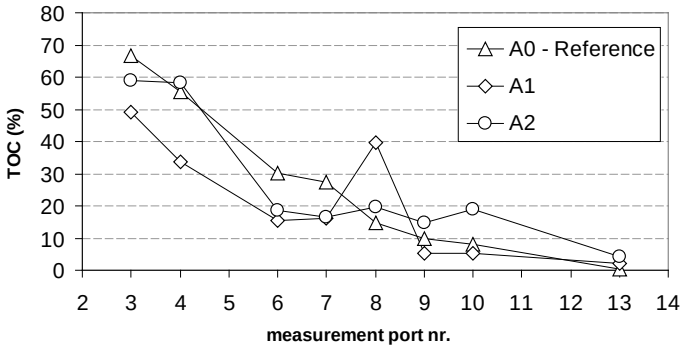

Figure 5.10a. Total Organic Carbon content (w. %) in fly ash samples taken in multiple levels along the furnace central axis

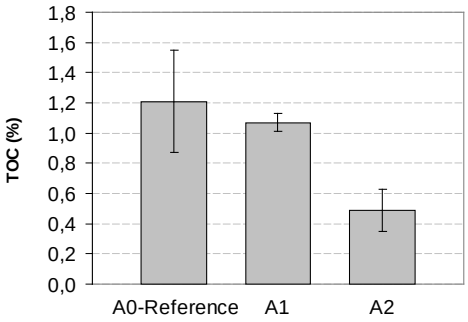

Figure 5.10b. Total Organic Carbon content (w. %) in ESP ash

5.2.3.4 Investigations of the deposition behaviour of the Greek lignite

Evaluation of the slagging behaviour based on calculated slagging indices

The slagging indices calculated for the Greek and Rhenish coals together with the derived estimations for the slagging behaviour are presented in Table 5.9. According to these values, the examined Greek lignites show lower slagging tendency compared to the Rhenish brown coals. This conclusion is confirmed by the performed ash fusibility tests for the Greek lignites presented in Table 5.10. The determined average softening temperatures for the Greek lignite from the “Mavropigi” mine are high, between 1240 and 1290 °C, while the relevant value for the Rhenish brown coal found in literature is lower, with a maximum value of about 1200 °C. One important aspect, however, which the calculated slagging indices fail to predict is the difference between the slagging and fouling behaviour of the three different Rhenish brown coals. According to experience with these three brown coal types, the first one, with the elevated sodium content, tends to exhibit intense slagging and fouling behaviour by forming low temperature melting points. The second one shows medium slagging behaviour, while the third one exhibits low slagging behaviour. This experience, gained from experimental investigations, is not clearly reproduced in the results of the evaluation by the slagging indices. Overall, however, the indices calculated succeed in predicting the difference between the depositon behaviour of the Greek and the Rhenish coals.

Table 5.9: Characterisation of deposition behaviour by different slagging indices

	Greek lignite ("Mavropigi" mine)	Greek lignite ("Kardia" mine)	Rhenish brown coal (high fouling tendency)	Rhenish brown coal (medium fouling tendency)	Rhenish brown coal (low fouling tendency)
Base to Acid Ratio	1.17 +++	1.70 +++	4.22 +++	1.06 +++	0.89 ++
Characteristic Alkali Number	0.72 ++	0.54 ++	4.83 +++	2.83 +++	0.83 ++
Fouling Index	1.13 ++	1.14 ++	21.10 ++	3.19 ++	0.89 ++
Iron Oxide	6.10 +	8.41 ++	15 +++	10 ++	15 +++
Fe to Ca Ratio	0.18 +	0.19 +	0.50 +++	0.50 +++	0.75 +++
Silica to Alumina Ratio	2.15 ++	2.04 ++	2.00 ++	7.00 +++	3.50 +++
Silica Ratio	0.37 +++	0.28 +++	0.14 +++	0.47 +++	0.47 +++

+ low deposition tendency, ++ medium deposition tendency, +++ high deposition tendency

Table 5.10: Results of the ash fusibility tests

	Sample 1	Sample 2
Softening Temperature [°C]	1242	1291
Hemisphere Temperature [°C]	n.a.	1356
Flow Temperature [°C]	1294	1363

Evaluation of the slagging behaviour based on experimental activities

The initial deposition measurements are performed during initial tests, in which the furnace exit temperature is set at 950˚C - 980˚C and the exposure time at 36 h. No deposits are observed in all four measurement positions after the initial investigations, thus confirming the low slagging tendency of the examined Greek lignite at flue gas temperatures below 1000˚C. The same behaviour is also noticed during similar observations in the large-scale boilers.

In order to investigate possible slagging and fouling phenomena at elevated temperatures representative of dry coal firing, the exposure temperature of the probes at the furnace outlet is set at 1050˚C during the main deposition tests. The main deposition investigations are performed during the "A test series" and the total exposure time of the probes is set at 16h. The temperature zones, at which each probe is exposed, are shown in Figure 5.6, and the photos of the deposits obtained at the probes located in measurement ports nr. 4 and 13 are presented in Figure 5.11.

	Case A0	Case A1	Case A2
Port 4	 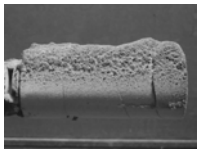	 	 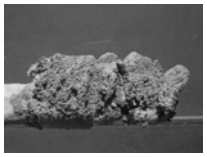
Port 13	 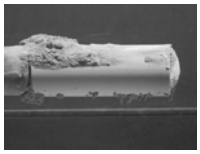	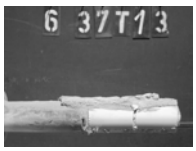 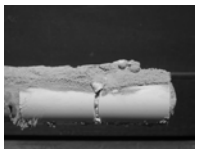	 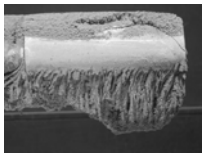

Figure 5.11: Photos of the metallic and the ceramic part of the deposition probes, at measuring ports nr. 4 and 13

No deposits are observed on the probes installed at ports 8 and 10. After evaluating this result and incorporating the outcome of the initial tests, it is concluded that the specific Greek lignite has a low deposition tendency in the temperature range between 950 and 1150˚C, either in reference or in dry coal firing conditions. This is an important outcome in favour of the suggestion that no radical changes of the slagging and fouling behaviour in Greek lignite boilers can be expected if dry coal co-firing is applied.

Increased deposits are observed at the ceramic part of the probe located at the facility outlet (measuring port nr. 13), but only during test point A2. Due to the difference between the observed behaviour in tests A0, A1 and the last one, no clear results can be drawn for the particular measurement location and further investigation is needed. It is argued that the noticed deposition in test A2 is caused by the reduced velocity magnitudes, which enable adhesive forces in the fly ash to overtake the effect of the high flue gas and particle momentum that would normally “decompose” this kind of “loose” deposits. However, such reduced flue gas mass flows and respective velocities are not expected in a realistic dry coal co-firing scenario in an existing boiler. Hence, no such increase of deposits at the particular region is either expected in large-scale conditions.

Increased slagging and fouling tendency is noticed for the “dry coal co-firing” cases at measurement port nr. 4 which corresponds to the near burner region. Sintered deposits are observed in the reference case (A0) and the first co-firing case (A1), and slagged deposits are further observed in case A2. This is most likely due to the increased amount of molten phases caused by the elevated furnace temperature, which lead to increased ash caking caused by the “adhesive effect” of the phases. These findings imply a definite slagging tendency for the investigated lignite in elevated temperatures above 1150˚C mainly at the near burner region.

In Figure 5.12a, b, c the oxide analysis of the deposits is presented together with the fuel ash analysis for the three test cases, A0, A1 and A2 respectively. An enrichment of the ash deposits on silicates, iron - and aliminum oxide compounds is observed. Similar composition for high temperature deposits of Greek lignite is also reported in the work of Maier [24].

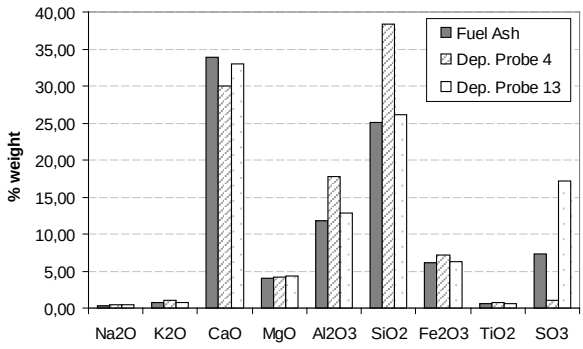

Figure 5.12a: Oxide analysis of fuel ash and deposits (A0 - Reference)

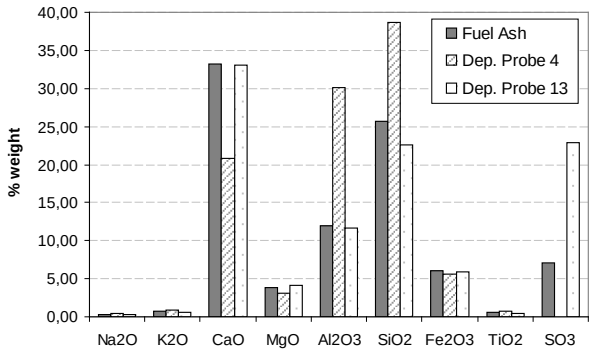

Figure 5.12b: Oxide analysis of fuel ash and deposits (A1)

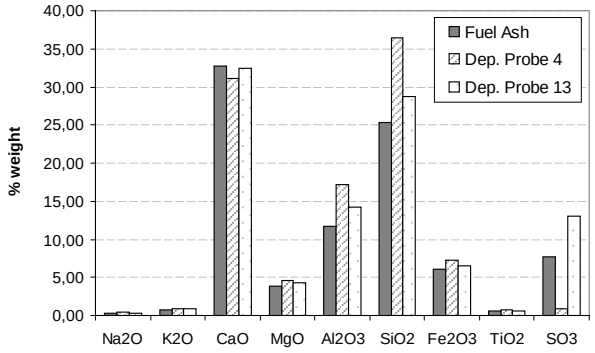

Figure 5.12c: Oxide analysis of fuel ash and deposits (A2)

The mineral phase analysis conducted by means of X-ray diffractometry is given in Table 5.11. It can be noticed that all deposits at the burner region (measurement port nr. 4) have similar mineral compositions, and the main components are silicate minerals, namely melilite, anorthite and pyroxenes. Further important components are amorphous constituents, indicating a high degree of molten ash in the deposits, which is among others the primary adhesive component of the deposit structure.

As a conclusion, the experimental investigations on the slagging and fouling behaviour of Greek lignite showed no specific tendency at the furnace outlet zone. Its deposition tendency is generally lower than that of Rhenish brown coals tested in the past at the particular facility. A definite slagging potential is, however, observed in the near burner region at flue gas temperatures above 1150°C , and this behaviour has to be further examined in future experimental investigations.

Table 5.11: Mineral phase analysis of the deposits

Test Nr.	Measurement Port Nr.	Part of the probe		Silica SiO_2	Anorthite $CaAl_2Si_2O8$	MelilitheAkermanite, Gehlenite $Ca_2(MG,Al)Si_2O_7$	Pyroxene $Ca(Mg, Fe,Al)Si_2O_6$	Larnite Ca_2SiO_4	Merwinite $Ca_3Mg(SiO_4)_2$	Albite $NaAlSi_3O_8$	Free lime CaO	Dicalciumferrite* $Ca_2Fe_2O_5$	Magnetite,Maghemite Fe_3O_4,Fe_2O_3	Periklase MgO	Anhydrite $CaSO_4$	Röntgen amorphous parts
		Metal-lic	ceramic													
A0	4		X	3.0	26.0	24.0	12.0	0	0	2.0	2.0	1.0	1.0	1.0	2.0	29.0
A1	4		X	1.0	16.0	30.0	7.0	0	0	1.0	0	0	1.0	0	0	45.0
A2	4		X	1.0	11.0	41.0	8.0	0	0	1.0	0	0	0	0	1.0	37.0
A0	13		X	4.0	10.0	18.0	9.0	0	0	2.0	1.0	1.0	1.0	1.0	24.0	28.0
A1	13		X	2.0	5.0	20.0	15.0	0	0	1.0	0	1.0	2.0	0	33.0	21.0
A2	13		X	3.0	7.0	23.0	14.0	6.0	4.0	1.0	0	0	3.0	0	22.0	16.0
A2	13	X		2.0	2.0	9.0	3.0	12.0	8.0	1.0	5.0	2.0	1.0	2.0	13.0	40.0

5.2.3.5 Investigations of heat transfer

Based on the presented methodology the energy balance of the facility for cases A0-A2 and B0-B2 is presented in Figures 5.13 and 5.14 respectively. It should be noted that high thermal losses are measured in all examined cases. The percentage of thermal input converted to useful heat (boiler efficiency) is lower than 30% in all examined cases, which testifies that the particular facility is designed for experimental purposes and not for power or heat production. Flue gas recirculation losses represent the highest percentage of the total losses. This result is, however, related to the specific reference volume chosen for the heat balance since one fraction of the outgoing flue gas is recirculated into the furnace. By adding the radiation losses to the furnace section and the heat flux to the cooling tubes, the total radiative heat flux to the furnace section is calculated. In series A, where dry coal co-firing and the 100% dry coal firing conditions are simulated, the radiative heat flux to the furnace increases by reducing the recirculation mass flow, while in series B, where the load decreases in order to keep the furnace outlet temperatures constant, the radiative heat flux almost remains constant. The convective heat flux to the heat exchanger decreases in both test series A0 to A2 as well as B0 to B2 due to the lower flue gas mass flow. A further analysis of the particular behaviour is attempted with the derived q-T plots. Finally, as regards the validation of the facility energy balance, a satisfying closure of the balance is obtained. For this scope, the initial thermal input is compared with the sum of the considered heat fluxes and thermal losses for each case.
In the second part of the evaluation the heat transfer in the facility is closely addressed by the evaluation of the respective q-T diagrams calculated for the flue gas side (Figure 5.15a, b). The main results of the q-T plots can be summarised in the following:

- The adiabatic temperature increases up to 70-80K when shifting from test point A0 to A1 and from A1 to A2, while it almost remains constant in cases B0, B1 and B2, which is expected due to the particular set up of the B cases.
- The radiative heat flux to the furnace increases in cases A1, A2 compared to the reference case due to the elevated flue gas temperatures. The relative increase is about 15% between cases A0 and A1, and about 22% between cases A0 and A2. On the other hand, the convective heat flux decreases due to the lower flue gas mass flow. As a result, the fraction of the radiative heat flux to the total heat flux of the facility increases (Figure 5.16a). This constitutes an expected change when firing dry coal also reported in the literature [V-27]. Similar behaviour is also mentioned in the case of pure oxygen combustion, where the absence of nitrogen as an inert component in the flue gas leads to increased flame temperatures and subsequently to higher radiative heat fluxes [V-28], [V-29].
- A different picture is obtained in the B series test, in which the radiative heat flux is almost stable due to the reduced load, and the convective heat flux decreases in absolute values. The total useful heat decreases considerably in these series. As a result, the fraction of the radiative heat flux devided by the total heat flux also increases in series B, although not to a very high percentage compared with the respective increase in series A (Figure 5.16b).

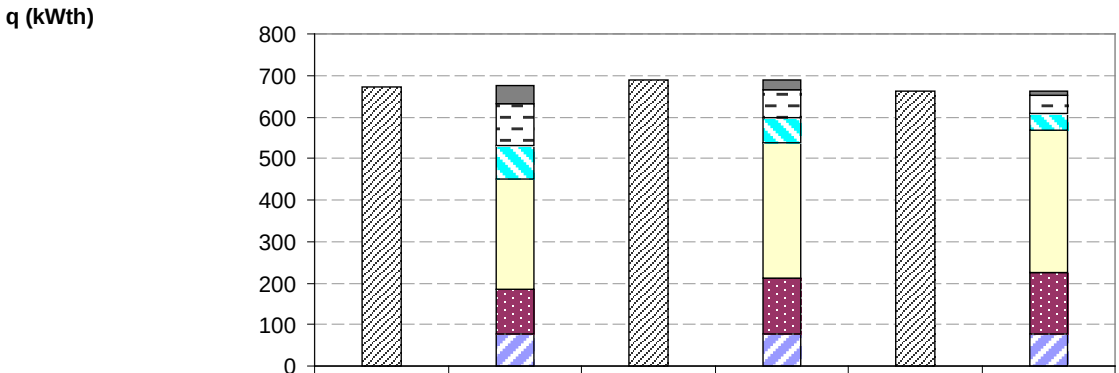

	A0: thermal input	A0: heat balance	A1: thermal input	A1: heat balance	A2: thermal input	A2: heat balance
Thermal input	673,5		688,1		662,5	
Flue gas losses		41,0		22,1		12,6
Heat Flux to convective HX		102,8		68,0		41,5
Radiation losses at intermediate part		79,5		58,4		42,2
Heat losses from FG recirculation		266,7		327,7		342,7
Radiation losses at furnace		106,6		134,2		147,2
Heat Flux to cooling tubes		77,5		77,5		77,5

Figure 5.13: Energy balance for cases A0, A1, A2

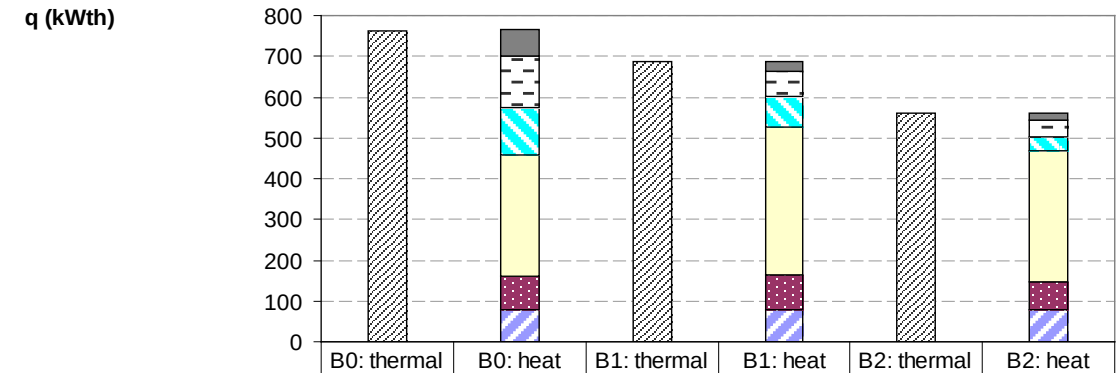

	B0: thermal input	B0: heat balance	B1: thermal input	B1: heat balance	B2: thermal input	B2: heat balance
Thermal input	763,6		686,8		560,2	
Flue gas losses		64,6		23,0		17,2
Heat Flux to convective heat exchanger		126,8		61,3		40,0
Radiation losses at intermediate part		115,4		76,8		36,0
Heat losses from FG recirculation		295,4		361,3		318,9
Radiation losses at furnace		84,5		87,6		71,1
Heat Flux to cooling tubes		77,5		77,5		77,5

Figure 5.14: Energy balance for cases B0, B1, B2

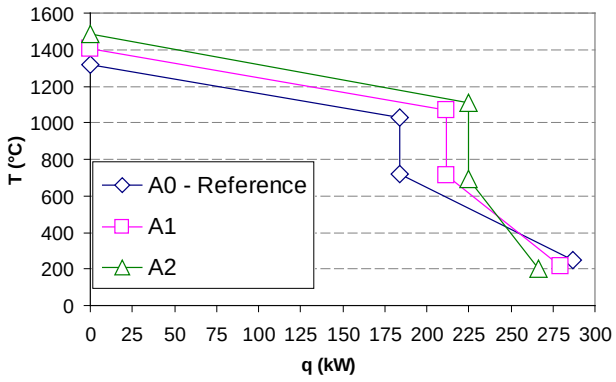

Figure 5.15a: q-T diagram, cases A

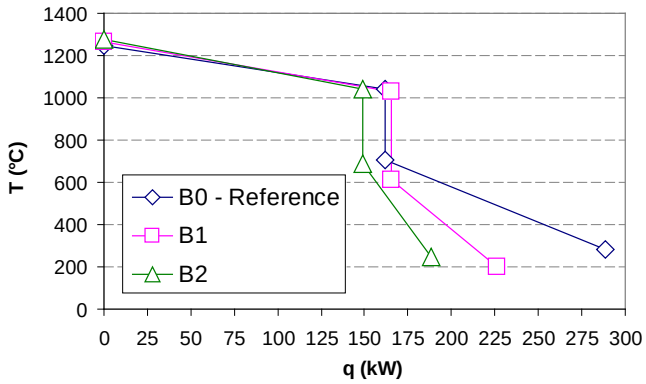

Figure 5.15b: q-T diagram, cases B

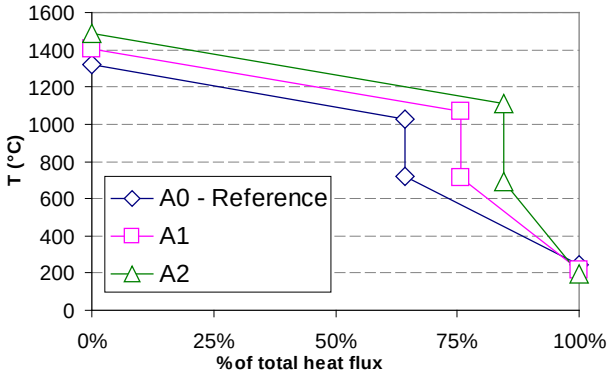

Figure 5.16a: q-T diagram (q in % of total heat flux), cases A

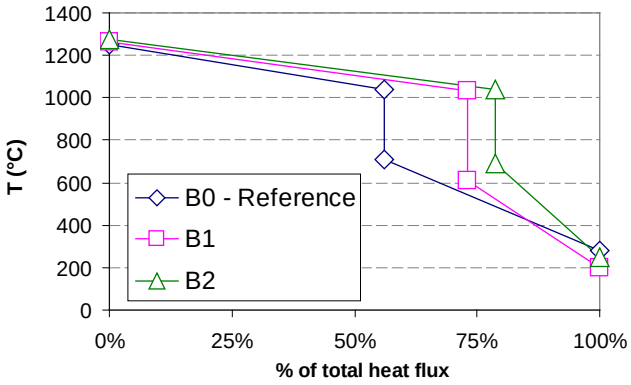

Figure 5.16b: q-T diagram (q in % of total heat flux), cases B

The results obtained are further interpreted in the case of large-scale power plants. Dry coal combustion or co-combustion namely leads to higher adiabatic and furnace exit temperatures. Radiative heat transfer is expected to play an increasingly important role when co-firing dry coal in large-scale plants, although this is not observed in the heat flux to the cooling tubes in the particular experimental facility due to high radiation losses. On the other hand, the reduction of the total flue gas amount due to the reduced amount of evaporated moisture, leads to a decrease of the heat transfer in the convective heat exchanger surfaces and has to be accounted in detail. The effect of these parameters on the heat transfer is clearly visible in the particular facility. However, it can be expected that the influence of dry coal firing in industrial boilers will be less pronounced since a moderate reduction of the flue gas mass flow is expected in the case of large-scale boilers co-firing dry lignite. The expected changes in large-scale conditions due to dry coal co-firing have to be further investigated by other computational tools also including CFD. This actually constitutes the subject of the next chapter.

5.2.4. Conclusions – Further work

The main results of the combustion campaign performed at the 1 MW_{th} semi-industrial-scale pulverized coal combustion facility are presented in this chapter. The scope of the tests is the investigation of the combustion behaviour of Greek lignite under "dry coal combustion" and "co-combustion" conditions. Both operation modes are simulated in the experimental facility by controlling the amount of the recirculated flue gas, while firing dried lignite with 12% remaining moisture. The examined parameters are temperature, emissions, burnout, ash quality, slagging and fouling tendency and heat transfer. A temperature increase of up to 200K in the near burner zone, and up to 80K in the furnace exit region is noticed while simulating dry coal firing. The deposition investigations indicate low slagging effects in the temperature range of 950˚C - 1150˚C and a specific slagging potential in the near burner region at increased temperatures above 1150˚C, which has to be further examined. The overall results of the tests imply that co-firing dry lignite in existing Greek power plants is feasible without exposing the operational behaviour of the boiler to great risk. Even in the case of future Greek power plants firing 100% dried lignite, no severe slagging and fouling effects are expected, at least in the furnace outlet region and the first heat exchanger surfaces, according to the evaluation of the current investigations. Further work should focus on the expected emission behaviour when co-firing dry lignite, which is not addressed in detail in the present analysis. Additional tests on the potential reduction of NO_x emissions by air staging could also be performed.

5.3 Numerical investigations at the 1 MW_{th} combustion facility

5.3.1 Introduction

The small-scale experimental investigations on dry coal co-firing are followed by the numerical investigations in the same facility. Numerical modeling is a useful tool in order to evaluate the influence of dry coal firing on combustion related parameters including among others, temperature fields, emissions, fuel burn out and wall heat fluxes. A specific model set up is proposed for the simulation of the dry coal combustion tests performed at the $1MW_{th}$ facility. It includes physical properties and combustion kinetics for the dried lignite and appropriate boundary conditions for the experimental facility. In order to evaluate the effect of the set values on simulation results, specific parametric investigations are carried out. The validation of the developed model set up is then based on the available experimental data. The CFD simulations of dry coal combustion at the $1MW_{th}$ facility are used as a necessary intermediate step in order to gain experience on the expected changes of the combustion behaviour when switching from raw coal to dry coal firing. Further simulation activities focus on the numerical simulation of a large-scale boiler at row coal and dry coal co-firing conditions. By means of this work the changes in the combustion behaviour of an existing boiler planned to be retrofitted in order to co-fire dry coal, can be predicted.

5.3.2 Methodology

5.3.2.1 Overview of the applied combustion submodels

The commercial code Fluent is used for the numerical simulations. A detailed overview of the standard models applied is presented in Appendix A. The RNG k-ε turbulence model is used to account for the swirl dominated flow in the experimental combustor [V-29]. For the calculation of the radiative heat fluxes the discrete ordinates model is applied [V-30]. Particle trajectories are calculated by integrating the particle force balance in a Lagrangian reference frame. The effect of radiation heat transfer on the particles is calculated after taking into account the Particle Radiation Interaction. One discrete phase calculation and update of the discrete phase source terms is performed every 50 continuous phase calculations, while about 12.000 particles are injected and tracked.

In Table 5.12 the kinetic parameters used for describing particle devolatilisation and char combustion are presented. The same kinetics are also applied in the lab-scale facility simulated in chapter 3. A single rate Arrhenius expression is used for coal devolatilization, and the applied devolatilisation kinetic rates are obtained from the literature. The Eddy-Break Up (EBU) model by Magnussen and Hjertager is applied for volatile combustion and the global two steps reaction mechanism is used. Volatiles are expressed as a hydrocarbon $C_xH_yO_z$, in which the corresponding x, y, z coefficients derive from the ultimate analysis of the fuel. Finally, for the last combustion step - char combustion - the kinetics/ diffusion limited reaction model of Baum and Street is considered.

Table 5.12: Proposed kinetic parameters for coal devolatilisation and char combustion

Kinetic Parameters	Value	Unit
Pre-exponential factor (k)	315,000	1/s
Activation energy (E)	$7.4 \cdot 10^{7}$	J/kmol
mass diffusion limited rate	$1 \cdot 10^{-11}$	kg/(m^2 s Pa)
kinetics limited pre-exponential factor	6.7	1/s
kinetics limited activation energy	$1.138 \cdot 10^{8}$	J/kmol

5.3.2.2 Simulation boundary conditions

For the combustion simulations of the 1 MWth semi-industrial-scale facility one quarter of the facility is simulated due axisymmetric periodic conditions, in order to save computational time. The developed hexahedral structured grid is composed of about 350,000 cells. A detail of the numerical mesh at the burner region is presented in Figure 5.17. The boundary conditions of the simulated cases are taken from the performed experimental campaign. Since the facility is equipped with one fuel inlet and a complete milling and drying system comparable with the large scale one, dried lignite with constant moisture content is fired during all tests. The proximate and ultimate analysis of the fired dried lignite has already been presented in Table 5.4. The Particle Size Distribution for the fired dried lignite is determined by screening. The fitted Rosin Rammler to the PSD data is presented in Figure 5.18. The following particle size data are used as boundary conditions in the numerical simulations. d_{min} = 5μm, d_{max} = 1500μm, d_{mean} = 103μm, spread parameter = 0.819.

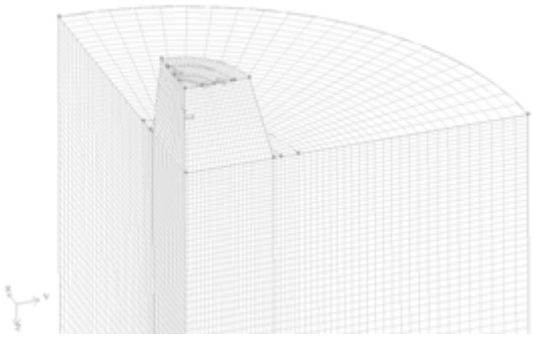

Figure 5.17: Detailed view of the numerical mesh at the near burner region.

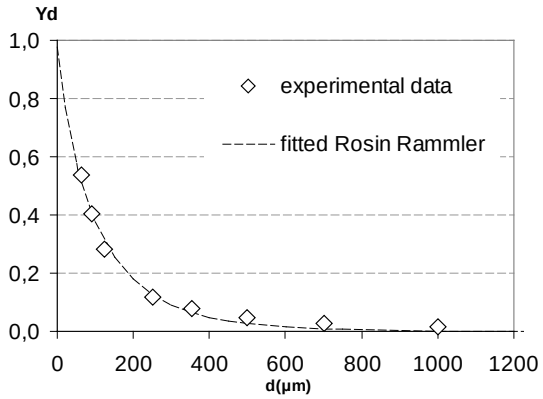

Figure 5.18: Measured PSD and fitted Rosin Rammler distribution of the fired dried Greek lignite

Experimental cases A0, A1 and A2 are chosen for the numerical simulations. These are also the most important cases from the technical point of view due to the observed temperature increase at the near burner region and the furnace exit. The objective of this work is the accurate quantitative prediction of this temperature rise through numerical simulations is the objective of this work. A satisfying result in this topic may facilitate the simulation of a large-scale boiler under dry coal firing conditions.
The furnace operating conditions during the three examined cases are given in Table 5.7. While setting up the simulation cases, some boundary conditions which are necessary for the simulations are not known, because they could not be accurately measured or determined during the experiments. In order to assess the influence of these parameters on the numerical results typical values are tested obtained from the literature when its is possible . The experimental values of the reference case (A0) are used for this scope. The investigation includes the following parameters:

- The temperature distribution and emissivity of the refractory lined furnace walls
- The swirl angle or swirl number of the secondary combustion air
- The devolatilization and char combustion kinetics of the specific lignite.

The most significant parameters among the undefined boundary conditions are the wall boundary conditions. Two different types of wall boundary conditions are adopted and evaluated: wall temperature boundary conditions and heat flux boundary conditions. Regarding the secondary air swirl, different angles are tested ranging from 30° to 50°. Different kinetic parameters for devolatilization and char combustion are also examined based on typical values available in the literature and presented in Chapter 3 (III-20), (III-21). The overall examined parameter set is given in Table 5.13.

Table 5.13: Investigated combustion related parameters

	Regarded parameters	Simulated values	Units
Wall boundary conditions	Constant wall temperature	800 - 900 - 1000 - 1100	°C
	Constant wall heat flux	0 - 10 - 20 - 14/10	kW/m2
Velocity inlet boundary conditions	Secondary air swirl	30 - 40 - 45 - 50	°
Devolatilisation and Char combustion kinetics	Devolatilisation pre exp. factor	$1.5 \cdot 10^5 – 3.15 \cdot 10^5$ (default) $– 6.0 \cdot 10^5$	1/s
	Devolatilisation activation energy	$7.4 \cdot 10^6 – 2.4 \cdot 10^7 – 7.4 \cdot 10^7$ (default)	J/kmol
	Char combustion pre exp. factor	0.67 – 6.7 (default) - 67	1/s
	Char combustion activation energy	$1.138 \cdot 10^8$ (default) $– 1.138 \cdot 10^7 – 1.138 \cdot 10^6$	J/kmol

After the parameter variation and the determination of the optimum parameter set, the dry coal co-firing cases A0, A1, A2 are simulated. Two different types of wall boundary conditions are applied: constant wall temperature boundary conditions and constant heat flux boundary conditions. The simulated results are compared with the respective experimental data.

5.3.3 Results

5.3.3.1 Parametric evaluation

The results of parametric variation are presented in Figures 5.18 – 5.24 together with the respective experimental values of the reference case. A detailed overview on the results obtained by the numerical investigations can be found in the literature [V-31]. The following conclusions can be drawn by the parametric investigation.

Figure 5.19 (wall BCs: temperature)

The value of the wall temperature boundary condition affects the overall temperature profile and flame ignition. Higher values lead to increased average temperatures and faster ignition. The value of 1000°C gives the best agreement with the available experimental data.

Figure 5.20 (wall BCs: heat flux)

The wall heat flux value affects the overall temperature profiles and flame ignition in a way similar to temperature boundary conditions. The best results are obtained by defining a couple of heat flux boundary conditions. The value of 14 kW/m^2 is set for the upper part of the facility wall including the near burner region and the value of 10 kW/m^2 is set for the remaining part of the furnace wall. These heat flux values are close to the calculated heat fluxes from the energy balance of the facility. Regarding the calculated high pick in the case of adiabatic walls it should be justified by the exponential type of the devolatilisation model and the assumptions of the used Eddy Dissipation Model.

Figure 5.21 (secondary air swirl)

Faster flame ignition is achieved when increasing swirl, which is also expected. The best fitted results are achieved with a swirl angle of 40°.

Figure 5.22 (devolatilisation pre exponential factor)

The increase of the devolatilisation pre-exponential factor leads to higher devolatilisation rates and thus to faster ignition. The overall flame shape is, however, retained in all simulations.

Figure 5.23 (devolatilisation activation energy)
The decrease of activation energy leads to higher devolatilisation rates and thus, to faster ignition, while by increasing the activation energy value no stable flame is achieved. A drastic change of the flame shape is observed in these simulations, which indicates the high sensitivity of the results obtained by the set value of the devolatilisation activation energy.

Figure 5.24 (char combustion pre exponential factor)
The simulated changes of the char combustion pre-exponential factor lead to small differentiations in temperature and O_2 profiles.

Figure 5.25 (char combustion activation energy)
By increasing the value of the char combustion activation energy no converged solution can be obtained. The decrease of the char combustion activation energy from $1.138 \cdot 10^8$ J/kmol to $1.138 \cdot 10^7$ J/kmol leads to higher char combustion rates, which is expected, while further decrease to $1.138 \cdot 10^6$ J/kmol leads to results similar to the default value. High sensitivity of the results obtained by the set value of char combustion activation energy is, in other words, noticed.

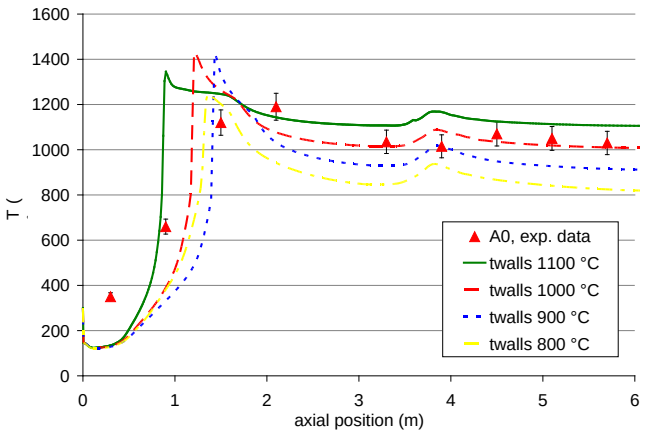

Figure 5.19a: Temperature profiles, (parameter: wall temperature)

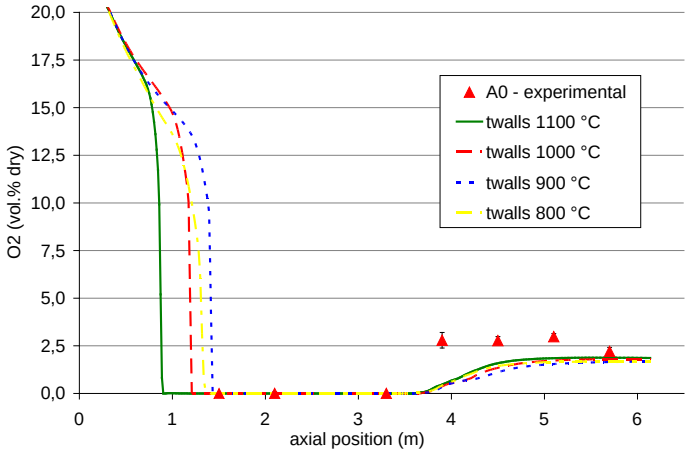

Figure 5.19b: O_2 profiles, (parameter: wall temperature)

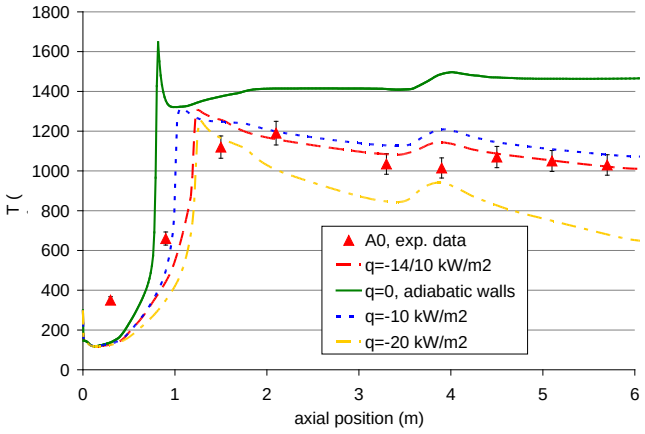

Figure 5.20a: Temperature profiles, (parameter: wall

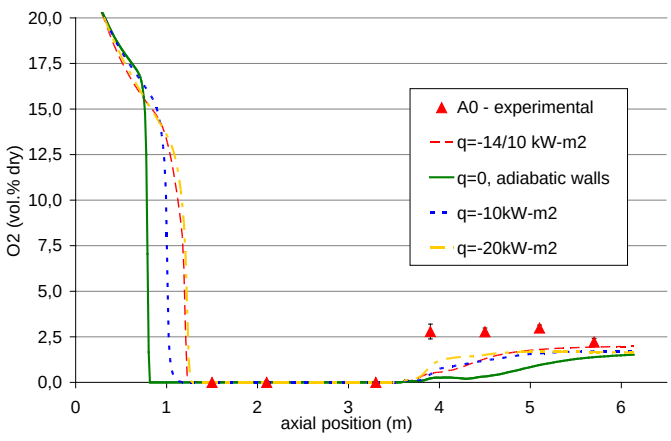

Figure 5.20b: O_2 profiles, (parameter: wall heat flux)

heat flux)

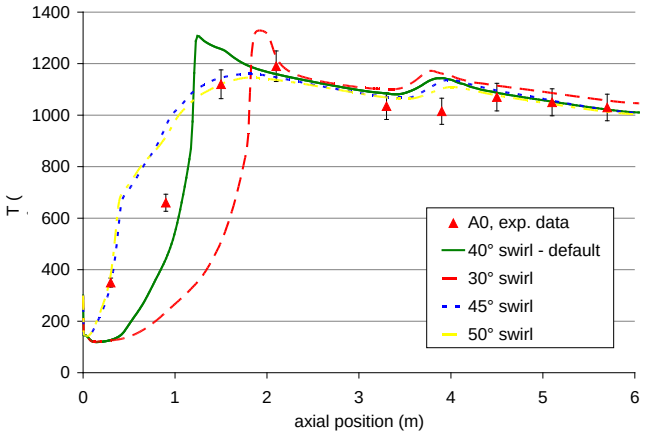

Figure 5.21a: Temperature profiles, (parameter: swirl)

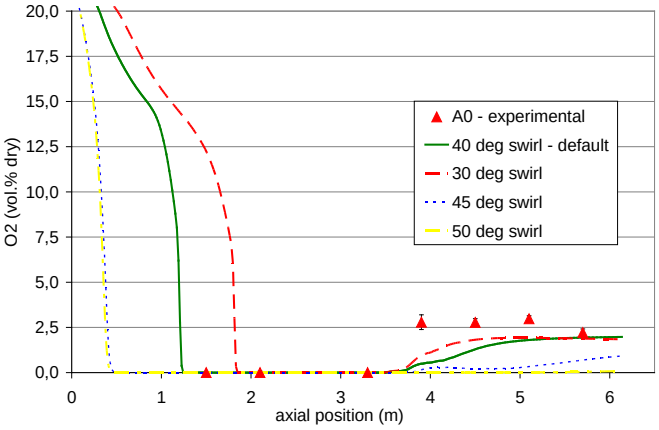

Figure 5.21b: O_2 profiles, (parameter: swirl)

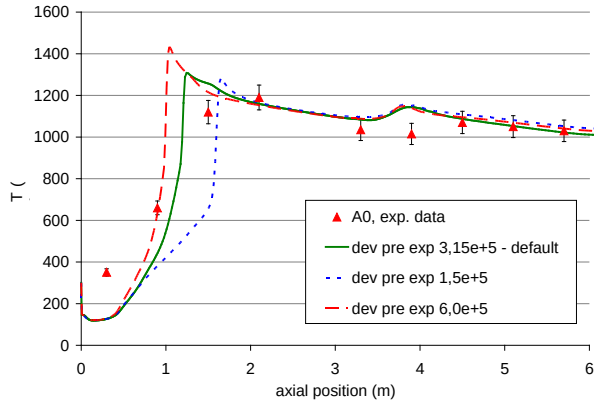

Figure 5.22a: Temperature profiles, (parameter: devolatilisation pre-exponential factor)

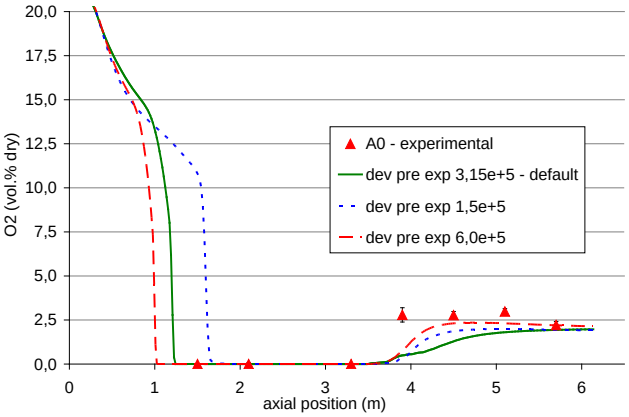

Figure 5.22b: O_2 profiles, (parameter: devolatilisation pre-exponential factor)

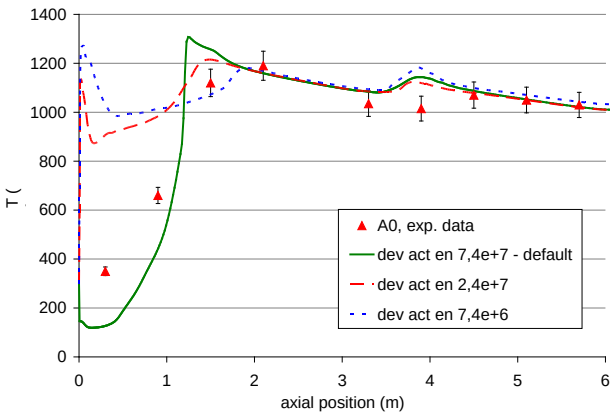

Figure 5.23a: Temperature profiles, (parameter: devolatilisation activation energy)

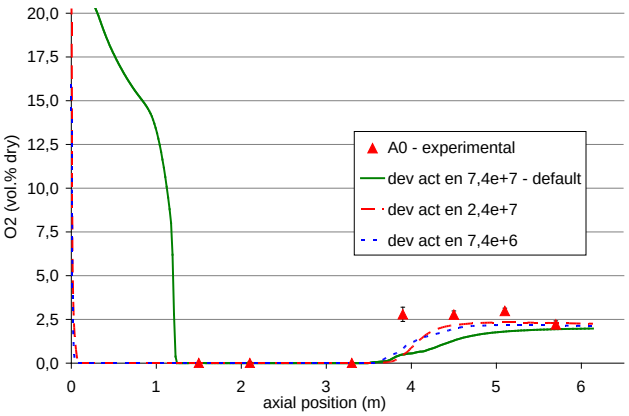

Figure 5.23b: O_2 profiles, (parameter: devolatilisation activation energy)

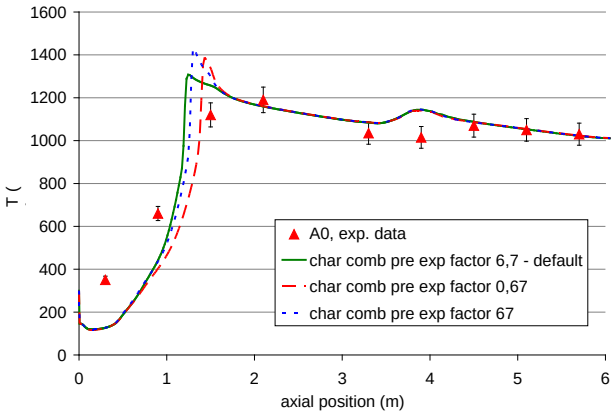

Figure 5.24a: Temperature profiles, (parameter: char combustion pre-exponential factor)

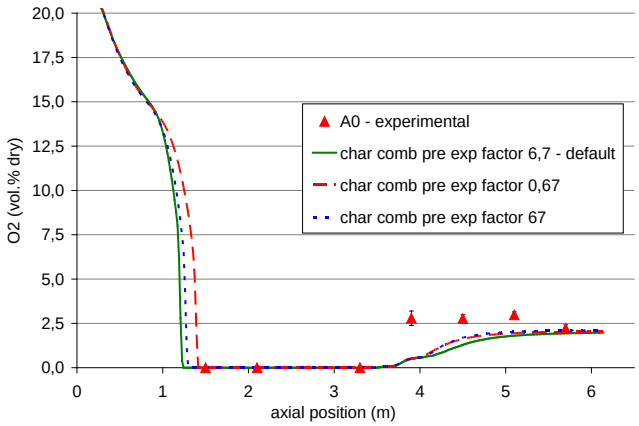

Figure 5.24b: O_2 profiles, (parameter: char combustion pre-exponential factor)

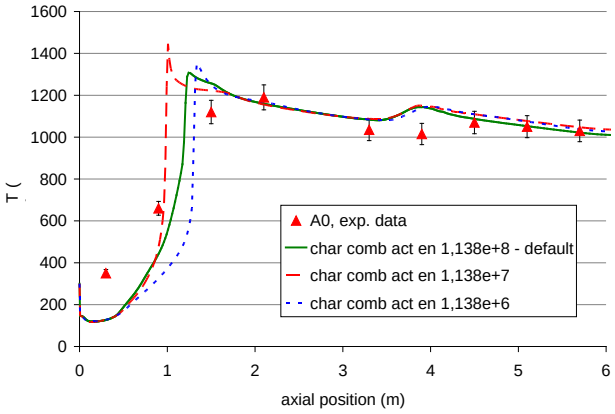

Figure 5.25a: Temperature profiles, (parameter: char combustion activation energy)

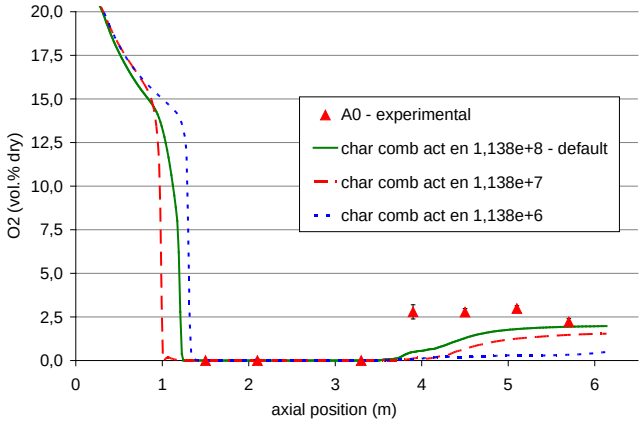

Figure 5.25b: O_2 profiles, (parameter: char combustion activation energy)

5.3.3.2 Co-firing simulations

In the initial numerical investigations [V-21] constant temperature boundary conditions are applied and cases A0, A1, A2 are simulated. The comparison between the simulated axial temperature profiles and the available experimental data for the three cases is presented in Figure 5.26. The temperature rise at the near burner region and the displacement of the temperature peak upstream when firing dry coal is successfully predicted. However, the expected elevated temperatures along the whole furnace length cannot be reproduced by the particular boundary condition type resulting in almost constant furnace exit temperatures in all three cases, which is not representative of the experimental trends. By using wall boundary conditions of constant heat flux, improved agreement with the experimental data is achieved. Specifically, the following trends observed during the experiments are successfully reproduced (Figure 5.27): (a) the increase of the furnace temperature throughout the furnace axis and also the increase of the furnace outlet temperature when increasing the dry coal share, and (b) shifting of the maximum temperature located in the near burner region upstream, indicating faster ignition. The simulated temperature contours of the experimental facility are also given in Appendix B.

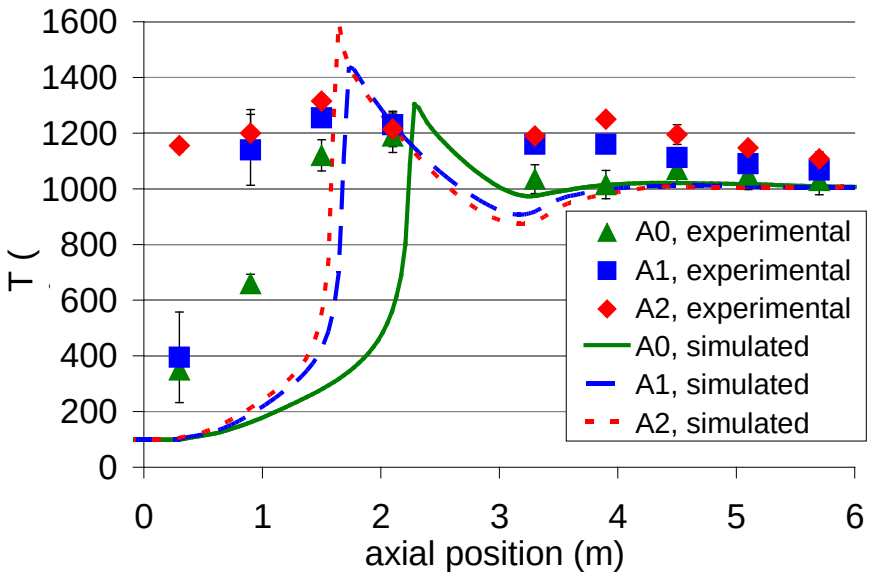

Figure 5.26: Validation based on temperature profiles, (wall boundary conditions: temperature)

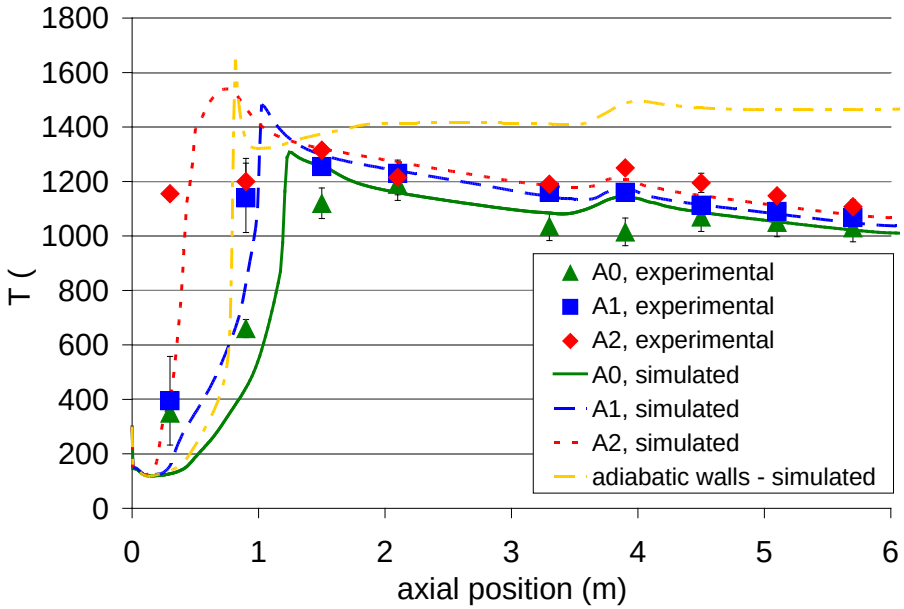

Figure 5.27: Validation based on temperature profiles, (wall boundary conditions: heat flux)

5.3.4 Conclusions - Further work

The substitution of raw lignite by dry lignite is investigated through numerical simulations in the particular section. The effect of dry coal co-firing on the combustion behaviour in terms of temperature fields, ignition - burnout and wall heat flux is simulated in the specific section. The heat flux boundary conditions successfully predict the temperature increase at the furnace exit, when increasing the dry coal co-firing share. A satisfying agreement is in overall achieved between the experimental and the simulation results in the case of the 1 MW_{th}

experimental facility. Further research work shall focus on NO_x formation modeling when firing dry coal. Initial investigations on NO_x formation in dry coal firing conditions have been performed in the past and can be found in the literature [V-21]. The elevated temperatures caused by the reduced flue gas mass flows when firing dried lignite are expected to facilitate the formation of thermal NO_x. Possible methods to mitigate the increase of NO_x emissions are fuel and air staging, and these have to be examined in detail in the future. Summing up, it should be noted that the small-scale investigations may provide a reliable qualitative picture on the expected changes in the operational behaviour of a boiler where dry coal co-firing is applied. These changes include among others the predicted temperature increase at the furnace exit, the improvement of fuel burn out and the potential increase of NO_x emissions. However, realistic values of these parameters and their respective changes cannot be obtained by the small-scale investigations. For this reason the research work is also extended to the large scale, and experimental and simulation work is carried out.

6 Dry lignite co-firing: Investigations in the large scale

Summary
The present chapter focuses on the investigations of dry lignite combustion in the large scale. The examinations performed in the small-scale facility determined a number of combustion related parameters which should be taken into account during any dry coal co-firing application. These parameters include among others the furnace outlet temperature, the fuel burnout, the wall heat flux and the flue gas emissions. On the other hand, the scope of the present work is the demonstration of the pre-drying and dry coal co-firing concept in the large scale and not only the evaluation of the proposed concepts in small, semi-industrial-scale facilities. Thus, in order to have reliable results in this field further research in the large scale is required since small-scale investigations may provide realistic trends; nevertheless, they cannot be directly extrapolated in the industrial scale. The work performed in the industrial scale includes (a) an experimental dry coal firing campaign at a $75MW_{th}$ Greek power plant, (b) the numerical simulation of the specific power plant under dry coal firing conditions, and (c) the thermodynamic study of a typical $350MW_e$ Greek power plant where a lignite pre-drying system is integrated in the existing steam cycle.

6.1 Large-scale experimental campaign on dry lignite co-firing

6.1.1 Introduction

The experimental part of the large-scale examinations focuses on the dry coal co-firing tests at the $75MW_{th}$ "Liptol" power plant operated by PPC. A number of measurements took place during the campaign including monitoring of operational data, fuel and ash analysis. Emission measurements at the stack and temperature profile measurements at the superheater region were also carried out. The overall evaluation of the results shows no clear influence of dry coal co-firing on the operation of the particular boiler. The changes of the operation mode are assumed to be more closely related to the old firing system and the changes in the lignite quality than to the effect of dry coal co-firing. According to the overall evaluation of the tests performed, dry coal co-firing is feasible in the particular boiler. The limiting factor for the co-firing share in the plant is the existing feeding system of dry coal and the aged firing system.

6.1.2 Experimental methods

6.1.2.1 Description of the plant

The large-scale dry coal co-combustion tests were performed at PPC's "Liptol" power station (Figure 6.1). The Liptol power station is a lignite-fired power plant operating since 1959. It consists of two boilers working in parallel and producing 80 t/h of steam each and feeding two steam turbines. The nominal electrical power of the first turbine is 10 MWel with a back pressure of 4.5 bar. A lignite drying and briquetting plant together with the district heating system of the city of Ptolemais are fed from the produced steam of the first turbine. The second turbine unit is a 33 MW_e condensing unit. The steam temperature is 485˚C and the steam pressure 64 bar. The feed water temperature is 154˚C. No reheat steam cycle is applied. Each boiler has two hammer mills firing at full load 48 t/h of raw lignite with a heating value of 5,6 MJ/kg and moisture of 58% from the front wall side.

Both boilers are capable of co-firing dry lignite dust up to a mass flow of 2 t/h per boiler. Dedicated dry lignite burners are used for this scope, which are located at the left and the right boiler walls at two different levels (Figure 6.2a). The dry lignite dust with a heating value of about 14.5 MJ/kg and moisture of about 12%, is collected in the ESPs of the nearby lignite drying and briquetting plant and can be fed in the boilers through separated, opposed fired dry lignite burners located at two different levels.. This results in a maximum thermal share of dry lignite of about 10%. The detailed boiler operational data can be found in Table 6.1.

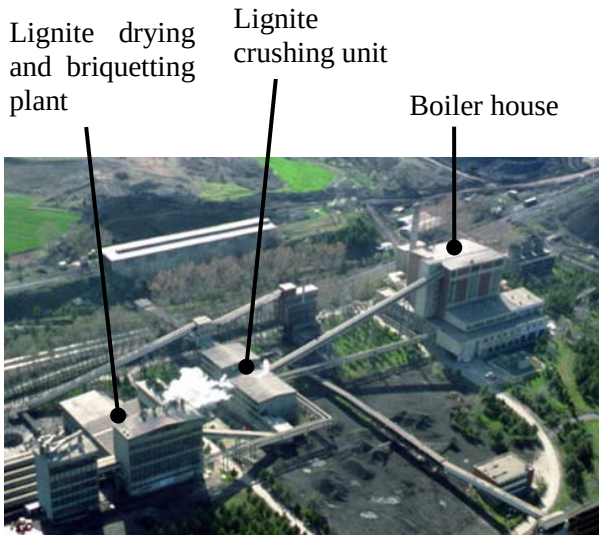

Figure 6.1: Overview of the "Liptol" power plant site

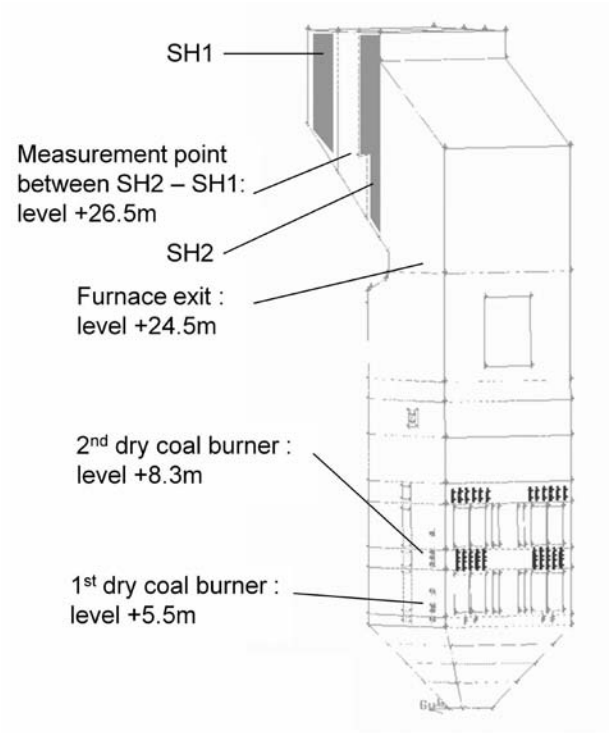

Figure 6.2a: Drawing of the "Liptol" boiler

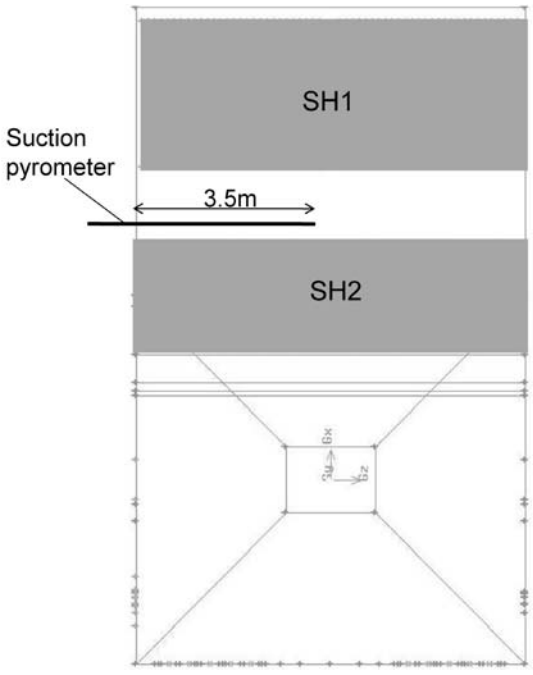

Figure 6.2b: Boiler cross-section at level 26.5m

Table 6.1: Main operational parameters of the Liptol boiler

Parameter	unit	value
Raw coal mass flow	t/h	48
Raw coal heating value	MJ/kg	5.6
Thermal input ($Q_{th\text{-}input}$)	MW	75
Steam mass flow	t/h	80
Superheated steam pressure	bar	64
Superheated steam temperature	˚C	495
Enthalpy superheated steam	kJ/kg	3,406
Temperature feeding water	˚C	154
Enthalpy feeding water	kJ/kg	645
Useful heat (Q_{useful})	MW	61
Boiler thermal efficiency	%	82
Maximum dry coal mass flow	t/h	2
Dry coal heating value	MJ/kg	14.5
Thermal share of substitution corresponding to maximum dry coal mass flow	%	10

6.1.2.2 Scope of the tests –Performed measurements

The dry coal co-firing tests were performed in boiler nr. 2 of the Liptol power station. The scope of the measurement campaign was the investigation of the effects of dry coal co-firing on the following aspects:

- The operational behaviour of the boiler including (a) the steam production, (b) the steam parameters (pressure, temperature), (c) the operation of the feeding system for raw and dry lignite
- the temperature profiles at the superheater (SH) section of the boiler
- the flue gas emissions in the stack
- the residue quality

For the characterisation of the operational behaviour of the boiler the following records are taken by the boiler data aquisitioning system: steam temperature at superheaters 1 and 2, flue gas temperature between superheater 1 and 2 and after the whole superheater section (before economiser). Flue gas temperatures are taken from ceramic shielded thermoelements which are placed in the furnace about 0,5m from the furnace wall. During the main experiments the produced electric power and steam production is also recorded by the boiler main control panel. Regarding the operation of the feeding systems of raw and dry lignite, both systems are monitored during the tests. No closer mechanical inspection is performed after the tests, since both systems stayed in the normal operation behaviour.

The profile measurements are performed at the 26.5m level between superheater 2 and superheater 1 (Figure 6.2a,b). The furnace exit level is considered to be the most important measurement level; however, no suitable measurement location is found at that level, and for this reason the next level is chosen. Pictures of the measuring level and the equipment used are presented in Figures 6.3, 6.4. A 6m-long water-cooled suction pyrometer equipped with a Ni-CrNi thermoelement, which is shielded from radiative heat transfer by a proper ceramic part, is used. An ejector is also used in order to generate sub pressure and extract flue gas out of the furnace by suction. The white vectors indicate its position at the specific measurement location. The pyromener is inserted at a 0.5m step inside the furnace up to 3.5m depth. The measuring time for each point is 4-5 minutes.

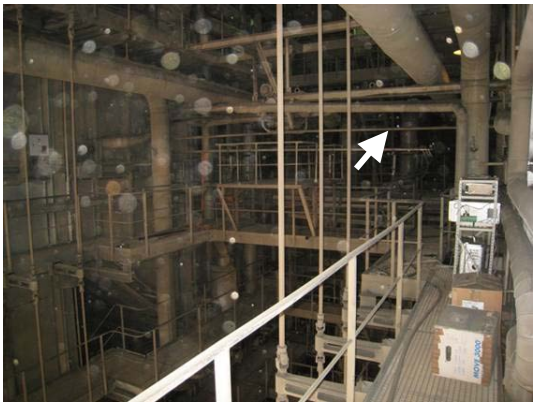

Fig. 6.3: Measurement location after SH2, level 26.5m

Fig. 6.4: View of the water-cooled pyrometer, level 26.5m

The flue gas measurements at the stack are performed with a portable flue gas analyser ("Madur GA40 plus"). Oxygen concentration in the flue gas and CO, NO_x emissions are continuously monitored for more than 10 min in the test cases. CO, NO_x are post-processed to a reference oxygen concentration of 6% vol.

6.1.3 Results

6.1.3.1 Characterisation of the operational behaviour

Baseline tests
The boiler operation in baseline conditions is initially evaluated. Due to the deterioration of the lignite quality of the "Mavropigi" mine in the recent period, dry lignite is used as a supporting fuel during the standard operation of the power plant. The support of the base fuel is considered as necessary, in order to avoid flame instabilities and unexpected boiler outages. When no dry lignite is co-fired, the flame is supported by the start-up oil burners, which results in increased operation costs for the plant.
Thus, in the presented reference case a low dry coal co-firing share, about 1% is continuosly applied with the exception of the marked interval, when the flame is supported by the start up oil burners The operational data recordings and temperature profile measurements at the superheater region are presented in Figures 6.5, 6.6. The steam and flue gas temperatures have a high variation range of more than 30K at some periods of the day. This high range is not typical for other larger boilers, such as PPC's standard 300 MW_e units, and is justified by the small boiler size and the boiler's aged firing and control system.

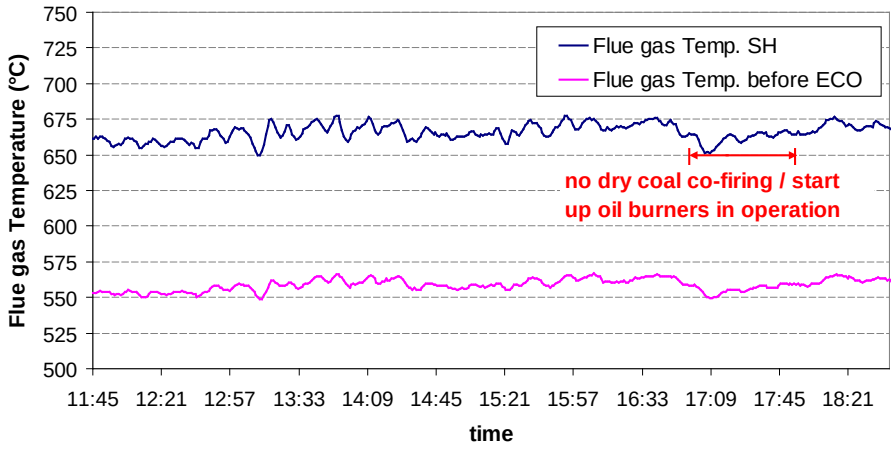

Figure 6.5: Records of flue gas temperatures (1st baseline test)

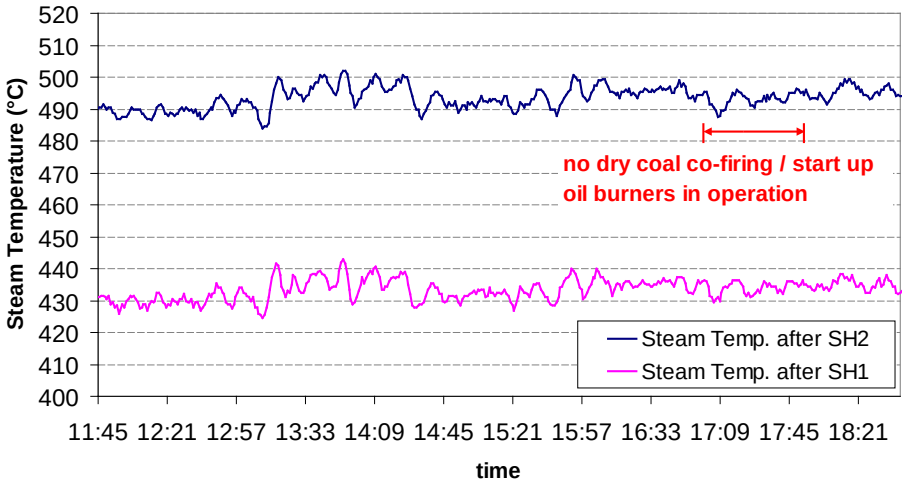

Figure 6.6: Records of steam temperatures (1st baseline test)

Main co-firing tests

The difficulties mentioned at the standard operation range led to necessary modifications of the measurement program during the main tests. Keeping the boiler at a totally stable operation for the entire test duration proved to be almost impossible. Particularly the raw lignite firing point was measured only for a limited period of time, during which the occurring flame instabilities led to the discontinuance of the measurements at the specific point. Taking into account that the boiler standard operating condition is the dry coal co-firing mode, due to deteriorated fuel quality and load requirements, the test points as decided are:

- Dry coal thermal share 6%
- Dry coal thermal share 3%
- Raw coal firing

Steam characteristics and power production data from the two turbines are given in Table 6.2. Although no high variations are observed in the data presented, this information shall not be further evaluated since the given data is manually taken from the operating personnel during the tests and does not represent any mean values of successive measurements. The flue gas and steam temperatures monitored are given in Figures 6.7 and 6.8. The variation range of the steam temperatures presented is relatively high, more than 30K at some periods of the day. This high range is not typical, as mentioned earlier, of other large-scale boilers and is justified

by the small boiler size and the old control system available. By comparing the time spaces indicating when the measurements took place and the daily variation of the particular data a definite conclusion is drawn. Dry coal co-firing seems to have no direct impact on plant operation as the variation of the temperatures examined stays within a certain range during the entire day and is not affected by the co-firing tests. The outdated steam temperature control system of the boiler has a more direct effect on steam temperatures, and the same applies to flue gas temperatures which are influenced to a greater extent by the change in the fuel quality and the outdated firing system. As a general result, it can be stated that dry coal co-firing does not have any particular effect on the operational behaviour of the specific boiler. The reason for this is the fairly old control systems of the boiler which allow operation with higher variations of the main values than current state-of-the-art systems.

Table 6.2: Average steam and power production during tests

	raw lignite firing	3% co-firing	6% co-firing
steam production (t/h)	79	76	78
steam pressure (bar)	60	61	62
MWe (back pressure turbine)	4.3	4.2	4.3
MWe (main turbine)	8.1	8.2	8,1
MWth (back pressure turbine)	21.8	21.7	21.8

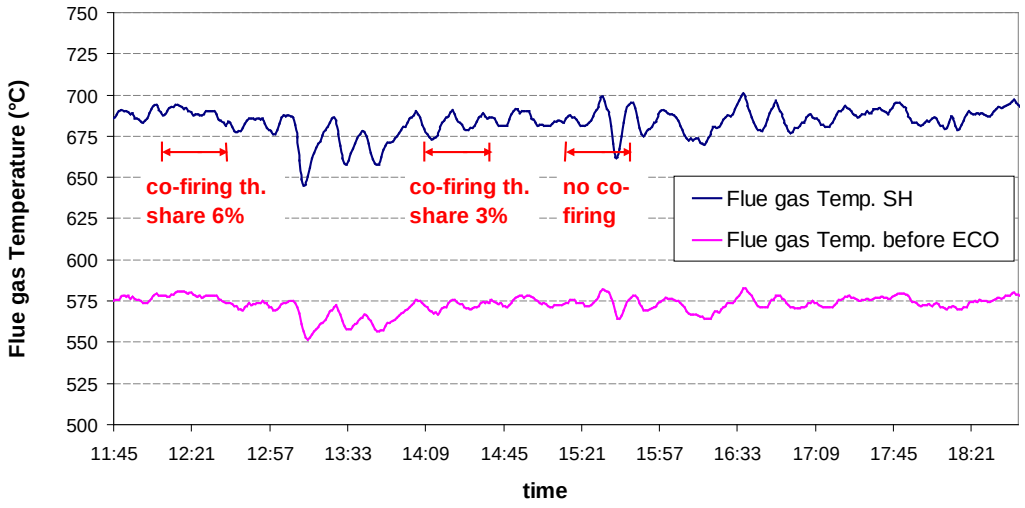

Figure 6.7: Records of flue gas temperatures (main co-firing tests)

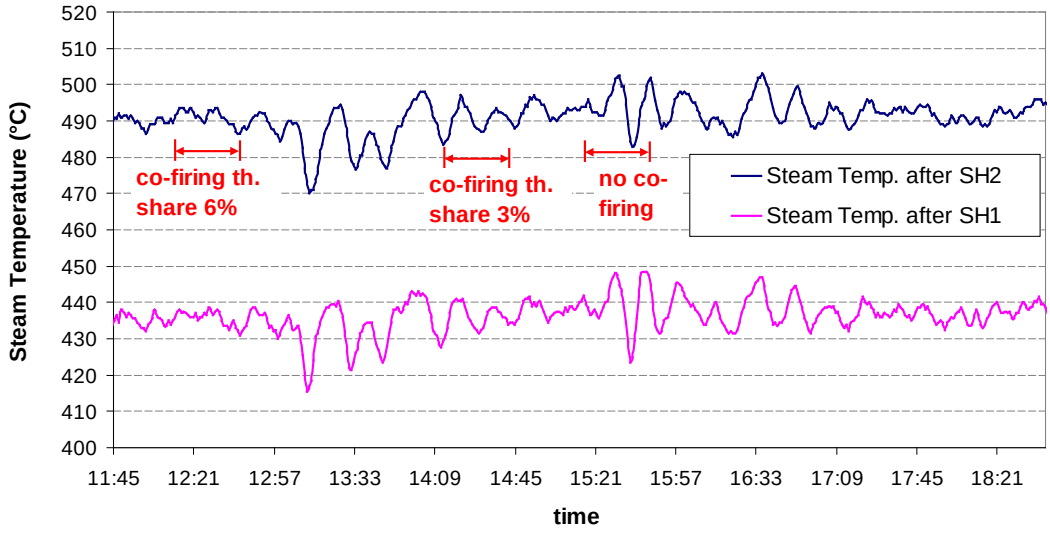

Figure 6.8: Records of steam temperatures (main co-firing tests)

6.1.3.2 Profile measurements in the superheater section

The temperature profiles obtained during the co-firing tests are presented in Figure 6.9. Although a slight increase of the flue gas temperature could be expected in the dry coal co-firing cases, this estimation is not confirmed by the measurement results. No clear tendency is noticed by the measured temperature profiles, while the standard deviation in the measured temperature values is generally high. The design of the particular firing system and the unstable character of the generated flow and temperature field, due to this firing system, may be the reason for this behaviour. It is further argued that the level of the temperature values recorded in the profile measurements, is representative for the given location, and therefore that the particular experimental data should be taken into consideration and not disregarded

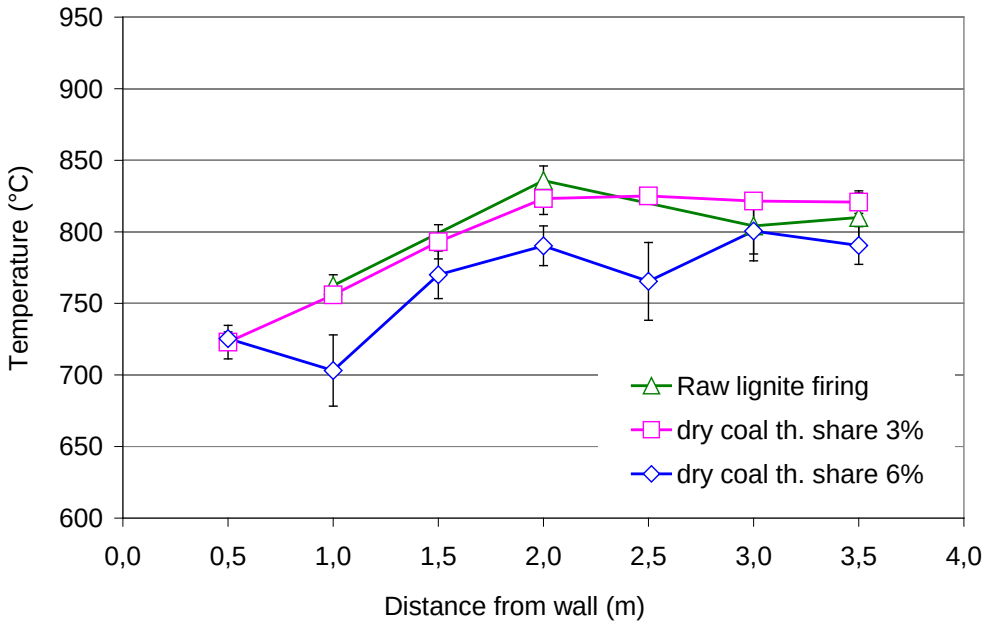

Figure 6.9: Temperature profiles at the main co-firing tests

6.1.3.3 Emission measurements at the stack

The average values of the flue gas emissions during the tests are presented in Table 6.3. The increased percentage of O2 in the flue gas is an indication of the increased amount of false air entering into the boiler and the electrostatic precipitators. NOx values tend to increase by increasing the co-firing share. Although no increase tendency of flue gas temperature at the furnace exit section was observed during the experimental investigation, local temperature picks, due to the increase of dry coal co-firing share could be expected primarily in the regions near the dry lignite burners. These temperature picks may provide an explanation for the increase tendency of NOx levels after taking into account the potential effect of the thermal NOx formation mechanism. Besides, on increase tendency of NOx when increasing the co-firing share is also predicted by the numerical simulations that will be presented below. CO emissions remain at a low level during the entire tests, and do not seem to be influenced by the different co-firing modes. SO2 emissions are measured in all tests and no clear effect of co-firing on SO2 emissions is noticed. No effect of the dry coal on SO2 formation is also expected since it is the sulphur content of the fuel that plays the main role in SO2 formation and not the combustion conditions in the furnace. The lack of a desulphurisation unit in the particular power plant is the reason for the increased SO2 emissions. To sum up, the relative increase of NOx emission values up to 16% compared to the reference case is the main influence of co-firing on the plant's emission behaviour. This trend is characteristic for the particular boiler only and cannot be directly extrapolated to typical Greek boilers of the 300 MWe class.

Table 6.3: Mean values and standard deviation of the measurements performed

		raw lignite firing	3% co-firing	6% co-firing
O_2 (% vol. dry)	mean	6.1	7.1	6.4
	st. dev.	0.6	0.7	0.4
NO_x (mg/Nm3 dry)	mean	290	319	340
	st. dev.	11	18	15
CO (mg/Nm3 dry)	mean	60	67	58
	st. dev.	5	4	3
SO_2 (mg/Nm3 dry)	mean	984	1040	991
	st. dev.	82	134	65

6.1.4 Conclusions – Further work

The influence of dry coal co-firing on several technical aspects related with the boiler operational behaviour is examined in the large-scale measurement campaign performed. Since the plant operates on a permanent co-firing mode, due to the deterioration of the raw lignite quality, no negative impact of co-firing on the plant behaviour is noticed. The changes in the operation conditions during the tests are assumed to be more closely related with the old firing system and the variation of the lignite quality than with the effect of dry coal co-firing. No negative impact of co-firing on residue quality is observed. The emission behaviour is also stable with the exception of NO_x emissions which show an increase tendency. The overall results indicate that dry coal co-firing is feasible in the particular plant, and that the current limitation on the co-firing share is based on the existing feeding system for dry coal. In order to evaluate the possible application of dry coal co-firing in a typical 300 MW_e unit, further investigations are necessary. These include the analysis of the combustion and heat transfer behaviour in the reference and the dry coal co-firing mode.

6.2 Large scale CFD simulations on dry lignite co-firing

6.2.1 Introduction

The investigation of dry lignite co-combustion in the 75 MW_{th} industrial-scale boiler is followed by numerical simulations in the present section. CFD simulations may provide a reliable picture on the changes expected in the boiler operational behaviour when increasing the dry coal co-firing share. The most significant technical parameters evaluated by the simulations are temperature profiles, NO_x emissions, coal burnout and heat flux to the evaporator. For the scope of the simulations the thermal share of substitution has been varied from 5% up to 20% of the boiler thermal input, despite the fact that in the experimental campaign performed a dry coal co-firing thermal share of up to 6% is realised, and that a maximum thermal share of 10% is feasible in the particular boiler due to limitations of the dry coal feeding system. In this way the potential influence of the elevated co-combustion thermal shares on the parameters chosen is evaluated. The simulated increase of the dry lignite co-firing share may not be implemented in the particular boiler because of its age and its planned shut down in the near future. However, the experience obtained from the simulations performed can be used in future numerical investigations of dry coal co-firing in other Greek power plants for which the issue of dry coal co-utilisation is of high importance. The 330MW_e Agios Dimitrios V unit could be one of the boilers to be simulated in the future since the integration of the pre-drying concept in the particular plant through a fluidised bed dryer is examined in the present thesis.

6.2.2 Methodology

6.2.2.1 Modeling of the 75MW_{th} large scale boiler - Numerical mesh and boundary conditions

The age of the boiler should also be noted in the firing system. The boiler is namely front-wall-fired and is equipped with two jet burners, each consisting of a lower and an upper part. The combination of the front wall firing system and of the jet burners does not allow the development of typical flow field conditions for pulverised coal boilers, i.e. a main central vortex in tangential fired boilers, or small recirculation zones in front of swirl burners in case of wall fired boilers equipped with swirl burners. As a result, some recirculation zones are predicted in the furnace section.

The final version of the mesh composed of 357,000 hexahedral cells is presented in Figure 6.10. A detail of the placement of the burners and the secondary air nozzles in the particular firing system is given in Figure 6.11. While setting up the reference case, information regarding inlet boundary conditions was not available. In particular, the distribution of combustion air between the different burner levels and the hopper was not available, due to the difficulty of measuring the specific air mass flows at site. For this reason different cases representing possible distributions of the combustion air were initially set and simulated. The parameter setup, which led to the most reasonable flow field and to no recirculation effects at the furnace outlet was finally chosen and considered as the main reference case.

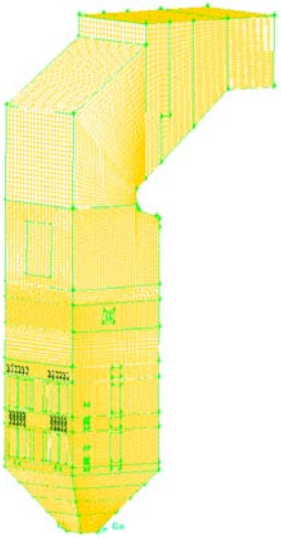

Figure 6.10: Overall view of the boiler numerical mesh

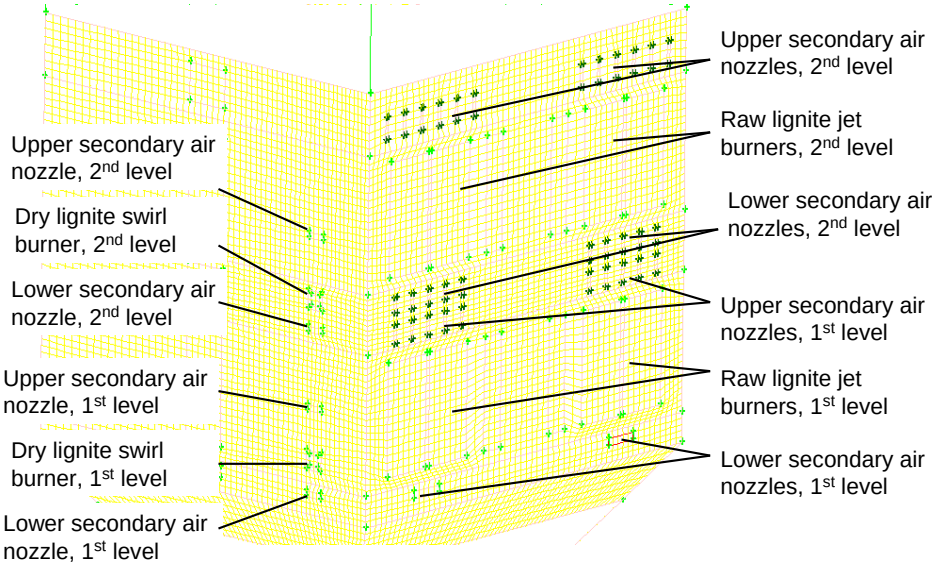

Figure 6.11: Detail of the boiler burners and air nozzles

The proximate and ultimate analysis of the dried lignite, used in the simulations, is given in Table 6.4. A mass balance in the recirculation ducts and the lignite mills is also carried out in order to calculate the composition of the carrier gas.

Table 6.4: Proximate and ultimate analysis of the Greek lignite

Proximate analysis (% a.r.)	Before mill	Ultimate analysis (%daf)	Mean
Water	56.25	C	63.81
Ash	13.35	H	4.87
Volatiles	18.33	N	2.07
Fixed C	12.07	O	27.60
Hu (kJ/kg K)	5,656	S	1.68

The primary and secondary air velocities are given in Table 6.5.

Table 6.5 Velocity values of primary and secondary air

		Combustion air velocities (m/s)			
		Baseline	Dry coal 5%	Dry coal 10%	Dry coal 20%
	Primary air (carrier gas)	6.1	5.7	5.4	4.6
Secondary air	Front Side	42.4	42.4	42.4	35.5
	Left-Right Side	24.9	24.9	24.9	20.9
	Rear Side	13.5	13.5	13.4	11.3
	Hopper	2.2	2.2	2.2	1.9

6.2.2.2 Overview of the applied combustion submodels

The commercial code Fluent is used for the numerical simulations. The k-ε turbulence model is used. P1 radiation model is used for the calculation of the radiative heat flux. Particle trajectories are calculated by the integration of the particle force balance in a Lagrangian reference frame. One discrete phase calculation and update of the discrete phase source terms is performed every 50 continuous phase calculations, while about 50,000 particles are injected and tracked in the boiler. The single rate kinetic model is used to account for coal devolatilisation and the kinetics / diffusion limited rate model is used to account for char combustion. The same kinetic constants used as default values for the combustion simulations of the Greek dried lignite in the 1 MW_{th} combustion facility are also used in the large-scale simulations.

The increase of NO_x emissions, through the formation of thermal NO_x, which was observed in the large-scale measurement campaign is an important technical aspect to be addressed in future large-scale boilers that will co-fire pre-dried lignite. The accurate prediction of NO_x emissions and the investigation of possible reduction measures is one of the key research objectives for the future dry lignite-fired boilers. Numerical simulations may play a key role in these investigations since experience of more than a decade in this field [VI-1], [VI-2], [VI-3] has proven that CFD is a reliable design tool for retrofitting existing power plants towards the optimization of combustion related aspects such as temperatures, fuel burn out and NO_x emissions. In the NO_x post-processing calculations performed the "thermal NO_x" and "fuel NO_x" formation mechanisms are used. More information on modeling NO_x formation can be found in Appendix A6.

6.2.3 Results

6.2.3.1 Temperature and O_2 profiles

The mean temperatures along the furnace height for the reference and the dry coal cases are presented in Figure 6.12. By rising dry coal co-firing share the average temperature at the near burner region at the level between 5 and 10m increases. In particular, according to the simulation results, a potential increase of the dry coal co-firing share up to the high percentage of 20%, which however can not be reached in the current operation mode of the particular boiler, would lead to a rise of the average temperature at the level of the lower raw and dry lignite burners (+4 to +5m) up to 80 K compared to the reference case. At the level of the upper raw and dry lignite burners (+7 to +8m) the predicted temperature rise for 20% co-firing is about 30 to 40 K, while at the furnace exit level is 20 to 30 K. These values should be considered as indicative for the expected influence of dry coal on the temperature fields in the furnace, when increasing the thermal share up to a very high percentage. Even in the 20% co-firing share, that is not realistic for the current boiler operation, no drastic increase is expected in the furnace exit temperature that could lead to overheating problems of the superheaters or even to melted deposits and fouling phenomena. This is an indication that moderate changes in the temperature fields are expected, when increasing the dry coal thermal share. This moderate behaviour was also noticed in the experimental investigations, where lower thermal shares were applied, and implies that dry coal co-firing in the investigated thermal shares in not expected to add any additional risks in the boiler's operational behaviour as regards the expected temperature levels.

In the same figure the calculated maximum temperatures along the furnace height are also presented. A similar behaviour as with the average temperature is also observed in the case of the maximum temperatures calculated. By raising the dry coal co-firing share the maximum

temperatures increase in the main burner region and slightly decrease in the region above the burner belt. In particular, an increase of the maximum temperature values of up to 100 K is calculated for the case of 20% dry lignite co-firing compared to the reference case. These elevated temperature peaks are expected to influence thermal NO_x formation. Detailed temperature contours for the baseline and the dry coal combustion cases are given in Appendix B5.

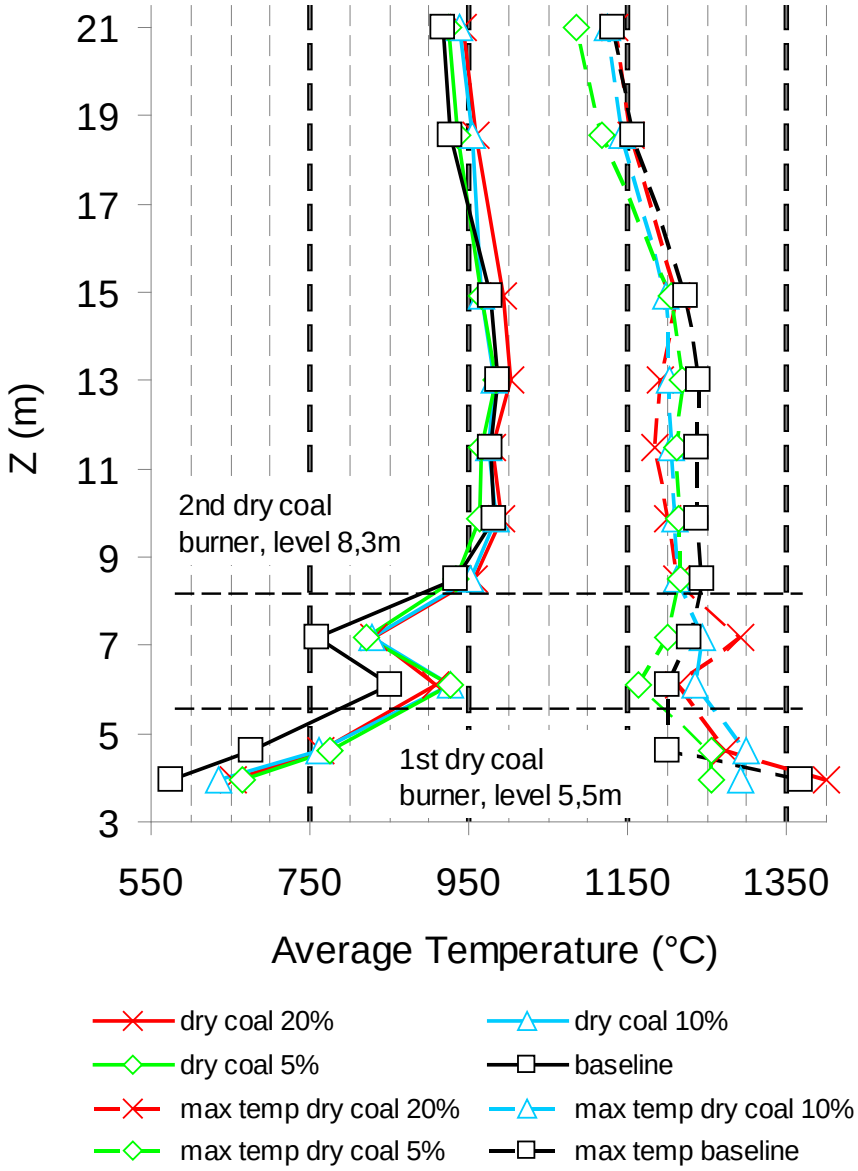

Figure 6.12. Average temperature along furnace height

The average oxygen concentration along the furnace height for the baseline and the dry lignite co-firing cases is presented in Figure 6.13. Dry lignite co-firing leads to a decrease of the mean O_2 concentration at the main burner region. This is explained by faster fuel ignition and faster oxygen consumption due to the dry coal. As an overall result, fuel burnout is improved by dry coal co-firing and for this reason the average oxygen concentration at the furnace exit slightly decreases. The decrease of oxygen concentration in the main burner region is also observed in the detailed O_2 contours which are presented in Appendix B5.

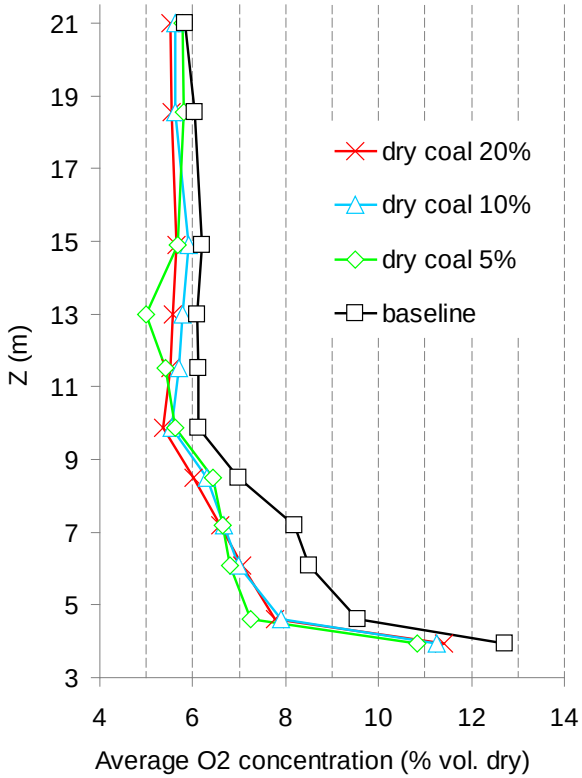

Figure 6.13 Average O_2 concentration along furnace height

6.2.3.2 Fuel burnout

The percentage of unburned carbon calculated in each simulated case is given in Figure 6.14. The burnout is clearly improved by applying dry lignite co-firing. In the maximum dry coal firing case of 20% the unburned carbon calculated is reduced to more than one fourth of the reference value. The improvement of the fuel burnout is also one of the main arguments in favour of the utilisation of dry lignite as a supporting fuel in existing Greek lignite boilers. Boiler efficiency is expected to increase in the dry coal co-firing cases, due to the reduced burnout losses. Furthermore, in cases of firing extremely low lignite qualities, co-firing of pre-dried lignite as a supporting fuel would assist in keeping the nominal load and avoiding potential flame instability issues. The increase of the fuel burnout predicted could not be measured in the experimental campaign since the duration of the tested co-firing cases was too short, and no representative bottom ash and fly ash samples could be collected for each co-firing mode tested. Nevertheless, although the calculated absolute values of coal burnout could not be verified by respective measurements in the large scale, the predicted trend of improvement for coal burnout is considered as realistic.

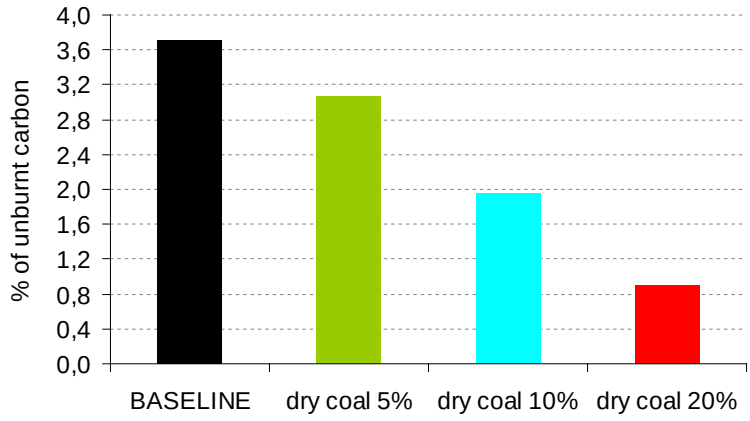

Figure 6.14. View of unburned carbon percentage

6.2.3.3 Heat flux

In order to evaluate the impact of dry coal co-firing on the boiler heat balance, the wall heat flux to the evaporator walls is calculated for each of the cases simulated. The heat flux to the furnace walls is composed of two different parts; the radiative one which is the major part and is generated by the radiation of the high flame temperature to the walls, and the convective one which represents the convective heat flux from the hot flue gas to the walls. Both parts are taken into account. The heat flux integral value (in kW) in the three main furnace zones, (a) the hopper, (b) the main burner zone and (c) the zone above the burner belt, as well as the overall heat flux to the whole furnace are presented in Figures 6.15 and 6.16, for the radiative and the total heat flux respectively. The total heat flux value to the furnace walls increases by raising the dry coal co-firing share; nevertheless, the relative changes are small. In particular, in the 20% co-firing case the calculated total heat flux is about 900 kW higher compared to the reference case, which corresponds to a relative increase of less than 4%. Moreover, the ratio of the radiative heat flux to the total heat flux almost remains constant indicating that dry coal co-firing does not extensively affect the heat transfer in the particular boiler.

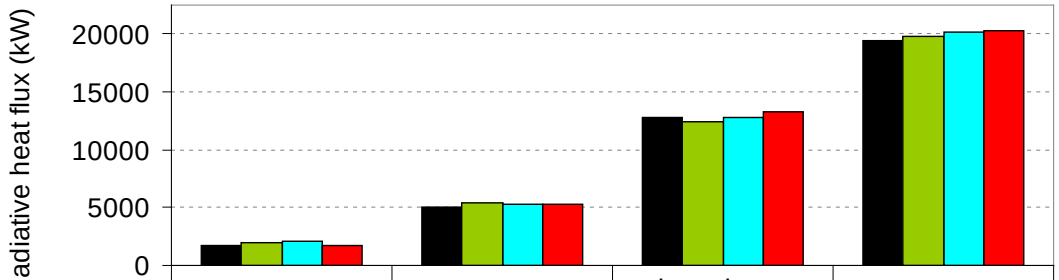

	hopper	burner zone	above burner zone	TOTAL
baseline	1691	5018	12778	19487
dry coal 5%	2003	5367	12461	19830
dry coal 10%	2091	5296	12725	20113
dry coal 20%	1701	5297	13312	20310

Figure 6.15. Radiative heat flux integral (kW) on furnace zones

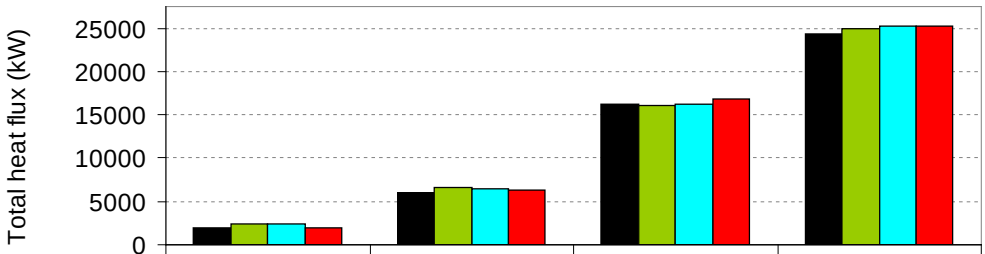

	hopper	burner zone	above burner zone	TOTAL
baseline	1962	6063	16251	24276
dry coal 5%	2347	6588	16020	24955
dry coal 10%	2478	6494	16263	25235
dry coal 20%	2027	6354	16793	25174

Figure 6.16. Total heat flux integral (kW) on furnace zones

In order to get detailed information on the possible effect of dry coal co-firing on the distribution of the wall heat flux along the furnace height, average values of total heat flux density (in kW/m2) are calculated for six different zones of the evaporator. Each zone corresponds to a different furnace level. According to the numerical results presented in Figure 6.17, dry coal co-firing has a moderate effect on the distribution of heat flux density over the furnace height and no major changes are expected. The specific heat flux density increases when increasing the dry coal firing share in most of the considered furnace zones; however, this rise is in relative terms less than 5% in most of the cases considered. Moreover, the values calculated for the average heat flux density of about 50 kW/m^2 are considered as low and are only representative of the specific furnace. Typical values for modern lignite fired furnaces are about 100 kW/m^2.

The change of the heat flux distribution due to dry coal co-firing is, therefore, expected to have a low impact on the operation of the evaporator of the specific boiler. More generally speaking, however, the possibility of potential damage on the evaporator surfaces due to overheating when co-firing dry lignite has to be investigated in detail for each potential application. Summing up, the impact of dry coal co-firing on the evaporator heat flux and in general, on the overall boiler heat balance is expected to be low in the case of the particular furnace.

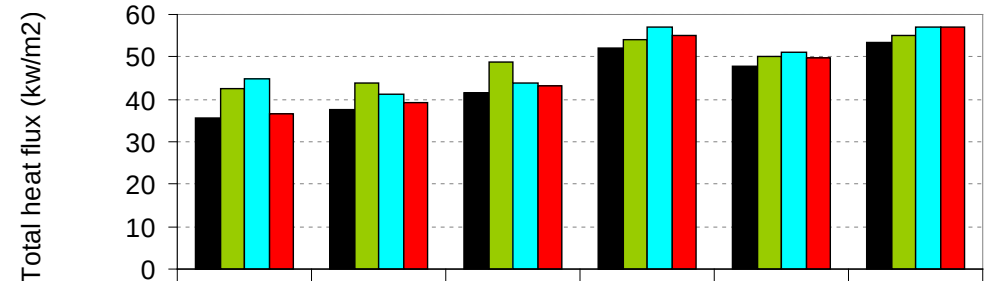

	hopper	lower zone	1st burner level	medium zone	2nd burner	upper zone
baseline	35,46	37,55	41,69	52,10	47,68	53,32
dry coal 5%	42,42	43,94	48,82	54,03	49,95	55,07
dry coal 10%	44,78	41,31	43,88	56,96	51,13	57,10
dry coal 20%	36,64	39,12	43,29	54,93	49,70	57,17

Figure 6.17. Distribution of total heat flux density (kW/m^2) on furnace zones

6.2.3.4 Predicted NO_x emissions

The calculated profiles of NO_x concentration are presented in Figure 6.18. By increasing the dry coal co-firing share, a clear increase of NO_x concentration along the whole furnace height is observed. The effect of the thermal NO_x formation mechanism, due to the increased temperature fields in case of dry coal co-firing, is assumed to be the reason for this behaviour. Previous investigations in the lab scale [V-24, 25] as well as the investigations performed in the particular boiler confirm this tendency. Further studies on possible NO_x reduction methods, like air and fuel staging practices, cannot be performed in the specific boiler due to its aged design and limited options for retrofitting works. Nevertheless, if dry coal co-firing is considered for a modern Greek boiler of the typical 300MW_e class, the investigation of the possible NO_x abatement measures is one of the key aspects, which have to be addressed in detail.

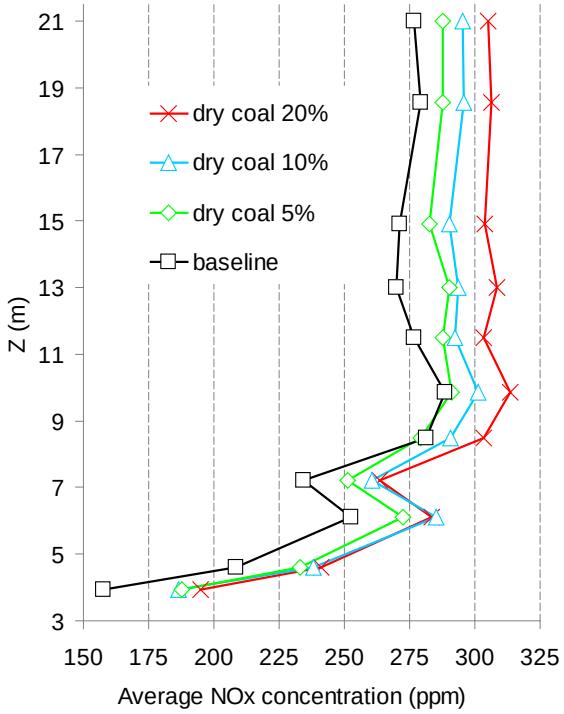

Figure 6.18. Calculated average NO_x concentration (ppm) along furnace height

6.2.4 Conclusions

Following the large-scale experimental campaign on dry coal co-firing, the numerical simulations of the same boiler under dry coal co-firing conditions are presented and analysed in the present section. Moderate changes of the combustion behaviour are predicted for all dry coal co-firing cases in terms of flue gas temperatures, burnout wall heat flux and emissions. An increase of the average furnace outlet temperature up to 30K is foreseen for the case of the 20% substitution compared to the baseline. The heat flux to the evaporator part increases only to a small percentage (less than 4%), while a clear improvement of the burnout is predicted by increasing the co-firing share. On the other hand, a clear increase of NO_x emissions when increasing the dry coal firing share is noticed, and this has to be further investigated. Summing up, the performed CFD simulations as well as the previous experimental investigations indicate that the substitution of raw lignite by pre-dried lignite of the same

origin is a feasible practice in existing lignite-fired power plants. The benefits expected on the boiler behaviour are related with the improvement of the combustion performance, by means of the increase of the fuel burnout and the improvement of the ignition and flame stability in the case of firing poor quality lignites.
Nevertheless, the main reason in favour of the application of dry lignite co-firing in an existing boiler is not only the improvement of the combustion behaviour but the improvement of the plant efficiency, if a state of the art pre-drying system is integrated in the current plant steam cycle. In order to quantify this efficiency gain, an atmospheric fluidized bed drying system with internal waste heat utilization (WTA-drying) is considered as a possible pre-drying concept for Agios Dimitrios V boiler. Thermodynamic steam cycle calculations of the plant are performed in reference and in pre-drying conditions where dry coal is co-fired up to a thermal share of 30% and the pre-dried lignite utilised is produced from a "WTA dryer".

6.3 Thermodynamic calculations on lignite pre-drying and dry lignite co-firing

6.3.1 Introduction - Scope of work

The experimental and numerical investigations on dry lignite co-firing, performed in the 75 MW_{th} Greek boiler and presented in the previous sections, indicate that the substitution of raw lignite by pre-dried lignite up to a certain thermal share is feasible without expected negative impacts on the operational boiler behaviour. In order to further evaluate dry lignite co-firing as a potential retrofitting option in a modern Greek boiler of the typical 300 MW_e class, the simulation of a specific boiler under reference and dry lignite co-firing conditions is required. The present analysis focuses on the thermodynamic simulation of the overall steam cycle and not on the numerical combustion simulation of the particular boiler. In this way the potential plant efficiency increase by the integration of a pre-drying system in an existing power plant can be estimated. This prediction is required for the examination of the feasibility of the retrofitting scenario proposed in terms of the technical and economic aspects. Apart from the plant efficiency increase expected, the change of the boiler heat balance is also predicted by the thermal cycle calculation tool. However, for a detailed prediction of the expected influence of dry coal co-firing on the boiler heat balance, the numerical simulation of the furnace and the convective part of the boiler is required and these simulation activities are proposed as future work.
The 375 MW_e Agios Dimitrios V boiler is considered as a candidate unit for the dry coal retrofitting scenario. Several aspects are taken into account for this decision: (a) the particular unit is relatively new and has a remaining lifetime of more than a decade. (b) The specific boiler is equipped with Over Fired Air firing system in order to comply with the reduced NO_x emission limits of the EU Large Combustion Plant Directive. Increased NO_x emissions which are expected in the case of dry coal co-firing could be, therefore, mitigated through the application of air staging. (c) The lignite fired by Agios Dimitrios V unit has high water content of about 54%. For this reason the efficiency increase expected when implementing lignite pre-drying is higher than in the case of other Greek power plants firing lignite qualities with lower water content, such as the Florina unit, where the utilized lignite has a moisture content of about 37%.

6.3.2 Methodology - Possible configurations studied

A commercial cycle calculation software (Ipsepro) is used for the thermodynamic cycle calculations performed. The co-firing thermal shares of substitution examined are 10%, 20%

and 30%. The fuel analysis of the raw lignite fired in Agios Dimitrios V boiler is given in Table 6.6. A secondary solid fuel injection cannot be simulated with the particular calculation software and for this reason the analysis of an equivalent fuel, which corresponds to the weighted mixture of raw and dry lignite for each considered thermal share, is used as input in the co-firing cases calculated. The analysis of the equivalent fuel for all co-firing cases is also presented in Table 6.6. Since the total thermal input remains constant in all cases considered, the fuel mass flow is accordingly calculated based on the heating value of the equivalent fuel in each co-firing case. An overview of the Agios Dimitrios V boiler including the arrangement of the convective heat exchanger surfaces is presented in Figure 6.19, while the overall flow sheet diagram of the Agios Dimitrios V steam cycle at reference conditions is given in Figure 6.20.

The particular steam cycle has four low pressure and two high pressure water pre-heaters. In order to keep the steam temperature at the high pressure and the medium pressure turbine below the maximum value allowed of 540 °C, steam coolers are integrated in the superheater and the reheater steam cycle. By injecting high pressure feeding water, extracted after the feeding pumps, steam temperature can be controlled. Steam coolers are incorporated in the cycle calculation tool through a “temperature controlled mixture box, TMX 1 and 2”, where the temperature of the outlet stream is set and the mass flow of the cooling water needed is calculated. The mass flow of the high pressure water injected in the reheated steam cooler directly affects plant performance. The feeding water consumed at the reheated steam cooler leads namely to a reduction of the available feeding water / steam mass flow passing through the evaporator, the superheater section and the high pressure steam turbine. This decrease of the steam mass flow in the high pressure cycle is, therefore, considered as a power loss and has to be calculated.

Table 6.6: Analysis of raw, dry lignite and of the equivalent fuel considered

Analysis	Units	Reference fuel	Pre-dried lignite, 12% moisture	10% dry lignite thermal share	20% dry lignite thermal share	30% dry lignite thermal share
C	% w.	18.00	34.43	18.75	19.61	20.58
H	“	1.45	2.77	1.51	1.58	1.66
N	“	3.00	0.96	0.52	0.54	0.57
O	“	8.50	16.26	8.86	9.26	9.72
S	“	0.44	0.84	0.46	0.48	0.50
water	“	54.00	12.00	52.08	49.90	47.40
ash	“	14.60	27.93	17.83	18.64	19.56
LHV	MJ/kg	5.464	12.682	5.794	6.169	6.597

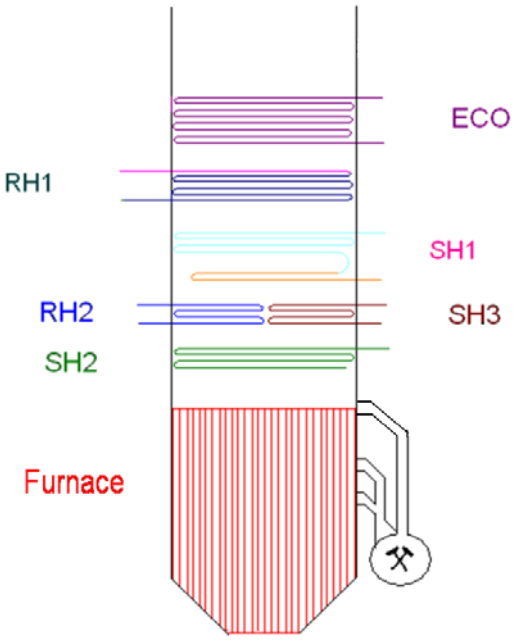

Figure 6.19: Overall layout of the Agios Dimitrios boiler

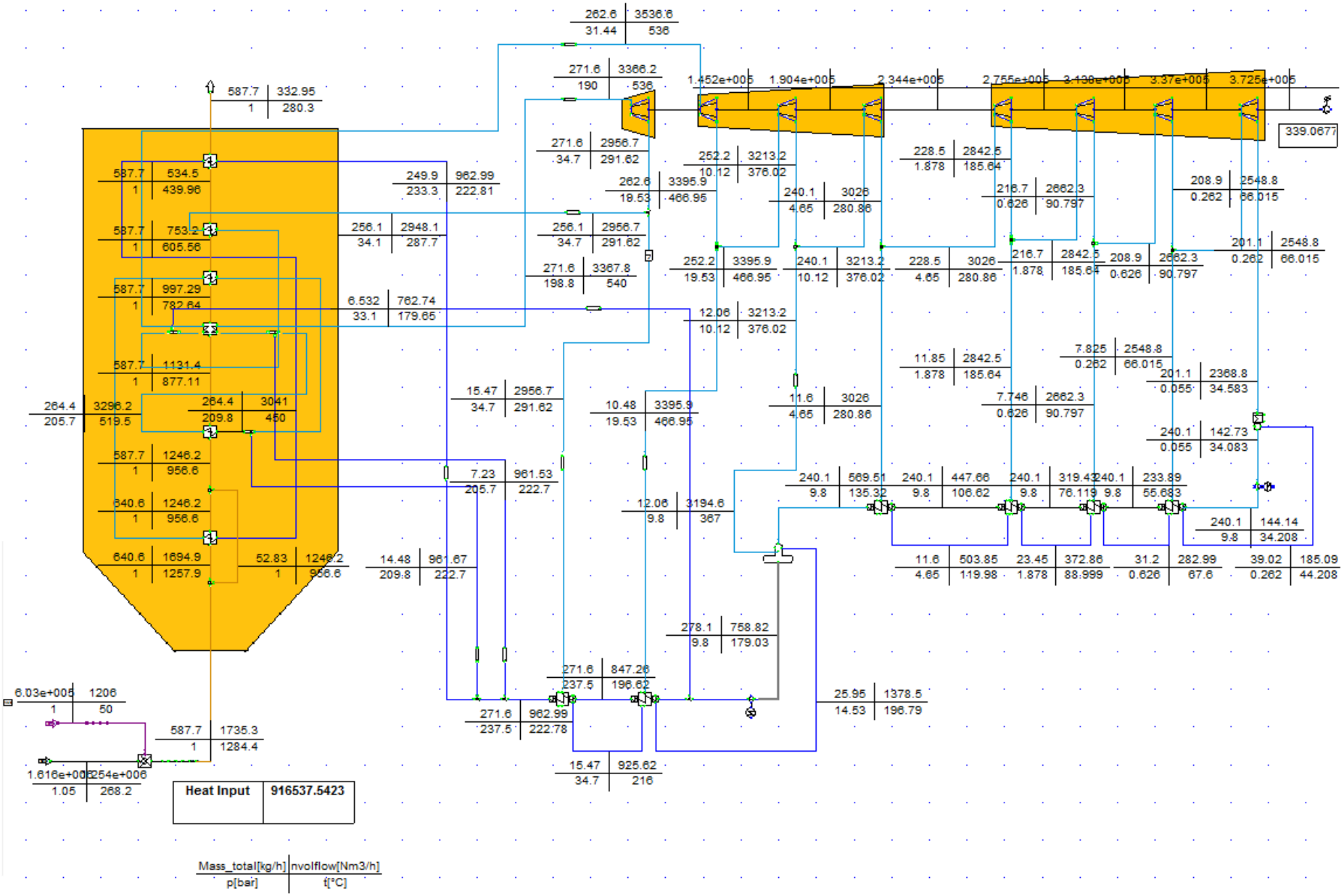

Figure 6.20: Flowsheet diagram of Agios Dimitrios V plant: Reference case

The WTA fluidised bed dryer is modelled in the calculation tool as a simple cross flow heat exchanger. The high temperature stream is the steam bleed from the steam turbine, and the low temperature stream is the water content of the lignite that is evaporated in the drying process. A more detailed modelling of the WTA dryer, which would include additional auxiliary streams and power consumptions, would require a detailed design of the pre-drying facility which is currently not available. The steam required for the operation of the fluidised bed lignite dryer is extracted from the first steam bleed of the low pressure steam turbine with parameters (188°C, 1.8 bar). The evaporated steam is used as heating medium on the first and the second low pressure feed water pre-heaters.

6.3.3 Results

The heat fluxes on the boiler heat exchanger surfaces for the reference and the dry coal co-firing thermal cases are given in Figure 6.21. An increase of the useful heat produced in the furnace section is predicted for the dry-coal firing cases, due to the higher adiabatic temperature and the increase of the radiative heat flux. More specific the radiative heat flux increases to about 11%, which is much higher than the relative increase calculated in the simulations of the Liptol power plant (about 4%). The total useful boiler heat flux increases from 824 to 840 MW_{th}. The calculated flue gas temperature at the furnace exit and the boiler exit is presented in Figure 6.22. The furnace exit temperature increases from 957 °C in the reference case to 1005 °C in the 30% co-firing case, while the boiler exit temperature decreases from 280 °C in the reference case to 270 °C in the 30% co-firing case. The elevated flue gas temperatures lead to an increase of the required cooling water mass flows (Figure 6.23).

The boiler efficiency calculated by the direct method increases accordingly 1.5 absolute percentage points (Figure 6.24). This improvement is also confirmed by the lower flue gas temperature values at the boiler exit. Furthermore, the installation of the WTA dryer brings an additional increase in the theoretical steam cycle efficiency through the reduced steam bleed to the first and the second low pressure feed water pre-heaters. A certain fraction of the particular steam mass flow is replaced by the evaporated moisture. The calculated plant efficiency rate increases 0.8 absolute points from 35.4% to 36.2% (Figure 6.24). A higher efficiency rise could be expected; this is however not feasible, due to the small power loss caused by the increased feed water mass flow in the steam coolers.

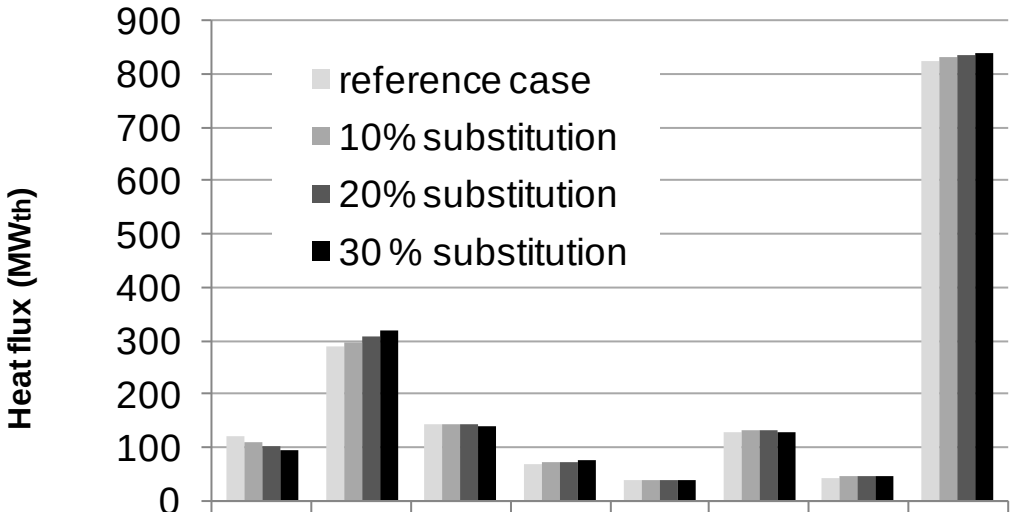

	ECO	FURNACE	SH1	SH2	SH3	RH1	RH2	TOTAL
reference case	118	287	143	67	36	129	43	824
10% substitution	109	298	143	70	37	131	43	831
20% substitution	103	309	142	72	38	130	44	837
30 % substitution	94	320	140	74	39	128	45	840

Figure 6.21: Prediction of the produced useful heat at each heat exchanger

The overall effect of dry coal co-firing on the plant net efficiency rate is summarised in the following:

- An increase of boiler efficiency by more than 1.5 absolute points may be achieved when co-firing dry coal up to a thermal share of 30% due to the reduced flue gas losses.
- An increase of net plant efficiency up to 0.8 percentage points may be achieved for a dry coal co-firing thermal share of 30%
- This increase trend may vary according to the plant configuration and is affected by the counterbalancing effect between the improvement from the pre-drying system integration and the expected losses, due to the increased demands for feed water.

The overall flow sheet diagrams for the dry lignite co-firing cases of 10%, 20% and 30% are presented in Figures 6.25, 6.26, 6.27 accordingly.

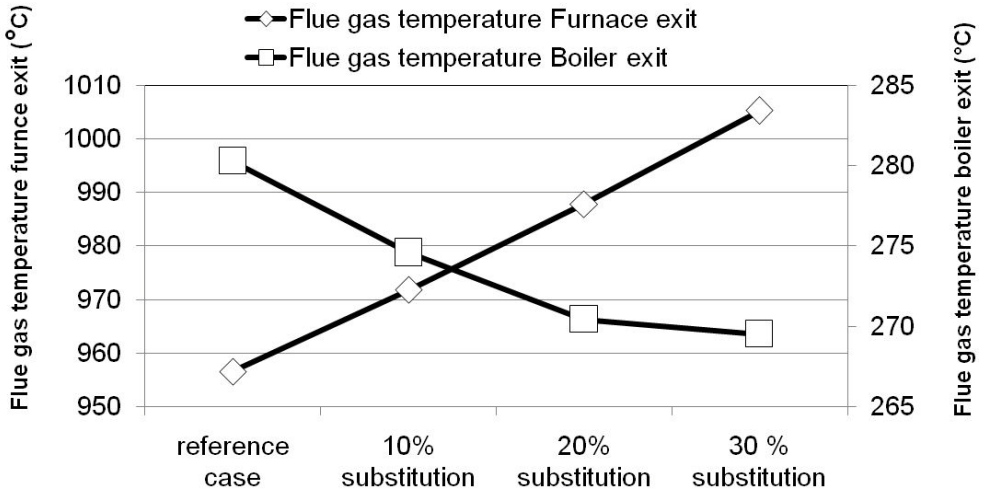

Figure 6.22: Calculated flue gas temperature at furnace and boiler exit

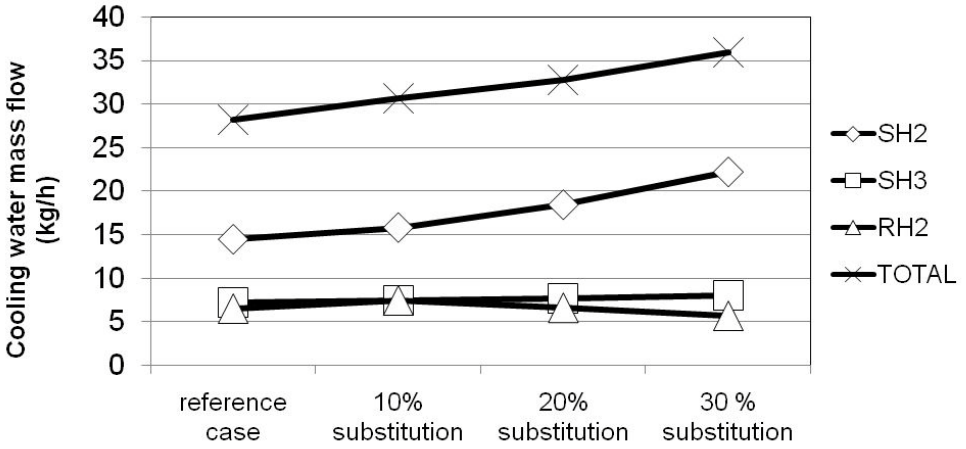

Figure 6.23: Calculated mass flows of cooling water at super heater and reheater steam coolers

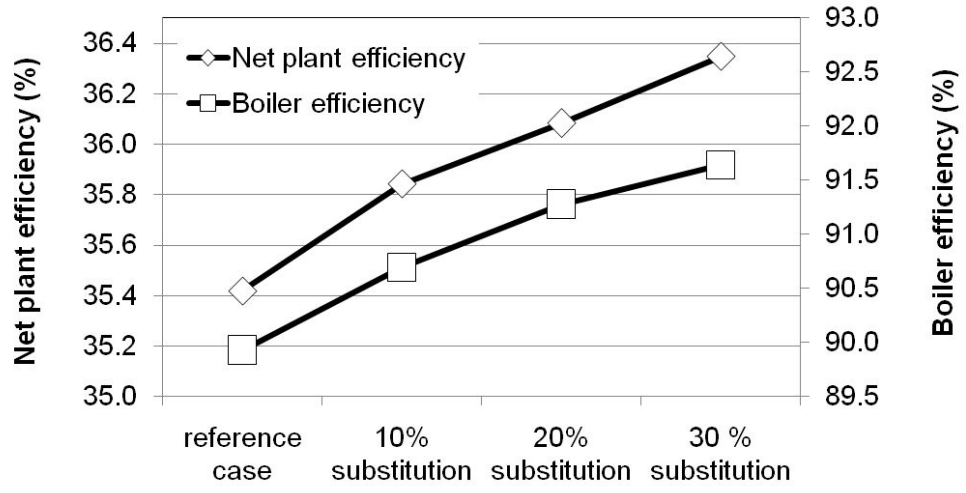

Figure 6.24: Calculated boiler efficiency rate and net plant efficiency rate

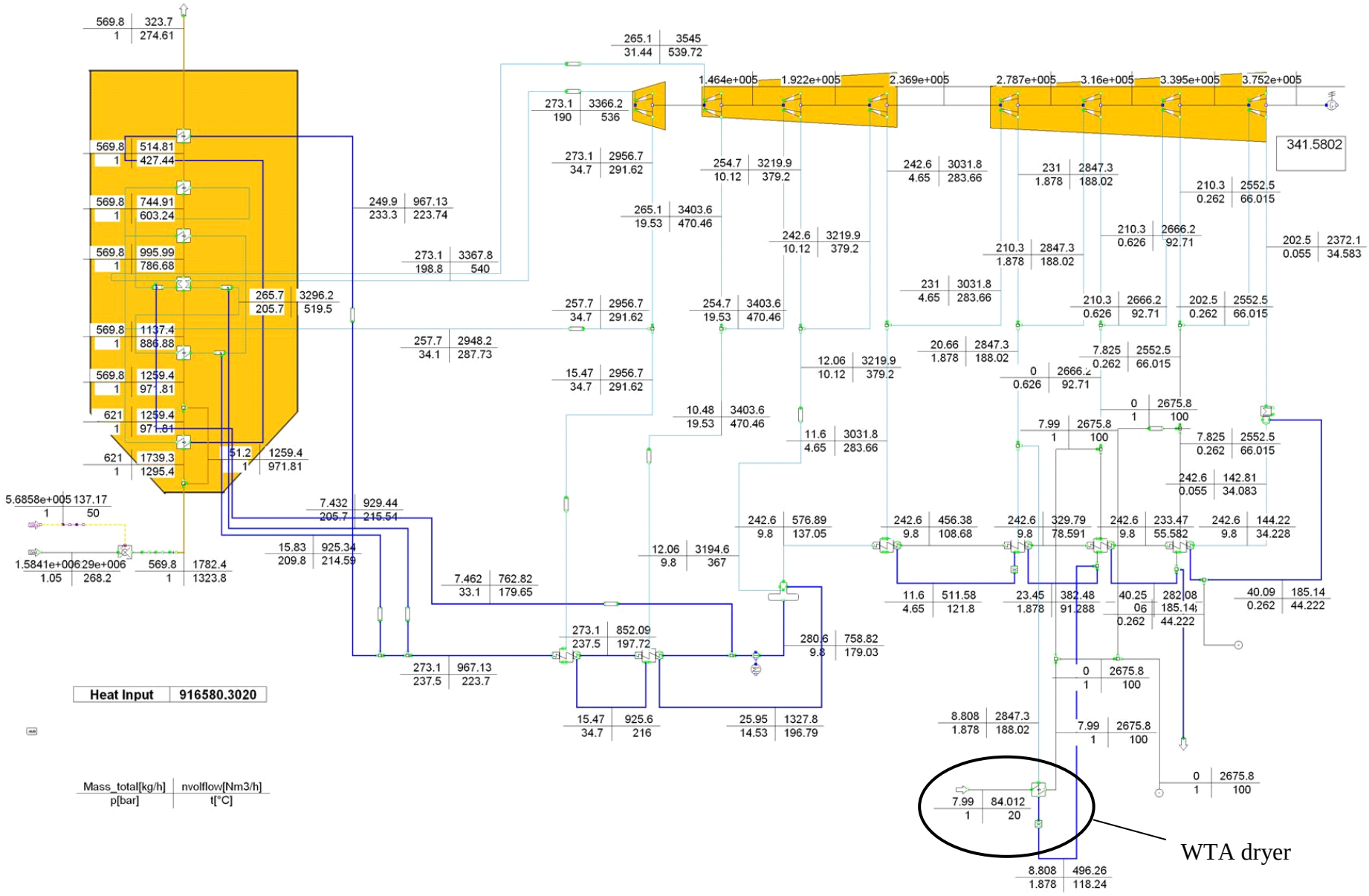

Figure 6.25: Flowsheet diagram of Agios Dimitrios V plant: Lignite dry-coal co-firing case, 10% thermal share

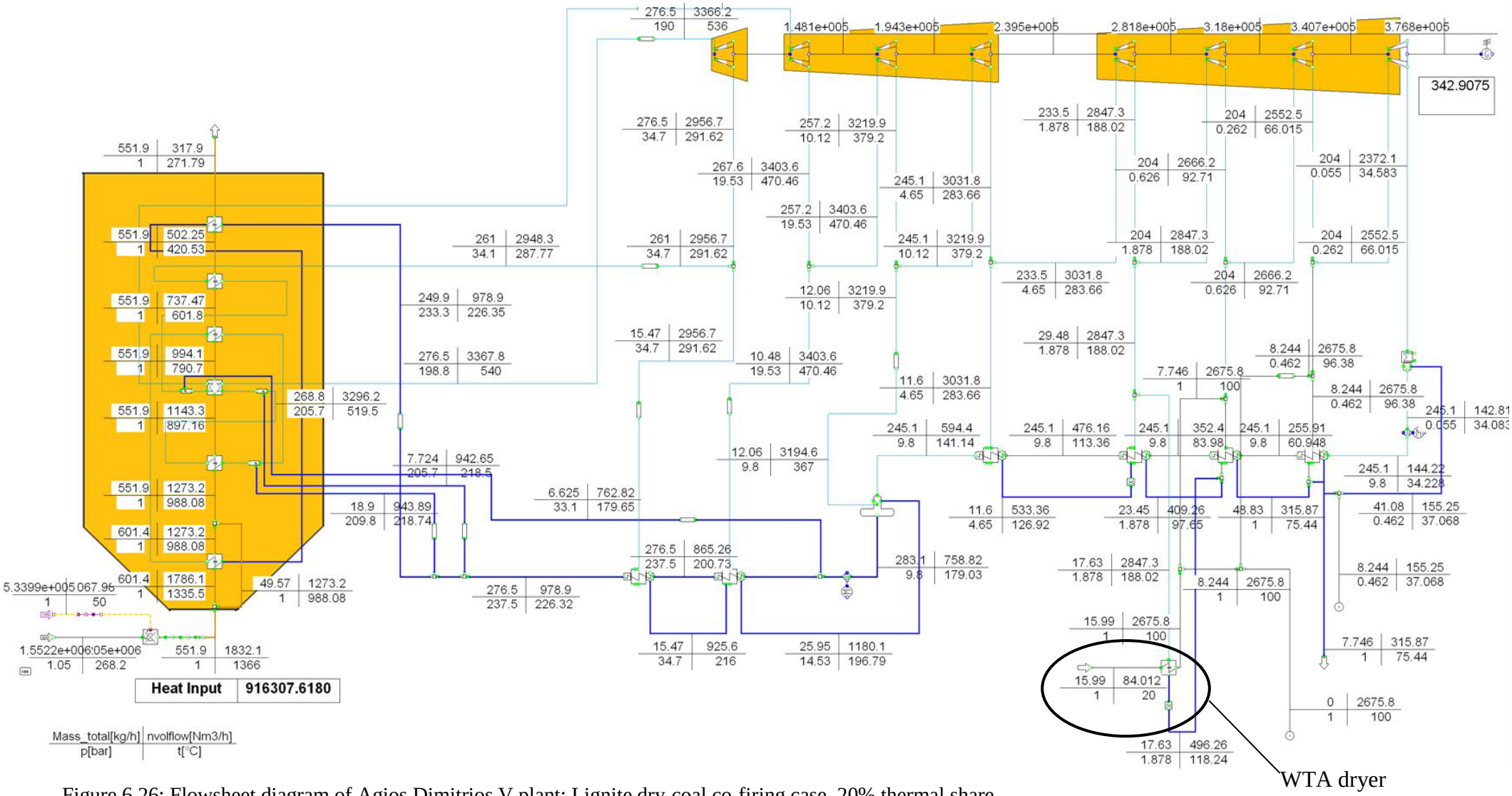

Figure 6.26: Flowsheet diagram of Agios Dimitrios V plant: Lignite dry-coal co-firing case, 20% thermal share

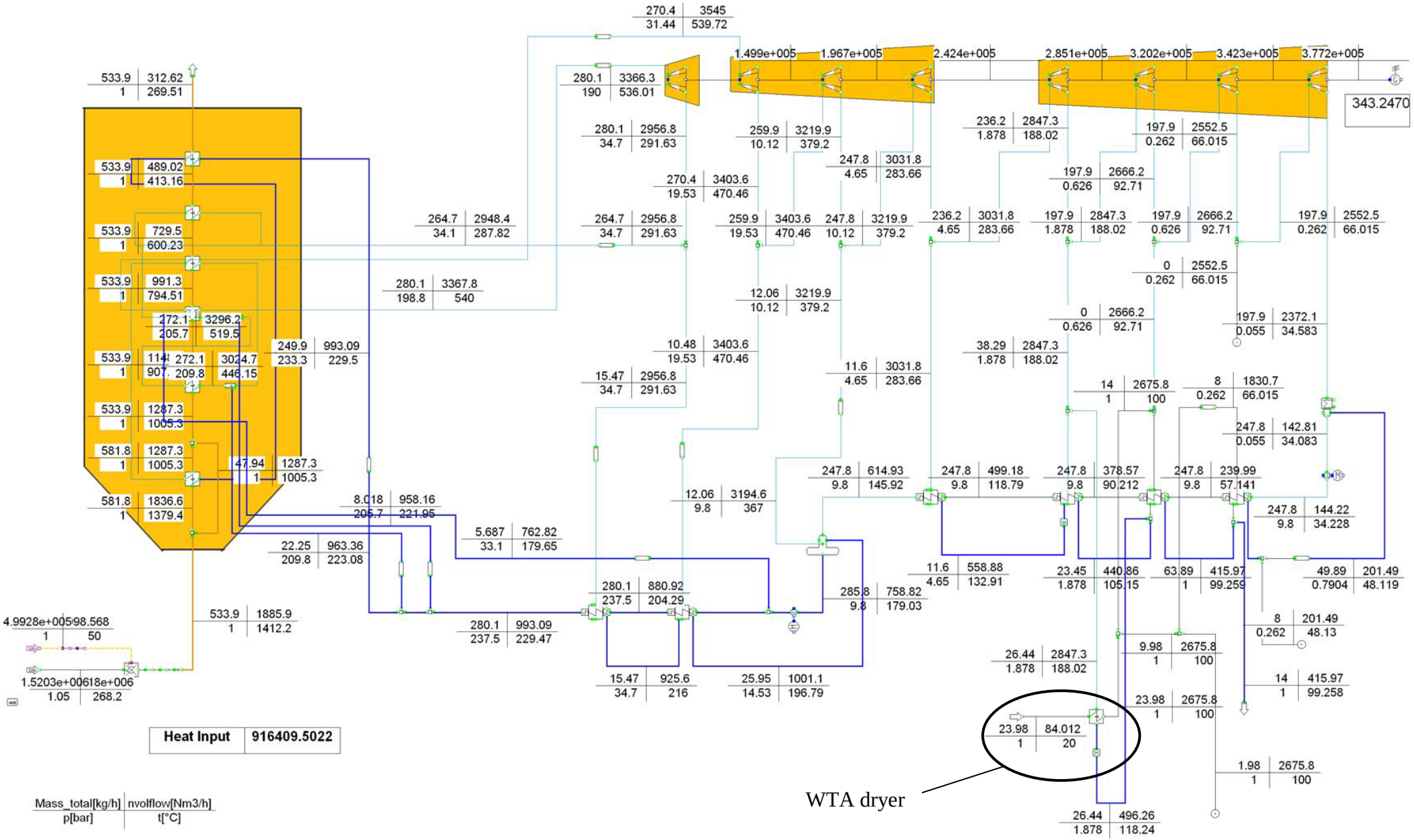

Figure 6.27: Flowsheet diagram of Agios Dimitrios V plant: Lignite dry-coal co-firing case, 30% thermal share

6.3.4 Conclusions – Further work

In the current section the integration of a WTA dryer in an existing Greek power plant is evaluated through thermodynamic cycle calculations. The moisture evaporated from the drying process is used as heating medium and partially replaces the steam bleed utilised for the first low pressure water pre-heater. The steam cycle of Agios Dimitrios V unit is taken into account for the examination. According to the calculation results, an increase of plant efficiency with the integration of the WTA dryer of up to 0.8 absolute percentage points is predicted. This value is lower than the equivalent values for power plants co-firing Rhenish pre-dried lignite. This is expected due to the lower moisture content of Greek lignite compared to the typical moisture content of Rhenish lignites, i.e. 56-59%. Nevertheless, the overall evaluation of the investigations performed indicates that the application of the WTA pre-drying concept is feasible in an existing Greek power plant without great risks to the operational behaviour of the boiler. The installation of dry lignite burners in an existing Greek power plant by replacing the start up oil burners with dedicated dual burners firing oil and dry lignite dust could be a next step towards the application of the particular technology in Greek power plants. This specific option should be numerically investigated.

6.4 Summary and evaluation of the large-scale investigations on lignite drying and dry lignite co-firing

The overall results of the investigations on pre-drying and dry coal co-firing are summarised and evaluated in this part. PPC's "Liptol" power plant was chosen for the large-scale dry lignite co-firing campaign due to the firing system for dry lignite available. Despite the age of the plant, the influence of the dry lignite on certain combustion related aspects was successfully investigated and the results obtained can be transferred to some extent to the newer Greek power plants of the 300 MW_e class. Satisfying results are obtained for the issue of the environmental performance of the boiler during dry lignite co-firing. Since the fired dry lignite is of the same quality as the main fuel, only conventional flue gas emissions were measured and no waste derived gas compounds, such as HCl or dioxins-furans, were recorded. However, the increase of NO_x emissions due to higher flame temperatures in the furnace was experimentally measured and predicted by the numerical simulations. A relative increase of up to 10% compared to the reference value is noticed in the simulation results. Therefore, direct NO_x abatement measures, such as fuel and air staging, should be taken into account in any existing boilers which will be retrofitted in order to co-fire dried lignite. An overview of the evaluation results on the environmental aspects is presented in Table 6.8.

Table 6.8: Evaluation table on the environmental aspects of SRF co-firing

		Proposed coal substitution concept : dry coal co-firing	
		Experimental methods	Numerical simulation methods/ mass balances
Environmental aspects	CO_2 emissions	n.i.	Annual savings of 208,000 t CO_2 for a co-firing thermal share of 20%
	Conventional flue gas emissions (NO_x, SO_2, CO)	!	!
	HM in the flue gas	n.r.	n.r.
	HCl	n.r.	n.r.
	Dioxines – Furans	n.r.	n.r.
	Ash quality: HM in the ash	n.r.	n.r.

"nr": no change is anticipated for the specific parameter and, therefore, it is considered as "not relevant" for the examination

"ni": the specific parameter is "not investigated"

A positive picture is also obtained in terms of the operational aspects investigated. Stable operational behaviour was observed during the large-scale tests performed, while no certain trend was measured at the temperature profiles at the superheater section, which are directly influenced by the furnace exit temperature. According to the large-scale numerical simulations, an increase of the furnace exit temperature is expected for the dry lignite co-firing cases. The predicted temperature rise is, however, moderate and the critical ash melting temperature of the Greek lignite will not be reached; therefore, no increased risk for slagging and fouling at the convective section is predicted from the numerical simulations. On the other hand, the tests performed at the 1 MW_{th} experimental combustor indicate that ash slagging could become a problem in the furnace walls at the near burner region due to the local temperature increase. This perspective should be examined in detail in the case of the application of the dry lignite co-firing concept in a Greek power plant. An improvement of the fuel burnout is numerically predicted, which could lead to an increase of boiler efficiency. Such an increase is also predicted by the thermal calculation tool due to the reduced flue gas losses when co-firing dry coal. Finally, another important technical aspect, which has to be carefully addressed, is the influence of dry lignite co-firing on the heat flux distribution to the boiler. According to the available literature and the performed small-scale tests, an increase of the radiative heat flux to the evaporator and a decrease of the convective heat flux to the heat exchangers are expected when increasing the dry coal co-firing share. Such a tendency was not clearly observed during the large-scale experiments or numerical simulations. It is, however, argued that the design of the particular boiler and the low specific heat flux density to the evaporator are the main reasons for this result. In other words, it is expected that the particular tendency will be apparent in a modern Greek boiler of the 300 MW_e class. Thus, it should be closely examined by dedicated numerical simulation tools which can combine the combustion calculations at the furnace section with the steam cycle calculations at the boiler convective part. An overview of the evaluation of the dry lignite co-firing concept based on the boiler technical and operational parameters is presented in Table 6.9.

Table 6.9: Evaluation table on the technical aspects of SRF co-firing

		Proposed coal substitution concept : dry coal co-firing	
		Experimental methods	Numerical simulation methods/ mass balances
Technological - operational aspects	Operational parameters (steam temperatures, Pel)	√	n.i.
	Heat flux to evaporator	n.i.	!
	Overall boiler heat balance /	n.i.	!
	Boiler Efficiency (η_{boiler}) Power plant efficiency (η_{PP})	n.i.	√
	Furnace exit conditions (temperature, O2)	√	√
	Combustion conditions in the furnace (temperature and O2)	n.i.	√
	Risk of potential operational problems due to slagging and fouling	! (investigations in the small scale facility)	√
	Ignition/ Burnout	√	√
	Risk of potential operational problems due to chlorine corrosion	n.r.	n.r.

7 Economical assessment of the investigated substitution concepts

7.1 Introduction

In this chapter the two brown coal substitution concepts previously presented are evaluated in terms of their economic feasibility. Considering the alternative fuels co-firing concepts, two different fuel types are investigated. The one is Solid Recovered Fuels (SRFs) presented in the previous chapters and the other is Solid Biofuels, which are produced from agricultural or forest residues. Solid biofuels are in the most cases fully biogenic and are also regarded as alternative substitute fuels to coal. In contrast to SRFs, which are regarded as waste according to the European legislation, Solid Biofuels, are ordinary fuels and have a definite price for purchase, although they derive from biomass residues. The presentation of these two different categories of alternative fuels and their comparison with pre-drying and dry lignite co-firing concept in terms of economic parameters is attempted in this chapter.

The expected types of costs and revenues, when implementing each substitution concept in the large scale are described and compared. Data for the required investment costs and running costs of the facilities is collected after a market research and through personal contact with industrial partners. The difficulty in collecting realistic data lays in the lack of standardised technical solutions for the proposed co-firing concepts. Although a significant number of SRF or biomass co-firing projects has been realised in coal power plants in central Europe, the respective investment costs vary extensively based on the technical solutions followed and the range of plant modifications carried out in each case. Furthermore, the investment costs of the pre-drying facility are estimated based on the costs of the first prototype erected. It is expected that the further commercialisation of the pre-drying concept will lead to decrease of the investment costs. At last, the economic feasibility of both concepts is compared based on a realistic co-firing scenario in a Greek large scale power plant. The 375 MW_e Agios Dimitrios V lignite boiler is regarded as the reference plant for the particular examination.

7.2 Estimation of expected costs and revenues by the implementation of the co-firing projects

In the first part of the economic evaluation of the two coal substitution concepts the expected additional costs and revenues are analysed. It should be underlined that the reduction of CO_2 emissions in the co-firing concepts regarded is achieved by different ways. Through the substitution of raw coal by SRF a certain amount of fossil fuels is saved. This leads to decreased CO_2 emissions, since SRF has a certain biogenic content. For the scope of the analysis a value of 50% is used as an average SRF biogenic content. This is a realistic value for Solid Recovered Fuels derived from MSW. In the case of biomass, it is assumed that the Solid Biofuels co-fired are fully biogenic and therefore their co-firing leads to further CO_2 savings. On the other side, by the integration of a brown coal pre-drying system in an existing power plant the reduction of CO_2 emissions is achieved through the increase of net plant efficiency and the decrease of the total fuel mass flow, due to the increased heating value of dry lignite. Thermal cycle calculations are performed, in order to quantify the expected plant efficiency increase when adopting the WTA pre-drying concept. The calculations are presented in chapter 6 and the respective results are also used in this chapter.

An overall comparison of the expected costs and revenues, when implementing the proposed co-firing concepts is given in Table 7.1. Regarding the co-firing scenario the two categories of alternative fuels regarded are: a) Solid Biofuels, which are 100% biogenic and are classified and standardised according to the work of CEN Technical Committee 335 and b) Solid Recovered Fuels, which derive from different types of non hazardous waste and their classification and standardisation is a subject of CEN Technical Committee 343. These two fuel types differ in their origin and respectively in their market price. Biomass fuels have a specific price in the market depending from fuel properties, such as heating value, moisture content and form of delivery to the plant (pellets, chips, dust). A broad range, from 50 €/t to 150 €/t, is given in Table 7.1 as a representative variation of the price of different biomass fuels. Solid Recovered Fuels on the other hand, are considered as waste in the European Legislation. Thus, they have a price for waste disposal, the so called "gate fee", expressed in €/Mg (1 mega gram = 1 tone). The gate fee is paid by the institution or company which disposes off the waste to the institution or company which accepts it, eg. from the municipality to the waste treatment plant, or from the waste treatment plant to the waste incinerator facility. The gate fee also varies extensively depending on the waste type and the local market situation in each country or region. A typical gate fee for unsorted Municipal Solid Waste in EU member states in Central Europe, as Germany and Austria, is 100 to 140 €/ Mg, while the gate fee of Solid Recovered Fuels may vary extensively (from 0 to 60 €/ Mg) according to the local market situation.

Investment costs

The required Total Plant Cost (TPC), which includes the costs of engineering, procurement construction and commissioning in a co-firing project for alternative fuels, either biomass or SRF, is presented in the first row of Table 7.1. Total plant costs of 2 - 3 M € are found in the literature as typical costs for co-firing projects with thermal input of 100 MW_{th}. The value represents only the thermal input of the substitute fuel Depending on the boiler size this thermal input corresponds to a co-firing thermal share of about 5-10%. In the case of the examined Greek power plant the given thermal input corresponds to a co-firing thermal share of about 11%. The corresponding specific plant costs expressed per kW_{th} of thermal input from the substitute fuel are 20 - 30 €/ kW_{th} . The same cost expressed per kWe of net produced power from the substitute fuel is in the range of 55 - 85 €/ kW_e. Co-firing projects, where extensive boiler modifications have been realised, and whose total budget greatly exceeds the aforementioned investment costs are not considered in the analysis. The prices are therefore obtained from implemented projects, where moderate technical solutions were followed and only the minimum required modifications are carried out in the boiler part. It is noticed that the particular values are very low compared with respective specific plant costs of a new combustion plant dedicated for 100% biomass firing, which may be in the range of 2500 – 3000 €/kW_e. The significant difference between the two costs is justified by the existing plant equipment, which is utilised in the case of a biomass co-firing project. Furthermore, due to the increased capacity of existing coal power plants, compared to dedicated biomass firing installations, the co-utilisation of increased biomass quantities under low co-firing shares is feasible without putting the boiler operation to a high risk. The Total Cost of Investment (TCI), or otherwise stated the Capital Expenditure (CAPEX) is calculated by adding to the initial TPC value extra 5% of Total Plant Cost as development cost and another 10% of TPC as cost for contingency.

Regarding the investment cost of a lignite pre-drying system, the reported figures are obtained from the first prototype erected. More specific, a Total Plant Cost (TPC) of approximately 35 M € is estimated for the engineering, procurement, construction and commissioning of an industrial scale fluidised bed dryer with a dry lignite production capacity of 110 t/h. This

capacity corresponds to a thermal input of about 400 MW_{th} in the case of Greek dry lignite. Another 3 to 5 M € are estimated as plant costs for the connection of the dryer with the boiler and the turbine house and the modification of the existing firing system. The overall sum is therefore about 40 M €, and the specific plant cost calculated is about 100 €/ kW_{th} of thermal input from the substitute fuel. The same cost expressed in €/ kW_e of electric power corresponding to the thermal input of the substitute fuel is then about 270 - 290 €/ kW_e when taking into account a typical Greek lignite boiler This price is considered as a guiding value for the investment costs of the particular technology. Since the WTA pre-drying concept is in the first demonstration phase, it is expected that the specific costs will decrease after the successful realisation of two or three future projects. The Capital Expenditure (CAPEX) is calculated by adding 5% of TPC to the initial value as development cost and another 10% as cost for contingency.

Another important aspect in the calculation of investment costs is the capacity of the facility and the respective range, for which the given specific investment costs are valid; in other words how scalable the investment costs are. In the case of alternative fuels co-firing, the value of 20-30 €/ kW_{th} is expected to be valid for a range of thermal inputs of 50 to 150 MW_{th}, as long as the thermal share of substitution is kept low, below 10% and no extensive modifications in the firing system of the considered boiler are required. The reason is that the required equipment for feeding and dosing of alternative fuels is highly scalable by choosing machinery of larger capacity (screw feeders, belt conveyors, radial fans for pneumatic feeding). Regarding fuel storage, a number of parallel storage bunkers can be installed, if the required capacity exceeds a specific limit. On the other side, the total investment costs of the pre-drying technology are expected to be kept more or less constant in the value previously reported. Although the pre-drying technology demonstrated is scalable for different dry lignite thermal inputs ranging from 40 to 400 MW_{th}, no linear decrease of the cost is expected for dryers of lower capacity. This behaviour is owed to the complexity of the process and the manufacturing costs of the dryer, which are about constant and are not in linear relation with the dryer capacity.

Furthermore, it has been shown in the previous chapter that a dry lignite co-firing thermal share of 25% is feasible in existing lignite power plants without any expected impact on boiler operation. In the case of the 375 MW_e Agios Dimitrios V unit the thermal share of 25% corresponds to a required thermal input from pre-dried lignite of about 260 MW_{th}. This in turn corresponds to a dry lignite production of 72 t/h. Compared to the capacity of the prototype WTA dryer erected in Germany (110 t/h) the calculated capacity for the Greek boiler (72 t/h) about 35% smaller. Since no linear dependency between capacity and Total Plant Cost is expected as mentioned above, the Total Plant Costs in the case of the Greek dryer should be decreased to less than 35%. A decrease of the initial plant costs to 25% is estimated as a representative value for the calculations indicating that no positive scale economies are found when trying to scale down the particular facility.

Operating and maintenance costs

In the next row of Table 7.1 the Operating and Maintenance (O&M) costs are given for each concept. They are separated to fixed and variable O&M costs. Fixed O&M costs include all fixed costs, which do not depend on the annual production, such as personnel costs, insurance and scheduled maintenance costs. They are expressed in € per kW_e of installed capacity. A value of 30 €/kW_e is taken for both coal substitution concepts. This value is typical for the fixed O&M costs of an overall coal power plant and can be found in relevant literature [VII-1], [VII-2]. The same value is given for the co-firing installations, although possible synergies in the operation of the power plant and the co-firing installation may reduce the costs. In this way the worst case scenario including the highest cost is taken into account. An example for

the application of synergies in the operation of the co-firing facilities can be provided by examining the personnel costs. More specific, no additional personnel costs are required for the operation of a biomass or SRF feeding system, if a fully automated system is installed. The automated operation of the feeding system can be then monitored in the control room by the shift personnel of the power plant. The fixed O&M of the co-firing installations are then reduced.
Variable maintenance costs are expressed as €/ MWh of produced net electric power corresponding to the substitute fuel co-fired. They correspond to the costs arising from the operation of the unit including mainly consumables. A value of 1.2 €/ kW_e of net electricity produced is determined in both co-firing cases. This value is typical to the variable operating costs of the whole coal power plant.

Fuel costs
The main difference between the running costs of the regarded coal substitution concepts lays in the fuel costs. In a biomass co-firing project the price of the biomass fuel may vary extensively from 50 €/t to 150 €/t. Since these values are higher than the lignite price, additional expenses are required from the power plant operator, in order to purchase and co-fire biomass. In this way the running costs increase and may also put to risk the economic feasibility of the investment, if the respective biomass price is too high compared to the expected revenues.
On the other side, Solid Recovered Fuels are considered as waste and they have no price for their purchase, but a gate fee for their disposal. This gate fee is then considered as a revenues of the power plant operator. As mentioned above the range of 0 to 60 €/Mg is a realistic variation range for the SRF gate fee according to the local market situation in each case.
The price of coal is also an important figure, since the savings achieved by the substitution practices have to be included in the economic calculations. Due to the considerable amounts of coal utilised, the constant substitution of coal even to a low thermal share may lead to considerable savings of coal throughout the period of one year. An estimation for the price of raw lignite extracted from open cast mines is obtained from the literature [VII-3]. The value 2.6 €/GJ is used, which corresponds to about 14 €/t in the case of Greek lignite. This value may considerably vary depending from the applied technology and the efficiency of lignite extraction in each mine.

Costs for CO_2 allowances
Last but not least, the costs for purchase of CO_2 allowances are regarded as variable costs. The reduction of CO_2 emissions, which is achieved by both co-firing concepts, corresponds to a decrease of the expenses for purchase of additional CO_2 credits. After the expiration of the Kyoto protocol in 2012, the whole amount of CO_2 emitted from coal power plants have to be included in the ETS. In other words, power plant operators will have to pay allowances for the whole amount of CO_2 emitted from their plants. It is therefore expected that the running costs of aged coal power plants with low efficiency rates will be significantly affected. In this framework co-firing practices are a realistic and reliable option, which may bring additional revenues or potential savings of future expenses for the existing coal power plants. A price of 15 €/ t CO_2 is considered in the present analysis as an indicative price for CO_2 allowances. This figure corresponds approximately to the average value in the last years (Figure 7.1) [VII-4]. According to relevant studies the CO_2 allowances price may increase to a level of 22 €/ t CO_2 in the coming years [VII-5]. Nevertheless, since forecasting is always related with uncertainty, the moderate price of 15 €/ t CO_2 is adopted for the calculations and the effect of its variation is later examined through parameter investigations.

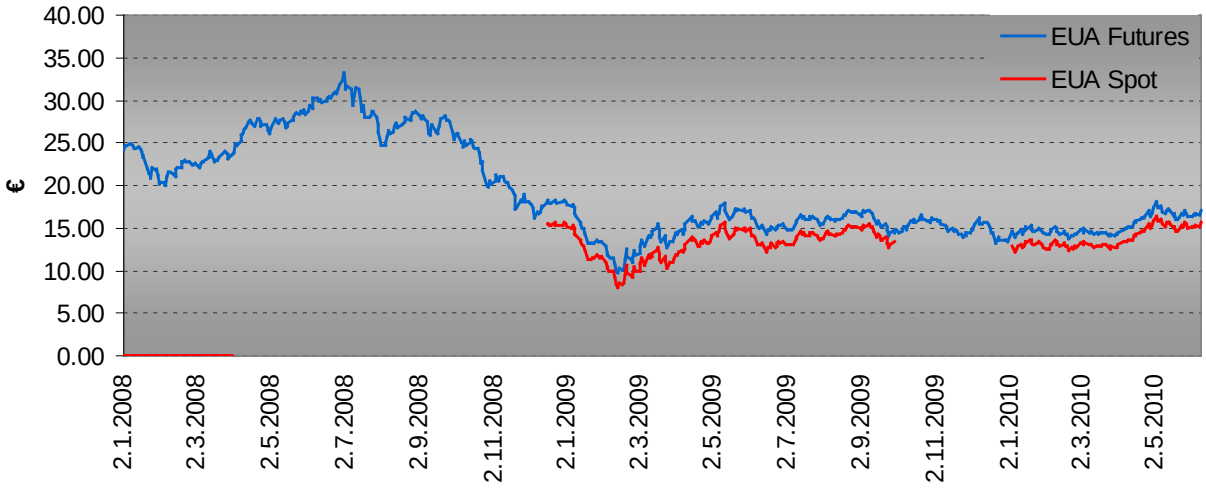

Figure 7.1: EU allowance in the years 2008-2010, Source: European Climate exchange, www.ecx.eu

Revenues

The expected revenues from the implementation of the co-firing projects are presented in Table 7.2. The first revenue is the subsidised electricity price for the electricity produced from biomass. A subsidised electricity price is applicable for Solid Biofuels, which are 100% biogenic as well as for Solid Recovered Fuels (SRF), which are only to a fraction biogenic. In the case of Greece, the new legislation on the promotion of RES [VII-6] determines the price for the electricity produced from biomass to 150 €/ MWh for applications with installed power larger than 5 MW_e and to 175 €/ MWh for applications with installed power between 1 and 5 MW_e. For electricity production from Solid Recovered Fuels the according price is 87.85 €/ MWh produced from the SRF biogenic share.

The main revenue for the power plant operator is the payment for the electricity produced on hourly rate according to the System's Marginal Price (SMP). The System's Marginal Price is determined by the electricity market and shows therefore significant fluctuations. In order to get a representative value for the calculations the monthly average of SMP in the years 2005-2010 is calculated and presented in Figure 7.2. A value of 55 €/MWh is finally considered as an indicative electricity price to be used in the calculations. The effect of the electricity price variation on the economic feasibility of the proposed concepts is then regarded through parametric investigations.

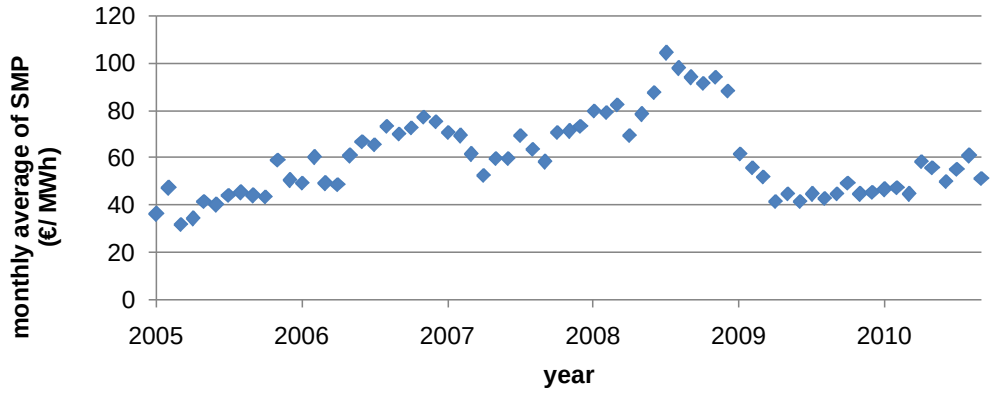

Figure 7.2: Monthly average of System's Marginal Price (SMP) in years 2005-2010, Source: Hellenic Transfer System Operator (HTSO)

Table 7.1: Comparison of costs for the investigated co-firing concepts

			Units	1. co-firing of alternative fuels		2. pre-drying and dry lignite co-firing
				a) Solid Biofuels (agricultural or forest residues)	b) Solid Recovered Fuels	
Cost categories	Investment costs	Additional fuel storage and handling system	€/ kW_e of capacity corresponding to thermal input of substitute fuel	55-85	55-85	-
		Lignite pre-drying system, connection to the boiler and the turbine house, modification of the firing system (based on data of WTA prototype)	"	-	-	270-290
	Operating and maintenance costs	Fixed Operating and Maintenance costs	€/ kWe of capacity corresponding to thermal input of substitute fuel	30	30	30
		Variable Operating and Maintenance costs	€/ MWhe from substitute fuel	1.2	1.2	1.2
	Fuel costs	Solid Biofuels	€/t	50-150	-	-
		SRF (gate fee is considered)	€/Mg of SRF co-fired	-	0-60	-
		Raw lignite (savings)	€/GJ - €/t	2.6 - 14		
	Cost for CO_2	Price of CO_2 allowances (savings)	€/ t CO_2	15		

Table 7.2: Comparison of revenues for the investigated co-firing concepts

		Units	1. co-firing of alternative fuels		2. pre-drying and dry lignite co-firing
			a. Solid Biofuels (agricultural or forest residues)	b. Solid Recovered Fuels	
Revenues	Subsidised electricity price	€/ MWh produced from substitute fuel	150	87.85 (only for the electricity from the biogenic content)	-
	Regular Electricity price	€/ MWh	55		

7.3 Calculation of CO_2 avoidance costs

In the present section the CO_2 avoidance costs for both co-firing concepts are calculated based on a realistic co-firing scenario in the Agios Dimitrios V unit. The CO_2 avoidance cost, (C_{avoid} in €/t CO_2) is given by the following expression (Eq. 7.1):

$$C_{avoid} = (C_{CO2} - C_{ref.}) / (em_{ref.} - em_{CO2}) \quad \text{Eq. 7.1}$$

whereas

$C_{ref.}$: The electricity production cost of the plant in the reference state (€/kWh)

C_{CO2}: The electricity production cost in the new plant configuration with reduced CO_2 emissions (€/kWh)

em_{ref}: The specific CO_2 emissions of the plant in the reference state (t CO_2/kWh)

em_{CO2}: The specific CO_2 emissions of the plant in the new plant configuration with reduced CO_2 emissions (t CO_2/kWh)

The electricity production cost of the lignite unit in the reference case is calculated after assuming that the unit is fully amortised. No annualised investment costs are therefore regarded. The electricity production cost of the considered unit in the reference case consist of a) Fixed Operation and Maintenance costs, b) Variable Operation and Maintenance costs, c) Fuel costs and d) costs for CO_2 allowances. The later is regarded as variable cost according to ministerial decision [VII- 7]. In order to have a projection of the electricity production costs of lignite power plants after the end of the second allocation period in 2012, the costs of CO_2 allowances are calculated according to the method to be implemented from 2013, i.e. trading of the total amount of the annual CO_2 emission allowances of a plant in the international carbon exchange markets. As CO_2 allowances price the value 15 €/ t CO_2 is taken as reference. After taking this situation as reference case, different coal substitution scenarios are considered. The first concept examined is the substitution of lignite by alternative fuels, including biomass (case 1a) or SRF (case 1b) and the second concept examined is pre-drying and dry coal co-firing (case 2). The electricity generation costs are calculated then each time for the new plant configuration. The difference in electricity production costs for the scenarios considered is related with the following factors:

- the additional operational costs of the plant, due to the continuous operation of the co-firing systems. As presented in Table 7.1 these include a) the annualised investment costs of the co-firing facilities b) the additional fuel costs, due to fuel switch or the respective savings due to the reduction of the raw coal input, c) the additional fixed Operation and Maintenance costs, d) the additional variable Operation and Maintenance costs, e) the expected savings from the CO_2 emissions reduction
- the additional revenues appearing from the operation of the co-firing systems. As presented in Table 7.2 these include the increased revenues from electricity production, due to the subsidised electricity price, when firing biomass fuels or SRF,

Concerning the SRF and biomass co-firing scenario, the thermal share proposed for the implementation of the co-firing concept in the power plant, greatly depends from aspects like fuel availability and technological parameters related with the boiler operation. In this framework a co-firing thermal share of 5% is considered for the biomass and the SRF co-firing scenario. A value of more than 5% is not favored, when utilising waste derived fuels, due to the increased chlorine content of these fuels, which may put to risk the boiler operation by increasing the chlorine corrosion and fouling potential in the boiler's convective section. Regarding fuel availability the thermal share of 5% in the particular boiler corresponds to a fuel quantity of 80.000 to 110.000 t/ a, depending from the heating value of the fuel regarded. Like in the previous section a heating value of 14 MJ/kg is regarded for SRF and 17 MJ/kg for biomass. The required fuel quantities are then about 90,000 t/a of biomass and about 109,000 t/a of SRF. The particular amount for biomass is available in the region according to previous survey [VII-8]. Concerning SRF there is no waste treatment plant in operation in the region in the present time. It is expected that such a plant will be built in the region of Western Macedonia in the coming years, because of the emerging need for alternative waste treatment options. The production capacity of such a plant would cover then the given amount of SRF regarded for the co-firing scenario.

A thermal share of 25% is considered in the case of pre-drying and dry lignite co-firing. Although the value is much higher than the thermal share in the case of SRF or biomass co-firing the investigations of the previous chapter have showed that high substitution rates up to 25% are feasible in the case of dry lignite co-firing in existing power plants, with no expected impacts on the operational behaviour of the boiler. In order to exploit the

The lifetime of all regarded co-firing facility is assumed to be fifteen years. The annual operation of the co-firing facility for alternative fuels is assumed to be 6,000 hours, while the annual operation of the pre-drying system is assumed to be 7,500 hours, the same as the annual hours of operation of the plant, since the particular system is designed for permanent operation in integration with the plant.

The installation of a lignite pre-drying system is regarded as a capital intensive investment, which has a longer pay back period and a longer lifetime, since it is regarded for a continuous operation as a basic part of the plant. Fuel availability is no issue in the case of pre-drying, since the dryer operates with the same lignite quality as of the raw lignite fired directly in the plant. On the other side, the implementation of a storage and feeding system for alternative fuels, such as SRF or biomass, in large scale boilers, requires a smaller investment, due to the lower co-firing thermal share applied and the small extend of technical modifications required in the boiler. Fuel availability or logistic issues may influence the total operational hours of the co-firing system for alternative fuels and for this reason the assumed total hours of operation of the plant in SRF or biomass co-firing mode are less than the total hours of operation of the plant.

The overall data of the regarded scenarios are given in Table 7.3. Assumptions are made for specific values, such as the electricity price, the price of CO_2 allowances, the price of biomass and the price of lignite. A sensitivity analysis is furthermore performed, in order to evaluate the effect of the variation of these prices on the CO_2 avoidance cost.

Table 7.3: Basic assumptions for the coal substitution scenarios

Data	Units	Alternative fuels co-firing		Pre-drying and dry lignite co-firing
		Solid biofuels	SRF	
Thermal share of substitution	%	5	5	25
Operational lifetime	years	15		
Hours of operation	h/a	6000	6000	7500
Biomass Price	€/ t	100	-	-
SRF Gate fee	€/Mg	-	0	-
Raw Lignite price	€/ GJ	-	-	2.6
Electricity price	€/MWh	55		
Subsidised electricity price	€/MWh	150	87.75	-

Based on the presented assumptions, the specific CO_2 emissions are calculated for the reference and the co-firing cases. In the cases of biomass and SRF co-firing the specific CO_2 emissions are decreased to 4.0% and to 2.44 % respectively, while a total decrease of about 6.64% is predicted for the dry lignite co-firing scenario, due to the high thermal share of substitution. About 2.2% from this value derives from the increase of plant efficiency (0.8 percentage points) and 4.4% derives from the fuel switch and the reduction of the lignite mass flow, due to the increased heating value of dry lignite (Figure 7.3).

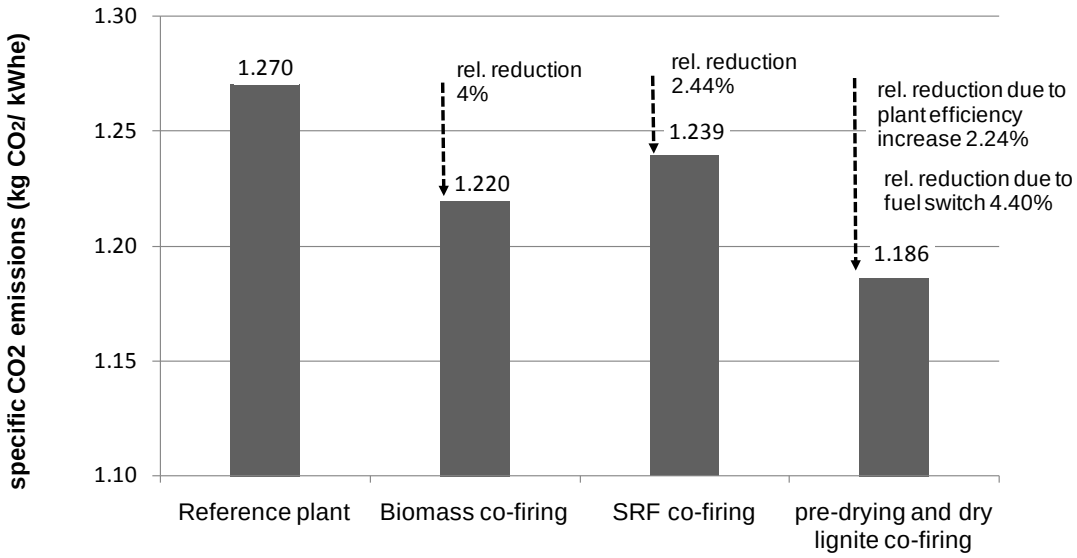

Figure 7.3: Reduction of specific CO_2 emissions by the proposed co-firing scenarios

Based on the break down of the expected additional costs of a co-firing case, presented in Table 7.1 the expected additional costs deriving from the installation and operation of the co-firing facilities are given in Table 7.4. The additional fuel costs in the biomass co-firing scenario is reasoned by the higher price of biomass compared to the price of lignite. More specific, additional fuel costs of 3.76 M € per year are registered. On the other side, in the case of SRF co-firing, respective raw lignite costs, corresponding to the SRF thermal share are saved, since SRF has no price but a gate fee of 0 €/Mg. Hence, the total fuel costs of the plant in case of SRF co-firing decrease to about 2.98 M € per year. Finally in the case of pre-drying and dry lignite co-firing lignite, fuel savings of about 4.85 M € per year are achieved through the increase of plant efficiency and the fuel switch. The annual cost in the case of SRF co-firing decreases, due to the reduced fuel expenses. In the dry coal co-firing case, the reduction of the fuel expenses is counterbalanced by the high investment costs for the pre-drying facility.

Table 7.4: Additional annual costs for the installation and operation of the co-firing facilities (in €/ a)

Annual costs	Unit	Alternative fuels' co-firing system		Pre-drying and dry lignite co-firing system
		Biomass co-firing	SRF co-firing	
Investment costs	M €/ a	0.278	0.278	4.70
Fuel costs	"	3.76	-2.98	-4.85
Fixed O&M costs	"	0.61	0.61	2.97
Variable O&M costs		0.14	0.14	0.82
Total	"	4.78	-1.95	3.65

Following these calculations the predicted CO_2 avoidance costs are 33.42 €/ t CO_2 in the case of biomass co-firing, -22.41 €/ t CO_2 in the case of SRF co-firing and 15.47 €/ t CO_2 in the case of pre-drying and dry lignite co-firing (Table 7.5). The negative avoidance cost for SRF implies that a reduction of the electricity production costs is achieved through the substitution of raw coal by SRF. In the case of biomass co-firing the calculated avoidance cost of 33.42 €/ t CO_2 is higher than the current price of CO_2 allowances, about 15 €/ t CO_2. This denotes that the particular co-firing scenario will not be economically feasible without a substitution of the electricity price for the share of energy deriving from biomass combustion. In the case of pre-drying and dry lignite co-firing the avoidance cost of about 11 €/ t CO_2 is marginally lower than the current price of CO_2 allowances. The proposed concept seems therefore to be economically feasible.

Table 7.5: CO_2 avoidance cost for the examined coal substitution cases (in €/ a)

	Unit	Reference plant	Plant with alternative fuels' co-firing system integrated		Plant with pre-drying and dry lignite co-firing system integrated
			Biomass co-firing	SRF co-firing	
CO_2 avoidance cost	€/ t CO_2	-	33.42	-22.41	15.37

In order to evaluate the effect of investment costs on electricity price and subsequently on CO_2 avoidance cost, a sensitivity analysis for the proposed substitution concepts is performed (Figure 7.4). The pre-drying concept, due to the high investment costs, is the most sensible concept to a potential change of CAPEX. The future development of pre-drying as a commercially available technology and the expected decrease of the investment costs, will further improve its economic performance, so as to become a competitive technology for reduction of CO_2 emissions in new lignite power plants. The avoidance costs of the alternative co-firing concepts are not essentially affected by a variation of the CAPEX, due to relatively low investment costs. Fuel costs represent the major part of costs in the alternative fuel co-firing concepts.

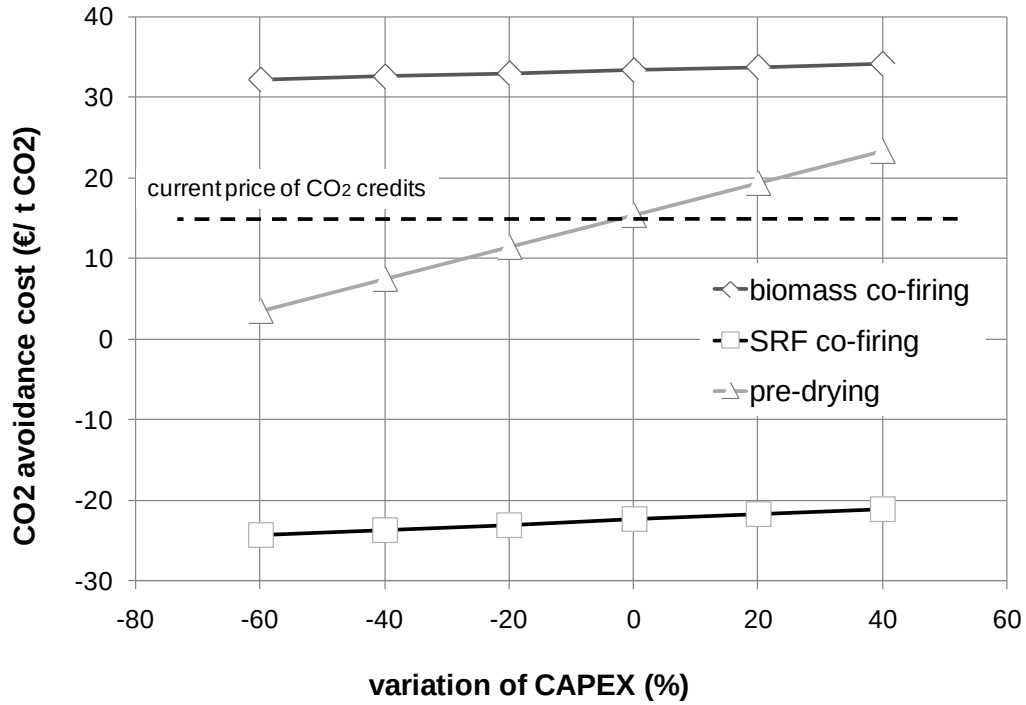

Figure 7.4: Sensitivity analysis of CO_2 avoidance cost (in €/ t CO_2) in relation with CAPEX

In order to evaluate the influence of the biomass price on the calculated CO_2 avoidance cost in the case of biomass co-firing, a sensitivity analysis is performed and presented in Figure 7.5. The operating cost and respectively the CO_2 avoidance cost of biomass co-firing are strongly affected by the biomass price. For a biomass price of about 60 €/t the avoidance cost reaches the current level of the CO_2 allowances price.

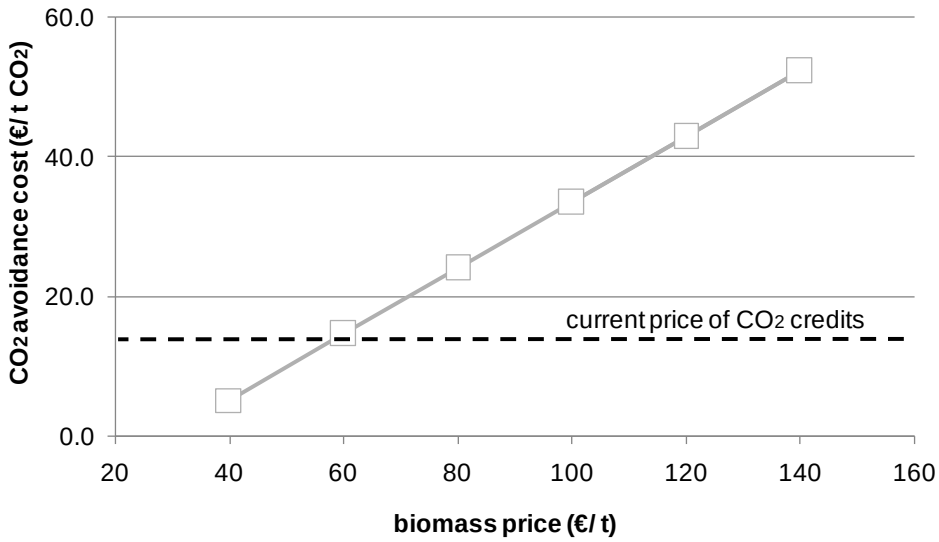

Figure 7.5: Sensitivity analysis of the CO_2 avoidance cost in the biomass co-firing scenario in relation with the biomass price

7.4 Electricity generation costs and revenues of Agios Dimitrios V unit for reference and co-firing cases

By adding the additional costs of the co-firing concepts of Table 7.4 to the annual costs (in M €/ a) of the reference plant, the new annual costs of the plant in the co-firing cases are calculated (Table 7.6) Additionally, the fifth row of the Table presents the expected costs for purchase of CO_2 emissions. The operational costs include a) the annualised investment costs of the co-firing systems, b) the new fuel costs including raw fuel savings and extra costs for purchase of alternative fuels c) new fixed operation and maintenance costs, d) new variable operation and maintenance costs, e) variable costs for CO_2 allowances to be purchased by the market by taking into account the future situation (after 2013).

Table 7.6: Annual electricity generation costs of Agios Dimitrios V unit for reference and co-firing cases (in €/ a)

Annual costs	Unit	Reference plant	Plant with alternative fuels' co-firing system integrated		Plant with pre-drying and dry lignite co-firing system integrated
			Biomass co-firing	SRF co-firing	
Investment costs	M €/ a		0.278	0.278	4.70
Fuel costs	"	74.36	78.12	71.39	69.52
Fixed O&M costs	"	12.15	12.76	12.76	15.12
Variable O&M costs		3.38	3.51	3.51	4.20
Variable costs from ETS (after 2013)		53.59	51.45	52.28	50.03
Total	"	143.68	146.11	140.22	143.57

The expected revenues when implementing the proposed co-firing concepts are given in Table 7.7, expressed in M €/a. Since the expected revenues are higher than the increase of the operating costs in all co-firing cases considered, it is concluded that the implementation of the proposed co-firing scenarios may be profitable for the plant operator. In other words, the implementation of any of the co-firing concepts regarded seems to be a profitable investment according to this first analysis. More detailed examination of the particular co-firing scenarios in terms of their economic competitiveness will be presented in the next section.

Table 7.7: Annual total revenues of Agios Dimitrios V unit for the reference and the co-firing cases (in €/ a)

Annual Revenues	Unit	Reference plant	Plant with alternative fuels' co-firing system integrated		Plant with pre-drying and dry lignite co-firing system integrated
			Biomass co-firing	SRF co-firing	
Electricity production	M €/ a	154.69	154.69	154.69	154.69
Subsidised el. price	"	-	10.69	1.85	-
Total	"	154.69	165.38	156.54	154.69

An overall picture of the expected costs and revenues in the reference and co-firing cases expressed in €/ MWh is given in Figure 7.6

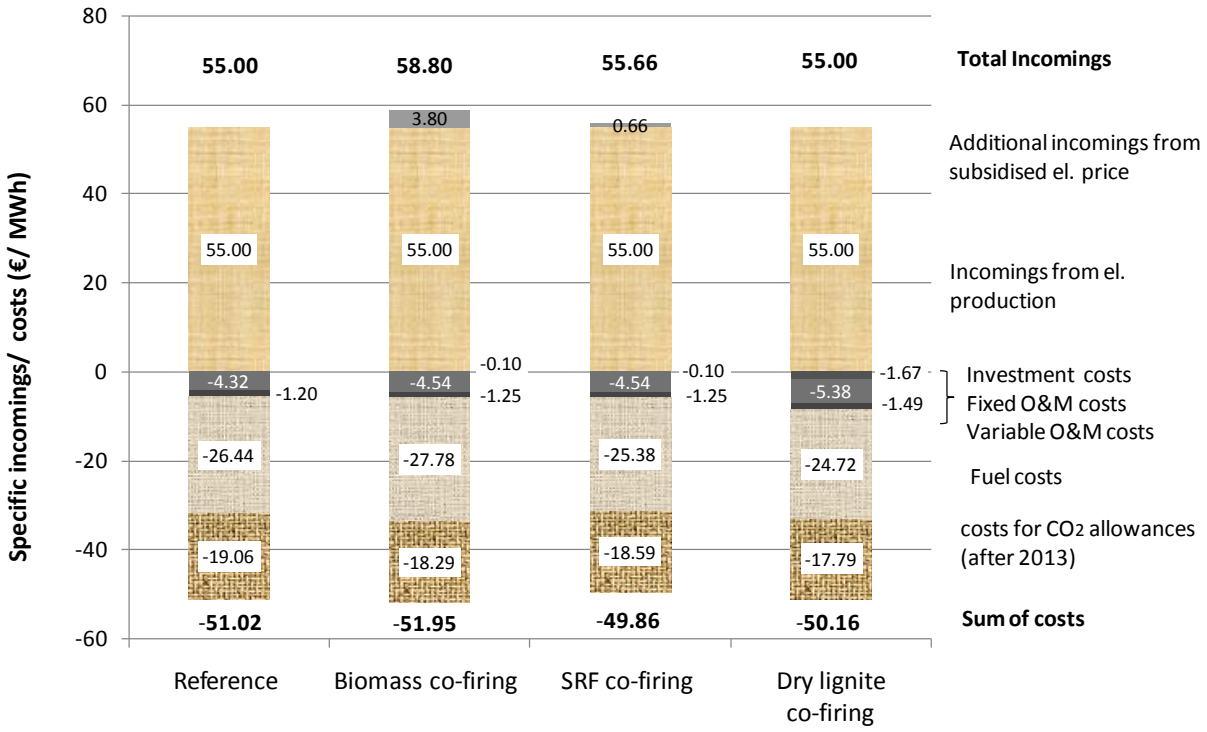

Figure 7.6: Electricity generation costs and revenues for the whole plant in reference and co-firing cases (in €/ MWh)

7.5 Economic viability of the proposed brown coal substitution concepts

The proposed co-firing concepts are compared in this section in terms of their economic competitiveness. The assumptions of the previous co-firing scenario are also taken into account in the present analysis: a) co-firing thermal share of 5% in one unit in the cases of biomass and SRF co-firing and b) thermal share of 20% in two units in the case of application of pre-drying and dry lignite co-firing. Three economic indices are calculated for the evaluation of the considered investments the Net Present Value (NPV), the Internal Rate of Return (IRR) and the payback period of investment

The Net Present Value is the sum of all years' discounted after-tax cash flows. It is an indicator for the time value of money. Projects, which have positive NPVs, are considered as attractive. NPV is calculated according to Equation 7.2

$$NPV = \sum_{t=0}^{n} \frac{CF_t}{(1+r)^t} \qquad \text{Eq. 7.2}$$

where

NPV: the Net Present Value of the project (s),

CFt : the cash flow of the investment in time period t (s),

r : the discount rate (%),

t : the time period from 0 to n (years).

NPVs of different projects can be summed up and the total benefits from the implementation of the regarded investments can be quantified. On the other side, no discount rate can be determined from NPV since it is an absolute variable and does not express the accurate rate of profitability.

The internal rate of return (IRR) is defined as the discount rate at which the NPV is zero, which means that the present value of the investment funds equals the net present revenues from operation. The calculated IRR is examined to determine if it exceeds a minimally acceptable return (sometimes called ‘‘the hurdle rate’’). IRR is defined in Equation 7.3

$$0 = \sum_{t=0}^{n} \frac{CF_t}{(1+IRR)^t} \qquad \text{Eq. 7.3}$$

where

IRR: the Internal Rate of Return,

CFt : the cash flow of the investment in time period t (s),

The main characteristic of IRR is that, it may be used for the comparison of projects of different sizes. If the calculated IRR of a project is higher than the discount rate, then the project is considered as attractive, otherwise it should be rejected. The higher the IRR, the more profitable is the project. As regards the payback period it is determined by the comparison of revenues with costs. It is the length of time required to recoup the initial investment. In the particular calculation of the payback period the time value of money is considered.

The main economic parameters, which are common for both proposed concepts and are considered in the investment plan are:
Inflation rate: 3.5%
Interest rate: 8%
Loan payback period: 10 years
Tax rate: 25%
Further economic parameters, which are different in the two investment plans, are presented in Table 7.8. A total project development and construction time of two years and a total investment lifetime of 20 years is regarded for the alternative fuel co-firing project, while in the case of the pre-drying and dry lignite co-firing project the total development and construction time regarded is 3 years and the total investment lifetime is also 20 years.
The two co-firing concepts regarded actually represent two different types of investment. The alternative fuels co-firing project is considered as a medium size investment with capital expenditures in the range of 2 to 3 M €, depending on the fuel handling technology to be installed. On the other side, the integration of a pre-drying system in the steam cycle of two power plants is considered as a large scale investment with estimated capital expenditures in the order of 60 M €. No additional revenues through subsidised electricity prices can be regarded in the case of pre-drying and for this reason a prolonged payback period is expected.
Another difference between the two co-firing projects considered is related with the financing program of investments. The investment on alternative fuels co-firing has medium capital requirements and for this reason it is assumed that it will be covered by the operator's own funds to 70% and by loan to 30%. In the case of predrying and dry lignite co-firing the the inclusion of the project in the development law and the retrieve of a public funding to 20% of the capital expenditures is regarded. The operator's own funds invested in the project would be then 50% of the total expenditures and the loan 30%.

Table 7.8: Economic parameters for the calculations

	Alternative fuels co-firing (biomass/ SRF)	Lignite pre-drying and dry lignite co-firing
Thermal share of substitution	5	25
Project development and construction time	2	3
Investment life time (years)	20	20
CAPEX (M €)	2.4	61.2
% of investment covered by own capital	70	50
% of investment covered by loan	30	30
% of investment covered by subsidy	0	20

The results of the calculated economic performance indices under the mentioned assumptions are presented in Table 7.9. The cumulative cash flows of the considered projects for a time

period of 20 years are presented in Figure 7.7. The two alternative fuel co-firing concepts show an exceptionally positive economic performance. The calculated IRR is very high and the payback period ends already in the first year of the operation of the co-firing facility. The calculated annual revenues and expenses of the two co-firing cases presented in Tables 7.4 and 7.7 are used. The implementation of the regarded biomass co-firing project would bring additional annual revenues of 10.69 M €/a to the power plant operator, while the expenses would increase to 4.78 M €/a. Accordingly, the implementation of SRF co-firing would bring additional annual revenues of about 1.85 M €/a, while the annual expenses would decrease to about 1.95 M €/a. The particular investment is much more profitable compared to a dedicated facility for biomass and/or SRF combustion, due to the utilisation of the existing capacity of the power plant (boiler, steam turbine, generator, flue gas cleaning system) and the minimum additional infrastructure required. The subsidised electricity price for biomass and SRF's biogenic content is another factor which influences positively the profitability of the investment.

On the other side, the project on the integration of pre-drying in existing steam cycle seems to be a large investment with a long payback period of 19 years and a low IRR. In other words it can hardly be considered as a short to medium term project for the reduction of CO_2 emissions in existing power plants with a limited remaining lifetime. It should be more regarded as a retrofitting option for new power plants or ideally as an option for increasing efficiency of new projects of brown coal power plants, which are currently in the design phase. If the integration of the dryer into the steam cycle is in detail planned during the initial design phase of the power plant, then considerable savings can be achieved, which may greatly reduce the additional investment cost considered in this analysis. More specific, savings are possible through the downsizing the whole conventional flue gas recirculation and milling system, due to the reduced raw coal input in the case of permanent dry coal co-firing.

Table 7.9: Calculated NPV, IRR and payback period for the regarded co-firing scenarios

	Biomass co-firing	SRF co-firing	Lignite pre-drying and dry lignite co-firing
Net Present Value (M €)	25.02	23.81	7.69
IRR (%)	116.5	95.6	9.2
Payback period (years)	2	2	18

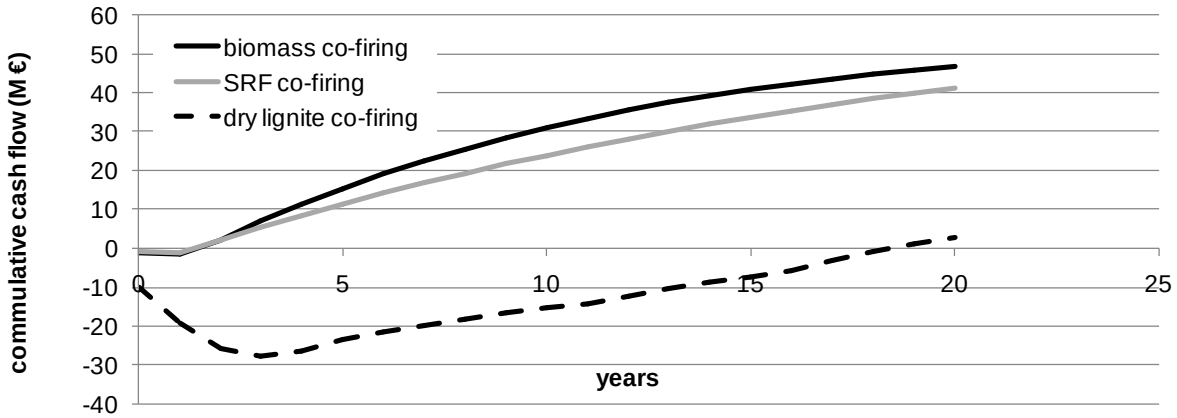

Figure 7.7: Cumulative cash flows (M €) for the regarded co-firing concepts

The influence of the price of CO_2 allowances on the feasibility of the investment is investigated by sensitivity analysis in the three co-firing cases. The predicted economic indices IRR and payback period are presented in Figure 7.8a, b. The interest should be focused on the pre-drying concept since the alternative co-firing concepts show exceptionally high IRR, due to their low investment costs and the high expected revenues. For a CO_2 price higher than 20 €/ t CO_2 the IRR becomes greater than 12% and the payback period is reduced to less than 15 years.

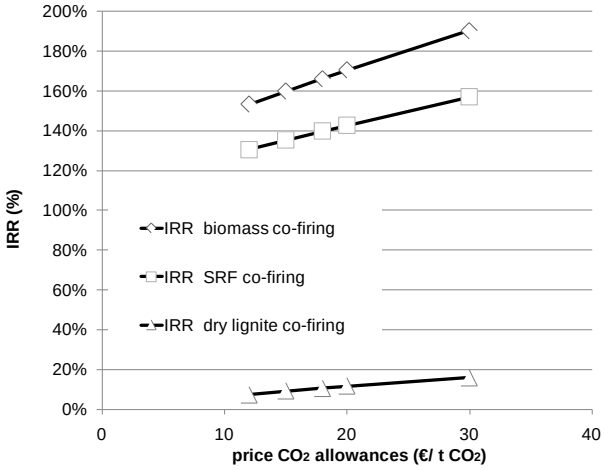

Figure 7.8 a: Sensitivity analysis of IRR in relation with price of CO_2 allowances

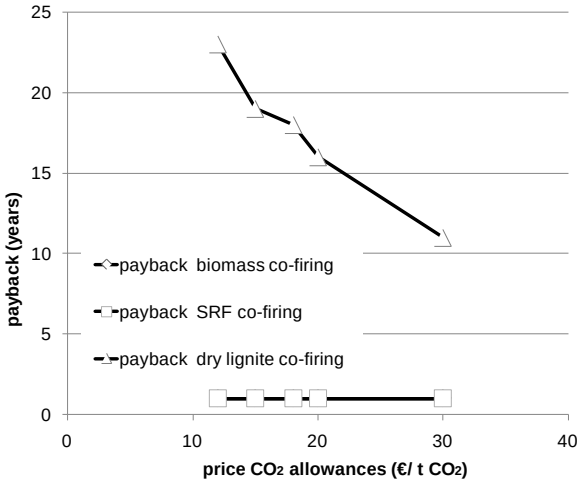

Figure 7.8 b: Sensitivity analysis of payback period in relation with price of CO_2 allowances

A similar picture is obtained in the evaluation of the effect of capital expenditures (CAPEX) on the project feasibility presented in Figure 7.9a, b. The regarded CAPEX of the pre-drying concept brings a marginally acceptable economic effectiveness for the particular project, while a further increase of the investment costs would lead to an insufficient economic performance. On the other side, a potential decrease of the initial investment costs to about 20%, which can be expected due to the commercialization of the technology, leads to an IRR greater than 15% and to a payback period less than 12 years.

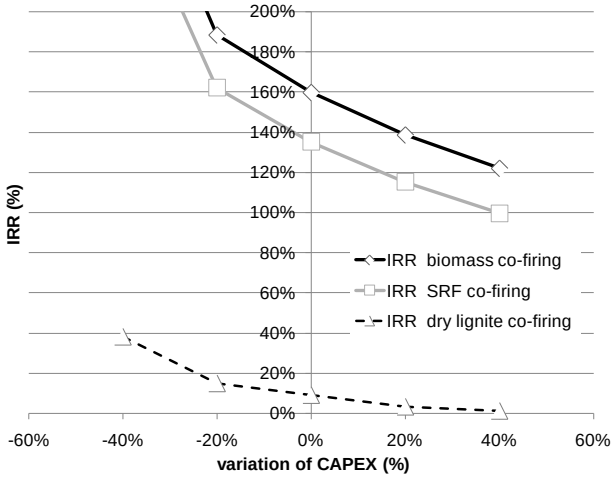

Figure 7.9 a: Sensitivity analysis of IRR in relation with variation of CAPEX

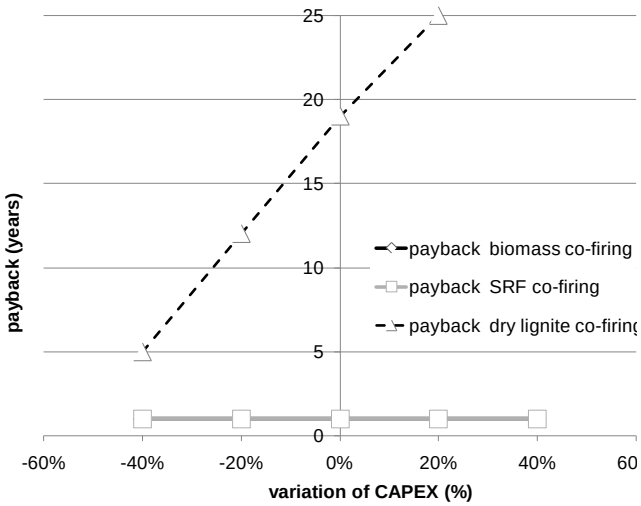

Figure 7.9 b: Sensitivity analysis of payback period in relation with variation of CAPEX

7.6 Contribution of the regarded co-firing concepts on the achievement of CO_2 reduction targets and the respective financial aspects

In the final part of the economic analysis the potential CO_2 emissions savings by the implementation of the proposed co-firing concepts are evaluated. The expected additional revenues from the implementation of the co-firing projects are compared with the estimated additional expenses of the plant operator, due to the implementation of the ETS mechanism in the second allocation period (2008-2012) and in the third allocation period (after 2013). Particularly for the Agios Dimitrios power plant, the annual allocated emissions for all five units are 11,049,784 t CO_2. [VII-9], [VII-10]. A calculation of the allocated emissions of unit V is attempted after the assumption of same operation time for all units. The breakdown of the emissions allocated for the whole plant is based then according to the installed power of each unit. The calculated amount of CO_2 allowances for unit V is 2,597,912 t CO_2/a. Based on the assumptions presented before regarding fuel quality, plant efficiency and operational time, the expected CO_2 emissions are calculated to about 3,573,000 t CO_2/a. The annual deficit is respectively calculated to about 975,000 t CO_2. The sum of annual deficits in the period 2008-2012 has to be covered until the end of the second allocation period in 2012. From 2013 no allocation is foreseen for the CO_2 emissions from coal power plants and 100% of the emissions will be traded. The particular results are presented in Figure 7.10 together with the expected emission savings from a potential implementation of the regarded co-firing concepts. It should be noticed that the real CO_2 emissions from unit V may be lower than calculated, due to a slightly higher efficiency rate, better fuel quality or reduced operating hours. However, the tendency will remain the same. In other words, the implementation of biomass co-firing in a thermal share of 5% may reduce the annual CO_2 allowances deficit for the years 2010-2012 to about 12%, while the implementation of pre-drying and dry lignite co-firing in a thermal share of 25% may reduce the expected deficit to about 24%.

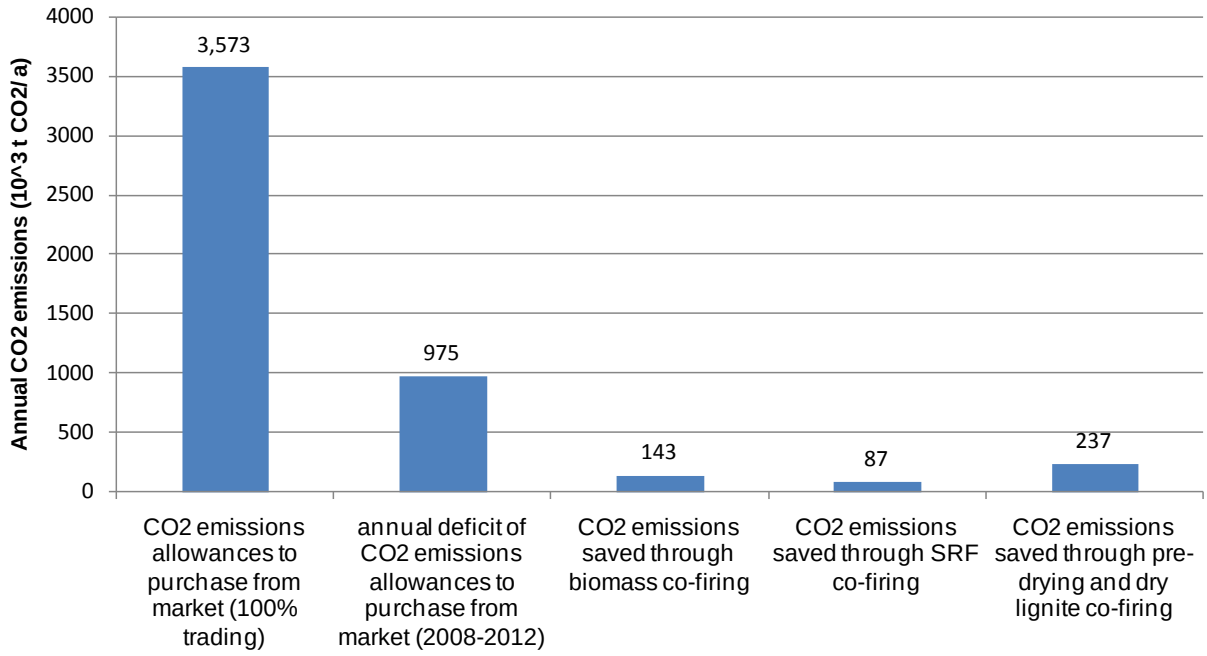

Figure 7.10: Expected annual CO_2 emission allowances to be traded in the second allocation time and after 2013 and respective CO_2 reduction through the realization of the considered substitution concepts

7.7 Conclusions of the economical assessment

The regarded coal substitution concepts are evaluated and compared in terms of their economic performance in the previous section. By the overall analysis it is concluded that the proposed concepts correspond to different investment practices. The implementation of alternative fuel co-firing is considered as a short to medium term, low risk investment, with low investment costs and significant revenues, due to the subsidized electricity price for biomass or SRF combustion or co-combustion. The payback period is respectively very short and the particular investment is characterized as highly profitable. The main difficulty for the realisation of such a project is securing fuel availability and the development of a logistic system for the continuous fuel supply of the power plant. The particular subject is not in the scope of this thesis. Because of the insecurity of fuel availability and the common difficulty in reaching long term supply contracts for biomass or SRF the regarded investment time was set to ten years for this co-firing scenario. It is not excluded that such a project may have a longer lifetime, however the initial financial calculations performed are based on this limited lifetime.

On the other side, the integration of a pre-drying concept into an existing power plant is a challenging project with increased capital expenditures and long payback period. It is characterised therefore as a long term investment. Based on the performed economic analysis the profitability of such a concept is marginal, and under the current price of specific investment costs and of CO_2 allowances it can hardly be proposed as an efficient practice to reduce CO_2 emissions in existing power plants. However, the specific investment costs of the particular technology are expected to decrease in the coming years through the application of the particular technology in the large scale, while the price CO_2 allowances is expected to increase above 15 €/ t CO_2, which is regarded as reference in the particular calculations. In this framework, pre-drying is expected to become economically feasible as a retrofitting option in the coming years. It should be noted that it is already an economically effective option for increasing plant efficiency in new lignite power plants, which are still in the planning phase. Savings in conventional plant equipment, such as in the milling and in the flue gas recirculation system, can be achieved, if the integration of the fluidized bed dryer is planned from the beginning, so that a considerable decrease of the total investment cost for the plant will be possible.

8 Summary and conclusions

In the previous chapters two different technological concepts for the reduction of CO_2 emissions from existing coal power plants through substitution practices of raw coal are presented and analysed. The first concept examined is the substitution of coal by alternative fuels with high biogenic content, while in the second concept the integration of a brown coal pre-drying concept and the substitution of raw brown coal by dried brown coal is assessed. Environmental, technological and economic parameters are used as performance indices for the analysis, while the considered analysis tools are experimental measurements, numerical simulations and thermal cycle calculations. Additional investigations in small-scale facilities are also performed as supportive actions for the evaluation of the large-scale substitution concepts. The results of the assessment of both proposed concepts are presented and compared in this section in a comparative way. Moreover, additional operational aspects, which are not analysed in the previous chapters and are important for the reliable plant operation in long-term perspective, are also addressed. In the final part a future outlook on the further development of the investigated substitution concepts is given.

8.1 Evaluation of examined environmental aspects

The main environmental aspects considered are the CO_2 emission reduction and the conventional and non-conventional flue gas emissions. The potential CO_2 emission reduction for both concepts was assessed in Chapter 2.3. A specific Greek power plant was considered for the scope of the analysis and a co-firing thermal share of 5% was regarded for both concepts. The annual emissions savings were calculated for the co-firing cases with alternative fuels: 1 a) co-firing solid biofuels such as agricultural or forrest residues, 1 b) co-firing SRF with a biogenic share of 50% and 2) for the pre-drying and dry lignite co-firing case. Following CO_2 emission savings are calculated for the three cases 1a) 178,642 t CO_2/a for biomass co-firing, 1b) 108,976 t CO_2/a for SRF co-firing and 2) 53,260 t CO_2/a for dry lignite co-firing. These amounts correspond to a reduction of annual CO_2 emissions of the considered plant to 5%, 3.1% and 1.5% accordingly. Co-firing of alternative fuels has therefore a higher potential of CO_2 emissions reduction compared to the pre-drying concept, while this potential naturally increases by increasing biogenic share. The particular result is presented in Table 8.1 by denoting two “+” signs for the alternative fuels co-firing concepts and one in the predrying concept. The only remark at this point would be that higher rates of substitution, up to 25% on thermal basis, are required for optimising efficiency increase in the integration of a lignite pre-drying concept in an existing power plant. In this case the expected relative reduction of CO_2 emissions would be about 6.6% corresponding to annual emission savings of about 237,000 t CO_2.

Considering the environmental performance in respect of conventional flue gas emissions (CO, SO_2, NO_x) it should be at first stated that the emission values stayed within the applicable legislative limits during both large scale co-firing tests. In the SRF co-firing case no significant change of the combustion behavior and the conventional flue gas emissions is expected, due to the low thermal share - up to 5% - that is usually applied. The nitrogen or sulfur content of SRF usually differ from the one of raw fuel. Specifically, in the performed large scale tests SRF had higher nitrogen content and comparable sulfur content compared to Rhenish brown coal. No tendency on increased NO_x or CO emissions was however observed during the co-firing tests. It is assumed that the low co-firing share and the unaltered combustion conditions do not facilitate a significant increase of NO_x production or a

significant increase of CO production that could be experimentally measured. The only parameter which could influence this behavior in a greater extend is the injection location of the alternative fuel. In the large scale SRF co-firing tests the injection locations of SRF remained the same with these of raw coal. A change of the respective injection may in turn affect the combustion behavior in a higher extend and this was investigated through numerical simulations.

A different picture is observed in the case of dry coal co-firing. The high co-firing shares up to 25% usually applied in this scenario may lead to a change in the NO_x formation mechanism. Increased NO_x production caused by the elevated flame temperatures and a respective promotion of the thermal NO_x formation mechanism can be expected. It should be also regarded that the average nitrogen concentration per mass of fuel input increases in the co-firing cases, due to the reduced moisture of pre-dried lignite. Although NO_x concentration did not exceed the given legislative limits during the performed experimental campaign, higher NO_x abatement rates may have to be reached in the case of future boiler co-firing pre-dried lignite through increased air or air and fuel staging. For this reason an exclamation mark is noted for the particular parameter on Table 8.1.

As regards the environmental performance of the co-firing concepts in respect of non conventional emissions such as HCl concentration in the flue gas, heavy metal concentration in the ash and the flue gas and dioxine and furanes concentration in the flue gas, only the SRF co-firing case is assessed. No change of the respective non conventional emissions is expected in the dry lignite co-firing case, since dry lignite, which is used as substitute fuel, has the same composition with the raw fuel. The effect of SRF on the above mentioned emissions was evaluated through respective measurements in the flue gas and the solid by products (fly ash, wet bottom ash, gypsum). No clear changes could be observed in the particular emission levels during the stack measurements and in the quality of the solid by products. An increase of the HCl concentration in the boiler exit was measured. This was however not reproduced in the stack measurements implying that HCl could be bound during the scrubbing process in the desulphurisation unit. The observed changes were in any case very low, due to the low thermal share of substitution while the stricter emission values imposed by the Waste Incineration Directive could easily be kept during the whole demonstration period, without altering the ordinary boiler operation. Regarding dioxins - furanes formation no tendency was observed in the dedicated measurements, while the respective concentration of dioxine stayed below the detection limit. Again the low co-firing share could be a reason for this results combined with the high residence time of the SRF particle in the high temperature regions of the boiler (more than 5s) expected that were also confirmed by the numerical simulations.

Table 8.1: Evaluation and comparison of environmental parameters

		Proposed coal substitution concepts	
		SRF co-firing	Lignite pre-drying and dry lignite co-firing
Environmental aspects	CO_2 emissions	√ (++)	√ (+)
	Conventional flue gas emissions (NO_x, SO_2, CO)	√	!
	HM in the flue gas	√	n.r.
	HCl	√	n.r.
	Dioxines - Furans	√	n.r.
	Ash quality: HM in the ash	√	n.r.

8.2 Evaluation of examined operational aspects

Several parameters are assessed related with the operational behavior of the regarded industrial boilers and the corresponding effect of co-firing on it. A qualitative picture is usually provided by the on line monitored process related parameters, among others the flue gas and steam temperatures and produced power. In both large scale measurement campaigns the online parameters are monitored and evaluated. No clear influence of co-firing on the boiler's process data is found indicating that the investigated concepts have a moderate impact on the related process parameters. A more general picture of the boiler's operational behavior is obtained by evaluating potential changes of the boiler's heat balance. SRF co-firing is not expected to have a considerable effect on the boiler's heat balance, due to the low co-firing share applied and the unaltered combustion conditions. An indication on expected changes of the heat balance is also provided by evaluating the heat flux to the evaporator. In case of a drastic change on the evaporator heat flux, it is expected that the boiler heat balance will be accordingly affected. In the case of SRF co-firing no such change is observed and even in the numerical simulations no considerable effect of co-firing on the evaporator heat flux is predicted. The effect of pre-drying and dry coal co-firing on the boiler heat balance is evaluated by thermal cycle calculations, since the industrial scale integration of the WTA dryer in an existing plant is still in a development phase, and no data is available from the industrial scale prototype. The 375 MW_e Agios Dimitrios V boiler is used as the reference unit for the thermal cycle calculations. Thermal shares of substitution of 10%, 20% and 30% are considered and the overall plant steam cycle is calculated for the reference and the co-firing cases. An increase of the evaporator heat flux is predicted by increasing the co-firing share due to the higher radiative flux caused by the increased adiabatic temperature. This in turn leads to increased quantities of cooling water in the steam coolers, which changes the whole energy balance also in the convective section. The total useful heat of the boiler increases leading to increased boiler efficiency. The net plant efficiency also increases. All these predicted changes imply that the effect of pre-drying and dry coal co-firing on the plant's heat balance cannot be neglected. It has to be studied in detail before the integration of any pre-drying system in existing power plants. For this reason the particular parameter is noted with an exclamation mark in Table 8.2.

The combustion conditions in the furnace and at the furnace exit are evaluated through experimental measurements and numerical simulations. Profile measurements of temperature and flue gas composition are carried out at the furnace exit during the large scale campaigns. No considerable changes of the combustion conditions at the furnace exit are observed in the case of SRF co-firing. This behaviour is also confirmed by the performed numerical simulations. A different tendency is noticed in the case of SRF co-firing. The average flue gas temperature increases, when increasing the dry coal co-firing share, because of the decrease of the flue gas mass flow. The particular tendency is noticed in the small scale experimental campaigns and in the respective numerical simulations. It could not be observed during the industrial scale measurements, probably, due to the low co-firing share and the increased fluctuations of the flue gas temperature. A temperature increase of the furnace exit temperature up to 50 K is predicted in the maximum thermal share of substitution, 30%. This value is obtained from thermal cycle calculations and numerical simulations. The respective increase of the furnace exit temperature may influence the overall boiler heat balance; however it is not expected to pose additional risks to the boiler operation. Nevertheless, in the case of a large scale dry coal co-firing demonstration it is recommended to continuously monitor the flue gas temperature at the convective section, so as to have a clear picture on changes in the temperature levels. Regarding the effect of the temperature increase on the ash

melting behavior detailed tests have been carried out in the 1 MW_{th} combustor. The Greek lignite has in general a low slagging and fouling propensity compared with the Rhenish lignite that is used as reference fuel. The expected temperature rise of 50 K is furthermore considered as moderate; hence no operational problems due to slagging and fouling are expected. It is nevertheless advised to monitor the respective tendency in case of a large scale demonstration through dedicated deposition probes. In this sense, the particular parameter is designated with an exclamation mark in Table 8.2.

The fuel burnout is another technical aspect evaluated during the examinations. Dry lignite co-firing leads to a clear improvement of the fuel burn out, due to the higher flame temperatures and the earlier ignition of lignite particles owed to the reduced water content of pre-dried lignite. A different picture is obtained in the case of SRF. The main fractions of SRF, the biogenic and plastic, have a different combustion behaviour. On the one side the biogenic fraction of SRF, which is composed of fluffy materials derived from paper or card board, usually shows a satisfying burnout due to its increased surface to volume ratio and its high residence time in the boiler. On the other side, plastic particles have to undergo several steps before being combusted, including melting and evaporation of the respective droplets. Depending on the point of injection and the particles diameter, they may have enough time for complete evaporation and combustion or they may fall into the hopper before being completely combusted. This behavior is also proven by the numerical simulations in the industrial scale boiler. The burnout of SRF has therefore to be closely assessed for each industrial facility, since there is no common effect expected in every application. For this reason the particular parameter is designated with an exclamation mark in Table 8.2.

The final technical aspect evaluated is the potential effect of SRF's chlorine content on corrosion induced phenomena at the boiler's superheater stages. The electrochemical corrosion potential was monitored by dedicated online monitoring probes during the large scale SRF co-firing campaign. The corrosion risk imposed by the increased chlorine content in SRF cannot be characterized as negligible. However, specific indications on increased risk for permanent damages at the superheater stages, due to corrosion were not found. The particular tendency has generally to be monitored and evaluated in each SRF co-firing case due to the high differences in coal quality. The coal quality considerably affects corrosion related phenomena. The successful long term operation of several brown coal power plants in SRF co-firing mode indicates that the corrosion issue may be successfully assessed and controlled, if additional parameters are closely monitored by online monitoring equipment and if the quality of alternative fuels co-fired is systematically monitored and evaluated by quality control and management systems.

Table 8.2: Evaluation and comparison of technical parameters in the substitution concepts proposed

		Proposed coal substitution concepts	
		SRF co-firing	Lignite pre-drying and dry lignite co-firing
Technological - operational aspects	Operational parameters (steam temperatures, P_e)	√	√
	Heat flux to evaporator	√	!
	Overall boiler heat balance	n.i.	!
	Boiler Efficiency (η_{boiler}) Power plant efficiency (η_{PP})	n.i.	√
	Furnace exit conditions (temperature, O_2)	√	√
	Combustion conditions in the furnace (temperature and O_2)	√	√
	Risk of potential operational problems due to slagging and fouling	n.i.	!
	Ignition/ Burnout	!	√
	Risk of potential operational problems due to chlorine corrosion	!	n.r.

"nr": no change is anticipated for the specific parameter and, therefore, it is considered as "not relevant" for the examination

"ni": the specific parameter is "not investigated"

8.3 Evaluation of other operational aspects

A number of additional operational aspects which are not closely related to the boiler operation are addressed in this section. The implementation of both coal substitution concepts requires several modifications in the boiler and the balance of plant, which have to be addressed. For the realization of an SRF co-firing concept in an existing coal power plant an area for the delivery and storage of SRF has to be established in the plant site. A closed storage is preferable so that spoiling is avoided and the fuel is adequately protected from weather and fire. The ventilation of the storage space has to be carefully designed so that smells from the biodegradable material of SRF, if an ongoing degradation process occurs, are eliminated. Feeding of the SRF can be realised by pneumatic transportation, while the existing coal conveyor belts can also be used in the case of feeding of SRF together with coal before the coal mills. Concerning the injection into the furnace, several scenarios were analysed and evaluated in Chapter 4. No optimum scenario can be determined. The scenarios which are considered the most problematic will not be further investigated in future evaluations.

Regarding the implementation of dry coal co-firing, larger retrofitting works are required than in the case of SRF co-firing. For the integration of a lignite fluidised bed dryer in an existing steam cycle, the construction of new piping connections between the steam turbine house and the dryer are necessary for: (a) the steam bleed required in the drying process and (b) the

evaporated coal moisture which is utilised as heating medium in the initial feed water pre-heaters. Furthermore, the construction of an additional pneumatic transportation system for dry lignite dust and the installation of dedicated dry lignite burners in the boiler is required. It is possible, however, to use dry lignite burners with integrated oil burners so that they can be placed in the location of the start-up burners in order to avoid new openings and major technical modifications in the furnace.

8.4 Evaluation of examined economical aspects

The evaluation of the economic aspects indicates that the proposed concepts correspond to different investment practices. The implementation of alternative fuel co-firing is considered as a short to medium term investment, with low investment costs and relatively high revenues, due to the subsidized electricity price for biomass or SRF combustion or co-combustion. The payback period is very short and the particular investment is characterized as highly profitable. The main difficulty for the realization of this project is related with fuel availability and the development of a logistic system for the continuous supply of the boiler with alternative fuels. On the other side, the integration of a pre-drying concept into an existing power plant is challenging with increased capital expenditures and long payback period. It is characterised therefore as a long term investment. Based on the performed economic analysis its profitability under the current price of specific investment costs and of CO_2 allowances is marginal. However, the specific investment costs of the particular technology are expected to decrease in the near future, while the price CO_2 allowances is expected to increase above 15 €/ t CO_2 regarded as reference in the particular calculations. In this perspective, pre-drying is expected to become economically feasible as a retrofitting option in the future. It is already an economically effective option to increase plant efficiency of new lignite power plants, which are still in the planning phase. Savings of investment costs may be achieved, if the integration of the fluidized bed dryer into the conventional steam cycle is effectively planned and overcapacity of the existing milling system, with respect to the continuous availability of the pre-drying system, is avoided.
The results of the economic assessment are summarised in Table 8.3. All economic indices are positive in case of alternative fuels co-firing, while in case of pre-drying and dry lignite co-firing the high investment cost combined with the limited economic revenues, due to the lack of subsidizes in the electricity generation, lead to marginal profitability.

Table 8.3: Evaluation and comparison of ecomomic parameters in the substitution concepts proposed

		Proposed coal substitution concepts	
		SRF- cofiring	Lignite pre-drying and dry lignite co-firing
Economical aspects	Expected investment and running costs	√	!
	CO_2 avoidance costs	√	√
	Feasibility of investment (IRR, NPV, payback)	√	!

8.5 Conclusions and future outlook

Two different coal substitution technologies were evaluated in detail by environmental, technological and economical parameters in the previous sections. Several topics, which are introduced and analysed in this thesis, have to be further investigated in future research activities. The accurate modeling of SRF particles motion and combustion, as well as the investigation, control and mitigation of chlorine induced corrosion phenomena are some of the most significant research targets regarding SRF co-firing. On the other hand, the mitigation of NO_x emissions through optimization of firing system, the investigation of effects of dry coal co-firing on slagging and fouling, and the prediction of the expected changes in the boiler's heat balance are important parameters to be further examined in the field of the pre-drying and dry lignite co-firing technologies.

A number of additional parameters, which may not be technology related, will influence the final decision between the two technologies. The availability of alternative fuels, the logistics, the capacity for investment and the operational plan of the plant operator, even the environmental concerns of the society may influence or even determine the decision making process. The particular study provides answers to issues regarding the environmental, technical and financial performance of both concepts. The important outcome of this thesis is that, from technological point of view, the realization of these co-firing scenarios is feasible in the short term. This message should be therefore considered as an additional motivation for power plant operators to act and undertake serious initiatives for the reduction of CO_2 emissions in existing coal power plants.

Appendices

A. Overview and physical basis of comprehensive combustion models

A1 Introduction

For the description of the overall physical phenomena applied during coal combustion in pulverised fuel boilers, many different submodels are considered addressing important physical and chemical processes which take part in the combustion process. The term "comprehensive combustion models" is used to indicate that these submodels have been modified and assembled into an integrated model with a specific solution approach which can adequately simulate the overall combustion process. Although the comprehensive combustion models known can simulate gaseous or liquid fuel combustion besides solid fuel combustion, the current examination will focus on the combustion related phenomena of solid fuels.

Since comprehensive combustion modelling aims at the prediction of combustion processes in sufficient accuracy in the cases of real geometries ranging from the lab up to industrial scale, simplified models derived from widely accepted modelling assumptions are used for the physical phenomena considered, in order to save computational time. A typical example is modelling coal volatile combustion. Global reaction mechanisms are usually adopted, despite the fact that detailed reaction mechanisms with more than 100 reactions are known for methane and other hydrocarbons. The implementation of such detailed mechanisms in industrial applications would, however increase the computational time several orders of magnitude, while it is doubtful whether the extended mechanisms are able to provide more realistic results as long as the detailed composition of coal volatiles in industrial-scale conditions cannot be accurately determined. For all submodels considered similar compromises are made between computational effort and accepted accuracy imposed by the models and the boundary conditions applied.

As a result of the special focus and the limitations of the models mentioned, accurate predictions of various combustion related parameters can be obtained by means of the numerical solution of the respective equations, including gas composition, velocities, particle trajectories, particle burnout, NO_x formation, wall heat fluxes. On the other hand, limited accuracy can be obtained in the prediction of flue gas properties which are usually related with detailed chemistry calculations, such as intermediate species like CO and radicals like OH^-.

An overview of the available submodels in a comprehensive combustion code is given in the work of Eaton et al. [A.1] as well as in the books of Goerner [A-2] and Epple and Leitner [A-3]. A representation of the coupling between the available submodels during the solution procedure is given in Fig. A.1. The main phenomena related with the physics of the reacting gaseous flows are: (a) gaseous, turbulent fluid mechanics with heat transfer; (b) gaseous, turbulent combustion; and (c) radiative energy transport. Additional phenomena modelled related with solid particles motion and combustion - as in the case of pulverised fuel firing - include multiphase, turbulent fluid mechanics and water vaporization, devolatilisation and char combustion steps of solid particles. Finally, depending on the information required by the simulations, additional submodels regarding pollutant formation can be incorporated as a post-processing step. The focus of this discussion of comprehensive combustion model features is on processes involving non premixed, turbulent diffusion flames, with emphasis on pulverised coal combustion.

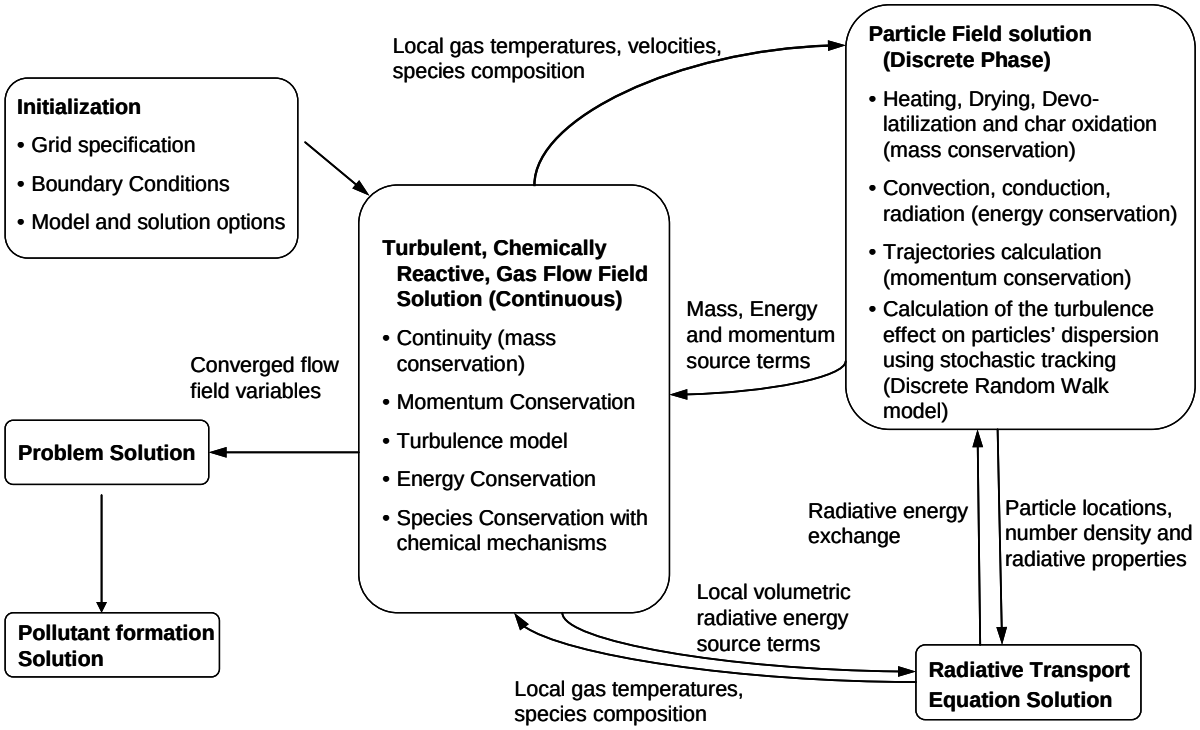

Fig. A.1 Overall parts and numerical solution procedure of a comprehensive combustion model, Source: [A.1]

A2 Modelling of basic fluid flow, energy, species and turbulence

In case of a non-reacting, incompressible, gaseous flow, there are five basic variables which must be considered for the modelling of fluid motion in a Cartesian reference frame: three velocity components (u_x, u_y, u_z) and two thermodynamic properties, pressure (p) and temperature (T). The determination of the respective values of the five variables as a function of space and time is the scope of the mathematical models of fluid motion. Five independent equations are used for the solution of the five variables: a) the conservation of mass; b) three equations for the momentum conservation for x, y, z; and c) the conservation of energy (first law of thermodynamics). These laws are used to derive integral relationships for control volumes, or differential relationships for local points in space. The differential relationships of the particular equations are presented in this part. The derivation of these equations is explained in introductory books on CFD [A-4], [A-5].

The conservation of mass is expressed in differential form by equation A.1

$$\frac{\partial \rho}{\partial t} + \nabla \cdot \left(\rho \vec{u}\right) = S_m \tag{A.1}$$

S_m is the mass-source added to the continuous phase through the dispersion of a second phase, for example from the vaporisation of liquid droplet, or from the devolatilisation in a solid fuel particle.

The conservation of momentum is expressed in differential form in equation A.2

$$\frac{\partial \rho}{\partial t} + \nabla \cdot \left(\rho \vec{u} \vec{u}\right) = \nabla p + \nabla \cdot \left(\bar{\bar{\tau}}\right) + \rho \vec{g} + \vec{F} \tag{A.2}$$

Where p is the static pressure, $\bar{\bar{\tau}}$ is the stress tensor, $\rho\vec{g}$ is the gravitational body force and $\vec{F}$ the external body force. The stress tensor in turn is described by the equation A.3

$$\bar{\bar{\tau}} = \mu\left[\left(\nabla\vec{u} + \nabla\vec{u}^{T}\right) - \frac{2}{3}\nabla\cdot\vec{u}I\right] \quad (A.3)$$

Where μ is the molecular viscosity and I the unit tensor.

For modelling of turbulence the standard k-ε model proposed by Launder and Spalding [A-6] is used in most of the simulated cases. Only in the simulation of the 1 MW_{th} combustor the RNG k- ε model is used, due to the high swirl dominated flow applied in the particular experimental conditions. More details on the RNG k-ε model can be found in the literature [A-7], [A-8].

For modeling the impact of turbulence in the flow field each flow property is expressed as the sum of an average value and a fluctuation. Equations (A.1), (A.2), (A.3) are then rewritten in the form of the "Reynolds equations" expressing only the average value of the respective properties. The molecular viscosity is then expressed as the sum of a laminar and a turbulent viscosity (Equation A.4).

$$\mu_{eff} = \mu_{lam} + \mu_t \quad (A.4)$$

In the k-ε model two additional transport equations are formulated for the conservation of the kinetic energy k (Equation A.5) and dissipation rate ε (equation A.6).

$$\frac{\partial}{\partial t}(\rho k) + \frac{\partial}{\partial x_i}(\rho k u_i) = \frac{\partial}{\partial x_j}\left[\left(\mu + \frac{\mu_t}{\sigma_k}\right)\frac{\partial k}{\partial x_j}\right] + G_k + G_b - \rho\varepsilon \quad (A.5)$$

$$\frac{\partial}{\partial t}(\rho\varepsilon) + \frac{\partial}{\partial x_i}(\rho\varepsilon u_i) = \frac{\partial}{\partial x_j}\left[\left(\mu + \frac{\mu_t}{\sigma_\varepsilon}\right)\frac{\partial \varepsilon}{\partial x_j}\right] + C_{1\varepsilon}\frac{\varepsilon}{k}(G_k + C_{3\varepsilon}G_b) - C_{2e}\rho\frac{\varepsilon^2}{k} \quad (A.6)$$

whereas
G_k: the generation of turbulent kinetic energy due to mean velocity gradients
G_b: the generation of turbulent kinetic energy due to buoyancy
$C_{1\varepsilon}, C_{2\varepsilon}, C_{3\varepsilon}$: constants
σ_k, σ_ε : the turbulent Prandtl numbers for k and ε

The turbulent viscosity is then calculated from the values of k and ε according to the expression

$$\mu_t = \rho C_\mu \frac{k^2}{\varepsilon} \quad (A.7)$$

Where C_μ is a specific constant

Regarding the conservation of energy, this is given in equation A.8

$$\frac{\partial}{\partial t}(\rho E) + \nabla\cdot\left(\vec{u}(\rho E + p)\right) = \nabla\cdot\left(k_{eff}\nabla T - \sum_j h_j\vec{J}_j + \left(\bar{\bar{\tau}}_{eff}\cdot\vec{u}\right)\right) + S_h \quad (A.8)$$

Where k_{eff} is the effective conductivity expressed as $k+k_t$ and k_t is the turbulent thermal conductivity. $\vec{J}_j$ is the diffusion flux of species j. The three terms in brackets in the right hand side represent heat transfer due to conduction, species diffusion and viscous dissipation

respectively. S_h represents the heat from chemical reactions. E in the former equation is defined as

$$E = h - \frac{p}{\rho} + \frac{u^2}{2} \tag{A.9}$$

where *h* is the sensible enthalpy of species defined for incompressible flows as

$$h = \sum_j Y_j h_j + \frac{p}{\rho} \tag{A.10}$$

where Y_j is the mass fraction of species j and $h_j = \int_{T_{ref}}^{T} c_{p,j} dT$

The general formulation for the chemical species conservation is given in Equation A.11.

$$\frac{\partial}{\partial t}(\rho Y_i) + \nabla \cdot (\rho \vec{u} Y_i) = -\nabla \cdot \vec{J}_i + R_i + S_i \tag{A.11}$$

Where R_i is the net rate of production of species i by chemical reaction and S_i the rate of addition of species from the discrete phase. The equation of species is solved for n-1 species, where n is the total number of available chemical species. The last species, which is usually the most abundant in the mixture (e.g. N_2 in case of air) is calculated by subtraction from the sum of the other species

Solution of the coupled problem

The pressure-based solver uses a solution algorithm where the governing equations are solved sequentially (i.e., segregated from one another). Because the governing equations are non-linear and coupled, the solution loop is carried out iteratively in order to obtain a converged numerical solution. The individual governing equations for the solution variables (e.g., u, v, w, p, t, k, ε, species etc.) are solved one after another, i.e. in a segregated manner. This means that each governing equation, while being solved, is "decoupled" or "segregated" from other equations. Following iterative steps are included in the solution procedure

1. Update fluid properties (e,g, density, viscosity, specific heat) including turbulent viscosity (diffusivity) based on the current solution.
2. Solution of the momentum equations, one after another, using the recently updated values of pressure and face mass fluxes.
3. Solution of the pressure correction equation using the recently obtained velocity field and the mass-flux.
4. Correction of face mass fluxes, pressure, and the velocity field using the pressure correction obtained from Step 3.
5. Solution of the equations for additional scalars including k, ε, energy, species, and radiation intensity using the current values of the solution variables.
6. Update of the source terms arising from the interactions between the continuous and the discrete phase.
7. Check for the convergence of the equations.

A3 Modeling gas reactions

For modeling of combustion of coal volatiles the Eddy Dissipation Model (EDM) model of Magnussen and Hjertager is used [A-9]. It is regarded as an extension of the Eddy Break Up (EBU) model of Spalding [A-10], which is only applicable for premixed flames. According to the Eddy Dissipation Model chemical reactions occur rapidly compared to mixing. The

limiting step is therefore only the turbulent mixing process, which is governed by the large eddy mixing time scale k/ε. The two respective rates are given in Equations A.12 and A.13. The net production rate of species i, $R_{i,r}$, due to reaction r is given by the smaller of the expressions below:

$$R_{i,r} = \nu'_{i,r} M_{w,i} A \rho \frac{\varepsilon}{k} \min_R \left(\frac{Y_R}{\nu'_{R,r} M_{w,R}} \right) \quad \text{(A.12)}$$

$$R_{i,r} = \nu'_{i,r} M_{w,i} AB \rho \frac{\varepsilon}{k} \frac{\sum_P Y_P}{\sum_j^N \nu''_{j,r} M_{w,j}} \quad \text{(A.13)}$$

Where

Y_P, Y_R the mass fractions of product species *P* and reactants *R* accordingly

$M_{w,i}$ the molar weight of species i

A is an empirical constant equal to 4.0

B is an empirical constant equal to 0.5

$\nu'_{i,r}$ the stoichiometric coefficient for reactant *i* in equation r

$\nu''_{j,r}$ the stoichiometric coefficient for product *j* in equation r

A global reaction mechanism is regarded for the combustion of coal or biomass volatiles with two reaction steps (Equations A.14, A.15). The volatiles are expressed as a hydrocarbon $C_xH_yO_z$, where coefficients x, y and z derive from the ultimate analysis of the fuel. The volatiles enthalpy of formation is calculated from the volatiles heating value, which is in turn calculated from the fuel's heating value and proximate analysis.

$$C_x H_y O_z + \frac{2x + y - 2z}{4} O_2 \rightarrow xCO + \frac{y}{2} H_2O \quad \text{(A.14)}$$

$$CO + \frac{1}{2} O_2 \rightarrow CO_2 \quad \text{(A.15)}$$

A4 Modeling discrete phase motion and reactions

Particle motion

In order to describe particle motion and combustion in pulverized fuel furnaces, the Euler - Lagrange approach is adopted. Unlike the Euler - Euler approach, where transport equations describing all phases (gas species, fuel and ash) are solved, the Euler - Lagrange approach is based on tracking of individual particles motion in the continuous gas phase. The particle tracks are calculated by integrating their force balance in the Lagrangian reference frame. The Euler - Euler approach is mostly applicable in dense flows, like granular flows or fluidized beds, where the description of particle flow as a continuum is valid. As a criterion for choosing between the two approaches available the volume fraction of the discrete phase is used. It is defined as the fraction of the particle volume to the total particle and gas volume. The Euler - Lagrange approach may be used for flows with volume fraction lower than 10%. In this case possible interaction between particles is neglected, and only the influence between discrete and continuous phase is considered. The continuous phase interacts with particles through the exchange of momentum, turbulence, species and energy source terms.

The trajectory of each particle is calculated by the integration of its force balance (Equation A.16)

$$\frac{du_p}{dt} = F_D\left(u - u_p\right) + \frac{g\left(\rho_p - \rho\right)}{\rho_p} + F_x \quad \text{(A.16)}$$

Where F_x is an additional acceleration term due to external body forces, and $F_D(u-u_p)$ the drag force as given in Equation A.17.

$$F_D = \frac{18\mu}{\rho_p d_p^2}\frac{C_D \,\mathrm{Re}}{24} \quad \text{(A.17)}$$

In the case of coal particles, these are considered to be spherical and so the standard expression of the drag coefficient for spherical particles is used.

Particle combustion

The fuel particle undergoes several steps including in a raw a) inert heating, b) vaporization and boiling c) devolatilisation and d) volatiles and char combustion. Particle's inert heating is calculated by a simple heat balance of the particle mass, where the particle's temperature is calculated by an integration of the energy equation (Equation A.14) at each time step

$$m_p c_p \frac{dT_p}{dt} = hA_p\left(T_\infty - T_p\right) + \varepsilon_p A_p \sigma\left(\theta_R^4 - T_p^4\right) \quad \text{(A.14)}$$

where T_p is the particles' temperature

The vaporisation process is calculated according to the energy equation taking also into consideration an additional term expressing the required latent heat of vaporization. The former expression takes the following form

$$m_p c_p \frac{dT_p}{dt} = hA_p\left(T_\infty - T_p\right) + \varepsilon_p A_p \sigma\left(\theta_R^4 - T_p^4\right) + \frac{dm_p}{dt} h_{fg} \quad \text{(A.15)}$$

Where dm_p/dt is the rate of the evaporation and h_{fg} is the latent heat. The evaporation rate is calculated as a molar flux (mole/s) from the following diffusion expression (Equation A.16).

$$N_i = k_c(C_{i,s} - C_{i,\infty}) \quad \text{(A.16)}$$

The molar flux of the vapour going into the gas phase (N_i) is related with the difference of the vapour concentration at the droplet surface ($C_{i,s}$) and the bulk gas ($C_{i,\infty}$). The mass transfer coefficient k_c is calculated from the Sherwood number correlation [A-11], [A-12]. $C_{i,s}$ is calculated from the saturated vapour pressure, which corresponds to the specific droplet temperature and $C_{i,\infty}$ is calculated from the concentration of vapour in the gas mixture, that is known from the solution of the species' transport equation. After determining the molar flux, Ni (moles/s) the mass flux of the evaporation rate, dm_p/dt (kg/s) is then calculated.

Droplet boiling starts when the droplet temperature reaches the boiling point, i.e. 100 °C for water. During the whole boiling process the droplet temperature remains the same and the liquid water quantity vaporises. The energy balance (Equation A.15) is then used to calculate the vaporisation rate, in terms of the decrease of droplet's diameter (Equation A.17).

$$-\frac{d(d_p)}{dt} = \frac{2}{\rho_p h_{fg}}\left[\frac{k_\infty Nu}{d_p}(T_\infty - T_p) + \varepsilon_p \sigma(\theta_R^4 - T_p^4)\right] \quad \text{(A.17)}$$

Nu is the Nusselt number and k_∞ is the thermal conductivity of the gas phase.

For devolatilisation a single rate expression is used meaning that the devolatilisation rate dm_{vol}/dt is in a first order dependency on the amount of volatiles remaining in the particle (Equation A.18).

$$\frac{dm_{vol}}{dt} = k \cdot f_{vol} \cdot m_p \quad \text{(A.18)}$$

f_{vol} is the fraction of volatiles remaining in the particle, m_p is the particle's mass and k is the kinetic rate defined by an Arrhenius type expression including a pre-exponential factor (A_1) and an activation energy (E) (Equation A.19).

$$k = A_1 \exp(-E / RT_p) \tag{A.19}$$

The values of the kinetic constants (A_1-the pre exponential factor and E-the activation energy) for coal devolatilisation are obtained from the literature [III-19]. In the case of simulation of biogenic fuels a constant devolatilisation rate is adopted as a default value in order to account for the high volatility of biomass [A-13].

Char combustion is modelled according to the kinetics/ diffusion limited reaction model of Baum and Street [A-14]. The model assumes that the reaction rate of char combustion is limited either by the oxygen's diffusion into the particle's mass expressed by the value of (D_0) or by the kinetics of the heterogeneous reaction (R_0) as presented in Equations A.20-A.22.

$$\frac{dm_p}{dt} = -A_p p_{ox} \frac{D_0 R_0}{D_0 + R_0} \tag{A.20}$$

where D_0 and R_0 are equal to

$$D_0 = C_1 \frac{\left[\left(T_p + T_\infty\right)/2\right]^{0.75}}{d_p} \tag{A.21}$$

$$R_0 = C_2 e^{-\left(E/RT_p\right)} \tag{A.22}$$

The default kinetic and diffusion constants used to model the char combustion process of brown coal and of the biogenic fraction of SRF, are obtained from the literature[III-21] and are presented in Table A.1. After the completion of the char burnout, the particle is considered as inert without any further chemical interaction with the fluid phase.

Table A.1: Kinetic constants of devolatilisation and char combustion used as default values

	Kinetic Parameters	Unit	Brown coal	biogenic fraction
Devolatilisation	Pre-exp. factor (A_1)	1/s	315,000 [III-20]	Constant rate
	Activation energy (E)	J/kmol	$7.4 \cdot 10^7$ [III-20]	50 (1/s) [A-12]
Char Combustion	mass diffusion limited rate (C_1)	kg/(m s Pa)	$1 \cdot 10^{-11}$ [III-21]	$1 \cdot 10^{-11}$
	kinetics limited pre-exp. Factor (C_2)	kg/(m^2 s Pa)	6.7 [III-21]	6.7
	kinetics limited activation energy	J/kmol	$1.138 \cdot 10^8$ [III-21]	$1.138 \cdot 10^8$

A5 Modeling radiation

The general radiative transport equation of a gas medium, where absorption, emission and scattering is also applicable, is given in equation A.23.

$$\frac{dI(\vec{r},\vec{s})}{ds} + (a + \sigma_s) I(\vec{r},\vec{s}) = an^2 \frac{\sigma \Gamma^4}{\pi} + \frac{\sigma_s}{4\pi} \int_0^{4\pi} I(\vec{r},\vec{s}') \Phi(\vec{s},\vec{s}') d\Omega' \tag{A.23}$$

where

$\vec{r}$:	position vector	σ_s :	scattering coefficient
$\vec{s}$:	direction vector	σ :	Stefan Boltzmann constant ($5.669\ 10^{-8}$ W/[m^2K^4])
$\vec{s}'$:	scattering direction vector	I :	radiation intensity

s :	path length	T :	local temperature
a :	absorption coefficient	Φ :	phase function
n :	refractive index	Ω′ :	solid angle

The portion $(\alpha+\sigma_s)s$ is the optical thickness of the medium. Through the expansion of the radiation intensity *I* into orthogonal series of spherical harmonics the general "P-N model" is derived [A-15], [A-16]. The P-1 model used for the radiative heat transfer calculations is the simplest case of the general P-N model. According to the P-1 model the radiation heat flux is calculated by Equation A.24

$$q_r = -\frac{1}{3(a+\sigma_s)-C\sigma_s}\nabla G \tag{A.24}$$

where G is the incident radiation and C the linear anisotropic phase function coefficient. The former expression can be written in the form

$$q_r = -\Gamma \nabla G \tag{A.25}$$

where Γ is defined as

$$\Gamma = \frac{1}{3(a+\sigma_s)-C\sigma_s} \tag{A.26}$$

The derived transport equation for G is then

$$\nabla \cdot (\Gamma \nabla G) - aG + 4an^2\sigma T^4 = S_G \tag{A.27}$$

Where n is the refractive index of the medium and S_G is any user defined radiation source
For the calculation of the absorption coefficient α the Weighted Sum of Gray Gases Model (WSGGM) is used, which takes into account the local concentrations of H_2O and CO_2 [A-17].

A6 Modeling NO_x formation

In the NO_x post-processing calculations performed the "thermal NOx" and "fuel NOx" formation mechanisms are applied. The "thermal NOx" formation model is based on the extended Zeldovich mechanism [A-18], and the principal reactions governing the formation of thermal NO_x from molecular nitrogen are given in the work of Diez et.al. [A-19], while the appropriate reaction rates are obtained by previous experimental investigations [A-20], [A-21]. For the "Fuel NO_x" formation mechanism the nitrogen in the fuel is considered. Nitrogen is assumed to be distributed between coal volatiles and char. Volatile nitrogen is converted firstly to HCN and NH_3 and then to NO or N_2 according to the reaction path given in [A-22], while char nitrogen is assumed to be converted to HCN before reacting to N_2 or NO, or oxidised directly to NO according to the mechanism described in [A-23], [A-24].

B. Additional data

B1 Detailed results of the lab scale SRF combustion simulations

B1.1 Grid independence study for the BTS facility
The results of the grid independence study are presented in Figure B1.1. Grid independence is achieved for numerical meshes with a size of more than 18.000 cells. The numerical meshes developed after grid adaption at the near burner region of the facility do not provide reliable results.

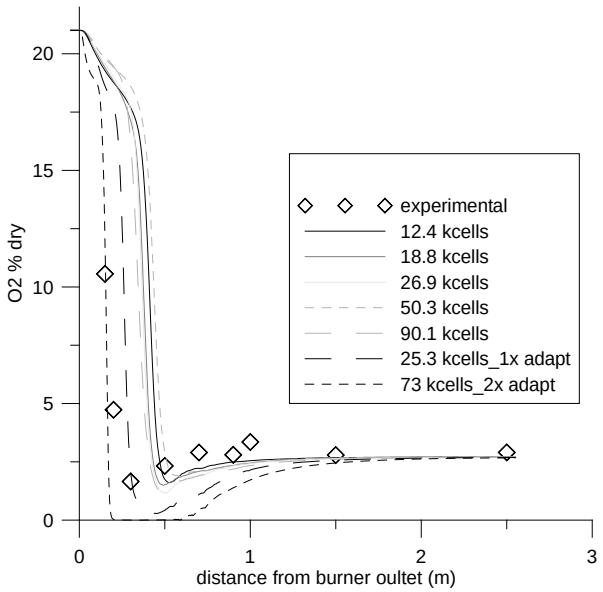

Fig. B1.1a:

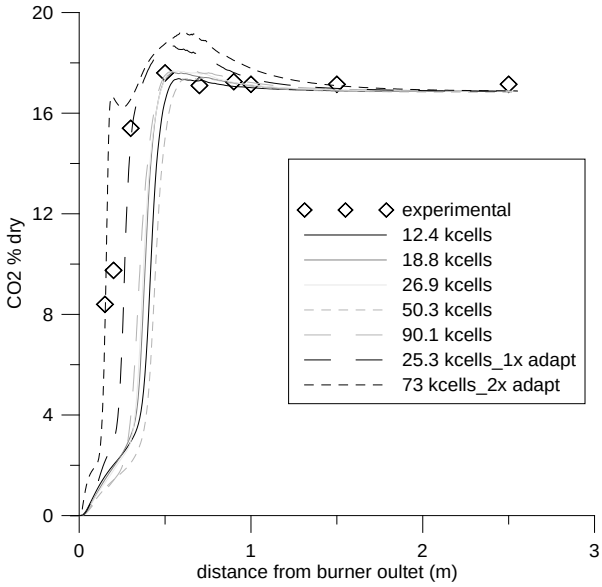

Fig. B1.1b

B1.2 Additional parametric study for the coal case
In order to further evaluate the effect of combustion related parameters, such as kinetics and volatile combustion reaction mechanisms, on the combustion behaviour, additional simulations are carried out. The parameters taken into consideration are, firstly, the pre-exponential factors of devolatilisation and char combustion steps. Four pre-exponential factors are tested for devolatilisation (a1, a2, a3, a4) and three for char combustion (a5, a6, a7). The parameter sets a1-a7 are given in Table B1.1. Additionally, three other combustion related parameters are investigated in cases a8, a9, a10. Case a8 includes default kinetics of the default case (a1) and a modified reaction mechanism for volatile combustion, according to which volatiles are directly combusted to CO_2 through one reaction step instead of two. In case a9 the constant expressions for heat capacities are used in all gas species instead of the polynomial expressions which are used in the default case.
O_2, and CO_2 and Temperature profiles of the simulation results are presented in FiguresB1.2-B1.4. Only the values on the symmetry axis are plotted in all cases and the additional values on the 3cm transposed axis are ignored in order to avoid the great number of simulation

curves in the same plot. Although no temperature measurements are available and therefore, no validation of the predicted temperature results is possible, the evaluation of the temperature profile is useful in order to predict in relative terms the influence of the examined parameters on the obtained temperature field. The results can be summarised as follows:

- Higher pre exponential factors lead, as expected, to higher devolatilisation and char combustion rates and therefore, to higher slopes of the curves and more abrupt decrease of the O_2 concentration.
- Satisfying results are achieved with all considered values of devolatilisation and char combustion pre-exponential factors, with the exception of case a5. No realistic trends are obtained with the low value of the char combustion pre-exponential factor set in a5. Therefore, it should be used with another parameter set such as set A3 in the main part of the analysis.
- No drastic changes are noticed by changing the number of reactions in the volatile combustion mechanism or the heat capacities of the species considered as performed in cases a8, a9. The minimum O_2 concentration in the profile of Fig.B1.4a is, however, shifted to higher levels in cases a8, a9 compared with the reference case a1. This is an indication that the produced volatiles are faster consumed either due to the presence of one combustion step instead of two or due to the higher temperatures. Therefore O_2 concentration in the gas mixture can not reach the minimum level of the reference case.
- It is further noticed that by setting constant cp for all considered gas species the predicted temperature peak is shifted to more than 100K higher compared to the baseline case, a1. In order to overcome this, the polynomial expressions of the heat capacities are used from the literature [B-1].

Table B1.1: Examined kinetic parameter sets

	Kinetic Parameters	Unit	Investigation of devolatilisation Pre-exp. Factor				Investigation of char combustion Pre-exp. Factor		
			a1 (=A1)	a2 (=A2)	a3	a4	a5	a6	a7
Devolatilisation	Pre-exp. factor (k)	1/s	200,000	**315,000**	**600,000**	**$2\cdot10^6$**	200,000	200,000	200,000
	Activation energy (E)	J/kmol	$7.4\cdot10^7$	$7.4\cdot10^7$	$7.4\cdot10^7$	$7.4\cdot10^7$	$7.4\cdot10^7$	$7.4\cdot10^7$	$7.4\cdot10^7$
Char Combustion	mass diffusion limited rate	Kg/(m^2 s Pa)	$5\cdot10^{-12}$	$5\cdot10^{-12}$	$5\cdot10^{-12}$	$5\cdot10^{-12}$	$5\cdot10^{-12}$	$5\cdot10^{-12}$	
	kinetics limited pre-exp. factor	1/s	6.7	6.7	6.7	6.7	**0.00208**	**0.67**	**67.0**
	kinetics limited activation energy	J/kmol	$1.138\cdot10^8$	$1.138\cdot10^8$	$1.138\cdot10^8$	$1.138\cdot10^8$	$1.138\cdot10^8$	$1.138\cdot10^8$	$1.138\cdot10^8$

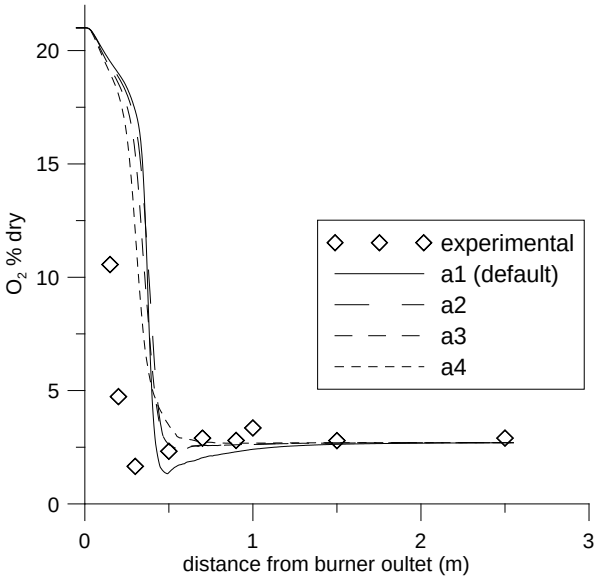

Fig. B1.2a: O_2 profiles cases a1-a4

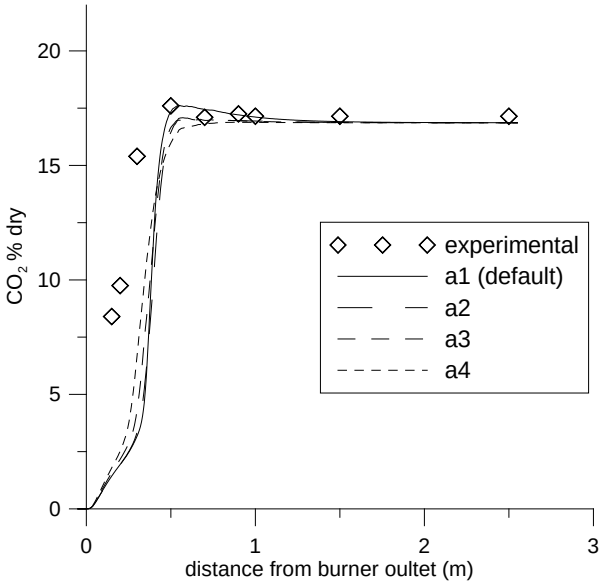

Fig. B1.2b: CO_2 profiles cases a1-a4

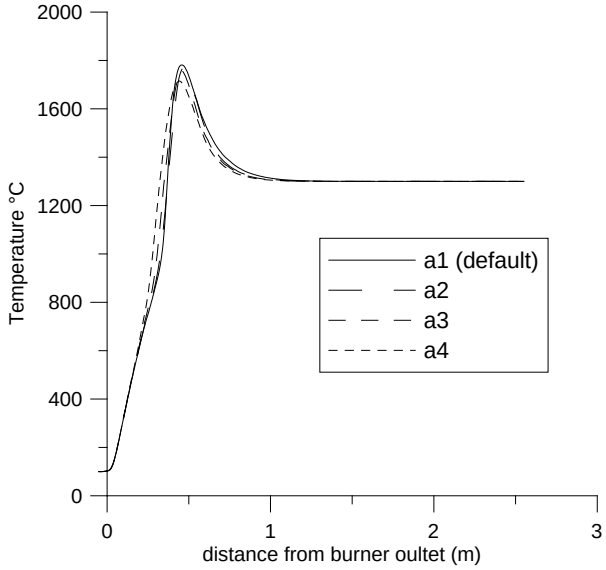

Fig. B1.2c: Temperature profiles cases a1-a4

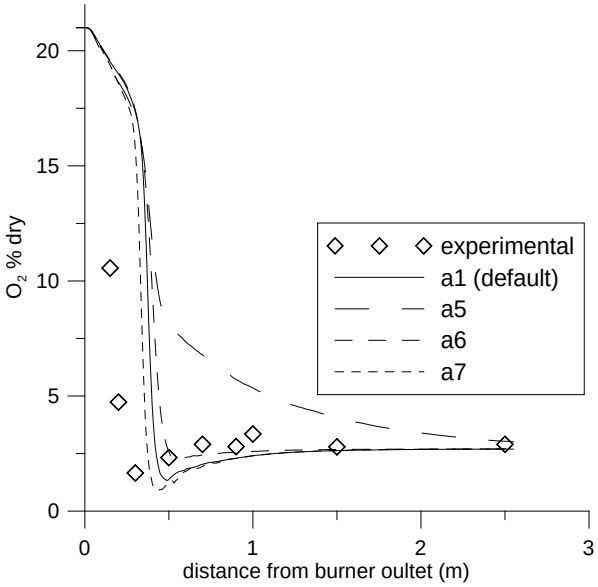

Fig. B1.3a: O_2 profiles cases a1,a5-a7

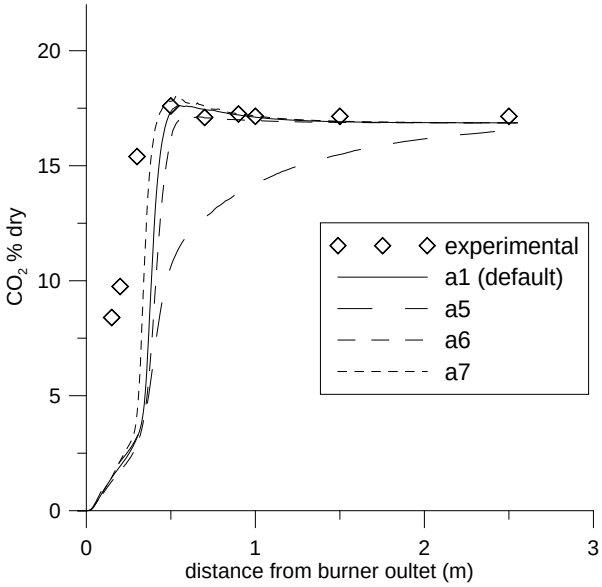

Fig. B1.3b: CO_2 profiles cases a1,a5-a7

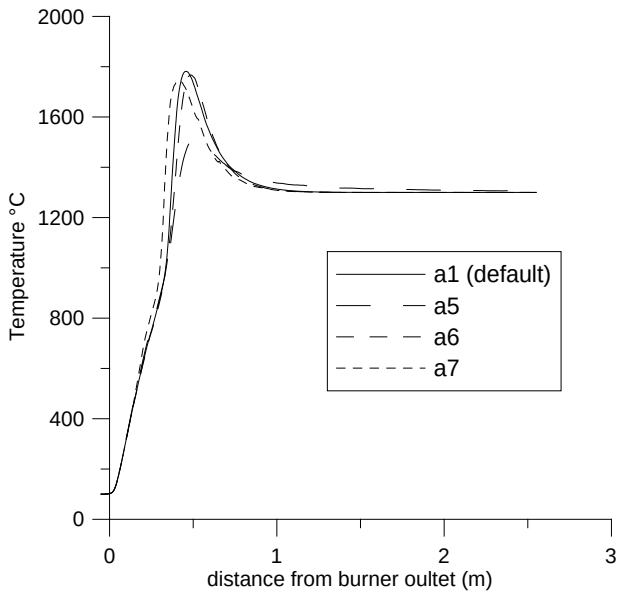

Fig. B1.3c: Temperature profiles cases a1,a5-a7

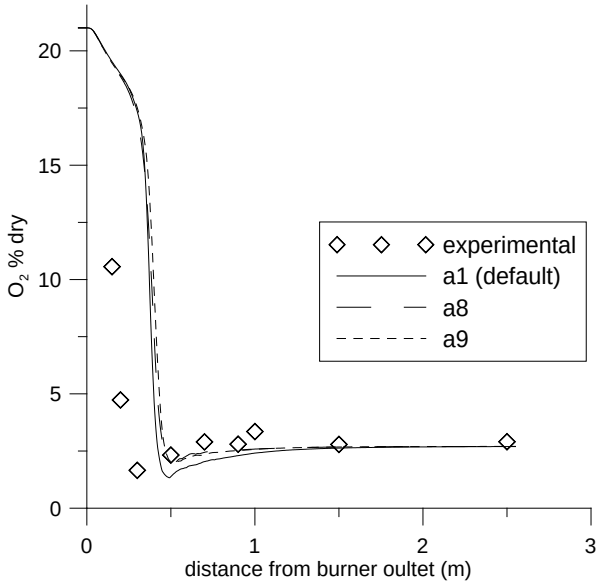

Fig. B1.4a: O_2 profiles cases a1,a8,a9

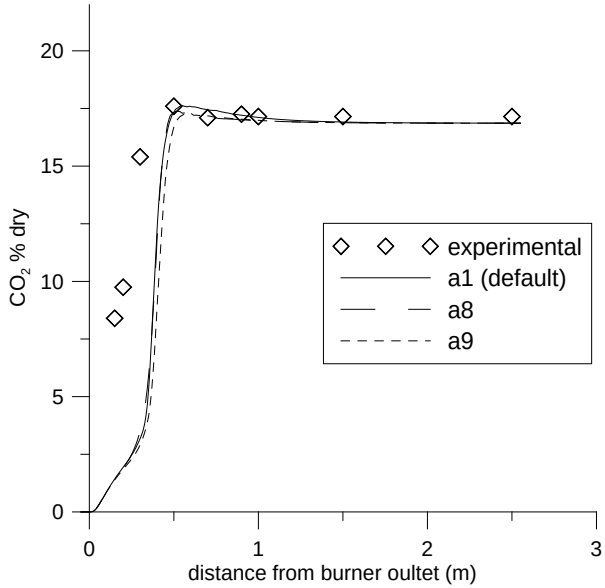

Fig. B1.4b: CO_2 profiles cases a1,a8,a9

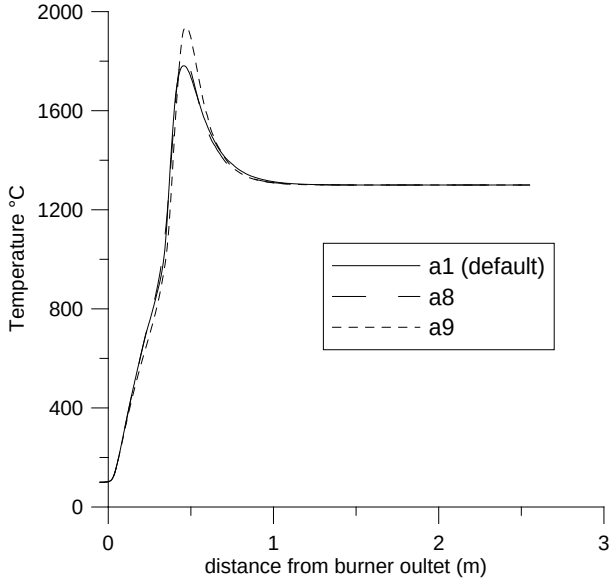

Fig. B1.4c: Temperature profiles cases a1,a8,a9

B1.3 Additional parametric study for the biomass case

An additional study on the influence of kinetics on the combustion behaviour is also performed in the biomass case. Since the char content of biogenic fuels is usually small, the parametric evaluation focuses on the devolatilisation kinetics. A large amount of the kinetic rates proposed can be found in the literature for different biogenic fuels and the great range of values should be also stressed. An overview of the activation energy and pre-exponential factor values proposed by other researchers for various biogenic fuels is given in Table B1.2. In this framework the parametric analysis included different values for the devolatilisation pre-exponential factor ranging from 50.000 until $3.15\ 10^{12}$. Two constant rates are also simulated for reasons of comparison. All tested kinetic data sets are given in Table B1.3 and the respective results are presented in Figure B1.5.

Similar trends are noticed in the simulation results to the ones noticed in the coal case. By increasing the value of the pre-exponential factor higher devolatilisation rates are achieved. The devolatilisation step is shorter and the combustion of volatiles starts and ends earlier as seen by the O_2 profiles which are slightly transposed to upstream. Very high devolatilisation rates such as the value $3.15\ 10^{12}$ do not provide realistic results since the predicted minimum in O_2 is very close to the burner outlet. Furthermore, the constant rate value of 8 (1/s) is evaluated as too low, while the value of 50 (1/s) is rather high for the particular biomass. An overall comment related with the available measurement data of the biomass case is that the translated profile at 3cm from the furnace symmetry axis tends to provide better results as shown in Figure 3.5 of the third chapter. However, as in the case of coal presented above, profile values at the symmetry axis are only presented in these extra parameter analyses of Annex B in order to avoid many curves on one plot that cannot be easily evaluated.

Table B1.2: Available literature data on devolatilisation kinetics

Literature sources	Biomass species	Pre-exponential factor A_1 (s^{-1})	Activation energy E (J/kgmol)
R.I Backreedy, L.M. Fletcher, J.M. Jones [A-13]	Pinewood	$2\ 10^{13}$, $6\ 10^{13}$, $12\ 10^{13}$, $6\ 10^{15}$	$1.8\ 10^{8}$, $2.5\ 10^{8}$
D. Gera, M. Mathur [III-22]	Switchgrass	$1.0\ 10^{6}$	$7.48\ 10^{7}$
D Gera, MC Freeman [III-23]	Switchgrass	$3.12\ 10^{6}$	$6.4\ 10^{7}$
Chr. Mueller, A. Brink [B-2]	Forest Residues	$3.12\ 10^{5}$	$7.4\ 10^{7}$

Table B1.3: Examined kinetic parameter sets

	Kinetic Parameters	Unit	Investigation of devolatilisation Pre-exp. Factor					
			b1	b2	b3	b4	b5	b6
Devolatilisation	Pre-exp. factor (k)	1/s	**Constant rate 8 (1/s)**	**Constant rate 50 (1/s)**	**50,000**	**3.15 10^{5}**	**3.15 10^{6}**	**3.15 10^{12}**
	Activation energy (E)	J/kmol			$7.4 \cdot 10^{7}$	$7.4 \cdot 10^{7}$	$7.4 \cdot 10^{7}$	$7.4 \cdot 10^{7}$
Char Combustion	mass diffusion limited rate	Kg/(m^2 s Pa)	$5 \cdot 10^{-12}$	$5 \cdot 10^{-12}$	$5 \cdot 10^{-12}$	$5 \cdot 10^{-12}$	$5 \cdot 10^{-12}$	$5 \cdot 10^{-12}$
	kinetics limited pre-exp. factor	1/s	6.7	6.7	6.7	6.7	6.7	6.7
	kinetics limited activation energy	J/kmol	$1.138 \cdot 10^{8}$	$1.138 \cdot 10^{8}$	$1.138 \cdot 10^{8}$	$1.138 \cdot 10^{8}$	$1.138 \cdot 10^{8}$	$1.138 \cdot 10^{8}$

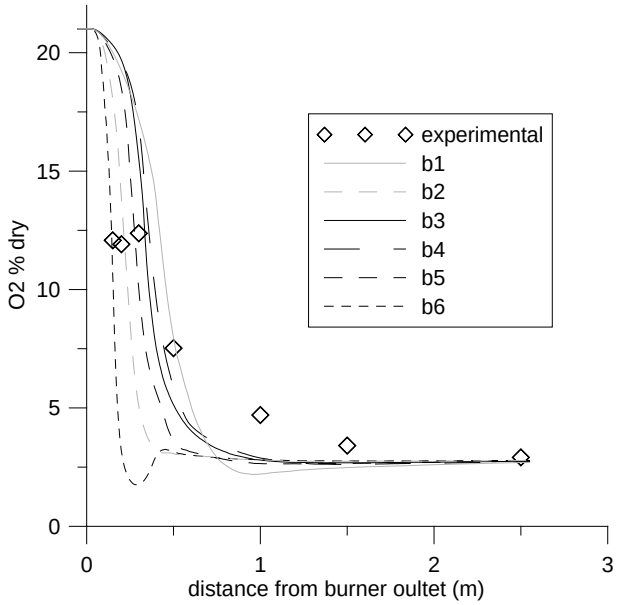

Fig. B1.5a: O_2 profiles cases b1-b6

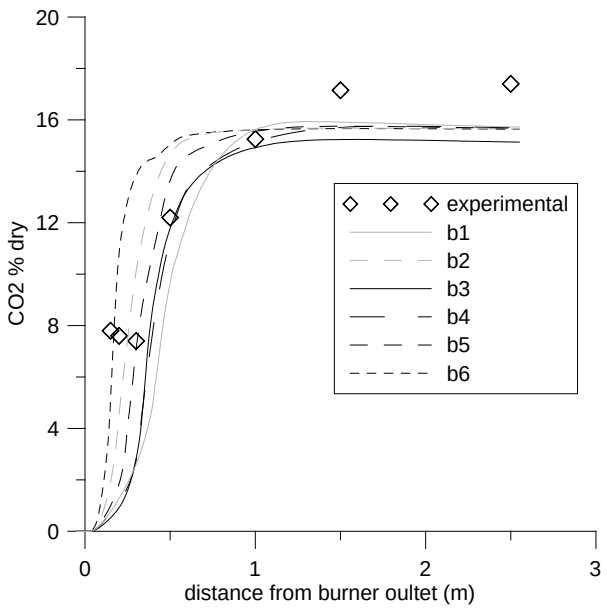

Fig. B1.5b: CO_2 profiles cases b1-b6

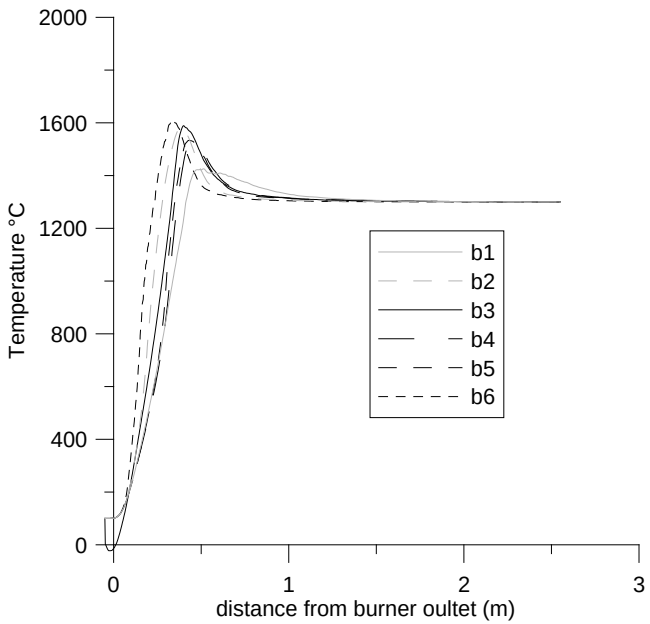

Fig. B1.5c: Temperature profiles cases b1-b6

B2 Additional data regarding the large scale SRF co-combustion tests at the 600MWe power plant

Table B2.1**:** Heavy Metals, Cl and F values of the fuels calculated in mg/kg (dry substance) ds and in mg/MJ, Source: Remondis – RWE-Power

Component	Lignite (*)	Paper Sludge (*)	SBS®1 (*)	Maximal values for SBS®1 measured during trials	Typical values for Hard Coal according to literature (**)	Lignite	Paper sludge	SBS®1
	mg/kg ds	mg/kg ds	mg/kg ds	mg/kg ds	mg/kg ds	mg/ MJ	mg/ MJ	mg/ MJ
Chlorine (Cl)	400	600	5.700	8000	0-2.000	17,241	73,26	263,69
Fluorine (F)	40	246	72	105	60-120	1,724	30,037	3,33
Cadmium (Cd)	<0,05	0,32	0,96	2,67	0,5-5	$2{,}16\ 10^{-3}$	0,039	0,044
Thallium (Tl)	<1,00	<1,00	<1,24	2,50	0,1-5	0,043	0,122	0,057
Mercury (Hg)	0,13	0,06	<0,17	0,28	0,01-10	$5{,}60\ 10^{-3}$	$7{,}33\ 10^{-3}$	$7{,}86\ 10^{-3}$
Antimony (Sb)	<1,50	1,52	12,4	39,50	0,5-1,6	0,064	0,186	0,573
Arsenic (As)	<1,00	1,35	<0,9	1,20	10-200	0,043	0,165	0,042
Lead (Pb)	3,62	20,9	58	137	10-100	0,156	2,552	2,683
Chromium (Cr)	<10,0	14,4	74	464,00	10-50	0,431	1,758	3,422
Cobalt (Co)	3,37	4,06	<4,6	11,1	1-20	0,145	0,496	0,213
Cooper (Cu)	4,3	156	639	3150,00	10-100	0,185	19,048	29,556
Manganese (Mn)	199	115	72	124,00	5-200	8,578	14,042	3,330
Nickel (Ni)	<3,00	9,80	44	343,00	10-50	0,129	1,197	2,035
Vanadium (V)	2,1	4,23	4,3	7,30	20-500	0,091	0,516	0,199
Tin (Sn)	<2,00	2,73	7,9	53,70	1-10	0,086	0,333	0,365

(*) average values of the daily samples during the trials

(**) Karl Krejci-Graf: "Über die Elemente in Kohlen", Erdöl und Kohle, Bd. 37 Heft 10, Okt. 84

Table B2.2: Ash components of SRF compared to lignite, Source: IVD University of Stuttgart

Oxides	Unit	Lignite, mean values	SRF, mean values
SiO_2	%	49,2	26,52
Al_2O_3	%	5,03	13,68
CaO	%	20,00	25,77
MgO	%	3,82	2,43
K_2O	%	0,31	2,02
Na_2O	%	0,32	5,27
Fe_2O_3	%	12,00	3,33
P_2O_5	%	0,10	1,26
TiO_2	%	1,50	2,28
MnO	%	0,20	0,05
SO_3	%	7,34	1,34

Table B2.3: Leaching behavior and legal limit for ash disposal to landfill, Source: RWE-Power

Component	Unit	Sample during SRF operation	Legal Limit
pH-Value		12	5,5-13
Conductivity	µS/cm	3990	10000
Total Organic Content (TOC)	mg/l	7,02	<20
Phenoles	mg/l	<0,02	<0,2
As	mg/l	<0,004	<0,2
Pb	mg/l	<0,005	<0,2
Cd	mg/l	<0,0002	<0,05
Cr	mg/l	<0,05	<0,05
Cu	mg/l	<0,002	<1
Ni	mg/l	<0,005	<0,2
Hg	mg/l	<0,0002	<0,005
Zn	mg/l	<0,02	<2
Cyanide	mg/l	<0,01	<0,1
AOX	mg/l	0,041	<0,3
Watersolubles	%	0,252	<3

Table B2.4: Heavy metal analysis of the fly ash samples taken during the reference case and during the SRF co-combustion, Source: RWE-Power

Component	Symbol	Unit	Blank test without SRF		SRF co-combustion	
			Range	Mean value	Range	Mean value
Cadmium	Cd	mg/kg	0.18 – 0.27	0.23	0.32-0.62	0.45
Thallium	Tl	mg/kg	< 1.00	< 1.00	< 1.00	< 1.00
Mercury	Hg	mg/kg	0.35-0.55	0.47	0.29-0.68	0.42
Antimony	Sb	mg/kg	< 1.50	< 1.50	< 1.50-6.70	5.20
Arsenic	As	mg/kg	6.01-7.68	6.74	6.37-11.7	8.86
Lead	Pb	mg/kg	9.22-14.3	12.0	10.8-32.8	22.0
Chromium	Cr	mg/kg	14.8-21.0	17.4	18.7-25.9	23.9
Cobalt	Co	mg/kg	20.6-26.1	22.5	11.3-19.3	15.1
Copper	Cu	mg/kg	37.8-80.9	63.77	45.8-97.6	58.9
Manganese	Mn	mg/kg	1910-2470	2207	971-3565	1719
Nickel	Ni	mg/kg	18.1-27.3	23.0	13.2-26.7	19.8
Vanadium	V	mg/kg	19.8-23.8	21.8	18.4-25.4	22.3
Tin	Sn	mg/kg	< 2.00	< 2.00	< 2.00-4.27	2.70
Zinc	Zn	mg/kg	65.1-79.0	71.6	112-222	137

B3 Additional data regarding the large scale SRF co-combustion simulations: grid independence study

An extensive study on the appropriate numerical meshes for the large-scale boiler simulations was performed in the initial steps of the particular work. Unstructured tetrahedral or hybrid meshes were initially tested without satisfying results as regards convergence behaviour. Hexahedral body-fitted meshes were afterwards developed ranging from about 150.000 cells to 1 million cells. It is proven by Figures B2.1 that the solutions with hexahedral meshes of 350.000 cells and more are grid independent.

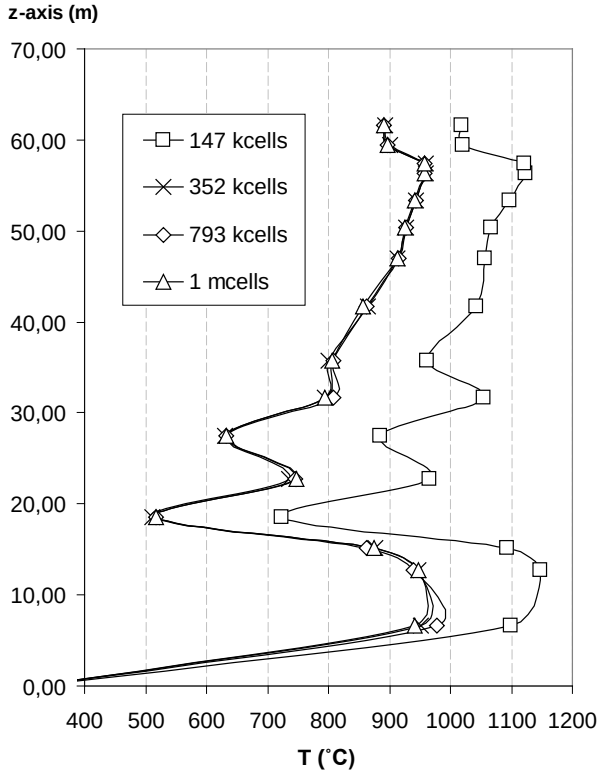

Fig. B3.1a Average temperatures along furnace height for different simulated meshes

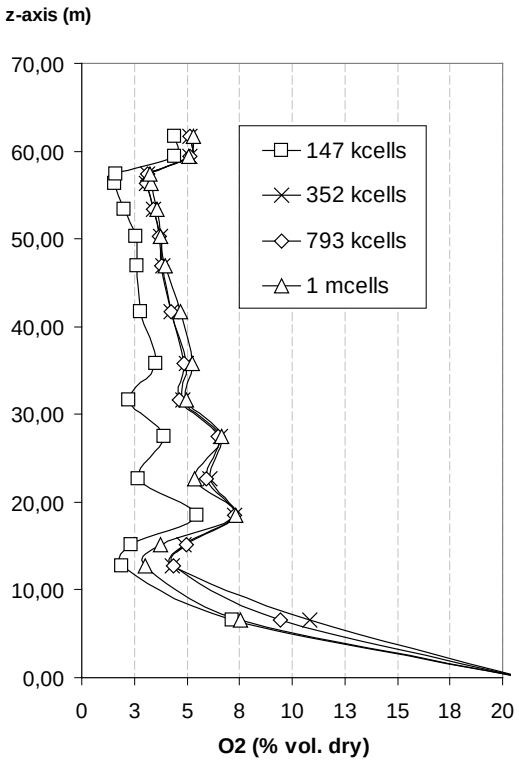

Fig. B3.1b Average oxygen concentrations along furnace height for different simulated meshes

B4 Additional data on dry coal combustion simulation at the semi industrial scale facility

Detailed results of the simulations performed for the 1 MW_{th} experimental facility are presented in this part. In the initial simulation set up constant temperature is used as a wall boundary condition. The simulated temperature, oxygen and axial velocity contours are given in Figures B4.1 to B4.3 respectively. An increase of the temperature peak and a shift of the flame ignition upstream is observed when increasing the dry coal share. This behaviour is also reproduced in the oxygen contours, while in the axial velocity contours a decrease of the mean axial velocity is noticed due to the reduction of the flue gas mass flow in cases A1 and A2. However, different behaviour is observed in the case of wall boundary conditions of constant

heat flux. Ignition takes place closer to the burner outlet compared to the cases of constant temperature boundary conditions. Additionally, the flow field varies in the three different cases, A0, A1, A2 and this is also noticed in the contours of vertical velocity, where the location and shape of the internal recirculation zone changes. As a result, the predicted temperature contours (Figure B4.4) and oxygen contours (Figure B4.5) are less “stable” compared to the contours of Figures B4.1-2. Summing up, wall boundary conditions of constant heat flux tend to provide more realistic results compared to the experimental data available. This constitutes a indication that this kind of wall boundary conditions should be used for future simulations of the particular experimental facility. On the other hand, the predicted flow and temperature fields are less “stable” in the case of heat flux boundary conditions, which should be further examined in future numerical investigations.

Fig. B4.1: Simulation results of the VVA facility for wall boundary conditions of constant temperature, Temperature contours (°C) for (a) case A0, (b) case A1, (c) case A2

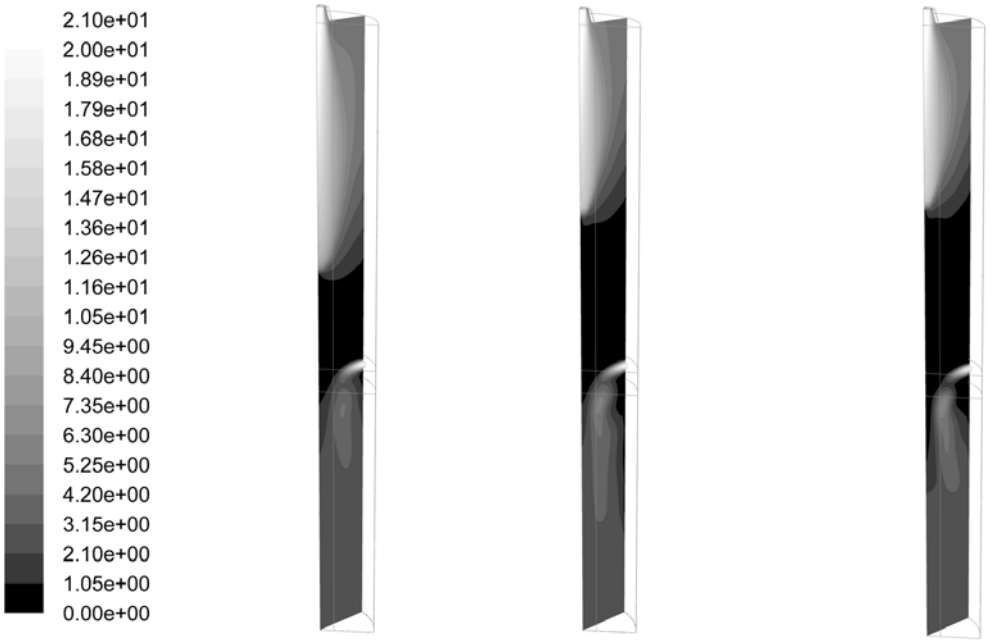

Fig. B4.2: Simulation results of the VVA facility for wall boundary conditions of constant temperature, Oxygen contours (% vol. dry) for (a) case A0, (b) case A1, (c) case A2

Fig. B4.3: Simulation results of the VVA facility for wall boundary conditions of constant temperature, axial velocity contours (m/s) for (a) case A0, (b) case A1, (c) case A2

Fig. B4.4: Simulation results of the VVA facility for wall boundary conditions of constant heat flux, temperature contours (°C) for (a) case A0, (b) case A1, (c) case A2

Fig. B4.5: Simulation results of the VVA facility for wall boundary conditions of constant temperature, Oxygen contours (% vol. dry) for (a) case A0, (b) case A1, (c) case A2

Fig. B4.6: Simulation results of the VVA facility for wall boundary conditions of constant temperature, axial velocity contours (m/s) for (a) case A0, (b) case A1, (c) case A2

B5 Additional data on dry coal combustion simulation at the industrial-scale boiler

Temperature and oxygen contours at two different vertical planes of the Liptol power plant are presented in the following figures. In Figures B5.1, B5.2 the temperature and oxygen contours at the boiler symmetry plane are given. An increase of the high temperature region located in the middle of the furnace, above the burner belt, is noticed by increasing the dry coal co-firing share. The region of low oxygen concentration also increases compared to the raw coal firing case indicating that fuel combustion begins earlier and lasts longer resulting in larger combustion zones. However, this low oxygen region is not enlarged when increasing the dry coal share, possibly due to the different flow field predicted after changing the inlet fuel and carrier gas mass flows. Similar pictures for the temperature and oxygen contours are also noticed in Figures B5.3, B5.4. The effect of the left side raw lignite burner and the left wall dry lignite burners on the temperature and oxygen contours at the specific plane is also apparent. Higher temperatures and definite increase of the oxygen concentration at the particular plane are namely noticed when increasing the dry coal firing share.

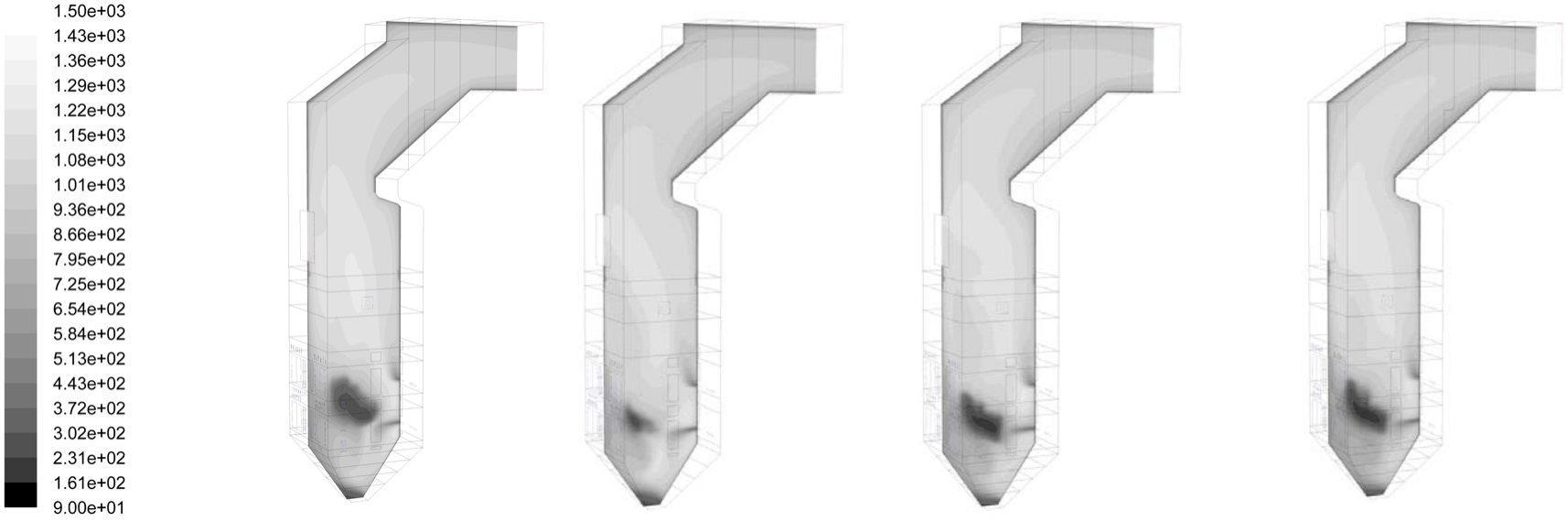

Figure B5.1 Temperature contours (°C) at the symmetry plane, from left to right: (a) reference case, (b) co-firing thermal share 5%, (c) co-firing thermal share 10%, (d) co-firing thermal share 20%

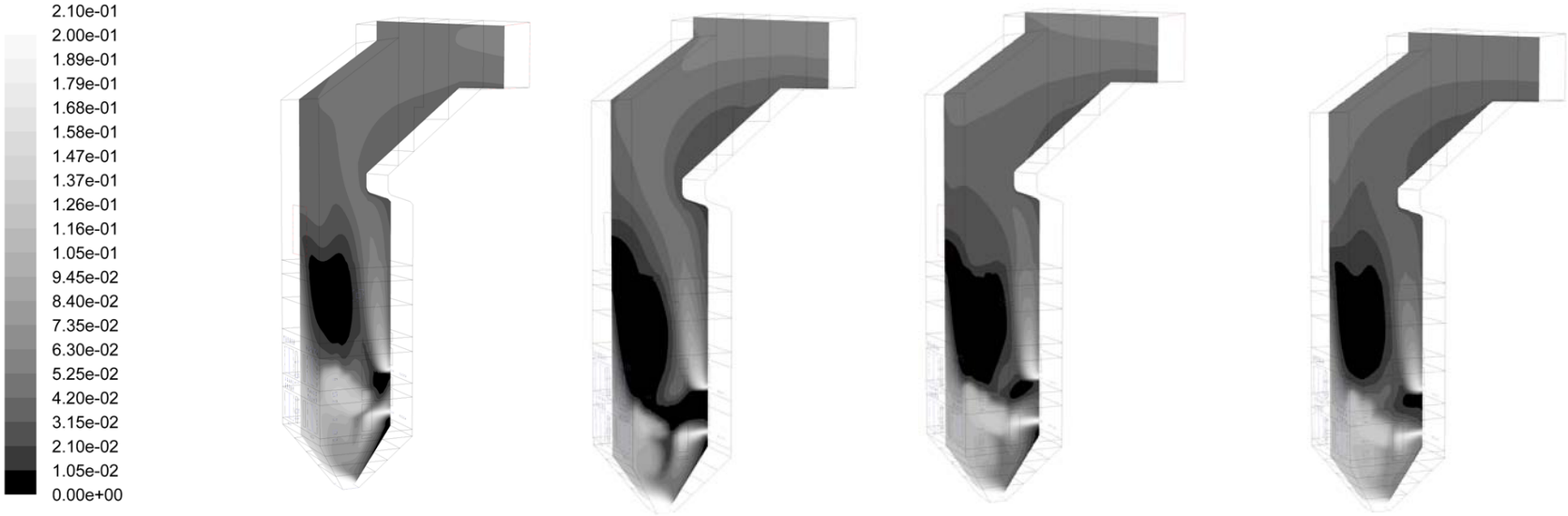

Figure B5.2 Oxygen contours (% vol. dry) at the symmetry plane, from left to right: (a) reference case, (b) co-firing thermal share 5%, (c) co-firing thermal share 10%, (d) co-firing thermal share 20%

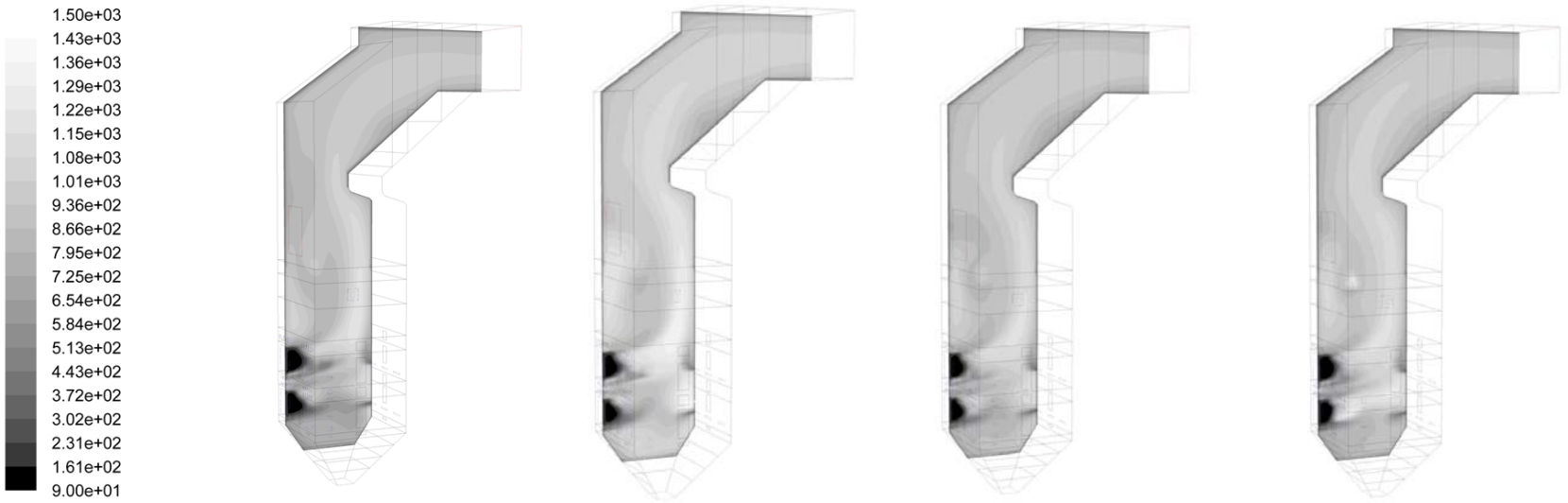

Figure B5.3 Temperature contours (°C) at the vertical plane of the raw lignite burners closer to the left wall, from left to right: (a) reference case, (b) co-firing thermal share 5%, (c) co-firing thermal share 10%, (d) co-firing thermal share 20%

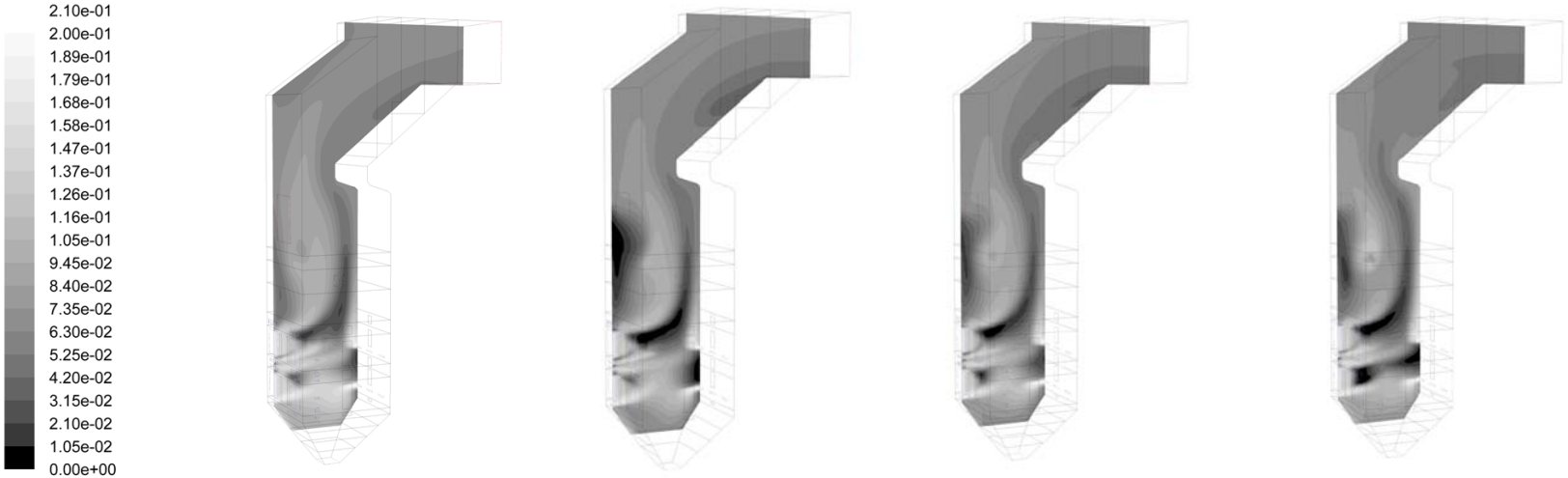

Figure B5.4 Oxygen contours (% vol. dry) at the vertical plane of the raw lignite burners closer to the left wall, from left to right: (a) reference case, (b) co-firing thermal share 5%, (c) co-firing thermal share 10%, (d) co-firing thermal share 20%

C. List of publications

During the doctor thesis the author had a contribution in the following publications

Publications in books

"Co-utilization of biomass based fuels in pulverized coal power plants in Europe", Panagiotis Grammelis, Michalis Agraniotis, Emmanuel Kakaras submitted to Wiley-VCH publishing in order to be included as a chapter in the book the handbook of combustion Vol. 4 (currently under review)

Publications in scientific Journals

"Solid Recovered Fuels as Coal Substitute in the Electricity Generation Sector", Emmanuel Kakaras, Panagiotis Grammelis, Michalis Agraniotis, Thermal Science Journal Vol. 9, 2/2005 , pp. 17-30

"Advantages and possibilities of Solid Recovered Fuel (SRF) co-combustion in the European Energy Sector", Thomas Hilber, Michalis Agraniotis, Jörg Maier, Günter Scheffknecht, Panagiotis Grammelis, Emmanuel Kakaras, Thomas Glorius, Uwe Becker, Hans-Peter Schiffer, Willy Derichs, Martin de Jong, Lucia Torri, Journal of the Air & Waste Management Association, Volume 57, Pages: 1178 - 1189, October 2007.

"Numerical investigation on the combustion behaviour of predried Greek lignite", Michalis Agraniotis, Dimitris Stamatis, Panagiotis Grammelis, Emmanuel Kakaras, Fuel, Volume 88, (2009), pp. 2385-2391

"Experimental investigation on the combustion behaviour of pre-dried Greek lignite" Michalis Agraniotis, Panagiotis Grammelis, Charalambos Papapavlou, Emmanuel Kakaras, Fuel Processing Technologies, Volume 90, (2009) pp.1071-1079

"Numerical investigation of Solid Recovered Fuels' co-firing with brown coal in large scale boilers – Evaluation of different co-combustion modes", Michalis Agraniotis, Nikos Nikolopoulos, Aris Nikolopoulos, Panagiotis Grammelis, Emmanouel Kakaras, Fuel 89 (2010), 3693-3709

"Dry lignite co-firing in a Greek utility boiler: Experimental activities and numerical simulations", Michalis Agraniotis, Dimitris Stamatis, Panagiotis Grammelis, Emmanouel Kakaras, (to be published in Journal "Energy and Fuels" DOI: 10.1021/ef1002843)

Publications in Conferences

"New mixtures of Solid Recovered Fuels with lignite", Em. Kakaras, P. Grammelis, M. Agraniotis, 3. National Congress, "The application of Renewable Energy Sources" (RENES) 23-25 February 2005 Athens, Greece, (Oral Presentation)

"Co-combustion of Solid Recovered Fuels (SRF) in coal fired power plants", Em. Kakaras, P. Grammelis, M. Agraniotis, International Science and Technology Conference "Wastes and Biomass Combustion and Co-combustion", Wroclaw University of Technology, 16-17 November 2005, Poland, (Oral Presentation)

"The utilization of recovered fuels for energy production", Em. Kakaras, P. Grammelis, M. Agraniotis, 2. National Congress on Biofuels and Alternative Fuels, 26-27 April 2007, Karditsa, Greece, (Poster Presentation)

"Experimental investigation on the combustion behaviour of Greek brown coal with varying moisture content", Emmanuel Kakaras, Panagiotis Grammelis, Michalis Agraniotis, Christoph Schlechter, Ioannis Nikolaides, Charalambos Papapavlou, International Clean Coal Technologies Conference, 14-18 May 2007, Sardinia Italy, (Oral Presentation)

"Demonstration of co-firing of Solid Recovered Fuels in European lignite fired power plants", Alexander Gerhardt, Jörg Maier, Günter Scheffknecht, Michalis Agraniotis, Panagiotis Grammelis, Emmanuel Kakaras, Thomas Glorius, Bernhard Roeper, Martin De Jong, International Energy from Biomass and Waste Conference, 25-27 September 2007, Pittsburgh, Pennsylvania, USA (Poster Presentation)

"Optimization of a superheater design towards decreasing ash deposition tendency and improving cleaning effectiveness", Michalis Agraniotis, Panagiotis Grammelis, Emmanuel Kakaras, Sergios Gkoudanis, 8th European Conference on Industrial Furnaces and Boilers (INFUB 8), 25-28 March 2008, Villamoura, Portugal (Poster Presentation)

"Co-firing Solid Recovered Fuels (SRF) with brown coal in large scale pulverized fuel power plants – a simulation approach", Michalis Agraniotis, Panagiotis Grammelis, Emmanuel Kakaras, Global Conference on Global Warming, 6-10 July 2008, Instanbul, Turkey (Oral Presentation)

"Numerical investigation on the combustion behaviour of predried Greek lignite", Michalis Agraniotis, Panagiotis Grammelis, Emmanuel Kakaras, 7th European Conference on Coal Research and its applications, 3-5 September 2008, Cardiff, UK, (Oral Presentation)

"Combustion simulations of predried Greek lignite at experimental and industrial scale facilities." International Clean Coal Technologies Conference, 18-21 May 2009, Dresden Germany, (Oral presentation)

"Utilisation of Solid Recovered Fuels (SRF) for energy production", Michalis Agraniotis, Panagiotis Grammelis, Emmanuel Kakaras, CEMEPE-Conference, 21-26 June 2009, Greece (Oral Presentation)

"CFD simulation of Solid Recovered Fuels' (SRF) co-firing with brown coal in large scale boilers", Michalis Agraniotis, Nikos Nikolopoulos, Panagiotis Grammelis, Emmanuel Kakaras, 24. Deutscher Flammentag, 16-17 September 2009 (Oral Presentation)

"Numerical investigation on the application of a lignite pre-drying concept in an existing Greek power plant", Michalis Agraniotis, Ioannis Violidakis, Aggelos Doukelis, Panagiotis Grammelis, Emmanuel Kakaras, 8th European Conference on Coal Research and its applications, 6-8 September 2010, Leeds, UK, (Poster Presentation)

D. Literature

Chapter 01

[I-1] International Energy Agency, "Key World Energy Statistics", 2008, www.iea.org

[I-2] Intergovernmental Panel on Climate Change, 4th Assessment Report Synthesis, 2007, www.ipcc.ch

[I-3] Office of Climate Change, "Stern Review on the Economics of Climate Change", www.occ.gov.uk, 2006

[I-4] United Nations Framework Convention on Climate Change, http://unfccc.int,

[I-5] Eurostat "Energy Transport and Environment Indicators", ISSN 1725-4566, 2008, http://epp.eurostat.ec.europa.eu

[I-6] European Union COM (2008) 30 Final, http://europa.eu/

[I-7] International Energy Agency, "World energy outlook 2007", ISBN: 978-92-64-02730-5, www.iea.org

[I-8] N. Tanaka, *What role for coal in a carbon constrained world?*, presentation, Clean Coal Technologies Conference, 18-21 May 2009, Dresden, Germany

[I-9] Eurelectric, Article 30-03-2009, Press Release 18-03-2009, www.eurelectric.org

[I-10] J. Topper, *Conclusive Remarks of CCT 2009*, presentation, Clean Coal Technologies Conference, 18-21 May 2009, Dresden, Germany

[I-11] Directive 2001/80/EC *On the propotion of electricity produced from renewable energy sources in the internal electricity market*

[I-12] IEA Report, *Emissions Trading and its possible impacts on investment decisions in the power plant sector, 2003*, www.iea.org

[I-13] IEA Report, *Clean Coal Technologies – Accelerating Commercial and Policy Drivers for Deployment, 2008*, www.iea.org

[I-14] P. Grammelis, N. Koukouzas et.al. *Refurbishment priorities at the Russian coal-fired power sector for cleaner energy production – Case studies*, Energy Policy, vol. 34, pages 3124-3136.

[I-15] Em. Kakaras, P. Grammelis, M. Agraniotis, *Solid Recovered Fuels as coal substitute in the electricity generation sector*, Thermal Science Journal, vol. 9, (2005), pages 17-30.

[I-16] Prognos AG, Institute of Environmental Research, University of Dortmund, *Resource savings and CO_2 reduction potentials in waste management in Europe and the possible contribution to the CO_2 reduction target in 2020*, Study 2008

[I-17] European Commission Directorate General for Environment *Refusal Derived Fuels Current Situation and Perspectives*, Final Report, 2003

[I-18] J. Maier, T. Hilber, G. Scheffknecht, *Current activities in terms of Solid Recovered Fuel (SRF) standardisation*, Presentation Conference Waste & Biomass Combustion and Co-combustion, Wroclaw University of Technology, Wroclaw, Poland, November 2005.

[I-19] Prognos AG, *European Atlas of secondary raw material, 2004 Status Quo and Potentials*, Study 2004

[I-20] Prognos AG, *The German waste managment market and perspectives till 2020 (In German) [Der Abfallmarkt in Deutschland und Perspektiven bis 2020]*, Study on behalf Deutscher Naturschutzbund (NABU), Berlin, Germany 2009

[I-21] C. Velis, V.S. Rotter, K. Lazaridi, *MBT-derived SRF: State of the art in Europe. Will Quality Management Deliver?* Hellenic Solid Waste Management Association, (ΕΕΔΣΑ), 3d International Congress on Waste management, 30-31 October 2009, Greece

[I-22] Eurocoal, EU statistics - Coal in European Power Generation 2007, www.eurocoal.be

[I-23] K. Kavouridis, *Current position and perspectives for Coal – A Greek and European view*, Third European Combustion Meeting, 2007

[I-24] K. Kavouridis, *Lignite and natural gas in the Greek electricity production sector*, workshop Technical Chamber of Greece, 2005

[I-25] K. Papanikolaou, M. Galetakis, A. Foskolos, *Quality characteristics of Greek brown coals and their relation ot the applied exploration and utilization methods*, Energy and Fuels, vol. 19 (1), 2005

[I-26] K. Kavouridis, F. Pavloudakis, *Determination of Ptolemon's lignite fluctuation – supportive fuels and homogenization methods to improve lignite quality for power generation purposes*, Surface Mining, Braunkohle and other minerals, vol. 1, (2001), p. 37-43

[I-27] PPC Report, *Co-combustion of lignite and hard coal in "Ptolemais IV" power plant*, (1985), in Greek

[I-28] K. Kavouridis, I. Nikolaides, A. Logothetis, *Improvement of the lignite quality produced from Ptolemais multi-seam deposits using dry lignite for power generation*, Workshop Proceedings: Pre-drying processes for the efficient and clean utilization of brown coals in the enlarged EU market, April 1999

[I-29] N. Orfanoudakis, *Co-generation and pre-drying of Greek lignite; the most effective method of upgrating of Greek lignites*, Workshop Proceedings: Pre-drying processes for the efficient and clean utilization of brown coals in the enlarged EU market, April 1999

[I-30] Directive 2001/80/EC *On the limitation of emissions of certain pollutants into the air from large combustion plants*

[I-31] Directive 2000/76/EC *On the Incineration of waste*

Chapter 02

[II-1] www.cen.eu/CENORM/Sectors/TechnicalCommitteesWorkshops/CENTechnicalCommittees/ CEN/TC 337

[II-2] www.cen.eu/CENORM/Sectors/TechnicalCommitteesWorkshops/CENTechnicalCommittees/ CEN/TC 343

[II-3] CEN/ TS 15357 Solid Recovered Fuels – Terminology, Definitions and descriptions

[II-4] CEN/ TS 15359 Solid Recovered Fuels – Specifications and classes

[II-5] "Bundesguetegemeinschaft Sekundaerbrennstoffe", www.bgs-ev.de

[II-6] European Recovered Fuel Organisation, www.erfo.info, *BREF Waste Treatment, Solid Recovered Fuels*

[II-7] CEN/TS 15358 Solid Recovered Fuels - Quality management systems - Particular requirements for their application to the production of solid recovered fuels

[II-8] Th. Glorius, *SRF production,* Recofuel workshop 29-05-2008, www.ivd.uni-stuttgart.de/recofuel-workshop

[II-9] European Commission, European Waste Catalogue (EWC) and hazardous waste list, established by Commission Decision 2000/532 EC

[II-10] IPPC, Best Available Techniques Reference Document BREF on Waste Treatment Industries

[II-11] S. Thiel, *Ersatzbrennstoffe in Kohlekraftwerken*, Dissertation (in German), 2007 Thome - Kozmiensky publishing, www.vivid.de

[II-12] CEN/ TS 15442 Solid Recovered Fuels – Methods for sampling

[II-13] CEN/ TS 15443 Solid Recovered Fuels – Methods for laboratory sample preparation

[II-14] CEN/ TS 15440 Solid Recovered Fuels – Determination of the biomass content

[II-15] CEN/ TR 15591 Solid Recovered Fuels – Determination of the biomass content based on the 14C method

[II-16] P. Grammelis, M. Agraniotis, Em. Kakaras, *Co-Utilization of Biomass Based Fuels in Pulverized Coal Power Plants in Europe*, Handbook of Combustion Volume 4, Wiley-VCH Books, (2009).

[II-17] F. Mielke, H.M. Kohde et. al., *Potentials and Operating Experiences of the Utilisation of Subsitute Fuels at the Jaenschwalde Lignite-fired Power Plant Site of the Vattenfall Europe Generation,* VGB – Powertech, vol. 12 2006

[II-18] R. Haasa, H. Breuer, *Co-combustion – The Power Producer' s point of view,* VGB – Powertech, vol. 4 2005

[II-19] EU Demonstration project Recofuel (TREN/04/FP6EN/S07.32813/503184), Final Report

[II-20] J. Ewers, W. Renzenbrick, Review and classification of different technologies for *CO_2 emissions reduction in coal power plants,* VGB Power Tech 4/2005

[II-21] S. Kjær, J. Bugge, R. Blum, *High efficiency coal-fired power plants development and perspectives*, Energy vol.31 (2006), p. 1437-1445

[II-22] E. Kakaras, A. Koumanakos, A. Doukelis, D. Giannakopoulos, *Ultra - supercritical power plant fired with low quality Greek Lignite*, ECOS 2007, Proceedings

[II-23] E. Kakaras, A. Koumanakos, A. Doukelis, D. Giannakopoulos, I. Vorrias *Oxyfuel boiler design in a lignite-fired power plant*, Fuel 86 (2007) 2144–2150

[II-24] E. Kakaras, A. Doukelis, D. Giannakopoulos, A. Koumanakos, *Economic implications of oxyfuel application in a lignite fired power plan*t, Article in Press Fuel (2007), doi:10.1016/ j.fuel.2007.03.035

[II-25] E. Kakaras, P. Ahladas, S. Syrmopoulos, *Computer simulation studies for the integration of an external dryer into a Greek lignite fired power plant*, Fuel 81 (2002), p.583-593

[II-26] H-J Klutz, C. Moser, D. Block, *WTA Fine Grain Drying – Module for Lignite –Fired Power Plants of the Future*, VGB - Powertech 11 (2006)

[II-27] *The WTA Technology, An advanced method for processing and drying lignite*, Report, www.rwe.com

[II-28] T. Porsche, L. Thannhaeuser, O. Hoehne, J.S. Martin, *Erste Testergebnisse von der Versuchsanlage zur Druckaufgeladenen Dampfwirbelschicht-Trocknung (DDWT) von Braunkohlen*, 24. German Flameday (2009), ISBN 978-3-18-092056-6

[II-29] USA fluidised bed system Presentation CCT 2007-2009

[II-30] F. Schwendig, H-J Klutz, J. Ewers, *The Dry Lignite Fired Plant*, VBG - Powertech 12 (2006)

[II-31] European Commission, The New Industrial Emissions Directive, draft, June 2010

[II-32] D. Metikanis, Presentation PPC, 25-06-2010

[II-33] I. Kopanakis, Presentation PPC, May 2010

Chapter 03

[III-1] CEN/TR 15716: 2008 Solid Recovered Fuels- Determination of combustion behaviour

[III-2] J. Maier, A. Gerhardt, G. Dunnu, *Experiences on co-firing Solid Recovered Fuels in the coal power sector*, Springer Biofuels Ch4

[III-3] G. Dunnu, Th. Hilber, U. Schnell, *Advanced size measurements and aerodynamic classification of solid recovered fuel particles*, Energy & Fuels, 20(4), (2006), 1685-1690

[III-4] G. Dunnu, J. Maier, Th. Hilber, G. Scheffknecht, *Characterisation of Large Solid Recovered Fuel Particles for Direct Co-firing in Large PF Power Plants.* Fuel (1009), doi:10.1016/j.fuel.2009.03.004

[III-5] L. Sorum, M. Gronli, J. Hustad, *Pyrolysis Characteristics of municipal solid wastes*, Fuel 80 (2001), 1217-1227

[III-6] A. Garcia, A. Marcilla, R. Font, *Thermogravimetric kinetic study of the pyrolysis of municipal solid waste*, Thermochimica Acta 254 (1995) 277-304

[III-7] P. Grammelis, P. Basinas, A. Malliopoulou, G. Sakellaropoulos, *Pyrolysis kinetics and combustion characteristics of waste recovered fuels*, Fuel vol. 88, (2009), p. 195-205

[III-8] Th. Hilber, M. Martensen, J. Maier, G. Scheffknecht, *A Method to characterise the volaitle release of solid recovered fuels (SRF)*, Fuel 86 (2007), 303-308

[III-9] M. Beckmann, S. Ncube, K. Gebauer, M. Pohl, *Characterisation of Refuse Derived Fuels in view of the Fuel Technical Properties*, VGB Powertech, 1/2-2009, p. 76-80

[III-10] T. Kolb, H. J. Gehrmann; M. Stein-Brzozowska; H. Seifert, *Characterisation of the Combustion Behaviour of Refuse Derived Fuel and Biomass with Lignite*, 8th European Conference on Industrial Furnaces and Boilers, INFUB08, 25-28 March 2008, Villamoura, Portugal

[III-11] N. Wolski, J. Maier, K.R.G. Hein, *Trace Metal Partitioning from co-combustion of RDF and bituminous coal*, IFRF Combustion Journal, (2002), article 200203,

[III-12] Th. Hilber, H. Thorwarth et. al., *Fate of mercury and chlorine during SRF co-combustion*, Fuel 86 (2007), 1935-1946

[III-13] W.E. Ranz, W. Marshal, Evaporation from Drops, Chemical Engineering Progress, 48 (3), 1952, 141-149

[III-14] Ch. Deeg, M. Schneider, U. Schnell, G. Scheffknecht, *A method for Modelling the Co-combustion of Solid Recovered Fuels in Pulverised Fuel Power plants,* 23. German Flameday 12.-13.09.2007 Berlin S. 345-354, ISBN: 978-3-18-091988-1; 2007

[III-15] Järvinen, M.: Numerical modelling of the drying, devolatilisation and char conversion processes of black liquor droplets, Academic Dissertation, Helsinki University of Technology, Helsinki, 2002

[III-16] Chr. Mueller, A. Brink, M. Huppa, Numerical simulation of the combustion behavior of different biomasses in a bubbling fluidized bed boiler, Proceeding 18. International Conference on Fluidised Bed Combustion, May 2005

[III-17] Perry's Chemical Engineers' Handbook 7th Ed. 1999, McGraw Hill, ISBN 0-07-049841-5

[III-18] Ch. Deeg, U. Schnell, G. Scheffknecht, M. Agraniotis, P. Grammelis, E. Kakaras, Deliverable 04, *Adaptation, Application and Validation of general particle models for the co-combustion of SRF*, EU-FP6 Project Recofuel, 2006

[III-19] Th. Hilber, Upswing An advanced waste treatment concept compared to the state of the art, *Dissertation*, Cuvillier Publishing, 2008, ISBN 978-3-86727-563-7

[III-20] Fluent Users' Guide Tutorial Coal Combustion using the Eddy Break Up (EBU) Model, Ansys Inc, (2008)

[III-21] S. Badzioch, P.G.W. Hawksley, *Kinetics of Thermal Decomposition of Pulverized Coal Particles.* Ind. Eng. Chem. Process Design and Development, 9:521-530, 1970.

[III-22] M.A. Field, *Rate of Combustion Of Size-Graded Fractions of Char from a Low Rank Coal between 1200 K-2000 K*, Combustion and Flame, 13:237-252, 1969.

[III-23] M. Agraniotis, N. Nikolopoulos, P. Grammelis, Em, Kakaras, *CFD simulation of Solid Recovered Fuels' (SRF) co-firing with brown coal in large scale boilers*, German Flameday, 16.-17.09.2007 Bochum, Germany

[III-24] C. Lin, L. Rosendahl, S. Kaer, *Use of numerical modelling in design for co-firing biomass in wall fired burners*, Chemical Engineering Schience 59 (2004), 3281-3292.

[III-25] D. Gera, M. Marthur, M. Freeman, A. Robinson, *Effect of Large Aspect Ratio of Biomass Particles on Carbon Burnout in a Utility Boiler*, Energy and Fuels 16 (2002), 1523-1532.

[III-26] D. Gera, M.C. Freeman, W. O'Dowd, M.P. Mathur, G. Walbert, A. Robinson, *Computational Fluid Dynamics modelling for biomass cofiring design in pulverised coal boilers*, Proceedings "Bioenergy" Congress, October 2000, Buffalo NY, USA

[III-27] D. Grow, *Mass and Heat Transfer to an Ellipsoidal Particle*, Combustion and Flame 80, 1990, 209-213

Chapter 04

[IV-1] European Recovered Fuel Organisation, J. van Tubergen, Th. Glorius, Classification of Solid Recovered Fuels, Report, 2005, www.erfo.info

[IV-2] RECOFUEL: TREN/04/FP6EN/S07.32813/503184, http://www.eu-projects.de/recofuel

[IV-3] Em. Kakaras, P. Grammelis, M. Agraniotis et.al. "Solid Recovered Fuels as Coal Substitute in the Electricity Generation Sector", Thermal Science Journal, Vol. 9, No2, pp.17-30, Jun. 2005

[IV-4] Th. Hilber, M. Agraniotis et. al.. *Advantages and possibilities of Solid Recovered Fuel (SRF) co-combustion in the European Energy Sector*, Journal of the Air & Waste Management Association, vol. 57, (2007), p. 1178 - 1189.

[IV-5] A. Gerhardt, B. Röper, J. Maier et. al., *Co-combustion of Solid Recovered Fuels with Rhenish Lignite*, VGB-Powertech vol. 11 (2008), p. 50-55

[IV-6] Th. Glorius, *Project Overview and SRF production*, Recofuel workshop 29-05-2008, www.ivd.uni-stuttgart.de/recofuel-workshop

[IV-7]S. Flamme, *Main conclusions of the EU-project Quovadis*, Recofuel workshop 29-05-2008, www.ivd.uni-stuttgart.de/recofuel-workshop

[IV-8] VDI Guideline 3480, Measurement of HCl in waste gases

[IV-9] B. Roepper, *SRF co-combustion at RWE*, Recofuel workshop 29-05-2008, www.ivd.uni-stuttgart.de/recofuel-workshop

[IV-10] Bundesministerium fuer Umwelt, Naturschutz und Reaktorsicherheit, 17. BimSchV, http://bundesrecht.juris.de/bundesrecht/bimschv_17

[IV-11] Directive 2000/76/EC *On the Incineration of waste*

[IV-12] R. Hassa, *Co-combustion from the operator's point of view, Vattenfall Europe Generation AG,* VGB-Congress Power Plants Cologne, 2004

[IV-13] A. Gerhardt, B. Röper et.al. *Investigation of the influence of SRF co-combustion on chlorine corrosion risk of superheaters at a CBF boiler*. 4th VGB Workshop, Operating Experiences with CFB-Systems, 2008

[IV-14] M. Agraniotis, P. Grammelis, Em. Kakaras, Co-firing Solid Recovered Fuels with Brown coal in large scale power plants – A simulation approach, Proceedings of the Global Conference on Global Warming, (2008), 1584-1596

Chapter 05

[V-1] D.l. Allardice, D.G. Evans, *The brown-coal/ water system: Part 1: The effect of temperature on the evolution of water on brown coal*, Fuel**,** 1971, 50, p. 201-210.

[V-2] D.l. Allardice, D.G. Evans, *The brown-coal/ water system: Part 2: Water sorption isotherms on bed – moist Yallourn brown coal*, 1971, 50, p. 236-253.

[V-3] David G. Evans, *The brown-coal/ water system: Part 4: shrinkage on drying*, Fuel 52 (1973), p. 186-190.

[V-4] G. Bongers, W. Jackson, F. Woskoboenko, *Pressurised steam drying of Australian low-rank coals, Part 1. Equilibrium moisture contents*, Fuel (57), 1998, p. 41-54

[V-5] G. Bongers, W. Jackson, F. Woskoboenko, *Pressurised steam drying of Australian low-rank coals, Part 2. Shrinkage and physical properties of steam dried coals, preparation of dried coals with very high porosity*, Fuel Processing Technologiy (64), 2000, p. 13-23

[V-6] Z. Chen, W. Wu, P.K. Agarwal, *Steam drying of coal. Part 1. Modelling the behaviour of a single particle*, Fuel 79 (2000), p. 961-973

[V-7] Z. Chen, P.K. Agarwal, J. Agnew *Steam drying of coal. Part 2. Modelling the operation of a fluidized bed drying unit*, Fuel 80 (2001), p. 209-223

[V-8] Allardice, D.J.: *The water in brown coal*, Ph.D. Thesis, University of Melbourne (1968)

[V-9] F. Buschsieveke, Dissertation, University of Stuttgart, Germany, 2006 (in German)

[V-10] Meschgbiz A., Krumbeck M, *Combined Combustion of Biomass and Brown Coal in a Pulverised Fuels and Fluidized Bed Combustion Plant*, Clean Coal Technology Programme 1992-1994, Vol. II Co-Combustion of Biomass, Sewage sludge and Coals, Final Reports, ISBN 3-928123-16-5

[V-11] Unsworth J.F., Barrat D. J., Park D., Titchener K.J., *Ash formation during pulverised fuel combustion. 3. The structure and strength of boiler deposits*, Fuel 67 (1988), p. 1503-1509

[V-12] Bryers R.W. *Fireside slagging, fouling and high temperature corrosion of heat-transfer surface due to impurities in steam-raising fuels*, Progress in Energy and Combustion Science 22 (1996), p. 29-120

[V-13] J. Barroso, J. Ballester, A. Pina *Study of coal ash deposition in an entrained flow reactor: Assessment of traditional and alternative slagging indices*, Fuel Processing Technology 88 (2007), p. 865-876

[V-14] J. Zelkowski, *Kohlecharakterisierung und Kohleverbrennung*, VGB Powertech Publishing, 2004

[V-15] E.C. Winegartner *Coal fouling and slagging parameters*, ASME Research Committee on Corrosion and Deposits from Combustion Gases, 1974

[V-16] E. Raask, *Mineral impurities in coal combustion, Behaviour, Problems and Remedial Measures*, Hemisphere Publishing Corporation, 1985

[V-17] G. Couch, *Understanding slagging and fouling in Pf Combustion*, IEA Coal Research London, 1994 IEA CR/72

[V-18] W. Gumz, *Kurzes Handbuch der Brennstoff und Feuerungstechnik* p. 416-426, Springer Publishing, 1962

[V-19] N. Papageorgiou Steam Boilers and Thermal installations I, in Greek

[V-20] M. Agraniotis, D. Stamatis, P. Grammelis, E. Kakaras, *Numerical investigation on the combustion behaviour of predried Greek lignite*, Fuel 88 (2009), 2385-2391

[V-21] M. Agraniotis, P. Grammelis, Ch. Papapavlou, E. Kakaras, *Experimental investigation on the combustion behaviour of predried Greek lignite*, Fuel Processing Technology 90 (2009), 1071-1079

[V-22] Goodarzi F., *Characteristics and composition of fly ash from Canadian coal-fired power plants*, Fuel 85 (2006), p. 1418-1427

[V-23] Maier J., Kluger F., Hocquel M., Spliethoff H., Hein K.R.G. *Investigation of Particle Behaviour of Raw and Pre-dried Brown Coal and Bituminous Coal in a 20 kW and in a 500 kW Test Facility*, 23rd Int. Conf. On Coal Utilization & Fuel Systems,Clearwater USA, 9 - 13 March, 1998

[V-24] Maier J., Heinzel T., Spliethoff H., Hein K.R.G.: *Milling, Drying and Combustion of Low Rank Coal in a 500 kWth Pulverized Coal Test Facility*, Proceedings of the International Symposium on Clean Coal Technology, Xiamen/ China, 1997

[V-25] Maier J., Hein K.R.G, *Effect of Pre-drying on P.F. Combustion, Fly Ash and Emission Behavior of Different European Low-Rank Fuels*, Tagungsband: 18th Annual International Pittsburgh Coal Conference, Dec. 3-7, 2001, Newcastle, NSW, Australia; 2001

[V-26] Spliethoff H., Maier J. *Effect of pre-drying on combustion behaviour and boiler design*, DG TREN Workshop “Pre drying processes for the efficient and clean utilisation of brown coals in the enlarged EU market”, Athens, Greece 1999

[V-27] Goanta, A., Becher, V., Bohn, J. - P., Gleis, S., & Spliethoff, S. *Controlled Staging with Non-Stoichiometric Burners for Oxy-fuel Pocesses – Numerical Validation*, 33nd International Technical Conference on Coal Utilization & Fuel Systems, Clearwater, Florida, (2008).

[V-28] Becher, V., Goanta, A., Gleis, S., & Spliethoff, H. *Controlled Staging with Non-Stoichiometric Burners for Oxyfuel Processes*, International Technical Conference on Coal Utilization & Fuel Systems, Clearwater Florida (2007).

[V-29] Shih TH, Liou WW, Shabbir A, Yang Z, Zhu J., *A new k–e eddy viscosity model for high Reynolds number turbulent flows – model development and validation*, Comput Fluids 1995;24(3):227–38.

[V-30] D. Raithby and E. H. Chui, *A Finite-Volume Method for Predicting a Radiant Heat Transfer in Enclosures with Participating Media*, J. Heat Transfer, 112:415-423, 1990

[V-31] Michalis Agraniotis, Dimitris Stamatis, Panagiotis Grammelis, Emmanuel Kakaras, Combustion simulation of predried Greek lignite at experimental and industrial scale facilities, International Clean Coal Technologies Conference, 14-18 May 2009, Dresden Germany

Chapter 06

[VI-1] Epple B., Schneider R., Schnell U., Hein K., *Computerised analysis of Low NOx Coal fired Utility Boilers*, Combustion Science and Technology (1995), 108:4, 383-401

[VI-2] Le Bris Thomas, Cadavid Francisco et al., *Coal Combustion modelling of large plant, for NOx abatement*, Fuel (2007), vol.86, 2213-2220

[VI-3] Diez Luis I., Cortes Cristobal, Pallares Javier *Numerical investigation of NOx emissions from tangentially-fired utility boiler under conventional and overfire air operation*, Fuel (2008), vol.87, 1259-1269

Chapter 07

[VII-1] NETL, *Cost and performance baseline for fossil energy plants*, Final report, 2007

[VII-2] P. A. Bouillon, S. Hennes, C. Mahieux, *ECO2: Post-combustion or oxyfuel- A comparison between coal power plants with integrated CO_2 capture*, Energy Procedia, 2009, 1, 4015- 4022.

[VII-3] Antonios Koumanakos. *Thermal cycles for fossil fuel fired power plants with integrated CO2 capture technologies,* PhD Thesis, NTUA 2009

[VII-4] European climate exchange www.ecx.eu

[VII-5] Committee on Climate Change, *Meeting Carbon budgets – The need for a step change*, report 12-10-2009, p. 68, www.theccc.org.uk

[VII-6] Greek legislation, Ministry of Environment and Climate Change, Electricity price for RES (nr. 3851 / 2010)

[VII- 7] Ministry of Energy, Environment and climate change, Ministerial decision, 28-09-2010

[VII-8] Anastasia Malliopoulou, *Co-combustion of biomass/ rdf with lignite in thermal power plant*, master thesis, 2006 (in Greek)

[VII-9] PPC, annual report 2009, p. 41

[VII-10] Greek Ministry of Environment, 2nd National Allocation Plan, 2008-2012 (in Greek)

Appendix A

[A-1] A.M. Eaton, L.D. Smoot, S.C. Hill, *Components formulations, solutions, evaluation, and application of comprehensive combustion models*, Progress in Energy and Combustion Science vol.25, p. 387-436, 1999

[A-2] Klaus Goerner, *Technische Verbrennungssysteme*, in German, ISBN 3-540-53947-6, Springer publications, 1991

[A-3] Bernd Epple, Reinhard Leithner, Wladimir Linzer, Heimo Walter, *Simulation von Kraftwerken und waermetechnischen Anlagen*, in German, ISBN 978-3-211-29695-0, Springer publications 2009

[A-4] J.D. Anderson, *Computational Fluid Dynamics: The basics with applications* ISBN 0070016852, McGraw Hill publications, 1995

[A-5] G. Bergeles, *Computational Fluid Mechanics*, in Greek, ISBN 960-7346-19, 1993

[A-6] B.E.Launder and D. B. Spalding. *The Numerical Computation of Turbulent Flows*. Computer Methods in Applied Mechanics and Engineering, 3:269-289, 1974.

[A-7] Yakhot V, Orszag SA. J Sci Comput 1986;1:1.

[A-8] Yakhot SA, Orszag S, Thangam S, Gatski TB, Speziale CG. Phys Fluids 1992;4:1510.

[A-9] B.F. Magnussen and B.H. Hjertager *On mathematical models of turbulent combustion with special emphasis on soot formation and combustion, In* 16th Symp. (Int'l.) on Combustion. The Combustion Institute, *1976.*

[A-10] D.B. Spalding *Mixing and chemical reaction in steady confined turbulent flames*. In *13th Symp. (Int'l.) on Combustion*. The Combustion Institute, 1970.

[A-11] W.E. Ranz and W.R. Marshall, Jr. *Evaporation from Drops, Part I. Chem. Eng. Prog. 1952*, 48(3):141-146.

[A-12] W.E. Ranz, W. Marshal. *Evaporation from Drops, Part II*. Chemical Engineering Progress 1952, 4: p. 173-180.

[A-13] R.I. Backreedy, L.M. Fletcher, J.M. Jones, L.Ma, M. Pourkashanian, A. Williams, *Co-firing pulverised coal and biomass: a modelling approach*, Proceedings of the Combustion Institute 30 (2005), pp. 2955-2964

[A-14] M.M. Baum, P.J. Street. *Predicting the Combustion Behaviour of Coal Particles*. Combustion Science and Technology 1971; 3: p. 231-243.

[A-15] P. Cheng. *Two-Dimensional Radiating Gas Flow by a Moment Method*. *AIAA Journal*, 2:1662-1664, 1964.

[A-16] R. Siegel and J. R. Howell. *Thermal Radiation Heat Transfer*. Hemisphere Publishing Corporation, Washington DC, 1992.

[A-17] T.F. Smith, Z.F. Shen, and J.N. Friedman. *Evaluation of Coefficients for the Weighted Sum of Gray Gases Model*. *J. Heat Transfer*, 104:602-608, 1982.

[A-18] Zeldovich Y.B.; Sadovnikov P.Y.; Kamentskii D.A. *Oxidation of nitrogen in combustion*. Moscow: Academy of Sciences of USSR, 1947

[A-19] Diez L.I.; Cortes C.; Pallares J., Fuel 87, 2008, 1259-1269

[A-20] Monat J. P.; Hanson R. K.; Kruger C. H.. 17th International Symposium on Combustion, 543, The Combustion Institute, 1979.

[A-21] Hanson R. K. ; Salimian S. Combustion Chemistry, 1984, 361

[A-22] Boardman RD; Smoot LD, *Pollutant formation and control*, Elsevier, 433-438, 1993.

[A-23] Arenillas A.; Backreedy R.I.; Jones J.M.; Pis J.J., Pourkashanian M., Rubiera F., Williams A.. Fuel 81, 2002, 627-636.

[A-24] Jones J.M., Patterson P.M., Pourkashanian M., Rowlands L., Williams A., 14th Annual International Pittsburgh Coal Conference (Clean Coal Technology and Coal Utilisation), Taiyuan, Shanxi, PRC, Sept. 23, 1997

Appendix B

[B-1] Fluent Inc. *Advanced Combustion Modeling*, Presentation, 2002

[B-2] Chr. Mueller, A. Brink and M. Hupa, *Numerical simulation of the Combustion Behavior of Different Biomasses in a Bubbling Fluidized Bed Boiler*, Proceedings of 18th Intenational Conferrence on Fluidised Bed Combustion, May 22-25, Toronto, Canada